FSTC-HT-23-829-70

U.S. ARMY FOREIGN SCIENCE AND TECHNOLOGY CENTER

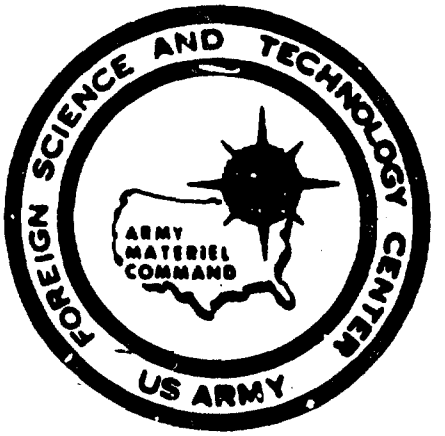

SHORTWAVE ANTENNAS

by

G. Z. Ayzenberg

COUNTRY: USSR

This document is a rendition of the original foreign text without any analytical or editorial comment.

TECHNICAL TRANSLATION

FSTC-HT-23-829-70

ENGLISH TITLE: SHORTWAVE ANTENNAS

FOREIGN TITLE: KOROTKOVOLNOVYYE ANTENNY

AUTHOR: G. Z. Ayzenberg

SOURCE: STATE PUBLISHING HOUSE FOR LITERATURE ON QUESTIONS OF COMMUNICATIONS AND RADIO (SVYAZ'IZDAT)
Moscow 1962

Translated for MID by Translation Consultants, LTD.

NOTICE

English Title:	Shortwave Antennas
Foreign Title:	Korotkovolnovyye Antenny
Author:	G. Z. Ayzenberg
Date and Place of Publication:	1962, Moscow
Publisher:	State Publishing House for Literature on Questions of Communications and Radio (Svyaz'izdat)

Foreword

This monograph is the result of the revision of the book titled Antennas for Main Shortwave Radio Communications, published in 1948.

The new book was written with an eye to the considerable progress made in the past in the engineering of shortwave antennas. This monograph presents a great deal of material on antennas which were virtually unused at the time the first monograph was published. Included among such antennas are broadside multiple-tuned antennas and, in particular, broadside antennas with untuned reflectors (Chapter XII), traveling wave antennas with pure resistance coupling (Chapter XIV), logarithmic antennas (Chapter XVI), multiple-tuned shunt dipoles (Chapter IX), and others.

The materials on rhombic antennas (Chapter XIII) have been expanded substantially. Included are data on rhombic antennas with obtuse angles (150°), as well as a great many graphics on the directional properties of antennas which take the parallel component of the field intensity vector into consideration. The question of the superposition of two rhombic antenna on a common area is discussed, as are other questions. A new chapter on single-wire traveling wave antennas (Chapter XV) has been added, as has a new chapter (Chapter XVII) on the comparative noise stability of various receiving antennas. Other materials not contained in the first monograph are included here. At the same time, much of the material which is no longer current has been deleted.

My coauthor for Chapter XIII (rhombic antennas) was S. P. Belousov.

My coauthors for Chapter XIV (single-wire traveling wave antennas) was written by S. P. Belousov and V. G. Yampol'skiy. Chapter XVII (comparative noise stability of receiving antennas) was written by L. K. Olifin. The section on transmitting antenna selectors (#4, Chapter XIX) was written by M. A. Shkud.

The graphics and computations for broadside multiple-tuned antennas were taken from the work done under the supervision of L. K. Olifin, for the most part.

The graphics for computing the mutual impedances of two balanced dipoles with arbitrary dimensions, contained in the handbook section, were compiled under the supervision of S. P. Belousov.

I express my appreciation to all the coauthors named.

I feel that it is my duty to express my deep appreciation to L. S. Tartakovskiy and Ye. G. Pol'skiy for the great help given me in selecting the materials and in editing the monograph. I also express my thanks to V. G. Ezrin and I. T. Govorkov for their great help in selecting the materials for the monograph.

I also feel that I must express my thanks to G. N. Kocherzhevskiy, the responsible editor, for the great assistance rendered in editing the manuscript, as well as for much valuable advice given me.

G. Z. Ayzenberg

List of Principal Symbols Used

A vector potential

B magnetic induction; susceptance; flux density; induction density; magnetic flux density

C capacitance; capacity; permittance; capacitor

C_l linear capacitance

c velocity of electromagnetic waves in a vacuum, $c = 3 \cdot 10^8$ meters/second

a,b,c sides of a spherical triangle; arbitary constants

A,B,C arbitary constants

D antenna directive gain; antenna front-to-back ratio

D_e electromotive force directive gain; electromotive force front-to-back ratio

D electrical displacement, k/m^2; dielectric flux density

D distance between conductors

d distance between dipoles; conductor diameter

E electric field intensity, volts/meter

e electromotive force (emf), volts

F surface

$F(\varphi\Delta)$ antenna radiation pattern formula

$F(\Delta)$ vertical plane antenna radiation pattern formula

$F(\varphi)$ horizontal plane antenna radiation pattern formula

f oscillation frequency, hertz

G conductance, mho

G_l linear conductance, mho

H magnetic field intensity

H_1,H difference in dipole heights; dipole height

h height of dipole above the ground

I electric current, amperes

I_{loop} loop current amplitude

I_{in},I_{re} incident and reflected waves of currents

I_{loop},I_{node} loop and node currents

j current volume density, amperes/meter^2

k traveling wave ratio

L inductance, henries

L_l linear inductance, henries/meter

l line length; conductor length; length of an unbalanced dipole; length of half a balanced dipole

l_{eff} antenna effective length

M mutual inductance, henries

M_l linear mutual inductance of coupled lines, henries/meter

n number of half-wave dipoles in a tier, SG or SGD antennas

n_1 number of tiers, SG or SGD antennas

P actual power

p feeder line reflection factor; arbitary constant

p_U, p_I voltage and current terminator reflection factors

q amount of electricity, charge, coulombs

R pure resistance, ohms

R_l linear impedance of uniform lines, ohms/meter

R_Σ radiation resistance

R_{nm} mutual radiation resistance of n and m dipoles in an antenna system

$|R_\parallel|$ modulus of reflection factor for a parallel polarized plane wave

$|R_\perp|$ modulus of reflection factor for a normally polarized plane wave

r radial coordinate in a spherical system of coordinates

S Poynting vector

T alternating current oscillation period

t time

U voltage; difference in potentials; volts

U_{in}, U_{re} incident and reflected waves of voltage

U_{loop}, U_{node} loop and node voltages

V voltage across points on a conductor; volume

v electromagnetic wave velocity, meters/second

W characteristic impedance of a lossless line

W_{med} characteristic impedance of the medium

X reactance

X_{nm} reactive component of the mutual radiation resistance of two dipoles, n and m

Y admittance

Y_l linear admittance of a line

Z impedance

Z_l linear impedance of a line

x, y, z rectangular coordinates

z coordinate along the axis of a cylindrical system of coordinates

Z_{eq} equivalent impedance

Z_{in} input impedance, $Z_{in} = R_{in} + iX_{in}$

Z_{load}, Z_2 line impedance

α phase factor (wave number), $\alpha = 2\pi/\lambda$

β attenuation factor

γ propagation factor

α, β, γ angles of a spherical triangle

γ_v specific conductivity, mhos/meter

Δ tilt angle

δ relative noise stability; energy leakage power ratio

ϵ permittivity of the medium, farads/meter

ϵ_0 permittivity of a vacuum, $\epsilon_0 = 1/4\pi \cdot 9 \cdot 10^9$ farads/meter

ϵ_r relative permittivity

ϵ antenna gain factor

η efficiency

η_A antenna efficiency

θ zenith angle in a spherical system of coordinates; the angle formed by the axis of a conductor with an arbitrary direction

λ wavelength, meters

μ magnetic inductivity, henries/meter

μ_0 magnetic inductivity of a vacuum, $\mu_0 = 4\pi \cdot 10^{-7}$ henries/meter

μ_r relative magnetic inductivity

ρ characteristic impedance of a line with losses; electric volume density

σ linear electric density

ξ magnetic flux; half a rhombic antenna obtuse angle

$\xi_{\parallel}$ argument (phase) for the reflection factor for a parallel polarized plane wave

$\xi_{\perp}$ argument (phase) for the reflection factor for a normally polarized plane wave

φ scalar potential

ω the azimuth in a cylindrical or spherical system of coordinates; the azimuth of antenna radiation patterns in the horizontal plane, read from a selected direction (the axis of the antenna conductor, or the normal to the axis of the antenna conductor)

ψ phase angle

ω oscillation angular frequency, $\omega = 2\pi f$

Chapter I

THE THEORY OF THE UNIFORM LINE

#I.1. Telegraphy Equations

The theory of long lines, which are systems with distributed constants, like the theory for systems with lumped constants (circuits) can be based on Kirchhoff's laws. However, the conclusions drawn from circuit theory cannot be applied directly to long lines.

Circuit theory is based on the following assumptions, and these are not applicable to long lines:

(1) a circuit consists of spatially dispersed elements in which electric or magnetic fields are concentrated. Electric field carriers are usually condensers, while magnetic field carriers are usually induction coils;

(2) currents are identical in magnitudes and phases at any given moment in time within the limits of each element (induction coils or condensers). This assumes that the time needed to propagate the electromagnetic processes within the limits of an element is so short that it can be ignored when compared with the time for one period.

These are not rigid assumptions. Even in circuits, every element which is an electric field carrier, say a condenser, is simultaneously a magnetic field carrier to some extent. A magnetic field carrier, say an induction coil, is also an electric field carrier to some extent (a shunt capacitance for the coils). Nor is the second assumption rigid.

However, in ordinary circuits the magnetic fields created around condensers, and the electric fields created around induction coils, are extremely weak. And the time required to propagate the electromagnetic processes within the limits of each element in the system is usually short. As a result, the conclusions based on the assumptions indicated are justified as a first approximation.

Neither the first, nor the second, assumption is applicable to long lines. Every element in the line, however small it may be, is a carrier of an electric, as well as of a magnetic field. Figure I.1.1 is included for purposes of illustration of what has been said to show the propagation of electric and magnetic lines of force through the cross section of a twin line. Line dimensions are usually sufficiently large, and the propagation time for the electromagnetic processes along the lines is commensurate with the time of one period. But if we cannot apply the laws governing the processes in circuits to the line as a whole, they can be applied in their entirety to a small element of the line which can be considered to be the sum of such elements. Each element in the line can be replaced by an equivalent circuit consisting of inductance and capacitance (fig. I.1.2).

Correspondingly, the line as a whole can be replaced by an equivalent circuit consisting of elementary inductances and capacitances, as shown in Figure I.1.3a. Since the line conductors have pure resistance, and since there is leakage conductance between them, the complete equivalent circuit for the line is as shown in Figure I.1.3b.

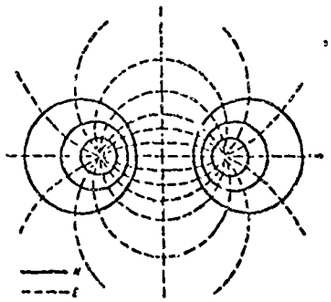

Figure I.1.1. Structure of the electromagnetic field through the transverse cross section of a twin line.

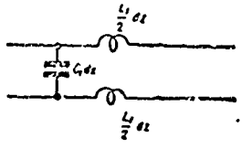

Figure I.1.2. Line element equivalent circuit.

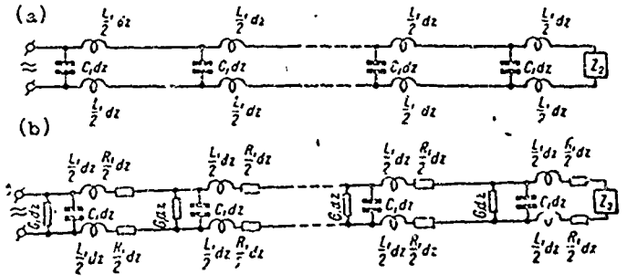

Figure I.1.3. Equivalent circuit for a line: (a) without impedance and leakage conductance considered; (b) with impedance and leakage conductance considered.

Telegraphy equations are based on Kirchhoff's laws for the formulation of the relationships between current and voltage applicable to an elementary section of a line replaced by equivalent inductance, capacitance, resistance, and leakage conductance. Solving the telegraphy equations will provide the relationships for the entire line.

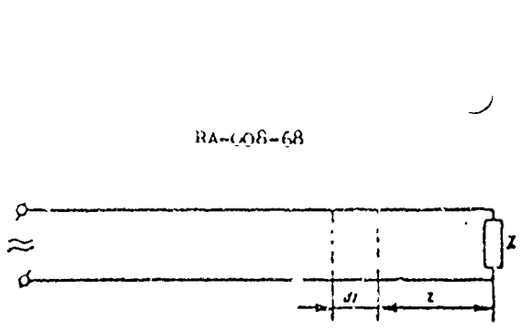

Figure I..4. Schematic diagram of an end-loaded line.

The concept of distributed constants for the line is introduced for analytical convenience:

L_1 is the inductance per unit line length;

C_1 is the capacitance per unit line length;

R_1 is the resistance per unit line length;

G_1 is the conductance per unit line length.

Telegraphy equations are derived as follows. Let us say we have a long line (fig. I.1.4), and let us isolate an infinitely small element of length dz at distance z from the termination. The isolated element, dz, has infinitely small inductance dL, capacitance dC, resistance dR, and conductance dG. They equal

$$\left.\begin{aligned} dL &= L_1 dz \\ dC &= C_1 dz \\ dR &= R_1 dz \\ dG &= G_1 dz \end{aligned}\right\}. \qquad \text{(I.1.1)}$$

The voltage drop, dU, across element dz is equal to the current, I, flowing through it multiplied by the element's impedance; that is

$$dU = I(dR + i\omega dL) = I(R_1 + i\omega L_1)dz = IZ_1 dz, \qquad \text{(I.1.2)}$$

where

ω is the angular frequency of the voltage applied to the line, while

$$Z_1 = R_1 + i\omega L_1.$$

Dividing both sides of the equation by dz, we obtain

$$\frac{dU}{dz} = IZ_1. \qquad \text{(I.1.3)}$$

The expression for the change in the current flowing in element dz can be derived in similar fashion.

The change in the current, dI flowing in element dz is equal to the current shunted in the capacitance and the conductance of this element.

This current is equal to the voltage multiplied by the element's impedance; that is

$$dI = U(dG + i\omega dC) = U(G_1 + i\omega C_1)dz = UY_1 dz. \qquad \text{(I.1.4)}$$

where

$$Y_1 = G_1 + i\omega C_1.$$

Dividing both sides of the equation by dz, we obtain

$$\frac{dI}{dz} = UY_1. \qquad \text{(I.1.5)}$$

Equations (I.1.3) and (I.1.5) are called telegraphy equations. They establish the association between the voltage and the current at any point in the line.

#I.2. Solving the Telegraphy Equations

(a) General expressions for voltage and current

In order to solve the telegraphy equations they are transformed so each contains only U or I. When the equations are differentiated with respect to z they take the following form

$$\left.\begin{aligned}\frac{d^2U}{dz^2} &= Z_1\frac{dI}{dz}\\ \frac{d^2I}{dz^2} &= Y_1\frac{dU}{dz}\end{aligned}\right\}. \qquad \text{(I.2.1)}$$

Substituting the values for dU/dz and dI/dz from I.1.3 and I.1.5 in (I.2.1), and converting, we obtain

$$\left.\begin{aligned}\frac{d^2U}{dz^2} - Z_1Y_1U &= 0\\ \frac{d^2I}{dz^2} - Z_1Y_1I &= 0\end{aligned}\right\}. \qquad \text{(I.2.2)}$$

The differential equations at (I.2.2) have the following solutions

$$\left.\begin{aligned}U &= A_1e^{\gamma z} + B_1e^{-\gamma z}\\ I &= A_2e^{\gamma z} + B_2e^{-\gamma z}\end{aligned}\right\}, \qquad \text{(I.2.3)}$$

where A_1, A_2, B_1 and B_2 are constants of integration,

$$\gamma = \sqrt{Z_1Y_1} = \sqrt{(R_1 + i\omega L_1)(G_1 + i\omega C_1)} = \beta + i\alpha. \qquad \text{(I.2.4)}$$

Here γ is the wave propagation factor;

β is the attenuation factor;

α is the phase factor.

Let us substitute the solutions found in equation (I.1.3) in order to determine the dependencies between A_1, B_1 and A_2, B_2. We then obtain

$$\gamma A_1e^{\gamma z} - \gamma B_1e^{-\gamma z} = Z_1(A_2e^{\gamma z} + B_2e^{-\gamma z}). \qquad \text{(I.2.5)}$$

The equality (I.2.5) should be satisfied identically for any value of z. This can only be so if the terms with the factors $e^{\gamma z}$ in the right and left hand sides are equal to each other. This applies as well to the terms with the factors $e^{-\gamma z}$ in the right and left hand-sides. Accordingly, we obtain two equations

$$\left.\begin{aligned} A_2 &= \frac{A_1}{\rho} \\ B_2 &= -\frac{B_1}{\rho} \end{aligned}\right\}. \qquad \text{(I.2.6)}$$

where the symbol introduced

$$\rho = \sqrt{\frac{Z_1}{Y_1}} = \sqrt{\frac{R_1 + i\omega L_1}{G_1 + i\omega C_1}}, \qquad \text{(I.2.7)}$$

is called the line's characteristic impedance. (See Appendix 1).

Substituting the values for A_2 and B_2 from (I.2.6) in (I.2.3), we obtain

$$\left.\begin{aligned} U &= A_1 e^{\gamma z} + B_1 e^{-\gamma z} \\ I &= \frac{1}{\rho}\left(A_1 e^{\gamma z} - B_1 e^{-\gamma z}\right) \end{aligned}\right\}. \qquad \text{(I.2.8)}$$

We will use the conditions at the termination, that is, at the point where z = 0, in order to determine the constants of integration.

Let us designate the voltage and current at the termination by U_2 and I_2. Substituting z = 0 in (I.2.8) and solving with respect to A_1 and B_1, we obtain

$$\left.\begin{aligned} A_1 &= \frac{1}{2}(U_2 + I_2\rho) \\ B_1 &= \frac{1}{2}(U_2 - I_2\rho) \end{aligned}\right\}. \qquad \text{(I.2.8a)}$$

Substituting the values for A_1 and B_1 in (I.2.8), we can present formula (I.2.8) in the form

$$\left.\begin{aligned} U &= U_2 \operatorname{ch}\gamma z + I_2\rho \operatorname{sh}\gamma z \\ I &= I_2 \operatorname{ch}\gamma z + \frac{U_2}{\rho}\operatorname{sh}\gamma z \end{aligned}\right\}. \qquad \text{(I.2.9)}$$

(b) Expressions for voltage and current in high-frequency lines. The ideal line.

At high frequencies $\omega L_1 \gg R_1$ and $\omega C_1 \gg G_1$. Therefore, when making engineering computations it is often possible to approximate a line's characteristic impedance as

$$W = \sqrt{\frac{L_1}{C_1}}. \qquad \text{(I.2.10)}$$

The characteristic impedance, W, is a real magnitude when R_1 and G_1 are disregarded.

Replacing ρ in (I.2.9) with W, we obtain

$$\left.\begin{aligned} U &= U_2 \operatorname{ch}\gamma z + I_2 W \operatorname{sh}\gamma z \\ I &= I_2 \operatorname{ch}\gamma z + \frac{U_2}{W} \operatorname{sh}\gamma z \end{aligned}\right\} \qquad \text{(I.2.11)}$$

It is sometimes preferable to use approximate formulas in analyzing short lines in order to simplify the calculations. These formulas are derived on the assumption that $R_1 = G_1 = 0$. And $\gamma = i\alpha$, while the expressions for voltage and current take the form

$$\left.\begin{aligned} U &= U_2 \cos\alpha z + iI_2 W \sin\alpha z \\ I &= I_2 \cos\alpha z + i\frac{U_2}{W} \sin\alpha z \end{aligned}\right\} \qquad \text{(I.2.12)}$$

A lossless line is called an ideal line.

#I.3. Attentuation Factor β, Phase Factor α, and Propagation Phase Velocity v

Squaring the right and left hand-sides of equation (I.2.4) and equating the real and imaginary components to each other respectively, we obtain two equations, from which we determine that

$$\alpha = \frac{2\pi}{\lambda} \sqrt{\frac{1}{2}\left\{\left(1 - \frac{R_1 G_1}{\omega^2 L_1 C_1}\right) + \sqrt{\left[1 + \left(\frac{R_1}{\omega L_1}\right)^2\right]\left[1 + \left(\frac{G_1}{\omega C_1}\right)^2\right]}\right\}}, \qquad \text{(I.3.1)}$$

$$\beta = \frac{\omega}{2\alpha}(R_1 C_1 + G_1 L_1) \approx \frac{1}{2}\left(\frac{R_1}{W} + G_1 W\right). \qquad \text{(I.3.2)}$$

where

λ is the wavelength in free space.

If line operating conditions are such that we can take $G_1 = 0$, then

$$\alpha = \frac{2\pi}{\lambda} \sqrt{\frac{1}{2}\left[1 + \sqrt{1 + \left(\frac{R_1}{\omega L_1}\right)^2}\right]}, \qquad \text{(I.3.3)}$$

$$\beta = \frac{R_1}{2W}. \qquad \text{(I.3.4)}$$

If $R_1 = G_1 = 0$, then

$$\left.\begin{aligned} \alpha &= \frac{2\pi}{\lambda} \\ \beta &= 0. \end{aligned}\right\} \qquad \text{(I.3.5)}$$

Substituting the expression for γ from (I.2.4) in (I.2.8), we obtain

$$\left.\begin{aligned} U &= A_1 e^{(\beta z + i\alpha z)} + B_1 e^{-(\beta z + i\alpha z)} \\ I &= \frac{1}{\rho}\left[A_1 e^{(\beta z + i\alpha z)} - B_1 e^{-(\beta z + i\alpha z)}\right] \end{aligned}\right\}. \qquad \text{(I.3.6)}$$

As will be seen from (I.3.6), the voltage and current amplitudes at any point in the line have two components. The first of these (with the coefficient A_1) decreases with decrease in z; that is, as a result of approaching the termination. The second (with coefficient B_1) increases as the termination is approached. Moreover, the closer to the source the first component is, the greater the phase lead, but conversely, the closer the second component is to the source the greater the phase lag.

What follows from what has been pointed out is that the first component is a voltage and current wave propagated from the source to the termination (incident wave), while the second component is a voltage and current wave propagated in the opposite direction (reflected wave)(fig. I.3.1).

Propagation of these voltage and current waves occurs at a velocity determined by the phase factor α. Let us find the absolute magnitude of the wave propagation phase velocity on the line. From formula (I.3.6) it will be seen that when wave passage is over a segment of length z the phase will change by angle φ, equal in absolute magnitude to

$$|\varphi| = \alpha z. \qquad (I.3.7)$$

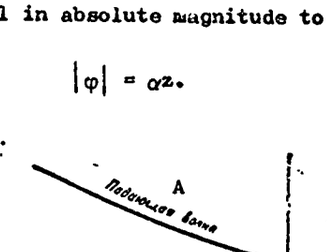

Figure I.3.1. Distribution of amplitudes of incident and reflected waves on a line.

A - incident wave; B - reflected wave.

On the other hand, the phase angle can be expressed in terms of the propagation phase velocity. In fact, let the wave be propagated with constant phase velocity v. Then the phase angle obtained as the wave passes over a path of length z will be equal to

$$\varphi = 2\pi \frac{t}{T} = 2\pi \frac{z}{v} \frac{1}{T}, \qquad (I.3.8)$$

where

T is the time of one period;

$t = z/v$ is the time needed to cover path z at velocity v.

Equating the right-hand sides of equations (I.3.7) and (I.3.8), we obtain

$$v = \frac{2\pi}{\alpha} \frac{1}{T}.$$

Expressing T in terms of the wavelength in free space, λ, and the propagation rate in free space by c, and then substituting $T = \lambda/c$, we obtain

$$v = \frac{2\pi}{\lambda\alpha} c, \qquad (I.3.9)$$

where

$c = 3 \cdot 10^8$ meters/second is the speed of light in free space.

As a practical matter, at high frequencies $\alpha \approx 2\pi/\lambda$, and, correspondingly, $v \approx c$.

Recapping what has been explained above, we can describe the processes taking place on a line as follows.

The electromotive force applied to a line causes voltage and current waves to appear on it and these waves are propagated from the source to the termination at velocity v, which is close to that of light, c. The current and voltage waves are respectively propagated at a phase velocity close to that of light, and the electromagnetic field is an electromagnetic wave.

In the general case the wave is partly reflected by and partly dissipated in the termination resistor. The reflected wave is back propagated from the termination to the point of supply at the same velocity as the incident wave. The wave is attenuated as it is propagated on the conductor. The magnitude of the attenuation is determined by the attenuation factor, and it, in turn, is determined by the line's distributed constants.

#I.4. The Reflection Factor

The reflection factor is the ratio between the reflected wave of voltage (U_{re}) or current (I_{re}) at the point of reflection and the incidence wave of voltage (U_{in}) or current (I_{in}) at the same point.

As will be seen from (I.2.8) and (I.2.8a), the voltage reflection factor equals

$$p_U = \frac{U_{re}}{U_{in}} = \frac{B_1}{A_1} = \frac{U_2 - I_2 \rho}{U_2 + I_2 \rho} = \frac{Z_2 - \rho}{Z_2 + \rho}. \qquad (I.4.1)$$

At high frequencies, when ρ can be replaced by W, we obtain

$$p_U = \frac{Z_2 - W}{Z_2 + W}. \qquad (I.4.2)$$

It can be shown in a similar manner that the current reflection factor equals

$$p_I = I_{re}/I_{in} = -p_U \qquad (I.4.3)$$

The reflection factor p_I can also be considered to be the magnetic field reflection factor; that is

$$p_I = Int_{re}/Int_{in} = p_{Int} \tag{I.4.4}$$

where

Int_{re} and Int_{in} are the magnetic field intensities of the reflected and incident waves in a transverse plane passing through the end of the line.

Similarly,

$$p_U = E_{re}/E_{in} = p_E \tag{I.4.5}$$

where

E_{re} and E_{in} are the electric field intensities of the reflected and incident waves in the transverse plane indicated.

$$p_{Int} = -p_E \tag{I.4.6}$$

The equality at (I.4.6) is self-evident because the Poynting vector for the reflected wave has a direction diametrically opposed to that of the Poynting vector for the incident wave (see Chapter IV).

Let us find the numerical values of the reflection factors for some special cases.

An open-end line ($Z_2 = \infty$):

$$\left.\begin{aligned} p_U &= \frac{\infty - \rho}{\infty + \rho} = 1 \\ p_I &= -1 \end{aligned}\right\}. \tag{I.4.7}$$

A closed-end line ($Z_2 = 0$):

$$\left.\begin{aligned} p_U &= \frac{0 - \rho}{0 + \rho} = -1 \\ p_I &= 1 \end{aligned}\right\}. \tag{I.4.8}$$

A high-frequency line, reactance loaded ($Z_2 = iX_2$):

$$p_U = \frac{iX_2 - W}{iX_2 + W}. \tag{I.4.9}$$

The absolute value (the modulus) of p_U equals

$$|p_U| = \sqrt{\frac{X_2^2 + W^2}{X_2^2 + W^2}} = 1. \tag{I.4.10}$$

A line loaded with impedance equal to its wave impedance ($Z_2 = \rho$):

$$p_U = \frac{\rho - \rho}{\rho + \rho} = 0. \tag{I.4.11}$$

The results obtained can be interpreted as follows.

The energy fed into the line continuously in the form of an incident wave can either be dissipated in the pure resistance installed at the end of the line, or it can be returned to the source in the form of a reflected wave. The wave is fully reflected by open-end or closed-end lines, as well as by a line, the end of which has installed in it a reactance which takes no energy. Accordingly, the modulus of the reflection factor will equal one. In this case, if there are no losses in the line proper, the energy circulates from the beginning to the end of the line and back, without being dissipated.

If the termination contains pure resistance, or complex impedance, the incident wave energy can be dissipated in the termination. However, we can only have complete dissipation of the incident wave energy when the termination contains a resistance across the terminals of which it is possible to retain that relationship between voltage and current created in the wave propagated along the line. For the incident wave the voltage to current ratio equals ρ. As a result, only when the end of the line contains impedance $Z_2 = \rho$ is it possible to actually have complete dissipation; that is, $p_U = p_I = 0$.

If the termination contains impedance $Z_2 \neq \rho$, U_2/I_2 at its terminals will equal Z_2 and will differ from ρ. Now complete dissipation is impossible, and some of the energy is reflected.

The reflection factor has a magnitude such that the relationship

$$Z_2 = U_{in} + U_{re}/I_{in} + I_{re} = \rho \cdot 1 + p_U/1 + p_I \qquad (I.4.12)$$

is satisfied at the end of the line.

Nor is it difficult to explain the sense of the concrete values of p_I and p_U given by formulas (I.4.7)-(I.4.11). For purposes of example, let us take formulas (1.4.7) and (I.4.8). What follows from these formulas is that in the case of the open-end line (fig. I.5.1) the current reflection factor equals (-1). This is understandable because the current corresponds to a moving charge which, naturally enough, begins to move in the opposite direction when it reaches the termination, and this is equivalent to rotating the phase 180°. On the other hand, in the case of the closed-end line the charge continues to move when it reaches the termination, and makes a transition from one conductor to the other at the point of short circuit. A charge on one, let us say the upper conductor, moves to the other (lower) conductor and, conversely, a charge moves from the lower conductor to the upper conductor. The direction of movement changes 180° when the transition is made to the other conductor, naturally enough. A charge changing direction at the site of the transition to the other conductor corresponds to a reflected wave of current. Reflected waves of current have no phase jumps at the reflection

site (p_I = 1) because the change in the direction in which the charges are propagated occurs at the site of the transition to the other conductor, which has a current with opposite phase flowing in it (the currents in conductors 1 and 2 have opposite phases). We can explain the sense of the values obtained for p_I and p_U, given other conditions at the end of the line, in a similar manner.

#I.5. Voltage and Current Distribution in a Lossless Line

(a) The open-end line

The current flowing in an open-end line is $I_2 = 0$. Substituting $I_2 = 0$ in equation (I.2.12), we obtain

$$\left.\begin{aligned} U &= U_2 \cos \alpha z \\ I &= i \frac{U_2}{W} \sin \alpha z \end{aligned}\right\}. \qquad \text{(I.5.1)}$$

Figure I.5.1 shows the curves for the distribution of voltage and current on an open-end line.

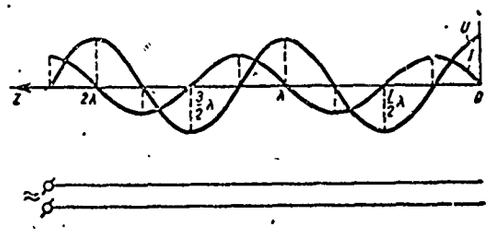

Figure I.5.1. Voltage and current distribution on an open-end line.

As will be seen, there is a voltage loop (maximum) and a current node (minimum) at the termination. Loops and nodes for both voltage and current occur at length segments equal to $\lambda/2$. Voltages and currents at the nodes equal zero.

The phases of voltage and current on the line change in 180° jumps as they pass through a node.

An electromagnetic wave on a line characterized by this type of current and voltage distribution, one in which phases change in jumps as they pass through zero, and remain constant within the limits of the segments between two adjacent nodes, is called a standing wave.

(b) The closed-end line

The voltage across the closed-end line equals zero ($U_2 = 0$). Here equation (I.2.12) takes the form

$$\left.\begin{aligned} U &= i I_2 W \sin \alpha z \\ I &= I_2 \cos \alpha z \end{aligned}\right\}. \qquad \text{(I.5.2)}$$

Figure I.5.2. shows the curves for the distribution of the voltage and current on a closed-end line. The curves have the same shape as those for the open-ended line, but the difference here is that there is a voltage node and a current loop at the end of the line.

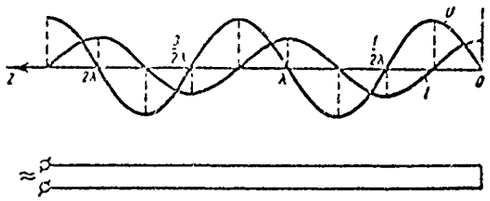

Figure I.5.2. Voltage and current distribution on a closed-end line.

(c) The reactance loaded line

Substituting $U_2/I_2 = Z_2 = iX_2$ in (I.2.12), and after making the transformations, we obtain

$$\left.\begin{aligned} U &= U_2 \frac{\cos(\alpha z - \varphi)}{\cos\varphi} \\ I &= i\frac{U_2}{W}\frac{\sin(\alpha z - \varphi)}{\cos\varphi} \end{aligned}\right\}, \qquad \text{(I.5.3)}$$

where

$$\varphi = \operatorname{arc\,tg}\frac{W}{X_2}.$$

A standing wave is formed on the line and there are no voltage or current nodes or loops at the termination. The first voltage loop is at distance

$$z_0 = \frac{\varphi}{\alpha} = \lambda\frac{\varphi}{2\pi}.$$

Figure I.5.3. shows the curves for current and voltage distribution for $X_2 = W(\varphi = \pi/4)$.

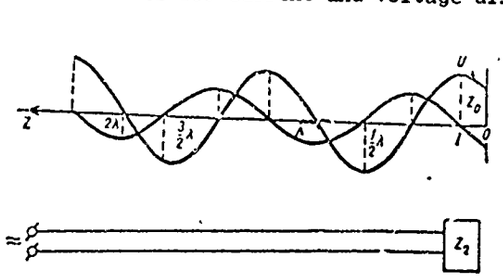

Figure I.5.3. Voltage and current distribution on a line for $R_2 = 0$, $X_2 = W$.

(d) The pure resistance loaded line

Substituting $U_2/I_2 = R_2$ in (I.2.12), we obtain

$$\left.\begin{aligned} U &= U_2\left(\cos\alpha z + i\frac{W}{R_2}\sin\alpha z\right) \\ I &= I_2\left(\cos\alpha z + i\frac{R_2}{W}\sin\alpha z\right) \end{aligned}\right\}. \qquad \text{(I.5.4)}$$

Figure I.5.4 shows the curves for the voltage distribution on a line for values of R_2/W equal to 0; 0.1; 0.2; 0.5; 1; 2; 5; 10; ∞.

The current distribution curves have the same characteristics as do the voltage distribution curves, but the displacement along the line with respect to the latter is by segments equal to 1/4 λ.

When $R_2 > W$ the voltage and current loops and nodes appear at the same points as they do on the open-end line, and when $R_2 < W$ they appear at the same points as they do on the closed-end line.

(e) The line with a load equal to the wave impedance

Substituting $R_2 = W$ in (I.5.4), we obtain

$$\left.\begin{aligned} U &= U_2 e^{i\alpha z} \\ I &= I_2 e^{i\alpha z} \end{aligned}\right\}. \qquad \text{(I.5.5)}$$

The line has only an incident wave. This mode on a line of finite length, when there is no reflected wave, is called the traveling wave mode.

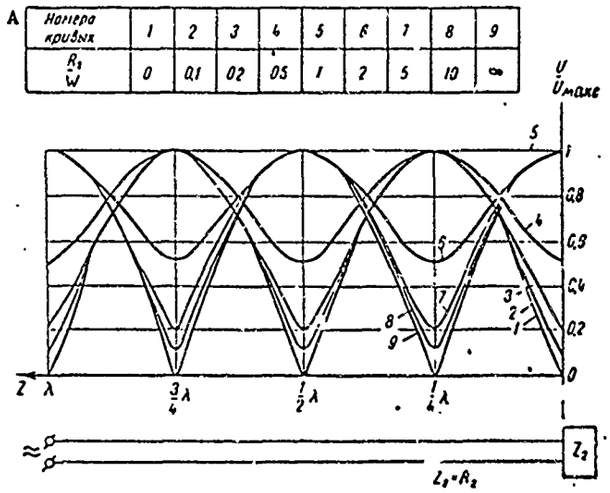

Figure I.5.4. Voltage distribution on a line for different values of R_2/W and $X_2 = 0$.
A - curve number.

(f) The complex impedance loaded line

Converting formula (I.2.12) and substituting $U_2/I_2 = Z_2$, we obtain

$$\left.\begin{aligned} U &= U_2\left(\cos\alpha z + i\frac{W}{Z_2}\sin\alpha z\right) \\ I &= I_2\left(\cos\alpha z + i\frac{Z_2}{W}\sin\alpha z\right) \end{aligned}\right\}. \qquad \text{(I.5.6)}$$

Here the coefficients of sin αz are complex magnitudes, as distinguished from formula (I.5.6), in which the coefficients of sin αz are imaginary. This latter indicates that when z = 0 there are neither voltage loops nor voltage nodes.

The formulas at (I.5.6) can also be given in the form for when the coefficients of the sines in the right-hand side are imaginary. This requires making a substitution

$$\alpha z = \alpha z_1 + \varphi = \alpha\left(z_1 + \frac{\varphi}{\alpha}\right), \qquad (I.5.7)$$

that is, the reading is not made at the termin[illegible], but at a point displaced from the termination by distance $z_0 = \varphi/\alpha$ (toward the energy source side), where φ can be determined from the relationship

$$\operatorname{tg} 2\varphi = \frac{2WX_2}{R_2^2 + X_2^2 - W^2}. \qquad (I.5.8)$$

The angle 2φ is taken to be in the quadrant in which the sign of $\sin 2\varphi$ coincides with the sign of the numerator, and the sign of $\cos 2\varphi$ coincides with the sign of the denominator in (I.5.8).

Substituting (I.5.7) in (I.5.6), we obtain

$$\left.\begin{aligned} U &= U_2\left(\cos\alpha z_1 + i\frac{W}{D}\sin\alpha z_1\right)Ce^{i\varphi} \\ I &= \frac{U_2}{D}\left(\cos\alpha z_1 + i\frac{D}{W}\sin\alpha z_1\right)Ce^{i\varphi} \end{aligned}\right\} \qquad (I.5.9)$$

where

$$C = \frac{2R_2W}{\sqrt{(R_2^2 + X_2^2 + R_2W)^2 + (X_2W)^2} - \sqrt{(R_2^2 + X_2^2 - R_2W)^2 + (X_2W)^2}}, \qquad (I.5.10)$$

$$D = W\frac{2R_2W}{(R_2^2 + X_2^2 + W^2) - \sqrt{(R_2^2 + X_2^2 + W^2)^2 - (2R_2W)^2}} \qquad (I.5.11)$$

$$\operatorname{tg} 2\psi = \frac{2R_2X_2W^2}{(R_2^2 + X_2^2)^2 - (R_2^2 - X_2^2)W^2}. \qquad (I.5.12)$$

The angle 2ψ is taken to be in the quadrant in which the sign of $\sin 2\psi$ coincides with the sign of the numerator, and the sign of $\cos 2\psi$ coincides with the sign of the denominator in (I.5.12).

Since $(R_2^2 + X_2^2 + W^2)^2 \geq (2R_2W)^2$, as as will be seen from formula (I.5.11), D is real. D has the dimensionality of impedance. A comparison between formula (I.5.9) and (I.5.4) shows that D is the line impedance at point $z_1 = 0$. From formula (I.5.11), D > W for any loads at the termination. Consequently, the voltage and current distribution, beginning at point $z_1 = 0$ (that is, beginning at a point displaced $z_0 = \varphi/\alpha$ with respect to the termination), is the same as in the case of the line loaded with pure resistance,

$R_2 > W$. There is a voltage loop at $z = z_0$. Accordingly, substitution of $\alpha z = \alpha z_1 + \varphi$ results in the equivalent transfer of the point at which the reading is made from the termination ($z = 0$) to the site where the voltage loop is found ($z_1 = 0$).

Figure I.5.5 shows the voltage and current distribution for $R_2 = X_2 = W$.

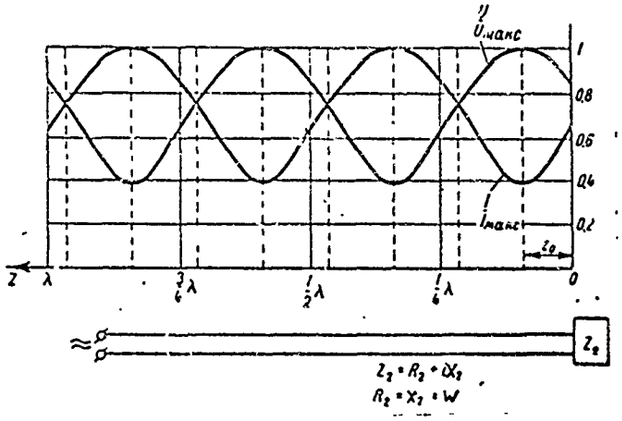

Figure I.5.5. Voltage and current distribution on a line for $R_2 = X_2 = W$.

#I.6. Voltage and Current Distribution in a Lossy Line

(a) The open-ended line

As in the case of the lossless line, we obtain

$$\left.\begin{aligned} U &= U_2 \operatorname{ch}\gamma z \\ I &= \frac{U_2}{\rho} \operatorname{sh}\gamma z \end{aligned}\right\}. \qquad (I.6.1)$$

These formulas can be reduced to the form

$$\left.\begin{aligned} U &= U_2(\operatorname{ch}\beta z \cos\alpha z + i \operatorname{sh}\beta z \sin\alpha z) \\ I &= \frac{U_2}{\rho}(\operatorname{sh}\beta z \cos\alpha z + i \operatorname{ch}\beta z \sin\alpha z) \end{aligned}\right\}. \qquad (I.6.2)$$

As will be seen, in the lossy line the voltage and current have two components 90° apart.

Formula (I.6.2) can be given in the form

$$\left.\begin{aligned} U &= U_2 \sqrt{\operatorname{sh}^2\beta z + \cos^2\alpha z}\, e^{i\varphi_U} \\ I &= \frac{U_2}{\rho} \sqrt{\operatorname{sh}^2\beta z + \sin^2\alpha z}\, e^{i\varphi_I} \end{aligned}\right\}, \qquad (I.6.3)$$

where

$$\varphi_U = \operatorname{arc\,tg}(\operatorname{th}\beta z \operatorname{tg}\alpha z), \qquad (I.6.4)$$

$$\varphi_I = \operatorname{arc\,tg}(\operatorname{cth}\beta z \operatorname{tg}\alpha z). \qquad (I.6.5)$$

Analysis of formula (I.6.3) reveals that in the lossy line the voltage and current loops and nodes are displaced relative to the loops and nodes on the ideal line. Given below are the formulas for computing the distances from the termination to the voltage and current loops and nodes on the open-ended lossy line:

$$z_{U\ \text{loop}} = \frac{n}{1-\left(\frac{\beta}{\alpha}\right)^2}\cdot\frac{\lambda}{2}, \qquad \text{(I.6.6)}$$

$$z_{U\ \text{node}} = \frac{2n+1}{1+\left(\frac{\beta}{\alpha}\right)^2}\cdot\frac{\lambda}{4}, \qquad \text{(I.6.7)}$$

$$z_{I\ \text{loop}} = \frac{2n+1}{1-\left(\frac{\beta}{\alpha}\right)^2}\cdot\frac{\lambda}{4}, \qquad \text{(I.6.8)}$$

$$z_{i\ \text{node}} = \frac{n}{1+\left(\frac{\beta}{\alpha}\right)^2}\cdot\frac{\lambda}{2}, \qquad \text{(I.6.9)}$$

where

n = 0, 1, 2, 3..

These are approximate formulas, based on the assumption that $\beta/\alpha \ll 1$.

The voltages and currents at the loops and nodes can be computed through the following formulas

$$U_{\text{loop}} = U_2 \operatorname{ch}\beta z \sqrt{1-\left(\frac{\beta}{\alpha}\right)^2 \operatorname{sh}^2\beta z}, \qquad \text{(I.6.10)}$$

$$U_{\text{node}} = U_2 \operatorname{sh}\beta z \sqrt{1+\left(\frac{\beta}{\alpha}\right)^2 \operatorname{ch}^2\beta z}, \qquad \text{(I.6.11)}$$

$$I_{\text{loop}} = \frac{U_2}{\rho} \operatorname{ch}\beta z \sqrt{1-\left(\frac{\beta}{\alpha}\right)^2 \operatorname{sh}^2\beta z}, \qquad \text{(I.6.12)}$$

$$I_{\text{node}} = \frac{U_2}{\rho} \operatorname{sh}\beta z \sqrt{1+\left(\frac{\beta}{\alpha}\right)^2 \operatorname{ch}^2\beta z}. \qquad \text{(I.6.13)}$$

Here z is the distance from the termination to the points where U_{loop}, U_{node}, I_{loop}, and I_{node} can be determined. They can be computed through formulas ((.6.6) - (I.6.9).

(b) The closed-end line

$$\left.\begin{aligned} U &= i_2 \rho \operatorname{sh}\gamma z \\ I &= I_2 \operatorname{ch}\gamma z \end{aligned}\right\}. \qquad \text{(I.6.14)}$$

The formulas at (I.6.14) can be given in the form

$$\left.\begin{aligned} U &= I_2 \rho \sqrt{\operatorname{sh}^2\beta z + \sin^2\alpha z}\, e^{i\varphi_U} \\ I &= I_2 \sqrt{\operatorname{sh}^2\beta z + \cos^2\alpha z}\, e^{i\varphi_I} \end{aligned}\right\}, \qquad \text{(I.6.15)}$$

where

$$\varphi_U = \operatorname{arc\,tg}(\operatorname{cth}\beta z \operatorname{tg}\alpha z), \qquad \text{(I.6.16)}$$

$$\varphi_I = \operatorname{arc\,tg}(\operatorname{th}\beta z \operatorname{tg}\alpha z). \qquad \text{(I.6.17)}$$

The locations of the voltage and current loops and nodes can be found through the approximate formulas

$$z_{U\ loop} = \frac{2n+1}{1-\left(\frac{\beta}{\alpha}\right)^2}\frac{\lambda}{4}, \tag{I.6.18}$$

$$z_{U\ node} = \frac{n}{1+\left(\frac{\beta}{\alpha}\right)^2}\frac{\lambda}{2}, \tag{I.6.19}$$

$$z_{I\ loop} = \frac{n}{1-\left(\frac{\beta}{\alpha}\right)^2}\frac{\lambda}{2}, \tag{I.6.20}$$

$$z_{I\ node} = \frac{2n+1}{1+\left(\frac{\beta}{\alpha}\right)^2}\frac{\lambda}{4}. \tag{I.6.21}$$

The expressions for U_{loop}, U_{node}, I_{loop}, and I_{node} are the same as in the case of the open-ended line.

(c) The reactance loaded line

Here, for convenience of analysis, the equations at (I.2.9), by substitution

$$Z_2 = U_2/I_2 \text{ and } \operatorname{tg}\theta = -\rho/Z_2 \tag{I.6.22}$$

can be converted into

$$\left.\begin{aligned} U &= U_2\frac{\operatorname{ch}(\gamma z-\theta)}{\operatorname{ch}\theta} \\ I &= \frac{U_2}{\rho}\frac{\operatorname{sh}(\gamma z-\theta)}{\operatorname{ch}\theta} \end{aligned}\right\} \tag{I.6.23}$$

In the general case θ is a complex magnitude

$$\theta = b + ia \tag{I.6.24}$$

Substituting $\gamma z = \beta z + i\alpha z$ and $\theta = b + ia$, in the formulas at (I.6.23), we obtain

$$\left.\begin{aligned} U &= \frac{U_2}{\operatorname{ch}(b+ia)}\left[\operatorname{ch}(\beta z-b)\cos(\alpha z-a)+i\operatorname{sh}(\beta z-b)\sin(\alpha z-a)\right] \\ I &= \frac{U_2}{\rho\operatorname{ch}(b+ia)}\left[\operatorname{sh}(\beta z-b)\cos(\alpha z-a)+i\operatorname{ch}(\beta z-b)\sin(\alpha z-a)\right] \end{aligned}\right\} \tag{I.6.25}$$

The formulas at (I.6.25) can be given in the form

$$\left.\begin{aligned} U &= \frac{U_2}{\operatorname{ch}(b+ia)}\sqrt{\operatorname{sh}^2(\beta z-b)+\cos^2(\alpha z-a)}\,e^{i\varphi_U} \\ I &= \frac{U_2}{\rho\operatorname{ch}(b+ia)}\sqrt{\operatorname{sh}^2(\beta z-b)+\sin^2(\alpha z-a)}\,e^{i\varphi_I} \end{aligned}\right\} \tag{I.6.26}$$

where

$$\varphi_U = \operatorname{arc\,tg}\left[\operatorname{th}(\beta z-b)\operatorname{tg}(\alpha z-a)\right], \tag{I.6.27}$$

$$\varphi_I = \operatorname{arc\,tg}\left[\operatorname{cth}(\beta z-b)\operatorname{tg}(\alpha z-a)\right]. \tag{I.6.28}$$

The magnitudes b and a can be determined from the relationship $\text{th}\,\theta = \text{th}(b + ia) = -\rho/Z_2$, and prove to be equal to

$$\text{th}\,2b = \frac{2B}{1 + A^2 + B^2}, \tag{I.6.29}$$

$$\text{tg}\,2a = \frac{2A}{1 - A^2 - B^2}, \tag{I.6.30}$$

where A and B are the imaginary and real components of the relationship $-\rho/Z_2$

$$B + iA = -\frac{\rho}{Z_2}. \tag{I.6.31}$$

The following approximate expression for the characteristic impedance (see Appendix 1) can be obtained from formula (I.2.7)

$$\rho = W\left(1 - i\frac{\beta}{\alpha}\right). \tag{I.6.32}$$

Substituting (I.6.32) in (I.6.31), and (I.6.31) in (I.6.29) and (I.6.30), we obtain

$$\text{th}\,2b = -\frac{2W\left(R_2 - \frac{\beta}{\alpha}X_2\right)}{\left(R_2^2 + X_2^2\right) + W^2\left[1 + \left(\frac{\beta}{\alpha}\right)^2\right]}, \tag{I.6.33}$$

$$\text{tg}\,2a = \frac{2W\left(X_2 + \frac{\beta}{\alpha}R_2\right)}{\left(R_2^2 + X_2^2\right) - W^2\left[1 + \left(\frac{\beta}{\alpha}\right)^2\right]}. \tag{I.6.34}$$

If $\beta/\alpha \ll 1$, then ρ can be replaced by W and formulas (I.6.33) and (I.6.34) will take the form

$$\text{th}\,2b = -\frac{2WR_2}{R_2^2 + X_2^2 + W^2}, \tag{I.6.35}$$

$$\text{tg}\,2a = \frac{2WX_2}{R_2^2 + X_2^2 - W^2}. \tag{I.6.36}$$

Comparing (I.6.36) and (I.5.8), we see that in this case

$$\text{tg}\,2a = \text{tg}\,2\varphi,$$

as should be expected.

The locations of the voltage and current loops and nodes can be determined through formulas

$$z_{U\ \text{loop}} = \frac{\left(n + \frac{\alpha}{\pi}\right) - \frac{\beta}{\alpha}\frac{\text{sh}\,2b}{2\pi}}{1 - \left(\frac{\beta}{\alpha}\right)^2 \text{ch}\,2b} \cdot \frac{\lambda}{2}, \tag{I.6.37}$$

$$z_{U\ node} = \frac{\left[(2n+1)+\frac{2a}{\pi}\right]+\frac{\beta}{\alpha}\frac{\sh 2b}{\pi}}{1+\left(\frac{\beta}{\alpha}\right)^2 \ch 2b}\frac{\lambda}{4}, \qquad (I.6.38)$$

$$z_{I\ loop} = \frac{\left[(2n+1)+\frac{2a}{\pi}\right]-\frac{\beta}{\alpha}\frac{\sh 2b}{\pi}}{1-\left(\frac{\beta}{\alpha}\right)^2 \ch 2b}\frac{\lambda}{4}, \qquad (I.6.39)$$

$$z_{I\ node} = \frac{\left(n+\frac{a}{\pi}\right)+\frac{\beta}{\alpha}\frac{\sh 2b}{2\pi}}{1+\left(\frac{\beta}{\alpha}\right)^2 \ch 2b}\frac{\lambda}{2}, \qquad (I.6.40)$$

where n = 0, 1, 2, 3...

Voltages and currents at nodes and loops equal

$$U_{loop} = U_2 \ch(\beta z - b)\sqrt{\frac{1-\left(\frac{\beta}{\alpha}\right)^2 \sh^2(\beta z - b)}{\sh^2 b + \cos^2 a}}, \qquad (I.6.41)$$

$$U_{node} = U_2 \sh(\beta z - b)\sqrt{\frac{1+\left(\frac{\beta}{\alpha}\right)^2 \ch^2(\beta z - b)}{\sh^2 b + \cos^2 a}}, \qquad (I.6.42)$$

$$I_{loop} = \frac{U_2}{\rho}\ch(\beta z - b)\sqrt{\frac{1-\left(\frac{\beta}{\alpha}\right)^2 \sh^2(\beta z - b)}{\sh^2 b + \cos^2 a}}, \qquad (I.6.43)$$

$$I_{node} = \frac{U_2}{\rho}\sh(\beta z - b)\sqrt{\frac{1+\left(\frac{\beta}{\alpha}\right)^2 \ch^2(\beta z - b)}{\sh^2 b + \cos^2 a}}; \qquad (I.6.44)$$

where z is the distance from the termination to the points at which U_{loop}, U_{node}, I_{loop}, and I_{node} are determined.

#I.7. The Traveling Wave Ratio for the Lossless Line

The concept of the traveling wave ratio can be used to characterize the line mode.

The traveling wave ratio is

$$k = U_{min}/U_{max} = I_{min}/I_{max}, \qquad (I.7.1)$$

where

U_{min} and U_{max} are the voltage amplitudes at the voltage node and loop;

I_{min} and I_{max} are the current amplitudes at the current node and loop.

The traveling wave ratio for the lossless line can be expressed in terms of the reflection factor (see Appendix 2)

$$k = \frac{1-|\rho|}{1+|\rho|}, \qquad (I.7.2)$$

where

$|\rho|$ is the modulus of the reflection factor.

As follows from (I.4.2)

$$|\rho| = \left|\frac{R_2 + iX_2 - W}{R_2 + iX_2 + W}\right| = \sqrt{\frac{(R_2 - W)^2 + X_2^2}{(R_2 + W)^2 + X_2^2}}. \qquad (I.7.3)$$

#I.8. The Traveling Wave Ratio for the Lossy Line

(a) The open-ended or closed-end line. The reactance loaded line.

As follows from formulas (I.6.10)-(I.6.13), the traveling wave ratio when $\beta/\alpha \ll 1$ is equal to

$$k = \frac{\operatorname{sh}\beta z_{node}}{\operatorname{ch}\beta z_{loop}}\sqrt{\frac{1 + \left(\frac{\beta}{\alpha}\right)^2 \operatorname{ch}^2\beta z_{node}}{1 - \left(\frac{\beta}{\alpha}\right)^2 \operatorname{sh}^2\beta z_{loop}}} \approx \frac{\operatorname{sh}\beta z_{node}}{\operatorname{ch}\beta z_{loop}}, \qquad (I.8.1)$$

where

z_{node} is the distance from the termination to the specified voltage or current node;

z_{loop} is the distance from the termination to the specified voltage or current loop.

If the distance from the termination to the point where the traveling wave ratio is to be determined is sufficiently great as compared with the distance between a loop and a node, $\beta z_{node} \approx \beta z_{loop}$, and the expression for the traveling wave ratio takes the form

$$k = \operatorname{th}\beta z_{loop}. \qquad (I.8.2)$$

If β is sufficiently small,

$$k \approx \beta z_{loop}. \qquad (I.8.3)$$

The expressions obtained for the traveling wave ratio can also be used for the reactance loaded line.

(b) The complex impedance loaded line

As follows from formulas (I.6.41)-(I.6.44), the traveling wave ratio will be equal to

$$k = \frac{\operatorname{sh}(\beta z_{node} - b)}{\operatorname{ch}(\beta z_{loop} - b)}\sqrt{\frac{1 + \left(\frac{\beta}{\alpha}\right)^2 \operatorname{ch}^2(\beta z_{node} - b)}{1 - \left(\frac{\beta}{\alpha}\right)^2 \operatorname{sh}^2(\beta z_{loop} - b)}} \approx \frac{\operatorname{sh}(\beta z_{node} - b)}{\operatorname{ch}(\beta z_{loop} - b)}. \qquad (I.8.4)$$

If z is very much larger than $\lambda/4$, then $\beta z_{node} \approx \beta z_{loop}$

and $$k \approx \operatorname{th}(\beta z_{loop} - b) \qquad (I.8.5)$$

where b can be found through formula (I.6.33).

#I.9. Equivalent and Input Impedances of a Lossless Line

(a). Determination of the equivalent and input impedances

The equivalent impedance of a line at a point distance z from its end is the ratio of the voltage across the line conductors to the current flowing in the line

$$Z_{eq} = U(z)/I(z) \qquad (I.9.1)$$

The input impedance is found from the expression for Z_{eq} by substitution z = l

$$Z_{in} = U(l)/I(l). \qquad (I.9.2)$$

(a) The open-ended line

Substituting the values for U and I from formula (I.5.1) in (I.9.), we obtain

$$Z_{eq} = \frac{U_2 \cos \alpha z}{i \frac{U_2}{W} \sin \alpha z} = -iW \operatorname{ctg} \alpha z = i X_{eq} \qquad (I.9.3)$$

Figure I.9.1 shows the curve for the change in the equivalent impedance with respect to z.

The equivalent impedance of the line is reactance at all points because the lossless line cannot absorb energy if it has no resistive load termination.

As Figure I.9.1 shows, the sign of the equivalent impedance changes every $\lambda/4$ segment. The impedance is negative, that is, there is capacitance, in the first segment from the termination.

Substituting z = l in (I.9.3), we obtain.

$$Z_{in} = -iW \operatorname{ctg} \alpha l. \qquad (I.9.4)$$

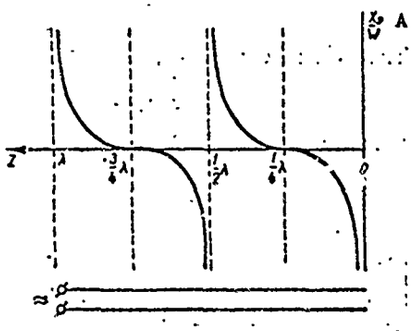

Figure I.9.1. Curve of change in equivalent impedance of an open-ended line.

A - X_{eq}/W.

(b) The closed-end line

In a manner similar to the foregoing, we obtain

$$Z_{eq} = iW \operatorname{tg} \alpha z = iX_{eq} \qquad (I.9.5)$$

A comparison between formulas (I.9.5) and (I.9.4) shows that the nature of the change in the equivalent impedance is the same as for the open-ended line. The difference is that curves for the equivalent impedance of a closed line are displaced along the axis of the abscissa by a distance equal to $\lambda/4$ with respect to the curves for the equivalent impedance of an open line.

(c) The reactance loaded line

$$Z_{eq} = -iW \operatorname{ctg}(\alpha z - \varphi) = iX_{eq} \qquad (I.9.6)$$

where

$$\operatorname{tg} \varphi = \frac{W}{X_2}.$$

The nature of the change in the equivalent impedance is the same as that in the first two cases.

The curve for the equivalent impedance is obtained with a displacement magnitude of φ/α as compared with the case of the open line.

(d) The pure resistance loaded line

Substituting the values for U and I from the expressions contained in formula (I.5.4) in formula (I.9.1) we obtain

$$Z_{eq} = R_{eq} + iX_{eq} = W \frac{\frac{W}{R_2} - 10{,}5\left[1 - \left(\frac{W}{R_2}\right)^2\right]\sin 2\alpha z}{\left(\frac{W}{R_2}\right)^2 \cos^2 \alpha z + \sin^2 \alpha z}, \qquad (I.9.7)$$

where

R_{eq} and X_{eq} are the active and reactive components of the equivalent impedance.

The curves for R_{eq}/W and X_{eq}/W with respect to line length for different values of R_2/W are shown in figures I.9.2 and I.9.3.

(e) The line with a load equal to the wave impedance

Substituting the expressions for U and I from formula (I.5.5) in formula (I.9.1), and putting $U_2/I_2 = W$, we obtain

$$Z_{in} = Z_{eq} = W. \qquad (I.9.8)$$

When an impedance equal to the characteristic impedance is inserted at the end of the line (a traveling wave mode on the line) the equivalent impedance at any point is made up of pure resistance and is equal to the line's characteristic impedance.

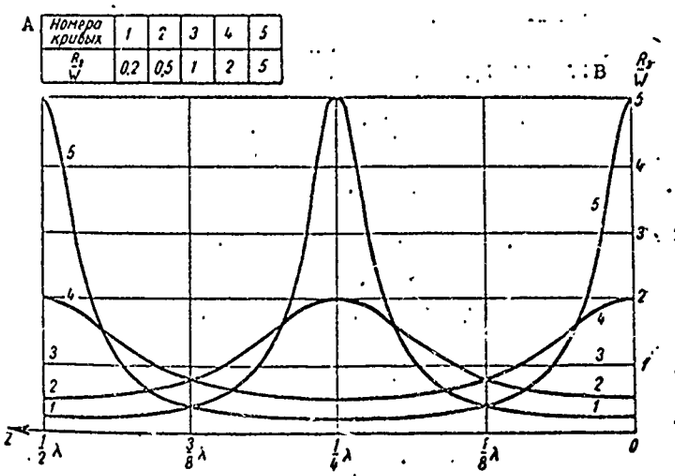

Figure I.9.2. Curves of change in R_{eq}/W for different values of R_2/W and $X_2 = 0$.

A - curve number; B - R_{eq}/W.

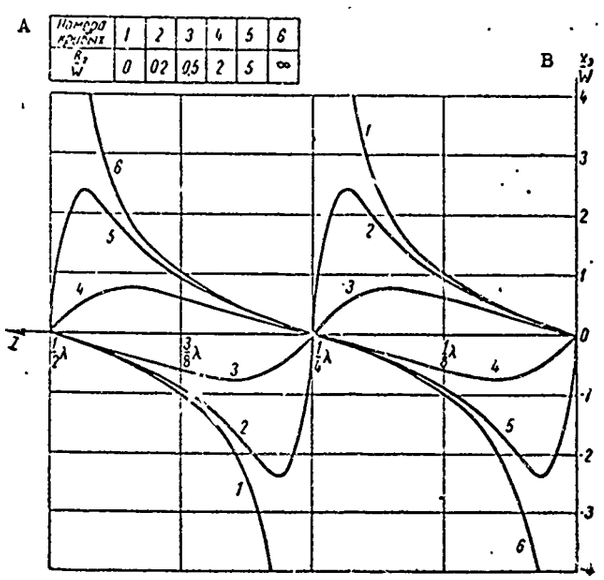

Figure I.9.3. Curves of change in X_{eq}/W for different values of R_2/W and $X_2 = 0$.

A - curve number; B - X_{eq}/W.

(f) The complex impedance loaded line

Substituting the expressions for U and I from formula (I.5.6) in formula (I.9.1), we obtain

$$Z_{eq} = W \frac{\cos \alpha z + i \frac{W}{Z_3} \sin \alpha z}{\frac{W}{Z_3} \cos \alpha z + i \sin \alpha z}. \qquad (I.9.9)$$

If the expressions for U and I from formula (I.5.9) are substituted in formula (I.9.1), and if it is taken that W/D = k [this equality can be obtained through formulas (I.5.11), (I.7.2), and (I.7.3)], then, after the transformations, we obtain

$$Z_{eq} = W \frac{k - i\, 0{,}5\,(1 - k^2) \sin 2\alpha z_1}{k^2 \cos^2 \alpha z_1 + \sin^2 \alpha z_1}. \qquad (I.9.10)$$

#I.10. Equivalent and Input Impedances of a Lossy Line

(a) The open-ended line

As for the lossless line, we obtain

$$Z_{eq} = \rho \operatorname{cth} \gamma z = \rho \frac{\operatorname{sh} 2\beta z - i \sin 2\alpha z}{\operatorname{ch} 2\beta z - \cos 2\alpha z}. \qquad (I.10.1)$$

If ρ is replaced by its expression from formula (I.6.32), the expression for Z_{eq} is transformed into

$$Z_{eq} = W \frac{\left(\operatorname{sh} 2\beta z - \frac{\beta}{\alpha} \sin 2\alpha z\right) - i\left(\frac{\beta}{\alpha} \operatorname{sh} 2\beta z + \sin 2\alpha z\right)}{\operatorname{ch} 2\beta z - \cos 2\alpha z}. \qquad (I.10.2)$$

(b) The closed-end line

$$Z_{eq} = \rho \operatorname{th} \gamma z = \rho \frac{\operatorname{sh} 2\beta z + i \sin 2\alpha z}{\operatorname{ch} 2\beta z + \cos 2\alpha z}. \qquad (I.10.3)$$

After the substitution of $\rho = W(1 - i\frac{\beta}{\alpha})$, expression (I.10.3) takes the form

$$Z_{eq} = W \frac{\left(\operatorname{sh} 2\beta z + \frac{\beta}{\alpha} \sin 2\alpha z\right) - i\left(\frac{\beta}{\alpha} \operatorname{sh} 2\beta z - \sin 2\alpha z\right)}{\operatorname{ch} 2\beta z + \cos 2\alpha z}. \qquad (I.10.4)$$

(c) The complex impedance loaded line

Substituting the expressions for U and I from formula (I.6.23), and the expression for θ from (I.6.24), in formula (I.9.1), we obtain

$$Z_{eq} = \rho \operatorname{cth}(\gamma z - \theta) = \rho \frac{\operatorname{sh} 2(\beta z - b) - i \sin 2(\alpha z - a)}{\operatorname{ch} 2(\beta z - b) - \cos 2(\alpha z - a)}. \qquad (I.10.5)$$

or, substituting $\rho = W(1 - \frac{\beta}{\alpha})$, we obtain

$$Z_{eq} = W \frac{\operatorname{sh} 2(\beta z - b) - \frac{\beta}{\alpha} \sin 2(\alpha z - a)}{\operatorname{ch} 2(\beta z - b) - \cos 2(\alpha z - a)} - i W \frac{\frac{\beta}{\alpha} \operatorname{sh} 2(\beta z - b) + \sin 2(\alpha z - a)}{\operatorname{ch} 2(\beta z - b) - \cos 2(\alpha z - a)}, \quad (I.10.6)$$

and a and b are found through formulas (I.6.33) and (I.6.34).

#I.11. Maximum and Minimum Values of the Equivalent Impedance of a Lossless Line

A knowledge of the maximum and minimum values of the active and reactive components of the equivalent impedance of a line is of interest.

If the line is open, closed, or reactance loaded, the maximum equivalent impedance can be infinitely large, while the minimum will equal zero. This follows from what has been cited above.

If the line is complex impedance loaded, both maximum and minimum equivalent impedances have a finite magnitude.

The maximum value of the equivalent impedance occurs at the voltage loop (the current node), whereas the minimum value occurs at the voltage node (current loop). These are pure resistances.

We can use formula (I.9.10) to obtain expressions for these. Voltage loops occur at points $\alpha z_1 = n\pi$, where n = 0; 1; 2; 3; ...

Substituting one of the stated values of αz_1 in formula (I.9.10) we obtain

$$Z_{eq\ max} = R_{eq\ max} = W/k \quad (I.11.1)$$

Voltage nodes occur at points $\alpha z_1 = (2n + 1)\pi/2$, where n = 0; 1; 2; 3; ...

Substituting one of the stated values of αz_1 in formula (I.9.10) we obtain

$$Z_{eq\ min} = R_{eq\ min} = Wk \quad (I.11.2)$$

The minimum value of the reactance (X_{eq}) of the equivalent impedance equals zero.

The maximum value of X_{eq} can be found by solving

$$dX_{eq}/dz = 0 \quad (I.11.3)$$

Substituting X_{eq} from equation (I.9.10) in equation (I.11.3), differentiating, and solving the equation obtained with respect to z_1, we obtain

$$z_1 = \pm \frac{1}{\alpha} \operatorname{arc\,tg} k. \quad (I.11.4)$$

Here z_1 is the distance from the voltage loop to the point where X_{eq} is a maximum.

Substituting this value for z_1 in formula (I.9.10), we find

$$X_{eq\ max} = \pm W \frac{1-k^2}{2k}. \qquad (I.11.5)$$

If $k \ll 1$, then

$$X_{eq\ max} \approx \pm W/2k + \pm 1/2\ R_{eq\ max}. \qquad (I.11.6)$$

#I.12. Maximum and Minimum Values of the Equivalent Impedance of a Lossy Line

(a) Open, closed, or reactance loaded lines

Let us consider the open-end line.

Let us limit ourselves to the case of $\beta/\alpha \ll 1$. It can be taken that $\rho \approx W$, and that the voltage loops are at distances $z = z_{loop} = n\ \lambda/2$ ($n = 0; 1; 2; 3; \ldots$) from the termination.

Substituting $\rho = W$ and $z_{loop} = n\ \lambda/2$ in formula (I.10.1), we find the maximum pure resistance equal to

$$R_{eq\ max} \approx \mathrm{cth}\ \beta\ z_{loop}. \qquad (I.12.1)$$

If βz_{loop} is small, it can be taken that $\mathrm{cth}\beta_{loop} \approx 1/\beta z_{loop}$, and then

$$R_{eq\ max} = W/\beta z_{loop}. \qquad (I.12.2)$$

Taking $G_1 = 0$, we obtain (see I.3.4)

$$R_{eq\ max} = 2W^2/R_1 z_{loop}, \qquad (I.12.3)$$

where

z_{loop} is the distance of the specified voltage loop from the termination.

Minimum reactance occurs when

$$z = z_{node} = (2n + 1)\ \lambda/4.$$

Substituting this value for z in formula (I.10.1), we obtain

$$R_{eq\ min} = W\ \mathrm{th}\ \beta z_{node} \approx W\ \beta_{node} = 1/2\ R_1 z_{node} \qquad (I.12.4)$$

where

z_{node} is the distance of the specified voltage node from the termination.

The expressions obtained for $R_{eq\ max}$ and $R_{eq\ min}$ are valid for a closed-end line and for a reactance loaded line.

(b) The complex impedance loaded line

The approximate expressions for maximum and minimum values of R_{eq} can be obtained through equation (I.10.5) if it is assumed that β/α is an extremely small magnitude. In this case the maximum values of R_{eq} occur at the points where $\alpha z - a = \alpha z_{loop} - a = n\pi$, while the minimums occur at the points where $\alpha z - a = \alpha z_{node} - a = (2n + 1)\pi/2$. They can be expressed by the formulas

$$R_{eq\ max} = W \operatorname{cth} (\beta z_{loop} - b), \qquad (I.12.5)$$

$$R_{eq\ min} = W \operatorname{th} (\beta z_{node} - b). \qquad (I.12.6)$$

#I.13. Maximum Voltages, Potentials, and Currents Occurring on a Line. The Maximum Electric Field Intensity.

It is important to know the maximum voltages, potentials, and currents for a line used for high power transmissions. We will limit ourselves to the case in which line losses can be neglected.

The effective voltage across the voltage loop equals

$$U_{loop} = \sqrt{PR_{loop}}, \qquad (I.13.1)$$

where

P is the power delivered to the line;

R_{loop} is the line resistance at the voltage loop, and is equal to W/k (see #I.11).

Substituting the value of R_{loop} in formula (I.13.1), we obtain

$$U_{loop} = \sqrt{PW/k} \qquad (I.13.2)$$

The maximum potential on a two-wire line is equal to half the maximum voltage.

The effective value of the current flowing at a current loop, where the line resistance equals Wk, is found through the formula

$$I_{loop} = \sqrt{P/Wk} \qquad (I.13.3)$$

Finding the maximum electric field strength on a line is of great interest. The maximum electric field strength is at the surface of the conductor and can be found in terms of the magnetic field strength at the surface of the conductor. A TEM type wave (a transverse electromagnetic wave) is propagated on the lines we are considering. When the line is functioning in the traveling wave mode we find that there is the relationship

$$E = W_i Int,$$

between the electric field strength, E, and the magnetic field strength, Int, at any point in space, and particularly at the surface of the conductor, where

E is the electric field strength, volts/meter;

Int is the magnetic field strength, amperes/meter;

W_i has the dimensionality of impedance (ohms), and can be called the characteristic impedance of the medium.

For TEM waves in free space

$$W_i = 120\pi, \text{ ohms.}$$

The magnetic field strength at the surface of the conductor can be found through the relationship

$$\oint_L H_l dl = \int_F j_n dF = I \qquad (I.13.4)$$

where the left-hand side is the circulation of vector H around the circumference of the conductor,

dl is an element of the circumference of the conductor;

j_n is the current volume density in the transverse cross section of the conductor, amperes/m^2;

dF is an element of the surface of the conductor's cross section.

Assuming the current and magnetic field strengths to be uniformly distributed around the circumference, we obtain

$$\oint_L H_l dl = H\pi d = I \qquad (I.13.5)$$

where

d is the conductor diameter.

The maximum electric field strength, E_{max}, equals

$$E_{max} = W_i I/\pi d \qquad (I.13.6)$$

Substituting I = U/W in (I.13.6), we obtain

$$E_{max} = W_i U/W\pi d \qquad (I.13.7)$$

or

$$E_{max} = 120U/Wd \qquad (I.13.8)$$

If the line is multi-conductor, that is, each balanced half of the line consists of n parallel conductors (for a four-wire balanced line n = 2), and if the distance between conductors is such that current distribution around the circumference of the conductors can be considered as uniform, the current flowing in one conductor will be reduced by a factor of n. Correspondingly, the maximum field strength equals

$$E_{max} = 120U/Wnd \qquad (I.13.9)$$

(non-uniformity in current distribution between conductors not considered).

If d is in centimeters, E_{max} is in volts/centimeter.

Formula (I.13.9) holds for any value of the traveling wave ratio for the line, since E in the formula is defined in terms of U. Substituting the value of U from (I.13.2), we obtain

$$E_{max} = 120\sqrt{P}/nd\sqrt{kW} \qquad (I.13.10)$$

Here E_{max} is the effective value of the field strength at the surface of the conductor at a voltage loop.

#I.14. Line Efficiency

By line efficiency is meant the ratio of the actual power dissipated in the terminator to the total actual power delivered to the line. The efficiency, η, can be expressed in terms of the reflection factor, p, as follows (see Appendix 3)

$$\eta = e^{-2\beta l}\frac{1-|p|^2}{1-|p|^2e^{-4\beta l}}. \qquad (I.14.1)$$

Substituting the expression for $|p|$ in terms of the traveling wave ratio $k(|p| = 1-k/1+k)$ in formula (I.14.1), we obtain

$$\eta = \frac{1}{\operatorname{ch} 2\beta l + \frac{1}{2}\left(k+\frac{1}{k}\right)\operatorname{sh} 2\beta l}. \qquad (I.14.2)$$

if $2\beta l \ll 1$ we can replace $\operatorname{sh} 2\beta l$ by $2\beta l$ and $\operatorname{ch} 2\beta l$ by one, whereupon

$$\eta = \frac{1}{1+\left(k+\frac{1}{k}\right)\beta l}. \qquad (I.14.3)$$

Formula (I.14.3) shows that efficiency is higher the closer the traveling wave ratio is to one and the smaller βl.

Figure I.14.1 shows the curves for the change in η with respect to βl for traveling wave ratios equal to 0.1, 0.2, 0.5, and 1. Formula (I.14.2) was used to construct the curves.

The efficiency of a line operating in the traveling wave mode equals

$$\eta = e^{-2\beta l}. \qquad (I.14.4)$$

If $2\beta l \ll 1$,

$$\eta \approx 1 - 2\beta l. \qquad (I.14.5)$$

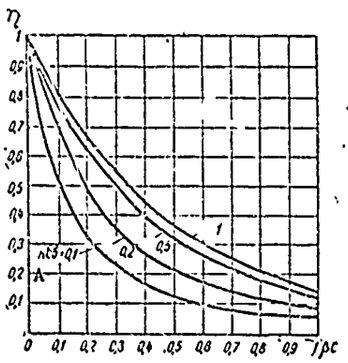

Figure I.14.1. Curves of change in line efficiency with respect to βl for different traveling wave ratios.

A - kbv, traveling wave ratio.

#I.15. Resonant Waves on a Line

The waves on a line, the input impedance of which has no reactive component, are called resonant waves.

The data presented in the foregoing indicate that resonant waves occur on a lossless line when there is a current loop, or node, at the point of supply for the line.

Every line has an infinitely large number of waves for which the reactive component of the input impedance equals zero. A line, therefore, has not one, but an infinitely large number of resonant waves. The maximum resonant wave is known as the line's natural wave.

#I.16. Area of Application of the Theory of Uniform Long Lines

In practice, the most widely used are uniform two-wire balanced and one-wire unbalanced open-wire or shielded lines. A line which is made up of two balanced conductors, or of two balanced systems of conductors, between which an emf source is connected, is called a balanced line.

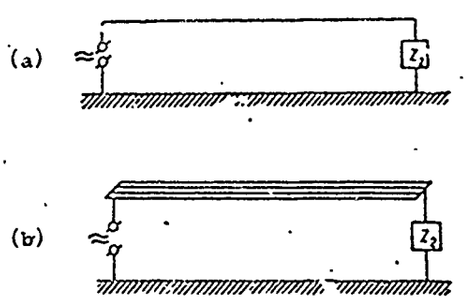

Figure I.16.1. Schematic diagrams of unbalanced single-wire lines: (a) single-wire unbalanced line; (b) unbalanced line consisting of a system of wires.

The open-wire one-wire line is understood to mean a line consisting of but one conductor (fig. I.16.1a), or of a system of conductors (fig. I.16.1b), to which one of the output terminals of the emf source is connected, while the other terminal is grounded. The shielded one-wire line is understood to mean a line consisting of a conductor (or of a system of conductors) surrounded by a shield which is connected to the generator shield and the load shield. The coaxial line is a special case of a shielded line.

The theory of uniform long lines is applicable to balanced lines, as well as to single-wire lines if they are uniform.

It is also possible to use the computational apparatus of the theory of uniform lines in the case of shielded one-wire lines if the penetration of the current into the external surface of the shield is excluded.

Chapter II

EXPONENTIAL AND STEP LINES

#II.1. Differential Equations for a Line with Variable Characteristic Impedance and Their Solution. Exponential Lines.[1]

Exponential and step transmission lines are widely used as broadband elements for matching lines with different characteristic impedances.

Let us take a line with a variable characteristic impedance (fig. II.1.1). The change in the characteristic impedance is shown in the drawing by the change in the distance between the line's conductors. In practice, the characteristic impedance is changed by changing the diameters of the conductors, or by using other methods, such as changing the parameters of the medium surrounding the conductor, all of them in addition to the method whereby the distance between the conductors is changed.

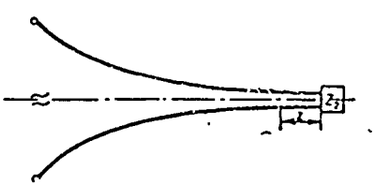

Figure II.1.1. Line with a variable characteristic impedance.

It is obvious that equations (I.1.3) and (I.1.5), derived for the uniform line, remain valid in this case; that is, the voltage/current ratio for any line element is in the form

$$\left.\begin{aligned}\frac{dU}{dz} &= IZ_1\\ \frac{dI}{dz} &= UY_1\end{aligned}\right\}, \qquad \text{(II.1.1)}$$

where

z is the distance between a specified point on the line and its termination.

Z_1 and Y_1 are functions of z for non-uniform lines.

Differentiating the second equation at (II.1.1) with respect to z, we obtain

$$\frac{d^2I}{dz^2} = \frac{dU}{dz}Y_1 + U\frac{dY_1}{dz}. \qquad \text{(II.1.2)}$$

---

1. M. S. Neyman. "Non-uniform Lines with Distributed Constants." IEST, No. 11, 1938.

Substituting the expressions for dU/dz and U from formula (II.1.1) in formula (II.1.2),

$$\frac{d^2I}{dz^2} - \frac{dI}{dz}\frac{1}{Y_1}\frac{dY_1}{dz} - IZ_1Y_1 = 0. \qquad \text{(II.1.3)}$$

Since $1/Y_1\ dY_1/dz = d/dz(\ln Y_1)$, equation (II.1.3) takes the form

$$\frac{d^2I}{dz^2} - \frac{dI}{dz}\frac{d}{dz}(\ln Y_1) - IZ_1Y_1 = 0. \qquad \text{(II.1.4)}$$

Similarly

$$\frac{d^2U}{dz^2} - \frac{dU}{dz}\frac{d}{dz}(\ln Z_1) - UZ_1Y_1 = 0. \qquad \text{(II.1.5)}$$

Let us designate

$$\gamma = \beta + i\alpha = \sqrt{Z_1Y_1}. \qquad \text{(II.1.6a)}$$

$$\rho = \sqrt{\frac{Z_1}{Y_1}}. \qquad \text{(II.1.6b)}$$

Then equations (II.1.5) and (II.1.4) can be transformed into

$$\left.\begin{aligned}\frac{d^2U}{dz^2} - \frac{dU}{dz}\frac{d}{dz}[\ln(\rho\gamma)] - U\gamma^2 = 0\\ \frac{d^2I}{dz^2} + \frac{dI}{dz}\frac{d}{dz}\left(\ln\frac{\rho}{\gamma}\right) - I\gamma^2 = 0\end{aligned}\right\}. \qquad \text{(II.1.7)}$$

As we see, in the general case the distribution of current and voltage in the non-uniform line can be described by linear differential equations with variable coefficients.

However, in the special case when ρ changes in accordance with an exponential law

$$\rho = \rho_0 e^{bz}, \qquad \text{(II.1.8)}$$

where ρ_0 is the characteristic impedance at the termination and the propagation factor γ remains constant along the line. The coefficients $d/dz[\ln(\rho\gamma)]$ and $d/dz(\ln \rho/\gamma)$ become constants and equal to b.

Lines for which ρ changes in accordance with an exponential law are called exponential lines.

Analysis of the exponential line follows.

After the substitution of (II.1.8), equation (II.1.7) is in the following form

$$\left.\begin{aligned}\frac{d^2U}{dz^2} - b\frac{dU}{dz} - \gamma^2U = 0\\ \frac{d^2I}{dz^2} + b\frac{dI}{dz} - \gamma^2I = 0\end{aligned}\right\}. \qquad \text{(II.1.9)}$$

The equations at (II.1.9) have the following solution

$$\left.\begin{aligned}U = A_1e^{\kappa_1'z} + B_1e^{\kappa_1''z}\\ I = A_2e^{\kappa_2'z} + B_2e^{\kappa_2''z}\end{aligned}\right\}. \qquad \text{(II.1.10)}$$

The coefficients k_1, k_2, k_1', and k_2' are determined from characteristic equations corresponding to the differential equations at (II.1.9).

The characteristic equations are in the form

$$\left.\begin{aligned} \kappa^2 - b\kappa - \gamma^2 = 0 \\ \kappa'^2 + b\kappa' - \gamma^2 = 0 \end{aligned}\right\}, \tag{II.1.11}$$

from whence

$$\left.\begin{aligned} \kappa_1 &= \frac{b}{2} + \sqrt{\gamma^2 + \left(\frac{b}{2}\right)^2} \\ \kappa_2 &= \frac{b}{2} - \sqrt{\gamma^2 + \left(\frac{b}{2}\right)^2} \\ \kappa_1' &= -\frac{b}{2} + \sqrt{\gamma^2 + \left(\frac{b}{2}\right)^2} \\ \kappa_2' &= -\frac{b}{2} - \sqrt{\gamma^2 + \left(\frac{b}{2}\right)^2} \end{aligned}\right\}. \tag{II.1.12}$$

Substituting (II.1.12) in (II.1.10),

$$\left.\begin{aligned} U &= e^{-\frac{b}{2}z}\left[A_1 e^{z\sqrt{\gamma^2+\left(\frac{b}{2}\right)^2}} + B_1 e^{-z\sqrt{\gamma^2+\left(\frac{b}{2}\right)^2}}\right] \\ I &= e^{-\frac{b}{2}z}\left[A_2 e^{z\sqrt{\gamma^2+\left(\frac{b}{2}\right)^2}} + B_2 e^{-z\sqrt{\gamma^2+\left(\frac{b}{2}\right)^2}}\right] \end{aligned}\right\}. \tag{II.1.13}$$

The connection between A_2 and A_1, as well as between B_2 and B_1, can be found by substituting the solution arrived at in one of the original differential equations.

Substituting that solution in the first of the equations at (II.1.1),

$$e^{z\sqrt{\gamma^2+\left(\frac{b}{2}\right)^2}}\left\{\left[\frac{b}{2} + \sqrt{\gamma^2 + \left(\frac{b}{2}\right)^2}\right]A_1 - \gamma\rho_0 A_2\right\} +$$

$$+ e^{-z\sqrt{\gamma^2+\left(\frac{b}{2}\right)^2}}\left\{\left[\frac{b}{2} - \sqrt{\gamma^2 + \left(\frac{b}{2}\right)^2}\right]B_1 - \gamma\rho_0 B_2\right\} = 0.$$

This equation should be identically satisfied for any value of z, so should be equal to zero in both expressions in the braces. Thus, we get two equations, from which we find

$$A_2 = A_1\left[\frac{b}{2\gamma} + \sqrt{1 + \left(\frac{b}{2\gamma}\right)^2}\right]\frac{1}{\rho_0}, \tag{II.1.14}$$

$$B_2 = B_1\left[\frac{b}{2\gamma} - \sqrt{1 + \left(\frac{b}{2\gamma}\right)^2}\right]\frac{1}{\rho_0}. \tag{II.1.15}$$

We will use the boundary conditions to determine the constants A_1 and B_1. Let us assume that at the termination, that is, when $z = 0$,

$$\left.\begin{aligned} U &= U_2 \\ I &= I_2 = \frac{U_2}{Z_2} \end{aligned}\right\}, \qquad \text{(II.1.16)}$$

where

Z_2 is the resistor inserted in the termination;

U_2 is the voltage across the termination;

I_2 is the current flowing in the termination.

Substituting (II.1.14), (II.1.15) and (II.1.16) in (II.1.13), and solving the equations obtained with respect to A_1 and B_1, we find

$$A_1 = \frac{U_2\left[-\frac{b}{2} + \sqrt{\gamma^2 + \left(\frac{b}{2}\right)^2}\right] + I_2\gamma\rho_0}{2\sqrt{\gamma^2 + \left(\frac{b}{2}\right)^2}}, \qquad \text{(II.1.17)}$$

$$B_1 = \frac{U_2\left[\frac{b}{2} + \sqrt{\gamma^2 + \left(\frac{b}{2}\right)^2}\right] - I_2\gamma\rho_0}{2\sqrt{\gamma^2 + \left(\frac{b}{2}\right)^2}}. \qquad \text{(II.1.18)}$$

What follows from equation (II.1.13) is that in a line in which the characteristic impedance changes smoothly, as it does in the uniform line, there are two waves of voltage and current; an incident wave, characterized by the coefficient A_1 and A_2, and a reflected wave, characterized by the coefficients B_1 and B_2.

The voltages of the incident and reflected waves change in direct proportion to $e^{1/2\ bz}$ in the exponential line; that is, the change is proportional to the square root of the characteristic impedance because

$$e^{\frac{1}{2}bz} = \sqrt{e^{bz}} = \sqrt{\frac{\rho}{\rho_0}}.$$

The changes in the incident and reflected wave currents are inversely proportional to the square root of the characteristic impedance.

Since traveling waves are propagated from an area of low characteristic impedances to an area of high characteristic impedances, voltage and current amplitudes are transformed; the voltage amplitude increases, the current amplitude decreases. Accordingly, the exponential line is a voltage and current transformer.

#II.2. The Propagation Factor

From the foregoing equations it is apparent that in this case the factor γ does not characterize the propagation of incident and reflected waves. Instead, it is the factor

$$\gamma' = \sqrt{\gamma^2 + \left(\frac{b}{2}\right)^2} = \gamma\sqrt{1 + \left(\frac{b}{2\gamma}\right)^2} = \beta' + i\alpha', \qquad \text{(II.2.1)}$$

where

β' and α' are the attenuation factor and the phase factor.

Substituting the expression for γ, we find

$$\beta'=\sqrt{\frac{1}{2}\left\{-\left[\alpha^2-\beta^2-\left(\frac{b}{2}\right)^2\right]+\sqrt{\left[\alpha^2-\beta^2-\left(\frac{b}{2}\right)^2\right]^2+4\alpha^2\beta^2}\right\}}, \qquad (II.2.2)$$

$$\alpha'=\sqrt{\frac{1}{2}\left\{\left[\alpha^2-\beta^2-\left(\frac{b}{2}\right)^2\right]+\sqrt{\left[\alpha^2-\beta^2-\left(\frac{b}{2}\right)^2\right]^2+4\alpha^2\beta^2}\right\}}. \qquad (II.2.3)$$

If $\beta \ll \alpha$, and this is customary and is the case at high frequencies, expressions β' and α' will take the form

$$\beta'=\frac{\beta}{\sqrt{1-\left(\frac{b}{2\alpha}\right)^2}}, \qquad (II.2.4)$$

$$\alpha'=\alpha\sqrt{1-\left(\frac{b}{2\alpha}\right)^2}. \qquad (II.2.5)$$

Formulas (II.2.4) and (II.2.5) demonstrate that the larger b is, that is, the less frequent the change in the line's characteristic impedance, the smaller the phase factor and, as a result the greater the phase velocity of wave propagation on the line ($v' = \omega/\alpha'$). Moreover, the attenuation factor increases with an increase in b.

#II.3. The Reflection Factor and the Condition for Absence of Reflection

As we noted above, the reflection factor is the ratio of the voltage (or current) associated with the reflected wave at the point of reflection to the voltage (or current) associated with the incident wave at the same place on the line. From (II.1.13) the reflection factor for the voltage equals

$$p_U = B_1/A_1 . \qquad (II.3.1)$$

Substituting the expressions for B_1 and A_1 from equations (II.1.17) and (II.1.18), we obtain

$$p_U=\frac{Z_2\left[\frac{b}{2}+\sqrt{\gamma^2+\left(\frac{b}{2}\right)^2}\right]-\gamma\rho_0}{Z_2\left[-\frac{b}{2}+\sqrt{\gamma^2+\left(\frac{b}{2}\right)^2}\right]+\gamma\rho_0}, \qquad (II.3.2)$$

where

Z_2 is the terminating impedance.

If line losses are neglected, that is, if it is taken that $\gamma = i\alpha$ and $\rho_0 = W_0$, the expressions for p_U will take the form

$$p_U=\frac{Z_2\left[\frac{b}{2}+i\alpha\sqrt{1-\left(\frac{b}{2\alpha}\right)^2}\right]-i\alpha W_0}{Z_2\left[-\frac{b}{2}+i\alpha\sqrt{1-\left(\frac{b}{2\alpha}\right)^2}\right]+i\alpha W_0}. \qquad (II.3.4)$$

Similarly, the reflection factor for the current when there are no line losses equals

$$p_i = \frac{\left[\frac{b}{i2\alpha} - \sqrt{1-\left(\frac{b}{2\alpha}\right)^2}\right]\left\{Z_2\left[\frac{b}{2} + \right.\right.}{\left[\frac{b}{i2\alpha} + \sqrt{1-\left(\frac{b}{2\alpha}\right)^2}\right]\left\{Z_2\left[-\frac{b}{2} + \right.\right.}$$
$$\frac{\left.\left. + i\alpha\sqrt{1-\left(\frac{b}{2\alpha}\right)^2}\right] - i\alpha W_0\right\}}{\left.\left. + i\alpha\sqrt{1-\left(\frac{b}{2\alpha}\right)^2}\right] + i\alpha W_0\right\}}. \qquad \text{(II.3.5)}$$

Equating the numerators in the right-hand sides of equations (II.3.4) and (II.3.5) to zero is the condition for absence of reflection. We find from these equalities that in order to eliminate reflection we must insert a complex impedance equal to

$$Z_2 = \frac{W_0}{-i\frac{b}{2\alpha} + \sqrt{1-\left(\frac{b}{2\alpha}\right)^2}}. \qquad \text{(II.3.6)}$$

in the end of the line.

But if $b/2\alpha$ is so much less than unity that we can ignore it

$$Z_2 = W_0,$$

and the reflection can be eliminated by inserting as the terminator a pure resistance equal to the characteristic impedance of an exponential line at its end.

#II.4. Line Input Impedance

The input impedance of an exponential line equals

$$Z_{in} = U_{(z=l)}/I_{(z=l)} \qquad \text{(II.4.1)}$$

We will limit ourselves to consideration of a lossless line.

Substituting the values for $U_{z=l}$ and $I_{z=l}$ found through equation (II.1.13) in equation (II.4.1), we obtain

$$Z_{in} = e^{bl}\frac{A_1 e^{|\alpha| l\sqrt{1-\left(\frac{b}{2\alpha}\right)^2}} + B_1 e^{-|\alpha| l\sqrt{1-\left(\frac{b}{2\alpha}\right)^2}}}{A_2 e^{|\alpha| l\sqrt{1-\left(\frac{b}{2\alpha}\right)^2}} + B_2 e^{-|\alpha| l\sqrt{1-\left(\frac{b}{2\alpha}\right)^2}}}. \qquad \text{(II.4.2)}$$

In the special case of the termination containing impedance Z_2, found through equation (II.3.6), and which is to say the impedance ensuring absence of reflection ($B_1 = B_2 = 0$), we obtain an input impedance equal to

$$Z_{in} = e^{bl}\frac{A_1}{A_2} = W_0\frac{e^{bl}}{-i\frac{b}{2\alpha} + \sqrt{1-\left(\frac{b}{2\alpha}\right)^2}} = Z_2 e^{bl}. \qquad \text{(II.4.3)}$$

Accordingly, when there is no reflection the input impedance, like the load impedance, is complex and depends on the wavelength.

But from equations (II.4.3) and (II.3.6), if $b/2\alpha$ is so small that it can be ignored when compared with unity, the input impedance, like Z_2, is active when there is no reflection and does not depend on the wavelength, whereupon

$$Z_{in} = W_0 e^{bl}. \qquad (II.4.4)$$

As we see, if b is sufficiently small, that is, when the change in the characteristic impedance is sufficiently slow, the exponential line can act as a wave transformer, transforming the pure resistance equal to W_0 in its termination into a pure resistance equal to $W_0 e^{bl}$. b can be either positive or negative.

We can prove that if the magnitude $b/2\alpha$ is ignored the input impedance will, for arbitrary load Z_2, equal

$$Z_{in} = W_0 e^{bl} \frac{\cos \alpha l + i \frac{W_0}{Z_2} \sin \alpha l}{\frac{W_0}{Z_2} \cos \alpha l + i \sin \alpha l}. \qquad (II.4.5)$$

The ratio Z_{in}/Z_2 is the exponential line impedance transformation ratio. Comparing equations (II.4.5) and (I.9.9), we see that the factor

$$\frac{W_0}{Z_2}\left[\frac{\cos \alpha l + i \frac{W_0}{Z_2} \sin \alpha l}{\frac{W_0}{Z_2} \cos \alpha l + i \sin \alpha l}\right]$$

is the transformation ratio for impedance Z_2 of a uniform line with unchanged characteristic impedance W_0, and that the factor e^{bl} is a supplemental transformation factor defined by the exponential nature of the change in the line's characteristic impedance.

The condition of smallness of the ratio $b/2\alpha$ in the case of a specified transformation ratio imposes a definite limitation on the length of the exponential line (l), which should be at least some minimum value.

#II.5. Dependence of the Needed Length of an Exponential Line on a Specified Traveling Wave Ratio

The exponential line, as was pointed out above, can be used as a transformer for matching lines with different characteristic impedances (fig. II.5.1).

The exponential line load is a line with some characteristic impedance, $W_2 = W_0$. The exponential line, together with line 2 connected to it, is the load for line 1, which has the characteristic impedance

$$W_1 = W_0 e^{bl}.$$

The exponential line should provide a sufficiently small reflection factor at the end of line 1, and in order to do so the input impedance of the exponential line (Z_{in}) should be close to $W_1 = W_0 e^{bl}$.

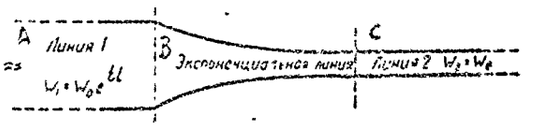

Figure II.5.1. Exponential transmission-line transformer.
A - line 1; B - exponential line; C - line 2.

Let us derive the expression for the reflection factor as

$$\rho_U = \frac{Z_{in} - W_1}{Z_{in} + W_1} = \frac{Z_{in} - W_0 e^{bl}}{Z_{in} + W_0 e^{bl}}, \qquad \text{(II.5.1)}$$

where

Z_{in} is the exponential line's input impedance.

Substituting the expression for Z_{in} from (II.4.2) and the values for A_1, A_2, B_1, and B_2 from (II.1.14)-(II.1.18), in (II.5.1), converting, and ignoring $(b/2\alpha)^2$, we obtain

$$|\rho_U| = \frac{b \sin \alpha l}{2\alpha}. \qquad \text{(II.5.2)}$$

The maximum reflection factor results when

$$l = \frac{2n+1}{4}\lambda,$$

where

n is any integer, or zero

$$|\rho_{U_{max}}| = \frac{b}{2\alpha}, \qquad \text{(II.5.3)}$$

By using the formula at (II.5.2), we can find the relationship between the reflection factor, the length of the exponential line, and the relationship of W_1 to W_2.

As a matter of fact,

$$W_1 = W_0 e^{bl} = W_2 e^{bl},$$

from whence

$$v = \left| \frac{1}{l} \ln \frac{W_1}{W_2} \right|. \qquad \text{(II.5.4)}$$

Substituting the value for b from (II.5.4) in (II.5.2), and omitting the factor characterizing the phase, we obtain

$$|p_U| = \frac{\left|\ln \frac{W_1}{W_2}\right| \sin \alpha l}{2\alpha l}. \qquad \text{(II.5.5)}$$

#II.6. General Remarks Concerning Step Transition Lines

Step transmission lines, that is, transmission lines comprising sections with different characteristic impedances, can be used for broadband matching of two lines with dissimilar characteristic impedances, W_0' and W_0''.

Step lines usually are made up of sections of equal lengths. The characteristic impedance within the limits of each section remains constant.

Different combinations of the number, n, length, l, and characteristic impedances of sections for satisfying a specific matching requirement are possible within the limits of a specified frequency band.

The requirements usually reduce to keeping the reflection factor for waves propagated from right to left, or from left to right, at a predetermined magnitude within the limits of the specified frequency band. And it is assumed that the line to which the energy is being fed has a resistive load equal to its characteristic impedance.

Let us pause here to consider the optimum, or Chebyshev, step transition. By optimum we mean that step transition which has a minimum overall length, $L = nl$, for a specified jump in the characteristic impedances $N = W_0''/W_0'(N > 1)$, a specified maximum reflection factor p_{max}, and an operating band $\lambda_2 - \lambda_1$. We shall not pause to consider the mathematical analysis, but will limit ourselves to citing the final results of such analysis, since they permit us to select the data for the step transmission line in accordance with specified requirements and problem conditions.

We will cite the data for two-step, three-step, and four-step transmission lines.[1]

#II.7. Step Normalized Characteristic Impedances

(a) Two-step line (n = 2)

The normalized (that is, equated to W_0') characteristic impedance of the first step is found through the formula

$$W_1 = \frac{N-1}{2\operatorname{tg}^2\theta_0} + \sqrt{\frac{(N-1)^2}{4\operatorname{tg}^4\theta_0} + N}, \qquad \text{(II.7.1)}$$

where

$$\theta_0 = \arccos\left(\Lambda \frac{\sqrt{2}}{2}\right), \qquad \text{(II.7.2)}$$

1. See the article by A. L. Fel'dshteyn and L. R. Yavich titled "The Engineering Computation for Chebyshev Step Transitions." Radiotekhnika [Radio Engineering], No. 1, 1960.

$$A = \frac{1}{\cos\left(\frac{1}{n}\arccos C\right)}, \qquad \text{(II.7.3)}$$

$$C = \frac{N-1}{2h\sqrt{N}}, \qquad \text{(II.7.4)}$$

$$h = \frac{|\rho|_{max}}{\sqrt{1-|\rho|^2_{max}}}, \qquad \text{(II.7.5)}$$

$|\rho|_{max}$ is the specified maximum permissible reflection factor.

The normalized characteristic impedance of the second step is

$$W_2 = N/W_1 \qquad \text{(II.7.6)}$$

(b) Three-step line (n = 3)

The normalized characteristic impedance of the first step can be found through the transcendental equation

$$\frac{N-1}{\operatorname{tg}^2\theta_0} = W_1^2 + 2W_1\sqrt{N} - \frac{N}{W_1^2} - \frac{2\sqrt{N}}{W_1}. \qquad \text{(II.7.7)}$$

The magnitude W_1 can be found graphically using equation (II.7.7):

$$\cos\theta_0 = A\frac{\sqrt{3}}{2}, \qquad \text{(II.7.8)}$$

$$W_2 = \sqrt{N}, \qquad \text{(II.7.9)}$$

$$W_3 = \frac{N}{W_1}. \qquad \text{(II.7.10)}$$

A can be found through formulas (II.7.3) - (II.7.6).

(c) Four-step line (n = 4)

$$W_1 = \sqrt{\xi}, \qquad \text{(II.7.11)}$$

$$\xi = -\frac{1}{2}\left\{\frac{2\sqrt{a}(a-N)}{(\sqrt{a}+N)^2} - \frac{a^2-N^2}{N(\sqrt{a}+N)^2}\left\{\operatorname{tg}^2\theta_1 + \operatorname{tg}^2\theta_2\right\}\right\} + \sqrt{\frac{1}{4}\left\{\frac{2\sqrt{a}(a-N)}{(\sqrt{a}+N)^2} - \frac{a^2-N^2}{N(\sqrt{a}+N)^2}\left(\operatorname{tg}^2\theta_1 + \operatorname{tg}^2\theta_2\right)\right\}^2 + \frac{a}{N}}, \qquad \text{(II.7.12)}$$

$$a = \frac{N(N-1)}{2\operatorname{tg}^2\theta_1\operatorname{tg}^2\theta_2} + \sqrt{\frac{N^2(N-1)^2}{4\operatorname{tg}^4\theta_1\operatorname{tg}^4\theta_2} + N^2}, \qquad \text{(II.7.13)}$$

$$\cos\theta_1 = A\cos\frac{\pi}{8}, \qquad \text{(II.7.14)}$$

$$\cos\theta_2 = A\cos 3\frac{\pi}{8}. \qquad \text{(II.7.15)}$$

A can be found through (II.7.3) - (II.7.6).

The characteristic (normalized) impedances of the second, third, and fourth steps equal

$$W_3 = \frac{\sqrt{a}}{W_1}, \qquad (II.7.16)$$

$$W_2 = \frac{N}{W_3}, \qquad (II.7.17)$$

$$W_4 = \frac{N}{W_1}. \qquad (II.7.18)$$

Tables II.8.1 - II.8.3 contain the values of the step characteristic impedances for specified values of $|p|_{max}$, N, and A, computed using the formulas given.

#II.8. Finding the Length of the Step, l, and the Waveband within which the Specified Value for the Reflection Factor $|p|_{max}$ Will Occur.

The length of a step is found through formula

$$l = \frac{\lambda_2}{2\pi} \arccos A, \qquad (II.8.1)$$

where

λ_2 is the longest wave in the specified operating band.

The ratio of the longest wave to the shortest wave in the operating band is found through

$$\frac{\lambda_2}{\lambda_1} = \frac{\pi - \arccos A}{\arccos A}. \qquad (II.8.2)$$

Here λ_2 and λ_1 should be understood to be the wavelengths in the step line

$$\lambda_2 = \lambda_{20} \frac{v}{c},$$

$$\lambda_1 = \lambda_{10} \frac{v}{c},$$

where

λ_{20} and λ_{10} are the wavelengths in free space;

v is the phase velocity at which propagation occurs on a step line;

c is the speed of light

If we are discussing step transmission lines made up of sections of open-wire lines we can take v = c.

The full length of the step transition equals

$$L = nl \qquad (II.8.3)$$

where

n is the number of steps.

Tables II.8.1 - II.8.3 list the corresponding values of λ_2/λ_1 for each value of A. We can, by using these tables, find the needed number of steps, n, the length of a step, l, and the characteristic impedances for a specified λ_2/λ_1 ratio if the magnitudes of N and $|p|_{max}$ are specified.

Table II.8.1

Two-step line n = 2

	$\lvert\rho\rvert_{max} = 0.02$					$\lvert\rho\rvert_{max} = 0.05$					$\lvert\rho\rvert_{max} = 0.1$				
N	A	W_1	W_2	$\frac{l}{\lambda_2}$	$\frac{\lambda_2}{\lambda_1}$	A	W_1	W_2	$\frac{l}{\lambda_2}$	$\frac{\lambda_2}{\lambda_1}$	A	W_1	W_2	$\frac{l}{\lambda_2}$	$\frac{\lambda_2}{\lambda_1}$
1,2	0,600	1,057	1,135	0,148	2,388	0,842	1,073	1,119	0,0907	4,513	—	—	—	—	—
1,4	0,460	1,099	1,274	0,174	1,875	0,676	1,102	1,271	0,132	2,792	0,864	1,144	1,224	0,084	4,954
1,6	0,394	1,136	1,407	0,186	1,695	0,590	1,153	1,387	0,150	2,343	0,772	1,183	1,353	0,110	3,561
1,8	0,355	1,170	1,538	0,192	1,601	0,536	1,188	1,516	0,160	2,126	0,710	1,218	1,478	0,124	3,021
2,0	0,327	1,201	1,665	0,197	1,538	0,498	1,219	1,640	0,167	1,993	0,665	1,250	1,600	0,134	2,725
2,2	0,307	1,230	1,789	0,200	1,496	0,469	1,245	1,760	0,172	1,902	0,631	1,277	1,720	0,141	3,537
2,4	0,290	1,257	1,909	0,203	1,461	0,447	1,271	1,880	0,176	1,837	0,603	1,304	1,840	0,147	2,402
2,6	0,278	1,283	2,027	0,205	1,437	0,428	1,297	2,000	0,180	1,783	0,580	1,330	1,950	0,151	2,300
2,8	0,268	1,307	2,147	0,207	1,418	0,413	1,323	2,110	0,182	1,744	0,561	1,357	2,060	0,155	2,222
3,0	0,259	1,329	2,256	0,208	1,400	0,400	1,349	2,223	0,184	1,710	0,545	1,384	2,168	0,158	2,159
3,2	0,251	1,351	2,369	0,210	1,385	0,388	1,370	2,340	0,187	1,680	0,530	1,404	2,280	0,161	2,103
3,4	0,244	1,372	2,479	0,211	1,372	0,376	1,390	2,440	0,188	1,656	0,517	1,425	2,350	0,163	2,058
3,6	0,238	1,391	2,587	0,212	1,361	0,369	1,410	2,550	0,190	1,634	0,507	1,446	2,490	0,165	2,020
3,8	0,233	1,410	2,694	0,213	1,352	0,361	1,430	2,660	0,191	1,615	0,496	1,466	2,590	0,167	1,987
4,0	0,228	1,428	2,800	0,213	1,343	0,354	1,450	2,758	0,192	1,599	0,486	1,487	2,691	0,169	1,955
4,2	0,224	1,446	2,905	0,214	1,336	0,347	1,467	2,860	0,194	1,582	0,478	1 504	2,790	0,171	1,929
4,4	0,220	1,463	3,008	0,215	1,329	0,341	1,483	2,960	0,195	1,569	0,470	1,521	2,890	0,172	1,905
4,6	0,216	1,479	3,110	0,215	1,322	0,336	1,500	3,060	0,195	1,558	0,462	1,538	2,990	0,174	1,881
4,8	0,212	1,495	3,211	0,216	1,315	0,330	1,517	3,160	0,196	1,545	0,455	1,555	3,080	0,175	1,863
5,0	0,209	1,510	3,311	0,216	1,310	0,326	1,533	3,261	0,197	1,536	0,449	1,572	3,180	0,176	1,843
5,2	0,206	1,525	3,410	0,217	1,304	0,321	1,548	3,360	0,198	1,525	0,444	1,587	3,280	0,177	1,829
5,4	0,203	1,540	3,507	0,217	1,299	0,317	1,562	3,450	0,199	1,517	0,438	1,602	3,360	0,178	1,812
5,6	0,201	1,554	3,604	0,218	1,296	0,313	1,576	3,550	0,199	1,508	0,433	1,616	3,460	0,179	1,798
5,8	0,198	1,567	3,700	0,218	1,291	0,309	1,590	3,650	0,200	1,500	0,428	1,631	3,550	0,180	1,784
6,0	0,196	1,581	3,795	0,219	1,287	0,306	1,605	3,739	0,200	1,494	0,423	1,646	3,646	0,180	1,770
6,2	0,194	1,594	3,890	0,219	1,284	0,303	1,618	3,830	0,201	1,487	0,419	1,658	3,730	0,181	1,759
6,4	0,192	1,606	3,981	0,219	1,280	0,299	1,630	3,930	0,202	1,479	0,415	1,671	3,830	0,182	1,749
6,6	0,190	1,619	4,077	0,220	1,277	0,296	1,643	4,020	0,202	1,473	0,411	1,684	3,920	0,183	1,738
6,8	0,188	1,631	4,169	0,220	1,274	0,294	1,656	4,110	0,203	1,469	0,407	1,697	4,010	0,183	1,728
7,0	0,186	1,643	4,264	0,220	1,270	0,291	1,669	4,194	0,203	1,463	0,404	1,710	4,093	0,184	1,720
7,2	0,184	1,654	4,352	0,221	1,267	0,288	1,680	4,280	0,203	1,457	0,400	1,722	4,180	0,184	1,710
7,4	0,183	1,666	4,442	0,221	1,266	0,286	1,690	4,370	0,204	1,453	0,397	1,733	4,270	0,185	1,702
7,6	0,181	1,677	4,531	0,221	1,262	0,283	1,701	4,460	0,204	1,447	0,394	1,745	4,350	0,186	1 695
7,8	0,179	1,688	4,621	0,221	1,259	0,281	1,712	4,550	0,205	1,443	0,391	1,756	4,440	0,186	1,687
8,0	0,178	1,698	4,710	0,221	1,257	0,279	1,722	4,646	0,205	1,439	0,388	1,768	4,525	0,187	1,680
8,2	0,177	1,709	4,796	0,222	1,256	0,277	1,733	4,730	0,205	1,435	0,385	1,778	4,610	0,187	1,673
8,4	0,176	1,720	4,885	0,222	1,254	0,275	1,744	4,810	0,206	1,431	0,382	1,789	4,690	0,188	1,665
8,6	0,174	1,730	4,972	0,222	1,251	0,273	1,755	4,900	0,206	1,428	0,379	1,800	4,770	0,188	1,658
8,8	0,173	1,740	5,059	0,222	1,249	0,271	1,765	4,980	0,206	1,423	0,377	1,810	4,860	0,188	1,653
9,0	0,172	1,749	5,145	0,222	1,247	0,269	1,776	5,067	0,207	1,419	0,374	1,821	4,942	0,189	1,646
9,2	0,171	1,759	5,230	0,223	1,246	0,267	1,785	5,150	0,207	1,416	0,372	1,831	5,020	0,189	1,641
9,4	0,170	1,769	5,315	0,223	1,244	0,266	1,795	5,230	0,207	1,414	0,370	1,841	5,100	0,190	1,636
9,6	0,169	1,778	5,400	0,223	1,243	0,264	1,804	5,320	0,207	1,410	0,368	1,850	5,180	0,190	1,632
9,8	0,168	1,787	5,483	0,223	1,241	0,262	1,814	5,400	0,208	1,406	0,365	1,860	5,260	0,191	1,624
10,0	0,166	1,796	5,568	0,223	1,237	0,261	1,823	5,486	0,208	1,404	0,363	1,870	5,348	0,191	1,619

Table II.8.2

Three-step line n = 3

	$\lvert\rho\rvert_{max} = 0{,}02$						$\lvert\rho\rvert_{max} = 0{,}05$						$\lvert\rho\rvert_{max} = 0{,}1$					
N	A	W_1	W_2	W_3	$\frac{l}{\lambda_2}$	$\frac{\lambda_2}{\lambda_1}$	A	W_1	W_2	W_3	$\frac{l}{\lambda_2}$	$\frac{\lambda_2}{\lambda_1}$	A	W_1	W_2	W_3	$\frac{l}{\lambda_2}$	$\frac{\lambda_2}{\lambda_1}$
1,2	0,781	1,047	1,095	1,149	0,107	3,657	0,924	1,065	1,095	1,127	0,0624	7,006	—	1,091	1,095	1,100		
1,4	0,682	1,067	1,183	1,312	0,131	2,830	0,830	1,090	1,183	1,284	0,0942	4,310	0,935	1,123	1,183	1,241	0,0577	7,668
1,6	0,621	1,087	1,265	1,472	0,143	2,487	0,775	1,113	1,265	1,438	0,109	3,592	0,866	1,155	1,265	1,385	0,0772	5,518
1,8	0,584	1,105	1,342	1,627	0,151	2,317	0,736	1,133	1,342	1,589	0,118	3,224	0,851	1,177	1,342	1,529	0,088	4,681
2,0	0,558	1,120	1,414	1,786	0,156	2,210	0,703	1,149	1,414	1,739	0,126	2,971	0,824	1,195	1,414	1,674	0,096	4,215
2,2	0,537	1,133	1,483	1,942	0,160	2,129	0,685	1,166	1,483	1,888	0,130	2,849	0,802	1,211	1,483	1,817	0,102	3,997
2,4	0,521	1,146	1,549	2,094	0,163	2,072	0,666	1,179	1,549	2,036	0,134	2,732	0,787	1,227	1,549	1,956	0,106	3,724
2,6	0,508	0,160	1,612	2,241	0,165	2,027	0,651	1,193	1,612	2,179	0,137	2,645	0,768	1,241	1,612	2,095	0,111	3,519
2,8	0,496	1,172	1,673	2,391	0,167	1,987	0,637	1,206	1,673	2,324	0,140	2,569	0,754	1,254	1,673	2,233	0,114	3,383
3,0	0,484	1,183	1,732	2,536	0,170	1,918	0,627	1,218	1,732	2,462	0,142	2,518	0,742	1,266	1,732	2,370	0,117	3,275
3,2	0,475	1,194	1,789	2,680	0,171	1,920	0,615	1,228	1,789	2,606	0,145	2,456	0,732	1,278	1,789	2,506	0,119	3,191
3,4	0,467	1,204	1,844	2,823	0,173	1,895	0,606	2,237	1,841	2,749	0,146	2,416	0,721	1,288	1,844	2,640	0,122	3,103
3,6	0,459	1,213	1,897	2,968	0,174	1,872	0,598	1,246	1,897	2,889	0,148	2,379	0,713	1,299	1,897	2,771	0,124	3,043
3,8	0,452	1,221	1,949	3,115	0,175	1,851	0,590	1,256	1,949	3,025	0,150	2,343	0,705	1,311	1,949	2,899	0,125	2,985
4,0	0,446	1,229	2,000	3,255	0,176	1,834	0,584	1,267	2,000	3,156	0,151	2,317	0,697	1,322	2,000	3,025	0,127	2,929
4,2	0,441	1,237	2,049	3,395	0,177	1,820	0,577	1,276	2,049	3,292	0,152	2,287	0,641	1,331	2,049	3,156	0,139	2,590
4,4	0,435	1,246	2,098	3,534	0,178	1,806	0,572	1,284	2,098	3,427	0,153	2,266	0,685	1,339	2,098	3,286	0,130	2,849
4,6	0,430	1,253	2,145	3,671	0,179	1,795	0,566	1,292	2,195	3,560	0,154	2,241	0,679	1,347	2,145	3,415	0,131	2,811
4,8	0,425	1,260	2,191	3,810	0,180	1,784	0,560	1,300	2,191	3,692	0,155	2,217	0,674	1,356	2,191	3,540	0,132	2,760
5,0	0,424	1,267	2,236	3,947	0,180	1,773	0,556	1,307	2,236	3,825	0,156	2,202	0,668	1,365	2,236	3,662	0,134	2,743
5,2	0,420	1,273	2,280	4,085	0,181	1,762	0,551	1,314	2,280	3,957	0,157	2,182	0,664	1,373	2,280	3,787	0,134	2,719
5,4	0,416	1,279	2,324	4,222	0,182	1,752	0,547	1,321	2,324	4,088	0,158	2,167	0,659	1,380	2,324	3,913	0,135	2,690
5,6	0,413	1,285	2,366	4,358	0,182	1,744	0,543	1,328	2,366	4,217	0,159	2,151	0,655	1,387	2,366	4,037	0,136	2,667
5,8	0,410	1,292	2,408	4,489	0,183	1,136	0,539	1,335	2,408	4,345	0,159	2,137	0,649	1,395	2,408	4,158	0,138	2,634
6,0	0,407	1,299	2,449	4,619	0,183	1,728	0,536	1,342	2,449	4,473	0,160	2,126	0,646	1,402	2,449	4,279	0,138	2,617
6,2	0,405	1,304	2,490	4,755	0,184	1,722	0,531	1,348	2,490	4,599	0,161	2,107	0,643	1,408	2,490	4,403	0,139	2,601
6,4	0,402	1,309	2,530	4,869	0,184	1,715	0,529	1,353	2,530	4,730	0,161	2,100	0,639	1,414	2,530	4,526	0,140	2,589
6,6	0,400	1,314	2,569	5,023	0,184	1,710	0,524	1,359	2,569	4,857	0,162	2,082	0,636	1,420	2,569	4,648	0,140	2,564
6,8	0,397	1,320	2,608	5,152	0,185	1,702	0,522	1,365	2,608	4,982	0,163	2,075	0,633	1,426	2,608	4,769	0,141	2,548
7,0	0,395	1,325	2,646	5,263	0,185	1,697	0,519	1,370	2,646	5,111	0,163	2,065	0,629	1,433	2,646	4,884	0,142	2,528
7,2	0,395	1,330	2,683	5,414	0,185	1,697	0,516	1,375	2,683	5,236	0,164	2,054	0,626	1,439	2,683	5,003	0,142	2,512
7,4	0,391	1,335	2,720	5,543	0,186	1,687	0,515	1,380	2,720	5,362	0,164	2,051	0,623	1,444	2,720	5,125	0,143	2,497
7,6	0,389	1,340	2,757	5,612	0,186	1,683	0,513	1,385	2,757	5,487	0,164	2,014	0,620	1,449	2,757	5,215	0,144	2,483
7,8	0,387	1,345	2,793	5,799	0,187	1,677	0,511	1,390	2,793	5,612	0,165	2,037	0,618	1,455	2,793	5,361	0,144	2,473
8,0	0,385	1,350	2,828	5,927	0,187	1,673	0,508	1,395	2,828	5,735	0,165	2,027	0,615	1,461	2,828	5,477	0,145	2,458
8,2	0,383	1,354	2,864	6,056	0,187	1,667	0,506	1,400	2,864	5,857	0,166	2,020	0,612	1,466	2,864	5,593	0,145	2,444
8,4	0,381	1,358	2,898	6,186	0,188	1,663	0,504	1,405	2,898	5,979	0,166	2,013	0,610	1,471	2,898	5,710	0,146	2,434
8,6	0,379	1,362	2,933	6,314	0,188	1,657	0,502	1,410	2,933	6,099	0,166	2,007	0,607	1,476	2,933	5,827	0,146	2,420
8,8	0,377	1,367	2,966	6,437	0,188	1,653	0,500	1,414	2,966	6,223	0,167	2,000	0,605	1,481	2,966	5,942	0,146	2,411
9,0	0,376	1,371	3,000	6,564	0,189	1,650	0,498	1,419	3,000	6,342	0,167	1,993	0,603	1,485	3,000	6,059	0,147	2,402
9,2	0,374	1,375	3,033	6,691	0,189	1,646	0,496	1,423	3,033	6,465	0,167	1,987	0,601	1,490	3,033	6,174	0,147	2,392
9,4	0,373	1,380	3,066	6,812	0,189	1,642	0,493	1,427	3,066	6,587	0,168	1,977	0,599	1,494	3,066	6,292	0,148	2,383
9,6	0,371	1,384	3,098	6,936	0,189	1,639	0,491	1,430	3,098	6,713	0,168	1,973	0,597	1,498	3,098	6,409	0,148	2,374
9,8	0,370	1,387	3,130	7,066	0,190	1,636	0,490	1,435	3,130	6,829	0,168	1,967	0,594	1,503	3,130	6,520	0,149	2,360
10,0	0,369	1,391	3,162	7,188	0,190	1,634	0,488	1,440	3,162	6,947	0,169	1,961	0,592	1,508	3,162	6,633	0,149	2,352

Table II.8.3

Four-step line n = 4

$\lvert\rho\rvert_{max}$ = 0,02								$\lvert\rho\rvert_{max}$ =		
N	A	W_1	W_2	W_3	W_4	$\frac{l}{\lambda_2}$	$\frac{\lambda_2}{\lambda_1}$	A	W_1	W_2
1,2	0,866	1,036	1,074	1,118	1,158	0,083	5,0	0,956	1,062	1,084
1,4	0,791	1,053	1,138	1,230	1,330	0,101	3,809	0,898	1,079	1,151
1,6	0,752	1,065	1,192	1,312	1,592	0,114	3,365	0,862	1,091	1,208
1,8	0,723	1,075	1,237	1,455	1,674	0,121	3,119	0,835	1,106	1,255
2,0	0,701	1,084	1,276	1,567	1,815	0,126	2,956	0,816	1,118	1,297
2,2	0,685	1,092	1,322	1,661	2,015	0,130	2,849	0,799	1,127	1,345
2,4	0,671	1,100	1,362	1,762	2,182	0,133	2,762	0,786	1,136	1,387
2,6	0,660	1,108	1,399	1,859	2,346	0,135	2,696	0,774	1,145	1,425
2,8	0,650	1,114	1,431	1,956	2,513	0,137	2,610	0,763	1,153	1,459
3,0	0,641	1,121	1,460	2,051	2,676	0,139	2,59	0,756	1,161	1,490
3,2	0,633	1,127	1,495	2,141	2,839	0,141	2,518	0,749	1,168	1,525
3,4	0,626	1,132	1,526	2,228	3,004	0,142	2,512	0,747	1,174	1,558
3,6	0,620	1,138	1,551	2,316	3,163	0,144	2,483	0,735	1,180	1,588
3,8	0,614	1,142	1,581	2,403	3,327	0,145	2,451	0,729	1,185	1,616
4,0	0,609	1,147	1,606	2,490	3,487	0,146	2,430	0,723	1,190	1,642
4,2	0,604	1,152	1,634	2,571	2,646	0,147	2,406	0,717	1,195	1,671
4,4	0,599	1,156	1,659	2,652	3,806	0,148	2,383	0,714	1,200	1,698
4,6	0,595	1,160	1,684	2,732	3,966	0,149	2,365	0,710	1,205	1,722
4,8	0,591	1,164	1,706	2,813	4,121	0,149	2,318	0,701	1,209	1,747
5,0	0,587	1,168	1,728	2,893	4,283	0,150	2,330	0,701	1,214	1,770
5,2	0,581	1,171	1,752	2,968	4,410	0,150	2,317	0,698	1,218	1,791
5,4	0,581	1,175	1,774	3,043	4,595	0,151	2,301	0,695	1,222	1,818
5,6	0,578	1,178	1,796	3,118	4,751	0,152	2,292	0,690	1,226	1,840
5,8	0,575	1,181	1,816	3,193	4,911	0,152	2,279	0,687	1,230	1,862

= 0,05				$\lvert\rho\rvert_{max}$ = 0,1						
W_3	W_4	$\frac{l}{\lambda_2}$	$\frac{\lambda_2}{\lambda_1}$	A	W_1	W_2	W_3	W_4	$\frac{l}{\lambda_2}$	$\frac{\lambda_2}{\lambda_1}$
1,107	1,130	0,047	9,547	—	—	—	—	—	—	—
1,216	1,297	0,072	5,897	0,958	—	—	—	—	0,0163	9,800
1,325	1,462	0,085	4,911	0,933	—	—	—	—	0,059	7,531
1,434	1,627	0,093	4,392	0,911	—	—	—	—	0,068	6,392
1,542	1,788	0,098	4,097	0,891	1,169	1,322	1,513	1,711	0,074	5,763
1,636	1,952	0,103	3,869	0,879	1,180	1,372	1,604	1,864	0,079	5,320
1,730	2,113	0,106	3,714	0,868	1,191	1,416	1,695	2,015	0,083	5,047
1,824	2,271	0,109	3,582	0,857	1,200	1,455	1,787	2,167	0,086	4,803
1,919	2,428	0,112	3,470	0,848	1,209	1,491	1,878	2,316	0,089	4,625
2,013	2,584	0,114	3,403	0,840	1,218	1,524	1,969	2,464	0,091	4,447
2,098	2,740	0,115	3,337	0,832	1,224	1,559	2,052	2,614	0,091	4,341
2,182	2,896	0,116	3,320	0,826	1,231	1,592	2,136	2,672	0,094	4,245
2,267	3,051	0,119	3,215	0,820	1,238	1,622	2,219	2,908	0,095	4,155
2,352	3,206	0,120	3,167	0,814	1,241	1,650	2,303	3,055	0,097	4,068
2,436	3,360	0,121	3,119	0,809	1,246	1,676	2,386	3,209	0,099	4,000
2,514	3,515	0,123	3,072	0,804	1,256	1,708	2,459	3,344	0,10	3,934
2,592	3,667	0,123	3,051	0,799	1,262	1,738	2,532	3,487	0,101	3,869
2,670	3,817	0,124	3,021	0,795	1,267	1,767	2,604	3,631	0,103	3,819
2,747	3,970	0,126	2,978	0,791	1,273	1,793	2,677	3,771	0,104	3,772
2,825	4,120	0,126	2,956	0,788	1,278	1,818	2,750	3,918	0,105	3,737
2,898	4,269	0,127	2,936	0,784	1,283	1,844	2,820	4,053	0,106	3,691
2,970	4,419	0,128	2,916	0,780	1,288	1,869	2,890	4,193	0,107	3,647
3,013	4,568	0,129	2,882	0,777	1,292	1,892	2,960	4,331	0,108	3,613
3,115	4,715	0,129	2,863	0,771	1,297	1,911	3,030	1,172	0,109	3,582

Table II.8.3 [cont.]

	$\lvert\rho\rvert_{max}=0,02$							$\lvert\rho\rvert_{max}=$		
N	A	W_1	W_2	W_3	W_4	$\frac{l}{\lambda_2}$	$\frac{\lambda_2}{\lambda_1}$	A	W_1	W_2
6,0	0,572	1,185	1,836	3,268	5,061	0,153	2,266	0,685	1,233	1,832
6,2	0,570	1,188	1,856	3,340	5,219	0,153	2,258	0,682	1,237	1,901
6,4	0,568	1,191	1,876	3,411	5,374	0,154	2,250	0,679	1,240	1,925
6,6	0,565	1,194	1,895	3,482	5,528	0,154	2,237	0,675	1,243	1,945
6,8	0,563	1,197	1,914	3,553	5,680	0,155	2,230	0,673	1,246	1,964
7,0	0,561	1,200	1,932	3,624	5,836	0,155	2,222	0,671	1,249	1,982
7,2	0,559	1,202	1,950	3,692	5,990	0,156	2,213	0,669	1,252	2,002
7,4	0,557	1,205	1,969	3,759	6,141	0,156	2,206	0,668	1,255	2,020
7,6	0,554	1,207	1,986	3,827	6,297	0,156	2,191	0,665	1,258	2,038
7,8	0,552	1,210	2,003	3,894	6,446	0,157	2,186	0,663	1,261	2,056
8,0	0,550	1,212	2,019	3,962	6,601	0,157	2,178	0,660	1,261	2,073
8,2	0,548	1,215	2,036	4,027	6,749	0,158	2,171	0,658	1,266	2,091
8,4	0,547	1,217	2,053	4,092	6,902	0,158	2,167	0,657	1,269	2,108
8,6	0,545	1,219	2,068	4,158	7,055	0,158	2,159	0,655	1,272	2,125
8,8	0,543	1,221	2,084	4,223	7,207	0,159	2,151	0,654	1,274	2,141
9,0	0,542	1,224	2,098	4,289	7,355	0,159	2,148	0,652	1,277	2,157
9,2	0,541	1,226	2,114	4,352	7,504	0,159	2,144	0,650	1,279	2,173
9,4	0,539	1,228	2,129	4,415	7,655	0,159	2,137	0,648	1,282	2,189
9,6	0,537	1,230	2,141	4 478	7,805	0,160	2,130	0,646	1,284	2,204
9,8	0,536	1,232	2,158	4,541	7,954	0,160	2,126	0,644	1,286	2,220
10,0	0,534	1,234	2,172	4,604	8,106	0,160	2,119	0,643	1,288	2,234

	$=0,05$				$\lvert\rho\rvert_{max}=0,1$						
W_2	W_4	$\frac{l}{\lambda_2}$	$\frac{\lambda_2}{\lambda_1}$	A	W_1	W_2	W_3	W_4	$\frac{l}{\lambda_2}$	$\frac{\lambda_2}{\lambda_1}$
3,188	4,865	0,130	2,819	0,771	1,300	1,936	3,100	4,614	0,110	3,551
3,256	5,012	0,131	2,830	0,768	1,305	1,958	3,166	4 752	0,111	3,519
3,325	5,161	0,131	2,811	0,766	1,308	1,980	3,232	4,889	0,111	3,500
3,394	5,310	0,132	2,786	0,763	1,312	2,001	3,298	5,030	0,112	3,470
3,463	5,457	0,132	2,774	0,761	1,316	2,021	3,361	5,167	0,112	3,450
3,532	5,603	0,133	2,762	0,759	1,319	2,041	3,430	5,303	0,113	3,432
3,597	5,751	0,133	2,749	0,756	1,323	2,059	3,497	5,446	0,114	3,403
3,663	5,896	0,134	2,743	0,754	1,326	2,077	3,563	5,581	0,114	3,383
3,729	6,041	0,134	2,725	0,752	1,329	2,094	3,630	5,719	0,114	3,365
3,791	6,186	0,135	2,714	0,750	1,332	2,110	3,696	5,856	0,115	3,346
3,860	6,331	0,135	2,696	0,748	1,335	2,126	2,763	5,993	0,115	3,329
3,922	6,477	0,136	2,685	0,746	1,338	2,147	3,820	6,129	0,116	3,311
3,985	6,619	0,136	2,678	0,745	1 341	2,167	3,877	6,264	0,116	3,303
4,047	6,761	0,136	2,667	0,741	1,344	2,186	3,934	6,399	0,117	3,267
4,110	6,907	0,136	2,662	0,739	1,347	2,205	3,991	6,533	0,118	3,250
4,173	7,048	0,137	2,651	0,738	1,349	2,223	4,048	6,670	0,118	3,242
4,234	7,193	0,137	2,610	0,736	1,352	2,241	4,106	6,805	0,118	3,225
4,294	7,332	0,138	3,628	0,735	1,355	2,257	4,164	6,937	0,119	3,215
4,355	7,477	0,138	2,617	0,734	1,358	2,273	4,223	7,069	0,119	3,207
4,415	7,620	0,139	2,606	0,732	1,360	2,289	4,281	7,206	0,119	3,191
4,476	7,763	0,139	2,601	0,729	1,362	2,305	4,339	7,310	0,120	3,167

#II.9. Finding the Reflection Factor within the Operating Band for a Step Transition

The reflection factor changes within the limits of the operating band. The dependence of the reflection factor on the wavelength is found through

$$|p| = \frac{\sqrt{|T_{11}|^2 - 1}}{|T_{11}|}. \qquad \text{(II.9.1)}$$

Here $|T_{11}|^2$ is the so-called effective attenuation function

$$|T_{11}|^2 = 1 + h^2 T_n^2\left(\frac{\cos\theta}{A}\right), \qquad \text{(II.9.2)}$$

where

$T_n(\cos\theta/A)$ is a Chebyshev polynomial of the first type of n^{th} order from the argument $\cos\theta/A$,

n is the number of steps.

$$\left.\begin{aligned} T_2\left(\frac{\cos\theta}{A}\right) &= 2\left(\frac{\cos\theta}{A}\right)^2 - 1 \\ T_3\left(\frac{\cos\theta}{A}\right) &= 4\left(\frac{\cos\theta}{A}\right)^3 - 3\frac{\cos\theta}{A} \\ T_4\left(\frac{\cos\theta}{A}\right) &= 8\left(\frac{\cos\theta}{A}\right)^4 - 8\left(\frac{\cos\theta}{A}\right)^2 + 1 \end{aligned}\right\}, \qquad \text{(II.9.3)}$$

where

$\theta = 2\pi l/\lambda$ is the electrical length of the step;

λ is the wavelength on the step line.

Substituting the value of T_{11} found through (II.9.3) in (II.9.1), we can find the dependence of p on λ.

Chapter III

COUPLED UNBALANCED TWO-WIRE LINES

#III.1. General

The preceding chapters reviewed balanced two-wire lines. One often encounters unbalanced two-wire lines in practice, and the computational apparatus in the foregoing is unsuited to an investigation of these latter lines.

Figure III.1.1 shows examples of two unbalanced lines. In the example in Figure III.1.1a, the unbalance is the result of dissimilar conditions at the end of conductors 1 and 2 of the line, while in the example in Figure III.1.1b, the unbalance is the result of the difference in the diameters of conductors 1 and 2. There are other reasons for an unbalance, such as unequal potentials at the generator end of conductors 1 and 2, unequal heights of the conductors above the ground, etc.

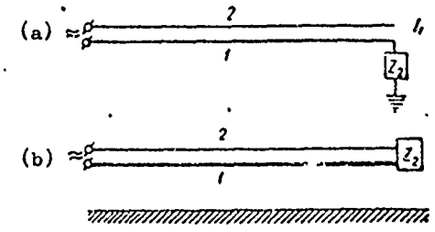

Figure III.1.1. Examples of unbalanced lines.
a - dissimilar conditions at terminations;
b - dissimilar conductor diameters.

Unbalanced lines, like balanced lines, have incoming distributed constants, inductance, capacitance, resistance, and leakage, per unit line length. We will limit ourselves to an analysis of unbalanced lines, disregarding their losses ($R_1 = G_1 = 0$).

#III.2. Determination of the Distributed Constants and Characteristic Impedances of Coupled Lines

(a) Distributed capacitances

The electrical system, which is an unbalanced line consisting of two conductors of identical length (l), should be considered in the light of three different distributed capacitances:

C_1, the capacitance of conductor 1 per unit length of the system;

C_2, the capacitance of conductor 2 per unit length of the system;

C_{12}, the capacitance between conductors 1 and 2 per unit length of the system.

In order to find capacitances C_1, C_2, and C_{12} let us use equations which associate the static charges and potentials in the system of conductors with

each other. In the case of two conductors, these equations are in the form

$$\left.\begin{aligned} V_1 &= q_1\varphi_{11} + q_2\varphi_{12} \\ V_2 &= q_2\varphi_{22} + q_1\varphi_{21} \end{aligned}\right\}, \qquad \text{(III.2.1)}$$

where

V_1 and V_2 are the potentials for conductors 1 and 2;

q_1 is the linear charge density, conductor 1;

q_2 is the linear charge density, conductor 2;

φ_{11} is the linear potential factor for conductor 1, numerically equal to the potential induced in conductor 1 by its own charge with linear density equal to one;

φ_{22} is the linear potential factor for conductor 2, numerically equal to the potential induced in conductor 2 by its own charge with linear density equal to one;

φ_{12} is the mutual linear potential factor, numerically equal to the potential induced in conductor 1 by the charge on conductor 2 with linear density equal to one;

φ_{21} is the mutual linear potential factor numerically equal to the potential induced in conductor 2 by the charge on conductor 1 with linear density equal to one.

Potentials φ_{11}, φ_{22}, φ_{12}, φ_{21} can be found through Academician M. V. Shuleykin's method, as well as by other known methods.[1] When the lengths of conductors 1 and 2 are the same, $\varphi_{12} = \varphi_{21}$.

We should note that it is not mandatory for conductors 1 and 2 to be single conductors. Each conductor can, in turn, consist of a system of conductors under a common potential.

Solving equation (III.2.1) for q_1 and q_2, we obtain

$$\left.\begin{aligned} q_1 &= \frac{\varphi_{22}}{\Delta}V_1 - \frac{\varphi_{12}}{\Delta}V_2 \\ q_2 &= \frac{\varphi_{11}}{\Delta}V_2 - \frac{\varphi_{21}}{\Delta}V_1 \end{aligned}\right\}, \qquad \text{(III.2.2)}$$

where

$$\Delta = \varphi_{11}\varphi_{22} - \varphi_{12}\varphi_{21} = \varphi_{11}\varphi_{22} - \varphi_{12}^2.$$

From formula (III.2.2), φ_{22}/Δ is the charge incoming per unit length of conductor 1, when the potential on this conductor is equal to one, and the potential on conductor 2 is zero; that is, there is capacitance C_1 for conductor 1 per unit length of the system.

Similarly, φ_{11}/Δ is the capacitance C_2 for conductor 2 per unit length of the system, and $\varphi_{12}/\Delta = \varphi_{21}/\Delta$ is the mutual capacitance C_{12} between conductors 1 and 2 per system unit length.

---

1. A. A. Pistol'kors. Antennas. Svyaz'izdat, 1947, pp. 227-238.

Accordingly,

$$\left.\begin{aligned} C_1 &= \frac{\varphi_{22}}{\Delta} = \frac{\varphi_{22}}{\varphi_{11}\varphi_{22} - \varphi_{12}^2} \\ C_2 &= \frac{\varphi_{11}}{\Delta} = \frac{\varphi_{11}}{\varphi_{11}\varphi_{22} - \varphi_{12}^2} \\ C_{12} &= \frac{\varphi_{12}}{\Delta} = \frac{\varphi_{12}}{\varphi_{11}\varphi_{22} - \varphi_{12}^2} \end{aligned}\right\} \qquad \text{(III.2.3)}$$

From formula (III.2.3), if the mutual capacitance between conductors 1 and 2 is zero, corresponding to $\varphi_{12} = 0$,

$$\left.\begin{aligned} C_1 = C_{10} &= \frac{1}{\varphi_{11}} \\ C_2 = C_{20} &= \frac{1}{\varphi_{22}} \end{aligned}\right\} \qquad \text{(III.2.4)}$$

Where C_{10} and C_{20} are the capacitances of conductors 1 and 2 per unit length when there is no link between them; that is, these are the capacitances of single conductors 1 and 2 per unit length.

When V and 2 are measured in volts and coulombs per meter, respectively, and ℓ is in meters, C is in farads per meter.

(b) Distributed inductances and line mutual inductance

Two magnitudes which characterize the distributed inductance in an unbalanced line must be considered:

L_{10},- the inductance of conductor 1 per unit length, the influence of conductor 2 not considered;

L_{20}, the inductance of conductor 2 per unit length, the influence of conductor 1 not considered.

The distributed mutual inductance of an unbalanced line can be characterized by the magnitude M_{12}, which is the mutual inductance per unit line length.

Using the known relationship

$$L_1 \text{ (henries/meter) } C_1 \text{ (farads/meter)} = 1/9\cdot10^6 (\text{seconds}^2/\text{meter}^2)$$

and taking equation (III.2.4) into consideration,

$$\left.\begin{aligned} L_{10} &= \frac{1}{9\cdot10^{16}C_{10}} = \frac{1}{9\cdot10^{16}}\varphi_{11} \\ L_{20} &= \frac{1}{9\cdot10^{16}C_{20}} = \frac{1}{9\cdot10^{16}}\varphi_{22} \end{aligned}\right\} \qquad \text{(III.2.5)}$$

Similarly,

$$M_{12} = \frac{1}{9\cdot10^{16}}\varphi_{12}. \qquad \text{(II.2.6)}$$

(c) Line characteristic impedances

A lossless unbalanced line consisting of two systems of conductors has three characteristic impedances which can be found through formulas (III.2.3), (II.2.5) and (I.2.10):

$$\left.\begin{aligned} W_1 &= \frac{1}{3\cdot10^8 C_1} = \frac{1}{3\cdot10^8}\,\frac{\varphi_{11}\varphi_{22}-\varphi_{12}^2}{\varphi_{22}} \\ W_2 &= \frac{1}{3\cdot10^8 C_2} = \frac{1}{3\cdot10^8}\,\frac{\varphi_{11}\varphi_{22}-\varphi_{12}^2}{\varphi_{11}} \\ W_{12} &= \frac{1}{3\cdot10^8 C_{12}} = \frac{1}{3\cdot10^8}\,\frac{\varphi_{11}\varphi_{22}-\varphi_{12}^2}{\varphi_{12}} \end{aligned}\right\} \qquad \text{(III.2.7)}$$

where

W_1 is the characteristic impedance of conductor 1 of the system;

W_2 is the characteristic impedance of conductor 2 of the system;

W_{12} is the mutual characteristic impedance of conductors 1 and 2 of the system.

If the mutual capacitance between conductors 1 and 2 equals zero ($C_{12} = 0$), by substituting the values for C_1 and C_2, taken from equation (III.2.4) in the case cited, we obtain

$$\left.\begin{aligned} W_1 = W_{10} &= \frac{1}{3\cdot10^8 C_{10}} = \frac{1}{3\cdot10^8}\varphi_{11} \\ W_2 = W_{20} &= \frac{1}{3\cdot10^8 C_{20}} = \frac{1}{3\cdot10^8}\varphi_{22} \end{aligned}\right\} \qquad \text{(III.2.8)}$$

When C_{12} falls to zero, W_{12} becomes infinite.

Example 1. Compute the linear potential factor for the unbalanced line shown in Figure III.2.1.

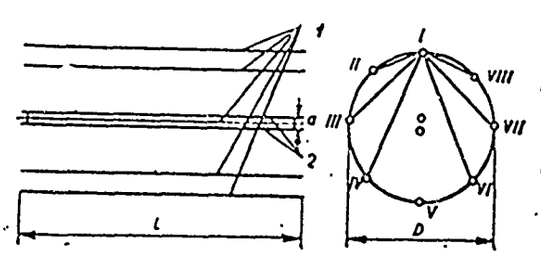

Figure III.2.1. Schematic diagram of an unbalanced line.

The line consists of two systems of conductors. The first system (1) consists of eight conductors, diameter d = 7.8 mm, length l = 120 meters, connected in parallel and positioned to form the generator of a cylinder of diameter D = 150 cm. The second system (2) consists of two conductors of the same diameter and length as the conductors in the first system, and these are connected to each other. The conductors in the second system are

parallel to the conductors in the first system and positioned close to the center of that system. The distance between the conductors in the second system is a = 20 cm.

1. Find the linear potential factor for the first system (φ_{11}).[1]

The average potential induced in conductor I (fig. III.2.1) by its own charge equals

$$\varphi_{IIav} = 9\cdot10^9\, 2\sigma_1\left(\ln\frac{2l}{d} - 0{,}307\right) = 9\cdot10^9\cdot 20\sigma_1.$$

where

σ_1 is the linear charge density for each of the conductors in the first system

$$\sigma_1 = q_1/8.$$

The distance between conductors I and II and I and VIII equal

$$a_{I\,II} = a_{I\,VIII} = 2\frac{D}{2}\sin\frac{360}{8\cdot2} = 57\ \text{cm}.$$

The average potential induced in conductors II or VIII by conductor I equals

$$\varphi_{I\,IIav} = \varphi_{I\,VIIIav} = 9\cdot10^9 2\sigma_1\left(\ln\frac{l}{a_{I\,II}} - 0{,}307\right) \approx 9\cdot10^9\cdot10\sigma_1.$$

Similarly we find

$$\varphi_{I\,IIIav} = \varphi_{I\,VIIav} = 9\cdot10^9\cdot 8{,}83\sigma_1;\quad \varphi_{I\,IVav} = \varphi_{I\,VIav} = 9\cdot10^9\cdot 8{,}31\sigma_1;$$
$$\varphi_{I\,Vav} = 9\cdot10^9\cdot 8{,}15\sigma_1.$$

The total average potential on conductor I from the charges carried by the conductors in the first system equals

$$\varphi_{Iav} = 9\cdot10^9(20 + 2\cdot10 + 2\cdot8{,}83 + 2\cdot8{,}31 + 8{,}15)\sigma_1 \approx 9\cdot10^9\cdot32{,}6\sigma_1 =$$
$$= 9\cdot10^9\cdot10{,}33q_1.$$

Since all the conductors in the first system are symmetrically positioned, their average potentials are the same. Accordingly, $\varphi_{I\ av}$ is the average potential for the entire first system.

The linear potential factor for the first system equals

$$\varphi_{11} = 9\cdot10^9\cdot10{,}33.$$

2. Find the linear potential factor for the second system of conductors (φ_{22}):

(1) The average potential for the second system from its charge equals

$$\varphi_{2av} = 9\cdot10^9 2\sigma_2\left[2\left(\ln\frac{l}{a} - 0{,}307\right) + \ln\frac{2a}{d}\right] =$$
$$= 9\cdot10^9\cdot32{,}2\sigma_2 = 9\cdot10^9\cdot16{,}1q_2.$$

where

σ_2 is the linear charge density for each of the conductors in the second system.

---

1. All formulas cited here for potential calculations were obtained using Howe's method.

(2) The linear potential factor for the second system equals

$$\varphi_{22} = 9 \cdot 10^9 \cdot 16.1.$$

3. Determine the mutual linear potential factor (φ_{12}).

(1) The average potential for the first system of conductors, induced by one of the conductors in the second system, equals

$$\varphi'_{12_{av}} \approx 9 \cdot 10^9 2\tau_2 \left(\ln \frac{2l}{D} - 0{,}307 \right) = 9 \cdot 10^9 \cdot 9{,}53\tau_2.$$

(2) The average potential for the first system of conductors, induced by both conductors in the second system, equals

$$\varphi_{12_{av}} \approx 2\varphi'_{12_{av}} = 9 \cdot 10^9 \cdot 2\ 9{,}53\tau_2 = 9 \cdot 10^9 \cdot 19{,}06\tau_2 = 9 \cdot 10^9 \cdot 9{,}53q_2.$$

The mutual linear potential factor is $\varphi_{12} = 9 \cdot 10^9 \cdot 9.53$

$$\varphi_{21} = \varphi_{12}.$$

Example 2. Find W_1, W_2, and W_{12} for an unbalanced line, the data for which are as given in Example 1.

The magnitudes C_1, C_2, C_{12}, W_1, W_2 and W_{12} are found through formulas (III.2.3) and (III.2.7).

Substituting

$$\begin{aligned} \varphi_{11} &= 10{,}33 \cdot 9 \cdot 10^9, \\ \varphi_{22} &= 16{,}1 \cdot 9 \cdot 10^9, \\ \varphi_{12} &= 9{,}53 \cdot 9 \cdot 10^9, \end{aligned}$$

we obtain

$$C_1 = 0{,}215 \frac{1}{9 \cdot 10^9} \text{ (farads/meter)},$$

$$W_1 = 140 \text{ ohms},$$

$$C_2 = 0{,}138 \frac{1}{9 \cdot 10^9} \text{ (farads/meter)},$$

$$W_2 = 217 \text{ ohms},$$

$$C_{12} = 0{,}127 \frac{1}{9 \cdot 10^9} \text{ (farads/meter)}$$

$$W_{12} = 236 \text{ ohms}.$$

#III.3. Pistol'kors' Equations for an Unbalanced Line

Let us introduce the notations

$$\left.\begin{aligned} X_1 &= \omega L_{10} = \omega \varphi_{11} \frac{1}{9 \cdot 10^{10}} \\ X_2 &= \omega L_{20} = \omega \varphi_{22} \frac{1}{9 \cdot 10^{10}} \\ X_{12} &= \omega M_{12} = \omega \varphi_{12} \frac{1}{9 \cdot 10^{10}} \end{aligned}\right\}; \qquad \text{(III.3.1)}$$

$$\left.\begin{aligned} b_1 &= \omega C_1 = \omega \frac{\varphi_{22}}{\Delta} \\ b_2 &= \omega C_2 = \omega \frac{\varphi_{11}}{\Delta} \\ b_{12} &= \omega C_{12} = \omega \frac{\varphi_{12}}{\Delta} \end{aligned}\right\}; \qquad \text{(III.3.2)}$$

I_1 is the current flowing in conductor 1; I_2 that flowing in conductor 2.

Let us select an infinitely small element of an unbalanced line at distance z from its end.

The potential drop across element dz of conductor 1 equals

$$dV_1 = iI_1X_1dz + iI_2X_{12}dz,$$

where

iI_1X_1dz is the emf of self-induction in element dz;

$iI_2X_{12}dz$ is the emf of mutual induction in element dz.

Dividing both sides of the equality by dz, and designating $V_1' = dV_1/dz$,

$$V_1' = iX_1I_1 + iX_{12}I_2. \qquad \text{(III.3.3)}$$

Similarly

$$V_2' = iX_2I_2 + iX_{12}I_1. \qquad \text{(III.3.4)}$$

The change in the current flowing in element dz of conductor 1 equals

$$dI_1 = I_1'dz = ib_1V_1dz - ib_{12}V_2dz,$$

where

ib_1V_1dz is the current leakage due to the capacitance of the element of conductor 1 to ground;

$ib_{12}V_2dz$ is the current leakage due to the capacitance of the element of conductor 1 to conductor 2.

Dividing both sides of the equality by dz,

$$I_1' = ib_1V_1 - ib_{12}V_2. \qquad \text{(III.3.5)}$$

Similarly,

$$I_2' = ib_2V_2 - ib_{12}V_1. \qquad \text{(III.3.6)}$$

The minus signs in front of the second terms in the right-hand sides of equations (III.3.5) and (III.3.6) are taken from the signs in the equations at (III.2.2). The minus sign means that mutual capacitance causes a reduction in current leakage in the case of potentials with the same names.

Let us reduce these equations to a form which will be convenient for analysis in order to integrate the differential equations at (III.3.3)-(III.3.6). Let us differentiate equations (III.3.3) and (III.3.4) with respect to z, and substitute the expressions for I_1' and I_2' from equations (III.3.5) and (III.3.6). Carrying out the operations indicated, and making the transformations,

$$\left.\begin{aligned} V_1'' + \alpha^2V_1 &= 0 \\ V_2'' + \alpha^2V_2 &= 0 \end{aligned}\right\} \qquad \text{(III.3.7)}$$

These equations are second-order homogeneous linear differential equations. They can be satisfied by the following functions

$$\left.\begin{aligned} V_1 &= A_1 \cos \alpha z + i B_1 \sin \alpha z \\ V_2 &= A_2 \cos \alpha z + i B_2 \sin \alpha z \end{aligned}\right\}, \qquad \text{(III.3.8)}$$

where A_1, A_2, B_1 and B_2 are constants of integration which can be found from the conditions at the ends of conductors 1 and 2.

Substituting the expressions V_1 and V_2 from (III.3.8) in equations (III.3.3) and (III.3.4), and solving them with respect to I_1 and I_2,

$$\left.\begin{aligned} I_1 &= \left(\frac{B_1}{W_1} - \frac{B_2}{W_{12}}\right)\cos \alpha z + i\left(\frac{A_1}{W_1} - \frac{A_2}{W_{12}}\right)\sin \alpha z \\ I_2 &= \left(\frac{B_2}{W_2} - \frac{B_1}{W_{12}}\right)\cos \alpha z + i\left(\frac{A_2}{W_2} - \frac{A_1}{W_{12}}\right)\sin \alpha z \end{aligned}\right\} \qquad \text{(III.3.9)}$$

Formulas (III.3.8) and (III.3.9) were derived by A. A. Pistol'kors.

#III.4. In-Phase and Anti-Phase Waves on an Unbalanced Line

Analysis of how unbalanced lines function can often be simplified by introducing the concept of in-phase and anti-phase waves. The in-phase wave on a twin line is a wave in which the currents and the potentials for any cross section of the line are identical in absolute magnitude and phase for both conductors (fig. III.4.1a).

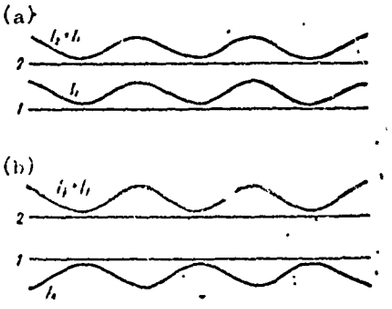

Figure III.4.1. In-phase (a) and anti-phase (b) waves on a line.

The anti-phase wave on a twin line is a wave in which the currents and the potentials for any cross section of the line are identical in absolute magnitude but opposite in phase for both conductors (fig. III.4.1b).

Regardless of the current and potential distributions along conductors 1 and 2, we can represent them as the sum of two components, the in-phase component, and the anti-phase component. In fact, let V_1 and V_2, the potentials for conductors 1 and 2, be functions of z.

Obviously, we can also find those magnitudes of V_c and V_n which satisfy the relationships

$$\left.\begin{aligned} V_1 &= V_c + V_n \\ V_2 &= V_c - V_n \end{aligned}\right\}. \qquad \text{(III.4.1)}$$

for any values of V_1 and V_2.

Solving (III.4.1) with respect to V_c and V_n,

$$\left.\begin{aligned} V_c &= \frac{1}{2}(V_1 + V_2) \\ V_n &= \frac{1}{2}(V_1 - V_2) \end{aligned}\right\}, \qquad \text{(III.4.2)}$$

where

V_c is the in-phase potential;

V_n is the anti-phase potential.

Accordingly, the potential across each conductor can be split into two components, one of which has identical values of absolute magnitude and phase for both conductors, while the other has values which are identical with respect to absolute magnitude, but opposite in phase.

The in-phase and anti-phase currents can be expressed in terms of similar formulas

$$\left.\begin{aligned} I_c &= \frac{1}{2}(I_1 + I_2) \\ I_n &= \frac{1}{2}(I_1 - I_2) \end{aligned}\right\}. \qquad \text{(III.4.3)}$$

Substituting the expressions for V_1, V_2, I_1 and I_2 from equations (III.3.8) and (III.3.9) in equations (III.4.2) and (III.4.3), we obtain

$$\left.\begin{aligned} V_c &= \frac{1}{2}\left[(A_1 + A_2)\cos\alpha z + i\,(B_1 + B_2)\sin\alpha z\right] \\ V_n &= \frac{1}{2}\left[(A_1 - A_2)\cos\alpha z + i\,(B_1 - B_2)\sin\alpha z\right] \end{aligned}\right\}; \qquad \text{(III.4.4)}$$

$$\left.\begin{aligned} I_c &= \frac{1}{2}\left\{\left[B_1\left(\frac{1}{W_1} - \frac{1}{W_{12}}\right) + B_2\left(\frac{1}{W_2} - \frac{1}{W_{12}}\right)\right]\cos\alpha z + \right. \\ &\quad \left. + i\left[A_1\left(\frac{1}{W_1} - \frac{1}{W_{12}}\right) + A_2\left(\frac{1}{W_2} - \frac{1}{W_{12}}\right)\right]\sin\alpha z\right\} \\ I_n &= \frac{1}{2}\left\{\left[B_1\left(\frac{1}{W_1} + \frac{1}{W_{12}}\right) - B_2\left(\frac{1}{W_2} + \frac{1}{W_{12}}\right)\right]\cos\alpha z + \right. \\ &\quad \left. + i\left[A_1\left(\frac{1}{W_1} + \frac{1}{W_{12}}\right) - A_2\left(\frac{1}{W_2} + \frac{1}{W_{12}}\right)\right]\sin\alpha z\right\} \end{aligned}\right\}. \qquad \text{(III.4.5)}$$

#III.5. Examples of Unbalanced Line Computations

Example 3. Find an expression for the voltage and current in a line, the sketch of which is shown in Figure III.1.1a.

Solution. Let Z_2 be the line load and I_{load} the current flowing in the line load. Conductors 1 and 2 have characteristic impedances W_1, W_2, and W_{12}.

Let us use the boundary conditions at the beginning and end of the line to find the constants A_1, A_2, B_1, and B_2 in formulas (III.3.8) and (III.3.9). At the end of the line, where z = 0,

$$\left.\begin{aligned} V_1 &= I_1 z_2 \\ I_1 &= I_{load} \\ I_2 &= 0 \end{aligned}\right\} \qquad \text{(III.5.1)}$$

At the beginning of the line, where z = l

$$I_1 = -I_2 \,. \qquad \text{(III.5.2)}$$

Substituting the expressions for V_1, V_2, I_1, and I_2 from formulas (III.3.8) and (III.3.9) in formulas (III.5.1) and (III.5.2), and assuming z = 0, or z = l, respectively, we obtain a system of equations for finding the sought-for constants

$$\left.\begin{aligned} A_1 &= \left(\frac{B_1}{W_1} - \frac{B_2}{W_{12}}\right) Z_2 \\ I_{load} &= \left(\frac{B_1}{W_1} - \frac{B_2}{W_{12}}\right) \\ \frac{B_2}{W_2} - \frac{B_1}{W_{12}} &= 0 \\ \left[\left(\frac{B_1}{W_1} - \frac{B_2}{W_{12}}\right)\cos\alpha l + i\left(\frac{A_1}{W_1} - \frac{A_2}{W_{12}}\right)\sin\alpha l\right] + & \\ + \left[\left(\frac{B_2}{W_2} - \frac{B_1}{W_{12}}\right)\cos\alpha l + i\left(\frac{A_2}{W_2} - \frac{A_1}{W_{12}}\right)\sin\alpha l\right] &= 0 \end{aligned}\right\} \qquad \text{(III.5.3)}$$

Using the system at (III.5.3) we can find the constants of integration, and using formulas (III.3.8) and (III.3.9), we can find the potential and current distributions in any of the conductors. These expressions are complex in their general form, and will not be cited here.

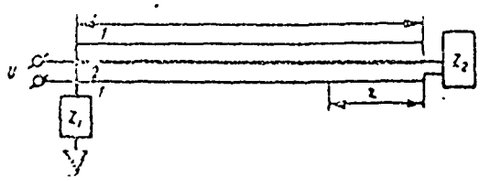

Figure III.5.1. Schematic diagram of a shielded coaxial line.

Example 4. Find expressions for the voltage and current for a shielded coaxial line, the schematic diagram for which is shown in Figure III.5.1. 1 is the line's shield, 2 is its inner conductor.

Solution. Let us introduce the notation:

U is the voltage applied to the line;

Z_1 is the impedance of line grounding;

Z_2 is the line load;

l is the line length.

Conductors 1 and 2 have characteristic impedances W_1, W_2, and W_{12}. Line unbalance can be established by the non-identity of the distributed constants on conductors 1 and 2, wherein $W_1 \neq W_2$, and one of the conductors (conductor 1 - the line shield) is grounded through impedance Z_1 at the point where the emf is supplied.

Let us assume that the inner conductor is completely shielded, that is, that the shield is solid, and $C_2 = C_{12}$, so

$$W_2 = W_{12}. \qquad \text{(III.5.4)}$$

The general equations for the unbalanced line (III.3.8) and (III.3.9), express the current and potential distributions for the line.

The line's boundary conditions are:

at the termination, where z = 0

$$\left.\begin{aligned} V_2 - V_1 &= I_2 Z_2 \\ I_1 &= -I_2 \end{aligned}\right\}. \qquad \text{(III.5.5)}$$

at the source, where z = l

$$\left.\begin{aligned} V_2 - V_1 &= U \\ V_1 &= -(I_1 + I_2) Z_1 \end{aligned}\right\}. \qquad \text{(III.5.6)}$$

Substituting the expressions for V_1, V_2, I_1 and I_2 from (III.3.8) and (III.3.9) in formulas (III.5.5) and (III.5.6), and assuming that z = 0, or that z = l, respectively, we obtain a system of equations for finding the constants of integration.

The solution, with formula (III.5.4) taken into consideration, yields the following expressions for the constants of integration

$$\left.\begin{aligned} B_1 = 0,\ B_2 &= U \frac{1}{\frac{Z_2}{W_2}\cos \alpha l + i \sin \alpha l} \\ A_1 = 0,\ A_2 &= U \frac{Z_2}{W_2} \frac{1}{\frac{Z_2}{W_2}\cos \alpha l + i \sin \alpha l} \end{aligned}\right\}. \qquad \text{(III.5.7)}$$

Substituting (III.5.7) in equations (III.3.8) and (III.4.2), we obtain expressions for the potentials across the outer and inner conductors of the line, V_1 and V_2, as well as for V_c and V_n. V_1 proves to be zero. This is as expected, because in the case of a complete shield all the electrical lines of force between the line's inner conductor and its shield are contained within the shield (they do not penetrate beyond the shield). Accordingly, V_2 is the anti-phase voltage across the line (U_n). The expression for U_n is

$$U_n = V_2 - V_1 = V_2 = U \frac{Z_1 \cos \alpha z + i W_2 \sin \alpha z}{Z_1 \cos \alpha l + i W_2 \sin \alpha l}. \qquad \text{(III.5.8)}$$

Substituting formula (III.5.7) in (III.3.9) and (III.4.3), we obtain the expressions for I_1 and I_2, as well as those for I_c and I_n. Further, $I_2 = -I_1$; $I_c = 0$, and

$$I_n = \frac{U}{W_2} \frac{W_2 \cos \alpha z + i Z_1 \sin \alpha z}{Z_1 \cos \alpha l + i W_2 \sin \alpha l}. \qquad \text{(III.5.9)}$$

The line's input impedance equals

$$Z_{in} = \frac{U_{n(z=l)}}{I_{n(z=l)}} = W_2 \frac{Z_1 \cos \alpha l + i W_2 \sin \alpha l}{W_2 \cos \alpha l + i Z_1 \sin \alpha l}. \qquad \text{(III.5.10)}$$

From formulas (III.5.8) and (III.5.10) we see that in the case of complete shielding of the line's inner conductor the expressions for voltage, current, and input impedance for the shielded line coincide with the corresponding expressions for the conventional twin (balanced) line.

Let us note that the results obtained do not change if the line is grounded at some point other than at the point of supply. We can prove this by considering the condition at (III.5.6), related to some point $z = z_1$ rather than to the point $z = l$.

The foregoing formulas were obtained for an arbitrary Z_1. It is apparent that they will remain valid when $Z_1 = 0$, which corresponds to the ideally grounded line, and when $Z_1 = \infty$, which corresponds to the ungrounded line.

So, from what has been discussed here, we can use the computational apparatus of the theory of two-wire balanced lines in the case of a completely shielded inner conductor of a shielded line.

The analysis made did not consider the conductivity to ground of the emf source and line load. When these conductivities are taken into consideration the analysis of the shielded line gets complicated and the computational apparatus of the theory of two-wire balanced lines would have to be discarded, even in the case of complete shielding of the inner conductor.

Example 5. Find the transmittance of a multi-conductor unbalanced line. Often used to feed unbalanced antennas are unbalanced transmission lines rather than cables. Here the solid shielded conductor is replaced by a series of conductors positioned around an inner conductor consisting of one, or of several conductors. The shielding conductors are grounded at the transmission line source and termination, the diagram of which is shown in Figure III.5.2.

In lines such as these, because the grounded shield is not solid, only some of the current flowing along the inner conductor has the shield as the

return. The rest of the current has the ground as its return. It is of interest to find the ratio of the current with the ground return to the total current flowing on the inner conductor. The higher this ratio, the greater the loss to ground.

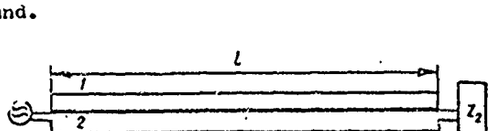

Figure III.5.2. Schematic diagram of an unbalanced line.

Solution. The current with the ground return is the in-phase component of the current (I_c). Accordingly, the problem is one of finding the ratio I_c/I_2. We shall call this ratio the shield transmittance.

In the case given

$$V_1 = 0. \tag{III.5.11}$$

From formula (III.3.8), and considering (III.5.11), we obtain $A_1 = B_1 = 0$. Equations at (III.3.9) can be transformed into

$$\left.\begin{aligned} I_1 &= -\frac{1}{W_{12}}(B_2\cos\alpha z + iA_2\sin\alpha z)\\ I_2 &= \frac{1}{W_2}(B_2\cos\alpha z + iA_2\sin\alpha z)\end{aligned}\right\}. \tag{III.5.12}$$

The in-phase component of the current equals

$$I_c = \frac{1}{2}(I_1 + I_2) = \frac{1}{2}\left(\frac{1}{W_2} - \frac{1}{W_{12}}\right)(B_2\cos\alpha z + iA_2\sin\alpha z). \tag{III.5.13}$$

The anti-phase component of the current equals

$$I_n = \frac{1}{2}(I_1 - I_2) = -\frac{1}{2}\left(\frac{1}{W_2} + \frac{1}{W_{12}}\right)(B_2\cos\alpha z + iA_2\sin\alpha z). \tag{III.5.14}$$

From formulas (III.5.12) and (III.5.13) the ratio of the in-phase current to the total current flowing on the inner conductor, that is, the transmittance, equals

$$\frac{I_c}{I_2} = \frac{W_{12} - W_2}{2W_{12}}. \tag{III.5.15}$$

The ratio of the in-phase component of the current to the anti-phase component, from formulas (III.5.13) and (III.5.14), equals

$$\frac{I_c}{I_n} = -\frac{W_{12} - W_2}{W_{12} + W_2}. \tag{III.5.16}$$

The ratio of the current flowing in the shield to the current in the inner conductor from formula (III.5.12), equals

$$I_1/I_2 = -W_2/W_{12}. \qquad \text{(XII.5.17)}$$

In the case of the line based on the data from examples 1 and 2, we obtain the following quantitative relationships

$$\frac{I_c}{I_s} = \frac{W_{12} - W_2}{2W_{12}} = \frac{236 - 217}{2 \cdot 236} = \frac{19}{472} = 0{,}04;$$

$$\frac{I_c}{I_n} = -\frac{W_{12} - W_2}{W_{12} + W_2} = -\frac{236 - 217}{236 + 217} = -\frac{19}{453} = -0{,}042;$$

$$\frac{I_1}{I_2} = -\frac{W_2}{W_{12}} = -\frac{217}{236} = -0{,}92.$$

Chapter IV

RADIO WAVE RADIATION

#IV.1. Maxwell's First Equation

Heinrich Hertz, in 1887, established experimentally that it was possible to radiate radio waves, that is, to radiate and propagate free electromagnetic fields in space. He established the theory of the elementary radiator of radio waves now known as the Hertz dipole. Hertz, in his investigations, relied on the writings of James Clark Maxwell, who, in 1873, published his "Treatise on Electricity and Magnetism." Maxwell's contribution was a mathematical theory for the electromagnetic field. He formulated the relationships between the strengths of electric and magnetic fields, and the densities of current and charge, in the form of a system of equations known as the Maxwell equations. It is from these equations, as well as from subsequent work done by Poynting, and other scientists, that the possibility of obtaining electromagnetic waves derives. Hertz provided the experimental confirmation.

The initiative and the practical solution to the problem of using radio waves for communications purposes belong to the Russian scientist Aleksandr Stepanovich Popov, who built the world's first radio communication line.

It was he who suggested and built transmitting and receiving antennas in the form of unbalanced dipoles. These are still widely used in various fields of radio engineering. The theory of these antennas is based directly on the work done by Maxwell, Hertz, and Poynting.

Maxwell's first equation expresses the dependence between the integral of the closed circuit magnetic intensity vector and the magnitude of the current penetrating this circuit.

Prior to Maxwell's treatise this dependence could have been formulated as follows.

The line integral of the magnetic intensity vector, H, for the closed circuit, L, equals the current, i, penetrating this circuit. Analytically, this law can be expressed through the formula

$$\oint_L H_l dl = i, \qquad \text{(IV.1.1)}$$

where

H_l is the component of the magnetic intensity vector tangent to the element dl;

dl is an element in the path of the closed circuit L;

i is the current penetrating the circuit.

Maxwell provided a generalized formulation of the law which associates magnetic field strength with the current, the while expressing it in differential form. The generalization provided by Maxwell reduces to the following.

Prior to Maxwell's formulation this law considered nothing other than the conduction current. Maxwell, in his formulation, took displacement currents into consideration. Using Faraday's writings as his base, Maxwell assumed that so far as the formation of the magnetic field was concerned the displacement current was equal in value to the conduction current.

An example of an electrical system in which the displacement current prevails is that of a condenser in an alternating current circuit. The alternating current can circulate between the plates of the condenser, even when they are separated by a perfect dielectric, or are in a vacuum, so no conduction current can form. Another example in which the displacement current plays a significant role is that of the circuit shown in Figure IV.1.1. Here the alternating emf is applied across the conductor and the conducting surface. The current flows over part of the path in the form of the conduction current, i, along the conductor and along the conducting surface, and over part of the path in the form of the displacement current, i_d, in the space between the conductor and the surface.

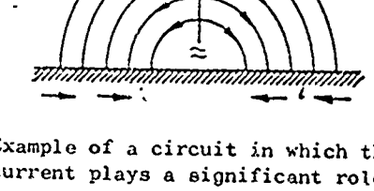

Figure IV.1.1. Example of a circuit in which the displacement current plays a significant role.

A - i_d.

Strictly speaking, the displacement current flowing in a circuit is alternating current. For example, even in an inductance coil, in which most of the current flows along the conductors in the form of conduction currents, some of the current always flows through the interturn capacitance in the form of a displacement current.

The displacement current is proportional to the product of the rate of change in electric field strength and the permittivity of the medium.

The displacement current density for an isotropic medium can be expressed analytically by the formula

$$j_d = \frac{\partial D}{\partial t} = \frac{\partial (\varepsilon E)}{\partial t} = \varepsilon \frac{\partial E}{\partial t}, \qquad \text{(IV.1.2)}$$

where

E is the electric field strength vector;

$D = \varepsilon E$ is the electric displacement vector;

j_d is the displacement current density;

ε is the dielectric constant of the medium.

From equation (IV.1.2), the unique current, the displacement current, the numerical value of which can be found through this equation, corresponds to the alternating electric field.

So, in accordance with Maxwell's opinions, formula (IV.1.1) is exceptional because it does not take displacement currents into consideration. In general form the ratio of H to i must be formulated as follows

$$\oint_L H_l dl = i + i_d, \qquad \text{(IV.1.3)}$$

where

i and i_d are the conduction and displacement currents penetrating circuit L.

Equation (IV.1.3), expressing Maxwell's first law, was derived for application to a circuit with finite dimensions.

Maxwell derived this equation in differential form for application to a point in space.

Let us transform equation (IV.1.3) so it will be applicable to an infinitely small circuit, to a point. Let us imagine a plane circuit encompassing an element of area ΔF, the spatial orientation of which is characterized by direction n, normal to its surface (fig. IV.1.2).

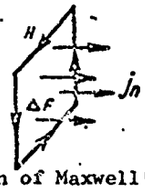

Figure IV.1.2. Derivation of Maxwell's first equation.

Let the normal components of the displacement current density vector and the conduction current density vector remain constant within the limits of area ΔF. Then the sum current flowing normal to area ΔF equals

$$i = (j_n + j_{n\,d})\Delta F, \qquad \text{(IV.1.4)}$$

where

j_n is the conduction current density for the current flowing in direction n;

$j_{n\,d}$ is the displacement current density for the current flowing in direction n.

The current densities j_n and $j_{n\,d}$ are associated with the electric field strength by the relationships

$$j_n = \gamma_v E_n, \qquad \text{(IV.1.5)}$$

$$j_{n\,d} = \frac{\partial D_n}{\partial t} = \varepsilon \frac{\partial E_n}{\partial t}, \qquad \text{(IV.1.6)}$$

where

γ_v is conductivity, measured in mhos per meter (mhos/m).

Substituting the value for $j_{n\,d}$ from formula (IV.1.6) in formula (IV.1.4),

$$I = \left(j_n + \frac{\partial D_n}{\partial t}\right) \Delta F. \qquad \text{(IV.1.7)}$$

In accordance with (IV.1.3), we have

$$\oint_L H_l dl = \left(j_n + \frac{\partial D_n}{\partial t}\right) \Delta F. \qquad \text{(IV.1.8)}$$

Dividing the right and left-hand sides of equation (IV.1.8) by ΔF and assuming that ΔF tends to zero,

$$\lim_{\Delta F \to 0} \frac{\oint_L H_l dl}{\Delta F} = j_n + \frac{\partial D_n}{\partial t}. \qquad \text{(IV.1.9)}$$

The expression shown in the left-hand side of equation (IV.1.9) is called the component of curl H in direction n, normal to the plane in which circuit L is located, and designated $\mathrm{rot}_n H$.

Accordingly,

$$\mathrm{rot}_n H = j_n + \frac{\partial D_n}{\partial t}. \qquad \text{(IV.1.10)}$$

Equation (IV.1.10) was composed as applicable to arbitrary direction n.

Shifting to a rectangular system of coordinates, x, y, z, we obtain the following three equations

$$\left.\begin{aligned} \mathrm{rot}_x H &= j_x + \frac{\partial D_x}{\partial t} \\ \mathrm{rot}_y H &= j_y + \frac{\partial D_y}{\partial t} \\ \mathrm{rot}_z H &= j_z + \frac{\partial D_z}{\partial t} \end{aligned}\right\}. \qquad \text{(IV.1.11)}$$

where $\mathrm{rot}_x H$, $\mathrm{rot}_y H$, $\mathrm{rot}_z H$, j_x, j_y, j_z, D_x, D_y, and D_z are the components of rot H and of vectors j and D on the x, y, and z axes.

The relationships expressed by the system of equations at (IV.1.11) can be written in vector form as

$$\mathrm{rot}\, H = \mathbf{j} + \frac{\partial \mathbf{D}}{\partial t}. \qquad \text{(IV.1.12)}$$

The equality at (IV.1.12) is Maxwell's first law.

We know from vector analysis that the components of the curl of some vector A in the rectangular system of coordinates can be determined as follows

$$\left.\begin{aligned} \mathrm{rot}_x A &= \frac{\partial A_z}{\partial y} - \frac{\partial A_y}{\partial z} \\ \mathrm{rot}_y A &= \frac{\partial A_x}{\partial z} - \frac{\partial A_z}{\partial x} \\ \mathrm{rot}_z A &= \frac{\partial A_y}{\partial x} - \frac{\partial A_x}{\partial y} \end{aligned}\right\} \qquad \text{(IV.1.13)}$$

Substituting equation (IV.1.13) in (IV.1.11), we obtain the following differential equations, which associate the components of vectors H, j, and D

$$\left.\begin{aligned}\frac{\partial H_z}{\partial y}-\frac{\partial H_y}{\partial z}&=j_x+\frac{\partial D_x}{\partial t}\\ \frac{\partial H_x}{\partial z}-\frac{\partial H_z}{\partial x}&=j_y+\frac{\partial D_y}{\partial t}\\ \frac{\partial H_y}{\partial x}-\frac{\partial H_x}{\partial y}&=j_z+\frac{\partial D_z}{\partial t}\end{aligned}\right\} \qquad \text{(IV.1.14)}$$

§IV.2. Maxwell's Second Equation

Maxwell's second equation is the formulation of Faraday's law, which associates the changing magnetic field and the changing electric field induced by it.

Faraday's law can be written

$$\oint_L E_l dl = -\frac{\partial \Phi}{\partial t}, \qquad \text{(IV.2.1)}$$

where

E_l is the component of the electric field strength vector tangent to element dl of circuit L, which encloses area ΔF;

Φ is the magnetic flux which penetrates circuit L;

$\oint_L E_l dl$ is the emf throughout the closed circuit L, induced by the changing magnetic field penetrating this circuit.

Equation (IV.2.1) can be formulated as follows. The emf across the closed circuit equals the rate of change in the magnetic flux penetrating this circuit.

Faraday derived this law during experiments with conductors placed in a changing magnetic field.

Maxwell's second equation expresses the relationship at (IV.2.1) in differential form. To obtain the second equation we will write (IV.2.1) so it will be applicable to plane area ΔF, the orientation of which in space is in some direction n, perpendicular to its surface (fig. IV.2.1).

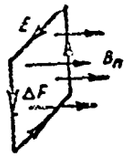

Figure IV.2.1. Derivation of Maxwell's second equation.

The magnetic flux penetrating area ΔF can be expressed as

$$\Delta\Phi = B_n \Delta F \qquad \text{(IV.2.2)}$$

where

B_n is the normal component of the magnetic induction vector, B, assumed constant within the limits of area ΔF.

$$B = \mu H,$$

where

μ is the magnetic conductivity of the medium.

(IV.2.1) takes the form

$$\oint_L E_l dl = -\frac{\partial B_n}{\partial t} \Delta F. \qquad \text{(IV.2.3)}$$

after the expression for Φ from equation (IV.2.2) is substituted in it.

Dividing both sides of (IV.2.3) by ΔF, and assuming that $\Delta F \to 0$,

$$\lim_{\Delta F \to 0} \frac{\oint_L E_l dl}{\Delta F} = -\frac{\partial B_n}{\partial t}. \qquad \text{(IV.2.4)}$$

The left-hand side of (IV.2.4) is the component of curl E in direction n. So (IV.2.4) can be written as

$$\mathrm{rot}_n E = -\frac{\partial B_n}{\partial t}. \qquad \text{(IV.2.5)}$$

Shifting to the rectangular system of coordinates x, y, z, we obtain these three equations

$$\left.\begin{aligned} \mathrm{rot}_x E &= -\frac{\partial B_x}{\partial t} \\ \mathrm{rot}_y E &= -\frac{\partial B_y}{\partial t} \\ \mathrm{rot}_z E &= -\frac{\partial B_z}{\partial t} \end{aligned}\right\}. \qquad \text{(IV.2.6)}$$

(IV.2.6) can be formulated in vector form as

$$\mathrm{rot}\ E = -\partial B/\partial t \qquad \text{(IV.2.7)}$$

(IV.2.7) is called Maxwell's second law. Expressing in (IV.2.6) the component of the curl in terms of the component of vector E, in accordance with (IV.1.13),

$$\left.\begin{aligned} \frac{\partial E_z}{\partial y} - \frac{\partial E_y}{\partial z} &= -\frac{\partial B_x}{\partial t} \\ \frac{\partial E_x}{\partial z} - \frac{\partial E_z}{\partial x} &= -\frac{\partial B_y}{\partial t} \\ \frac{\partial E_y}{\partial x} - \frac{\partial E_x}{\partial y} &= -\frac{\partial B_z}{\partial t} \end{aligned}\right\}. \qquad \text{(IV.2.8)}$$

#IV.3. Maxwell's System of Equations

The following are also a part of Maxwell's system of equations

$$\operatorname{div} D = \rho, \tag{IV.3.1}$$

$$\operatorname{div} B = 0, \tag{IV.3.2}$$

where

ρ is the electric volume density, that is, the charge incoming per unit volume.

The divergence of some vector A at the point specified is a limit to which tends the ratio of the flux of vector A over the surface (ΔS) surrounding this point, to the magnitude of the volume (ΔV) limited by this surface when ΔV tends to zero

$$\operatorname{div} A = \lim_{\Delta V \to 0} \frac{\oint_{\Delta S} A_n dS}{\Delta V}.$$

In the rectangular system of coordinates the divergence of vector A equals

$$\operatorname{div} A = \frac{\partial A_x}{\partial x} + \frac{\partial A_y}{\partial y} + \frac{\partial A_z}{\partial z}.$$

Formula (IV.3.2) demonstrates that the flux of the magnetic induction vector (B) has no outlets; the magnetic field force lines are closed. Consequently, the total flux of the magnetic induction vector over any closed surface always equals zero.

Similarly, formula (IV.3.1) demonstrates that in those expanses in space which have no charges ($\rho = 0$), the flux of the displacement vector (D) over any closed surface too equals zero. If there are distributed charges in space every point in space will become a source of the displacement vector flux, that is every point in space will become the origin of new lines of force. And the displacement vector flux, equated to unit volume, equals the charge density (ρ).

So, we have the following system of equations, which is the basis of classical electrodynamics and, in particular, the basis of the theory of radiating systems

$$\left.\begin{aligned}
&\operatorname{rot} H = j + \frac{\partial D}{\partial t} && (a)\\
&\operatorname{rot} E = -\frac{\partial B}{\partial t} && (b)\\
&\operatorname{div} D = \rho && (c)\\
&\operatorname{div} B = 0 && (d)\\
&D = \varepsilon E && (e)\\
&B = \mu H && (f)\\
&j = \gamma_e E && (g)
\end{aligned}\right\} \tag{IV.3.3}$$

#IV.4. Poynting's Theorem

Emerging directly from Maxwell's equations is an equation which characterizes the energy balance in an electromagnetic field and points to the possibility of radiating electromagnetic energy and propagating it in space. Let us derive this equation.

Making a scalar multiplication of both sides of the equality at (IV.3.3a) by E, and both sides of the equality at (IV.3.3b) by H, and subtracting the first product from the second, we obtain

$$(\mathrm{H}\,\mathrm{rot}\,\mathrm{E}) - (\mathrm{E}\,\mathrm{rot}\,\mathrm{H}) = -\left(\mathrm{H}\frac{\partial \mathrm{B}}{\partial t}\right) - \left(\mathrm{E}\frac{\partial \mathrm{D}}{\partial t}\right) - (\mathrm{EJ}), \qquad \text{(IV.4.1)}$$

From vector analysis data

$$(\mathrm{H}\,\mathrm{rot}\,\mathrm{E}) - (\mathrm{E}\,\mathrm{rot}\,\mathrm{H}) = \mathrm{div}\,[\mathrm{EH}].$$

Let us transform the terms in the right-hand side of the equality at (IV.4.1):

$$\left(\mathrm{H}\frac{\partial \mathrm{B}}{\partial t}\right) = \left(\mathrm{H}\frac{\partial}{\partial t}(\mu \mathrm{H})\right) = \frac{\partial}{\partial t}\left(\frac{\mu \mathrm{H}^2}{2}\right);$$

$$\left(\mathrm{E}\frac{\partial \mathrm{D}}{\partial t}\right) = \left(\mathrm{E}\frac{\partial}{\partial t}(\varepsilon \mathrm{E})\right) = \frac{\partial}{\partial t}\left(\frac{\varepsilon \mathrm{E}^2}{2}\right);$$

$$(\mathrm{EJ}) = \gamma_v(\mathrm{EE}) = \gamma_v E^2.$$

Equation (IV.4.1) takes this form after the transformations indicated

$$\mathrm{div}\,[\mathrm{EH}] = -\frac{\partial}{\partial t}\left(\frac{\varepsilon E^2}{2} + \frac{\mu H^2}{2}\right) - \gamma_v E^2. \qquad \text{(IV.4.2)}$$

Integrating both sides of (IV.4.2) with respect to some volume V,

$$\int_V \mathrm{div}\,[\mathrm{EH}]\,dV = -\frac{\partial}{\partial t}\int_V \left(\frac{\varepsilon E^2}{2} + \frac{\mu H^2}{2}\right)dV - \int_V \gamma_v E^2 dV. \qquad \text{(IV.4.3)}$$

In accordance with Gauss' theorem, the volume integral from the divergence of a vector for the volume V can be replaced by the surface integral for this same vector for surface F limiting this volume.

Considering Gauss' theorem then, and transposing the terms in equation (IV.4.3),

$$-\frac{\partial}{\partial t}\int_V \left(\frac{\varepsilon E^2}{2} + \frac{\mu H^2}{2}\right)dV = \int_F [\mathrm{EH}]_n dF + \int_V \gamma_v E^2 dV, \qquad \text{(IV.4.4)}$$

where

dF is an element of closed surface F, limiting volume V.

The subscript n means that the component of the [EH] vector normal to the element of surface dF must be taken.

This is the Poynting equation.

Let us explain the physical sense of this equation.

Here $\varepsilon E^2/2$ is the electric field energy in unit volume;

$\mu H^2/2$ is the magnetic field energy in unit volume;

$(\varepsilon E^2/2 + \mu H^2/2)$ is the total energy of the electromagnetic field in unit volume.

Accordingly, $W = \int_V (\varepsilon E^2/2 + \mu H^2/2) dV$ is the energy in some volume V, of the electromagnetic field.

The derivative $\partial W/dt$ [the left-hand side of equation (IV.4.4)] expresses the reduction in the supply of electromagnetic energy in volume V per unit time, that is, the consumption of electromagnetic energy in this volume per unit time. The expression standing in the right-hand side of equation (IV.4.4) shows that the energy being consumed consists of two summands.

The summand $\int_V \gamma_v E^2 dV$ is the energy dissipated as a result of the conductivity of the medium (γ_v). This energy is dissipated within volume V itself, becoming Joule heat.

The summand $\int_F [EH]_n dF$ is the flux of the [EH] vector along surface F limiting volume V. The S=[EH] vector is called the Poynting vector.

So, from what has been said, $\int_F [EH]_n dF$ is the energy leaving volume V, that is, the energy being put out (radiated) by the source of the electromagnetic field into the surrounding space.

Poynting's theorem demonstrates that electromagnetic energy can be propagated in space and that it is possible, in principle, to create that source of an electromagnetic field, a considerable part of the energy from which will be expended in radiation. In radio engineering installations this source is the generator feeding the antenna.

The simplest antenna is the Hertz dipole, the theory of which will be discussed below.

#IV.5. Vector and Scalar Potentials. Electromagnetic Field Velocity.

Maxwell's equations give the dependence between E, H, j, ρ and the parameters of the medium ε, μ and γ_v, in general form. As a practical matter, it is often necessary to solve problems in which the distribution of the current and charge densitities, as well as medium parameters, are given, and what must be found will be E and H. In cases such as these it is convenient to find E and H by introducing new magnitudes, specifically the vector potential A, and the scalar potential, φ.

From vector analysis it is known that the divergence in the curl of any vector equals zero, so, on the basis of (IV.3.3d), it is convenient to represent B as the curl of some vector A, called the vector potential

$$B = \text{rot } A \quad \text{or} \quad H = 1/\mu \text{ rot } A. \qquad \text{(IV.5.1)}$$

Substituting equation (IV.5.1) in (IV.3.3b), and replacing B by μH,

$$\operatorname{rot} E = -\frac{\partial}{\partial t}(\operatorname{rot} A),$$

from whence

$$\operatorname{rot}\left[-\left(E+\frac{\partial A}{\partial t}\right)\right]=0.$$

According to the data from vector analysis the curl of the gradient of any scalar magnitude equals zero, with the result that the $-(E + \partial A/dt)$ vector can be considered to be the gradient of some scalar function called the scalar potential

$$-\left(E+\frac{\partial A}{\partial t}\right)=\operatorname{grad}\varphi, \qquad \text{(IV.5.2)}$$

from whence

$$E=-\left(\frac{\partial A}{\partial t}+\operatorname{grad}\varphi\right). \qquad \text{(IV.5.3)}$$

By the gradient of a scalar at a specified point we mean a vector in the direction of maximum change in this scalar, numerically equal to the scalar's increase per unit length in this direction. In the rectangular system of coordinates, by designating the unit vectors along the x, y, and z axes as i, j, and k, the expression for the gradient of scalar φ can be written

$$\operatorname{grad}\varphi=\mathrm{i}\frac{\partial\varphi}{\partial x}+\mathrm{j}\frac{\partial\varphi}{\partial y}+\mathrm{k}\frac{\partial\varphi}{\partial z}.$$

Let us find A and φ. Considering the fact that $D = \varepsilon E$, substituting the expressions for H and E from formulas (IV.5.1) and (IV.5.3) in formula (IV.3.3a), and taking it that there are no losses in the medium ($\gamma_v = 0$),

$$\operatorname{rot}\operatorname{rot} A=\mu\mathrm{j}-\varepsilon\mu\operatorname{grad}\frac{\partial\varphi}{\partial t}-\varepsilon\mu\frac{\partial^2 A}{\partial t^2}. \qquad \text{(IV.5.4)}$$

It is known that

$$\operatorname{rot}\operatorname{rot} A=\operatorname{grad}\operatorname{div} A-\nabla^2 A,$$

where

$\nabla^2 A$ can be expressed in the following manner in the rectangular system:

$$\nabla^2 A=\frac{\partial^2 A}{\partial x^2}+\frac{\partial^2 A}{\partial y^2}+\frac{\partial^2 A}{\partial z^2}. \qquad \text{(IV.5.5)}$$

Substituting this expression in formula (IV.5.4), and converting,

$$-\operatorname{grad}\left(\operatorname{div} A+\varepsilon\mu\frac{\partial\varphi}{\partial t}\right)+\nabla^2 A-\varepsilon\mu\frac{\partial^2 A}{\partial t^2}=-\mu\mathrm{j}. \qquad \text{(IV.5.6)}$$

Let us impose the additional condition

$$\operatorname{div} A+\varepsilon\mu\frac{\partial\varphi}{\partial t}=0. \qquad \text{(IV.5.7)}$$

Then equation (IV.5.6) takes the form

$$\nabla^2 A - \varepsilon\mu \frac{\partial^2 A}{\partial t^2} = -\mu j. \qquad \text{(IV.5.8)}$$

Substituting the expression $D = \varepsilon E$ in (IV.3.3c), replacing the expression for E from formula (IV.5.3), and considering the condition at (IV.5.7),

$$\nabla^2 \varphi - \varepsilon\mu \frac{\partial^2 \varphi}{\partial t^2} = -\frac{1}{\varepsilon}\rho. \qquad \text{(IV.5.9)}$$

Equations (IV.5.8) and (IV.5.9) define the wave-like process in space and are therefore called wave equations.

These equations have the following solutions

$$A = \frac{\mu}{4\pi}\int_V \frac{j\left(t - \frac{r}{v}\right) dV}{r}, \qquad \text{(IV.5.10)}$$

$$\varphi = \frac{1}{4\pi\varepsilon}\int_V \frac{\rho\left(t - \frac{r}{v}\right) dV}{r}, \qquad \text{(IV.5.11)}$$

where

dV is an element of the volume in which current density j and charge density ρ are given;

is the distance from the element of the volume to a point at which A and φ are determined;

v is the velocity at which the electromagnetic oscillations are propagated,

$$v = 1/\sqrt{\varepsilon\mu}. \qquad \text{(IV.5.12)}$$

The symbol $(t - r/v)$ means that the values of A and φ (and consequently of E and H) at time t can be defined by the values of j and ρ occurring at time $t - r/v$. What this signifies is that electromagnetic perturbations are propagated at a velocity equal to v.

In free space, and approximately in air

$$\varepsilon = \varepsilon_0 \approx 1/4\pi \cdot 9 \cdot 10^9 \text{ (farads/meter)}, \quad \mu = \mu_0 = 4\pi/10^7 \text{ (henries/meter)}$$

and the electromagnetic perturbation propagation rate equals

$$v = c = 1/\sqrt{\varepsilon_0\mu_0} = 2.998 \cdot 10^8 \approx 3 \cdot 10^8 \text{ (meters/second)}.$$

By using the relationships at (IV.5.1), (IV.5.3), ((V.5.10), and (IV.5.11) we can find E and H if the distribution of the conduction current density j, and the charge density ρ are known. These equations can be used to calculate fields around antennas for which it is assumed the current and charge distributions are known.

When computing the fields around line conductors in a non-conducting medium the fact that in this case the conduction and charge currents are only concentrated along the axes of the conductors should be taken into consideration, and that correspondingly the volume integrals in expressions for A and φ can be replaced by line integrals

$$A = \frac{\mu}{4\pi}\int_L \frac{I\left(t-\frac{r}{v}\right)}{r}dl, \qquad \text{(IV.5.13)}$$

$$\varphi = \frac{1}{4\pi\varepsilon}\int_L \frac{\sigma\left(t-\frac{r}{v}\right)}{r}dl, \qquad \text{(IV.5.14)}$$

where

i is the conduction current flowing in the conductor;

σ is the linear charge density.

But if it is the harmonic oscillations of the linear current that are under discussion then $i(t - r/v) = Ie^{i(\omega t-\alpha r)}$; $\sigma(t - r/v) = \sigma_0 e^{i(\omega t-\alpha r)}$ and the expressions for A and φ become

$$A = \frac{\mu}{4\pi}\int_L \frac{I e^{i(\omega t-\alpha r)}}{r}dl, \qquad \text{(IV.5.15)}$$

$$\varphi = \frac{1}{4\pi\varepsilon}\int_L \frac{\sigma_0 e^{i(\omega t-\alpha r)}}{r}dl, \qquad \text{(IV.5.16)}$$

where

α is the conduction current flowing in the conductor;

$\alpha = \omega/v = 2\pi f/v = 2\pi/\lambda$;

f is the frequency.

There is a definite physical sense to the above accepted condition at (IV.5.7).

Substituting the expressions for A and φ from formulas (IV.5.10) and (IV.5.11) in formula (IV.5.7),

$$\frac{\mu}{4\pi}\operatorname{div}\int_V \frac{j\left(t-\frac{r}{v}\right)}{r}dV + \frac{\mu}{4\pi}\frac{\partial}{\partial t}\int_V \frac{\rho\left(t-\frac{r}{v}\right)}{r}dV = 0.$$

This equation will reduce to

$$\frac{\mu}{4\pi}\int_V \left(\operatorname{div} j + \frac{\partial \rho}{\partial t}\right)\frac{dV}{r} = 0,$$

from whence

$$\operatorname{div} j + \frac{\partial \rho}{\partial t} = 0. \qquad \text{(IV.5.17)}$$

The relationship at (IV.5.17) is the formulation of the law for the conservation of an amount of electricity in differential form (the equation of continuity).

Substituting the expression for ρ from formula (IV.3.1) in formula (IV.5.17),

$$\operatorname{div} j + \operatorname{div}\left(\frac{\partial D}{\partial t}\right) = \operatorname{div}\left(j + \frac{\partial D}{\partial t}\right) = 0. \qquad \text{(IV.5.18)}$$

Formula (IV.5.18) demonstrates that the sum of the conduction currents and the displacement currents outgoing from a unit of volume equals zero. For the case of current flowing along a conductor in space which has no conductivity, formula (IV.5.17) becomes

$$\frac{\partial I}{\partial z} + \frac{\partial \sigma}{\partial t} = 0, \qquad \text{(IV.5.19)}$$

where

I is the current flowing along a conductor oriented along the z axis;

σ is the linear charge density on the conductor.

#IV.6. Radiation of Electromagnetic Waves

The possibility of radiating and propagating electromagnetic energy in space without conductors follows, in essence, directly from the theses propounded by Faraday and Maxwell, in accordance with which electric current can circulate in a dielectric and in free space in the form of a displacement current. And so far as the formation of a magnetic field is concerned, the displacement current exhibits the same physical properties as does the conduction current. Faraday and Maxwell, in their assumptions, assigned the properties of a conductor, a conductor of the displacement current, so to speak, to the dielectric and to free space. The propagation of the displacement current in space is associated with the propagation of electromagnetic energy because the field current corresponding to it is the electromagnetic energy carrier. Hence, any electrical circuit which can create a displacement current in space can be used as a radiator of electromagnetic energy.

Suppose we take a circuit consisting of a condenser supplied by an alternating emf source (fig. IV.6.1). A displacement current will circulate in the space between the plates. Since the space surrounding the condenser can conduct the displacement current, it is only natural that the latter should branch out into that space, just as would the conduction current if the condenser were located in space possessing conductivity. The process of this branching of displacement currents, and consequently of electromagnetic energy, into the space surrounding the condenser is, from the point of view of Maxwell's theory, as natural a process as is the branching of energy in a conductor connected to some source of emf.

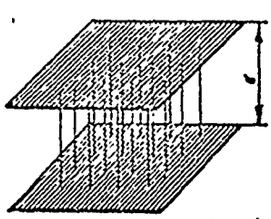

Figure IV.6.1. Explanation of the radiation process.

The principle that it is possible for electromagnetic energy to branch (radiate) into space can be proven by Poynting's theorem, which is the direct consequence of Maxwell's equations.

Keep in mind that while in principle any circuit which can create displacement currents can be a source, or as usage has it a radiator, of electromagnetic waves, in practice the circuits used as radiators of electromagnetic waves (antennas) meet predetermined requirements. A basic requirement imposed on the practical radiator is that the energy involved be a minimum, that is, that the energy not be radiated into surrounding space (minimum reactive energy). The greater the coupled (reactive)energy, the greater the loss, and the narrower the antenna passband.

The radiator shown in Figure IV.6.1 in the form of a condenser made of two parallel plates is an example of an unsuccessful circuit, in the sense of the foregoing, for in this circuit the coupled portion of the energy is relatively great and much of the energy is concentrated in the space between the plates.

The reason is that the space between the plates of the condenser is highly conductive so far as displacement currents are concerned.

A relative reduction in the coupled part of the energy can be obtained by turning the condenser plates and positioning them as shown in Figure IV.6.2.

One variant of the circuit permitting intensive radiation for a comparatively small part of the coupled energy is the one shown in Figure IV.6.3, in which the plates have been replaced by thin conductors with spheres on their ends. Heinrich Hertz was the first to devise this circuit, and the radiator made in accordance with the circuit shown in Figure IV.6.3 is known as the Hertz dipole.

Figure IV.6.2. Explanation of the radiation process.

Figure IV.6.3. The Hertz dipole.

#IV.7. Hertz' Experiments

The purpose of Hertz' experiments was to verify experimentally the probability that the electromagnetic waves anticipated by Maxwell's theory did in fact exist. Hertz conducted a series of extremely complicated experiments. We shall limit ourselves here to just a brief description of these experiments.

Hertz used a dipole, a conductor with a Ruhmkorff coil inserted in the middle of its spark gap, to excite electromagnetic waves. Metallic spheres were connected to the ends of the conductor (fig. IV.6.3). When the sparks shoot the spark gap in the dipole damped oscillations, the fundamental frequency of which is determined by the natural frequency at which the dipole oscillates, are excited.

Considering the displacement current density proportional to the rate of change in the electric field strength

$$j_d = \epsilon \, \partial E/dt \ .$$

Hertz tried to obtain the shortest possible waves. He tried to increase the natural frequency by reducing the dipole dimensions. Hertz began his first experiments with dipoles about 1 meter long and obtained waves several meters long.

Later on Hertz experimented with dipoles a few decimeters long and obtained waves some 60 cm long.

The loop with the spark gap served at the field strength indicator.

The maximum possible length of the spark was proportional to the field strength. Hertz used the simple apparatus described to prove that the electromagnetic field around the dipole matches the theoretical data obtained by using Maxwell's equations.

Hertz used this same apparatus to prove experimentally that it was possible to reflect electromagnetic waves and he measured the coefficients of reflection from the surfaces of certain materials.

Hertz, using the analogy of optics in order to obtain directional radiation, used a parabolic mirror with the dipole located in the focal plane of the mirror.

Hertz also made a theoretical analysis of the functioning of the infinitesimal, or elementary, dipole, and this was in addition to the experimental verification he undertook of the general conclusions of the theory of the radiation of electromagnetic waves.

#IV.8. The Theory of the Elementary Dipole

(a) Expressions for electric field strength and the vector potential of the elementary dipole

Hertz, in his mathematical analysis of radiators used in the experiments, considered them as elementary dipoles, that is as extremely short conductors compared with the wavelength, along the entire length of which the current has the same amplitude and phase. It is impossible to have a dipole of finite dimensions with unchanged current amplitude and phase over its entire length, so the elementary dipole is simply an idealized radiating system convenient to use for analysis. However, the dipole used by Hertz in his experiments

(fig. IV.6.3) is an extremely successful practical approximation of this idealized radiator. Because the spheres on the ends of the dipole have a high capacitance, there is little change in current amplitude along the length of the conductor.

Equations (IV.5.3) and (IV.5.1) can be used to find the strengths of the electric and magnetic fields around the elementary dipole.

If it is assumed that oscillations are harmonic, we can readily express φ in terms of A. In point of fact, in the case of harmonic oscillations $\partial\varphi/\partial t = i\omega\varphi$. Substituting this relationship in equation (V.5.7),

$$\varphi = i\frac{1}{\varepsilon\mu\omega}\operatorname{div} A. \qquad \text{(IV.8.1)}$$

Substituting equation (IV.8.1) in (IV.5.3), and taking it that in the case of harmonic oscillations $\partial A/\partial t = i\omega A$,

$$E = -i\omega A - i\frac{1}{\varepsilon\mu\omega}\operatorname{grad}\operatorname{div} A. \qquad \text{(IV.8.2)}$$

This equation, in conjunction with equation (IV.5.1) makes it possible to compute all the components of an electromagnetic field, if the vector potential A is known. For linear currents A can be computed through formula (IV.5.15).

In the case specified, and according to the definition of an elementary dipole, I remains fixed over the entire length l, and can be taken from under the integral sign. Moreover, assuming that $l \ll r$, the terms dependent on r can also be taken from under the integral sign. Accordingly,

$$A = \frac{\mu}{4\pi}\frac{Ie^{i(\omega t - \varepsilon r)}}{r}l. \qquad \text{(IV.8.3)}$$

(b) Components of the dipole electric and magnetic field strength vectors in a rectangular system of coordinates

Using formulas (IV.5.1), (IV.8.2) and (IV.8.3), we can determine the E and H components along the three coordinate axes. Let us select the coordinate system such that the z axis coincides with the dipole axis, and the origin with the center of the dipole. In this system the A vector has no components on the x and y axes,

$$A_x = A_y = 0, \qquad \text{(IV.8.4)}$$

$$A_z = A. \qquad \text{(IV.8.5)}$$

Based on formulas (IV.8.2) and (IV.8.3), we have these expressions for the components of the E and H vectors

$$E_x = -i\omega A_x - i\frac{1}{\varepsilon\mu\omega}\operatorname{grad}_x \operatorname{div} A = -i\frac{1}{\varepsilon\mu\omega}\frac{\partial^2 A}{\partial x \partial z}; \quad \text{(IV.8.6)}$$

$$E_y = -i\omega A_y - i\frac{1}{\varepsilon\mu\omega}\operatorname{grad}_y \operatorname{div} A = -i\frac{1}{\varepsilon\mu\omega}\frac{\partial^2 A}{\partial y \partial z}; \quad \text{(IV.8.7)}$$

$$E_z = -i\omega A_z - i\frac{1}{\varepsilon\mu\omega}\operatorname{grad}_z \operatorname{div} A = -i\omega A - i\frac{1}{\varepsilon\mu\omega}\frac{\partial^2 A}{\partial z^2}. \quad \text{(IV.8.8)}$$

Similarly, taking formulas (IV.5.1) and (IV.1.13) into consideration,

$$H_x = \frac{1}{\mu}\operatorname{rot}_x A = \frac{1}{\mu}\frac{\partial A}{\partial y}; \quad \text{(IV.8.9)}$$

$$H_y = \frac{1}{\mu}\operatorname{rot}_y A = -\frac{1}{\mu}\frac{\partial A}{\partial x}; \quad \text{(IV.8.10)}$$

$$H_z = \frac{1}{\mu}\operatorname{rot}_z A = 0. \quad \text{(IV.8.11)}$$

Note that formulas (IV.8 6) through (IV.8.11) are correct for any linear dipole oriented along the x axis.

Substituting the expression for A from formula (IV.8.3) in formulas (IV.8.6) through (IV.8.10), and taking it that

$$r = \sqrt{x^2 + y^2 + z^2}, \quad \text{(IV.8.12)}$$

$$\alpha = \frac{\omega}{v} = \omega\sqrt{\varepsilon\mu},$$

we obtain

$$\left.\begin{aligned} E_x &= \frac{1}{4\pi\varepsilon}\frac{xz}{r^5}\frac{Il}{\omega}\left(-i\frac{3}{r^3} + \frac{3\alpha}{r^2} + i\frac{\alpha^2}{r}\right)e^{i(\omega t - \alpha r)} \\ E_y &= \frac{1}{4\pi\varepsilon}\frac{yz}{r^5}\frac{Il}{\omega}\left(-i\frac{3}{r^3} + \frac{3\alpha}{r^2} + i\frac{\alpha^2}{r}\right)e^{i(\omega t - \alpha r)} \\ E_z &= \frac{1}{4\pi\varepsilon}\frac{1}{r^3}\frac{Il}{\omega}\left[-i\frac{3z^2 - r^2}{r^3} + \frac{(3z^2 - r^2)\alpha}{r^2} + \right. \\ &\qquad \left. + i\frac{(z^2 - r^2)\alpha^2}{r}\right]e^{i(\omega t - \alpha r)} \end{aligned}\right\}; \quad \text{(IV.8.13)}$$

$$\left.\begin{aligned} H_x &= -\frac{1}{4\pi}\frac{y}{r}Il\left(\frac{1}{r^2} + i\frac{\alpha}{r}\right)e^{i(\omega t - \alpha r)} \\ H_y &= \frac{1}{4\pi}\frac{x}{r}Il\left(\frac{1}{r^2} + i\frac{\alpha}{r}\right)e^{i(\omega t - \alpha r)} \\ H_z &= 0. \end{aligned}\right\} \quad \text{(IV.8.14)}$$

In formulas (IV.8.13) and (IV.8.14) all lengths are in meters, current is in amperes, electric field strength in volts per meter, and magnetic field strength in amperes per meter.

So, knowing the current and the dielectric constant for the medium, we can determine the strengths of the electric and magnetic fields at any point around a dipole, so long as the condition $r \gg 1$ is satisfied.

(c) Components of the electric and magnetic field strength vectors in spherical and cylindrical systems of coordination

In view of the axial symmetry of the elementary dipole, it is extremely convenient to use formulas which define the field in spherical or cylindrical systems of coordinates.

Components E_r, E_θ, E_φ and H_r, H_θ, H_φ (fig. IV.8.1)[1] characterize the electric and magnetic field strengths when the spherical system is used, while E_R, E_φ, E_z and H_R, H_φ, H_z (fig. IV.8.2) do the same when the cylindrical system is used.

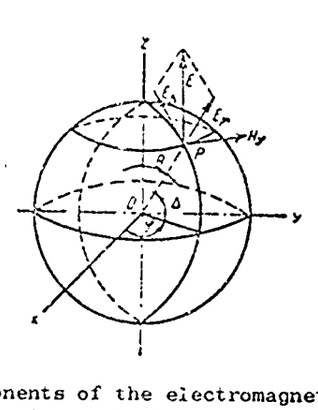

Figure IV.8.1. Components of the electromagnetic field of a dipole in a spherical system of coordinates.

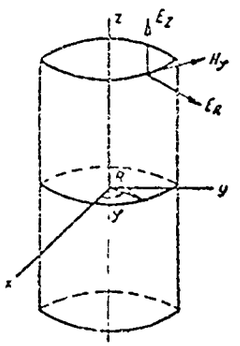

Figure IV.8.2. Components of the electromagnetic field of a dipole in a cylindrical system of coordinates.

Determination of the relationship between the components of the field strengths in the rectangular and spherical systems of coordinates is very much simplified by the introduction of the component E_R, directed perpendicular to the z axis (fig. IV.8.2). Nor is it difficult to prove that

1. Figures IV.8.1 and IV.8.2 only show those components of the E and H vectors applicable to the dipole. The component $E_\Delta = -E_\theta$ is shown in Figure IV.8.1.

$$\left.\begin{aligned} E_R &= E_x\cos\varphi + E_y\sin\varphi \\ E_r &= E_R\sin\theta + E_z\cos\theta \\ E_\theta &= E_R\cos\theta - E_z\sin\theta \\ E_\varphi &= -E_x\sin\varphi + E_y\cos\varphi \end{aligned}\right\}; \qquad \text{(IV.8.15)}$$

$$\cos\theta = \frac{z}{r};\ \sin\theta = \frac{R}{r};$$

$$\cos\varphi = \frac{x}{R};\ \sin\varphi = \frac{y}{R}.$$

Substituting the expressions for E_x, E_y, E_z and E_R in formula (IV.8.15) and converting, we obtain the following expressions for the E and H components in a spherical system of coordinates

$$\left.\begin{aligned} E_r &= \frac{1}{4\pi\varepsilon}\frac{2Il}{\omega}\cos\theta\left(-i\frac{1}{r^2}+\frac{\alpha}{r^2}\right)e^{i(\omega t-\alpha r)} \\ E_\theta &= \frac{1}{4\pi\varepsilon}\frac{Il}{\omega}\sin\theta\left(-i\frac{1}{r^2}+\frac{\alpha}{r^2}+i\frac{\alpha^2}{r}\right)e^{i(\omega t-\alpha r)} \\ H_\varphi &= \frac{1}{4\pi}Il\sin\theta\left(\frac{1}{r^2}+i\frac{\alpha}{r}\right)e^{i(\omega t-\alpha r)} \\ E_\varphi &= H_r = H_\theta = 0 \end{aligned}\right\}, \qquad \text{(IV.8.16)}$$

The E and H vectors are mutually perpendicular, as will be seen from (IV.8.16).

The expressions for the components of the E and H vectors in a cylindrical system of coordinates are in the form

$$\left.\begin{aligned} E_R &= \frac{1}{4\pi\varepsilon}\frac{Rz}{r^2}\frac{Il}{\omega}\left(-i\frac{3}{r^2}+\frac{3\alpha}{r^2}+i\frac{\alpha^2}{r}\right)e^{i(\omega t-\alpha r)} \\ E_z &= \frac{1}{4\pi\varepsilon}\frac{1}{r^2}\frac{Il}{\omega}\left[-i\frac{3z^2-r^2}{r^3}+\frac{(3z^2-r^2)\alpha}{r^2}+\right. \\ &\quad \left.+i\frac{(z^2-r^2)\alpha^2}{r}\right]e^{i(\omega t-\alpha r)} \\ H_\varphi &= \frac{1}{4\pi}\frac{R}{r}Il\left(\frac{1}{r^2}+i\frac{\alpha}{r}\right)e^{i(\omega t-\alpha r)} \\ E_\varphi &= H_R = H_z = 0 \end{aligned}\right\}, \qquad \text{(IV.8.17)}$$

where

$$r = \sqrt{R^2 + z^2}.$$

#IV.9. The Three Zones of the Dipole Field

(a) Division of the space around a dipole into zones

Three dipole field zones can be differentiated: the near, the far (wave) and the intermediate. Let us use formula (IV.8.16) to arrive at the best explanation of the criterion for dividing the space around a dipole

into zones. Introducing the value $2\pi/\lambda$ for the phase factor α, we can render the formulas at (IV.8.16) in the forms

$$E_r = \frac{1}{4\pi\varepsilon}\frac{2Il}{\omega}\left(\frac{2\pi}{\lambda}\right)^3\cos\theta\left[-i\left(\frac{\lambda}{2\pi r}\right)^3+\left(\frac{\lambda}{2\pi r}\right)^2\right]e^{i(\omega t-} \quad . \qquad \text{(IV.9.1)}$$

$$E_\theta = \frac{1}{4\pi\varepsilon}\frac{Il}{\omega}\left(\frac{2\pi}{\lambda}\right)^3\sin\theta\left[-i\left(\frac{\lambda}{2\pi r}\right)^3+ \right.$$

$$\left.+\left(\frac{\lambda}{2\pi r}\right)^2+i\left(\frac{\lambda}{2\pi r}\right)\right]e^{i(\omega t-\alpha r)}, \qquad \text{(IV.9.2)}$$

$$H_\varphi = \frac{1}{4\pi}Il\left(\frac{2\pi}{\lambda}\right)^2\sin\theta\left[\left(\frac{\lambda}{2\pi r}\right)^2+i\left(\frac{\lambda}{2\pi r}\right)\right]e^{i(\omega t-\alpha r)}. \qquad \text{(IV.9.3)}$$

(b) The near zone

The near zone is the zone within the limits of which $r \ll \lambda/2\pi$. Here the term $(\lambda/2\pi r)^2$ in formula (IV.9.1), the terms $(\lambda/2\pi r)^2$ and $i(\lambda/2\pi r)$ in formula (IV.9.2), and the term $i(\lambda/2\pi r)$ in formula (IV.9.3) can be ignored.

Whereupon we obtain

$$E_r = -i\frac{2Il}{4\pi\varepsilon\omega r^3}\cos\theta\, e^{i(\omega t-\alpha r)}, \qquad \text{(IV.9.4)}$$

$$E_\theta = -i\frac{Il}{4\pi\varepsilon\omega r^3}\sin\theta\, e^{i(\omega t-\alpha r)}, \qquad \text{(IV.9.5)}$$

$$H_\varphi = \frac{Il}{4\pi r^2}\sin\theta\, e^{i(\omega t-\alpha r)}. \qquad \text{(IV.9.6)}$$

Substituting the expression for current I in terms of charge $q(I=i\omega q)$ in equations (IV.9.4) and (IV.9.5),

$$E_r = \frac{ql}{2\pi\varepsilon r^3}\cos\theta\, e^{i(\omega t-\alpha r)}, \qquad \text{(IV.9.7)}$$

$$E_\theta = \frac{ql}{4\pi\varepsilon r^3}\sin\theta\, e^{i(\omega t-\alpha r)}. \qquad \text{(IV.9.8)}$$

The factors in the right-hand sides of equations (IV.9.7) and (IV.9.8)

$$\frac{ql}{2\pi\varepsilon r^3}\cos\theta \text{ and } \frac{ql}{4\pi\varepsilon r^3}\sin\theta$$

do not depend on time and therefore coincide with known expressions for components of the electric field strength of an electrostatic dipole consisting of two charges with opposite signs (+q and -q) at distance l from each other. The phase factor $e^{-i\alpha r}$, because of the smallness of the magnitude αr, can be ignored. Thus, the electric field strength of the dipole changes in-phase with the change in the moment ql at short distances, and the amplitude of the dipole's electric field strength is the same as that of the electrostatic dipole.

If one ignores the phase factor $e^{-i\alpha r}$ in formula (IV.9.6), and discards the time factor $e^{i\omega t}$, the result is an expression which coincides with the expression for DC magnetic field strength, that is, we obtain Bio-Savar's formula

$$H_\varphi = \frac{Il}{4\pi r^2}\sin\theta.$$

Thus, the field in the dipole's near zone can be characterized by the following features:

(1) the amplitude of the dipole's electric field strength is equal to the electrostatic dipole's field strength when both have the same charges (+q and -q);

(2) the amplitude of the dipole's magnetic field strength equals the magnetic field strength created by a conductor of the same length, l, as that of the dipole and passing DC equal in amplitude to that of the current flowing in the dipole;

(3) the electric field strength is inversely proportional to the dielectric constant of the medium for a specified current magnitude;

(4) the electric and magnetic field vectors are 90° out of phase with respect to each other.

(c) The far (wave) zone

The far, or wave, zone is that zone within the limits of which $r \gg \lambda/2\pi$. And we can ignore the terms $(\lambda/2\pi r)$ of powers higher than the first in formulas (IV.9.2) and (IV.9.3). Moreover, as compared with E_θ, we can ignore E_r.

As a result, substituting $2\pi/\lambda = \sqrt{\omega\,\varepsilon\mu}$, we obtain

$$E_\theta = i\frac{Il\omega\mu}{4\pi r}\sin\theta\, e^{i(\omega t - \alpha r)}, \qquad \text{(IV.9.7)}$$

$$H_\varphi = i\frac{Il\omega}{4\pi r}\sqrt{\varepsilon\mu}\sin\theta\, e^{i(\omega t - \alpha r)}, \qquad \text{(IV.9.8)}$$

$$E_r \cong E_\varphi = H_r = H_\theta = 0.$$

From formulas (IV.9.7) and (IV.9.8),

$$E_\theta = H_\varphi\sqrt{\frac{\mu}{\varepsilon}}. \qquad \text{(IV.9.9)}$$

The factor

$$W_c = \sqrt{\frac{\mu}{\varepsilon}} \qquad \text{(IV.9.10)}$$

has the dimensionality of impedance and is called the characteristic impedance of the medium.

As will be seen, the field in the far zone can be characterized by the following features:

(1) the strengths of the electric and magnetic fields are inversely proportional to the first power of the distance r;

(2) the electric field strength is proportional to the magnetic conductivity of the medium and will not depend on the medium's dielectric constant for a specified frequency and magnitude of current flowing in the dipole;

(3) the magnetic field strength is proportional to the square root of the product of the medium's magnetic conductivity and dielectric constant, that is, it is inversely proportional to the propagation velocity, for a specified frequency and magnitude of current flowing in the dipole;

(4) the electric field strength is equal to the magnetic field strength multiplied by the characteristic impedance of the medium;

(5) the electric and magnetic field vectors are in phase;

(6) the electric and magnetic field strengths are proportional to the ratio of l/λ, for a specified current magnitude. Electric and magnetic field strengths are greater the shorter the wavelength for a specified dipole length (l).

(d) The intermediate zone

The intermediate zone is the transition zone from the near to the far zone. None of the summands in the expressions for electric and magnetic field components can be ignored in this zone. Figure IV.9.1 shows the curves for the change in the three summands of E_θ (see formula IV.9.2). Curve 1 is that for the summand proportional to (λ/r), while curves 2 and 3 are those for the summands proportional to $(\lambda/r)^2$ and $(\lambda/r)^3$. Scale is relative. They can be used to determine the degree to which some particular distance corresponds to some particular zone.

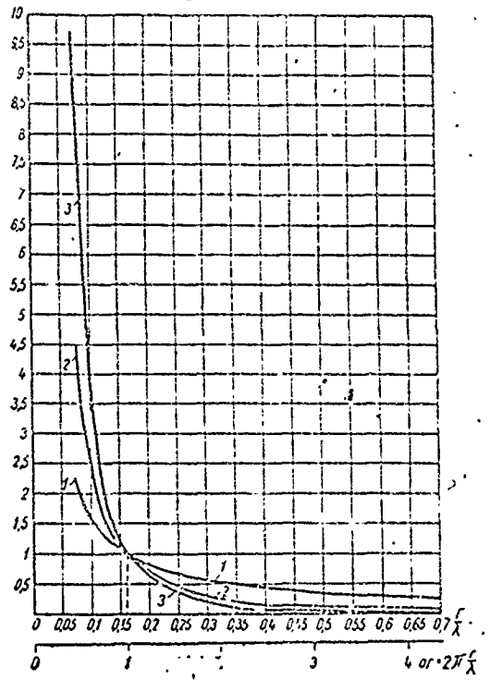

Figure IV.9.1

Curves of change in the three summands of E_θ with respect to r/λ.

$E_r = 0$ (because $\cos\theta = 0$) in the equatorial plane of the dipole, that is, in the plane normal to its axis and passing through its center. Consequently, the curves in Figure IV.9.1 give the characteristic of the full magnitude of the electric field strength vector for the equatorial plane.

#IV.10. Electric Field Strength in the Far Zone in Free Space

In free space, $\omega\mu = 240\pi^2/\lambda$. Substituting the value of this magnitude in formula (IV.9.7), and omitting the time factor,

$$\dot{E}_\theta = i\frac{60\pi \dot{I}(a)\, l(\kappa)}{\lambda(\kappa)\, r(\kappa)}\sin\theta\, e^{-i\kappa r} \quad \text{(volts/meter)} \qquad \text{(IV.10.1)}$$

If the distance is expressed in kilometers, and if the electric field strength is expressed in microvolts per meter, formula (IV.10.1) will take the form

$$E_\theta = i\frac{0.1884\cdot 10^4 \dot{I}(a)\, l(\kappa)}{\lambda(\kappa)\, r(\kappa)}\sin\theta\, e^{-i\kappa r} \quad \text{microvolts/meter} \qquad \text{(IV.10.2)}$$

Plots, or charts, of the dependence of the magnitude of the field strength on the direction at the point of observation are called radiation patterns. Radiation patterns are usually constructed in polar or rectangular systems of coordinates.

Figure IV.10.1 shows the radiation pattern for an elementary dipole plotted in a polar system of coordinates.

The field strength at the point of observation defines the magnitude (amplitude), as well as the phase, which, in the general case too can depend on the direction at this point. Therefore, the concept of phase radiation pattern, understood to mean the dependence of the field strength phase on the direction at the point of observation, is sometimes introduced.

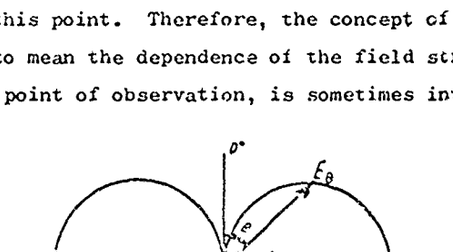

Figure IV.10.1. Radiation pattern for an elementary dipole in a polar system of coordinates.

#IV.11. Power Radiated by a Dipole

Let us imagine a spherical surface, in the center of which we have located a dipole. The flow of energy per unit time over this surface is the radiated power. This power can be expressed analytically by

$$P_\Sigma = \oint S_n dF, \qquad \text{(IV.11.1)}$$

where

dF is the elemental area on the closed surface surrounding the dipole;

S_n is the component of Poynting's vector normal to surface dF,

$$dF = r^2 \sin\theta \, d\theta \, d\varphi.$$

Substituting the expression for dF in formula (IV.11.1),

$$P_\Sigma = \int_0^{2\pi} d\varphi \int_0^{\pi} S_n r^2 \sin\theta \, d\theta. \qquad \text{(IV.11.2)}$$

The energy flowing in direction r over 1 m^2 of the surface of the sphere is determined by the components of the vectors for the strengths of the electric and magnetic fields normal to r, that is, E_θ and H_φ.

From Poynting's theorem and the rules for multiplying vectors,

$$S_n = r_0 S_n = [\theta_0 E_\theta \, \varphi_0 H_\varphi] = [\theta_0 \varphi_0] E_\theta H_\varphi = r_0 E_\theta H_\varphi; \qquad \text{(IV.11.3)}$$

where

r_0, θ_0 and φ_0 are unit vectors directed toward the increase in radius r and of angles θ and φ.

From (IV.11.3),

$$S_n = E_\theta H_\varphi. \qquad \text{(IV.11.4)}$$

E_θ and H_φ are harmonic functions of time. If their expressions from formula (IV.8.16) are substituted in formula (IV.11.4), we obtain an expression for the instantaneous value of S_n. We are interested in the average value of S_n for the period, however. The average value for the period of the product of the two magnitudes A and B, which are harmonic functions of time, and which have the complex amplitudes A_0 and B_0, equal the real part of the product

$$1/2 \; A_0 B_0^*,$$

where

B_0^* is a complex magnitude conjugate with B_0.

Thus, the average value of the component S_n of Poynting's vector equals

$$S_{n\,cp} = \frac{1}{2} E_{0\theta} H_{0\varphi}^*, \qquad \text{(IV.11.5)}$$

where

$E_{0\theta}$ and $H_{0\varphi}^*$ are the complex amplitudes of the magnitudes E_θ and H_φ.

. The result of the integration of the power with respect to the spherical surface in a lossless medium is not dependent on the radius of this surface. In order to simplify the calculations we will assume that the radius of the sphere is so great that the spherical surface passes through the radiation zone. In this zone

$$H_{0\varphi} = \frac{E_{0\theta}}{\sqrt{\frac{\mu}{\varepsilon}}}.$$

Substituting the expressions obtained in (IV.11.2), we obtain the following formula for the average radiated power

$$P_{\Sigma} = \frac{1}{2\sqrt{\frac{\mu}{\varepsilon}}} \int_0^{2\pi} d\varphi \int_0^{\pi} E_0^2 r^2 \sin\theta \, d\theta. \qquad \text{(IV.11.6)}$$

The subscript θ for E_0 is omitted because there is only one component of the E_0 vector in the far zone.

Equation (IV.11.6) is the general expression for the power radiated by any antenna if we understand E_0 to be the amplitude of the field strength in the far zone.

Taking the expression for the amplitude of the field strength vector from equation (IV.9.7) and integrating, we obtain the following formula for the power radiated by the elementary dipole.

$$P_{\Sigma} = \pi \frac{I^2}{3} \left(\frac{l}{\lambda}\right)^2 \sqrt{\frac{\mu}{\varepsilon}} = \frac{\pi I^2}{3} \left(\frac{l}{\lambda}\right)^2 W_i. \qquad \text{(IV.11.7)}$$

where

W_i is the characteristic impedance of the medium.

#IV.12. Dipole Radiation Resistance

By analogy with other electrical circuits, the proportionality factor for power expended and half the square of the current amplitude can be called the dipole's pure resistance. This pure resistance is called the radiation resistance and is designated by R_{Σ}.

Thus,

$$R_{\Sigma} = \frac{2P_{\Sigma}}{I^2} = \frac{2\pi}{3} \left(\frac{l}{\lambda}\right)^2 W_i. \qquad \text{(IV.12.1)}$$

In free space $W_i = \sqrt{\mu_0/\varepsilon_0} = 120\pi \approx 377$ ohms, and

$$R_{\Sigma} = 80\pi^2 \left(\frac{l}{\lambda}\right)^2. \qquad \text{(IV.12.2)}$$

The radiation resistance is only a part of the active component of the dipole resistance, measured at the point where the emf source is connected. The real dipole has other components, in addition to the radiation resistance, which determine losses in the dipole conductors and in the surrounding medium.

Chapter V

ANTENNA RADIATION AND RECEPTION THEORY

#V.1. Derivation of the Single Conductor Radiation Pattern Formula

A long conductor can be considered as the sum of the elementary dipoles, and the field strength in any direction can be found by integrating field strength for the components of its elementary dipoles with respect to the length of the conductor. The field strength of an elementary dipole depends on the current, so, in order to solve the problem posed here it is first necessary to determine current distribution along the conductor. This is an extremely complicated problem. Moreover, current distribution along the conductor and the field structure in the space around it are interdependent, and it is impossible to solve these two problems separately.

We will limit ourselves here to an exposition of a rather imprecise solution which assumes the radiating conductor to be a line with characteristic impedance unchanged along its length. Now current distribution can be established by using the laws contained in the theory of uniform long lines. Actually, there is no basis for this assumption. The distributed constants and the characteristic impedance of a radiating conductor do not remain constant over the entire length of the conductor. But experience is that the actual current distribution along the conductor coincides extremely closely with the distribution this assumption stipulates. The smaller the conductor diameter, the greater the coincidence.

Long line theory data tell us current distribution along a conductor with constant characteristic impedance along its length can be determined through the following formula,

$$I = I_{in}[e^{-\gamma z} + p_I e^{-\gamma(2l-z)}], \qquad (V.1.1)$$

where

I_{in} is the incident wave current at the generator end;

z is the distance from the point of application of the emf to a specified point on the conductor;

p_I is the current reflection coefficient.

We will consider the conductor as the sum of the elementary dipoles. Then the field of element dz can be determined through formula (IV.10.1). Substituting the expression for I from formula (V.1.1) in formula (IV.10.1), we obtain the following expression for the field strength created in the far zone by element dz

$$dE_\theta = i\frac{60\pi}{r\lambda} I_{in} \left[e^{-\gamma z} + p_I e^{-\gamma(2l-z)}\right] \sin\theta \, e^{-ikr} dz. \qquad (V.1.2)$$

Let us express the distance r from any element of the conductor to the point of observation by the fixed distance from the generator end of the conductor to the point of observation. This we will designate as r_0.

Then, from Figure V.1.1,

$$r = r_0 - z\cos\vartheta.$$

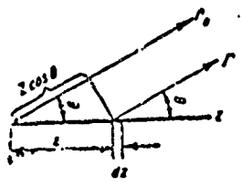

Figure V.1.1. Determination of the difference in propagation from two elements of a radiating conductor.

Substituting this expression in formula (V.1.2), and considering that $r \gg z$,

$$dE_\vartheta = i\frac{60\pi}{r_0\lambda} I_{in} \left[e^{-\gamma z} + p_I e^{-\gamma(2l-z)}\right] \sin\vartheta\, e^{-i\alpha(r_0 - z\cos\vartheta)}\, dz.$$

Integrating this expression along the entire length of the conductor, and taking it that in the far zone the directions to the point of observation from all elements of the conductor are parallel to each other, that is, that θ does not depend on z,

$$E_\vartheta = i\frac{60\pi}{r_0\lambda} I_{in} \sin\vartheta\, e^{-i\alpha r_0}\left[\frac{e^{(i\alpha\cos\vartheta-\gamma)l}-1}{i\alpha\cos\vartheta-\gamma} + p_I\frac{e^{(i\alpha\cos\vartheta+\gamma)l}-1}{i\alpha\cos\vartheta+\gamma}\, e^{-\gamma l}\right] \quad (V.1.3)$$

The component of the electric field strength vector expressing the above formulas has a direction perpendicular to r_0, and lies in the plane zr_0.

#V.2. Special Cases of Radiation from a Single Conductor in Free Space

(a) Single conductor passing a traveling wave of current ($p_I = 0$)

Formula (V.1.3) takes the form

$$E_\vartheta = i\frac{60\pi}{r_0\lambda} I_0 \sin\vartheta\, \frac{e^{(i\alpha\cos\vartheta-\gamma)l}-1}{i\alpha\cos\vartheta-\gamma}. \quad (V.2.1)$$

in the traveling wave mode, when the reflection factor, p_I, equals zero, and the current I_{in} equals zero at the generator end of the conductor, I_0.

If we ignore attenuation, that is, if we take $\gamma = i\alpha$, after transformation the following expression for the field strength modulus is obtained

$$E_\vartheta = \frac{60 I_0}{r_0}\frac{\sin\vartheta}{1-\cos\vartheta}\sin\left[\frac{\alpha l}{2}(1-\cos\vartheta)\right]. \quad (V.2.2)$$

Figures V.2.1 through V.2.3 contain a series of radiation patterns for various values of l/λ, charted without regard for attenuation. As will be seen, the patterns are symmetrical with respect to the dipole axis and asymmetrical with respect to the normal to this axis. The larger l/λ, the greater this asymmetry. As l/λ increases the angle formed by the direction of the maximum concentration of energy and the axis of the conductor decreases.

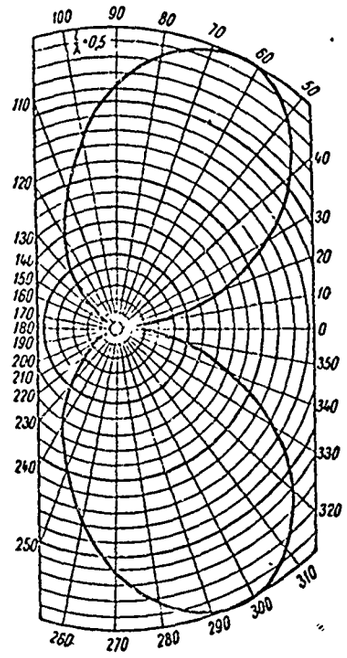

Figure V.2.1. Radiation pattern for a single conductor passing a traveling wave of current, computed without taking current attenuation in the conductor into consideration; $l/\lambda = 0.5$.

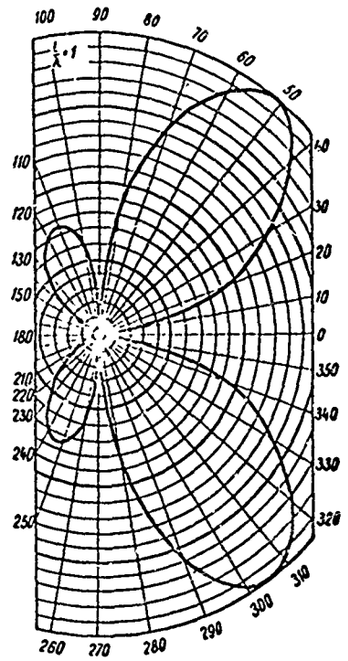

Figure V.2.2. Radiation pattern for a single conductor passing a traveling wave of current, computed without taking current attenuation in the conductor into consideration; $l/\lambda = 1.0$.

Figure V.2.4 shows the radiation pattern charted with attenuation considered for $l = 3\lambda$ and $\beta l = 0.6$. The magnitude of βl is taken from design data for attenuation in conductors passing a traveling wave of current when the characteristic impedance is 300 ohms.

As will be seen, the outstanding feature of the radiation pattern charted with attenuation considered is the absence of a direction in which radiation is equal to zero, with the exception of the direction along the axis of the conductor.

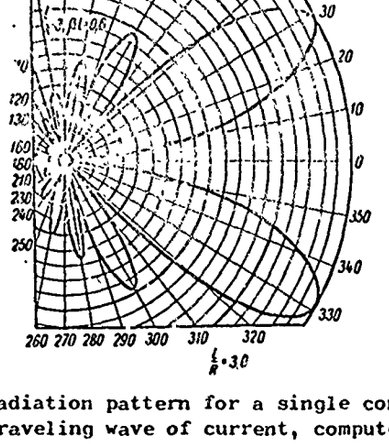

Figure V.2.3. Radiation pattern for a single conductor passing a traveling wave of current, computed without taking current attenuation in the conductor into consideration; $l/\lambda = 3.0$.

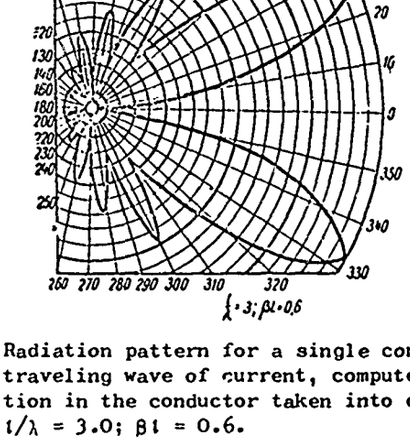

Figure V.2.4. Radiation pattern for a single conductor passing a traveling wave of current, computed with current attenuation in the conductor taken into consideration; $l/\lambda = 3.0$; $\beta l = 0.6$.

(b) Single conductor, open-ended

If the conductor is open-ended the reflection factor is $p_I = -1$. In this case it is convenient to express the field strength in terms of the current at the generator end (I_0). The dependence between I_{in} and I_0 can be determined through formula (V.1.1) by substituting $p_I = -1$ and $z = 0$. Substituting, we obtain

$$I_{in} = I_0 \frac{1}{2\operatorname{sh}\gamma l e^{-\gamma l}}. \qquad (V.2.3)$$

Substituting $p_I = -1$ and the expression for I_{in} from formula (V.2.3) in formula (V.1.3), and omitting the factor characterizing the field phase, we obtain

$$E_\theta = i\frac{30 I_0}{r_0}\frac{\sin\theta}{\operatorname{sh}\gamma l}\times$$

$$\times\frac{\left(\frac{\gamma}{\alpha}\operatorname{ch}\gamma l + i\cos\theta\operatorname{sh}\gamma l\right) - \frac{\gamma}{\alpha}\left[\cos\left(\alpha l\cos\theta\right) + i\sin\left(\alpha l\cos\theta\right)\right]}{\cos^2\theta + \left(\frac{\gamma}{\alpha}\right)^2}. \qquad (V.2.4)$$

If the attenuation ($\gamma = i\alpha$) in the factor which takes directional properties into consideration is disregarded, formula (V.2.4) becomes

$$E_\theta = \frac{30 I_0}{r_0 \operatorname{sh}\gamma l}\,\frac{\left[\cos\left(\alpha l\cos\theta\right) - \cos\alpha l\right] + i\left[\sin\left(\alpha l\cos\theta\right) - \sin\alpha l\cos\theta\right]}{\sin\theta} \qquad (V.2.5)$$

Figures V.2.5 through V.2.8 show a series of radiation patterns for a conductor passing a standing wave of current for different values of l/λ. Formula (V.2.5) was used to chart the curves in figures V.2.6 through V.2.8.

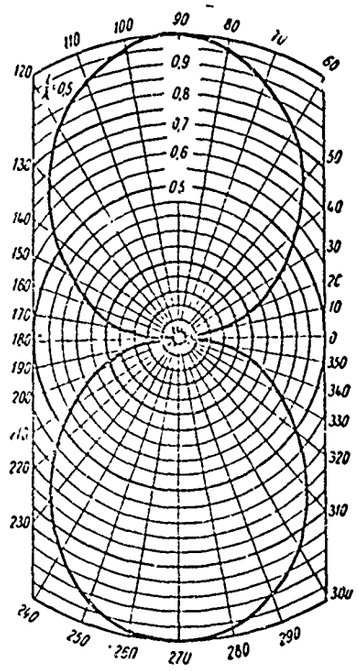

Figure V.2.5. Radiation pattern for a single conductor passing a standing wave of current, computed without taking attenuation into consideration; $l/\lambda = 0.5$.

The radiation patterns are, as we see, symmetrical with respect to the normal to the axis of the conductor. This should have been expected since the conductor with total reflection at its end will pass two traveling waves of identical intensity, an incident wave and a reflected wave, provided there is no attenuation.

Each wave of current matches its own radiation pattern asymmetrical relative to the normal to the conductor axis. The summed radiation pattern

obtained is symmetrical relative to the normal to the conductor axis.

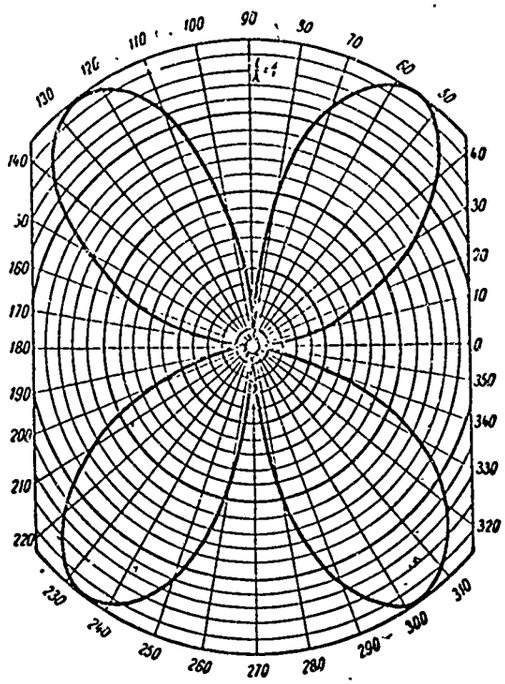

Figure V.2.6. Radiation pattern for a single conductor passing a standing wave of current, computed without taking attenuation into consideration; $l/\lambda = 1.0$.

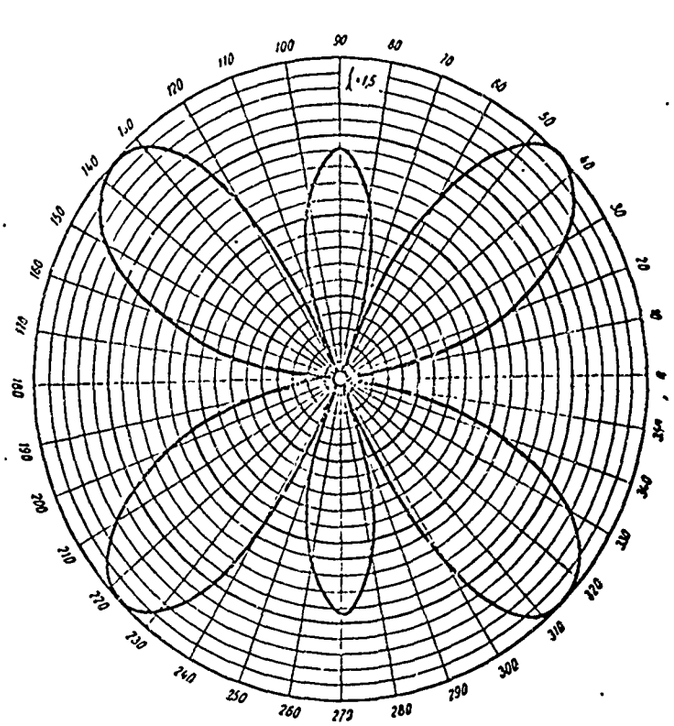

Figure V.2.7. Radiation pattern for a single conductor passing a standing wave of current, computed without taking attenuation into consideration; $l/\lambda = 1.5$.

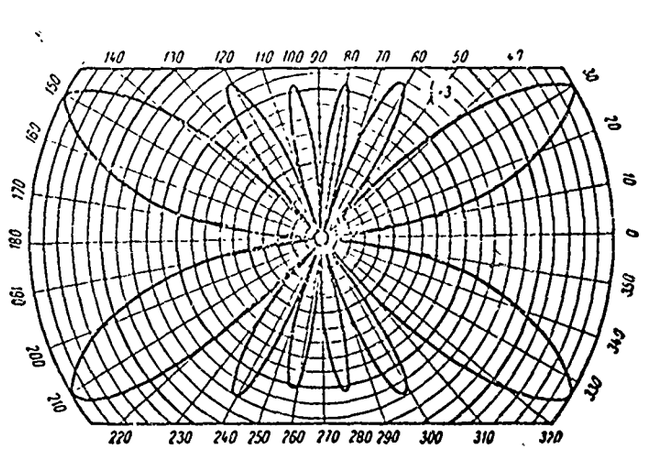

Figure V.2.8. Radiation pattern for a single conductor passing a standing wave of current, computed without taking attenuation into consideration; $l/\lambda = 3.0$.

#V.3. The Balanced Dipole. Current Distribution in the Balanced Dipole.

A balanced dipole is a straight conductor of length 2l, center-fed, the ends of which are not terminated. The balanced dipole is a distribution type antenna and is the basic radiating element in many complex antennas.

First of all, let us find the current distribution in the balanced dipole. Let us use formula (V.1.1) for this purpose. Let us designate the distance from the center of the dipole to a point under consideration in one of the halves by z (fig. V.3.1.).

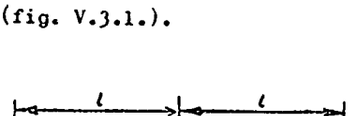

Figure V.3.1. Schematic diagram of a balanced dipole.

Since the conductor is not terminated $p_I = -1$ must be substituted in formula (V.1.1). Making this substitution, and using the relationship at (V.2.3), we obtain the following expression for the current,

$$I_z = I_0 \frac{\operatorname{sh}\gamma(l-z)}{\operatorname{sh}\gamma l}. \qquad (V.3.1)$$

If current attenuation in the conductors is disregarded, that is, if we assume that $\gamma = i\alpha$, then

$$I_z = I_0 \frac{\sin\alpha(l-z)}{\sin\alpha l} = I_{loop} \sin\alpha(l-z), \qquad (V.3.2)$$

where

I_{loop} is the current flowing in a current loop.

Figure V.3.2 shows several curves for current distribution along a balanced dipole.

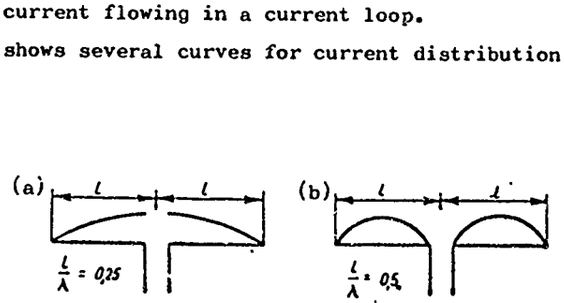

Figure V.3.2. Current distribution along a balanced dipole for different l/λ ratios.

#V.4. The Radiation Pattern of a Balanced Dipole in Free Space

Formula (V.2.4) expresses the field strength for each of the conductors of a balanced dipole in the radiation zone.

The field strength of a balanced dipole can be represented in the form of the sum of two terms expressed by formula (V.2.4). And, in accordance with the system of coordinates selected in the derivation of formula (V.2.4) (fig. V.1.1), the expression for field strength created by the right conductor is in complete coincidence with (V.2.4), but θ must be replaced by $180° + \theta$ in the expression for the field strength created by the left conductor. Moreover, if it is taken that positive for the current is to the right of the origin, then I_0 in the expression for the field strength created by the left conductor must be replaced by $-I_0$. From what has been said, then

$$E_\theta = \frac{60 I_0}{r_0} \frac{\sin\theta}{\operatorname{sh}\gamma l} \frac{\operatorname{ch}\gamma\frac{l}{4} - \cos\left(\frac{\pi}{4}\cos\theta\right)}{\cos^2\theta} \cdot \qquad (V.4.1)$$

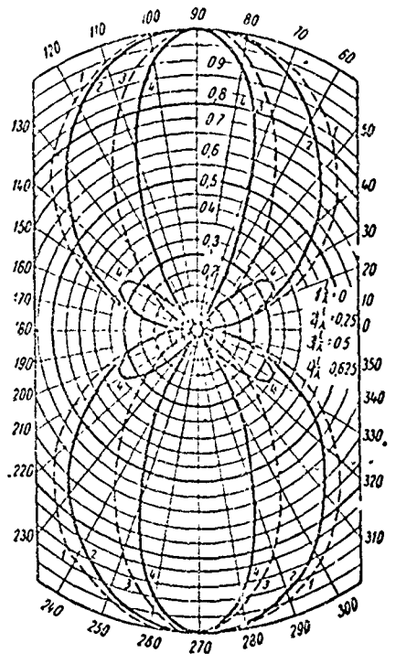

Figure V.4.1. Radiation pattern for a balanced dipole for different l/λ ratios.

Disregarding current attenuation in the dipole ($\gamma = i\alpha$) during the calculation of directional properties, and dropping the factors which characterize phase, we obtain

$$E_\theta = \frac{60 I_0}{r_0 \operatorname{sh}\gamma l} \frac{\cos\left(\frac{\pi}{2}\cos\theta\right) - \cos\pi l}{\sin\theta} \cdot \qquad (V.4.2)$$

Expressing the current flowing at the point of supply (I_0) in terms of the current flowing in the loop (I_{loop}) through formula $I_0 = I_{loop}$ sh γl,

$$E_\theta = 60 I_{loop}/r_0 \cos(\alpha l \cos\theta) - \cos \alpha l / \sin\theta \qquad (V.4.3)$$

Putting $l = \lambda/4$ in formula (V.4.3), we obtain an expression for the radiation pattern of a half-wave dipole

$$E_\theta = 60 I_{loop}/r_0 \frac{\cos(\pi/2 \cos\theta)}{\sin\theta} . \qquad (V.4.4)$$

Figure V.4.1 charts a series of radiation patterns of a balanced dipole in free space for different values of l/λ. As we see, the increase in the l/λ ratio is accompanied by narrowing of the radiation pattern. When $l/\lambda > 0.5$, there are parasitic lobes, in addition to the major lobe, which has a maximum radius vector normal to the dipole axis. When $l/\lambda = 1$, there is no radiation in the direction normal to the dipole axis.

#V.5. The Effect of the Ground on the Radiation Pattern of a Balanced Dipole

(a) General considerations

The foregoing discussed radiation from a balanced dipole in free space. Let us now consider a dipole located near the earth's surface.

Electric currents flow in the ground as a result of the effect produced by the dipole's electromagnetic field. In the general case these currents are the conduction and displacement currents. The conduction current density is determined by the ground conductivity, and equals $j = \gamma_v E$, while displacement current density is determined by the dielectric constant for the ground, ϵ, and is equal to $j_d = \epsilon\, dE/dt$, where E is the electric field strength vector at the point on the ground under consideration. Distribution of currents on the ground depends on the height at which the dipole is located, its length, tilt with respect to the earth's surface, wavelength, and ground parameters.

The current flowing in the ground is equivalent to a secondary field. The interference generated by primary and secondary field interaction causes dipole field strength to change, not only in the immediate vicinity of the dipole, but at distant points as well. Change in the field structure near the dipole leads to some change in the distribution of current flowing in the dipole, and to a corresponding change in the dipole's input impedance.

A precise calculation of the influence of the ground on antenna radiation is a very complicated problem, and has not yet been completely resolved. If the ground is represented as an ideal flat conductor ($\gamma_v = \infty$) of infinite extent the problem is easy to solve. In this case it is comparatively simple

to establish the change in the radiation pattern, as well as the change in the dipole's input impedance.

(b) Radiation pattern of a balanced dipole in the vertical plane, dipole over flat ideal ground

In the ideal ground case ($\gamma_y = \infty$), electric currents in the ground are present only in the form of surface conduction currents.[1] The system of ground currents is such that as a result of the superposition of the field of the ground currents on the field of the dipole currents a field is formed such that a field satisfying the boundary conditions at the surface of the ideal conductor is formed at the ground surface. The tangential component of the E vector and the normal component of the H vector equal zero.

It is relatively simple to explain why boundary conditions at ground level can be satisfied if we replace the system of ground currents with a mirror image of dipole currents (fig. V.5.1).

In the horizontal dipole case (fig. V.5.1a) the current flowing in the mirror image has an amplitude equal to the amplitude of the current flowing in the dipole, but 180° out of phase.

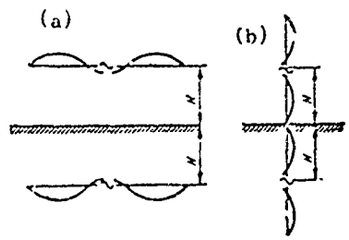

Figure V.5.1. Horizontal and vertical dipoles and their mirror images.

In the vertical dipole case (fig. V.5.1b) the current flowing in the mirror image equals the dipole current, in amplitude and in phase.

The fact that the dipole field and the mirror image satisfy the boundary conditions over an entire infinite surface of an air-ground section is sufficient reason for asserting that a field created by currents flowing at ground level is exactly like the field created by the mirror image, and this is so for any point. Therefore, we can replace the ground with the dipole's mirror image when charting the pattern (charting the field at a long distance from the dipole).

Let us consider the radiation patterns of a balanced dipole in the vertical plane passing through the dipole axis in the vertical dipole case (the meridional plane), and in the horizontal dipole case that in the plane passing through the center of the dipole normal to its axis (equatorial plane).

---

1. For the vertical dipole current flow in the ground is radial; for the horizontal d pole it is parallel to the dipole axis.

E_1 is the electric field strength of the wave formed by the dipole, and E_2 is the electric field strength of the wave formed by the mirror image. Moreover, H is the distance from the center of the dipole to the ground surface (fig. V.5.2).

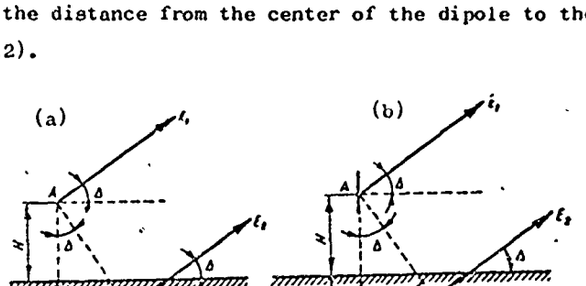

Figure V.5.2. Determination of the difference in propagation between beams emanating from a dipole and its mirror image.

a - horizontal dipole; b - vertical dipole.

Let us assume that $r \gg H$, in which case the beams from the dipole and those from the mirror image can be taken as parallel (they have the same angle of tilt, Δ).

The field strength resulting from the mirror image of the vertical dipole equals

$$E_2 = E_1 e^{i\varphi_p} .$$

The field strength resulting from the mirror image of the horizontal dipole equals

$$E_2 = -E_1 e^{i\varphi_p} ,$$

where

φ_p is the phase displacement, determined by the difference in the propagation of the beams from the dipole and from its mirror image.

The difference in propagation is equal to CB = 2H sin Δ,

$$\varphi_p = -2\alpha H \sin \Delta ,$$

Accordingly, the vertical dipole field strength equals

$$E_v = E_1 + E_2 = E_1 (1 + e^{-i2\alpha H \sin\Delta}) .$$

Horizontal dipole field strength equals

$$E_h = E_1 + E_2 = E_1 (1 - e^{-i2\alpha H \sin\Delta}) .$$

From formula (V.4.3), for the vertical dipole ($\theta = 90° - \Delta$)

$$E_1 = 60I_{loop}/r_0 \cos(\alpha l \sin\Delta)-\cos \alpha l/\cos \Delta \qquad (V.5.1)$$

and for the horizontal dipole ($\theta = 90°$)

$$E_1 = 60I_{loop}/r_0 (1 - \cos \alpha l) . \qquad (V.5.2)$$

Substituting the values for E_1 from (V.5.1) and (V.5.2) in the expressions for E_v and E_h, replacing the exponential functions with trigonometric functions, and omitting the factors which characterize the phase,

$$E_v = 120\ I_{loop}/r_0 \cos(\alpha l \sin \Delta)-\cos \alpha l/\cos \Delta\cdot\cos(\alpha l \sin \Delta), \qquad (V.5.3)$$

$$E_h = 120\ I_{loop}/r_0 (1 - \cos \alpha l)\sin(\alpha l \sin \Delta). \qquad (V.5.4)$$

(c) Radiation pattern of a balanced dipole in the vertical plane, dipole over flat ground of finite conductivity. Approximate and precise solution to the problem.

In the real ground case the ground carries a system of currents created by the effect of the dipole field which is not the equivalent of the dipole's mirror image. But, as we shall see, when we compute field strength at extremely long distances from the dipole we can use a method for so doing which is similar to that for mirror images.

Let us suppose we have an elementary dipole set up over the ground surface. The elementary dipole radiates spherical waves. A precise analysis of the effect of the ground on the structure of the field which is the source of spherical waves is extremeley complicated, and a full explanation is not one of our tasks. We shall give a brief explanation of the precise analysis in what follows, and we shall prove that if reception occurs at an extremely long distance from the point of radiation it is permissible to analyze the effect of the ground, regardless of the height at which the dipole may be above it, and assuming the dipole is radiating a plane wave. This will make it possible to use the theory of the reflection of plane waves (the geometric optics method), in order to determine field strength at a long distance from the dipole.

Data from this theory tell us that a plane wave incident to a flat, infinitely large surface will be reflected from it at an angle equal to the angle of incidence.

The angle of incidence is that angle formed by the direction in which the beam is propagated end the normal to the reflecting surface.

The amplitude of the reflected wave is, in the general case, less than the amplitude of the incident wave because some of the energy is lost in the

reflecting medium. The phase of the reflected wave will depend on ground parameters, the angle of incidence, and the polarization of the vector for the electric field strength for the incident wave.

Let us distinguish between parallel and normal polarization. A wave is said to have parallel polarization when the electric field strength vector is normal to the plane of incidence. The plane of incidence is a plane normal to the reflecting surface and containing the direction in which the beam is propagated.

The vertical dipole builds up an electromagnetic field only with parallel polarization.

The horizontal dipole builds up an electromagnetic field only with normal polarization in the equatorial plane. The horizontal dipole builds up electromagnetic fields with both normal and parallel polarization in other planes.

The relationship between the field strength of the reflected wave and the field strength of the incident wave at the point of reflection is

$$R_{\parallel} = |R_{\parallel}| e^{i\varphi_{\parallel}} = \frac{\varepsilon_r' \sin\Delta - \sqrt{\varepsilon_r' - \cos^2\Delta}}{\varepsilon_r' \sin\Delta + \sqrt{\varepsilon_r' - \cos^2\Delta}} \qquad (V.5.6)$$

when the electric field strength vector is parallel to the plane of incidence, and

$$R_{\perp} = |R_{\perp}| e^{i\varphi_{\perp}} = \frac{\sin\Delta - \sqrt{\varepsilon_r' - \cos^2\Delta}}{\sin\Delta + \sqrt{\varepsilon_r' - \cos^2\Delta}} \qquad (V.5.7)$$

when the electric field strength vector is normal to the plane of incidence.

Here $|R_{\parallel}|$ and $|R_{\perp}|$ are the ratios of the amplitudes of the field strength vector for the reflected beam to the amplitudes of the field strength vector for the incident beam for parallel and normal polarizations, respectively (the moduli of the reflection factors); $\varphi_{\parallel}$ and $\varphi_{\perp}$ are the phase displacements between the field strength vectors for the incident and reflected waves for parallel and normal polarizations, respectively (arguments for the reflection factors);

ε_r' is the relative complex dielectric constant for the ground, $\varepsilon_r' = \varepsilon_r - i60\gamma_v\lambda$, where $\varepsilon_r = \varepsilon/\varepsilon_0$ is the relative dielectric constant for the ground; that is, the ratio of the dielectric constant for the ground to the dielectric constant for free space.

The magnitudes $R_{\parallel}$ and $R_{\perp}$ are known as the reflection factors, or the Fresnel coefficients.

Utilizing the data cited from the theory of the reflection of plane waves, we obtain the following expression for field strength at a long distance from the source

$$E \approx E_1 + E_2 ,$$

where

E_1 is the field strength of a beam directly incident at the point of observation. E_1 is found through the formula for a dipole in free space;

E_2 is the field strength of a beam reflected from the ground.

If the distance from the dipole to the point of observation is very much greater than H the directions in which these two beams are propagated can be considered as parallel (both beams have the same angle of tilt).

The reflected beam field strength equals

$$E_2 = E_1 |R| e^{i(\phi+\varphi_p)},$$

where

$|R|$ and ϕ are modulus and argument for the reflection factor, found through formula (V.5.6) in the case of the vertical dipole, and through formula (V.5.7) in the case of the horizontal dipole, if reception is in the equatorial plane;

φ_p is the angle of the phase displacement, determined by the difference in propagation between the incident and the reflected beams.

The difference in propagation equals AC-AB (fig. V.5.3). Correspondingly

$$\varphi_p = -\alpha(AC-AB).$$

Substituting

$$AC = H/\sin\Delta$$

and

$$AB = AC\cos 2\Delta = \frac{H\cos 2\Delta}{\sin\Delta}$$

and converting,

$$\varphi_p = -\alpha 2H\sin\Delta.$$

Thus,

$$E = E_1 + E_2 = E_1\left[1 + |R| e^{i(\phi-2\alpha H\sin\Delta)}\right]. \qquad (V.5.8)$$

If we imagine the ground as absent and that an identical dipole is located at distance 2H from the dipole in a direction normal to the plane of the section (fig. V.5.3), the difference in propagation between the beams from the main and the second dipoles will equal $A_1D = 2H\sin\Delta$, that is, the same relationship as exists between the outgoing and the reflected beams.

And if, in addition, it is assumed that the current flowing in the second dipole equals $I_2 = I_1R$, the amplitude and phase of the second dipole's field strength will be exactly those of the reflected beam.

So, in the case specified, as in the case of the ideally conducting ground, when the field is established as being at a great distance from the

dipole, the ground can be replaced by a distorted mirror image of the dipole, and the current flowing in the image should equal the current flowing in the dipole multiplied by the reflection factor. As follows from formulas (V.5.6) and (V.5.7), the reflection factor depends on the angle of tilt. Correspondingly, the amplitude and phase of the image current depend on the location of the point of observation.

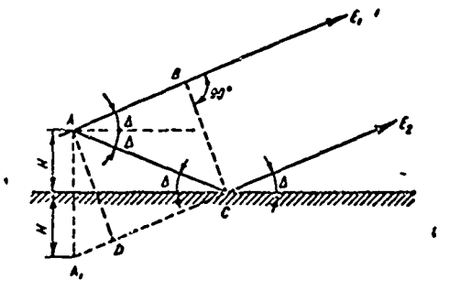

Figure V.5.3. Analysis of the directional properties of a dipole.

This method of establishing the field strength at a long distance from the elementary dipole can be used to establish the field strength of a balanced dipole, taking it as the sum of the elementary dipoles.

The field strength of a vertical balanced dipole equals

$$E_v = E_{v1} + E_{v2} = E_{v1}[1 + |R_{\parallel}| e^{i(\varphi_{\parallel} - 2\alpha H \sin\Delta)}].$$

The field strength of a horizontal dipole in the equatorial plane equals

$$E_h = E_{h1} + E_{h2} = E_{h1}[1 + |R_{\perp}| e^{i(\varphi_{\perp} - 2\alpha H \sin\Delta)}].$$

E_{v1} and E_{h1} are the field strengths of the outgoing beams from the vertical and horizontal dipoles. E_{v1} and E_{h1} can be established through the formulas for free space;

E_{v2} and E_{h2} are the field strengths of the reflected beams, or, what is the same thing, the field strengths of images equivalent to real ground;

H is the height at which the horizontal dipole is suspended. H is the height of suspension of the mean point in the case of the vertical dipole.

Substituting the expressions for E_{h1} and E_{v1} from (V.5.1) and (V.5.2), converting, and omitting the factors which characterize field strength phase, we obtain the following expressions for the vertical plane radiation patterns for vertical and horizontal dipoles:

$$F_v = 60 I_{loop}/r_0 \frac{\cos(\alpha l \sin\Delta) - \cos\alpha l}{\cos\Delta} \sqrt{1 + |R_1|^2 + 2|R_1|\cos(\psi_1 - 2\alpha H \sin\Delta)}, \quad (V.5.9)$$

$$E_h = 60I_{loop}/r_0\,(1-\cos\alpha l)\sqrt{1+|R_\perp|^2+2|R_\perp|\cos(\Phi_\perp - 2\pi l/\lambda\sin\Delta)}. \quad (V.5.10)$$

What follows is a brief explanation of Weyl's work, which provides a precise analysis of the elementary dipole, and what follows from this analysis is that the approximate theory of the radiation from a dipole close to the ground discussed here and based on the theory of the reflection of plane waves (the geometric optics method) provides correct results at long distance from the dipole if the error resulting because the earth is not flat is disregarded.

The components of the electromagnetic field are established by vector potential A (see #IV.8).

From formula (IV.8.3), the vector potential for the elementary dipole in free space equals

$$A_1 = \frac{\mu}{4\pi}\frac{Idl\,e^{-i\alpha r}}{r} = A_0\frac{e^{-i\alpha r}}{r},$$

where

A_0 is a coefficient which does not depend on r.

This expression for the vector potential corresponds to a spherical wave.

It can be proven that

$$\frac{e^{-i\alpha r}}{r} = -i\frac{\alpha}{2\pi}\int_0^{2\pi} d\psi \int_0^{\frac{\pi}{2}+i\infty} e^{-i\alpha r\cos\eta}\sin\eta\, d\eta. \quad (1')$$

In fact, let us designate the right-hand side of equation (1') by the letter Π. Integrating the right-hand side with respect to ψ,

$$\Pi = -i\alpha\int_0^{\frac{\pi}{2}+i\infty} e^{-i\alpha r\cos\eta}\sin\eta\, d\eta = -\frac{1}{r}\int_0^{\frac{\pi}{2}+i\infty} e^{-i\alpha r\cos\eta}\, d(-i\alpha r\cos\eta). \quad (2')$$

Let us put $-i\alpha r\cos\eta = \xi$. Then $d\xi = i\alpha r\sin\eta d\eta$. Let us make a change in the limits of integration

when $\eta = 0$ $\xi = -i\alpha r$,

when $\eta = \pi/2 + i\infty$ $\xi = -i\alpha r\cos(\pi/2 + i\infty) = i\alpha r\sin(i\infty) = -\infty$.

Substituting the new variable,

$$\Pi = -\frac{1}{r}\int_{-i\alpha r}^{-\infty} e^{\xi}\, d\xi = -\frac{1}{r}\,e^{\xi}\Big|_{-i\alpha r}^{-\infty} = \frac{e^{-i\alpha r}}{r}.$$

Substituting (1') in (IV.8.3),

$$A_1 = A_0\frac{e^{-i\alpha r}}{r} = -iA_0\frac{\alpha}{2\pi}\int_0^{2\pi} d\psi \int_0^{\frac{\pi}{2}+i\infty} e^{-i\alpha r\cos\eta}\sin\eta\, d\eta. \quad (3')$$

The expression under the integral sign in the right-hand side of (3') is a plane wave propagated in some direction at angle η to the direction of vector r; that is, at angle η to a line joining the dipole and the point of observation.

Thus, equation (3') demonstrates that spherical waves radiated by an elementary dipole in free space can be represented in the form of the sum of an infinitely large number of plane waves propagated at angle η to the direction of vector r lying in the limits from 0 to $\pi/2 + i\infty$. The integration is with respect to the surface of some sphere with radius equal to unity ($\sin\eta d\eta d\psi$ is an element of a sphere with radius equal to unity). Integration with respect to the azimuth angle (ψ) is from 0 to 2π.

If the elementary dipole is above the earth's surface it becomes obvious that the geometric optics method discussed above can be applied to each of the plane waves, and the expression for the vector potential of an elementary dipole located at height H above ground can be represented as follows

$$A = -iA_0\frac{\alpha}{2\pi}\int_0^{2\pi}\int_0^{\frac{\pi}{2}+i\infty} e^{-i\alpha r\cos\gamma}\sin\eta\left[1+|R_1|e^{i(\Phi_1-2\alpha H\sin\Delta_1)}\right]d\psi\,d\eta. \qquad (4')$$

where

Δ_1 is the angle of tilt to the ground of a plane wave propagated in a direction fixed by angles η and ψ; the limits of change in angle Δ_1 are fixed by the limits of change in angles η and ψ; $|R_1|$ and Φ_1 are the modulus and argument for Fresnel's coefficient for angle Δ_1.

Equation (4') can be rewritten

$$A = A_0\frac{(-i\alpha r)}{2\pi}\frac{e^{-i\alpha r}}{r}\int_0^{2\pi}\int_0^{\frac{\pi}{2}+i\infty} e^{-i\alpha r(\cos\gamma-1)}\sin\gamma P(\Delta_1)\,d\psi\,d\gamma, \qquad (5')$$

where

$$P(\Delta_1) = 1 + |R_1|\,e^{i(\Phi_1-2\alpha H\sin\Delta_1)}.$$

Let us introduce the new variable $\tau = i\alpha(\cos\eta - 1)$, whereupon $d\tau = -i\alpha\sin\eta d\eta$; when $\eta = 0$, $\tau = 0$; when $\eta = \pi/2 + i\infty$, $\tau = \infty$.

Substituting the new variable in (5')

$$A = A_0\frac{e^{-i\alpha r}}{r}\int_0^{\infty} e^{-\tau r}\left[\frac{1}{2\pi}\int_0^{2\pi}P(\Delta_1)\,d\psi\right]r\,d\tau =$$

$$= A_0\frac{e^{-i\alpha r}}{r}\int_0^{\infty} e^{-r\tau}\varphi(\tau)\,r\,d\tau = A_0\frac{e^{-i\alpha r}}{r}p(r), \qquad (6')$$

where

$$\varphi(\tau) = \frac{1}{2\pi}\int_0^{2\pi}P(\Delta_1)\,d\psi, \qquad (7')$$

$$p(r) = \int_0^{\infty} e^{-r\tau}\varphi(\tau)\,r\,d\tau. \qquad (8')$$

Let us expand the function $\varphi(\tau)$ into Maclaurin's series

$$\varphi(\tau) = a_0 + a_1\tau + a_2\tau^2 + \ldots + a_n\tau^n + \ldots, \qquad (9')$$

where

$$a_0 = \varphi(0);\ a_1 = \frac{\varphi'(0)}{1!};\ a_2 = \frac{\varphi''(0)}{2!};\ \ldots a_n = \frac{\varphi^{(n)}(0)}{n!};\ \ldots$$

Substituting (9') in (8'), we obtain

$$p(r) = a_0\int_0^\infty e^{-r\tau} r\,d\tau + a_1\int_0^\infty e^{-r\tau} r\tau\,d\tau +$$

$$+ a_2\int_0^\infty e^{-r\tau} r\tau^2\,d\tau + \ldots + a_n\int_0^\infty e^{-r\tau} r\tau^n\,d\tau + \ldots. \qquad (10')$$

Let us introduce a new variable $x = r\tau = i\alpha r(\cos\eta - 1)$.

Substituting the new variable, we obtain

$$p(r) = a_0\int_0^\infty e^{-x}\,dx + \frac{a_1}{r}\int_0^\infty e^{-x}x\,dx + \frac{a_2}{r^2}\int_0^\infty e^{-x}x^2\,dx + \ldots$$

$$\ldots + \frac{a_n}{r^n}\int_0^\infty e^{-x}x^n\,dx + \ldots = b_0 + \frac{b_1}{r} + \frac{b_2}{r^2} + \ldots + \frac{b_n}{r^n} + \ldots. \qquad (11')$$

where

$$b_0 = a_0\int_0^\infty e^{-x}\,dx,$$

$$b_1 = a_1\int_0^\infty e^{-x}x\,dx,$$

. . . . . .

$$b_n = a_n\int_0^\infty e^{-x}x^n\,dx.$$

. . . . . .

The coefficients b_0, b_1, b_2, ..., b_n, do not depend on r.

Let us find the expressions for these coefficients. Applying the method of integration by parts

$$b_n = a_n\int_0^\infty e^{-x}x^n\,dx = -a_n x^n e^{-x}\Big|_0^\infty + na_n\int_0^\infty x^{n-1}e^{-x}\,dx = 0 + na_n\int_0^\infty x^{n-1}e^{-x}\,dx.$$

Continuing the integration by parts

$$b_n = a_n n! \qquad (12')$$

Substituting the expression for a_n,

$$b_n = \varphi^{(n)}(0). \qquad (13')$$

Correspondingly,

$$b_0 = \varphi(0),$$
$$b_1 = \varphi'(0),$$
$$b_2 = \varphi''(0), \qquad (14')$$
. . . . . .

With (6'), (14') and (11') in mind, we obtain the following expression for the vector potential of an elementary dipole above ground level

$$A = A_0 \frac{e^{-i\alpha r}}{r} p(r) = A_0 \frac{e^{-i\alpha r}}{r} \left[\varphi(0) + \frac{\varphi'(0)}{r} + \frac{\varphi''(0)}{r^2} + \ldots \right.$$
$$\left. \ldots + \frac{\varphi^{(n)}(0)}{r^n} + \ldots \right]. \qquad (15')$$

Thus, the vector potential of an elementary dipole can be expressed by a series in negative powers of r.

Let us prove that the first term in this series is a magnitude determined by the above discussed approximate geometric optics method.

What follows from the expression $\tau = i\alpha r(\cos \eta - 1)$ is that when $\tau = 0$, $\eta = 0$; that is, the wave can be propagated in a direction from the dipole to the point of observation.

Correspondingly, we have $\Delta_1 = \Delta$, where Δ is the angle of tilt of the wave being propagated from the elementary dipole to the point of observation. Thus, when $\tau = 0$, $\Delta_1 = \Delta$, and Δ does not depend on ψ. With this in mind,

$$\varphi(0) = \left[\frac{1}{2\pi} \int_0^{2\pi} P(\Delta_1) d\psi \right]_{\Delta_1 = \Delta} = \frac{1}{2\pi} \int_0^{2\pi} \left[1 + |R| e^{i(\Phi - 2\alpha l \sin\Delta)} \right] d\psi =$$
$$= \left[1 + |R| e^{i(\Phi - 2\alpha l \sin\Delta)} \right]. \qquad (16')$$

Substituting the value for $\varphi(0)$ found in (15'),

$$A = A_0 \frac{e^{-i\alpha r}}{r} \left[1 + |R| e^{i(\Phi - 2\alpha l \sin\Delta)} \right] +$$
$$+ A_0 \frac{e^{-i\alpha r}}{r^2} \varphi'(0) + A_0 \frac{e^{-i\alpha r}}{r^3} \varphi''(0) + \ldots \qquad (17')$$

As we see, the first term in the series actually coincides with the approximate expression arrived at by the geometric optics method. When $\Delta = 0$, the first term of the series equals zero. Therefore, only the last terms in the series establish the surface (ground) waves. Without pausing to establish these latter terms here, we will simply point out that analysis too reveals that their sum has a maximum when $\Delta = 0$.

We can, therefore, confirm that if r is so large that the ground wave field strength is very much less than the sky wave field strength the first term in the series is the complete expression for A for any value of Δ, that is,

$$A = A_0 \frac{e^{-i\alpha r}}{r} \left[1 + |R| e^{i(\Phi - 2\alpha l \sin\Delta)} \right]. \qquad (V.5.11)$$

The expression at (V.5.11) corresponds to formula (V.5.8) for field strength.

What has been presented here demonstrates that a completely reliable criterion for establishing the value of r, beginning with which we can use the geometric optics method to chart the pattern, is the attenuation of the ground wave. The geometric optics method will yield results which are correct if the point of reception is at a distance from the dipole such that there is practically no ground wave present.

In the shortwave area the field attenuation at ground level is so great that within a few tens of waves the radiation patterns charted through the formulas obtained here coincide well with the experimental patterns, particularly in the case of the horizontal dipole suspended at a height on the order of $\lambda/4$, and higher.

If it is assumed that the ground is an ideal conductor ($\gamma_v = \infty$), then $|R_\parallel| = |R_\perp| = 1$, $\Phi_\parallel = 0$ and $\Phi_\perp = 180°$. And formulas (V.5.9) and (V.5.10) become identical with formulas (V.5.3) and (V.5.4).

(d) Radiation pattern of a balanced dipole in the horizontal plane for an arbitrary value of Δ

The radiation pattern of a vertical dipole is circular in the horizontal plane.

The composition of the expression for the field strength of a horizontal dipole in an arbitrary direction breaks each element, dl, of the dipole down into two component elements; one normal to the plane of incidence, and one lying in this plane.

The length of the first element equals dl sin φ, that of the second dl cos φ.

The element normal to the plane of incidence only gives the normal component of the field strength vector. The reflection factor for this element equals $R_\perp$.

The element lying in the plane of incidence only gives the parallel component of the field strength vector. The reflection factor for it equals $-R_\parallel$. The minus sign is shown because in the case of horizontal orientation of the conductor the positive direction of the field strength vector of the wave propagated toward the ground and creating a reflected wave is opposite in direction to the positive direction of the field strength vector of a wave directly incident to the point of reception (fig. V.5.4).

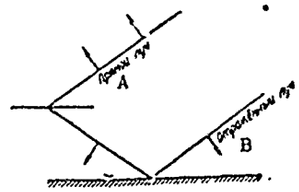

Figure V.5.4. Explanation of sign selection in the case of the reflection factor for a parallel polarized wave.
A - outgoing wave; B - reflected wave.

The corresponding incident and reflected waves are established as a result of breaking the elements of the balanced dipole down into two components in this same way. Doing the integration with respect to the entire length of the dipole, we find the normal ($E_\perp$) and parallel ($E_\parallel$) components of the field strength vector at the point of reception.

Carrying out the mathematical operations indicated, we obtain the following expressions for the field strength of a horizontal dipole in an arbitrary direction.

$$E_\perp = \frac{60I_0}{r_0 \operatorname{sh}\gamma l} \frac{\operatorname{ch}\gamma l - \cos(\alpha l \cos\varphi\cos\Delta)}{\frac{\alpha}{\gamma}\cos^2\varphi\cos^2\Delta + \frac{\gamma}{\alpha}} \sin\varphi \times$$
$$\times \sqrt{1 + |R_\perp|^2 + 2|R_\perp|\cos(\Phi_\perp - 2\alpha H\sin\Delta)}, \qquad (V.5.12)$$

$$E_\parallel = \frac{60I_0}{r_0 \operatorname{sh}\gamma l} \frac{\operatorname{ch}\gamma l - \cos(\alpha l \cos\varphi\cos\Delta)}{\frac{\alpha}{\gamma}\cos^2\varphi\cos^2\Delta + \frac{\gamma}{\alpha}} \cos\varphi\sin\Delta \times$$
$$\times \sqrt{1 + |R_\parallel|^2 - 2|R_\parallel|\cos(\Phi_\parallel - 2\alpha H\sin\Delta)}. \qquad (V.5.13)$$

The field strength vector exhibits elliptical polarization. The average value of Poynting's vector for the period, S_{av}, equals

$$S_{av} = \frac{|E_\perp|^2 + |E_\parallel|^2}{2W_i}. \qquad (V.5.14)$$

We can introduce the concept of an equivalent field strength value, establish it through

$$E_{eq} = \sqrt{2W_i S_{av}} = \sqrt{|E_\perp|^2 + |E_\parallel|^2}. \qquad (V.5.15)$$

E_{eq} is the field strength of a linearly polarized wave with the same average Poynting vector value as the elliptically polarized wave considered.

In the special case of ideally conducting ground, the field strength vector becomes linearly polarized, and formula (V.5.15) gives us an expression for the real summed value of the field strength. So, for ideally conducting ground,

$$E = \sqrt{|E_\perp|^2 + |E_\parallel|^2} =$$
$$= \frac{120I_0}{r_0 \operatorname{sh}\gamma l} \frac{\operatorname{ch}\gamma l - \cos(\alpha l\cos\varphi\cos\Delta)}{\frac{\alpha}{\gamma}\cos^2\varphi\cos^2\Delta + \frac{\gamma}{\alpha}} \sqrt{1 - \cos^2\varphi\cos^2\Delta}\sin(\alpha H\sin\Delta) \qquad (V.5.16)$$

In the general case, when there are two components of the field strength vector (E_1 and E_2), not parallel and out of phase, at the point of reception, the equivalent value of the field strength can be expressed by the formula

$$E_{eq} = \sqrt{|E_1|^2 + |E_2|^2 + 2|E_1|\cdot|E_2||\cos\rho|\cos(\nu_1 - \nu_2)}, \qquad (V.5.17)$$

where

σ is the solid angle between the E_1 and E_2 vectors;

v_1 and v_2 are the phase angles for the E_1 and E_2 vectors.

#V.6. Directional Properties of a System of Dipoles

Modern shortwave antennas are often built in the form of a complex system of dipoles positioned in a predetermined manner with respect to each other. In what follows we shall discuss in detail the methodology used to analyze directional properties as they apply to individual types of multi-element arrays. At this point we will simply comment that the directional properties of a system of dipoles can be analyzed by summing the fields of the individual elements in the system, in the same way that the directional properties of a line conductor can be analyzed by summing the fields of its component, elementary dipoles.

Variously shaped radiation patterns are obtained, depending on the number, the positioning, and the relationship of current amplitudes and phases for the individual dipoles.

#V.7. General Formulas for Calculating Radiated Power and Dipole Radiation Resistance

The Poynting vector method is one way in which to calculate the power radiated by an antenna.

This method is based on establishing the radiated power by integrating Poynting's vector in terms of the surface of a sphere, with the radiating antenna positioned in the center of the sphere. The radius of the sphere is selected such that the surface of the sphere is in the far zone for the antenna.

This method was described in detail in Chapter IV as applicable to the elementary dipole. The following general expression was obtained for radiated power

$$P_{\Sigma} = \frac{1}{2}\sqrt{\frac{\varepsilon}{\mu}}\int_0^{2\pi} d\varphi \int_0^{\pi} E^2 r^2 \sin\theta \, d\theta, \qquad (V.7.1)$$

where

r is the radius of the sphere for which power integration will be made;

θ is the wave's zenith angle;

φ is the wave's azimuth angle.

In general form, field strength E can be expressed as

$$E = 60I/r\ F(\varphi,\Delta), \qquad (V.7.2)$$

where

$\Delta = 90° - \theta$.

Substituting $\theta = 90° - \Delta$, and replacing the expression for E from formula (V.7.2) in formula (V.7.1), and taking it that for free space and air

$$\sqrt{\frac{\mu}{\varepsilon}} = \sqrt{\frac{\mu_0}{\varepsilon_0}} = W_l = 120\pi,$$

we obtain

$$P_\Sigma = \frac{15}{\pi} I^2 \int_0^{2\pi} d\varphi \int_{-\frac{\pi}{2}}^{\frac{\pi}{2}} F^2(\varphi, \Delta) \cos\Delta \, d\Delta. \qquad (V.7.3)$$

Conversely, the power radiated by an antenna can be expressed as

$$P_\Sigma = \frac{I^2}{2} R_\Sigma, \qquad (V.7.4)$$

where

R_Σ is the antenna's radiation resistance, equated to the current, I.

Comparing formulas (V.7.3) and (V.7.4), we obtain the following general expression for radiation resistance equated to current I,

$$R_\Sigma = \frac{30}{\pi} \int_0^{2\pi} d\varphi \int_{-\frac{\pi}{2}}^{\frac{\pi}{2}} F^2(\Delta, \varphi) \cos\Delta \, d\Delta. \qquad (V.7.5)$$

If the antenna is located above a flat, ideally conducting surface which coincides with the equatorial plane of the sphere, the integration need only be done with respect to the upper hemisphere. Then, in place of (V.7.5) we will have

$$R_\Sigma = \frac{30}{\pi} \int_0^{2\pi} d\varphi \int_0^{\frac{\pi}{2}} F^2(\Delta, \varphi) \cos\Delta \, d\Delta. \qquad (V.7.6)$$

Expressions (V.7.5) and (V.7.6) establish the fixed relationship between the shapes of the radiation patterns and the radiation resistance. These formulas can be used for any antenna.

#V.8. Calculating the Radiation Resistance of a Balanced Dipole

We will use the general expression at (V.7.5) to establish the radiation resistance of a balanced dipole in free space, and we will direct the axis of the dipole along the polar axis of the sphere. The radiation pattern of the dipole will not depend on angle φ, and (V.7.5) will take the form

$$R_\Sigma = 60 \int_{-\frac{\pi}{2}}^{\frac{\pi}{2}} F^2(\Delta) \cos\Delta \, d\Delta. \qquad (V.8.1)$$

Here we substitute the expression for $F(\Delta)$, for which we will use the expression at (V.4.3), taking it at the same time that $\theta = 90° - \Delta$. Making the integration, we obtain the following expression for radiation resistance equated to the current in the loop, I_{loop},

$$R_{\Sigma} = 30\{2(E + \ln 2\alpha l - \mathrm{ci}\, 2\alpha l) + \sin 2\alpha l(\mathrm{si}\, 4\alpha l - 2\,\mathrm{si}\, 2\alpha l) + \cos 2\alpha l(E + \ln \alpha l + \mathrm{ci}\, 4\alpha l - 2\,\mathrm{ci}\, 2\alpha l)\}, \quad (V.8.2)$$

where

si x is the sine integral from the argument for x

$$\mathrm{si}\, x = \int_0^x \frac{\sin u}{u}\, du = x - \frac{1}{3}\frac{x^3}{3!} + \frac{1}{5}\frac{x^5}{5!} - \ldots,$$

ci x is the cosine integral from the argument for x

$$\mathrm{ci}\, x = -\int_x^{\infty} \frac{\cos u}{u}\, du = E + \ln x - \frac{1}{2}\frac{x^2}{2!} + \frac{1}{4}\frac{x^4}{4!} - \ldots,$$

ln x is the natural logarithm from the argument for x;

E = 0.57721 is Euler's constant.

For the case when $l/\lambda \ll 1$, formula (V.8.2) will reduce to

$$R_{\Sigma} = 20\,(\alpha l)^4. \quad (V.8.3)$$

As a practical matter, formula (V.8.3) can be used for values for l/λ within the limits $0 < l/\lambda < 0.1$.

Figures V.8.1a and V.8.1b show the curves for the dependence of R_{Σ} on l/λ.

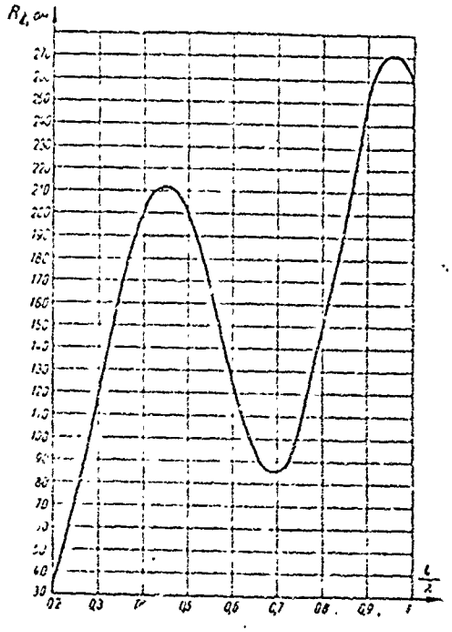

Figure V.8.1a. Dependence of the radiation resistance of a balanced dipole on the l/λ ratio.

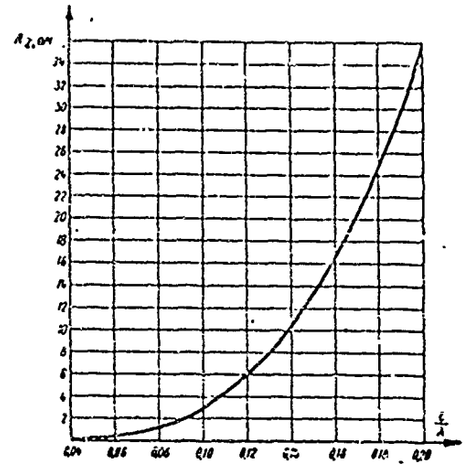

Figure V.8.1b. Dependence of the radiation resistance of a balanced dipole on the l/λ ratio.

The formulas obtained for calculating radiation resistance are approximate because they are based on the assumption concerning a sinusoidal shape for the distribution curve for current along the conductor which actually does not take place. Experience does demonstrate, however, that the results obtained through the use of these formulas agree well with actual data.

Particularly good coincidence is obtained for thin and short conductors in which the current distribution obtained is extremely close to sinusoidal in practice.

#V.9. Radiation Resistance of a Conductor Passing a Traveling Wave of Current

The method for calculating radiation resistance above can be applied as well to a conductor passing a traveling wave. Analysis demonstrates that the radiation resistance of a single conductor passing a traveling wave equals

$$R_{\Sigma} = 60\left(\ln 2\pi l - \operatorname{ci} 2\pi l + \frac{\sin 2\pi l}{2\pi l} - 0{,}423\right), \qquad (V.9.1)$$

where

l is conductor length.

Figure V.9.1 shows the curve for the dependence of R_{Σ} on l/λ.

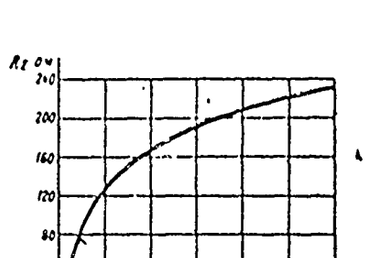

Figure V.9.1. Dependence of the radiation resistance of a conductor passing a traveling wave of current on the l/λ ratio.

#V.10. Calculation of the Input Impedance of a Balanced Dipole

On the basis of the assumption made in this chapter that the current distribution along a radiating conductor is subject to the law of the theory of uniform long lines, the formula for this theory can be used to calculate the input impedance.

The calculation for the influence of radiation on the input impedance can be made by introducing an attenuation factor which it can be assumed is equal to

$$\beta = R_1/2W \qquad (V.10.1)$$

where

R_1 is the radiation resistance per unit length of the dipole; the magnitude of R_1 is assumed to be identical along the entire length of the dipole;

W is the characteristic impedance of the dipole.

Thus, we will consider the balanced dipole to be an open-ended twin line. The length of the equivalent twin line is equal to the length of one arm of the dipole.

The input impedance of an open-circuit line can, in accordance with the long-line theory specified, be calculated through the formula

$$Z_{in} = W\frac{\operatorname{sh} 2\beta l - \frac{\beta}{\alpha}\sin 2\alpha l}{\operatorname{ch} 2\beta l - \cos 2\alpha l} - iW\frac{\frac{\beta}{\alpha}\operatorname{sh} 2\beta l + \sin 2\alpha l}{\operatorname{ch} 2\beta l - \cos 2\alpha l}, \qquad (V.10.2)$$

An approximation of the characteristic impedance, W, can be made through

$$W = 120\left(\ln\frac{2l}{d} - 1\right), \qquad (V.10.3)$$

where

d is conductor diameter.

Formula (V.10.1) can be used to establish the attenuation factor β.

If loss resistance is disregarded, the distributed resistance R_1 can be established as follows.

The power radiated by element dz of the conductor equals

$$dP_z = \frac{I_z^2}{2} R_1 \, dz,$$

where

I_z is the current flowing in the element;

$R_1 dz$ is the radiation resistance of element dz.

The power radiated by all dipoles, defined as the sum of the powers radiated by the elementary dipoles, equals

$$P_\Sigma = \int_0^l \frac{1}{2} I_z^2 R_1 dz. \qquad \text{(V.10.4)}$$

Conversely, the power radiated by the dipole equals

$$P_\Sigma = I_{loop}^2/2 \; R_\Sigma \qquad \text{(V.10.5)}$$

Equating the right sides of formulas (V.10.4) and (V.10.5),

$$I_{loop}^2 R_\Sigma = R_1 \int_0^l I_z^2 dz. \qquad \text{(V.10.6)}$$

Substituting the value of the current flowing in the dipole, $I_z = I_{loop} \sin \alpha(l-z)$, at this point and integrating,

$$R_1 = \frac{2R_\Sigma}{l\left(1 - \frac{\sin 2\alpha l}{2\alpha l}\right)}. \qquad \text{(V.10.7)}$$

From formulas (V.10.1) and (V.10.7),

$$\beta l = \frac{R_1 l}{2W} = \frac{R_\Sigma}{W\left(1 - \frac{\sin 2\alpha l}{2\alpha l}\right)}. \qquad \text{(V.10.8)}$$

Formula (V.10.2), after substituting the value for βl from formula (V.10.8), reduces to the following approximate form for short dipoles

$$Z_{in} = \frac{R_\Sigma}{\sin^2 \alpha l} - i\,W \operatorname{ctg} \alpha l. \qquad \text{(V.10.9)}$$

Formula (V.10.9) gives precise enough results for dipoles with arm lengths $l \leqslant 0.3\ \lambda$.

If the characteristic impedance of a balanced dipole is greater than 600 to 700 ohms, formula (V.10.9) can be used for values of l lying in the limits (0.to 0.4)λ and (0.6 to 0.9)λ.

If the dipole has noticeable losses, $R_{\Sigma} + R_{loss}$ should be introduced in place of R_{Σ}, where R_{loss} is the loss resistance, equated to the current loop.

Chapter IX contains the curves for the dependence of R_{in} and X_{in} on l/λ, calculated for different values of W. This same chapter points out the area in which the formulas obtained here can be used.

#V.11. General Remarks About Coupled Dipoles

The methodology discussed above for calculations involving radiation resistance and input impedance is suitable for the case of the single dipole.

The practice in the shortwave field, as well as in other wavebands, is to make widespread use of multi-element antennas consisting of many dipoles. Moreover, even in the case of the single dipole its mirror image, which is established by the ground effect, sets up conditions similar to those when two dipoles are functioning in conjunction with each other.

Dipoles located close to each other induce emfs in each other. This creates cross-coupling between the dipoles similar to that taking place when circuits with lumped constants are positioned close to each other. Cross-coupling results in a change in radiation resistance and input impedance in each of the dipoles. The radiation resistance of each of the coupled dipoles is made up of two resistances, own and induced. The induced resistances, which occur in the special case when the currents flowing in the coupled dipoles is made up of two resistances, own and induced. The induced resistances, which occur in the special case when the currents flowing in the coupled dipoles are identical in amplitude and phase, are called mutual radiation resistances.

We shall, in what follows, prove that the currents and input impedance for any combination of coupled dipoles can be calculated if the totals of own and mutual radiation resistances are known.

The resistive component of own radiation resistance can be established by the Poynting vector method explained above.

The reactive component of own radiation resistance, as well as the mutual radiation resistances, can be established by the induced emf method.

#V.12. Induced emf Method. Calculation of Induced and Mutual Resistances. Approximate Formulas for Calculating Mutual Resistances.

(a) General expression for induced radiation resistance

The induced emf method was devised by I. G. Klyatskin and developed by A. A. Pistol'kors and V. V. Tatarinov. The general theoretical hypotheses formulated by F. A. Rozhanskiy and Brillouin are the basis for the method, the substance of which is as follows. Suppose we locate two dipoles in arbitrary fashion with respect to each other (fig. V.12.1). The current

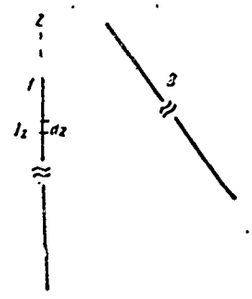

Figure V.12.1. Explanation of the substance of the induced emf method.

flowing in dipole 2 will set up a field near dipole 1. Now let the tangential component of the field strength vector for the field set up by the current flowing in dipole 2 at the surface of element dz of dipole 1 equal $E_{z\,12}$. Then the emf induced by the current flowing in dipole 2 in element dz of dipole 1 will equal

$$de_{12} = E_{z\,12}dz \ . \qquad (V.12.1)$$

The tangential component of the electric field strength vector at the conductor surface should equal zero. Therefore, the dipole 2 field causes a redistribution of dipole 1 own field to occur in such a way that there is a self-emf at the surface of element dz equal to $-de_{12}$, and the resultant tangential component of the field strength vector is zero. And so, as a result of the current flowing in dipole 2 we have emf $-de_{12}$, generated by the power source connected to dipole 1, acting acrosss element dz.

The power developed by the emf source equals

$$P = eI^*/2 \ ,$$

where

e is the complex amplitude of the source emf;

I is the complex amplitude of the current flowing at the point of application of the emf;

I* is a magnitude, conjugate of I.[1]

For the case under consideration, the effect of conductor 2 on conductor 1 is

$$dP_{12} = -\frac{1}{2} I_z^* de_{12} = -\frac{1}{2} I_z^* E_{z12} dz, \qquad (V.12.2)$$

where

I_z is the complex amplitude of the current flowing in element dz;

I^*_z is a magnitude, conjugate of current I_z.

---

1. The conjugate magnitude of a complex number is that complex magnitude with an argument of opposite sign. If current I equals $I=I_0 e^{i\varphi}$, the magnitude conjugate of I equals $I^*=I_0 e^{-i\varphi}$.

The magnitude of dP_{12} characterizes the power efficiency of the energy source for dipole 1 sustaining the emf $-de_{12}$ in the space around the dipole where the counter-emf, de_{12}, is concentrated. In other words, dP_{12} is the power radiated into space.

The power expended in dipole 1 as a result of the field of dipole 2 equals

$$P_{12} = -\frac{1}{2}\int_{\gamma} I_1^* E_{z12}\,dz. \qquad \text{(V.12.3)}$$

Formula (V.12.3) expresses total power, consisting of the resistive and reactive components.

The analogy of the resistance of conventional circuits can be used to establish the radiation resistance as the ratio of power to half the square of current amplitude for current $|I|^2$,

$$Z_{\text{induced}} = \frac{P_{12}}{\frac{1}{2}|I|^2} = -\frac{1}{|I|^2}\int_{\gamma} I^* E_{z12}\,dz. \qquad \text{(V.12.4)}$$

The real and the imaginary components in the right-hand side of equation (V.12.4) yield the resistive and reactive components of the impedance equated to current I.

The resistive component of P_{12} characterizes the energy leaving the dipole for surrounding space, or received by the dipole from that space. The reactive component of P_{12} characterizes the energy of the electromagnetic field coupled with the dipole (not radiated into surrounding space).

According to established terminology the resistive component of Z_{induced} is called the resistive impedance of the radiation, while the reactive component of Z_{induced} is called the reactive impedance of the radiation, although the latter component in essence characterizes the coupled (unradiated) electromagnetic field energy.

The methodology described for calculating the induced radiation resistance is applicable to any coupled dipoles located in any manner chosen with respect to each other. Given below is the application of this methodology to the special case, although one very often found in practice, when dipoles 1 and 2 have identical geometric dimensions and are parallel to each other. In accordance with what has been said in the foregoing (see #V.11), we shall limit ourselves to establishing the induced resistance when the currents flowing in both dipoles are identical in magnitude and phase. In other words, what we will be seeking is the mutual radiation resistance.

(b) The use of the induced emf method to calculate the mutual radiation resistance of two parallel dipoles

Let us take two balanced dipoles, 1 and 2 (fig. V.12.2), and, as for the calculation of radiation power using the Foynting vector method, we will take current distribution to be sinusoidal.

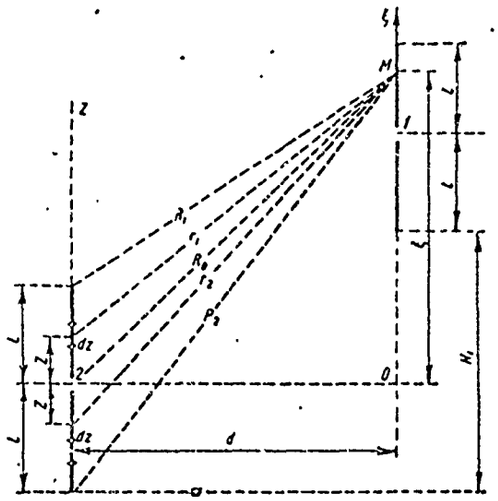

Figure V.12.2. Derivation of the formula for mutual radiation resistance.

Let us designate the axis passing through dipole 2 by z, and the axis passing through dipole 1 by ξ. We will take the mid-point of dipole 2 as the origin of the z axis, and we will take as the origin of the ξ axis the point of intersection of this axis with a normal to the z axis passing through the origin of this axis.

Current distribution over the upper half of dipole 2 can be expressed by

$$I_2 = I_{loop}\sin[\alpha(l-z)]e^{i\omega t} \qquad (V.12.5)$$

and the current distribution over the lower half of dipole 2 can be expressed by

$$I_2 = I_{loop}\sin[\alpha(l+z)]e^{i\omega t}. \qquad (V.12.6)$$

Upper half current for dipole 1 can be expressed by

$$I_1 = I_{loop}\sin[\alpha(l+H_1-\xi)]e^{i\omega t}, \qquad (V.12.7)$$

and lower half current by

$$I_1 = I_{loop}\sin[\alpha(l-H_1+\xi)]e^{i\omega t} \qquad (V.12.8)$$

(for the value of H_1 see Figure V.12.2).

Let us find the expression for the strength of the field created by dipole 2 at an arbitrary point M on dipole 1. We will only be interested in the component of the field strength vector parallel to the dipole axis, and we designate this component $E_{\xi 12}$.

The component parallel to the axis of a linear dipole is established through the vector potential through formula (IV.8.8) in the case of harmonic oscillations.

Thus, in the case specified,

$$E_{\xi 12} = -i\omega A - \frac{1}{\varepsilon\mu\omega}\frac{\partial^2 A}{\partial \xi^2}. \qquad (V.12.9)$$

Substituting the expression for A from formula (IV.8.3), and taking it that in the case specified the current can be established through formulas (V.12.5) and (V.12.6), we obtain

$$E_{\xi 12} = -i\frac{\omega}{4\pi} I_{loop} \int_0^l \frac{e^{i(\omega t-\alpha r_1)}}{r_1} \sin[\alpha(l-z)]dz - i\frac{1}{4\pi\varepsilon\omega} \times$$

$$\times I_{loop} \frac{\partial^2}{\partial \xi^2} \int_0^l \frac{e^{i(\omega t-\alpha r_1)}}{r_1} \sin[\alpha(l-z)]dz - i\frac{\mu\omega}{4\pi} I_{loop} \int_{-l}^0 \frac{e^{i(\omega t-\alpha r_2)}}{r_2} \times$$

$$\times \sin[\alpha(l+z)]dz - i\frac{1}{4\pi\varepsilon\omega} I_{loop} \frac{\partial^2}{\partial \xi^2} \int_{-l}^0 \frac{e^{i(\omega t-\alpha r_2)}}{r_2} \sin[\alpha(l+z)]dz. \qquad (V.12.10)$$

Here r_1 and r_2 are the distances from the arbitrary, symmetrically located elements, dz, of the upper and lower halves of dipole 2 to the arbitrary point M on dipole 1:

$$r_1 = \sqrt{d^2 + (\xi - z)^2},$$

$$r_2 = \sqrt{d^2 + (\xi + z)^2};$$

where

d is the distance between the axes of dipoles 1 and 2.

The first two integrals yield the component of the vector for the field strength established by the currents in the upper half, while the other two integrals yield the component of the vector for the field strength established by the currents in the lower half of dipole 2 (fig. V.12.3). Making the integration and the necessary transformations, substituting $\omega=\alpha/\sqrt{\varepsilon\mu}$, and taking it that for air $\varepsilon = \varepsilon_0 = 1/36\pi\cdot 10^9$ and $\mu = \mu_0 = 4\pi/10^7$, we obtain the following expression for the component of the vector for the field strength created by dipole 2,

$$E_{\xi 12} = -i30 I_{loop}\left(\frac{e^{-i\alpha R_1}}{R_1} + \frac{e^{-i\alpha R_2}}{R_2} - 2\frac{e^{-i\alpha R_0}}{R_0}\cos\alpha l\right)e^{i\omega t}, \qquad (V.12.11)$$

where

$R_1 = \sqrt{(\xi - l)^2 + d^2}$ is the distance from point M to the upper end of dipole 2;

$R_2 = \sqrt{(\xi + l)^2 + d^2}$ is the distance from point M to the lower end of dipole 2;

$R_0 = \sqrt{\xi^2 + d^2}$ is the distance from point M to the center of dipole 2.

Let us find the expression for the mutual impedance by using general formula (V.12.4). Whereupon

$$Z_{12} = -\frac{1}{I_{loop}^2}\int_{H_1-l}^{H_1} E_{\xi 12} I_1^* \, d\xi - \frac{1}{I_{loop}^2}\int_{H_1}^{H_1+l} E_{\xi 12} I_1^* d\xi . \qquad (V.12.12)$$

The first summand yields the component of Z_{12} for the lower half of dipole 1, the second summand the component of Z_{12} for the upper half of dipole 1.

Substituting the expression for $E_{\xi 12}$ from formula (V.12.11), and the expression for I_1 from formula (V.12.7) and (V.12.8) for the lower and upper halves of dipole 1, and omitting the time factor, we obtain

$$Z_{12} = i30\left[\int_{H_1-l}^{H_1}\left(\frac{e^{-ikR_1}}{R_1} + \frac{e^{-ikR_2}}{R_2} - 2\cos kl\,\frac{e^{-ikR_0}}{R_0}\right)\times\right.$$

$$\times \sin k(l - H_1 + \xi)\,d\xi + \int_{H_1}^{H_1+l}\left(\frac{e^{-ikR_1}}{R_1} + \frac{e^{-ikR_2}}{R_2} -\right.$$

$$\left.\left. - 2\cos kl\,\frac{e^{-ikR_0}}{R_0}\right)\sin k(l + H_1 - \xi)\,d\xi\right]. \qquad (V.12.13)$$

The result of integrating (V.12.13) is the following formula for calculating mutual radiation resistance, equated to a current loop

$$Z_{12} = R_{12} + iX_{12}, \qquad (V.12.14)$$

where

$$R_{12} = 15\{(K_1\sin q + L_1\cos q) + [(K_2\sin(q+2p) + L_2\cos(q+2p)] + [K_3\sin(q-2p) + L_3\cos(q-2p)]\}, \qquad (V.12.15)$$

$$X_{12} = 15\{(M_1\sin q + N_1\cos q) + [M_2\sin(q+2p) + N_2\cos(q+2p)] + [M_3\sin(q-2p) + N_3\cos(q-2p)]\}, \qquad (V.12.16)$$

$$
\left.\begin{aligned}
K_1 &= 2\,[2f_2(\delta, q) - f_2(\delta, q+p) - f_2(\delta, q-p)]\\
L_1 &= 2\,[2f_3(\delta, q) - f_3(\delta, q+p) - f_3(\delta, q-p)]\\
K_2 &= f_2(\delta, q) - 2f_2(\delta, q+p) + f_2(\delta, q+2p)\\
L_2 &= f_3(\delta, q) - 2f_3(\delta, q+p) + f_3(\delta, q+2p)\\
K_3 &= f_2(\delta, q) - 2f_2(\delta, q-p) + f_2(\delta, q-2p)\\
L_3 &= f_3(\delta, q) - 2f_3(\delta, q-p) + f_3(\delta, q-2p)\\
M_1 &= 2\,[2f_4(\delta, q) - f_4(\delta, q+p) - f_4(\delta, q-p)]\\
N_1 &= -2\,[2f_1(\delta, q) - f_1(\delta, q+p) - f_1(\delta, q-p)]\\
M_2 &= f_4(\delta, q) - 2f_4(\delta, q+p) + f_4(\delta, q+2p)\\
N_2 &= -f_1(\delta, q) + 2f_1(\delta, q+p) - f_1(\delta, q+2p)\\
M_3 &= f_4(\delta, q) - 2f_4(\delta, q-p) + f_4(\delta, q-2p)\\
N_3 &= -f_1(\delta, q) + 2f_1(\delta, q-p) - f_1(\delta, q-2p)
\end{aligned}\right\} \qquad \text{(V.12.17)}
$$

The following notations have been adopted in formulas (V.12.15 to V.12.17)

$$p = \alpha l = 2\pi \frac{l}{\lambda}, \quad q = \alpha H_1 = 2\pi \frac{H_1}{\lambda}, \quad \delta = \alpha d = 2\pi \frac{d}{\lambda}.$$

The functions $f(\delta,u)$ contained in the expressions for coefficients K, L, M and N have the following form

$$
\begin{aligned}
f_1(\delta, u) &= \mathrm{si}\left(\sqrt{u^2+\delta^2}+u\right) + \mathrm{si}\left(\sqrt{u^2+\delta^2}-u\right),\\
f_2(\delta, u) &= \mathrm{si}\left(\sqrt{u^2+\delta^2}+u\right) - \mathrm{si}\left(\sqrt{u^2+\delta^2}-u\right),\\
f_3(\delta, u) &= \mathrm{ci}\left(\sqrt{u^2+\delta^2}+u\right) + \mathrm{ci}\left(\sqrt{u^2+\delta^2}-u\right),\\
f_4(\delta, u) &= \mathrm{ci}\left(\sqrt{u^2+\delta^2}+u\right) - \mathrm{ci}\left(\sqrt{u^2+\delta^2}-u\right).
\end{aligned}
$$

In the expressions for the coefficients K, L, M, and N the variable δ is a parameter, and the variable u is an argument, taking the following values

$$q = 2\pi \frac{H_1}{\lambda}; \quad q+p = 2\pi\left(\frac{H_1}{\lambda}+\frac{l}{\lambda}\right); \quad q-p = 2\pi\left(\frac{H_1}{\lambda}-\frac{l}{\lambda}\right);$$

$$q+2p = 2\pi\left(\frac{H_1}{\lambda}+2\frac{l}{\lambda}\right); \quad q-2p = 2\pi\left(\frac{H_1}{\lambda}-2\frac{l}{\lambda}\right).$$

The curves for the functions $f(\delta,u)$ are shown in the handbook section (#H.III.1).

The handbook section also shows the curves for the dependence of R_{12} and X_{12} on d/λ for the special case when $H_1 = 0$ for different values of αl (figs. H.III.25 - H.III.38), and curves for R_{12} and X_{12} (figs. H.III.6 to H.III.21) for half-wave dipoles ($2l = \lambda/2$) for different values of H_1/λ.

(c) The use of the induced emf method to calculate own radiation resistance

Formula (V.12.11) for the induced tangential component of the vector for electric field strength can be converted into a formula for the tangential

eigen component of the field if we put $H_1 = 0$ and $d = \rho$ (ρ is the radius of the conductor).

The interaction between the dipole current and the tangential component of the vector for the strength of own field is of the same nature as that described above as occurring between the dipole current and the tangential component of the vector for the field strength induced by an adjacent dipole, and also causes power radiation.

Own radiation resistance is related to the power radiated as a result of own field. The expression for own radiation resistance can be obtained by substituting $H_1 = 0$ and $d = \rho$ into formulas (V.12.15) and (V.12.16), whereupon, as related to a current loop

$$R_{11} = 30\{2(E + \ln 2\alpha l - \operatorname{ci} 2\alpha l) + \sin 2\alpha l(\sin 4\alpha l - 2\operatorname{si} 2\alpha l) + \\ + \cos 2\alpha l(E + \ln \alpha l + \operatorname{ci} 4\alpha l - 2\operatorname{ci} 2\alpha l)\}, \qquad (V.12.18)$$

$$X_{11} = 30\{2\operatorname{si} 2\alpha l + \sin 2\alpha l(E + \ln \alpha l + \operatorname{ci} 4\alpha l - \\ - 2\operatorname{ci} 2\alpha l - 2\ln\frac{l}{\rho}) + \cos 2\alpha l(-\operatorname{si} 4\alpha l + 2\operatorname{si} 2\alpha l)\}. \qquad (V.12.19)$$

As will be seen, own radiation resistance has a reactive component.

The expression for the resistive component of the radiation resistance coincides with the corresponding expression obtained above by Poynting's vector method, as should be expected, because both methods reduce to the integration of the power radiated by the dipole in the suggested sinusoidal shape for the current distribution curve.

The principal difference between Poynting's vector method and the induced emf method is that in the former the power integration is done in the far zone, where reactive power equals zero, whereas in the latter the power integration is done in direct proximity to the dipole where there is reactive power associated with the dipole. Hence, the former yields only the resistive component of the radiation resistance, whereas the latter gives not only the resistive component, but the reactive component of the radiation resistance as well.

We note that the above cited references to the error in Poynting's vector method (#V.8) established by the postulation of a sinusoidal shape for the current distribution curve applies equally to the induced emf method.

This error manifests itself to a greater degree in the computation of own radiation resistance than it does in the computation of radiation resistance induced by adjacent dipoles.

Figure V.12.3 shows the curve for the dependence of X_{11} on l/λ. The reactive component of the radiation resistance equals 42.5 ohms when $l/\lambda = 0.25$.

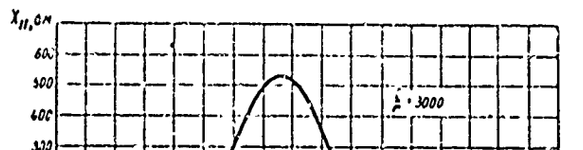

Figure V.12.3. Dependence of the reactive component of own radiation resistance of a balanced dipole equated to a current loop on l/λ in the case of a standing wave of current along the conductor; $l/D = 3000$.

When $l/\lambda = 0.25$ the radiation resistance, equated to a current loop, equals the dipole's input impedance. Thus, the induced emf method demonstrates that the first resonant length of a radiating conductor (the length at which the reactive component of the input impedance equals zero) is shorter than the resonant length of a conventional line, that is, the phase velocity of propagation along the dipole is less than the speed of light. Formula (V.10.2) for calculating input impedance does not take this into consideration. Chapter IX will discuss the calculation for the reduction in propagation phase velocity, as well as other circumstances which result in displacement of the resonant wave from the radiating conductor.

(d) Approximate formulas for calculating the mutual impedance of dipoles

Formulas for calculating mutual impedances are extremely cumbersome. For example, the formula for the case of parallel dipoles of the same length contains 72 summands. Similar formulas for the general case are even more complex. The graphics on the subject in the literature (see the Handbook Section, H.III) are far from all-inclusive, so far as all the practical cases of interest are concerned.

Given below are the approximate formulas for calculating mutual impedances, obtained by V. G. Yampolskiy and V. L. Lokshin. They were derived for the most interesting case, that of two parallel, unloaded dipoles of the same length. It should be noted that the methodology specified can also be used for the general case.

The general formula for establishing the mutual impedance of two parallel dipoles (formula V.12.13) will, after the new variable $u=l\pm(H_1-\xi)$ is introduced, take the form

$$Z_{12} = i30\alpha \int_0^l [\varphi(A_0) + \varphi(A_2) - 2\cos\alpha l\,\varphi(A_1)] \sin\alpha u\,du, \tag{V.12.20}$$

where

$$\varphi(A_\kappa) = \frac{e^{-i\alpha\sqrt{(H_1-\kappa l+u)^2+d^2}}}{\alpha\sqrt{(H_1-\kappa l+u)^2+d^2}} + \frac{e^{-i\alpha\sqrt{(H_1+\kappa l-u)^2+d^2}}}{\alpha\sqrt{(H_1+\kappa l-u)^2+d^2}}, \tag{V.12.21}$$

$$\kappa = 0,1,2.$$

The concept behind the derivation of the approximate formula involves "averaging" the present distances $R_k = \sqrt{(H_1 \pm kl \pm u)^2 + d^2}$ contained in formula (V.12.21).

Calculations have shown that when the constant of integration with respect to dipole length is changed the change in the integrand

$$F(u) = \varphi(A_0) + \varphi(A_2) - 2\cos\alpha l\,\varphi(A_1)$$

will be relatively slight if the distance between the centers of the dipoles, $\rho_0 = \sqrt{H_1^2 + d^2}$, are not very small. Therefore, the integrand F(u) can be taken from under the integral sign without appreciable error, putting $u = u_0 = l/2$. This selection of u_0 will yield the smallest error.

The approximate formula will be in the form

$$Z_{12} = i30(1 - \cos\alpha l)\,F\left(\frac{l}{2}\right). \tag{V.12.22}$$

after the integration is made.

Analysis has revealed that formula (V.12.22) is applicable when calculating mutual impedances of parallel dipoles with arm lengths $\alpha l < 200°$ to 220°. Use of formula (V.12.22) to compute the resistive component of the mutual impedance will result in an error of a few percentage points for any distances between dipoles. Accuracy increases with increase in the distance between dipoles when the approximate formula is used.

The reactive component of the mutual impedance can be computed through formula (V.12.22), but only when the distances between the centers of the dipoles are

$$\rho_0 = \sqrt{H_1^2 + d^2} \geqslant 1.5l \text{ to } 2l,$$

and the accuracy provided is at least 2 to 5%.

Figures V.12.4 and V.12.5 show the curves of the resistive and reactive components of the mutual resistance of two half-wave dipoles ($\alpha l = 90°$) with relation to αd for the cases $H_1 = 0$ and $H_1 = 2l$ by way of illustrating the accuracy provided by the approximate formula. The solid lines are based on the precise formula, the dotted ones on the approximate formula.

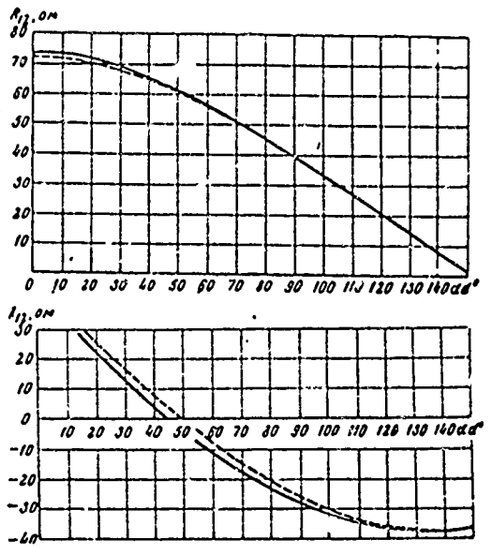

Figure V.12.4. Curves of the resistive and reactive components of the mutual impedance of two half-wave dipoles ($\alpha l = 90°$); $H_1 = 0$.

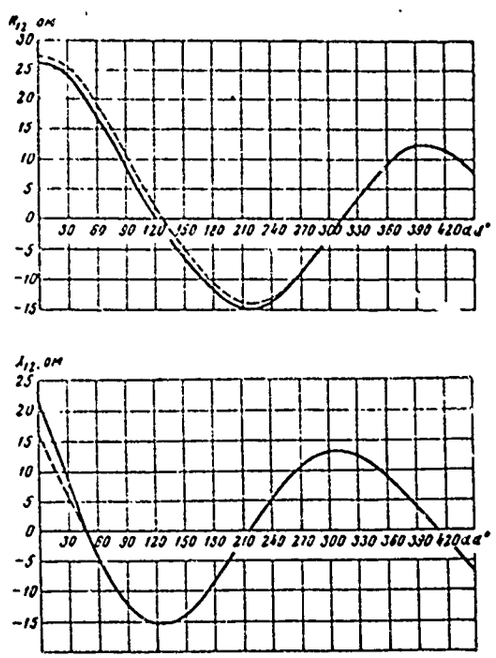

Figure V.12.5. Curves of the resistive and reactive components of the mutual impedance of two half-wave dipoles ($\alpha l = 90°$); $H_1 = 2l$.

#V.13. Use of the Induced emf Method to Calculate Radiation Resistance and Currents in the Case of Two Coupled Dipoles

Let there be two dipoles arbitrarily positioned with respect to each other. Let the emf induced by dipole 2 in dipole 1 at a current loop in dipole 1 equal e_{12}, and the emf induced by dipole 1 in dipole 2 at a current loop in dipole 2 equal e_{21}. Obviously,

$$U_1 = I_{1\ loop}Z_{11} + e_{12} = I_{1\ loop}Z_{11} + I_{1\ loop}Z_{12\ induced},$$

$$U_2 = I_{2\ loop}Z_{22} + e_{21} = I_{2\ loop}Z_{22} + I_{2\ loop}Z_{21\ induced}, \qquad (V.13.1)$$

where

U_1 and U_2 are the voltages applied across dipoles 1 and 2 converted to the current loops;

$I_{1\ loop}$ and $I_{2\ loop}$ are the currents flowing in the current loops of dipoles 1 and 2;

Z_{11} and Z_{22} are self radiation resistances of dipoles 1 and 2;

$Z_{12\ induced}$ is the radiation resistance induced in dipole 1 by the current flowing in dipole 2;

$Z_{21\ induced}$ is the radiation resistance induced in dipole 2 by the current flowing in dipole 1.

Obviously, $Z_{12\ induced}$ is proportional to the current flowing in dipole 2, while $Z_{21\ induced}$ is proportional to the current flowing in dipole 1. Thus,

$$\left.\begin{aligned} Z_{12\ induced} &= Z_{12}\, I_{2\ loop}/I_{1\ loop} \\ Z_{21\ induced} &= Z_{21}\, I_{1\ loop}/I_{2\ loop} \end{aligned}\right\} \qquad (V.13.2)$$

where

Z_{12} and Z_{21} are the mutual impedances, that is, the induced resistances for the condition $I_{1\ loop} = I_{2\ loop}$.

Substituting (V.13.2) in (V.13.1),

$$\left.\begin{aligned} U_1 &= I_{1\ loop}Z_{11} + I_{2\ loop}Z_{12} \\ U_2 &= I_{2\ loop}Z_{22} + I_{1\ loop}Z_{21} \end{aligned}\right\} \qquad (V.13.3)$$

Based on the reciprocity principle, $Z_{21} = Z_{12}$.

The equations at (V.13.3) are similar to Kirchhoff's equations derived as applicable to two coupled circuits and known from the theory of coupled circuits.

Let us designate

$$I_{2\ loop}/I_{1\ loop} = me^{i\psi}.$$

Substituting in formula (V.13.3),

$$\left.\begin{aligned} U_1 &= I_{1\ loop}(Z_{11} + me^{i\psi}Z_{12}) \\ U_2 &= I_{2\ loop}(Z_{22} = 1/m\ e^{-i\psi}Z_{12}) \end{aligned}\right\} \qquad (V.13.4)$$

Total radiation resistance of the dipoles equals

$$\left.\begin{aligned} Z_1 &= U_1/I_{1\ loop} = Z_{11} + me^{i\psi}Z_{12} \\ Z_2 &= U_2/I_{2\ loop} = Z_{22} + 1/m\ e^{-i\psi}Z_{12} \end{aligned}\right\} \qquad (V.13.5)$$

The second terms in the right-hand sides of the formulas at (V.13.5) are the radiation resistances induced by adjacent dipoles.

All the impedances figured here are complex in the general case,

$$\left.\begin{aligned} Z_{11} &= R_{11} + i\,X_{11} \\ Z_{22} &= R_{22} + i\,X_{22} \\ Z_{12} &= R_{12} + i\,X_{12} \end{aligned}\right\}. \qquad (V.13.6)$$

Substituting (V.13.6) in (V.13.5) and converting the entry for the magnitude $e^{i\psi}$ to trigonometric form, we obtain the following equations suitable for making the calculations

$$\left.\begin{aligned} Z_1 &= [R_{11} + m(R_{12}\cos\psi - X_{12}\sin\psi)] + i\,[X_{11} + \\ &\quad + m(R_{12}\sin\psi + X_{12}\cos\psi)] \\ Z_2 &= \left[R_{22} + \frac{1}{m}(R_{12}\cos\psi + X_{12}\sin\psi)\right] + \\ &+ i\left[X_{22} + \frac{1}{m}(-R_{12}\sin\psi + X_{12}\cos\psi)\right] \end{aligned}\right\}. \qquad (V.13.7)$$

The power expended on radiation by the source of emf for the first dipole equals

$$P_{\Sigma 1} = 1/2\ I^2_{1\ loop}[R_{11} + m(R_{12}\cos\psi - X_{12}\sin\psi)] \qquad (V.13.8)$$

while that for the second dipole equals

$$P_{\Sigma 2} = 1/2\ I^2_{2\ loop}[R_{22} + 1/m(R_{12}\cos\psi + X_{12}\sin\psi)]. \qquad (V.13.9)$$

Total power expended on radiation by the sources of emf for both dipoles equals

$$P_{\Sigma} = P_{\Sigma 1} + P_{\Sigma 2}. \qquad (V.13.10)$$

Using equation (V.13.3), we can establish the current flowing in the loops of each of the dipoles if the voltage applied to the dipoles is known. In fact, solving (V.13.3) with respect to $I_{1\ loop}$ and $I_{2\ loop}$,

$$\left.\begin{aligned} I_{1\ loop} &= U_1 \frac{Z_{22}}{Z_{11}Z_{22}-Z_{12}^2} - U_2 \frac{Z_{12}}{Z_{11}Z_{22}-Z_{12}^2} \\ I_{2\ loop} &= U_2 \frac{Z_{11}}{Z_{11}Z_{22}-Z_{12}^2} - U_1 \frac{Z_{12}}{Z_{11}Z_{22}-Z_{12}^2} \end{aligned}\right\}, \qquad (V.13.11)$$

and the current ratio equals

$$\frac{I_{2\ loop}}{I_{1\ loop}} = \frac{Z_{11} - \frac{U_1}{U_2} Z_{12}}{Z_{22} - \frac{U_2}{U_1} \cdot Z_{12}} \frac{U_2}{U_1}. \qquad (V.13.12)$$

#V.14. Use of the Induced emf Method to Establish Radiation Resistance and Currents in the Case of Two Coupled Dipoles, One of Which is Parasitic.

Let us consider the case when one of the dipoles is parasitic, that is, it is not fed directly from a source of emf. Parasitic elements are widely used as reflectors and directors (see #IX.15).

Let us assume that dipole 1 is directly fed, and that dipole 2 is parasitic, that is, that $U_2 = 0$.

Substituting $U_2 = 0$ into formula (V.13.11),

$$\left.\begin{aligned} I_{1\ loop} &= \frac{U_1 Z_{22}}{Z_{11}Z_{22} - Z_{12}^2} \\ I_{2\ loop} &= -\frac{U_1 Z_{12}}{Z_{11}Z_{22} - Z_{12}^2} \end{aligned}\right\}, \qquad (V.14.1)$$

from whence

$$I_{2\ loop} = -I_{1\ loop} Z_{12}/Z_{22} \qquad (V.14.2)$$

If resistance is connected to the parasitic element

$$I_{2\ loop} = -I_{1\ loop} Z_{12}/Z_{22} + Z_{2\ load} \qquad (V.14.3)$$

where

$Z_{2\ load}$ is the connected resistance converted to the current loop.

The conversion of the connected resistance from the point of connection to the current loop can be made through the approximate formula

$$Z_{2\ load} = Z_{20} \sin^2 \alpha l \qquad (V.14.4)$$

[see formula (V.10.9)], or more accurately through

$$Z_{2\ load} = Z_{20} \operatorname{sh}^2(\beta + i\alpha) l, \qquad (V.14.5)$$

where Z_{20} is the resistance connected to the input terminals of antenna 2;

βl is a magnitude calculated for dipole 2 through formula (V.10.8) without regard for the effect of the first dipole.

If the magnitude of l is close to n $\lambda/2$ (n = 1, 2, 3...), formula (V.14.5) must be used.

$Z_{2\ load}$ is usually a reactive component ($Z_{2\ load} = iX_{2\ load}$).

Substituting the values of Z_{12} and Z_{22} from formula (V.14.6) in formula (V.14.3), we obtain the following expression for the current flowing in the parasitic element,

$$I_{2\ loop} = mI_{1\ loop}e^{i\psi}, \qquad (V.14.6)$$

where

$$m = \sqrt{\frac{R_{12}^2 + X_{12}^2}{R_{22}^2 + (X_{22} + X_{2H})^2}}, \qquad (V.14.7)$$

$$\psi = \pi + \operatorname{arc\,tg}\frac{X_{12}}{R_{12}} - \operatorname{arc\,tg}\frac{X_{22} + X_{2H}}{R_{22}}. \qquad (V.14.8)$$

When $X_{2\ load} = -X_{22}$ (the parasitic element tuned to resonance)

$$m = \sqrt{\frac{R_{12}^2 + X_{12}^2}{R_{22}^2}}, \qquad (V.14.9)$$

$$\psi = \pi + \operatorname{arc\,tg}\frac{X_{12}}{R_{12}}. \qquad (V.14.10)$$

Since $|Z_{12}| < |Z_{22}|$, and as follows from formula (V.14.7), when there is no tuned reactive component ($X_{2\ load}$) in the parasitic element, m < 1; that is, the amplitude of the current flowing in the parasitic element is less than the amplitude of the current flowing in the directly fed dipole. When the parasitic element is tuned to resonance m can be greater than 1 if Z_{12} does not differ greatly from Z_{22}, as is the case when the distances between elements 1 and 2 are small.

So, from formula (V.14.1), the total radiation resistance of the directly fed dipole equals

$$Z_1 = U_1/I_{1\ loop} = Z_{11} - Z_{12}^2/Z_{22}. \qquad (V.14.11)$$

If the parasitic element is tuned to resonance and, if both elements are identical, as is often the case

$$Z_1 = Z_{11} - \frac{Z_{12}^2}{R_{11}} = (R_{11} + iX_{11}) - \frac{R_{12}^2 - X_{12}^2}{R_{11}} - i\frac{2R_{12}X_{12}}{R_{11}}. \qquad (V.14.12)$$

Kirchhoff's system of equations cited here for coupled dipoles makes it possible to establish the currents flowing in the loops and the total radiation resistances if own and mutual radiation resistances are known.

#V.15. The Calculation for Radiation Resistance and Current Flowing in a Multi-Element Array Consisting of Many Dipoles

The theory of the coupling of two dipoles discussed above can be applied to the calculation of the radiation resistance of dipoles in a multi-element system.

Let us suppose we have n dipoles. Let us designate the voltage and currents at the current loops of the dipoles by U_1, U_2, ..., U_n and I_1, I_2, ..., I_n. The equations associating currents, voltages, and resistances are

$$\left.\begin{aligned} \dot{U}_1 &= I_1 Z_{11} + I_2 Z_{12} + \ldots + I_n Z_{1n} \\ \dot{U}_2 &= I_1 Z_{21} + I_2 Z_{22} + \ldots + I_n Z_{2n} \\ &\cdots\cdots\cdots\cdots\cdots\cdots \\ \dot{U}_n &= I_1 Z_{n1} + I_2 Z_{n2} + \ldots + I_n Z_{nn} \end{aligned}\right\}. \qquad (V.15.1)$$

These equations enable us to establish the radiation resistance of each of the dipoles in the system

$$\left.\begin{aligned} Z_1 &= \frac{U_1}{I_1} = Z_{11} + \frac{I_2}{I_1} Z_{12} + \ldots + \frac{I_n}{I_1} Z_{1n} \\ Z_2 &= \frac{U_2}{I_2} = \frac{I_1}{I_2} Z_{12} + Z_{22} + \ldots + \frac{I_n}{I_2} Z_{2n} \\ &\cdots\cdots\cdots\cdots\cdots\cdots \\ Z_n &= \frac{U_n}{I_n} = \frac{I_1}{I_n} Z_{n1} + \frac{I_2}{I_n} Z_{n2} + \ldots + Z_{nn} \end{aligned}\right\}. \qquad (V.15.2)$$

By solving the system of equations at (V.15.1) with respect to currents I_1, I_2, I_3, ..., I_n, we can establish the current flowing in any of the dipoles.

If the system consists of two groups of broadside dipoles with currents of identical amplitudes the solution to the system of equations at (V.15.1) can be much simplified. This requires the introduction of the equivalent dipole concept, wherein this latter replaces a group of broadside dipoles.

This will be discussed in detail below during the analysis of the type SG antenna.

#V.16. Use of the Induced emf Method to Establish the Effect of the Ground on the Radiation Resistance of a Single Balanced Dipole

#5 of this chapter reviewed the question of calculating the effect of the ground on the directional properties of dipoles. This same effect must also be taken into consideration when calculating radiation resistance. The ground is usually assumed to be an ideal conductor[1] when this problem is

1. "The Engineering Calculation of the Impedance of Linear Conductors with the Effect of the Real Ground Taken Into Consideration," by A. S. Knyazev, which appeared in Radiotekhnika [Radio Engineering], No. 9, 1960, develops the method of induced emfs for the case of the real ground.

posed because it is a complex one. When this is done the mirror image method is used, that is, the effect of the ground on radiation resistance is replaced by the effect of the dipole's mirror image.

This hypothesis is entirely acceptable in the case of a horizontal dipole suspended sufficiently high above ground ($H/\lambda \geq 0.25$), because the ground actually exerts an effect similar to that exerted by the mirror image. This is so because the reflection factor for the mirror image of a horizontal dipole is approximately equal to -1.

So far as the vertical dipole is concerned, this hypothesis will only hold when artificial metallization is used instead of the ground (the dipole is grounded).

Thus, the task of calculating the radiation resistance of a dipole located close to the ground reduces to calculating the coupling of two identical dipoles carrying currents identical as to magnitude and phase in the case of the vertical dipole and identical as to magnitude, but opposite in phase in the case of the horizontal dipole.

Using formula (V.13.5) and considering the foregoing relative to the amplitude and phase of the current in the mirror image,

$$Z_1 = Z_{11} - Z'_{11} \qquad \text{(V.16.1)}$$

in the case of the horizontal dipole, and

$$Z_1 = Z_{11} + Z'_{11} \qquad \text{(V.16.2)}$$

in the case of the vertical dipole, where Z'_{11} is the mutual impedance between the dipole and its mirror image.

Example. Find the total radiation resistance equated to a current loop for a horizontal half-wave dipole suspended at height $H = \lambda/4$.

Solution. From the curves in figures V.8.1a and V.12.3, we establish

$$Z_{11} = (73.1 + i42.5) \text{ ohms.}$$

The distance between the dipole and its mirror image equals $2H = \lambda/2$.

Using the curves in figures H.III.6 and H.III.14 in the Handbook Section,

$$Z'_{11} = -13 - i30 = -(13 + i30) \text{ ohms,}$$

$$Z_1 = Z_{11} - Z'_{11} = (86.1 + i72.5) \text{ ohms.}$$

#V.17. Use of the Induced emf Method to Establish the Effect of the Ground on the Radiation Resistance of a Multi-Element Antenna

If the antenna is a complex system consisting of a series of dipoles, the effect of the ground on its radiation resistance can also be established by computing the resistances induced by the mirror images of the dipoles.

Total radiation resistance for each of the dipoles consists of own resistance, the resistance induced by all the other dipoles, and the resistance induced by all the mirror images.

To illustrate this, let us take Kirchhoff's equations applicable to two horizontal, coupled, directly fed dipoles near the ground

$$\left.\begin{aligned} U_1 &= I_{\text{loop }1}(Z_{11} - Z'_{11}) + I_{\text{loop }2}(Z_{12} - Z'_{12}) \\ U_2 &= I_{\text{loop }2}(Z_{22} - Z'_{22}) + I_{\text{loop }1}(Z_{21} - Z'_{21}) \end{aligned}\right\} \qquad \text{(V.17.1)}$$

where

Z'_{11} is the mutual impedance between dipole 1 and its mirror image;

Z'_{22} is the mutual impedance between dipole 2 and its mirror image;

Z'_{12} is the mutual impedance between dipole 1 and the mirror image of dipole 2;

Z'_{21} is the mutual impedance between dipole 2 and the mirror image of dipole 1.

Let us designate

$$I_{\text{loop }2}/I_{\text{loop }1} = me^{i\psi}.$$

Expressing the impedance Z in terms of the resistive and reactive components, and taking it that $Z_{21} = Z_{12}$ and $Z'_{21} = Z'_{12}$, we obtain

$$Z_1 = U_1/I_{\text{loop }1} = \left\{(R_{11} - R'_{11}) + m[(R_{12} - R'_{12})\cos\psi - (X_{12} - X'_{12})\sin\psi]\right\} +$$

$$+ i\left\{(X_{11} - X'_{11}) + m[(X_{12} - X'_{12})\cos\psi + (R_{12} - R'_{12})\sin\psi]\right\}; \qquad \text{(V.17.2)}$$

$$Z_2 = U_2/I_{\text{loop }2} = \left\{(R_{22} - R'_{22}) + 1/m[(R_{12} - R'_{12})\cos\psi + (X_{12} - X'_{12})\right.$$

$$\left.\sin\psi]\right\} + i\left\{(X_{22} - X'_{22}) + 1/m[(X_{12} - X'_{12})\cos\psi - (R_{12} - R'_{12})\sin\psi]\right\}. \qquad \text{(V.17.3)}$$

Similarly, for the case of two horizontal dipoles, one of which is parasitic,

$$Z_1 = (Z_{11} - Z'_{11}) - \frac{(Z_{12} - Z'_{12})^2}{(Z_{22} - Z'_{22}) + iX_{2\text{load}}}. \qquad \text{(V.17.4)}$$

$$m = \sqrt{\frac{(R_{12} - R'_{12})^2 + (X_{12} - X'_{12})^2}{(R_{22} - R'_{22})^2 + (X_{22} - X'_{22} + X_{2\text{load}})^2}}, \qquad \text{(V.17.5)}$$

$$\psi = \pi + \operatorname{arc\,tg}\frac{X_{12} - X'_{12}}{R_{12} - R'_{12}} - \operatorname{arc\,tg}\frac{X_{22} - X'_{22} + X_{2\text{load}}}{R_{22} - R'_{22}} \qquad \text{(V.17.6)}$$

The signs for the mutual impedances between dipoles and mirror images should be reversed in the case of the vertical dipoles in equations (V.17.1) through (V.17.6).

#V.18. Calculation of Input Impedance in a System of Coupled Dipoles

Formula (V.10.2) can be used to approximate the input impedance of each of the dipoles in a system. However, the fact that parameters W and β change as a result of the cross-coupling should be taken into consideration.

Thus, we obtain the following formulas for computing the input impedance of each of the dipoles in the system

$$Z_{in} = W_c \frac{\operatorname{sh} 2\beta_c l - \frac{\beta_c}{a} \sin 2al}{\operatorname{ch} 2\beta_c l - \cos 2al} - i W_c \frac{\frac{\beta_c}{a} \operatorname{sh} 2\beta_c l + \sin 2al}{\operatorname{ch} 2\beta_c l - \cos 2al}, \qquad (V.18.1)$$

where

W_c and β_c are the characteristic impedance and attenuation factor, with the cross-coupling of the dipoles taken into consideration.

The effect of cross-coupling on W and β can be approximated by assuming the induced resistive and reactive resistances are uniformly distributed over the entire length. Given this assumption, we have for W_c and β_c

$$W_c = \sqrt{\frac{\omega L_1 + X_{1ind}}{\omega C_1}} = W \sqrt{1 + \frac{X_{1ind}}{aW}}; \qquad (V.18.2)$$

$$\beta_c l = \frac{R_{11} + R_{ind}}{W_c \left(1 - \frac{\sin 2al}{2al}\right)}, \qquad (V.18.3)$$

where

R_{ind} is the resistive component of radiation resistance induced by all adjacent dipoles and all mirror images, including own mirror image;

$X_{1\,ind}$ is the induced reactive resistance per unit length.

Similar to formula (V.10.7) for computing the distributed reactive resistance is

$$X_{1ind} = \frac{2X_{ind}}{i\left(i - \frac{\sin 2al}{2al}\right)}, \qquad (V.18.4)$$

where

X_{ind} is the reactive component of the radiation resistance induced by all adjacent dipoles and all mirror images, including own mirror image;

R_{ind} and X_{ind} are computed through the formulas given in the preceding paragraphs.

If the length of the dipoles does not exceed 0.25 to 0.3 λ, we can use formula (V.10.9) to compute the input impedance, replacing R by $R_\Sigma + R_{ind}$, and W by W_c, respectively.

#V.19. Generalization of the Theory of Coupled Dipoles

The equations cited above for coupled dipoles were derived as applicable to the voltages and currents at a current loop. This is the result of the specifics of the manner in which the methodology for computing the input impedance and other electrical parameters of shortwave antennas is constructed. In principle, the equations indicated retain their effect with respect to any point on the dipole, and particularly to the point of feed. In the latter case the mutual impedance too must be equated to the point of feed for the dipoles. Similar equations can also be obtained for conductors passing a traveling wave.

#V.20. Application of the Theory of the Balanced Dipole to the Analysis of a Vertical Unbalanced Dipole

Radio communications is a field in which unbalanced dipoles, and particularly vertical unbalanced dipoles, are widely used. Figure V.20.1 is a schematic of a vertical unbalanced dipole.

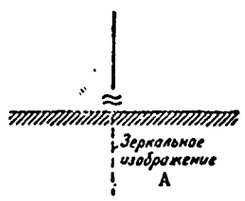

Figure V.20.1. Unbalanced vertical dipole with mirror image.
A - mirror image.

The field of the vertical dipole creates a system of currents in the ground. If it is assumed that the ground has infinitely high conductivity, similar to that indicated above, the currents flowing at its surface create a secondary field which corresponds precisely to the field of the dipole's mirror image. The mirror image is shown by the dotted line in Figure V.20.1.

The unbalanced dipole and its mirror image form a system completely analogous to that of a balanced dipole in free space. Therefore, if ground conductivity is ideal all the above data regarding directional properties, radiation resistance, input impedance, etc., for the balanced dipole in free space can be applied in toto to the unbalanced dipole. We need only consider the fact that the source of the emf applied to the balanced dipole carries twice the load the source feeding the unbalanced dipole does. Therefore, for the same design of leg, the input impedance, Z_{in}, the radiation resistance, R_{Σ}, and the characteristic impedance, W_i, of the unbalanced dipole are half those of the balanced dipole. The values obtained for Z_{in}, R_{Σ}, and W_i, using the methods indicated, are very close to the actual values if a bonding system (a ground system) has been developed under the dipole. Since ground parameters approximate the parameters of an ideally conducting medium as

wavelength is lengthened, the accuracy of the results obtained by making a similar analysis of the unbalanced dipole will improve with increase in the wavelength.

We note that it is impossible to use the balanced dipole theory to analyze the directional properties of a vertical unbalanced dipole above real ground. The radiation pattern is usually charted with respect to a point of observation at a very great distance from the dipole. The field at distant points is not only established by the currents flowing in the ground in direct proximity to the dipole, but also by the whole system of currents flowing in the ground. Therefore, even if an extremely sophisticated ground system is used the radiation pattern of the unbalanced dipole differs substantially from that of the unbalanced dipole over an ideally conducting ground under actual conditions.

The degree to which the surface beam is attenuated can be used as the criterion for establishing the distance at which the theory of the unbalanced dipole over ideally conducting ground is no longer applicable. If the distance from the dipole is so great that the surface beam is substantially attenuated because of ground losses the directional properties of a real unbalanced dipole will differ a great deal from those of an unbalanced dipole over ideally conducting ground, even when a sophisticated ground system is installed.

The shortwave communications field mainly uses beams reflected from the ionosphere because reception usually is so far away from the dipole that the ground wave is almost completely attenuated. Hence, the theory of the unbalanced dipole over ideally conducting ground cannot be used in the shortwave field to analyze directional properties.

#V.21. The Reception Process

Let an antenna, a balanced dipole for example, be set up in the field of a plane wave (fig. V.21.1). The electric field strength vector will form angle θ with the axis of the dipole. The component of the field strength vector tangent to the conductor equals $E \cos \theta$. The tangent component of the electric field strength vector excites currents in the conductor. These currents cause energy scattering at the input to the receiver connected to the dipole. Thus, the process of transferring energy from a propagated wave to a load (the receiver) is accomplished. The currents flowing in the dipole are sources of a secondary field. The tangential component of the secondary field E vector is such that boundary conditions are satisfied at the surface of the conductor. If it is assumed that the conductor has ideal conductivity the resultant (primary and secondary) tangential component of the electric field strength vector at the surface of the conductor should equal zero. To be so the tangential component of the secondary field E vector

should equal in magnitude to, but be opposite in phase to the tangential component of the primary field E vector.

Maxwell's equations provide definitive association between the secondary field and the current distribution through the dipole. The computation of this association and the requirement with respect to the magnitude of the tangential component of the electric field strength vector stemming from the need to satisfy the boundary conditions, together with the requirements stemming from the law of continuity of current at the terminals of the load resistor, is enough to establish current distribution in the conductor. In particular, because these conditions must be satisfied, we can establish the magnitude of the current at the input to the load. However, there are mathematical difficulties involved in using this method of establishing the currents flowing in the conductor and in the load, and as of this time this problem has not yet been finally resolved.

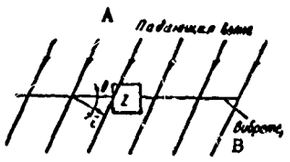

Figure V.21.1. Description of the reception process.
A - incident wave; B - dipole.

The principle of reciprocity can be used to establish the currents flowing in the receiving antenna and in the load. This principle enables us to find the currents flowing in the receiving antenna, based on known data with respect to how current is distributed on an antenna such as this, as well as on the field in the space around the antenna when it is used as a radiator. However, the accuracy of the results obtained will be determined by the accuracy of the formulas used to establish antenna data when the antenna is radiating.

#V.22. Use of the Reciprocity Principle to Analyze Properties of Receiving Antennas

Let there be two antennas, type immaterial, separated by some distance and oriented arbitrarily with respect to each other. We shall review two cases.

First case. Antenna 1 is the transmitting antenna; antenna 2 is the receiving antenna (fig. V.22.1). Let us connect a generator with emf e_1 to antenna 1. The current flowing at the input to antenna 1 equals

$$I_1 = \frac{e_1}{Z_1 + Z_{1in}}, \qquad (V.22.1)$$

where

Z_1 is the impedance connected to antenna 1;

$Z_{1\,in}$ is the input impedance of antenna 1.

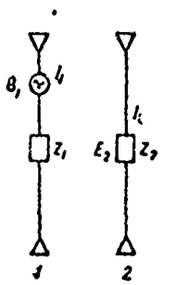

Figure V.22.1. The derivation of formula (V.22.3).

Connected to antenna 2 is a receiver with impedance Z_2. Antenna 1 field will cause electric field E_2 to act on antenna 2, and some current I_2 will flow in load Z_2. The strength of the field created by antenna 1 equals

$$E_2 = \frac{60k_1I_1}{r_0} F_1(\Delta, \varphi), \qquad \text{(V.22.2)}$$

where

r_0 is the distance between antennas;

$F_1(\Delta,\varphi)$ is an expression establishing the shape of antenna 1 radiation pattern;

$$k_1 = I_0/I_1$$

I_0 is the current used to express the field strength of the specific type of antenna;

I_1 is the current flowing at the input terminals of the antenna.

Substituting the expression for I_1 from formula (V.22.1) in formula (V.22.2), we find the relationship between the emf acting across the transmitting antenna and the field strength at the receiving antenna

$$e_1 = \frac{E_2(Z_1 + Z_{1in})r_0}{60k_1F_1(\Delta, \varphi)}. \qquad \text{(V.22.3)}$$

Second case. Antenna 2 is the transmitting, antenna 1 the receiving antenna (fig. V.22.2). Let us connect a generator with emf e_2 to antenna 2, and a receiver with impedance Z_1 to antenna 1. Field strength E_1 caused by antenna 2 field, will act on antenna 1, and current I_1 will flow in load Z_1. By analogy with the first case we obtain the relationship

$$e_2 = \frac{E_1(Z_2 + Z_{2in})r_0}{60k_2F_2(\Delta, \varphi)}, \qquad \text{(V.22.4)}$$

where

Z_2 is the impedance connected to antenna 2;

$Z_{2\,in}$ is the input impedance of antenna 2;

$F_2(\Delta,\varphi)$ is an expression establishing the shape of antenna 2 radiation pattern.

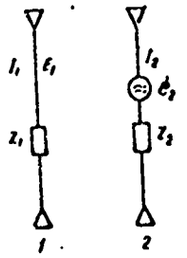

Figure V.22.2. The derivation of formula (V.22.4).

According to the reciprocity principle emf e_1 fed to antenna 1 is related to current I_2 flowing as a result of this emf in the load on antenna 2, as emf e_2 fed to antenna 2 is related to current I_1 flowing as a result of this antenna in the load on antenna 1,

$$e_1/I_2 = e_2/I_1 \,. \qquad (V.22.5)$$

Substituting the values for e_1 and e_2 from formulas (V.22.3) and (V.22.4) in formula (V.22.5), and grouping factors, we obtain

$$\frac{I_1(Z_1+Z_{1in})}{E_1k_1F_1(\Delta,\varphi)} = \frac{I_2(Z_2+Z_{2in})}{E_2k_2F_2(\Delta,\varphi)}. \qquad (V.22.6)$$

All magnitudes in the left-hand side of (V.22.6) are related to one antenna, and all those in the right-hand side are related to the other antenna. Accordingly, $I(Z+Z_{in})/EkF(\Delta,\varphi)$ is a constant, not dependent on type of antenna. We thus obtain the following equality

$$\frac{I(Z+Z_{in})}{EkF(\Delta,\varphi)} = c, \qquad (V.22.7)$$

from whence

$$I = Ekc/Z_{load}+Z_{in}\ F(\Delta,\varphi) \qquad (V.22.8)$$

where

Z_{load} is the impedance of the load connected to the receiving antenna.

The constant c can be established by comparing formula (V.22.8) with the expression for I obtained by direct analysis of the antenna as a receiving system. It can be proven that $c = \lambda/\pi$.

Thus

$$I = kE\lambda/\pi(Z_{load}+Z_{in})\ F(\Delta,\varphi) \qquad (V.22.9)$$

Formula (V.22.9) establishes an extremely important dependence between the current in the receiving antenna and the electric field strength of the incoming wave. What follows directly from this formula is that the receiving pattern of any receiving antenna coincides with the radiation pattern obtained when the same antenna is used as a transmitting antenna if the receiver is connected at the same point as was the transmitter.

Formula (V.22.9), in the more general form, is

$$I = kE\lambda \cos x/\pi(Z_{load}+Z_{in})\ F(\Delta,\varphi)e^{i\psi}, \qquad (V.22.9a)$$

where

x is the angle between the plane of polarization of waves incoming to the antenna and the plane of polarization of waves leaving the antenna in the same direction as when the antenna was used for transmitting;

ψ is the antenna's directional phase diagram.[1]

#V.23. Receiving Antenna Equivalent Circuit. Conditions for Maximum Power Output.

Formula (V.22.9) demonstrates that every receiving antenna has an equivalent circuit, shown in Figure V.23.1. As will be seen, the equivalent circuit consists of an emf source, e_{rec}, load impedance, Z_{load}, and internal impedance Z_{in}. The internal impedance in the equivalent circuit equals the input impedance of the same antenna when it is used for transmitting. The equivalent emf equals

$$e_{rec} = \lambda kE/\pi\ F(\Delta,\varphi). \qquad (V.23.1)$$

Power supplied by the antenna to the load equals

$$P_{rec} = e^2_{rec}/2\left|Z_{in}+Z_{load}\right|^2\ R_{load}, \qquad (V.23.2)$$

where

R_{load} is the resistive component of load impedance.

The conditions for maximum output of power to the load connected to the antenna will obviously be those for any generator; that is, maximum output will be obtained when $R_{in} = R_{load}$ and $X_{in} = -X_{load}$. Thus, maximum power supplied by the antenna to the load equals

$$P_{rec\ max} = e^2_{rec}/8R_{in}. \qquad (V.23.3)$$

---

1. A. R. Vol'pert. "Phase Relationships in Receiving Antenna Theory and Some Applications of the Principle of Reciprocity." Radiotekhnika [Radio Engineering], No. 11, 1955.

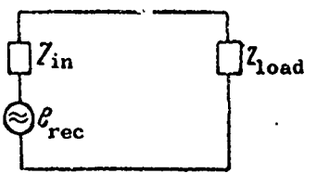

Figure V.23.1. Receiving antenna equivalent circuit.

#V.24. Use of the Principle of Reciprocity for Analyzing a Balanced Receiving Dipole

We shall limit ourselves to the case of a balanced dipole in free space. For this dipole, from a comparison of formulas (V.4.3) and (V.22.2),

$$F(\Delta,\varphi) = F(\theta) = \frac{E}{60I_{loop}/r} = \frac{\cos(\alpha l\cos\theta)-\cos\alpha l}{\sin\theta};$$

$$k = I_{loop}/I_1 = 1/\mathrm{sh}\,\gamma l.$$

Substituting in (V.22.9),

$$I = \frac{E\lambda}{\pi(Z_{load}+Z_{in})\mathrm{sh}\gamma l}\,\frac{\cos(\alpha l\cos\theta)-\cos\alpha l}{\sin\theta}, \qquad (V.24.1)$$

where

Z_{in} is the input impedance of the balanced dipole.

The emf fed to the balanced dipole and reduced to the site where the load is connected equals

$$e_{rec} = E\,\frac{\lambda}{\pi}\,\frac{1}{\mathrm{sh}\gamma l}\,\frac{\cos(\alpha l\cos\theta)-\cos\alpha l}{\sin\theta}. \qquad (V.24.2)$$

For a half-wave dipole ($2l = \lambda/2$) during reception of beams propagated in its equatorial plane ($\theta = 90°$),

$$e_{rec} = E\,\lambda/\pi \qquad (V.24.3)$$

The power supplied by the half-wave dipole to the load when match is optimum and when waves incoming have been propagated in the equatorial plane, in accordance with (V.23.3) and (V.24.3), equals

$$P_{\frac{\lambda}{2}} = \frac{E^2\lambda^2}{8\pi^2 73,1} \approx \frac{E^2\lambda^2}{5800}. \qquad (V.24.4)$$

E is understood to be the amplitude of the field strength.

Currents flowing in the receiving dipole create a secondary field which can be superimposed on the primary field of the excitation wave. The result is the creation of standing waves around the dipole which are particularly clearly defined in the direction from the receiving dipole to the source of the incoming wave.

Chapter VI

ELECTRICAL PARAMETERS CHARACTERIZING TRANSMITTING AND RECEIVING ANTENNAS

#VI.1. Transmitting Antenna Directive Gain

The basic requirement imposed on a transmitting antenna is that the strongest possible field be produced in the specified direction, and here two factors are involved; the directional characteristics of the antenna, and the absolute magnitude of the radiated power. The first is characterized by the directive gain, D, the second by the efficiency η.

Directive gain in a particular direction is the ratio of the square of the field strength created by the antenna in that direction (E_0^2) to the average value of the square of the field strength (E_{av}^2) in all directions

$$D = E_0^2/E_{av}^2 . \qquad \text{(VI.1.1)}$$

Since radiated power and the square of field strength are directly proportional, the directive gain can also be defined as a number indicating how many times the radiated power must be reduced if an absolutely non-directional antenna is replaced by the antenna specified, on the condition that the same field strength be retained. Obviously, both definitions are the same.

Let us find the general expression for directive gain.

The field strength produced by the antenna can be expressed in general form by the formula

$$E = \frac{60I}{r} F(\Delta, \varphi), \qquad \text{(VI.1.2)}$$

where

I is the current flowing at no matter which point on the antenna;

$F(\Delta,\varphi)$ is a function expressing the dependence of field strength on angle of tilt Δ, and azimuth angle φ.

Let us designate the angle of tilt and the azimuth angle for the direction in which the directive gain is to be established by Δ_0 and φ_0. Now the field strength in this direction equals

$$E_0 = \frac{60I}{r} F(\Delta_0, \varphi_0). \qquad \text{(VI.1.3)}$$

For purposes of establishing the average value of the square of the field strength let us imagine a sphere with its center at the point where the antenna is located and radius r.

The average on the surface of the sphere equals

$$E_{av}^2 = \frac{\int_F E^2 dF}{F}, \qquad \text{(VI.1.4)}$$

where

E is the field strength at the infinitesimal area dF on the surface of the sphere,

$$dF = r^2 \cos\Delta \, d\Delta \, d\varphi,$$

F is the total surface of the sphere, $F = 4\pi r^2$.

Substituting values for E, F, and dF in formula (VI.1.4), and replacing integration with respect to the surface by integration with respect to angles Δ and φ,

$$E_{av}^2 = \frac{1}{4\pi}\left(\frac{60I}{r}\right)^2 \int_0^{2\pi} d\varphi \int_0^{\frac{\pi}{2}} F^2(\Delta, \varphi) \cos\Delta \, d\Delta. \qquad \text{(VI.1.5)}$$

The integration with respect to Δ is done from 0 to $\pi/2$ only, since it is assumed that radiated energy resulting from ideal conductivity of the ground applies only to the upper hemisphere. If a hypothetical antenna in free space is under discussion, or if the fact that ground conductivity is not ideal is taken into consideration, integration with respect to Δ must be done from $-\pi/2$ to $\pi/2$.

Substituting the values for E_0 and E_{av} from formulas (VI.1.3) and (VI.1.5) in formula (VI.1.1),

$$D = \frac{4\pi F^2(\Delta_0, \varphi_0)}{\int_0^{2\pi} d\varphi \int_0^{\frac{\pi}{2}} F^2(\Delta, \varphi) \cos\Delta \, d\Delta}. \qquad \text{(VI.1.6)}$$

If $F(\Delta)$ is normalized to $F(\Delta_0, \varphi_0)$, formula (VI.1.6) becomes

$$D = \frac{4\pi}{\int_0^{2\pi} d\varphi \int_0^{\frac{\pi}{2}} F_1^2(\Delta, \varphi) \cos\Delta \, d\Delta}, \qquad \text{(VI.1.7)}$$

where

$F_1(\Delta, \varphi)$ is a function of $F(\Delta, \varphi)$, normalized to $F(\Delta_0, \varphi_0)$.

If it is customary to have the pattern symmetrical with respect to some azimuth, and if the reading is taken relative to this azimuth,

$$D = \frac{2\pi}{\int_0^{\pi} d\varphi \int_0^{\frac{\pi}{2}} F_1^2(\Delta, \varphi) \cos\Delta \, d\Delta}. \qquad \text{(VI.1.8)}$$

If the radiation pattern has axial symmetry with respect to the vertical axis, $\Delta = 90°$, the integration with respect to φ will yield the factor π in the denominator. Recognizing this, and introducing the angle $\theta = 90° - \Delta$,

$$D = \frac{2}{\int_0^{\frac{\pi}{2}} F_1^2(\theta) \sin\theta \, d\theta}. \qquad \text{(VI.1.9)}$$

Difficulties resulting from the complexity involved in computing the integrals are often encountered when values for D are established through formulas (VI.1.6) through (VI.1.9). If the antenna's radiation resistance is known, we can do away with the need to compute the integrals. Let us make use of formula (V.7.6). Substituting the expression for the double integral established through formula (V.7.6) in formula (VI.1.6),

$$D = \frac{120F^2(\Delta_0, \varphi_0)}{R_\Sigma}. \qquad \text{(VI.1.10)}$$

Here R_Σ is the radiation resistance equated to current I.

Let us establish the value of D for a half-wave dipole in free space. The radiation resistance of the half-wave dipole in free space, equated to the current flowing in a loop, equals

$$R_\Sigma = 73.1 \text{ ohms.}$$

The field strength produced by the half-wave dipole, expressed in terms of the loop current (I_{loop}), equals

$$E = \frac{60I_{loop}}{r} \frac{\cos(\pi/2 \cos\theta)}{\sin\theta}. \qquad \text{(VI.1.11)}$$

The function $F(\Delta,\varphi)$ can be established as a particular solution by dividing the expression for the field strength by $60I_{loop}/r$

$$F(\Delta,\varphi) = \frac{E}{(60I_{loop}/r)} = \frac{\cos(\pi/2 \cos\theta)}{\sin\theta}. \qquad \text{(VI.1.12)}$$

In the case specified the function expressing the dependence of E on the angle of tilt and on the azimuth angle can be replaced by a function which expresses the dependence on angle θ; that is, on the angle formed by the direction of the beam and the axis of the dipole.

Substituting the values for R_Σ and $F(\Delta,\varphi)$ in formula (VI.1.10),

$$D_{\frac{\lambda}{2}} = 1{,}64\frac{\cos^3\left(\frac{\pi}{2}\cos\theta\right)}{\sin^3\theta}. \qquad \text{(VI.1.13)}$$

In the equatorial plane ($\theta = 90°$), $\sin\theta = 1$, $\cos\theta = 0$ and $D = 1.64$. The elementary dipole has a directive gain of 1.5.

#VI.2. Transmitting Antenna Efficiency

Efficiency is found through the formula

$$\eta = P_\Sigma/P_0, \qquad \text{(VI.2.1)}$$

where

P_0 is the power applied to the antenna;

P_Σ is the power radiated by the antenna.

#VI.3. Transmitting Antenna Gain Factor

Just how good an antenna is can be characterized by yet another parameter in addition to directive gain and efficiency, and that is the antenna gain factor, which depends on directional properties, as well as on antenna efficiency.

The antenna gain factor in a specified direction is the ratio of the square of field strength produced by the antenna in this direction to the square of the field strength produced by a standard antenna.

The non-directional (isotropic) antenna is used as the standard antenna in the field of meter and shorter waves. A half-wave dipole in free space is usually used as the standard antenna in the short-wave antenna field. Accordingly, the gain factor equals

$$\varepsilon = \frac{E^2}{E^2_{\frac{\lambda}{2}}}. \qquad \text{(VI.3.1)}$$

The following assumptions are made when establishing the gain factor:

(1) the power applied to the antenna and to the half-wave dipole is the same in magnitude;

(2) the half-wave dipole is in free space;

(3) the efficiency of the half-wave dipole equals 1.

The gain factor can also be defined as a number indicating how many times the input must be reduced if the half-wave dipole is replaced by the antenna specified, the while retaining field strength unchanged. The second definition assumes that the second and third conditions for the first definition are observed.

Both gain factor definitions are unique.

Let us express the gain factor in terms of D and η. From formula (VI.1.1) it follows that the square of the field strength of any antenna can be expressed by the formula

$$E^2 = DE^2_{av}. \qquad \text{(VI.3.2)}$$

Substituting (VI.3.2) in (VI.3.1),

$$\varepsilon = \frac{DE^2_{av}}{D_{\frac{\lambda}{2}} E^2_{\frac{\lambda}{2}av}}, \qquad \text{(VI.3.3)}$$

D is the directive gain for the antenna specified in the direction in which the gain factor is to be established.

$D_{\lambda/2}$ is the directive gain in the equatorial plane of the half-wave dipole in free space. It is self-evident that E^2_{av} does not depend on the antenna's directional properties. E^2_{av} is proportional to antenna efficiency for a given power. Taking the efficiency of the half-wave dipole as equal to 1, we obtain

$$\frac{E^2_{av}}{E^2_{\frac{\lambda}{2}\,av}} = \eta.$$

Substituting this expression in formula (VI.3.3), and considering that $D_{\lambda/2} = 1.64$,

$$\varepsilon = D\eta/1.64. \qquad \text{(VI.3.4)}$$

The relationship at (VI.3.4) is true for any antenna, and can be used to find one of the three antenna parameters if the other two are known. If the expression for D from formula (VI.1.10) is substituted into (VI.3.4), then

$$\varepsilon = \frac{F^2(\delta_\varepsilon, \varphi_0)\eta 73.1}{R_\Sigma}. \qquad \text{(VI.3.5)}$$

We note that when an isotropic antenna with an efficiency of 1 is used as the standard antenna the relationship at (VI.3.4) becomes

$$\varepsilon = D\eta. \qquad \text{(VI.3.6)}$$

#VI.4. Receiving Antenna Directive Gain

The quality of receiving antennas too can be characterized by the directive gain, the efficiency, and the gain factor.

The receiving antenna's directive gain in a specified direction is the ratio of the power, P_{rec}, applied to the receiver input when reception is from that direction to the average (in all directions) value of reception power, P_{av}.

Thus

$$D = P_{rec}/P_{av}. \qquad \text{(VI.4.1)}$$

Since the power at the receiver input is proportional to the square of the voltage across the input, the directive gain can also be defined as the ratio

$$D = U^2/U^2_{av}, \qquad \text{(VI.4.2)}$$

where

U is the voltage across the receiver input upon reception from the direction specified;

U^2_{av} is the average value of the square of the voltage across the receiver input.

#VI.5. Receiving Antenna Gain Factor. The Expression for the Power Applied to the Receiver Input in Terms of the Gain Factor.

The receiving antenna gain factor in a specified direction is the ratio of the power applied to the receiver input during reception from that direction to the power supplied to the receiver input during reception with a standard antenna. A non-directional antenna is used as the standard antenna in the meter and shorter wave bands. The half-wave dipole in free space is usually used as the standard antenna in the shortwave band.

Accordingly,

$$\varepsilon = P_{rec}/P_{\lambda/2} \quad , \qquad \text{(VI.5.1)}$$

where

P_{rec} is the power supplied to the receiver input during reception by the antenna specified;

$P_{\lambda/2}$ is the power supplied to the receiver input during reception by a half-wave dipole.

The following assumptions are made in defining the gain factor:

(1) the field strength is the same when reception is by the antenna specified and when by the half-wave dipole;

(2) the half-wave dipole is in free space;

(3) antenna and dipole have an optimum match with the receiver;

(4) the half-wave dipole is receiving from the direction of maximum reception; that is, from the direction passing through the equatorial plane.

The gain factor can be defined as the ratio

$$\varepsilon = \frac{U^2}{U^2_{\frac{\lambda}{2}}} , \qquad \text{(VI.5.2)}$$

where

U is the voltage across the receiver input when reception is by the antenna specified;

$U_{\lambda/2}$ is the voltage across the receiver input when reception is by a half-wave dipole.

The relationship at (VI.5.2) assumes the input impedance of the receiver during reception to be the same for both antennas, and that conditions 1 through 4 above are satisfied.

Knowing the gain factor for the receiving antenna, we can establish the power applied to the receiver input for optimum match,

$$P_{rec} = \varepsilon P_{\lambda/2} .$$

Substituting the value for $P_{\lambda/2}$ from formula (V.24.4),

$$P_{rec} = E^2\lambda^2\varepsilon/5800 \quad . \qquad \text{(VI.5.3)}$$

If the efficiency of the transmission line, η_F, connecting antenna and receiver is taken into consideration,

$$P_{rec} = E^2\lambda^2\varepsilon\eta_F/5800 \qquad \text{(VI.5.4)}$$

#VI.6. Receiving Antenna Efficiency

Receiving antenna efficiency is the efficiency of this same antenna when it is used for transmitting.

#VI.7. Equality of the Numerical Values of ε and D when Transmitting and Receiving

What has been proven above is that the patterns are the same when transmitting or receiving, regardless of the antenna used. Comparing the definitions for antenna directive gain when transmitting and receiving, it is not difficult to conclude that sameness of the patterns predetermines the sameness of the numerical values of the directive gains when transmitting and receiving.

The reciprocity principle is the basis for proving the sameness of the numerical values of the gain factor for any antenna when transmitting and when receiving.

It follows, therefore, that (VI.3.4) and (VI.3.6) will remain valid when equated to any receiving antenna.

#VI.8. Effective Length of a Receiving Antenna

The concept of effective length can also be used to evaluate how well a receiving antenna will function.

The effective length of a receiving antenna is the ratio of the emf across the receiver input to the electric field strength. Let us find the effective length of a half-wave dipole in free space.

According to (V.24.3), the effective length of a half-wave dipole equals

$$l_{\frac{\lambda}{2}} = \frac{e_{\frac{\lambda}{2}}}{E} = \frac{\lambda}{\pi}. \qquad \text{(VI.8.1)}$$

This expression for effective length assumes that the receiver is connected directly to the center of the dipole.

Let us now suppose that the half-wave dipole is connected to the receiver by a transmission line with characteristic impedance W_F. Let a transforming device, Tr, which matches the characteristic impedance of the transmission line to the dipole's input impedance, the resistive component of which equals 73.1 ohms (fig. VI.7.1), be inserted between the transmission line and the dipole. The input impedance of the transmission line will equal W_F where it is connected to the receiver. The relationship between the emf, e_{rec}, supplied

to the receiver by the transmission line and the emf, $e_{\lambda/2}$, acting in the middle of the dipole can be established from the equality

$$e_{rec} = e_{\lambda/2}\sqrt{W_F\eta_F/73.1} \qquad \text{(VI.8.2)}$$

where

η_F is the transmission line efficiency; losses in the transforming device are taken into consideration.

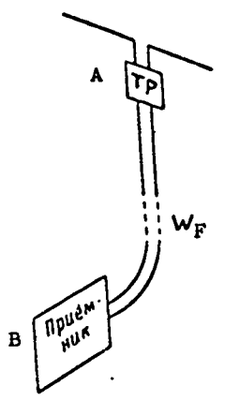

Figure VI.7.1. Block schematic of a receiving antenna with a transformer for matching the antenna input impedance to the transmission line characteristic impedance.

A - transformer; B - receiver.

The effective length of the half-wave dipole connected to a receiver through a transmission line with characteristic impedance W_F equals

$$l'_{\lambda/2} = e_{rec}/E = \lambda/\pi\sqrt{W_F\eta_F/73.1}\ . \qquad \text{(VI.8.3)}$$

According to the definition of gain factor, the effective length of any antenna can be expressed in terms of the effective length of a half-wave dipole through the formula

$$l_{eff} = l_{\lambda/2}\sqrt{\epsilon}\ . \qquad \text{(VI.8.4)}$$

Substituting the value for $l'_{\lambda/2}$ in (VI.8.4),

$$l_{eff} = \lambda/\pi\sqrt{W_F\eta_F\epsilon/73.1}\ . \qquad \text{(VI.8.5)}$$

#VI.9. Independence of Receptivity of External Non-Directional Noise from Antenna Directional Properties. Influence of Parameters ε, D, and η of a Receiving Antenna on the Ratio of Useful Signal Power to Noise Power.

A distinction should be made between directional and non-directional noise. Receptivity of directional noise depends on the shape of the receiving antenna's receiving pattern and on the direction from which the noise is arriving. When circumstances are right, the direction from which the noise is arriving can coincide with the direction of maximum antenna reception. The directional antenna can, in this case, greatly reduce the absolute value of the noise emf. Conversely, the directional antenna will provide no increase in noise resistance when noise direction and maximum antenna reception direction coincide.

Of definite interest is investigation of the receiving antenna when noise arrives simultaneously from all directions, since the likelihood that the relationship between the amplitudes and phases of the noise fields incoming from different directions will be arbitrary is quite probable. This never happens in actual practice, but there are individual cases of noise coming in from many directions at once, and it is this which creates conditions approximating those when noise arrives from all directions at once.

Let us find a general expression for emf and power across the receiver input produced by the noise acting in the manner described. Let us imagine that there is a sphere, its center coinciding with the antenna's phase center, around the receiving antenna, and let the noise sources be located outside this sphere. Let us designate the square of the field strength created at the antenna by the noise passing through unit solid angle, by E_n^2. Then the square of the field created by the noise and passing through the elementary solid angle $d\omega_s$ equals

$$E_n^2 d\omega_s.$$

The square of the emf across the receiver input, produced by this noise field equals

$$d(e_n^2) = E_n^2 l_{eff}^2 d\omega_s , \qquad (VI.9.1)$$

where

l_{eff} is the effective length of the antenna in the case of reception from a direction passing through the elementary angle $d\omega_s$.

Substituting the value for l_{eff} from formula (VI.8.5) in formula (VI.9.1) and expressing ε in terms of D [using formula (VI.3.4)], we obtain

$$d(e_n^2) = E_n^2 \lambda^2/\pi^2 W_F \eta_F \eta/120 D d\omega_s . \qquad (VI.9.2)$$

Based on data from the theory of probability, the average resultant vector A_{av} over a long interval of time, obtained from the sum of the vectors A_1, A_2, A_3 ..., which have a disordered phase relationship, can be defined from

$$A_{av}^2 = A_1^2 + A_2^2 + A_3^2 + \ldots$$

According to this then, the average value of the square of the emf produced by the noise, $e_{n\,av}^2$, passing through unit solid angle, and with expression (VI.1.6) taken into consideration, equals

$$e_{n\,av}^2 = E_n^2 \left(\frac{\lambda}{\pi}\right)^2 \frac{W_F \eta_F \eta}{120 \cdot 4\pi} \cdot \frac{4\pi \int_{\omega_s} F^2(\Delta_0, \varphi_0)\, d\omega_s}{\int_0^{2\pi} d\varphi \int_0^{\frac{\pi}{2}} F^2(\Delta, \varphi) \cos\Delta\, d\Delta}. \qquad \text{(VI.9.3)}$$

Substituting in (VI.9.3)

$$d\omega_s = \cos\Delta_0\, d\Delta_0\, d\varphi_0; \quad \int_{\omega_s} F^2(\Delta_0, \varphi_0)\, d\omega_s =$$

$$= \int_0^{2\pi} d\varphi_0 \int_0^{\frac{\pi}{2}} F^2(\Delta_0, \varphi_0) \cos\Delta_0\, d\Delta_0 = \int_0^{2\pi} d\varphi \int_0^{\frac{\pi}{2}} F^2(\Delta, \varphi) \cos\Delta\, d\Delta,$$

we obtain

$$e_{n\,av}^2 = E_n^2 \left(\frac{\lambda}{\pi}\right)^2 \frac{W_F \eta_F \eta}{120}, \qquad \text{(VI.9.4)}$$

from whence

$$e_{n\,av} = E_n \left(\frac{\lambda}{\pi}\right) \sqrt{\frac{W_F \eta_F \eta}{120}}. \qquad \text{(VI.9.5)}$$

What follows from formula (VI.9.5) is that the effective length of any antenna receiving non-directional noise equals

$$l_{eff\,n} = \frac{\lambda}{\pi} \sqrt{\frac{W_F}{120}\, \eta_F \eta}. \qquad \text{(VI.9.6)}$$

The noise intensity at the receiver input when match is optimum, that is, when input impedance of the receiver equals W_F, can be expressed by the formula

$$U_{n\,in} = e_{n\,av}/2 = \lambda/2\pi\, E_n \sqrt{\frac{W_F \eta_F \eta}{120}} \qquad \text{(VI.9.7)}$$

The power developed by the noise across the receiver input when match is optimum and when $\eta_F = 1$, equals

$$P_n = \frac{U_{n\,in}^2}{2W_F} = \left(\frac{\lambda}{2\pi}\right)^2 E_n^2 \frac{\eta_F \eta}{240}. \qquad \text{(VI.9.8)}$$

Then, from formula (VI.9.8), the average power produced across the receiver input by non-directional noise over a long time interval does not depend on the antenna directive gain, but only on its efficiency.

Thus, the use of directional receiving antennas will not result in a weakening of the verage noise power across the receiver input when conditions

that noise is arriving from all directions. The effect derived from the use of a directional receiving antenna, as compared with that obtained from the use of a non-directional antenna under these conditions simply reduces to an increase in the ratio of the power produced across the receiver input by the incoming signal, P_s, to the power produced by the noise P_n. This is obvious when the ratio P_s/P_n for an arbitrary antenna and a half-wave dipole are compared.

According to the definition of gain factor,

$$P_s = \varepsilon P_{s\,\lambda/2}, \qquad \text{(VI.9.9)}$$

where

$P_{s\,\lambda/2}$ is the power supplied across the receiver input when reception is by a half-wave dipole in free space.

The non-directional noise power, with reception by any antenna, equals

$$P_n = \eta P_{n\,\lambda/2}, \qquad \text{(VI.9.10)}$$

where

$P_{n\,\lambda/2}$ is the noise power supplied across the receiver input when reception is by a half-wave dipole.

Comparing formulas (VI.9.9) and (V.9.10),

$$\frac{P_s}{P_n} = \frac{P_{s\frac{\lambda}{2}}\varepsilon}{P_{n\frac{\lambda}{2}}\eta},$$

from whence

$$\frac{P_s}{P_n} : \frac{P_{s\frac{\lambda}{2}}}{P_{n\frac{\lambda}{2}}} = \frac{\varepsilon}{\eta} = \frac{D}{1.64}. \qquad \text{(VI.9.11)}$$

Thus, if the noise arrives from all directions at once the gain in the magnitude of the ratio of useful signal power to noise power provided by any antenna, as compared with the half-wave dipole, equals D/1.64.

When compared with a completely non-directional (isotropic) antenna, the gain equals D.

When compared with an isotropic antenna, the gain in the ratio of the useful signal emf to the noise emf equals $\sqrt{D}$.

#VI.10. Emf Directive Gain

The ratio

$$x = e_s/e_n$$

is the characteristic ratio for reception quality, where

e_s is the emf across the receiver input produced by the useful signal;

e_n is the emf across the receiver input produced by unwanted signals.

The magnitude x can be called the coefficient of excess.

Let us introduce the concept of relative noise stability for antennas, understanding this to be the ratio

$$\delta = \frac{e_s/e_n}{e_{s\ non}/e_{n\ non}} = \frac{x}{x_{non}} ,$$

where

x is the ratio e_s/e_n when reception is by a specified antenna;

x_{non} is the ratio $e_{s\ non}/e_{n\ non}$ when reception is by a non-directional (isotropic) antenna.

It is assumed that the ratio between the useful signal and unwanted signals is the same when reception is by a given antenna and by an isotropic antenna.

Under real conditions the magnitude of δ changes constantly, the result of constant change in useful and unwanted signal field strengths and the directions from which these signals arrive. The concept of an average operational value of δ can be introduced in order to evaluate the operational properties of receiving antennas. We can call this magnitude δ_{av}. It is sometimes taken that

$$\delta_{av} = \sqrt{D} . \qquad \text{(VI.10.1)}$$

Formula (VI.10.1) is valid if noises incoming from all directions are applied to the receiver input simultaneously, and this follows from the data in #V.9. Practically speaking, the evaluation of the operational noise stability based on formula (VI.10.1) is satisfactory when the noise is from individual discrete directions, provided that several emfs produced by the individual noises coming from different directions are applied across the receiver input.

In the latter case, in view of the arbitrariness of the phases of the emfs of the individual noises, the resultant emf equals

$$e_{n\ res} = \sqrt{e_{n1}^2 + e_{n2}^2 + \ldots + e_{nn}^2} \qquad \text{(VI.10.2)}$$

where

e_{n1}, e_{n2}, ..., e_{nn} are the emfs developed across the receiver input by the noises coming from different directions.

Since noise powers across the receiver input are proportional to the square of the emfs of the noises, in this case D, arrived at through formula (VI.4.1), establishes δ_{av} quite well if its connection with the magnitude of D is arrived at through formula (VI.10.1). Practically speaking, the external noise is, for the most part, produced by radio stations operating on frequencies within the receiver's passband, and, as a rule, the interfer . at any given time can be established by the emf developed across the receiver input by the operation of any one of the interfering stations. Given conditions

such as these, the magnitude of $\sqrt{D}$ does not adequately describe the relative noise stability. It is more correct to evaluate the magnitude of δ_{av} through the formula

$$\delta_{av} = D_{emf}^{-1} \qquad \text{(VI.10.3)}$$

where

D_{emf} is the emf directive gain, established through

$$D_{emf} = \frac{|F(\Delta_0, \varphi_0)|}{\int_0^{2\pi} d\varphi \int_0^{\frac{\pi}{2}} |F(\Delta, \varphi)| \cos\Delta \, d\Delta}. \qquad \text{(VI.10.4)}$$

Normalizing $|F(\Delta,\varphi)|$ to $|F(\Delta_0,\varphi_0)|$, and recognizing that ordinarily the function $F(\Delta,\varphi)$ is symmetrical with respect to some azimuth, reading from that azimuth, we obtain

$$D_{emf} = \frac{2\pi}{\int_0^{\pi} d\varphi \int_0^{\frac{\pi}{2}} |F_1(\Delta, \varphi)| \cos\Delta \, d\Delta}, \qquad \text{(VI.10.5)}$$

$$|F_1(\Delta, \varphi)| = \frac{|F(\Delta, \varphi)|}{|F(\Delta_0, \varphi_0)|}.$$

The relative noise stability of two arbitrary receiving antennas, 1 and 2, can be defined by the expression

$$\delta_{av} = x_1/x_2 = D_{emf\ 1}/D_{emf\ 2} \qquad \text{(VI.10.6)}$$

where

x_1 and x_2 are the average operational values for the x factors for antennas 1 and 2;

$D_{emf\ 1}$ and $D_{emf\ 2}$ are the emf directive gains for antennas 1 and 2.

Two antennas with identical values for the directive gain, D, can have different values for D_{emf}. Let us, for example, take antennas 1 and 2, the first of which has a narrower major lobe than the second. Let the side lobes of antenna 1 be so much larger than those of antenna 2 that their D factors are identical. Then, as follows from simple calculations, D_{emf} for antenna 2 is larger than D_{emf} for antenna 1.

But the conclusion that D does not generally characterize the noise stability of receiving antennas does not follow from the foregoing. However,

---

1. G. Z. Ayzenberg. "The Traveling Wave Antenna With Resistive Coupling." Radiotekhnika, No. 6. 1959.

proper use of this factor can, to some degree, enable us to orient ourselves when we are evaluating the qualities of receiving antennas. With this in mind, as well as because an accurate computation of D_{emf} involves even greater computational difficulties, we will henceforth cite the data which characterize the value of D for these antennas when we describe the properties of individual types of receiving antennas.

Chapter VII

PRINCIPLES AND METHODS USED TO DESIGN SHORTWAVE ANTENNAS

#VII.1. Required Wave Band

The wave band required for day-long and year-round communications is extremely inportant in designing antennas for radio communications, and must be known.

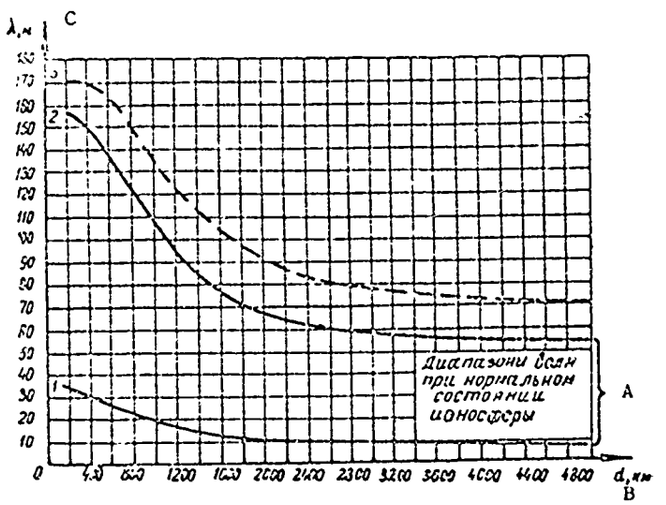

Figure VII.1.1 Required wave bands: 1 - shortest waves, used during the summer, in the daytime, during the period of maximum solar activity; 2 - longest waves, used during the winter, at night, during the period of minimum solar activity; 3 - longest waves, used during the winter, at night, during the period of minimum solar activity during ionospheric perturbations.

A - wave bands for normal ionosphere; B - d, kilometers; C - λ, meters.

Figure VII.1.1 shows the curves which establish the operating wave bands required for day-long and year-round communications during years of minimum and maximum solar activity. The shortest waves are required in the daytime during years of maximum solar activity. Curve 1 shows the shortest waves required during a period of maximum solar activity in the summer in daytime. Even shorter waves (5 to 6 meters) can be used in the winter on long main lines during periods of maximum solar activity during the short periods of daylight. The longest waves are required at night in the winter during years of minimum solar activity (curve 2).

Even longer waves can be used during the winter, at night, during periods of minimum solar activity during ionospheric perturbations (curve 3).

The curves in Figure VII.1.1 were graphed for a northern geographic latitude $\varphi = 56°$. The value of the wavelengths obtained from the curves in Figure VII.1.1 must be multiplied by the correction factor k_1 in order to determine the required wavelengths in other latitudes. Figure VII.1.2 shows the dependence of this factor on the geographic latitude.

The data cited were taken from materials provided by the Scientific Research Institute of the Ministry of Communications of the USSR and show that an extremely broad band is needed to service shortwave main lines.

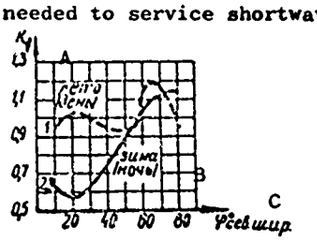

Figure VII.1.2. Correction factors for determining wave bands required in latitudes other than 56°.

A - summer (day); B - winter (night); C - north latitude.

#VII.2. Tilt Angles and Beam Deflection at the Reception Site

(a) Tilt angles

Knowledge of the tilt angles of the beams reaching the reception site is of great significance in designing shortwave antennas. Transmitting antennas must be designed so their radiation patterns provide maximum beam intensity upon reaching the reception site, that is, that attenuation be a minimum, while the directional diagram for receiving antennas should, in so far as possible, provide for maximum intensity in the reception of these beams. Beams are propagated from transmission point to reception point in various ways. For example, in communicating over a distance of 5,000 km, when the height of the reflecting layer is 300 km, the beam can be reflected two, three, or even more times between the transmission point and the reception point. The tilt angle is 7° for two reflections, and 10° for three. This example shows that beams with different tilt angles can reach the reception site.

Beam tilt angles at the reception site change with time because of daily, seasonal, and annual changes in the height of the reflecting layer. Tilt angles can also change because of the appearance of unevenness in the reflecting surface, as well as because of the beam diffusion (scattering) phenomenon. Diffusion is a phenomenon which usually occurs at night, particularly in years of reduced solar activity.

Generalization of the results of measurements made of beam tilt angles at the reception sites by various countries for lines of various lengths leads to the following conclusions.

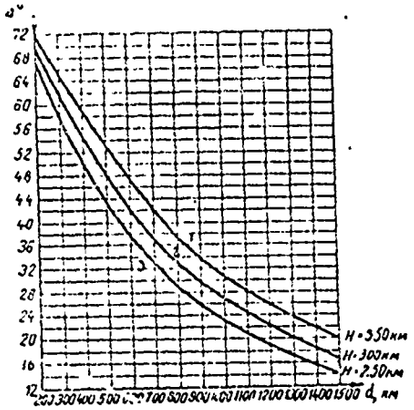

Figure VII.2.1. Dependence of beam tilt angle on length of main line.

The highest degree of probability of carrying on communications on lines ranging in length from 200 to 1500 to 2000 km is with beams with one reflection off the F_2 layer. Figure VII.2.1 shows the curves for the dependence of the beam tilt angle Δ on the length of the main line, d, for one reflection. The curves were constructed for heights of the reflecting layer, H, equal to 250, 300, and 350 km.

Antenna design for main lines 200 to 1500 km long should take the range of angles bounded by the curves constructed for heights of 250 and 350 km, since maximum radiation will be obtained in this way.

When main lines are longer, the most probable values for the tilt angles will change within limits

from 2 to 3° to 20° for a main line 2000 to 3000 km long;

from 2 to 3° to 18° for a main line 3000 to 5000 km long;

from 2 to 3° to 12° for a main line 5000 to 10000 km long.

It should be borne in mind that the range of beam tilt angles at the reception site can spread wider than the limits indicated. For example, maximum tilt angles on long main lines can be 20 to 25.

(b) Beam deflection

Radio waves are normally propagated from the point of transmission to the point of reception over an arc of a great circle on the earth. When the condition of the ionosphere changes in certain ways there is a deflection (deviation) in the direction in which the radio waves are propagated away from this arc. Unevenness, or slopes, on the reflecting surface of the ionosphere can cause beam deflection.

When deflection occurs the beams arriving at the reception site appear to have been radiated on an azimuth which fails to coincide with the direction

of the arc of the great circle. Also possible is the simultaneous arrival of beams propagated along the arc of a great circle and of beams which have some deflection. And those which have been deflected can be more intense than those propagated along the arc.

Currently available are experimental data demonstrating that there is practically no deflection when waves are propagated over the illuminated track, but that deflection is observed for the most part at times of partial track illumination.

Deflection is slight in the overwhelming majority of cases, no more than a few degrees, but there are times, particularly during magnetic storms, when it can be tens of degrees.

The possibility of beam deflection must be taken into consideration when designing antennas. The directional patterns of antennas designed for operation under conditions of partial track illumination should be wide enough to make communications possible when operation is with beams which have some deflection. The question of the limits into which the directional pattern in the horizontal plane can be constructed when operation is over a partially, or wholly unilluminated track, while not causing any considerable increase in the number of hours of non-communications attributable to deflection, cannot now be considered as having been finally resolved. It can be assumed that an adequate width for a half-power pattern is 4 to 6°.

#VII.3. Echo and Fading. Selective Fading

(a) Echo

Beams with different propagation paths do not arrive at the reception site at the same time. The greater the number of reflections, the later the beam will arrive at the reception site. This failure to arrive simultaneously is called echoing, and manifests itself in signal repetition during reception.

Experimental data demonstrate that the difference in the times of arrivals of beams can be as much as 2 to 3 microseconds. The time difference in the travel of adjacent beams will be greater the greater the number of times they are reflected. For example, this difference on the main line between Moscow and New York is about 0.8 microsecond for the first and second beams, and about 1.2 microseconds between the third and fourth beams. This travel time difference can be increased by shortening the main line when the beams have the same number of reflections.

Echoing causes distortion in telephone and telegraph operations alike. In telegraph operations echoing causes plus bias, that is, an increase in the duration of transmitted pulses, and a corresponding decrease in the duration of the spacing, in turn leading to a requirement that keying speed be limited.

Example. Let the travel difference for the beams equal $\tau_{diff} = 1.5$ microseconds. Operation is by Morse code using Creed equipment with a speed of N = 300 international words per minute. It is known that the number of bauds[1] per second when using Morse code is an average 0.8N. In this case the number of bauds per second equals $N_b = 0.8 \cdot 300 = 240$.

Duration of one baud equals

$$\tau_b = 1/240 = 0.00415 \text{ sec} = 4.15 \text{ microseconds.}$$

The shortest spaces have a one-baud duration.

The percentage of plus bias equals

$$1.5/4.15\ 100\% = 36\%.$$

There are various ways to cope with echoing. One effective method is to reduce the number of beams accepted by the antenna, and this is done by appropriate selection of the shape of the directional patterns for transmitting and receiving antennas. Beams following different paths as a rule have dissimilar tilt angles and deflections, so when the directional pattern is constricted and oriented accordingly the desired beams, or groups of beams, can be separated. Chapter XVII will describe one version of an antenna which makes it possible to separate desirable beams.

We note that in addition to the above-described echoing, which occurs as a consequence of receiving beams which differed in the number of reflection enroute from the radiation site to the reception site, there is also a so-called round-the-world echo, which occurs as a result of the reception of beams traveling the same arc of a great circle as the main signal, but in the opposite direction. Now the difference in beam travel can be in the tens of milliseconds. A high-degree of unidirectionality should be the goal for both transmitting and receiving antennae in order to cope with this type of echo.

(b) Fading. Selective fading.

The presence of beams which have covered different paths at the reception site causes a continuous fluctuation in the magnitude of the field strength. This is the phenomenon known as fading. Fading occurs as a result of constant

---

1. A baud is a conventional equivalent, the duration of which equals the duration of one dot in the Morse code. The number of bauds per word equals

$$\tau_{word}/\tau_{time},$$

where

τ_{word} is the average incoming time for one word;

change in the phase relationships of the field strengths of the individual beams. In addition, the beam itself is usually heterogenous. Each beam, in turn, consists of a bundle of homogenous beams, between which there are extremely small differences in travel, yet these are sufficient to cause fading. This reduces to the fact that the individual beams too are subject to fading.

Variations in the field strengths of the individual beams also occur as a result of rotation of the plane of polarization. This is why fading also occurs when a single homogenous beam is present at the reception site.

From what has been said, then, we can see that the picture of the variation in field strength is extremely complicated.

When radiotelephone, or radiotelegraph stations propagate a frequency spectrum there is either simultaneous fading over the entire spectrum, or fading of individual frequencies within the spectrum. The latter is known as selective fading. Selective fading will be found when beams, or bundles of beams, traveling greatly different paths, are present at the reception site.

Selective fading can be explained in this way. Let there be two beams with difference in time of arrival equal to τ at the reception site. Then the difference in the phases of the field strengths of these beams, established by the path difference, equals

$$\Phi_{diff} = \omega\tau = 2\pi f\tau \ , \qquad \text{(VII.3.1)}$$

where

f is the frequency in hertz.

Let us designate the carrier frequency for the radiated spectrum by f_0, and the modulating frequency by F_1, F_2, ..., F_n. The side frequencies equal

$$\begin{aligned} f_1 &= f_0 \pm F_1, \\ f_2 &= f_0 \pm F_2, \\ &\cdots\cdots \\ f_n &= f_0 \pm F_n. \end{aligned}$$

The phase shifts between the beam field strength vectors at different frequencies equal

$$\left.\begin{aligned} \Phi_0 &= 2\pi f_0\tau \\ \Phi_1 &= 2\pi f_0\tau \pm 2\pi\frac{\tau}{T_1} \\ \Phi_2 &= 2\pi f_0\tau \pm 2\pi\frac{\tau}{T_2} \\ &\cdots\cdots\cdots \\ \Phi_n &= 2\pi f_0\tau \pm 2\pi\frac{\tau}{T_n} \end{aligned}\right\}, \qquad \text{(VII.3.2)}$$

where

ϕ_0 is the phase shift in the carrier frequency;

ϕ_1, ϕ_2 ... ϕ_n are the phase shifts in the side frequencies;

T_1, T_2 ... T_n are the oscillation periods for the modulating frequencies.

As we see from formula (VII.3.2), the phase shift consists of two components in the general case. The first of these is the same for all frequencies in the spectrum, but the second depends on the modulating frequency, and establishes the possibility of selective fading. If τ is so small that the angle $2\pi\ \tau/T$ is extremely small, equal to a few degrees for example, for all values of F_{diff}(diff = 1, 2, 3 ...), then the phase shift between the field strength vectors for both beams is approximately the same for all frequencies in the spectrum and fading will occur on all frequencies in the spectrum simultaneously. But if τ is commensurate with T, fading will be selective, that is, will not occur simultaneously on all frequencies.

Example. There are two beams with a travel time difference of 1 microsecond at the reception site. Determine the nature of the fading of a radiotelephone transmission modulated by a frequency spectrum from 50 to 3000 hertz.

Solution. For purposes of simplification we will assume that angle $2\pi f_0\tau$ is a multiple of 2π. Then the resultant field strength for both beams can simply be determined by the angle $2\pi\ \tau/T$.

Maximum fading occurs at frequencies determined from the relationship

$$2\pi\ \tau/T = (2n + 1)\pi, \qquad \text{(VII.3.3)}$$

where

n is any number, or zero.

From formula (VII.3.3) we establish the period of the modulating frequency at which maximum fading occurs

$$T = 2\tau/2n + 1,$$

from whence

$$T_0 = 2\tau = 2 \text{ microseconds},$$

$$T_1 = 2/3\ \tau = 0.666 \text{ microsecond},$$

$$T_2 = 2/5\ \tau = 0.4 \text{ microsecond}.$$

The obtained values for T correspond to the modulating frequencies

$$F_0 = 1/T_0(\text{sec}) = 500 \text{ hertz},$$

$$F_1 = 1/T_1(\text{sec}) = 1500 \text{ hertz},$$

$$F_2 = 1/T_2(\text{sec}) = 2500 \text{ hertz}.$$

Higher modulating frequencies are outside the spectrum specified.

Maximum field strength occurs at frequencies determined from the relationships

$$2\pi\ \tau/T = 2\pi\ n, \qquad \text{(VII.3.4)}$$

where

$$n = 1, 2, 3,$$

from whence

$$T_1 = \tau/1 = 1 \text{ microsecond},$$

$$T_2 = \tau/2 = 0.5 \text{ microsecond},$$

$$T_3 = \tau/3 = 0.33 \text{ microsecond}.$$

Corresponding modulating frequencies equal

$$F_1 = 1/T_1(\text{sec}) = 1000 \text{ hertz},$$

$$F_2 = 1/T_2(\text{sec}) = 2000 \text{ hertz},$$

$$F_3 = 1/T_3(\text{sec}) = 3000 \text{ hertz}.$$

Maximum field strength will also be observed at the carrier frequency.

In the example cited fading and maximum field strength occur simultaneously on both symmetrical side frequencies. This is because of the assumption made that $2\pi f_0 \tau$ is a multiple of 2π. In the general case fading and growth in field strength on symmetrical frequencies is not simultaneous.

In practice, the magnitude of τ does not remain constant but changes continuously, and this causes a continuous change in the amplitude and phase relationships for the radiated frequency spectrum.

The picture of selective fading described is that of two beams at the reception site. When there are several beams the picture is more complex. However, the general nature of fading, and of its selectivity in particular, when there is a considerable difference in beam travel remains in all cases.

Selective fading is accompanied by considerable distortion of the transmission, particularly in telephone and phototelegraph operation.

What follows from the data cited with respect to selective fading is that it can be avoided by eliminating reception of many beams.

One way in which this can be done is to use antennas with narrow and controlled directional patterns.

#VII.4. Requirements Imposed on Transmitting Antennas and Methods for Designing Them.

The basic requirement imposed on the transmitting antenna is to obtain the maximum field strength for assigned radiation power in the necessary direction; that is, obtain the highest gain factor.

Only by reducing the radiation intensity in other directions can the intensity of radiation in a specified direction be obtained for assigned power; that is, by constricting the radiation pattern and orienting the antenna accordingly.

Contemporary professional shortwave antennas achieve constriction of the radiation pattern, and the corresponding field amplification in the assigned direction by distributing the energy among a great many simple dipoles located and excited in such a way that their fields in the assigned direction can be added in phase, or with small mutual phase shifts.

Let us illustrate what has been said by the use of a concrete example. Suppose we have some radiator, say a balanced dipole. And suppose the power applied to the dipole equals P. Then current

$$I = \sqrt{\frac{P}{R_0}}, \qquad \text{(VII.4.1)}$$

will flow in the dipole, and R_0 is the resistive component of the dipole's input impedance.

The field strength at some point M in direction r_0 perpendicular to the dipole axis (fig. VII.4.1) can be expressed as follows in the general case:

$$E_0 = AI = A\sqrt{\frac{P}{R_0}}, \qquad \text{(VII.4.2)}$$

where

A is a proportionality factor which depends on the distance, propagation conditions, and dipole dimensions.

Let another such dipole, II, be added to dipole I, while retaining total input at the same level (fig. VII.4.2).

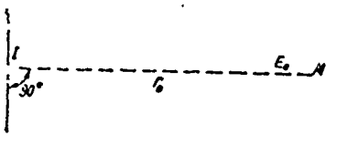

Figure VII.4.1. Derivation of formula (VII.4.4).

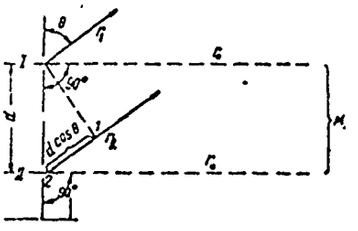

Figure VII.4.2. Derivation of formula (VII.4.4).

Let us assume that the input is halved between dipoles I and II, and that the current flowing in them is in phase. Obviously, the field strengths of both dipoles will add in phase in direction r_0 because the beam paths from both dipoles to the reception site are the same in this direction. Field strength at the reception site equals

$$E = E_1 + E_2 = 2E_1 = 2A\sqrt{\frac{P}{2R_1}} = A\sqrt{\frac{2P}{R_1}}, \qquad \text{(VII.4.3)}$$

where

E_1 and E_2 are the field strengths for dipoles I and II; in this case $E_1 = E_2$;

R_1 is the resistive component of the input impedance of one dipole.

It it is assumed that dipoles I and II are positioned such that their mutual influence can be ignored, $R_1 = R_0$.

And, as will be seen when (VII.4.3) and (VII.4.2) are compared,

$$E = A\sqrt{\frac{2P}{R_0}} = \sqrt{2}E_0. \qquad \text{(VII.4.4)}$$

Thus, field strength is increased by the $\sqrt{2}$, and the gain factor is doubled.

Similarly, replacement of a single dipole by N dipoles will be accompanied by an increase in the gain factor by a factor of N. Equivalent power radiated in direction r_0 is increased by a factor of N.

It goes without saying that the assumptions we have made with respect to the mutual spacing of the dipoles, and the lack of phase shift between currents flowing in the dipoles, are not mandatory. The only thing that is important is that the mutual spacing of the dipoles and the current phase relationships be such that the individual dipoles will add in phase in the necessary direction.

It must not be forgotten that the conclusion made is only valid when the assumption made concerning the mutual effect of the individual dipoles on their pure resistance being small is correct. This requires considerable separation between dipoles. What follows from the foregoing is that the use of the method described to obtain large gain factors involves an increase in antenna size.

Virtually all types of antennas used in the shortwave band are designed by this method. The difference between the individual types of antennas is only in the difference in the methods used to achieve co-phasality of the fields of the individual dipoles comprising the antenna.

As was pointed out above, an increase in field strength in a definite direction can be achieved by constricting the radiation pattern; that is, by reducing the intensity of radiation in other directions. The latter

follows from simple computations. As a matter of fact, we can take the above-cited example (fig. VII.4.2). The dipoles are spaced in such a way that their fields add in phase in direction r_0. The field strengths of dipoles I and II are displaced in phase in other directions. For example, in direction r_1, which forms angle θ with the axes of the dipoles, the difference in the beam paths equals $d \cos \theta$, and the phase displacement between the field strength vectors for these beams equals

$$\varphi = a\, d \cos \theta = 2\pi \frac{d}{\lambda} \cos \theta.$$

When the distances between dipoles in certain directions are sufficiently large angles φ can equal $\pi(2n + 1)$, where $n = 0, 1, 2, \ldots$, and the resultant field strength equals zero. The greater the number of dipoles, the greater the difference in phase of the dipole fields in directions other than the main direction of transmission, and the narrower the major lobe of the spatial radiation pattern.

Accordingly, increasing field strength in a specified direction by distributing the energy among a great many dispersed dipoles definitely constricts the radiation pattern.

The method of designing antennas described here, one involving the distribution of available energy among a great many radiating elements positioned and excited such that the elements add in phase, or with a small phase displacement, in the required direction, provides the radiation pattern shape yielding the maximum radius vector for the pattern in that direction. However, it does not provide the narrowest radiation pattern for specified antenna dimensions.

In principle, it is possible to obtain radiation patterns as narrow as desired for any assigned antenna dimensions, and, as a result, as high a gain in the magnitude of field strength as desired for the corresponding out of phase summation of fields produced by the individual radiations. The above indicated dependence between gain in field strength and antenna dimensions is only valid when fields of individual antenna elements at the reception site are in phase. Accordingly, it is possible, in principle, to design highly efficient, small antennas. However, small antennas have certain shortcomings as a natural consequence of their size. When the dipoles are excited so they produce a field which sums out of phase the required field strength at the reception site for assigned radiated power is such that very much greater current amplitudes are excited in the antenna than is the case for co-phased excitation. This causes an increase in reactive energy. The ratio of reactive energy to radiated energy increases very rapidly with reduction in antenna size, and this growth is accompanied by a corresponding constriction in the pasband and an increase in losses. Moreover, the strong cross coupling between elements of small, highly directional antennas makes it difficult to tune them.

Hence small, highly directional antennas are not used. The possibility of reducing the size of highly directional antennas with out of phase fields created by their individual elements has, to a limited extent, seen practical realization in the form of traveling wave antennas, and in certain other types of antennas.

#VII.5. Types of Transmitting Antennas

(a) Balanced dipole

One of the simplest types of antennas using the above method for increasing field strength in a specified direction is the balanced dipole, each leg of which is no longer than $\lambda/2$. This dipole consists of two identical halves, excited in phase. Maximum radiation is obtained in a direction normal to the dipole axis because in this direction the fields of both halves and of all elements in each half of the dipole sum in phase. The radiation pattern of this dipole was shown in Figure V.4.1.

(b) The Tatarinov antenna

The antenna suggested by V. V. Tatarinov is another way in which the method described for increasing the gain factor in a specified direction can be used. The operating principle is as follows. Suppose we have a balanced dipole, the length of which is considerably greater than the wave length. If we disregard attenuation, the current distribution is as shown in Figure VII.5.1.

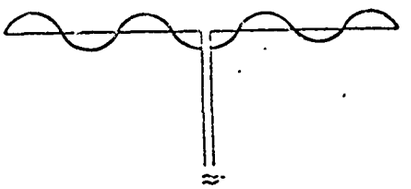

Figure VII.5.1. Current distribution on a long balanced dipole.

As will be seen from Figure VII.5.1, both halves of the dipole are excited in phase and there are sections $\lambda/2$ long in each in which the currents are opposite in phase.

This dipole is unsuited for use as a radiator in a direction normal to its axis because the fields created by the excitation in the sections of the dipole in which phases are opposite will cancel each other. However, if, in some way, the radiation from the segments passing currents of one phase can be eliminated the dipole will be a system of half-wave dipoles excited in phase and providing an increase in the field strength in a direction normal to the axis.

The antenna arrangement suggested by Tatarinov (fig. VII.5.2) solves this problem. Segments of the conductor carrying currents of one phase

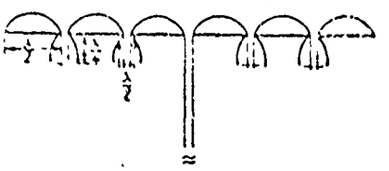

Figure VII.5.2. Schematic diagram of the Tatarinov antenna.

convolute, becoming two-wire lines, while the segments of the conductor passing currents of the opposite phase remain involute and act as radiators. Out of phase currents flowing in the two-wire lines(loops) provide very slight radiation.

The Tatarinov arrangement is a comparatively simple way in which to distribute energy between a great many co-phasally excited dipoles. The fields of all dipoles add in phase in the direction normal to the antenna axis and the gain factor in this direction increases in proportion to the number of half-wave dipoles.

The Tatarinov antenna has two directions in which radiation is a maximum, so it is fitted with a reflector (fig. VII.5.3) in order to make it unidirectional. The reflector is a system similar in all respects to the antenna proper. The reflector is usually suspended at a distance of from 0.2 to 0.25 λ from the antenna.

The reflector is excited in such a way that the field strengths of reflector and antenna are in phase in direction r_1 (fig. VII.5.3), and opposite in phase in direction r_2. The reflector produces a unidirectional radiation pattern and the field strength in direction r_1 is increased approximately $\sqrt{2}$. Figure VII.5.4 shows the radiation pattern in the horizontal plane for the Tatarinov antenna with four half-wave dipoles in each half.

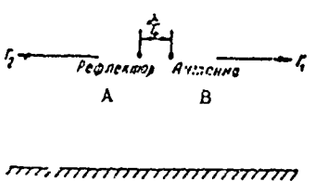

Figure VII.5.3. Antenna with reflector.
A - reflector; B - antenna.

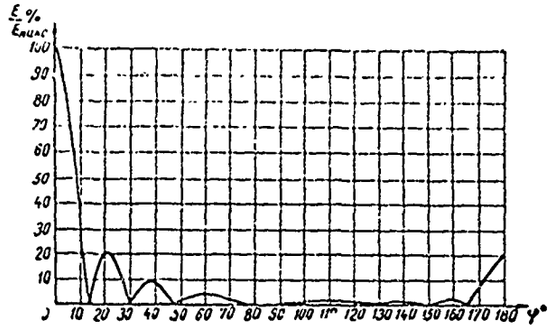

Figure VII.5.4. Radiation pattern in the horizontal plane for the Tatarinov antenna consisting of eight half-wave dipoles.

(c) Broadside vertical antenna

Figure VII.5.5 is a schematic diagram of a broadside vertical antenna.

The antenna consists of several sections (four in this case) fed from one source over transmission lines 1 and 2.

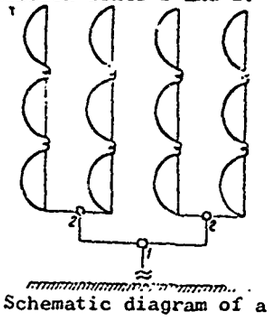

Figure VII.5.5. Schematic diagram of a vertical broadside antenna.

Each section is a vertical conductor functioning on the same principle as does the Tatarinov antenna. The difference is that radiation from the segments and out of phase carrier currents are eliminated by their convolution into a coil. The radiation produced by the current flowing in the coils is very weak, as in the case of the segments of the conductor in the Tatarinov antenna convoluted into a loop.

The vertical broadside antenna can be developed upward (increasing the number of tiers), as well as broadwise (by increasing the number of sections).

The antenna is fitted with a reflector to make it unidirectional.

The vertical broadside antenna was used on many main radio lines in the first years of shortwave main radio communications.

The chief shortcoming of the vertical broadside antenna is the vertical orientation of the dipole. The use of vertical dipoles in the shortwave band simply means that much of the power applied to the antenna is dissipated in the ground. Use of an artificially metallized ground can reduce these losses, but this is, as a practical matter, extremely complicated and uneconomical.

(d) Horizontal broadside antenna (SG)

A somewhat different, and extremely convenient, method distributes energy between matched fed dipoles in a horizontal broadside antenna, the basic elements of which were developed in the USSR, in the Nizhegorod Radio Laboratory.

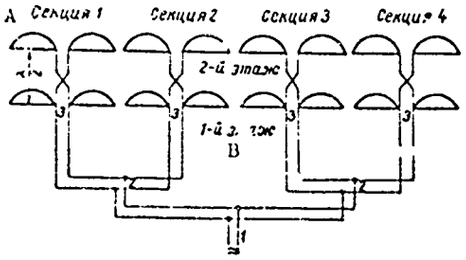

Figure VII.5.6. Schematic diagram of a horizontal broadside antenna.

A - section; B - tier.

One version of the antenna is shown in Figure VII.5.6. It has four sections. In phase excitation of the sections is ensured because the current paths from source to each section are identical, a factor which also provides identical current amplitudes in all sections. The identity of current amplitudes for dipoles in the first and second tiers of each section is ensured because the tiers are interconnected by two-wire lines $\lambda/2$ long. The voltages across two points displaced $\lambda/2$ from each other are identical in absolute value in lossless lines. However, in the absence of special measures the currents flowing in the first and second tiers will be 180° apart because the voltages across lines $\lambda/2$ apart will be 180° out of phase. The inter-tier lines are crossed, and this is the equivalent of creating an additional 180° phase shift, so this eliminates the phase shift mentioned. The horizontal broadside antenna can be developed upward by increasing the number of tiers, as well as broadwise by increasing the number of dipoles in each tier.

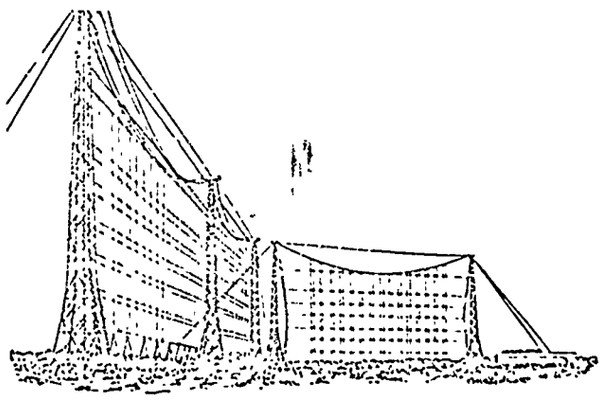

Figure VII.5.7. General view of horizontal broadside antennas.

Figure VII.5.7 shows a general view of horizontal broadside antennas built for one of the radio centers. Horizontal broadside antennas are usually fitted with reflectors. Antennas of this type are used by modern shortwave transmitting radio centers. A detailed analysis is made in Chapter XI.

(e) Slant wire antenna

The elements of this particular antenna is a conductor installed in the form of a broken line and consisting of straight line sections $\lambda/2$ long, in the same vertical plane (fig. VII.5.8). Current flows in the dipoles are conventionally designated by arrows. Each slant segment of the conductor produces a field which can be represented in the form of horizontal and vertical components. The vertical components of the field strength vectors for all dipoles are in phase in the direction normal to the plane in which the antenna elements are located, but the horizontal components are out of phase in pairs and are therefore mutually compensatory.

Figure VII.5.8. Schematic diagram of a single-tier slant wire antenna.

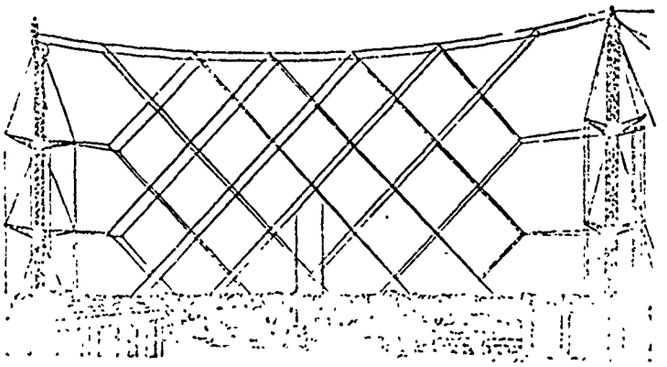

Figure VII.5.9. General view of a slant wire antenna.

The slant wire antenna is usually made up of several co-phasally excited elements located one above the other in the vertical plane. The antenna is usually fitted with a reflector. The direction of maximum radiation of this antenna (like that of all the above-described antennas) is normal to the plane in which its curtain is located, and the antenna produces only the vertical component of the field strength vector in this direction. The shortcomings of the vertical antennas indicated above are characteristic of the slant wire antenna as well.

A general view of the antenna is shown in Figure VII.5.9.

(f) V-antenna

Figure VII.5.10 is a general view of a V-antenna. It consists of two horizontal, or slant, wires positioned at some angle to each other.

The operating principle of this antenna is as follows. We have explained in Chapter V that a long conductor produces intense radiation at some angle to its axis. For example, the maximum radiation produced by a conductor $l = 8\lambda$ is at an angle of 17.5° to its axis. The angle between the conductors is selected such that the field in the direction of the bisector, or at some height angle to the bisector, produced by both conductors adds in phase, resulting in an increase in the gain factor in this direction.

Complex antennas, consisting of two and more V-antennas, are used to further increase the gain factor.

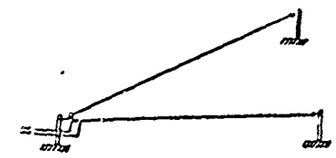

Figure VII.5.10. General view of a V-antenna.

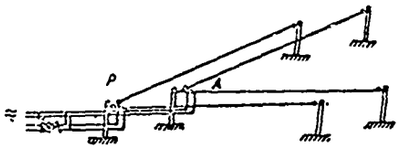

Figure VII.5.11. Schematic diagram of a V-antenna with reflector.

Figure VII.5.11 is a sketch of a complex V-antenna consisting of the main curtain A, and the reflector P.

(g) Rhombic antenna

Figure VII.5.12 is the schematic diagram of the rhombic antenna. The operating principle of this antenna will be taken up in detail later on. Here we will simply note that the arrangement of the rhombic antenna too is based on the above explained method of designing directional antennas, that of distributing energy among matched working dipoles. In this case the energy is distributed among four conductors passing the current of a traveling wave. The conductors themselves have sharply defined directional properties (figs. V.2.1 - V.2.4). The four conductors of the rhombic antenna are positioned such that their fields add in phase in the necessary direction.

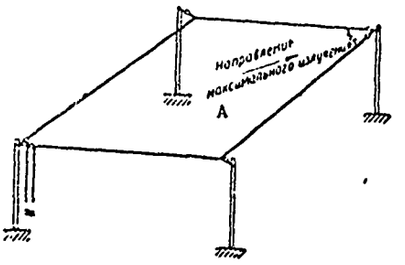

Figure VII.5.12. Schematic diagram of a rhombic antenna.
A - direction of maximum radiation.

Complex rhombic antennas are often used in practice (double rhombic antennas, and others).

The big advantage of the rhombic antenna is that it can be used over a broad, continuous band of frequencies.

Rhombic antennas are widely used throughout the world.

There are, in addition to the antennas discussed above, a great many other types of antennas which we will not discuss here.

#VII.6. Requirements Imposed on Receiving Antennas

The receiver input always has an emf, e_i, which interferes with reception across it, and this emf is in addition to the useful signal emf.

Let us call the expression

$$x_i = e_s/e_i$$

the coefficient of excess, x_i. This data is taken from #VI.10.

The basic requirement imposed on the receiving antenna is that it provide the maximum possible coefficient of excess.

Let us distinguish between internal and external noise sources. External sources are those which induce extraneous emfs in the antenna. These are carried to the receiver input by the transmission line. Sources such as these include the noise produced by stations radiating on frequencies close to each other, by atmospheric charges, by industrial sources of radio interference, and others.

Internal noise sources are tube noises caused by fluctuations in the electron flows through the tubes, and circuit noises caused by the thermal movement of electrons along the conductors.

All stages of the receiver have tube and circuit noises, but tube and circuit noise emfs can be replaced by equivalent emfs at the receiver input, or as they say, they can be reduced to the receiver input.

Accordingly

$$x_i = e_s/e_{ex} + e_n, \qquad \text{(VII.6.1)}$$

where

e_{ex} is the external noise emf across the receiver input;

e_n is the receiver's internal noises reduced to the receiver input.

The requirements imposed on the receiving antenna depend on the ratio of e_{ex} to e_n.

Two extreme main line operating modes can be distinguished.

The first mode occurs when $e_{ex} \gg e_n$, the second when $e_{ex} \ll e_n$.

In the first mode

$$x_i = x = e_s/e_{ex}, \qquad \text{(VII.6.2)}$$

because reception quality is determined only by the ratio of signal emf to external noise emf received by the antenna.

What follows from the data in #VI.10 is that in the first mode reception quality is determined by the directive gain, D_{emf}, or $\sqrt{D}$.

The gain factor has no significant value in this case because when the shape of the directive pattern is retained change in reception strength is not accompanied by a change in the coefficient of excess.

In the second receiving antenna operating mode

$$x_i = x_n = e_s/e_n, \qquad \text{(VII.6.3)}$$

that is, the reception quality is determined by the ratio of signal emf to receiver internal noise emf.

Substituting the expression for e_s we obtain

$$x_n = \lambda E_s/\pi e_n \sqrt{W_F \eta_F/73.1}\ \sqrt{\varepsilon}. \qquad \text{(VII.6.4)}$$

As will be seen, the antenna gain factor is of decisive importance in the second mode.

It should be noted that the lower the antenna gain factor, the greater the probability that the main line is operating in the second mode. There is marked predominance of the first regime in the case of modern receiving antennas on shortwave main lines. The second regime is most often observed during years of reduced solar activity, particularly at night. The intermediate operating mode, when e_x and e_n are commensurable, is rare, but when encountered the coefficient of excess must be computed through formula (VII.6.1).

What follows from what has been said is that increase in directive gain is particularly important for the receiving antenna. Increase in the gain factor is also material.

#VII.7. Methods Used to Design Receiving Antennas

The methods used to design shortwave receiving antennas are similar to those used to design shortwave transmitting antennas.

The growth in field strength in the necessary direction when transmitting is obtained by the distribution of energy among the radiating dipoles, the latter positioned and excited in such a way that the field strengths of the individual dipoles add in phase in the assigned direction, or with minimum mutual phase displacement.

The growth in power applied to the receiver input when reception occurs is arrived at similarly. The receiving dipoles are positioned in space and connected to each other and to the receiver input in such a way that the emfs induced in all dipoles by the wave arriving from a specified direction produce co-phased voltages, or voltages with small mutual phase displacements, at the receiver input.

Let us take the concrete example of an antenna consisting of two balanced dipoles to illustrate this. Let the incoming wave arrive from direction r_0, normal to the dipole axis. Let us suppose that initially reception is by one dipole and that transmission line l_1 feeds emf e_1 to the receiver input (fig. VII.7.1). Let the input impedance of the transmission line at the receiver input equal $Z_F = R_F + iX_F$. Maximum energy at receiver input is obtained if the receiver input impedance equals $R_F - iX_F$.

In this case the power applied to the receiver input equals

$$P_{rec} = e_1^2/8R_F. \qquad \text{(VII.7.1)}$$

Let us now suppose that instead of one dipole we have two identical dipoles oriented relative to the direction of the incoming wave in the same way as was the first dipole (fig. VII.7.2). We will assume the same transmission lines used in the first case are used here to carry the emf from the dipoles to the receiver.

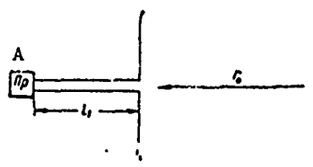

Figure VII.7.1. Explanation of the methods used to design receiving antennas.

A - receiver.

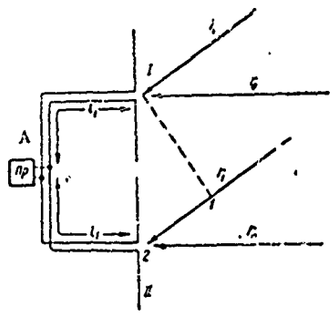

Figure VII.7.2. Explanation of the methods used to design receiving antennas.

A - receiver.

Since the transmission lines to both dipoles are of equal length and since both dipoles are located in a straight line oriented along the wave front, the emfs from both dipoles are identical in amplitude and phase at the receiver input. Emf amplitude for two dipoles will remain what it was in the case of one dipole.

If dipoles I and II are separated in such a way that the input impedance of each can be taken as equal to the input impedance of a single dipole, the impedance of two transmission lines connected to the receiver input in parallel equals

$$R_F/2 + i\,X_F/2$$

The power applied to the receiver input, efficiency is optimum, equals

$$P'_{rec} = e_1^2/8\,\frac{R_F}{2} = 2P_{rec}. \qquad \text{(VII.7.2)}$$

As will be seen, the power supplied to the receiver is doubled, while the voltage across the grid of the input tube of the receiver is increased by the $\sqrt{2}$. It goes without saying that the gain in the power supplied to the receiver will not change if transmission lines other than those used with one dipole are used with two dipoles. What is necessary, regardless of the case involved, is to have optimum match with receiver input and equal transmission line efficiencies.

The increase in power indicated is applied to the receiver input when the beams picked up by the antenna arrive from a predetermined direction, but if the beams arrive from other directions, say r_1 (fig. VII.7.2), the emfs induced in dipoles I and II will be displaced in phase, one from the other, because of the beam propagation difference, and there will be a corresponding decrease in the power applied to the receiver. There can also be directions from which the power applied to the receiver input will equal zero.

It is not difficult to prove that if there are N dipoles instead of just one, correspondingly phased, the gain factor will be increased N times and the voltage across the grid of the input will be increased $\sqrt{N}$ times.

Accordingly, the increase in the power received from one direction is significantly linked to the reduction in the power received from other directions; that is, linked with the increase in the directional properties of the antenna, and this too follows from formula (VI.3.4).

This is the method used to design all modern shortwave receiving antennas for main radio communications and the antennas are matched, in one way or another, to the operating system of dipoles. Individual types of receiving antennas differ from each other only in the manner ir which the co-phased operation of the elements are arrived at, and in the manner in which the elements proper are made.

The general considerations cited here lead to the conclusions that any transmitting antenna capable of increasing field strength in a specified direction can be used as a receiving antenna, and that the antenna will provide for an increase in power incoming from a specified direction (when the match to the receiver is made accordingly).

These conclusions, based on general considerations, also follow from the principle of reciprocity, which was the basis for the proof of the identity of the directional properties of any antenna during reception and transmission given above.

#VII.8. Types of Receiving Antennas

(a) General remarks

All of the transmitting antenna types described in the foregoing are widely used, or have been used, for reception as well. The rhombic antenna has been particularly widely used in the reception field. There are certain types of receiving antennas which have not, however, been used in the transmission field. These include the zigzag antenna, the traveling wave antenna, and others.

(b) Zigzag antenna

In its day the zigzag antenna was widely used in reception centers. The schematic is shown in Figure VII.8.1.

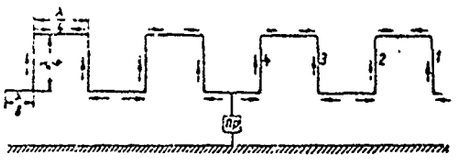

Figure VII.8.1. Schematic diagram of a zigzag antenna.
A - receiver.

Maximum reception is from the direction normal to the curtain plane, and the voltages developed across the receiver input induce in phase emfs in the antenna's vertical elements. The emfs induced in the horizontal elements are out of phase in pairs and thus cancel each other.

It is convenient to illustrate what has been said by using the principle of reciprocity as a base and considering the antenna as if it were used to transmit. Figure VII.8.1 shows the distribution of the currents along the antenna when it is excited by a generator. As will be seen, all vertical elements are excited in phase. The horizontal elements consist of two equal segments excited in such a way that phases are opposite.

(b) Traveling wave antenna

The traveling wave antenna (fig. VII.8.2) is widely used in the reception field.

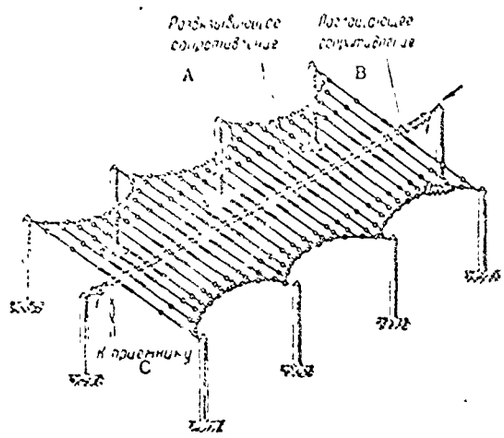

Figure VII.8.2. Schematic diagram of a traveling wave antenna.

A - decoupling resistor; B - terminating resistor; C - to receiver.

It consists of a collection line, 1-1, connected to balanced dipoles at equal intervals along its length. The dipoles are usually impedance connected to the line. One end of the line goes to the receiver, the other to the impedance, which is equal to the line's characteristic impedance. The emfs induced in the individual dipoles by the incoming wave cause a current to flow in the collection line to the receiver input. The best current phasing from the individual dipoles is obtained when a wave moving in the direction shown in the figure by the arrow is incoming.

The principle of operation of the traveling wave antenna will be described in detail later on. We will simply note here that the significant advantage of this antenna is the possibility of using it over a broad, continuous band of frequencies.

Chapter VIII

MAXIMUM PERMISSIBLE POWER TO OPEN-WIRE FEEDERS AND ANTENNAS

#VIII.1. Maximum Power Carried by the Feeder

The maximum power carried by the feeder is determined by the dielectric strength of the insulators used and of the air surrounding the feeder. Let us first deal with the question of the dielectric strength of air.

If field strength exceeds a permissible value ionization of the air will set in and air breakdown will occur. This phenomenon can be explained as follows. Free electrons are present in space, particularly near the surface of a conductor. These electrons acquire additional velocity as a result of the field effect. The greater the field strength at the surface of the conductor, the higher the velocity attained by the electrons, and the more frequent the ionization of the neutral molecules of air colliding with these electrons, that is the dislodging of electrons from their orbits. The dislodged electrons in turn accelerate the process of further ionization. The positive ions, that is molecules with excess positive charges, bombard the negatively charged conductor, causing an additional flow of electrons from the surface of the conductor into the air, and, at the same time also intensifying the ionization process. Acceleration of ionization is also caused by the direct activity of ions on neutral particles.

Ionization is accompanied by a process which decreases available ionized particles, the latter the result of recombination, and in part the result of the dissipation of the charged particles into surrounding space. If field strength is not too great the process whereby charged particles are reduced quickly results in curtailment of the ionization process initiated. When fields are strong the ionization process initiated is sustained. The result is the appearance of stable volumes of ionized air around the conductor.

Radiation of electromagnetic waves within the limits of the optical wave band occurs as the molecules are ionized, causing the ionized air mass to glow.

Field strength is not everywhere the same along the line, the result of standing waves, as well as because of local nonuniformities (bends, protrusions, and others) where elevated field strengths are established. This is why the ionization process is usually initiated at definite sites and not all along the conductor and why ionization is accompanied by elevated air temperatures at these sites. A column of ionized air will rise, like an ordinary flame, in the form of a torch, and hence the term "torch emanation." Even when the wind is light the torch formed will move with the wind, and if it enters an area with a weaker field it will be extinguished. A torch occurring on vertical or slant wires will usually move upward.

Torch emanation on lines is not permitted, because it can lead to overheating and melting of the conductors. Too, torch emanation causes high frequency energy loss, since the HF energy is converted into heat.

The field strength at which spontaneous torch formation takes place is called the initiating field strength, and once the torch is formed it can be sustained at a field strength below that of initiation. Minimum field strength at which the torch emanation, once established, can be sustained is called critical field strength. If field strength is higher than critical torch emanation can occur as a result of random spark formation caused by a conducting body, such as a falling leaf, a bird, an insect, a drop of water, and other bodies, coming in contact with a current-carrying conductor. It is therefore recommended that field strength be below critical.

The initiating field strength is approximately equal to 30 kv/cm. While no exhaustive data on critical field strength are available at this time, the experience in the construction of powerful shortwave stations is broad enough to allow the following conclusions to be drawn. Critical field strength does not always remain the same, but depends on temperature and humidity. Critical field strength decreases with increase in temperature and humidity, with the result that it is somewhat lower in the summer than in the winter. Experience, as well as theoretical considerations, indicate that critical field strength in the long wave portion of the shortwave band is somewhat greater than in the short wave portion.

Available experience confirms the fact that the permissible amplitude of the field strength is approximately equal to 6 to 8 kv/cm. Permissible power, in accordance with (1.13.10) can be found through

$$P_{max} = E_{per}^2 d^2 kWn^2/28800 \qquad \text{(VIII.1.1)}$$

where

E_{per} is the permissible amplitude of field strength.

When telephone transmission is amplitude modulated and the transmitter is operating at assigned power output, the peak amplitude of the field strength is twice what it is in the telegraph mode, so a reduction in permissible power by a factor of four can be expected. The experimental investigations made by I. S. Gonorovskiy revealed however that as a practical matter, because the peak field strength lasts but a very short time, one can, if necessary, permit peak field strength amplitude to be $\sqrt{2}$ greater.

Accordingly, the peak field strength amplitude in the case of AM telephony can, if need be, be 8.4 to 11.2 kv/cm. Correspondingly, the permissible power in the case of telephony is not reduced by a factor of 4, but only by a factor of 2, so in the case of telephone transmission maximum power can be established through

$$P_{max} = k_1 \cdot E^2_{per} d^2 kwn^2/28800 \qquad \text{(VIII.1.2)}$$

where

k_1 is a constant which takes the permissible increase in field strength amplitude to peak into consideration. From what has been said, k_1 can be taken as equal to 0.5.

Let us now look at the question of the dielectric strength of insulators. Since antenna and feeder insulators are in the open air the permissible potentials can be determined by the dielectric strength of insulators covered with moisture, which is considerably below the dielectric strength of a dry surface.

It can be taken that it is permissible to apply potentials to wet insulators such that the voltage drop across the insulator will be no more than 1 to 1.5 kv/cm, or, putting it another way, the potential gradiant should be no more than 1 to 1.5 kv/cm. Insulators used in shortwave feeder lines are usually made in the form of long rods or sticks with smooth surfaces, and the purpose is to reduce the shunt capacitance created by the insulators. An insulator such as that described has a potential drop per unit length of path approximately the same along the entire length of the insulator,

$$\partial V/\partial t \approx V/t \qquad \text{(VIII.1.3)}$$

where

V is the potential applied to the insulator;

t is the length of the path over the surface of the insulator from the point of application of the potential to the point of zero potential.

The insulator must be metal-tipped in order to satisfy the equality at (VIII.1.3), otherwise there will be an increase in the potential gradient at the point of voltage application.

One version of this metal tip is shown in Figure H.V.1.

We note that in a balanced line the potential is half the voltage across a U line.

#VIII.2. Maximum Permissible Antenna Power

Any typical shortwave antenna (balanced dipole, rhombic antenna, and others) can be reduced to an equivalent line, or to a system of lines between which energy can be distributed (broadside antenna and others). Therefore, maximum permissible power can be established through the same formulas, (VIII.1.1) and (VIII.1.2), as in the case of the line. But we must, however, pay attention to the manner in which individual units (the transpositions,

the end surfaces of the dipoles, etc.) are made in order to eliminate heavy local field gradients. The requirements imposed on antenna insulation are the same as those imposed for feeder insulation.

It should be noted that data cited here concerning permissible powers do not coincide with the data cited in our monograph titled Antennas for Main Line Communications (Svyaz'izdat, 1948). Data in the latter were based on a generalization of M. S. Neyman's experimental investigations. Obviously, while his investigations were correct, in and of themselves, they were not adequate for generalization purposes.

Chapter IX

THE BALANCED HORIZONTAL DIPOLE

#IX.1. Description and Conventional Designations

The balanced dipole is one of the simplest and most widely used of the shortwave antennas. Figure IX.1.1 is a schematic, and as will be seen the dipole is a conductor, to the center of which an emf is applied through a feeder, or transmission line.

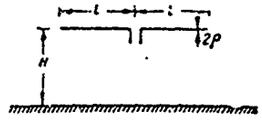

Figure IX.1.1. Balanced horizontal dipole.

Chapter V discussed the general theory of the balanced dipole, and here we will use the results of that theory to establish the properties of balanced dipoles used in the shortwave field.

The balanced horizontal dipole has come to be designated by the letters VG (dipole, horizontal). A balanced dipole with low characteristic impedance designed for broadband use is designated by the letters VGD (dipole, horizontal, broadband). A fraction, the numerator of which indicates the length of one arm, l, and the denominator of which indicates the height, H, at which the dipole is suspended, is added to the letter designation to indicate suspension height and arm length. For example, VG 10/15 signifies a horizontal dipole with an arm length of 10 meters suspended at a height of 15 meters.

#IX.2. General Equation for Radiation Pattern

Engineering computations of the radiation pattern can ignore attenuation in the dipole, that is, it can be taken that $\gamma = i\alpha$. The radiation pattern formulas, according to (V.5.12) and (V.5.13) and without taking the factor characterizing the phase into consideration become

$$E_{\perp} = \frac{60I_{loop}}{r} \frac{\cos(\pi l \cos\varphi \cos\Delta) - \cos\pi l}{\sin^2\varphi + \cos^2\varphi \sin^2\Delta} \sin\varphi \times$$

$$\times \sqrt{1 + |R_{\perp}|^2 + 2|R_{\perp}| \cos(\Psi_{\perp} - 2\pi H \sin\Delta)}, \qquad \text{(IX.2.1)}$$

$$E_{\parallel} = \frac{60I_{loop}}{r} \frac{\cos(\pi l \cos\varphi \cos\Delta) - \cos\pi l}{\sin^2\varphi + \cos^2\varphi \sin^2\Delta} \cos\varphi \sin\Delta \times$$

$$\times \sqrt{1 + |R_{\parallel}|^2 - 2|R_{\parallel}| \cos(\Psi_{\parallel} - 2\pi H \sin\Delta)}, \qquad \text{(IX.2.2)}$$

where

I_{loop} is the current flowing in a dipole current loop;

φ is the beam azimuth angle, that is, the angle formed by the projection of the beam on the horizontal plane and the direction of the axis of the dipole;

Δ is the beam tilt angle, that is, the angle formed by the direction of the beam with the horizontal plane;

l is the length of one dipole arm;

$|R_\perp|$, $|R_\parallel|$, $\phi_\perp$ and $\phi_\parallel$ are moduli and arguments for the reflection factors for normally polarized and parallel polarized beams.

The reflection factors are established through formulas (V.5.7) and (V.5.6)

$$|R_\perp|e^{i\Phi_\perp} = \frac{\sin\Delta - \sqrt{\varepsilon_r' - \cos^2\Delta}}{\sin\Delta + \sqrt{\varepsilon_r' - \cos^2\Delta}},$$

$$|R_\parallel|e^{i\Phi_\parallel} = \frac{\varepsilon_r' \sin\Delta - \sqrt{\varepsilon_r' - \cos^2\Delta}}{\varepsilon_r' \sin\Delta + \sqrt{\varepsilon_r' - \cos^2\Delta}}.$$

Here $\varepsilon_r' = \varepsilon_r - i60\gamma_v\lambda$,

where

ε_r is the relative dielectric strength of the soil (see #V.5);

γ_v is the specific conductivity of the soil in mho/meter.

Table IX.2.1 lists values for ε_r and γ_v for various types of soils and waters.

Table IX.2.1

Types of waters and soils	ε_r		γ_v (mho/meter)	
	from	to	from	to
Sea water	80	-	$700\cdot10^{-3}$	$7000\cdot10^{-3}$
Fresh water	80	-	$1\cdot10^{-3}$	$5\cdot10^{-3}$
Wet soil	5	25	$1\cdot10^{-3}$	$11\cdot10^{-3}$
Dry soil	2	6	$0.1\cdot10^{-3}$	$4\cdot10^{-3}$

It is convention to characterize the directional properties of antennas by the radiation patterns in the vertical and horizontal planes, with the vertical plane taken to be in the direction of maximum radiation. Accordingly, in this case the vertical plane is selected as passing through the center of the dipole and normal to its axis (its equatorial plane). In this plane $E_\parallel = 0$.

#IX.3. Radiation Pattern in the Vertical Plane

Substituting $\varphi = 90°$ in formula (X.2.1), we obtain the following expression for the radiation pattern in the vertical plane

$$F(\Delta) = \frac{E}{\frac{60I_{loop}}{r}} = (1 - \cos\alpha l)\sqrt{1 + |R_\perp|^2 + 2R_\perp \cos(\Phi_\perp - 2\alpha H \sin\Delta)} \qquad (IX.3.1)$$

Figures IX.3.1 - IX.3.11 show a series of radiation patterns in the vertical plane for various values of H/λ. The diagrams were charted in a rectangular system of coordinates, and because of the symmetry of the patterns with respect to the direction $\Delta = 90°$ only patterns for one quadrant were charted in figures IX.3.1 - IX.3.11.

The solid curves chart the patterns for ideally conducting ground ($\gamma_v = \infty$). The dashed lines chart the diagrams for ground of average conductivity ($\varepsilon_r = 8$, $\gamma_v = 0.005$). The dotted lines chart the patterns for dry ground ($\varepsilon_r = 3$, $\gamma_v = 0.0005$).

This series of patterns characterizes the limits of change in the shape of the radiation patterns for various ground parameters. Patterns for non-ideal ground were computed for a wavelength of 30 meters.

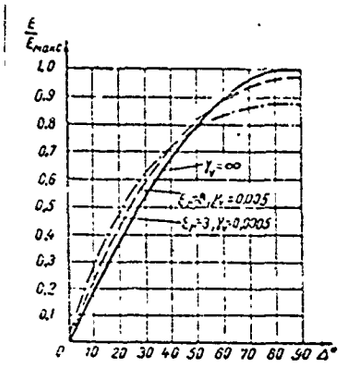

Figure IX.3.1. Radiation patterns in the vertical plane for a VG antenna for various ground parameters; $H/\lambda = 0.1$.

Vertical scale: E/E_{max}.

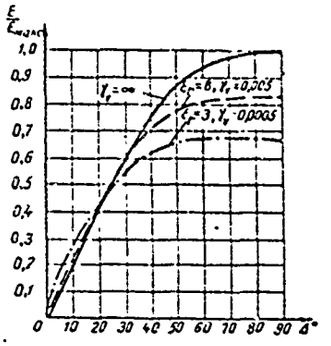

Figure IX.3.2. Radiation patterns in the vertical plane for a VG antenna for various ground parameters; $H/\lambda = 0.2$

1. The engineering computations for horizontal dipole radiation patterns usually assume that the ground is ideally conducting ($|R_\perp| = 1$, $\Phi_\perp = \pi$), and the computation is made through formula (V.5.4).

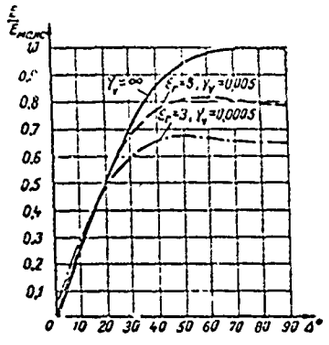

Figure IX.3.3. Radiation patterns in the vertical plane for a VG antenna for various ground parameters; $H/\lambda = 0.25$.

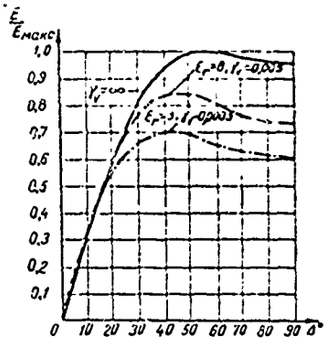

Figure IX.3.4. Radiation patterns in the vertical plane for a VG antenna for various ground parameters; $H/\lambda = 0.3$.

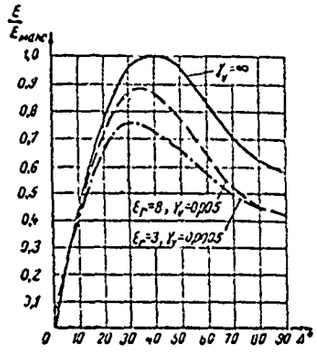

Figure IX.3.5. Radiation patterns in the vertical plane for a VG antenna for various ground parameters; $H/\lambda = 0.4$.

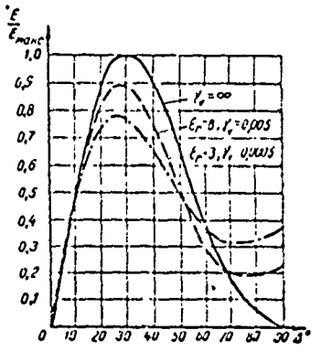

Figure IX.3.6. Radiation patterns in the vertical plane for a VG antenna for various ground parameters; $H/\lambda = 0.5$.

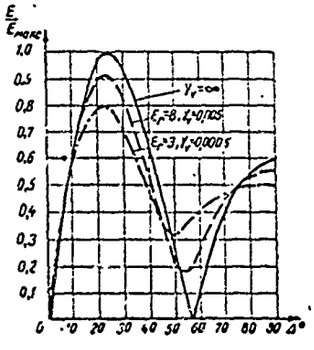

Figure IX.3.7. Radiation patterns in the vertical plane for a VG antenna for various ground parameters; $H/\lambda = 0.6$.

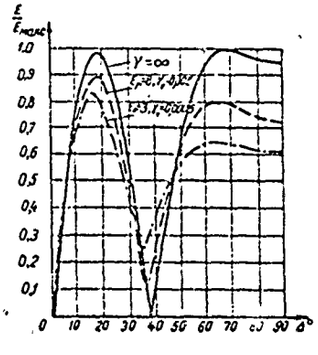

Figure IX.3.8. Radiation patterns in the vertical plane for a VG antenna for various ground parameters; $H/\lambda = 0.8$.

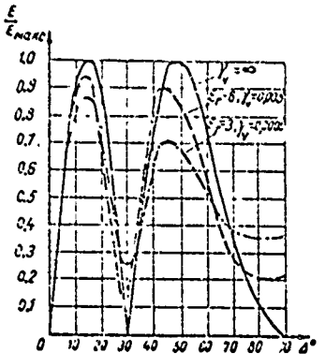

Figure IX.3.9. Radiation patterns in the vertical plane for a VG antenna for various ground parameters; $H/\lambda = 1.0$.

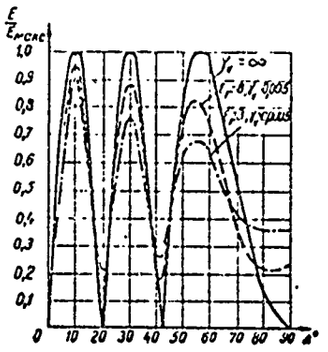

Figure IX.3.10. Radiation patterns in the vertical plane for a VG antenna for various ground parameters; $H/\lambda = 1.5$.

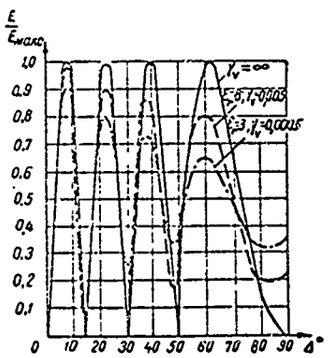

Figure IX.3.11. Radiation patterns in the vertical plane for a VG antenna for various ground parameters; $H/\lambda = 2.0$.

These curves are characteristic enough for any wave in the shortwave band. Figures IX.3.12 and IX.3.13 show values for $|R_{\perp}|$ and $\varphi_{\perp}$ for various types of ground and wave lengths of 15 and 80 meters by way of illustrating what has been said. As will be seen from these curves, $|R_{\perp}|$ and $\varphi_{\perp}$ have little dependence on the wavelength within the limits of the shortwave band.

The relationship

$$E/E_{max}$$

where

E is the field strength in the specified direction;

E_{max} is the field strength in the direction of maximum radiation for ideally conducting ground,[1]

is laid out on the axis of the ordinates in Figures IX.3.1 - IX.3.11.

---

1. The computation for E assumed the resistive component of the antenna impedance remains the same regardless of ground parameters.

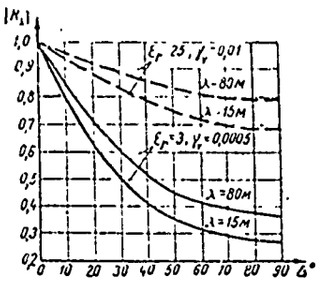

Figure IX.3.12. Dependence of the modulus of the reflection factor for a normally polarized beam on the angle of tilt for 15 and 80 meter wavelengths for dry (ε_r = 3, γ_v = 0.0005) and damp (ε_r = 25, γ_v = 0.01) soil.

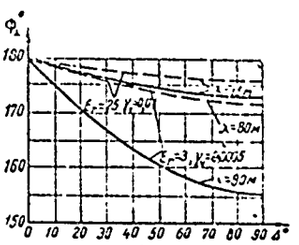

Figure IX.3.13. Dependence of the argument for the reflection factor for a normally polarized beam on the angle of tilt for 15 and 80 meter wavelengths for dry (ε_r = 3, γ_v = 0.0005) and damp (ε_r = 25, γ_v = 0.01) soil.

When the radiation patterns for ideally conducting ground and real ground are compared we see that field strength maxima decrease because of the reduction in conductivity, and that the values of the minima increase.

Curve 1 in Figure IX.3.14 shows the dependence of tilt angles for the maximum beam of the first lobe (read from the direction $\Delta = 0$) on the ratio H/λ.

Plotted in this same figure are the tilt angles for beams the intensity of which (power) is less than that of the maximum beat. For example, the curves designated by the figure 0.3 show the values for angle Δ corresponding to beams the intensity of which is 0.9 the intensity in the direction of maximum radiation. All curves were plotted applicable to the first lobe of the pattern.

The curves in Figure IX.3.14 were plotted for ideally conducting ground.

#IX.4. Radiation Pattern in the Horizontal Plane

Formulas (IX.2.1) and (IX.2.2) are used to compute the radiation patterns in the horizontal plane for specified value of angle Δ. Formula (V.5.16) can be used in the case of ideally conducting ground, substituting $\gamma = i\alpha$ into

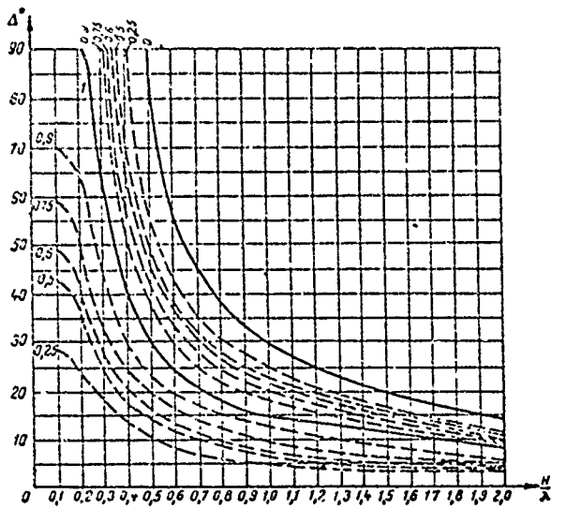

Figure IX.3.14. Dependence of the angles of tilt of the beam of the first lobe of the radiation pattern in the vertical plane of a VG antenna on suspension height: 1 - curve for tilt angles for maximum beam; 0.9; 0.75; ...; 0.25 - curves for angles of tilt of beams, the intensity of which is 0.9; 0.75; ... 0.25 on intensity of maximum beam (with respect to power); 0 - boundary of first lobe.

it. The relationship between the field strength in the specified direction and the field strength in the direction of maximum radiation can be expressed through

$$E/E_{max} = A \frac{\cos(\alpha l \cos\Delta \cos\varphi) - \cos\alpha l}{\sqrt{\sin^2\varphi + \cos^2\varphi \sin^2\Delta}}, \qquad (IX.4.1)$$

where

A is a factor which does not depend on φ.

The radiation pattern for very small angles Δ is of particular interest because it can be checked experimentally very readily by measuring the field intensity at ground level. When $\Delta \to 0$

$$E/E_{max} = B \frac{\cos(\alpha l \cos\varphi) - \cos\alpha l}{\sin\varphi}. \qquad (IX.4.2)$$

Here B is a constant not dependent on angle φ. From formula (V.5.16) B should equal zero when $\Delta = 0$. However, this is the result of an inaccuracy in the geometric optics method used to derive the formula. More precise analysis reveals that $B \neq 0$.

Figure IX.4.1 shows a series of radiation patterns in the horizontal plane when $\Delta = 0$ and various values for l/λ.

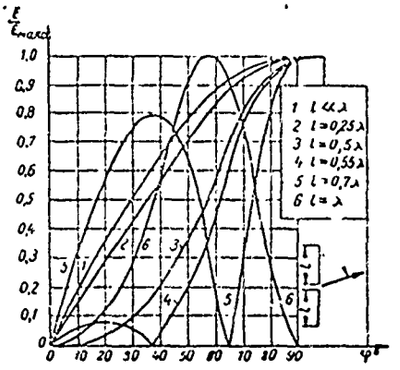

Figure IX.4.1. Radiation pattern in the horizontal plane for a VG antenna when $\Delta = 0$ for various values of l.

Vertical: E/E_{max}.

Figures IX.4.2 - IX.4.9 show a series of radiation patterns of a balanced dipole in the horizontal plane, computed for definite values of the ratio l/λ and various values of angle of tilt Δ.

As will be seen from the curves in figures IX.4.1 - IX.4.9, the balanced dipole has maximum radiation in a direction normal to its axis for values of l/λ, lying within the limits from 0 to ~ 0.7, that is, from the longest waves to wavelengths on the order of 1.4 l. Radiation in this direction begins to diminish very quickly upon further shortening of waves.

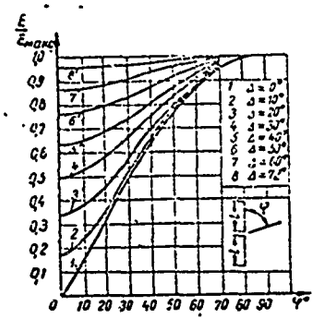

Figure IX.4.2. Radiation patterns in the horizontal plane for a VG antenna for various angles of tilt Δ; $l \ll \lambda$.

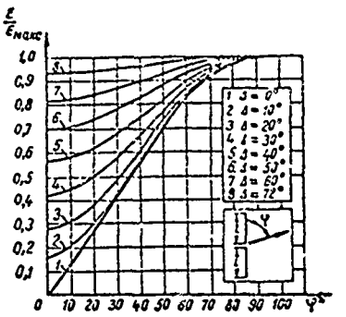

Figure IX.4.3. Radiation patterns in the horizontal plane for a VG antenna for various angles of tilt Δ; $l = 0.25\ \lambda$.

There is no radiation in the direction normal to the axis when the wavelength is equal to l. Practically speaking, however, there will be some radiation in the direction $\varphi = 90°$ on this wavelength, the result of attenuation of the current flowing in the dipole's conductors.

What follows from figures IX.4.1 - IX.4.9 is that the larger angle Δ, the less defined will be the directional properties obtained for the antennas.

The latter reveals that it is possible to use the balanced dipole for non-directional radiation if communications are conducted on beams with large angles of tilt.

According to the data cited in Chapter VII, beams with large angles of tilt are not worked when communications are over short distances (fig. VII.2.1).

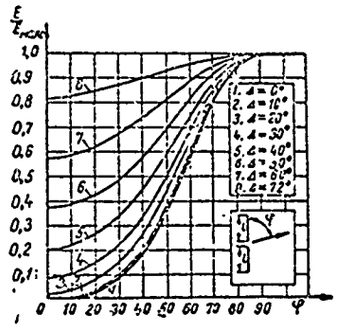

Figure IX.4.4. Radiation patterns in the horizontal plane for a VG antenna for various angles of tilt Δ; t = 0.5 λ.

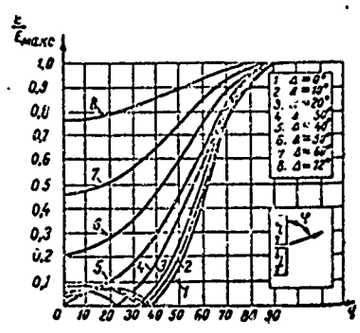

Figure IX.4.5. Radiation patterns in the horizontal plane for a VG antenna for various angles of tilt Δ; t = 0.55 λ.

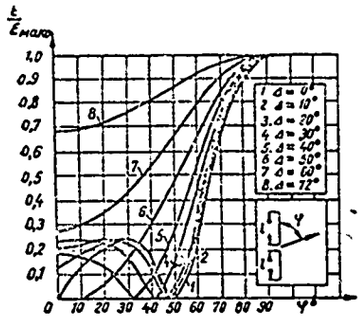

Figure IX.4.6. Radiation patterns in the horizontal plane for a VG antenna for various angles of tilt Δ; t = 0.61 λ.

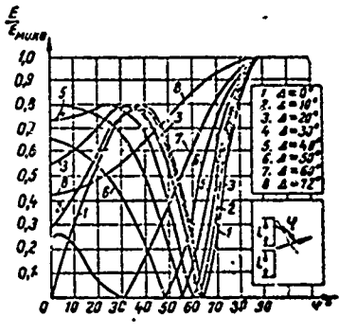

Figure IX.4.7. Radiation patterns in the horizontal plane for a VG antenna for various angles of tilt Δ; t = 0.7 λ.

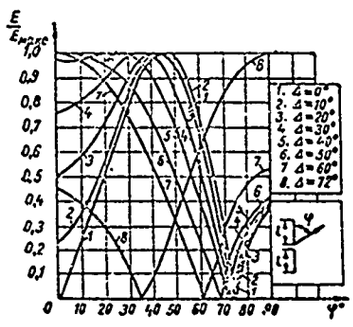

Figure IX.4.8. Radiation patterns in the horizontal plane for a VG antenna for various angles of tilt Δ; t = 0.8 λ.

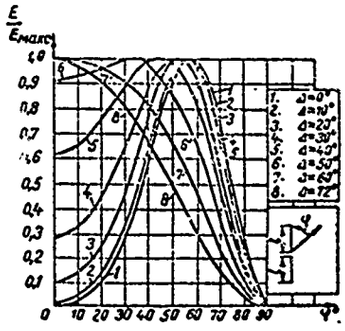

Figure IX.4.9. Radiation patterns in the horizontal plane for a VG antenna for various angles of tilt Δ; t = λ.

#IX.5. Radiation Resistance

Formula (V.12.18) is used to find the radiation resistance of a balanced dipole in free space. It yields the radiation resistance relative to a current loop and is deduced without the effect of the ground being taken into consideration. When suspension heights are on the order of $\lambda/4$ and more the influence of the ground on the radiation resistance can be computed approximately if the ideal conductivity of the ground is assumed, for this assumption makes it possible to replace the ground by the mirror image of the dipole. V. S. Knyazev (see the footnote to #V.16, p.136) analyzed the effect of the real ground on the radiation resistance of the dipole.

In the case of ideal ground conductivity the mirror image is a radiator wholly similar to the balanced dipole, but passing current shifted 180° in phase with respect to dipole current. Thus, radiation resistance can be computed through the formula

$$R_{\Sigma} = R_{11} - R'_{11} , \qquad (IX.5.1)$$

which takes the effect of the ground into consideration, and in which

R_{11} is the dipole's own radiation resistance computed through formula (V.12.18), and

R'_{11} is the mutual radiation resistance of two dipoles positioned at distance 2H.

R'_{11} can be computed through formula (V.12.15), or from the curves in the Handbook Section.

Figure IX.5.1 is a curve computed to show the dependence of radiation resistance of a balanced dipole with arm length $l = \lambda/4$ on suspension height. The curve was computed by the approximation method pointed out here.

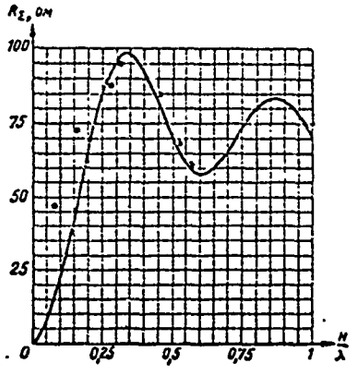

Figure IX.5.1. Dependence of radiation resistance of a half-wave dipole on the H/λ ratio (H is the dipole suspension height).

V. V. Tatarinov's experimental data on the resistive component of the input impedance of the dipole were used to plot the points on this curve.

As will be seen from Figure IX.5.1, when $H/\lambda > 0.25$ the experimental values for pure resistance and the values for radiation resistance, computed through formula (IX.5.1), agree well. When suspension heights are low the experimental values of the pure resistance are considerably in excess of the computed values for radiation resistance. Non-coincidence of experimental and theoretical curves can be explained by the losses to ground, as well as by the divergence between actual and computed values for radiation resistance caused by the finite conductivity of the ground.

Figures V.8.1a and b show the curves for dipole radiation resistance equated to a current loop and computed without considering ground effect ($R_\Sigma = R_{11}$).

#IX.6. Input Impedance

Formula (V.10.2) can be used to calculate the input impedance of a balanced dipole, the influence of the ground not considered,

$$Z_{in} = W \frac{\operatorname{sh} 2\beta l - \frac{\beta}{\alpha} \sin 2\alpha l}{\operatorname{ch} 2\beta l - \cos 2\alpha l} - i W \frac{\frac{\beta}{\alpha} \operatorname{sh} 2\beta l + \sin 2\alpha l}{\operatorname{ch} 2\beta l - \cos 2\alpha l}.$$

The attenuation factor, β, can be calculated through the following formula, which stems from formula (V.10.8)

$$\beta = \frac{R_\Sigma}{W\left(1 - \frac{\sin 2\alpha l}{2\alpha l}\right)}. \qquad \text{(IX.6.1)}$$

Approximate formula (V.10.9)

$$Z_{in} = \frac{R_\Sigma}{\sin^2 \alpha l} - i W \operatorname{ctg} \alpha l.$$

can be used to calculate Z_{in} for values of l/λ between 0 and 0.35 and from 0.65 to 0.85.

Formula (V.10.3)

$$W = 120\left(\ln \frac{2l}{d} - 1\right),$$

where d is dipole conductor diameter, can be used to make an approximate calculation of characteristic impedance of a single-conductor dipole.

The influence of the ground on characteristic impedance can be ignored for real suspension heights. Formula (V.18.2) can be used in case of need to make an approximate calculation of the ground effect on characteristic impedance.

Analysis of formula (V.10.2) demonstrates that the input impedance curve will pass through a maximum for l as a multiple of $\lambda/2$. Here the input

impedance has only the effective component, and equals

$$R_{max} = W^2/R_{\Sigma} . \qquad (IX.6.2)$$

When l equals an odd number for $\lambda/4$ the input impedance passes through a minimum and it too has only the effective component, equal to

$$R_{min} = R_{\Sigma}. \qquad (IX.6.3)$$

A comparison of formulas (IX.6.2) and (IX.6.3) reveals that the dependence of the input impedance on l/λ will be less the smaller W.

Moreover, what also follows from formulas (V.10.2) and (V.10.9) is that with a reduction in W comes a reduction in the absolute value of the reactive component of the input impedance for all values of the ratio l/λ.

Figures IX.6.1 and IX.6.2 provide a series of curves which characterize the dependence of the resistive, R_{in}, and reactive, X_{in}, components of Z_{in} on the ratio l/λ.

It has already been pointed out (Chapter V, #12), that the effect of the distributed induced emfs is to reduce the phase velocity of propagation along the dipole conductor. There is some corresponding increase in α, and the curves for R_{in} and X_{in} shift in the direction of lesser values of l/λ. Change in the phase velocity can also occur as a result of the secondary field established by currents flowing in the ground.

The influence of the capacitance of the ends of the dipole arms, as well as the influence of insulator capacitance, is manifested by a significant distortion in dipole current distribution and a corresponding deformation of input impedance curves. The lower the characteristic impedance the greater the distortion of the input impedance curves as compared with the curves shown in figures IX.6.1 and IX.6.2. The shift to lesser values of l/λ is a characteristic feature of the effective curves for the input impedance as compared to the calculated curves, as has already been pointed out. This shift differs with different l/λ ratios, however. The shift is particularly marked when the l/λ values are close to 0.5. For example, in practice maximum R_{in} does not occur when $l/\lambda = 0.5$, but when $l/\lambda \approx 0.46$ if W equals 700 to 1000 ohms, when $l/\lambda \approx 0.42$ if W equals 400 to 500 ohms, and when $l/\lambda \approx 0.4$ if W equals 200 to 300 ohms.

Ultrashort-Wave Antennas (Svyaz'izdat, 1957), Chapter XIII, #2, contains detailed data dealing with effective input impedance curves.

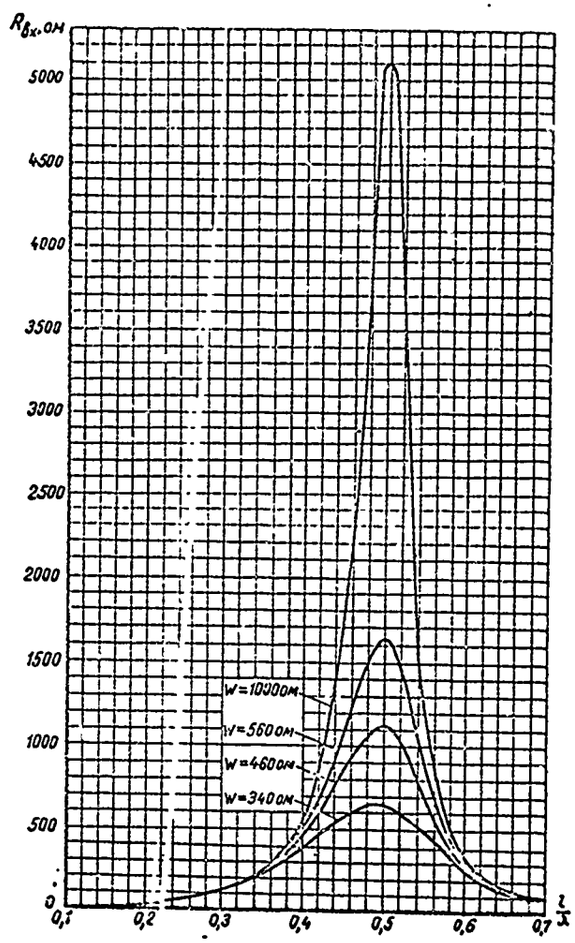

Figure IX.6.1. Dependence of the resistive component of the input impedance of the VG antenna on l/λ for various characteristic impedances.

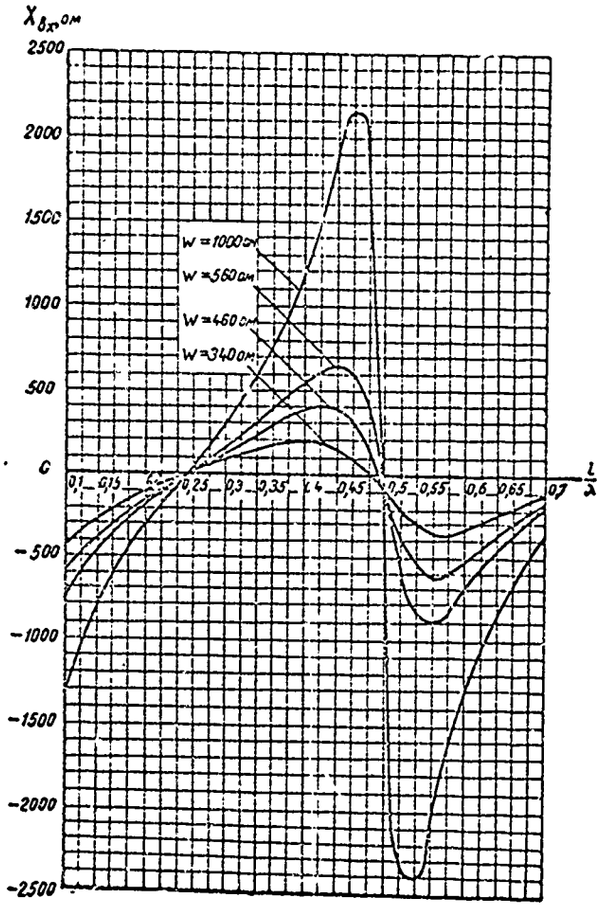

Figure IX.6.2. Dependence of the reactive component of the input impedance of a VG antenna on l/λ for various characteristic impedances.

#IX.7. Directive Gain, D, and Antenna Gain Factor, ε

We have already explained that directive gain has the following expression [formula (VI.1.10)]

$$D = \frac{120F^2(\Delta, \varphi)}{R_\Sigma},$$

where

$$F(\Delta, \varphi) = \frac{E}{\frac{60I}{r}}.$$

Let us find the value of D for the vertical plane passing through the center of the dipole, and normal to its axis.

Let us substitute the value of $F(\Delta,\varphi)$ from formula (IX.3.1) in formula (VI.1.10), whereupon

$$D = 120\frac{(1-\cos\alpha l)^2}{R_\Sigma}\left[1+|R_\perp|^2+2|R_\perp|\cos\left(\Phi_\perp - 2\pi H\sin\Delta\right)\right]. \qquad \text{(IX.7.1)}$$

Formula (IX.7.1) will become

$$D = \frac{480}{R_\Sigma}(1-\cos\alpha l)^2\sin^2(\alpha H\sin\Delta). \qquad \text{(IX.7.2)}$$

for ground with infinite conductivity.

Formula

$$D = \frac{480}{R_\Sigma}(1-\cos\alpha l)^2. \qquad \text{(IX.7.3)}$$

establishes the efficiency in the direction of maximum radiation in the case of ideally conducting ground.

The gain factor is established by the relationship at (VI.3.4)

$$\varepsilon = D\eta/1.64,$$

where

η is the efficiency, equal to

$$\eta = R_\Sigma/R_\Sigma + R_{loss} \qquad \text{(IX.7.4)}$$

where

R_{loss} is the loss resistance, equated to a current loop.

R_{loss} consists of losses attributable to the ground, antenna conductors and insulators used to suspend the antenna, as well as to other dielectrics if they are close to the antenna. The cables supporting the antenna can also be a source of loss. All losses other than ground losses can be ignored if the antenna is properly made, and if the antenna is on the order of 0.2 to 0.25 λ above the ground, or higher, losses attributable to the ground are not high either. Accordingly, when calculating the gain factor we can take η equal to unity, and make the calculation through the formula

$$\varepsilon = D/1.64. \qquad \text{(IX.7.5)}$$

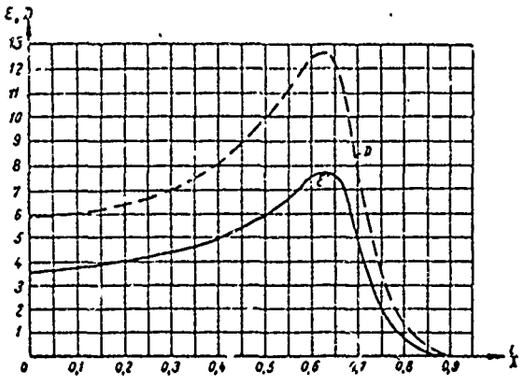

Figure IX.7.1. Dependence of the gain factor (ε) and directive gain (D) in the direction of maximum radiation by a VG antenna on the l/λ ratio.

Figure IX.7.1 shows the curves providing the dependence of the gain factor and directive gain on l/λ. The curves were calculated assuming ground with infinitely great conductivity. The influence of the ground on the radiation resistance was not taken into consideration.

As will be seen from these curves the gain factor increases initially with increase in l/λ, and maxima for gain factor and directive gain occur when $l/\lambda = 0.63$. But further increase in l/λ results in a sharp drop in the gain factor, and this must be taken into consideration when establishing the dipole's working wave band.

The curves for the dependence of ε and D on l/λ, like the input impedance curves, actually shift womewhat to the lesser values of l/λ and this too must be taken into consideration in antenna design. For example, the maximum gain is actually obtained when the l/λ ratio is 5 to 20% less than theoretical.

The curves in figures IX.3.1 - IX.3.11 can be used to establish ε for real ground, remembering that the gain factor is proportional to the square of the field strength.

Example 1. Establish the gain factor in the direction of maximum radiation when $l/\lambda = 0.4$; $H/\lambda = 0.5$, and the soil is dry.

Using the curve in Figure IX.7.1, we can establish the fact that for ideally conducting ground and $l/\lambda = 0.4$, $\varepsilon = 4.9$. From the curve in Figure (X.3.6 we can establish the fact that in the direction of maximum radiation the ratio of field strength and dry soil to field strength when $\gamma_v = \infty$ equals 0.78. The gain factor in the direction of maximum radiation and dry soil equals $\varepsilon = (0.78)^2 \cdot 4.9 \approx 3$.

The formula

$$\varepsilon_{eff} = \varepsilon\left(\frac{1+|R_{\perp}|}{2}\right)^2, \qquad (IX.7.6)$$

where

$|R_{\perp}|$ is the modulus of the reflection factor for a specified angle of tilt, and can be used to make an approximate calculation of the reduction in the gain factor in the direction of maximum radiation for any wave in the case of real ground.

What follows from the data concerning the magnitude of $|R_{\perp}|$ graphed in Figure IX.3.12, is that when the soil is dry the gain factor can be reduced by a factor of from 1.1 to 2, depending on the direction of maximum radiation.

Using the series of radiation patterns in the vertical plane we can establish ε and D for any value of Δ. The reduction in ε and D for a direction other than that of maximum radiation is proportional to the reduction in the E^2/E^2_{max} ratio.

#IX.8. Maximum Field Strength and Maximum Permissible Power for A Balanced Dipole

The maximum permissible antenna power for proper selection of insulation can be established by the dielectric strength of the air surrounding the antenna (see Chapter VIII). There is danger of torch emanation if the electric field strength at the surface of the antenna conductors should exceed some predetermined magnitude. As in the case of feeders, we can take the maximum permissible amplitude of the field strength to be on the order of 6000 to 8000 volts/cm for telegraph transmission, or for FM telephone transmission. If necessary, the peak amplitude of the field strength can go to 10000 to 11000 volts/cm in the case of AM telephone transmission. In accordance with (I.13.9), and considering the balanced dipole as a unique two-wire line, we obtain the following expression for maximum field strength at the dipole surface

$$E_{max} = 120U/ndW, \qquad (IX.8.1)$$

where

n is the number of conductors in each arm of the dipole;

d is the diameter of the conductors used in the dipole, cm;

W is the dipole's characteristic impedance, ohms;

U is the voltage across symmetrical points on both arms of the dipoles, volts.

The field around the antenna is not a potential field. A field is called a potential field if the voltage drop across two arbitrary points does not depend on the path over which movement occurs from one point to the other. Practically speaking, this only occurs when antenna dimensions

are small compared with the wavelength. In the case of the balanced dipole, which has a length commensurate with the wavelength, the voltage drop depends on the path. Specifically, the voltage drop across two symmetrically located points on the two arms of the dipole depends on the path over which the drop is established. For example, the voltage drop along path r_1 (fig. IX.8.1) generally speaking, differs from the voltage drop along path r_2. In view of what has been said, then, the magnitude of U is non-uniform for the dipole.

Nevertheless, formula (IX.8.1) can be used to establish E_{max} in designing an antenna, because the practical aspects are satisfied.

This is so because in the direct proximity of the conductors the dipole's field structure does not differ significantly from the field structure near the conductors of a conventional twin line with small spacing between conductors, the field of which can be taken to be a potential field. Therefore, in establishing E, we can, as we did in a number of other cases, use the representation of an equivalent twin line and assume U to be the voltage across the conductors of this equivalent line. We will call this voltage the equivalent voltage, and its distribution along the line can be established through the formulas cited in Chapter I, #6. The maximum equivalent voltage can be obtained at the end of the line, that is, at the ends of the dipole arms and at the line input, if the l/λ ratio is close to 0.5.

The equivalent voltage across the end of the line equals

$$U_{end} = U_{in}/\operatorname{ch} \gamma l \qquad \text{(IX.8.2)}$$

The effective voltage across the input, U_{in}, is found through

$$U_{in} = Z_{in}\sqrt{P/R_{in}} \qquad \text{(IX.8.3)}$$

where

P is the input power to the dipole.

The effective value of the field strength at the end of the dipole can be found through

$$E_{end} = 120U_{end}/ndW. \qquad \text{(IX.8.4)}$$

The effective value of the field strength at the dipole input can be found through

$$E_{in} = 120U_{in}/ndW\ . \qquad \text{(IX.8.5)}$$

Substituting the U_{in} for U_{end} and P and Z_{in} for U_{in} in (IX.8.4) and converting,

$$E_{end} = \frac{120\sqrt{\frac{P}{R_{in}}}}{nd\sqrt{(\operatorname{ch}\beta l\cos\alpha l)^2 + (\operatorname{ch}\beta l\sin\alpha l)^2}}\ . \qquad \text{(IX.8.6)}$$

We can take $\gamma = i\alpha$ for l/λ values less than 0.35, as well as for l/λ values between 0.65 and 0.85, whereupon (IX.8.6) will become

$$E_{end} = \frac{120 \sqrt{\frac{P}{R_{in}}}}{nd \sin \pi l} \approx \frac{120 \sqrt{\frac{P}{R_{\Sigma}}}}{nd} . \qquad (IX.8.7)$$

Figures IX.8.2 and IX.8.3 show the dependencies of U_{in} and U_{end} on the l/λ ratio for various values of W and input power of 1 kw. By suing these curves and formulas (IX.8.4) and (IX.8.5) we can find E_{end} and E_{in} for specified values of n and d.

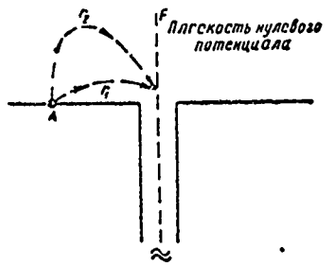

Figure IX.8.1. Determination of the voltage across two points on a dipole.

F - zero potential plane.

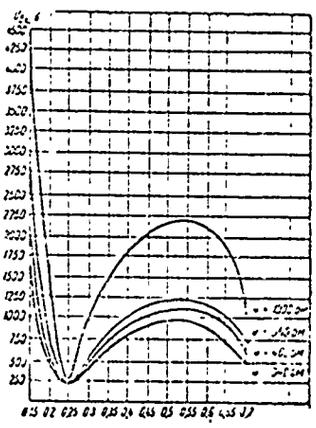

Figure IX.8.2. Dependence of input voltage (effective value) across a VG antenna on the l/λ ratio for input P = 1 kw.

Vertical: U_{in}, volts.

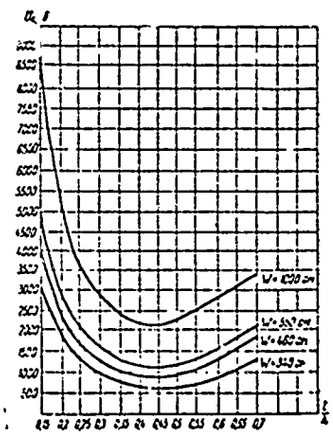

Figure IX.8.3. Dependence of the effective equivalent voltage across the ends of the dipole of a VG antenna on the l/λ ratio for input P = 1 kw.

Vertical: U_{end}, volts.

Figure IX.8.4 graphs the values of E_{end} and E_{in} when P = 1 kw. computed for two characteristic versions of balanced dipoles.

The values for E_{end} and U_{end} graphed in figures IX.8.2 - IX.8.4 must be multiplied by $\sqrt{P}$, with P the input in kilowatts, to obtain values for E_{end} and U_{end} when the input differs from 1 kw.

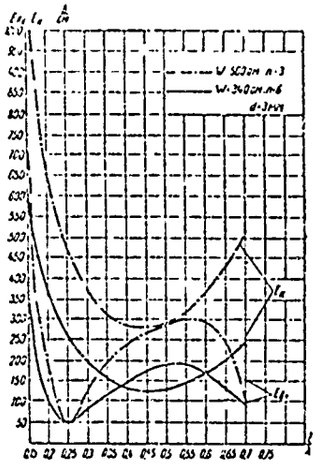

Figure IX.8.4. Dependence of the effective value of the field strength at the input (E_{in}) and at the end (E_{end}) of a dipole on the l/λ ratio for input P = 1 kw. Vertical: E_{in}; E_{end}, volts/cm.

What follows from Figure IX.8.4, and taking the remarks contained in #VIII.2 into consideration, is that the multiple-tuned dipole with characteristic impedance W = 340 ohms used in the wave band between λ = 3 to 4 l and λ = 1.7 l can accommodate up to 300 kw in the case of telegraphy operations and half that in the case of AM telephony.

The multiple-tuned shunt dipole, the operating wavelength of which begins with λ = 6 l, can accommodate a maximum of 100 kw in the case of telegraphic transmission and 50 kw in the case of telephony for the n and d values indicated in Figure IX.8.4. Either n or d must be increased correspondingly to increased accommodated power.

#IX.9. Use Band

The band in which the balanced dipole can be used is determined primarily by its directional properties in the horizontal plane. The patterns for the balanced dipole (figs. IX.4.1 - IX.4.9) show that the direction of maximum radiation remains the normal to the axis of the dipole for waves longer than ~1.4 l.

So from the point of view of the directional properties in the horizontal plane the same dipole can be used for communications in a specified direction on any wave longer than 1.4 l.

The second factor which establishes the band in which the balanced dipole can be used is the possibility of matching its input impedance to the characteristic impedance of the supply feeder. This possibility is established by the natural traveling wave ratio for the feeder, understood to mean the traveling wave ratio when there are no tuning devices in the line. But one must distinguish between working a fixed wavelength and working a broad, continuous band of frequencies.

An inductive stub, or some other method (see Chapter XX) can be used to match the dipole's input impedance and the feeder's characteristic impedance when operating on a fixed wavelength. A good match can be made for any value of l/λ. However, in practice tuning is unstable when the natural traveling wave ratio for the feeder is small. The antenna input impedance changes somewhat with changes in the weather, so when the natural traveling wave ratio is low the match made by the inductive stub, or by some other method, is upset.

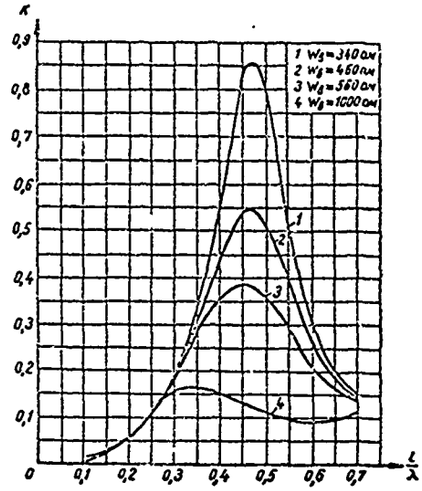

Figure IX.9.1. Dependence of the natural traveling wave ratio for a supply feeder on the l/λ ratio; W_F = 600 ohms.

It can be taken that the minimum natural traveling wave ratio at which the balanced dipole can be tuned so that changes in the weather will not detune is 0.1 to 0.15. Figures IX.9.1 and IX.9.2 show calculated curves for the dependence of the natural traveling wave ratio, k, on l/λ for various values of W_d and W_F.

The traveling wave ratio, k, is calculated through

$$k = \frac{1-|\rho|}{1+|\rho|}, \qquad \text{(IX.9.1)}$$

where

$|\rho|$ is the modulus of the reflection factor, calculated through (see #I.4.)

$$|\rho| = \sqrt{\frac{(R_{in} - W_F)^2 + X_{in}^2}{(R_{in} + W_F)^2 + X_{in}^2}}, \qquad \text{(IX.9.2)}$$

where

W_F is the characteristic impedance of the feeder.

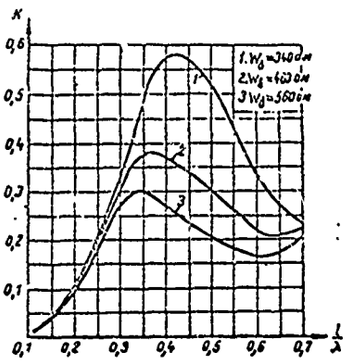

Figure IX.9.2. Dependence of the natural traveling wave ratio for a supply feeder on the l/λ ratio; W_F = 350 ohms.

As will be seen from the curves in figures IX.9.1 and IX.9.2, the natural traveling wave ratio will become less than the minimum indicated when the relationship is $l/\lambda < 0.2$ to 0.25.

Thus, operation can take place on any wavelength, beginning at 4 to 5 l and shorter, when fixed wavelengths are used, at least from the point of view of providing for a stable match.

The dipoles with reduced characteristic impedances described in what follows can be used when operating on a broad, continuous band of frequencies. These dipoles have a satisfactory match with feeder characteristic impedance over an extremely broad band. As a practical matter, that match for which the traveling wave ratio is at least 0.3 to 0.5 can be taken to be satisfactory. This match can be provided on wavelengths on the order to 3 to 4 l and shorter, depending on W_F. Satisfactory match is obtained up to ~6 l when the multiple-tuned shunt dipole is used.

These considerations with respect to the use band for the balanced dipole make it possible to draw the following conclusions. So far as providing for maximum radiation in the direction normal to the dipole axis is concerned, the minimum permissible wave length equals 1.4 to 1.5 l. Practically speaking, this value must be increased somewhat, considering the relative shift in the curves for $\epsilon = f(l/\lambda)$ toward the lesser values of l/λ, as we indicated above. When the dipole's characteristic impedance is on the order of 1000 ohms we must limit ourselves to wavelengths equal to 1.5 to 1.6 l, and when on the order of 300 ohms to those equal to 1.7 to 1.8 l. The requirement that a suitable match be made between dipole and feeder will not permit us to operate on wavelengths longer than 3 to 6 l.

An additional factor, and an extremely important one, limiting the use band is the need to provide intensive radiation at predetermined angles to the horizontal plane. This limitation will depend on main line operating conditions.

The use band can also be limited by the maximum field strength produced by the antenna (see #8 in this chapter) when operating at high powers.

#IX.10. Design Formulation and the Supply for a Dipole Made of a Single Thin Conductor

The balanced dipole can be a single wire (fig. IX.10.1) when used for a fixed wavelength. The characteristic impedance can be calculated through formula (V.10.3).

The dipole is made of hard-drawn bronze or bimetallic wire. Diameter is based on considerations of mechanical and electrical strength and is usually between 3 and 6 mm.

Characteristic impedance is on the order of 1000 ohms.

If permissible field strength is taken as 8 kv/cm, the curves in Figure IX.8.2 and IX.8.3 will show this dipole capable of accommodating 50 to 70 kw. If the transmitter produces more power than this a dipole with less characteristic impedance will have to be used.

The insulators used in the center and at the ends of the dipole should be as low in capacitance as possible to avoid heavy losses in the insulators which cause a deterioration in the natural traveling wave ratio. The use of stick insulators is desirable.

Additional insulators must be inserted in the cables supporting the dipole in order to avoid high induction currents, and should be installed 2 to 3 meters from the ends of the dipole. Based on this, the distance between supports should be at least $2l$ + (5 to 6) meters.

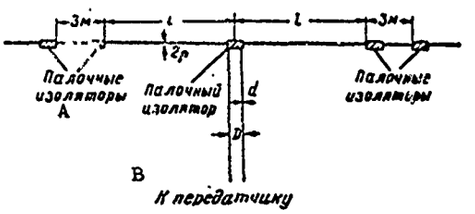

Figure IX.10.1. Schematic diagram of a VG antenna made of a single thin conductor.
A - stick insulators; B - to transmitter.

The balanced dipole is usually suspended on wooden supports. It is desirable to insert insulators in the guys in such a way that segments are no longer than $\lambda/4$ (λ is the working length of the dipole).

Suspension height must be selected so direction of maximum radiation and angles of beam tilt at the reception site match.

A two-wire transmission line with a characteristic impedance on the order of 600 ohms is usually used to feed a balanced dipole.

Chapter XX describes the methods used to tune a transmission line to the traveling wave mode.

#IX.11. Design Formulation and the Supply for a Dipole with Reduced Characteristic Impedance. The Nadenenko Dipole.

Balanced dipoles designed for broad band use are made with reduced characteristic impedance. Recourse is also had to reduction in characteristic impedance when high power is applied to the dipole.

The reduction in characteristic impedance is usually arrived at by making the balanced dipole from a series of conductors positioned around the generator of a cylinder (fig. IX.11.1). This type of dipole was first suggested by S. I. Nadenenko and is known as the Nadenenko (VGD) dipole.

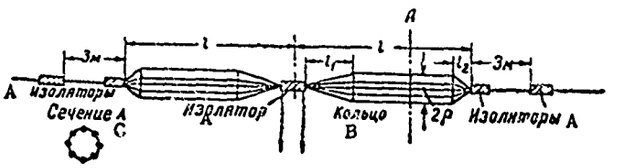

Figure IX.11.1. Schematic diagram of the VGD [Nadenenko] antenna; l_1 = 3 to 5 meters; l_2 = 1 meter.
A - insulators; B - ring; C - section through A.

The characteristic impedance of this dipole is calculated through

$$W = 120 \left(\ln \frac{l}{\rho_{eq}} - 1\right), \qquad \text{(IX.11.1)}$$

where

l is the length of one dipole arm;

ρ_{eq} is the dipole's equivalent radius; that is, the radius of a dipole made of an unbroken length of tubing with the same characteristic impedance as that of the particular dipole; ρ_{eq} can be calculated through

$$\rho_{eq} = \rho \sqrt[n]{\frac{nr}{\rho}}, \qquad \text{(IX.11.2)}$$

where

n is the number of conductors used in the dipole;

r is the radius of dipole conductors;

ρ is the radius of the cylindrical surface of the dipole.

ρ is usually taken as equal to 0.5 to 0.75 meters, the number of conductors n = 6 to 8. The characteristic impedance of the antenna is on the order of 250 to 400 ohms (figs. IX.11.2 and IX.11.3).

Figure IX.11.4 shows the curves for the dependence of ρ_{eq} on ρ for various values of n (4, 6, and 8) and conductor radius r = 1.5 mm. Approximate

values of ρ_{eq} can also be obtained for other practically possible values of r.

As will be seen from the curves in figures IX.9.1 and IX.9.2, k is considerably increased when a dipole with reduced characteristic impedance is used. The best match with the transmission line occurs when $W_F \approx 300$ ohms.

Steps should be taken to reduce the distributed capacitance near the center of the dipole, that is, near the site where the supply emf is brought in, so a good match between dipole and supply line will be maintained. It is at this site that increased distributed capacitance results because of the mutual effect of both arms of the dipole, the result of which is to cause a deterioration in the match. The reduction in distributed capacitance can be obtained by reducing radius ρ at this site. The dipole conductors gradually converge as they near the center, where they are brought together in one bundle (fig. IX.11.1).

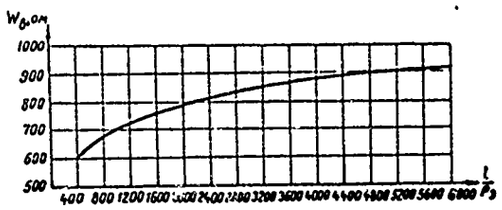

Figure IX.11.2. Dependence of the characteristic impedance of the VGD antenna on the l/ρ_{eq} ratio (ρ_{eq} is the equivalent radius of the dipole).

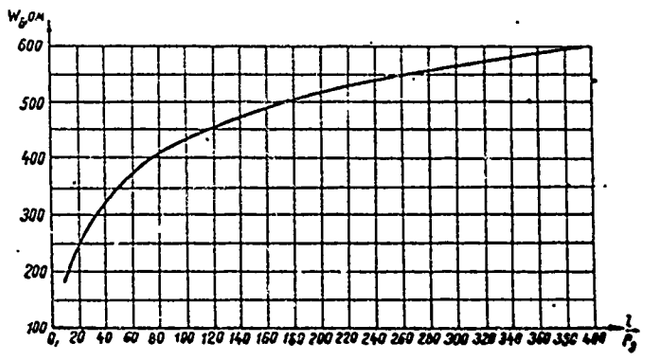

Figure IX.11.3. Dependence of the characteristic impedance of the VGD antenna on the l/ρ_{eq} ratio.

Convergence should begin 3 to 5 meters from the center of the dipole.

All of the foregoing with respect to insulation and supporting cables for a dipole made of one thin conductor applies as well to the dipole with reduced characteristic impedance.

It is recommended that the VGD antenna mast guys be made such that none of the segments contained in the guys are longer than $\lambda_{sh}/4$ (λ_{sh} is the shortest wave length in the band). As a practical matter, it is desirable to obtain the characteristic impedance of the feeder by making it of four conductors in the form of a square (see Chapter XIX). However, a four-conductor feeder is a much more complicated design than a two-conductor feeder and use brings with it certain inconveniences. It is inconvenient, in particular, to bring the four-conductor feeder into the space in which the transmitter is located. Hence, a two-conductor feeder is often used to feed a multiple-tuned dipole. And an exponential feeder transformer, the characteristic impedance of which can be changed smoothly from 300 to 600 ohms (see Chapter XIX), is used to improve the feeder-dipole match.

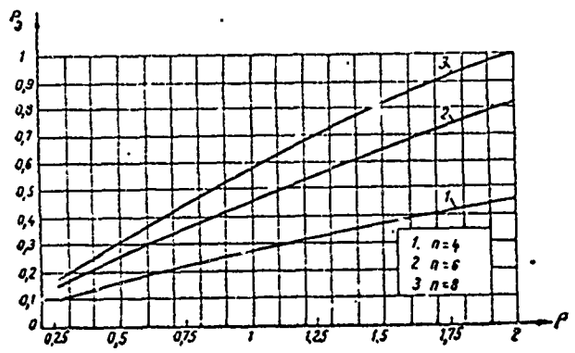

Figure IX.11.4. Dependence of the equivalent radius of the dipole on the radius of the cylindrical surface on which the conductor is located. Conductor diameter 2r = 3 mm. Vertical: ρ_{eq}.

The feeder transformer is connected directly to the dipole input and is positioned in part horizontally, and in part vertically, while, at the same time undergoing reduction. The ends of the horizontel section are connected to the two-conductor feeder.

The general arrangement of the supply to the balanced dipole through an exponential feeder transformer is shown in Figure IX.11.5. Transformer details are contained in Chapter XIX.

Suspension heig.+ for the VGD antenna is selected so as to provide for the closest possible approach of angles of maximum radiation to angles of tilt of the beams at the reception site within the band in which the antenna is used.

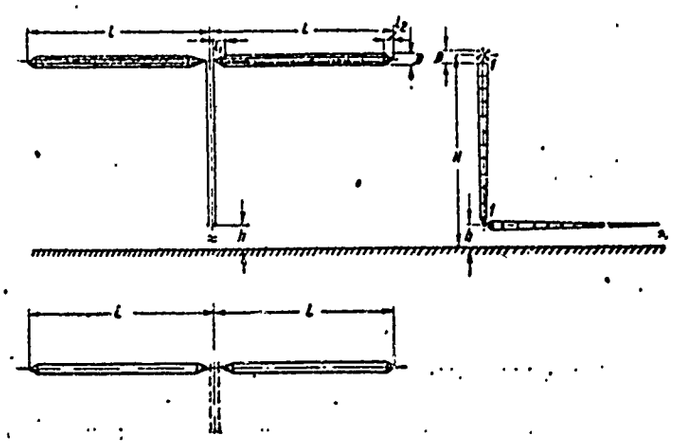

Figure IX.11.5. Schematic diagram of how the VGD antenna is designed. Designations: H - average suspension height (chosen in accordance with main line length); l_1 = (3 to 5) meters; $l_2 \approx 1$ meter; D = (1 to 1.5) meters; h = (2 to 4) meters; diameter of antenna conductors (2 to 4) mm; 1-1-1 - exponential feeder transformer TF4 300/600 40 for maximum wavelength 60 meters and TF4 300/600 60 for maximum wavelength over 60 meters.

Note 1. A reduction can be made in VGD receiving antennas by a standard four-conductor feeder with a characteristic impedance of 208 ohms.

Note 2. In VGD transmitting antennas the vertical section of the exponential feeder transformer can be made of stranded conductors to facilitate the design.

#IX.12. Wideband Shunt Dipole

Shunt dipoles (conventional designation VGDSh) have found widespread application in recent years as wideband dipoles.

The first version of this dipole, suggested by the author, was built of rigid tubing (fig. IX.12.1). As will be seen, the dipole consists of two symmetrical arms, 1-5 and 2-6, shunted by stub 3-7-4. The arms are metal tubing surrounded by wires. Shunt 3-7-4 is made of metal tubing. The dipole made of rigid metal tubing can be secured in place on a metal mast or tower, without insulators. The author, together with V. D. Kuznetsov, subsequently suggested a wire version of the shunt dipole suitable for suspending on two supports like a conventional balanced dipole.

Chapter XII contains detailed information on the construction and parameters of the rigid shunt dipole. At this point we will concern ourselves only with the wire version.

Several versions of this type of dipole were investigated. The recent development of the dipole has taken the form shown in Figure IX.12.2, from which it will be seen that the arrangement is no different from that used when the dipole is made of rigid tubing. The wire-type dipole consists of

six conductors, with only four of them connected to the supply. The other two are connected to the main conductors at points 4 and 3.

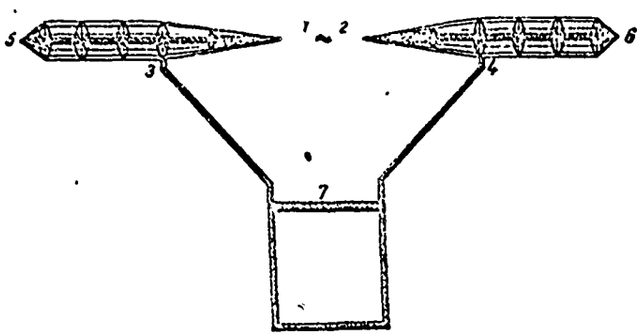

Figure IX.12.1. General view of the wideband shunt dipole.

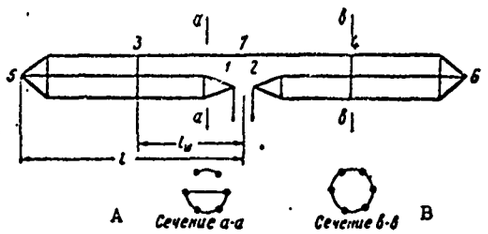

Figure IX.12.2. Schematic diagram of the wire-type shunt dipole; $l_{shunt} = l/2$.
A - section through a-a; B - section through b-b.

Section 3-7-4 forms the shunt, and sections 3-5 and 4-6, which are connected to the four main conductors, form a six-conductor cylindrical wire-type dipole comprising the two sections and the sunt section. Replacement of the shunt dipole by an equivalent two-wire line will take the form shown in Figure IX.12.3. As will be seen, the equivalent circuit comprises the open-end line 1-5-2-6, which has two sections, 1-3 - 2-4 and 3-5 - 4-6 with non-identical characteristic impedances, and the closed stub 3-7-4. There is extensive distributed electromagnetic coupling, not shown in the equivalent circuit diagram, between shunt 3-7-4 and line sections 1-2 - 2-4. Because the dipole has two branches (one open, one closed) conditions are favorable for maximum constancy of input impedance. This makes it possible to arrive at a close match of dipole input impedance to transmission line characteristic impedance over a broad band of frequencies when the proper geometric data for the dipole are selected.

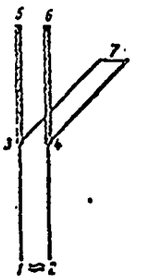

Figure IX.12.3. Equivalent shunt dipole circuit.

The shunt also causes an increase in the input impedance, of some advantage because a feeder line with a characteristic impedance on the order of 400 to 600 ohms can be used without feeder transformers, or other types of transformers.

Without pausing here to calculate the input impedance[1] let us discuss the results of experimental investigation.

Figures IX.12.4 and IX.12.5 contain curves characteristic of the input impedances and the match with the supply feeder of a shunt dipole. As will be seen, the traveling wave ratio is above 0.3 to almost the quintuple range. It is of particular importance that the working range of the shunt dipole be expanded to the long wave side, that is to the side of small l/λ ratios, so dipoles with arms of minimum length can be used. The shunt dipole has a satisfactory match beginning at an l/λ ratio equal to 0.16 to 0.17. In many instances one shunt dipole can replace two conventional dipoles with reduced characteristic impedance.

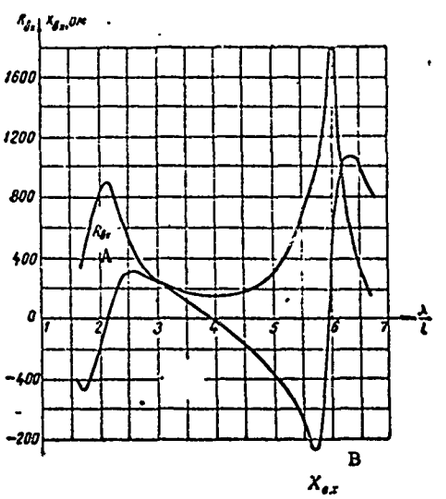

Figure IX.12.4. Dependence of the input impedance of a wire-type shunt dipole on the λ/l ratio.
Vertical: R_{in}, X_{in} in ohms. A - R_{in}; B - X_{in}.

1. An analysis of the input impedance of the shunt dipole is given in V. D. Kuznetsov's article titled "Shunt Dipoles," which appeared in Radiotekhnika, No. 10, 1955.

The possibility of grounding the antenna is essential in areas in which unusual thunderstorm activity occurs. The conventional wideband dipole cannot be grounded unless chokes are used. The shunt dipole can be grounded at point 7 (fig. IX.12.2).

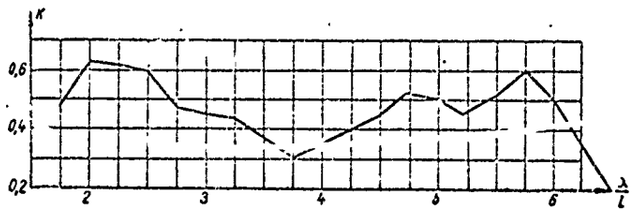

Figure IX.12.5. Experimental curve for the dependence of the traveling wave ratio on a line with a characteristic impedance of 500 ohms feeding a shunt dipole on the λ/l ratio.

Figure IX.12.6 shows a general view of a grounded wideband shunt dipole.

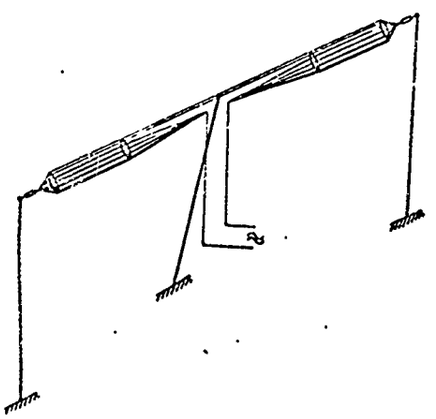

Figure IX.12.6. General view of a grounded wideband shunt dipole.

#IX.13. Balanced Receiving Dipoles

The balanced dipole is very widely used as a receiving antenna.

All of the foregoing data relative to the electrical parameters of a balanced transmitting dipole apply with equal force to the balanced receiving dipole.

Design-wise the balanced receiving dipole is similar to the transmitting. As was the case for transmission, it is desirable to use dipoles with reduced characteristic impedance (type VGD and VGDSh) for reception in order to provide the best possible match of dipole input impedance to supply feeder characteristic impedance.

A standard four-conductor feeder with a characteristic impedance of 208 ohms can be used to connect the dipole to the receiver. When the VGDSh dipole is used an exponential transition with a transformation ratio of 500/208 must be used to make the transition to a standard four-wire crossed receiving feeder.

It should be noted that the match of the antenna to the supply feeder is not as great in value for reception as it is for transmission. Deterioration in the match with the feeder leads primarily to a reduction in the gain factor. Directive gain remains the same.

#IX.14. The Pistol'kors Corner Reflector Antenna

One version of the balanced dipole is the antenna shown in Figure IX.14.1. As will be seen the antenna is a balanced dipole with the difference that the arms form an angle of 90° with each other rather than being in line. This antenna type was suggested by A. A. Pistol'kors, and is known as a "V-antenna."

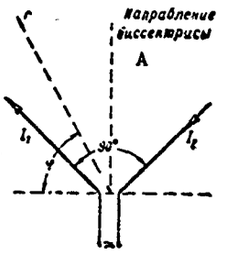

Figure IX.14.1. Schematic diagram of the corner reflector; conventional designation UG.

A - direction of bisector.

Characteristic of the V-antenna is weak directivity in the horizontal plane, because the direction of maximum radiation of both conductors comprising the V are mutually perpendicular.

The space radiation pattern of the Pistol'kors antenna, calculated for E_{eq} in accordance with (V.5.17), for a perfectly conducting ground, can be expressed through the formula

$$E = \frac{60I_{loop}}{r}\left[\sqrt{\Psi_1^2 + \Psi_2^2 + 2\Psi_1\Psi_2\cos(\nu_1 - \nu_2)}\,|\cos\rho|\right] \times \times \sin(\alpha H \sin\Delta)\,^{1)}, \qquad \text{(IX.14.1)}$$

where

Ψ_1 and Ψ_2 are magnitudes proportional to the field strengths produced by conductors 1 and 2 of the V;

1. Formulas IX.14.1 through IX.14.6 were derived by L. S. Tartakovskiy.

ν_1 and ν_2 are the phase angles of the field strength vectors for conductors 1 and 2;

$$\Psi_1 = \left| \{\cos [\alpha l \cos \Delta \cos (\varphi - 45)] - \cos \alpha l\} \times \right.$$
$$\left. \times \frac{1}{\cos \nu_1 \sqrt{1 - \cos^2 \Delta \cos^2 (\varphi - 45)}} \right|, \qquad \text{(IX.14.2)}$$

$$\nu_1 = \operatorname{arc\,tg} \frac{\sin [\alpha l \cos \Delta \cos (\varphi - 45)] - \sin \alpha l \cos \Delta \cos (\varphi - 45)}{\cos [\alpha l \cos \Delta \cos (\varphi - 45)] - \cos \alpha l}, \qquad \text{(IX.14.3)}$$

$$\Psi_2 = \left| \{\cos [\alpha l \cos \Delta \cos (\varphi + 45)] - \cos \alpha l\} \times \right.$$
$$\left. \times \frac{1}{\cos \nu_2 \sqrt{1 - \cos^2 \Delta \cos^2 (\varphi + 45)}} \right|, \qquad \text{(IX.14.4)}$$

$$\nu_2 = - \operatorname{arc\,tg} \frac{\sin [\alpha l \cos \Delta \cos (\varphi + 45)] - \sin \alpha l \cos \Delta \cos (\varphi + 45)}{\cos [\alpha l \cos \Delta \cos (\varphi + 45)] - \cos \alpha l}, \qquad \text{(IX.14.5)}$$

where

Δ is the beam tilt angle;

φ is the beam azimuth, read from the direction of the normal to the angle bisector between the sides of the V;

ρ is the solid angle between the vectors for the field strengths of sides 1 and 2 of the V;

$$|\cos \rho| = \frac{1}{\sqrt{1 + \left(\frac{2 \operatorname{tg} \Delta}{\cos \Delta \cos 2\varphi} \right)^2}}. \qquad \text{(IX.14.6)}$$

Substituting $\Delta = 0$ and converting, we obtain the following expression for the radiation pattern in the horizontal plane when $\Delta = 0$,[1]

$$F_h(\varphi) = \sqrt{(\Psi_{1a} + \Psi_{2a})^2 + (\Psi_{1r} + \Psi_{2r})^2}, \qquad \text{(IX.14.7)}$$

where

$$\Psi_{1a} = \frac{1}{\sin (\varphi - 45)} \{\cos [\alpha l \cos (\varphi - 45)] - \cos \alpha l\}, \qquad \text{(IX.14.8)}$$

$$\Psi_{2a} = \frac{1}{\sin (\varphi + 45)} \{\cos [\alpha l \cos (\varphi + 45)] - \cos \alpha l\}, \qquad \text{(IX.14.9)}$$

$$\Psi_{1r} = \frac{1}{\sin (\varphi - 45)} \{\sin [\alpha l \cos (\varphi - 45)] - \sin \alpha l \cos (\varphi - 45)\}, \qquad \text{(IX.14.10)}$$

$$\Psi_{2r} = - \frac{1}{\sin (\varphi + 45)} \{\sin [\alpha l \cos (\varphi + 45)] - \sin \alpha l \cos (\varphi + 45)\}. \qquad \text{(IX.14.11)}$$

---

1. When $\Delta = 0$ sin (H sin Δ) = 0. And in accordance with (IX.14.1), field strength should equal zero. In fact, because the ground is not a perfect conductor, and because it is rough, the field strength vector has some finite value in the horizontal plane which will change in accordance with formula (IX.14.7) with change in φ.

Figure IX.14.2 shows a series of radiation patterns in the horizontal plane when $\Delta = 0$ for various l/λ ratio values.

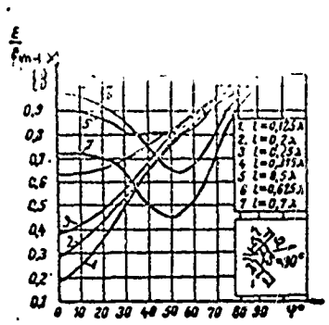

Figure IX.14.2. Radiation patterns of a UG antenna in the horizontal plane ($\Delta = 0$) for various values of l.

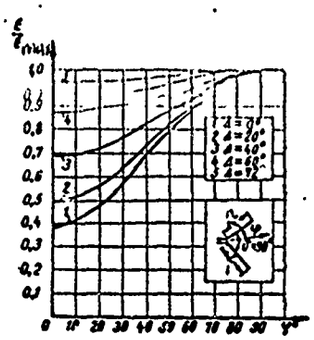

Figure IX.14.3. Radiation patterns of a UG antenna in the horizontal plane for various angles of tilt Δ and $l = 0.25\ \lambda$.

Figure IX.14.3 shows a series of radiation patterns in the horizontal plane for the relationship $l/\lambda = 0.25$ and values of Δ changing from 0° to 72°. Figures IX.14.4 to IX.14.7 show similar curves for values of l/λ equal to 0.375, 0.5, 0.625, and 0.7.

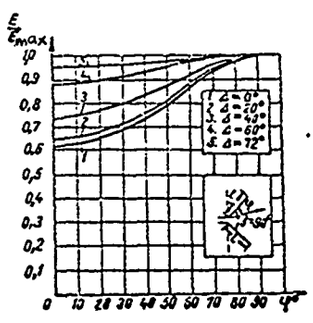

Figure IX.14.4. Radiation patterns of a UG antenna in the horizontal plane for various angles of tilt Δ and $l = 0.375\ \lambda$.

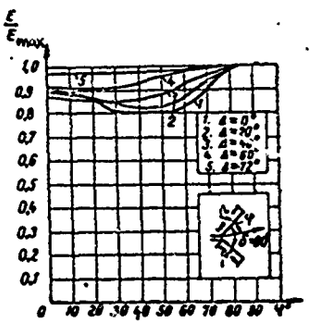

Figure IX.14.5. Radiation patterns of a UG antenna in the horizontal plane for various angles of tilt Δ and $l = 0.5\ \lambda$.

As will be seen from the curves in figures IX.14.3 - IX.14.7, an increase in angle Δ will increase the uniformity of radiation in all directions.

Arm length has a definite effect on the shape of the radiation pattern. Most uniform radiation in all directions results when l/λ is close to 0.5.

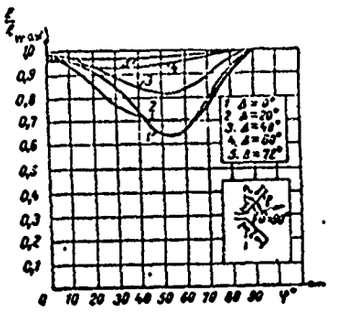

Figure IX.14.6. Radiation patterns of a UG antenna in the horizontal plane for various angles of tilt Δ and ℓ = 0.625 λ.

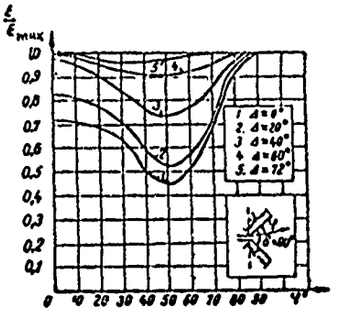

Figure IX.14.7. Radiation patterns of a UG antenna in the horizontal plane for various angles of tilt Δ and ℓ = 0.7 λ.

Uniformity of horizontal radiation can be increased substantially by making the antenna from two balanced dipoles placed at an angle of 90° to each other (fig. IX.14.8).

The vertical radiation patterns of the corner reflector antenna are close to those of the conventional balanced dipole.

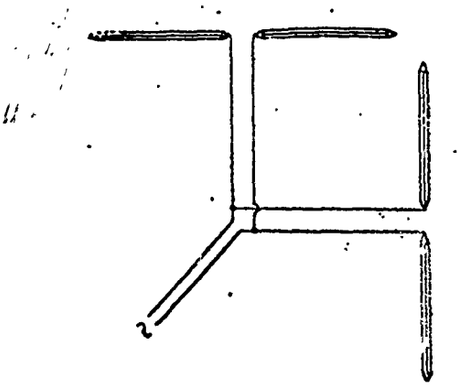

Figure IX.14.8. Corner reflector consisting of two balanced dipoles.

The gain factor for angles of tilt corresponding to the maximum beam in the vertical radiation pattern is approximately $4/1.64 \approx 2.4$ when the ground is a perfect conductor. For real ground the gain factor will change in proportion to the magnitude of $(1+|R_{\perp}|)^2/4$.

What has been said with respect to the gain factor applies when the ℓ/λ ratio is such that weak horizontal antenna directivity results.

The Pistol'kors antenna is usually made with reduced characteristic impedance to facilitate its broad band use.

Figure IX.14.9 shows the schematic diagram of the elements of a wideband corner reflector antenna.

The corner reflector antenna can be used for transmission and for reception.

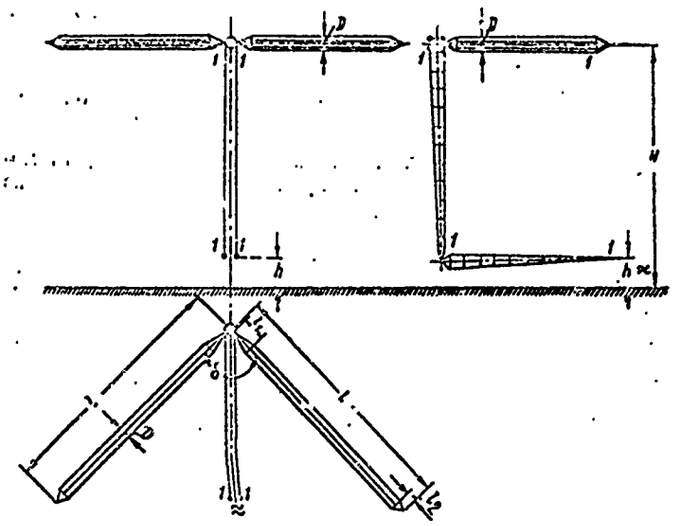

Figure IX.14.9. Structural arrangement of a wideband corner reflector. Designations: H - average suspension height (chosen in accordance with main line length); l_1 = (3 to 5) m; l_2 = 1 m; D = (1 to 1.5) m; δ = (90°; h - (2 to 4) m; 1-1 - exponential feeder transformer TFCh 300/600 40 for a maximum wavelength of 60 m and TFCh 300/600 60 for a maximum wavelength of over 60 m; diameter of antenna conductors 3 to 4 mm.

Note: In corner reflector receiving antennas the reduction can be made by a standard four-conductor feeder with a characteristic impedance of 208 ohms.

The use of wideband corner reflector shunt dipoles can be recommended to improve the match over a wide range of frequencies. The arrangement shown in Figure IX.14.8 can also apply to the use of VGDSh dipoles.

#IX.15. Dipole with Reflector or Director

(a) Schematic and principle of operation of a dipole with a reflector or a director

A horizontal balanced dipole has two directions in which radiation is maximum. Under conditions prevailing in radio communications or radio broadcasting it can be desirable to increase radiation intensity in one of these directions at the expense of weakening the radiation intensity in the other direction. This can be done by using a reflector, or a director.

The principle of operation of the reflector is as follows. Suppose we have dipole A (fig. IX.15.1) radiating identically in directions r_1 and r_2. Let it be required to intensify radiation in direction r_1 and decrease radiation direction in direction r_2.

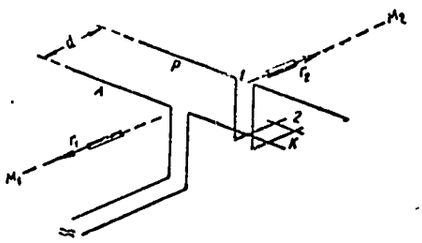

Figure IX.15.1. Schematic diagram of a dipole with a parasitic reflector.

One way in which to do away with radiation in direction r_2 is to install a reflector, in the form of a flat screen impenetrable by electromagnetic waves, in this direction. This type of reflector will be reviewed in Chapter XII.

Another way in which the desired result can be obtained is to use an additional dipole (R) positioned and excited in such a way that the field produced by it in direction r_2 weakens, and in direction r_1 intensifies the field produced by dipole A. This additional dipole is also called a reflector. Henceforth the main dipole will be referred to as the antenna.

One of the most frequently used versions of a reflector is a dipole made similar to the antenna and set up distance $d \approx \lambda/4$ from it. And good results can be obtained when the current flowing in the reflector is equal in amplitude to the current flowing in the antenna and leads the latter by $\pi/2$. Now let us investigate what the field strengths in directions r_1 and r_2 will be in this case.

Suppose we take some point, say M_2, in direction r_2. The field strength at this point equals

$$E = E_A + E_R,$$

where

E_A and E_R are the antenna and reflector field strengths, respectively.

Let us assume the antenna and reflector are identical in design, and that the currents flowing in them are identical in amplitude. In such case E_A and E_R are iuentical in absolute magnitudes.

There is a phase angle, Ψ, between E_A and E_R such that

$$E_R = E_A e^{i\Psi}; \quad \Psi = \psi + \psi_R,$$

where

ψ is the lag between antenna and reflector currents equal to $\pi/2$ in this case;

ψ_R is the lag determined by the difference in the path of the beams from antenna and reflector.

Since point M_2 is closer to the reflector than to the antenna by $\lambda/4$,

$$\psi_R = \alpha\frac{\lambda}{4} = \frac{2\pi}{\lambda}\frac{\lambda}{4} = \frac{\pi}{2}.$$

Thus,

$$\Psi = \frac{\pi}{2} + \frac{\pi}{2} = \pi, \quad E_R = -E_A.$$

The summed field equals

$$E = E_A + E_R = E_A - E_A = 0.$$

At arbitrary point M_1, located in direction r_1, the summed field also equals

$$E = E_A + E_R = E_A + E_A e^{i\varphi} = E_A + E_A e^{i(\psi+\psi_R)}.$$

At point M_1

$$\psi_R = -\frac{\pi}{2} \quad \text{and} \quad E = E_A + E_R = 2E_A.$$

Thus, for the mode we have chosen the system comprising an antenna and reflector meets the requirements imposed; no radiation in direction r_2, increased radiation in direction r_1.

The reflector can be either driven or parasitic. The driven reflector is one which, like the antenna, is fed directly from the transmitter, while the parasitic reflector is one which is not directly connected to the transmitter. Current flowing in the parasitic antenna is induced by the antenna field. Figure IX.15.1 shows the schematic of a dipole with a parasitic reflector.

Figure IX.15.2 is the schematic of a dipole with a driven reflector. Here T_1 and T_2 are transforming devices serving to regulate the amplitude and phase relationships between the currents flowing in the antenna and reflector.

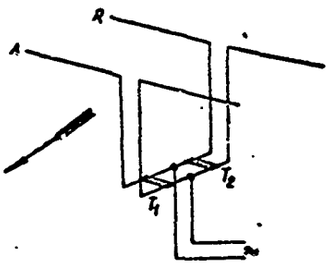

Figure IX.15.2. Schematic diagram of a dipole with a driven reflector. T_1 and T_2 - conversion transformers.

Because use of a driven reflector complicates the feed system, the parasitic reflector has been used to advantage. Reactance inserted in the reflector is used to regulate the relationships between current amplitudes and phases in the antenna and the parasitic reflector.

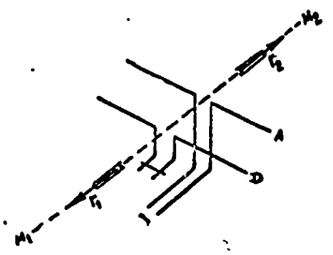

Figure IX.15.3. Schematic diagram of a dipole with director.
r_1 - direction to correspondent; D - director.

A short-circuited line, 1-2 (Fig. IX.15.1), is used as the reactance in shortwave antennas. The magnitude and sign of the reactance are regulated by switching the shorting plug, k.

As a practical matter, precise observance of the above-indicated distance between antenna and reflector ($d = \lambda/4$) is not mandatory in order to arrive at a substantial reduction in field strength in direction r_2 and amplification of field strength in direction r_1, because analysis has shown that if current amplitudes and phases are properly adjusted good results can be obtained for d values in the range from 0.1 λ to 0.25 - 0.3 λ.

Everything commented upon here refers to the parasitic dipole installed in direction r_2 from the antenna; in a direction opposite to that over which the correspondent can be reached. The parasitic dipole, D, can also be installed in direction r_1 from the dipole (fig. IX.15.3), and by making the corresponding current amplitude and phase adjustments an increase in field strength in direction r_1, and a weakening of the field strength in direction r_2 can be arrived at. In this case the parasitic dipole is called a director.

Parasitic dipoles are customarily used as reflectors in the shortwave field.

(b) Reflector current calculation

The relationship between amplitude m and phase ψ of the currents flowing in reflector and antenna must be known when calculating the radiation pattern, the gain factor and the directive gain, the radiation resistance, and other parameters. The magnitudes m and ψ can be arbitrary in the case of the driven reflector, and selected such that optimum desired reflector mode is obtained. In the case of the parasitic reflector current amplitude and phase are controlled by changing the reactance (stub 1-2 in fig. IX.15.1) inserted in the reflector. Range of such change is limited, and moreover, the magnitudes m and ψ are associated in a definite way. They can be established through the formulas in #V.17,

$$I_2 = I_1 m e^{i\psi}, \qquad \text{(IX.15.1)}$$

$$m = \frac{(R_{12}-R'_{12})^2 + (X_{12} - X'_{12})^2}{(R_{22}-R'_{22})^2 + (X_{22}-X'_{22}+X_{2load})^2} \qquad \text{(IX.15.2)}$$

$$\psi = \pi + \text{arc tg}\,\frac{X_{12}-X'_{12}}{R_{12}-R'_{12}} - \text{arc tg}\,\frac{X_{22}-X'_{22}+X_{2load}}{R_{22} - R'_{22}} \qquad \text{(IX.15.3)}$$

where

I_1 and I_2 are the amplitudes of the currents flowing in the current loops on antenna and reflector;

R_{22} and X_{22} are the resistive and reactive components of the reflector's radiation resistance;

R'_{22} and X'_{22} are the resistive and reactive components of the mutual impedance of the reflector and its mirror image;

R_{12} and X_{12} are the resistive and reactive components of the mutual impedance of reflector and antenna;

R'_{12} and X'_{12} are the resistive and reactive components of the mutual impedance of the reflector and of the mirror image of the antenna;

X_{2load} is the reactance inserted in the reflector and converted at the reflector current loop.

As was pointed out above, X_{2load} is usually made in the form of a segment of a short-circuited line.

If losses in the reflector are noticeable, we should write $R_{22} + R_{2\ loop}$ in place of R_{22} in the above formulas, where $R_{2\ loop}$ is the resistance of the losses in the reflector equated to the current loop.

As a practical matter, $X_{22} + X_{2load}$ can change within any limits by changing X_{2load}. The magnitude of X_{2load} can be selected such that the highest gain factor, or the most favorable radiation pattern shape, can be obtained. Calculation of R_{22}, R_{12}, X_{22} and X_{12} is made using the methods described in Chapter V.

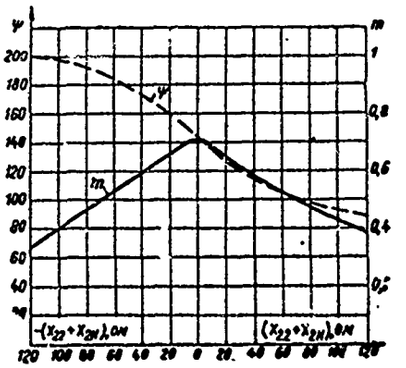

Figure IX.15.4. Dependence of ratio of amplitude (m) and phase angle (ψ) on the tuning of the parasitic reflector of a balanced dipole; $l = d = \lambda/4$.

Figure IX.15.4 shows the curves for the dependence of m and ψ on $X_{22} + X_{2load}$ when $t = d = \lambda/4$. X'_{22}, R'_{22}, X'_{12} and R'_{12} can be assumed equal to zero in the calculations, and this is permissible when the antenna is installed at a great height.

Example. Find the relationship between the currents flowing in the antenna and the parasitic reflector under the following conditions:

(1) $t = 0.5\ \lambda$;

(2) both dipoles are suspended at the same height, $H = 0.25\ \lambda$;

(3) $d = 0.25\ \lambda$;

(4) radius of the conductor of each of the dipoles is $\rho = t/3000$;

(5) the reflector is tuned to resonance,

$$X_{22} - X'_{22} + X_{2load} = 0.$$

Distances between dipoles 1 and 2 and their mirror images equal $2H = 0.5\ \lambda$.

Solution. The distance between the reflector and the antenna's mirror image equals

$$\sqrt{(0,5\lambda)^2 + (0,25\lambda)^2} \approx 0\ 56\lambda.$$

Using the curves in figures V.8.1 and V.12.3, we obtain

$$R_{22} = 198 \text{ ohms}, \quad X_{22} = 125.8 \text{ ohms}.$$

Using the curves in figures H.III.27, 35, 28, and 36 in the Handbook Section, we obtain

$$R_{12} = 105 \text{ ohms}, \quad X_{12} = -80 \text{ ohms}$$

$$R'_{22} = -48 \text{ ohms}, \quad X'_{22} = -75 \text{ ohms}$$

$$R'_{12} = -70 \text{ ohms}, \quad X'_{12} = -42.5 \text{ ohms}$$

$$m = \sqrt{\frac{(105+70)^2 + (-80+42,5)^2}{(198+48)^2}} = 0,72,$$

$$\psi = 180^\circ + \operatorname{arc\,tg}\frac{-80+42,5}{105+70} - \operatorname{arc\,tg}\frac{0}{198+48} = 167,5^\circ.$$

(c) Radiation pattern of a dipole with reflector

The field strengths of antenna and reflector in any direction can be expressed through the formula

$$E = E_A + E_R = E_A(1 + me^{i\Psi}), \qquad \text{(IX.15.4)}$$

$$\Psi = \psi + \psi_R, \qquad \text{(IX.15.5)}$$

where

ψ_R is the component of the phase angle between the antenna and reflector field strength vectors, established by the difference in beam paths.

For arbitrary direction r we have angle of tilt Δ and azimuth angle φ, read from the direction of the dipole axis, and difference in beam path from antenna and reflector equal to (see fig. IX.15.5)

$$d_R = d \sin\varphi \cos\Delta, \qquad \text{(IX.15.6)}$$

$$\psi_R = -\alpha d_R = -\alpha d \sin\varphi \cos\Delta, \qquad \text{(IX.15.7)}$$

$$\Psi = \psi - \alpha d \sin\varphi \cos\Delta. \qquad \text{(IX.15.8)}$$

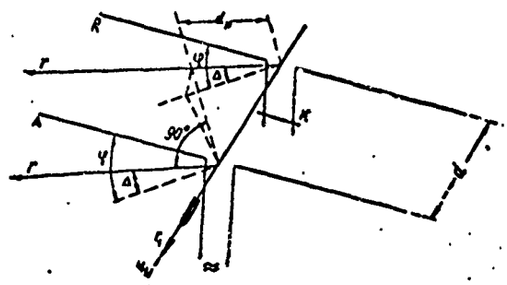

Figure IX.15.5. Determination of the difference in beam travel from antenna and reflector; arrow r_1 - direction to correspondent.

Substituting the expression for Ψ in formula (IX.15.4) and converting, we obtain the following expression for the field strength modulus

$$E = E_A \sqrt{1 + m^2 + 2m\cos(\psi - \alpha d \sin\varphi \cos\Delta)}; \qquad \text{(IX.15.9)}$$

Formulas (IX.2.1) and (IX.2.2) can be used to find E_A in the general case.

Substituting the value for E_A from formulas (IX.3.1) and (IX.4.2), we obtain the following formula for the radiation patterns in the vertical ($\varphi = 90°$) and horizontal ($\Delta = 0$) planes

$$F_v(\Delta) = (1-\cos\alpha l)\sqrt{1 + |R_\perp|^2 + 2|R_\perp|\cos(\Psi_\perp - 2\alpha H \sin\Delta)} \times \times \sqrt{1 + m^2 + 2m\cos(\psi - \alpha d \cos\Delta)}, \qquad \text{(IX.15.10)}$$

$$F_h(\varphi) = \frac{\cos(\alpha l \cos\varphi) - \cos\alpha l}{\sin\varphi} \sqrt{1 + m^2 + 2m\cos(\psi - \alpha d \sin\varphi)}. \qquad \text{(IX.15.11)}$$

In the case of infinite ground conductivity $|R_\perp| = 1$, $\Phi_\perp = \pi$, and formula (IX.15.1) becomes

$$F_v(\Delta) = 2(1-\cos\alpha l)\sin(\alpha H \sin\Delta)\sqrt{1 + m^2 + 2m\cos(\psi - \alpha d \cos\Delta)}. \qquad \text{(IX.15.12)}$$

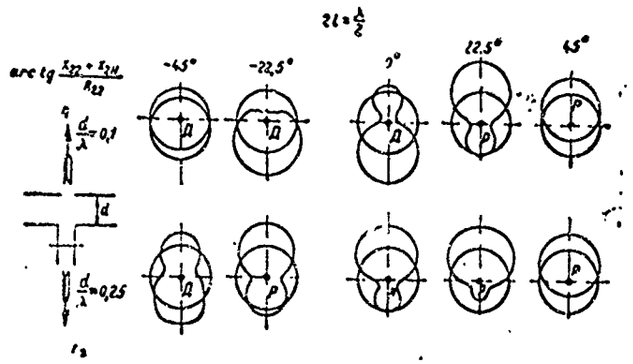

Figure IX.15.6. Effect of various parasitic dipole tuning regimes on the radiation pattern of a system consisting of horizontal driven and parasitic dipoles.

Figure IX.15.6 shows a series of curves characterizing the effect of a parasitic dipole on the radiation pattern in the horizontal plane for two values of d/λ (0.1 and 0.25), and for various parasitic dipole tuning modes. The curves do not take the effect of the ground on the radiation resistance into consideration, but this is permissible, practically speaking, when suspension is high. All curves were graphed as applicable to a half-wave dipole ($2l = \lambda/2$).

As will be seen from Figure IX.15.6, in certain of the modes we have intensification of the field strength in the r_1 direction, in others this is true of the r_2 direction. In the former the parasitic dipole is a reflector, in the latter a director.

(d) Radiation resistance and input impedance

Based on the data in Chapter V, #17, the resistive and reactive components of the dipole's radiation resistance can be calculated through the following formulas, which take the effect of the ground and of the parasitic dipole into consideration:

$$R_{\Sigma} = (R_{11} - R'_{11}) + m\,[(R_{12} - R'_{12})\cos\psi - (X_{12} - X'_{12})\sin\psi], \qquad \text{(IX.15.13)}$$

$$X_{\Sigma} = (X_{11} - X'_{11}) + m\,[(R_{12} - R'_{12})\sin\psi + (X_{12} - X'_{12})\cos\psi]. \qquad \text{(IX.15.14)}$$

The input impedance is calculated through formula (V.10.2), and W is replaced by $W_{coupling}$ and β by $\beta_{coupling}$, where $W_{coupling}$ and $\beta_{coupling}$ are the characteristic impedance and attenuation factor, with induced impedances taken into consideration,

$$W_{coupling} = W\sqrt{1 + \frac{X_{1\ ind}}{\alpha W}}\ . \qquad \text{(IX.15.15)}$$

In the case specified,

$$X_{1\ ind} = \frac{2X_{ind}}{l\left(1-\frac{\sin 2\alpha l}{2\alpha l}\right)} = \frac{2(X_{\Sigma} - X_{11})}{l\left(1-\frac{\sin 2\alpha l}{2\alpha l}\right)} \quad , \tag{IX.15.16}$$

$$\beta_{coupl}{}^{1} = \frac{R_{11} + R_{ind}}{W_{coupl}\left(1-\frac{\sin 2\alpha l}{2\alpha l}\right)} = \frac{R_{\Sigma}}{W_{coupl}\left(1-\frac{\sin 2\alpha l}{2\alpha l}\right)}, \tag{IX.15.17}$$

where

R_{ind} and X_{ind} are the resistive and reactive components of the radiation resistance induced in the antenna by its mirror image, by the reflector, and by the mirror image of the reflector;

$X_{1\ ind}$ is the induced reactive impedance occurring per unit antenna length.

(e) Directive gain and gain factor

Directive gain equals

$$D = 120\,\frac{F_v^2(\Delta)}{R_{\Sigma}} \quad . \tag{IX.15.18}$$

The gain factor equals

$$\varepsilon = D/1.64 \quad . \tag{IX.15.19}$$

We can set the efficiency equal to unity.

$F_v(\Delta)$ can be established through formulas (IX.15.10) or (IX.15.12), and R_{Σ} through formula (IX.15.13). The calculation reveals that when X_{2load} is properly selected the factors D and ε for the dipole with reflector are approximately double what they are for the same dipole without reflector.

Figure IX.15.7 shows curves for the dependence of the ratio $\varepsilon/\varepsilon_0$ on the magnitude of $X_{22} + X_{2load}$, that is, on reflector tuning.

ε and ε_0 are the gain factors with and without reflector.

X'_{12}, R'_{12}, X'_{11} and R'_{11} are taken equal to zero, a practical approach when antenna suspension is quite high.

Curves were plotted for two values of d/λ (0.1 and 0.25) when $2l = \lambda/2$.

As will be seen, the increase in the gain factor is somewhat greater when $d = 0.1\ \lambda$ than is the case when $d = 0.25\ \lambda$, thanks to the reflector.

As a practical matter, however, it is recommended that the reflector be located so it is not too close to the antenna because if it is the radiation resistance is extremely low, making it difficult to obtain the match with the feeder line and resulting in a reduction in efficiency.

By way of illustration, we have included Figure IX.15.8 to show the curves for the dependence of the radiation resistance on the magnitude $X_{22} + X_{2load}$ for a half-wave dipole for d/λ values equal to 0.1 and 0.25.

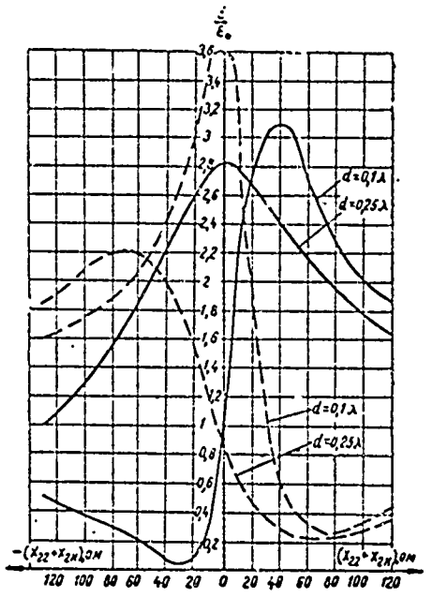

Figure IX.15.7. Dependence of the ratio $\varepsilon/\varepsilon_0$ for a half-wave dipole on reflector or director tuning when $d/\lambda = 0.1$ and $d/\lambda = 0.25$; ε is the gain factor for a dipole with reflector or director; ε_0 is the gain factor for the dipole alone; ——— reflector; - - - - director.

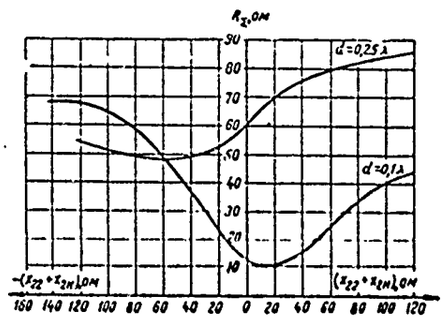

Figure IX.15.8. Dependence of half-wave dipole radiation resistance on reflector tuning. Scales in ohms.

A comparison of the curves in Figure IX.15.7 with those of Figure IX.15.8 shows that the considerable increase in the gain factor corresponds to the drop in radiation resistance. When $d/\lambda = 0.1$ the radiation resistance in the field of high values for $\varepsilon/\varepsilon_0$ is extremely low as compared with the antenna's own radiation resistance (73.1 ohms).

Figure IX.15.7 uses the dotted lines to show the curves for the $\varepsilon/\varepsilon_0$ ratio when the radiation coupled dipole is a director.

Chapter X

BALANCED AND UNBALANCED VERTICAL DIPOLES

#X.1. Radiation Pattern

The short wave field also utilizes reception and transmission vertical dipoles without directional properties in the horizontal plane. Vertical dipoles can be either balanced (fig. X.1.1) or unbalanced (fig. X.1.2).

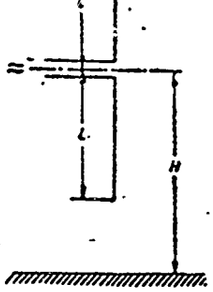

Figure X.1.1. Schematic diagram of a balanced vertical dipole.

Characteristic of the vertical dipole is stronger radiation and reception of ground waves, useful for short-range communications, but also damaging because the result is stronger local noise pickup.

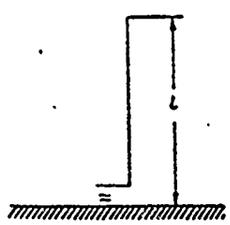

Figure X.1.2. Schematic diagram of an unbalanced vertical dipole.

The radiation pattern of a balanced vertical dipole in the vertical plane can be computed through the formula

$$E_b \sim \frac{60I}{r}\,\frac{\cos(\pi l/\sin\Lambda)-\cos\pi l}{\cos\Lambda}\times \\ \times\sqrt{1+|R_{\parallel}|^2+2|R_{\parallel}|\cos(\Phi_{\parallel}-2\pi H/\sin\Delta)}, \qquad (X.1.1)$$

where

l is the length of one arm of the dipole;

$|R_{\parallel}|$ and $\Phi_{\parallel}$ are the modulus and the argument for the reflection factor for a parallel polarized beam;

H is the height of an average point on the dipole above the ground.

The radiation pattern of an unbalanced dipole in the vertical plane can be computed through the formula

$$E_{unb} = \frac{30I}{r\cos\Delta}\left\langle\left\{\left[\cos(\alpha l\sin\Delta)-\cos\alpha l\right](1+|R_{\parallel}|\cos\Phi_{\parallel})+\right.\right.$$
$$+|R_{\parallel}|\sin\Phi_{\parallel}\left[\sin(\alpha l\sin\Delta)-\sin\alpha l\sin\Delta\right]\Big\}+i\Big\{\left[\sin(\alpha l\sin\Delta)-\right.$$
$$\left.\left.-\sin\alpha l\sin\Delta\right](1-|R_{\parallel}|\cos\Phi_{\parallel})+|R_{\parallel}|\sin\Phi_{\parallel}\left[\cos(\alpha l\sin\Delta)-\right.\right.$$
$$\left.\left.\left.-\cos\alpha l\right]\right\}\right\rangle. \qquad \text{(X.1.2)}$$

Chapter V, #5, contains the derivation of formula (X.1.1).

Formula (X.1.2) is derived in a manner similar to that used to derive formula (X.1.1) by replacing the ground with the mirror image. The reflection factor establishes the magnitude and phase of the current flowing in the mirror image.

Figures X.1.3 - X.1.6 show the values of $|R_{\parallel}|$ $\Phi_{\parallel}$ for wet soil (ε_r = 25, γ_v = 0.01) and dry soil (ε_r = 5 and γ_v = 0.001). The curves were plotted for waves in the 15 to 100 meter range. The curves in figures X.1.3 - X.1.6 show that $|R_{\parallel}|$ and $\Phi_{\parallel}$ are quite dependent on the ground and wavelength parameters. Moreover, $|R_{\parallel}|$ and $\Phi_{\parallel}$ will change greatly with the angle of tilt.

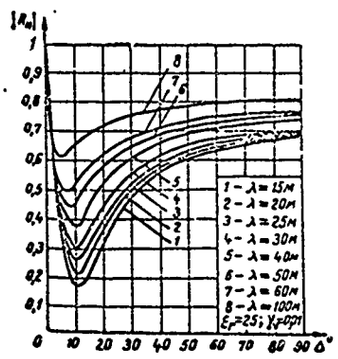

Figure X.1.3. Dependence of the modulus of the reflection factor $|R_{\parallel}|$ for a parallel polarized wave on the angle of tilt for wet soil (ε_r = 25; γ_v = 0.01).

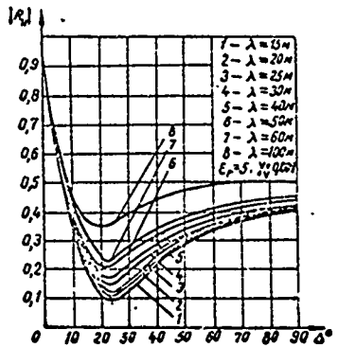

Figure X.1.4. Dependence of the modulus of the reflection factor $|R_{\parallel}|$ for a parallel polarized wave on the angle of tilt for dry soil (ε_r = 5; γ_v = 0.001).

Figures X.1.7 - X.1.14 show a series of radiation patterns of a balanced dipole.

The patterns were charted for the special case when l = 10 meters, H = 20 meters, and two types of soil.

Similar curves are shown in figures X.1.15 - X.1.22 for an unbalanced dipole when l = 10 meters.

Note that these diagrams fail to consider the effect of ground metallization near the antenna on its directional properties. This effect is slight, however (see #V.20).

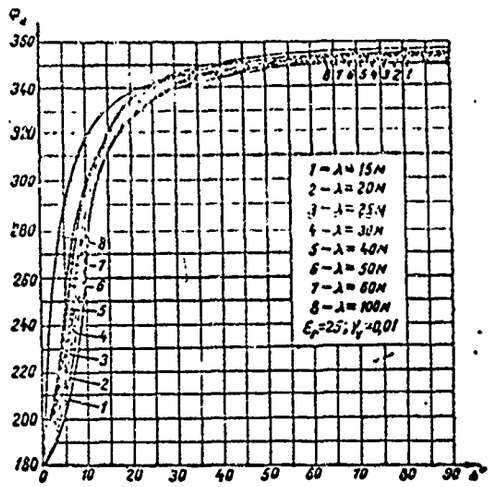

Figure X.1.5. Dependence of the argument for the reflection factor ($\tilde{\varrho}_{\parallel}$) for a parallel polarized wave on the angle of tilt for wet soil ($\varepsilon_r = 25$; $\gamma_v = 0.01$).

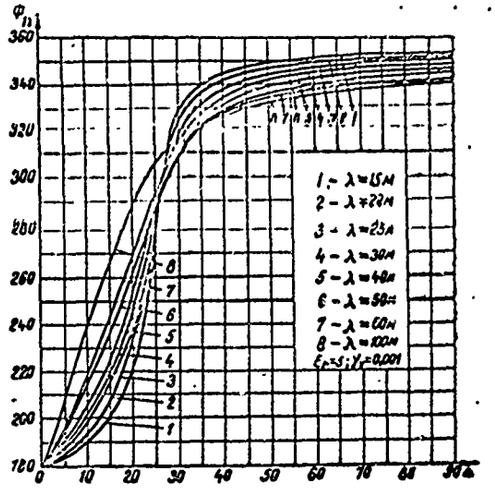

Figure X.1.6. Dependence of the argument for the reflection factor ($\tilde{\varrho}_{\parallel}$) for a parallel polarized wave on the angle of tilt for dry soil ($\varepsilon_r = 5$; $\gamma_v = 0.001$).

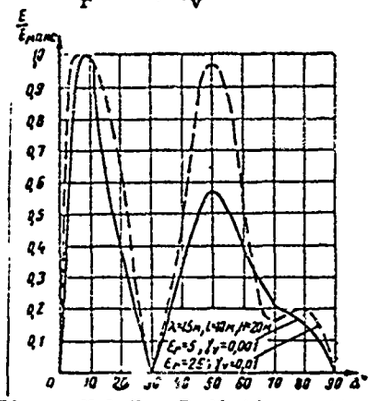

Figure X.1.7. Radiation pattern of a balanced dipole (l = 10 m; H = 20 m) for wet ($\varepsilon_r = 25$; $\gamma_v = 0.01$) and dry ($\varepsilon_r = 5$; $\gamma_v = 0.001$) soil; λ=15 m.

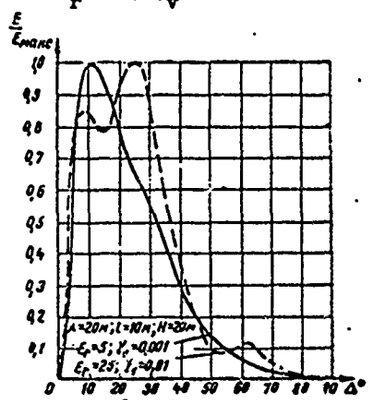

Figure X.1.8. Radiation pattern of a balanced dipole (l = 10 m; H = 20 m) for wet ($\varepsilon_r = 25$; $\gamma_v = 0.01$) and dry ($\varepsilon_r = 5$; $\gamma_v = 0.001$) soil; λ=20 m.

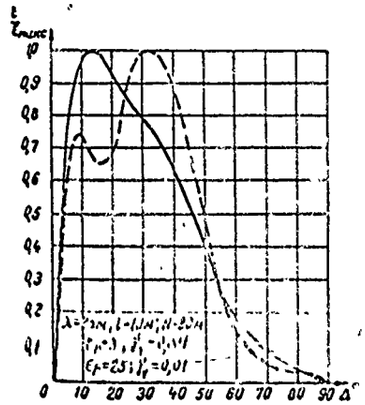

Figure X.1.9. Radiation pattern of a balanced dipole (ℓ = 10 m; H = 20 m) for wet (ε_r = 25; γ_y = 0.01) and dry (ε_r = 5; γ_v = 0.001) soil; λ= 25 m.

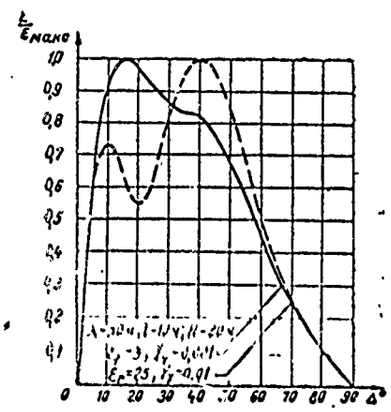

Figure X.1.10. Radiation pattern of a balanced dipole (ℓ = 10 m; H = 20 m) for wet (ε_r = 25; γ_y = 0.01) and dry (ε_r = 5; γ_v = 0.001) soil; λ= 30 m.

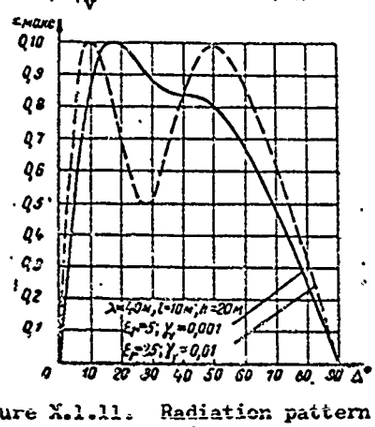

Figure X.1.11. Radiation pattern of a balanced dipole (ℓ = 10 m; H = 20 m) for wet (ε_r = 25; γ_y = 0.01) and dry (ε_r = 5; γ_v = 0.001) soil; λ = 40 m.

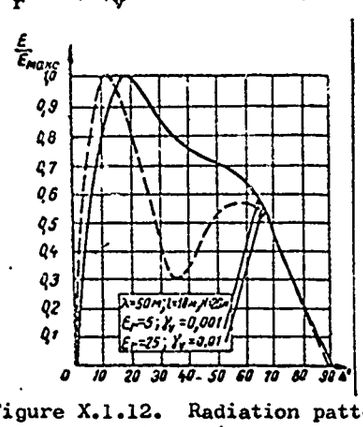

Figure X.1.12. Radiation pattern of a balanced dipole (ℓ = 10 m; H = 20 m) for wet (ε_r = 25; γ_y = 0.01) and dry (ε_r = 5; γ_v = 0.001) soil; λ = 50 m.

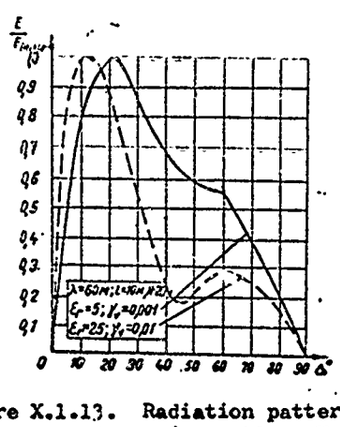

Figure X.1.13. Radiation pattern of a balanced dipole (ℓ = 10 m; H = 20 m) for wet (ε_r = 25; γ_y = 0.01) and dry (ε_r = 5; γ_v = 0.001) soil; λ = 60 m.

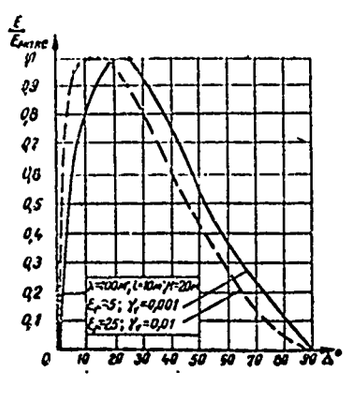

Figure X.1.14. Radiation pattern of a balanced dipole (ℓ = 10 m; H = 20 m) for wet (ε_r = 25; γ_y = 0.01) and dry (ε_r = 5; γ_v = 0.001) soil; λ = 100 m.

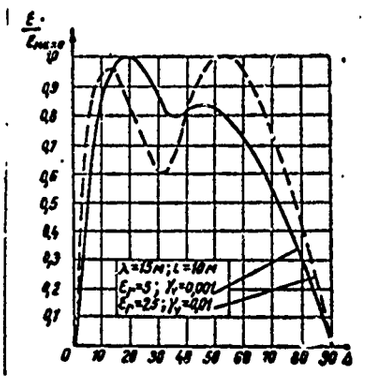

Figure X.1.15. Radiation pattern of an unbalanced dipole (l = 10 m) for wet (ε_r = 25; γ_v = 0.01) and dry (ε_r = 5; γ_v = 0.001) soil; λ = 15 m.

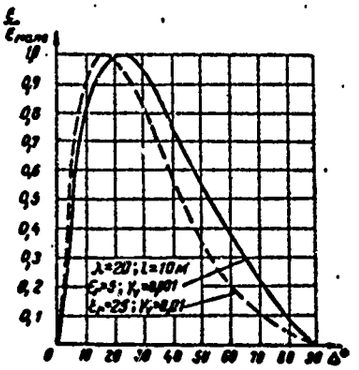

Figure X.1.16. Radiation pattern of an unbalanced dipole (l = 10 m) for wet (ε_r = 25; γ_v = 0.01) and dry (ε_r = 5; γ_v = 0.001) soil; λ = 20 m.

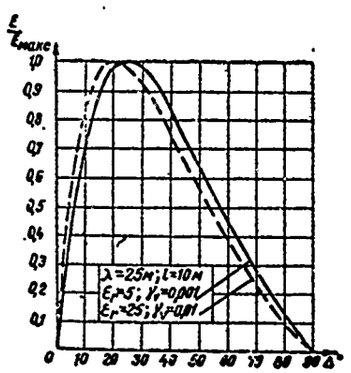

Figure X.1.17. Radiation pattern of an unbalanced dipole (l = 10 m) for wet (ε_r = 25; γ_v = 0.01) and dry (ε_r = 5; γ_v = 0.001) soil; λ = 25 m.

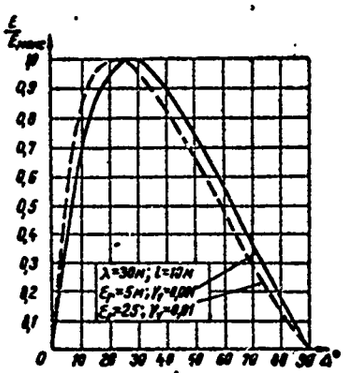

Figure X.1.18. Radiation pattern of an unbalanced dipole (l = 10 m) for wet (ε_r = 25; γ_v = 0.01) and dry (ε_r = 5; γ_v = 0.001) soil; λ = 30 m.

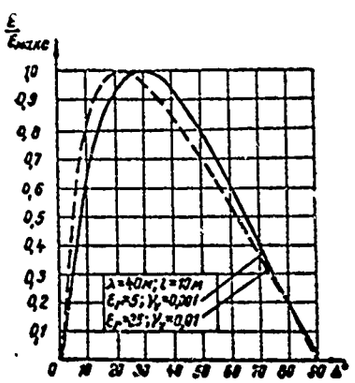

Figure X.1.19. Radiation pattern of an unbalanced dipole (l = 10 m) for wet (ε_r = 25; γ_v = 0.01) and dry (ε_r = 5; γ_v = 0.001) soil; λ = 40 m.

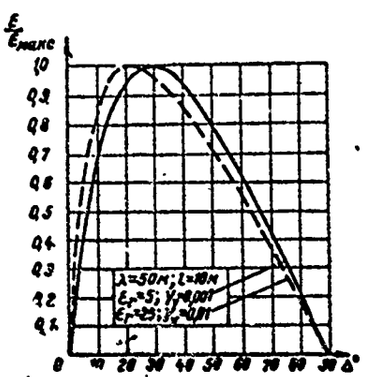

Figure X.1.20. Radiation pattern of an unbalanced dipole (l = 10 m) for wet (ε_r = 25; γ_v = 0.01) and dry (ε_r = 25; γ_v = 0.001) soil; λ = 50 m.

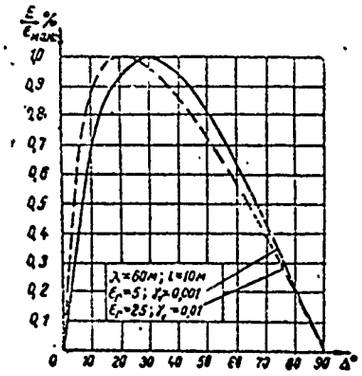

Figure X.1.21. Radiation pattern of an unbalanced dipole (l = 10 m) for wet (ε_r = 25; γ_v = 0.01) and dry (ε_r = 5; γ_v = 0.001) soil; λ = 60 m.

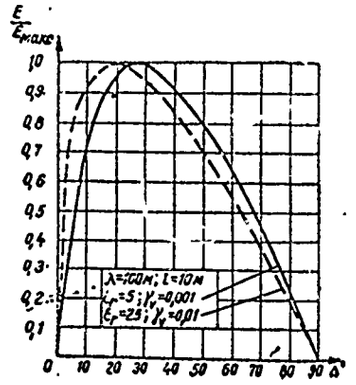

Figure X.1.22. Radiation pattern of an unbalanced dipole (l = 10 m) for wet (ε_r = 25; γ_v = 0.01) and dry (ε_r = 5; γ_v = 0.001) soil; λ = 100 m.

#X.2. Radiation Resistance and Input Impedance

The radiation resistance and the input impedance of a vertical dipole are readily computed if the ground near the dipole is carefully metallized, for in such case the approximation is that the field structure near the dipole is the same as it would be were the ground a perfect conductor, with the result that the radiation resistance, as well as the input impedance, can be calculated through the formulas obtained above for the balanced dipole. But what must be borne in mind is that for a specified value of l the radiation resistance and the characteristic impedance of an unbalanced dipole are half what they are for a balanced dipole. Based on what has been said we can also use the curves in figures V.8.1, IX.6.1, IX.6.2, and figures IX.11.2, IX.11.3 to establish the radiation resistance and the input impedance.

The use of the formulas and curves mentioned is permissible in the case of the unbalanced dipole for computing radiation resistance and input impedance if the dipole is fitted with radial ground system comprising 80 to 120 conductors, the lengths of which are on the order of the wavelength and longer. If a developed ground system is not used the calculations for radiation resistance and input impedance are complex, and will not be taken up here.[1]

#X.3. Directive Gain and Gain Factor

In the case specified the directive gain can be computed through formula (VI.1.9) because field strength is independent of azimuth angle.

The gain factor ε can be computed through formula (VI.3.5), and the radiation resistance computation is made as indicated in the preceding paragraph in the case of well-metallized ground near the antenna.

---

1. See the footnote at page 136.

The results of the D and ε computations for the special case of the unbalanced dipole (ℓ = 10 m) and for two types of soils are shown in figures X.3.1 and X.3.2.

Integration of the expression in the numerator of formula (VI.1.9) is carried out graphically to calculate D.

The values for D and ε shown in figures X.3.1 and X.3.2 equate to the direction of maximum radiation.

The D values obtained are only valid when distances from the dipole are such that we can ignore the ground waves, as compared with sky waves.

ε is computed assuming the field structure near the dipole remains as it is in the case of perfect ground, an assumption based on a developed ground system being installed. Efficiency is taken equal to one.

Let us note that in the case specified formula (VI.3.4) pays no attention to the relationship between ε and D, and this can be explained by the fact that D was established through the radiation pattern charted for real ground parameters without taking energy radiated into the ground into consideration. When the reflection factor from the ground does not equal one, some of the energy radiated by the antenna is entering the ground. If the relationship at (VI.3.4) is to be satisfied for ground with less than perfect conductivity we must either take the energy penetrating the ground into consideration when calculating D, or consider the energy radiated into the ground as a loss. In the latter case it is necessary to introduce in formula (VI.3.4) a factor equal to the transmission efficiency (η_t), and by which we understand to mean the ratio of the energy remaining in the upper half-space to the total energy radiated.

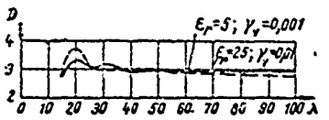

Figure X.3.1. Dependence of the directive gain of an unbalanced dipole (ℓ = 10 m) on the wavelength for wet (ε_r = 25; γ_v = 0.01) and dry (ε_r = 5; γ_v = 0.001) soil.

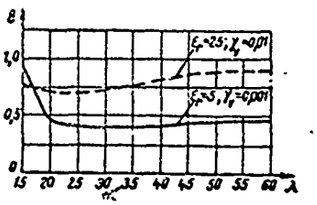

Figure X.3.2. Dependence of the gain factor for an unbalanced dipole (ℓ = 10 m) on the wavelength for wet (ε_r = 25; γ_v = 0.01) and dry (ε_r = 5; γ_v = 0.001) soil.

#X.4. Design Formulation

Figure X.4.1 shows one way in which to make a balanced [sic] vertical dipole with reduced characteristic impedance. As will be seen, segments of the guys used on the wooden mast are used in part as a dipole. Supply is by a two-conductor feeder.

An exponential feeder transformer is inserted in the line to improve the match between the two-conductor line and the dipole. The angle formed by the exponential line and the axis of the dipole is made as close to 90° as possible in order to avoid asymmetry in current distribution in the dipole and feeder.

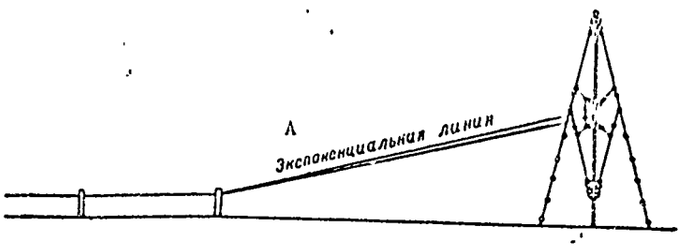

Figure X.4.1. Design formulation of one version of an unbalanced [sic] vertical dipole with reduced characteristic impedance.
A - exponential line.

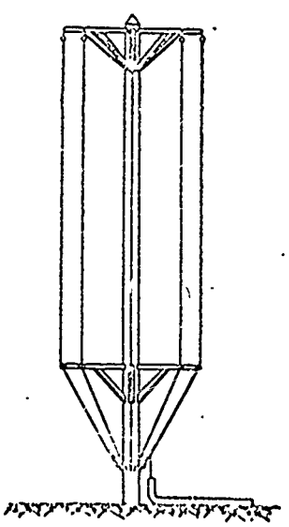

Figure X.4.2. Design formulation of one version of an unbalanced vertical dipole with reduced characteristic impedance.

Figure X.4.2 shows one version of a design for an unbalanced vertical dipole with reduced characteristic impedance. Mast guys can also be used to obtain a dipole with low characteristic impedance.

A high-frequency cable (fig. X.4.2), or a coaxial line can be used to feed the unbalanced dipole.

One possible version of a coaxial line is shown in Figure X.4.3. The external conductors, which play the same part as the cable shield, have one end connected to the grounding bus, the other to the transmitter (receiver)

frame. The end of the feeder running to the base of the antenna should be dipped toward the ground to reduce the reactive component of the conductor connecting the outer conductors of the feeder to the grounding system.

There are other ways to make an unbalanced wire feeder. When the feeder circuit is selected attention must be given to reducing the transmittance, which ought not exceed 0.03 to 0.05 (see #III.5).

A developed grounding system should be used with unbalanced dipoles to provide a high efficiency.

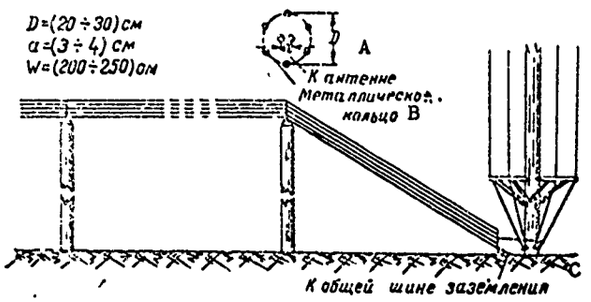

Figure X.4.3. Schematic diagram of the supply to an unbalanced vertical dipole by a coaxial feeder.

A - to antenna; B - metal ring; C - to common grounding bus.

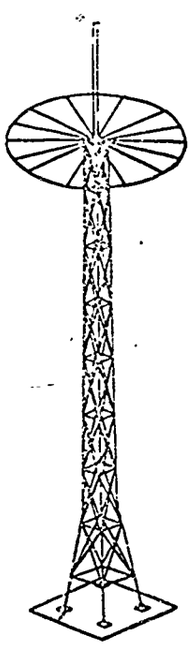

Figure X.4.4. Variant in the design of an unbalanced vertical dipole high above the ground.

Recommended is a grounding system consisting of from 80 to 120 conductors 1.5 to 2ℓ long. The system is buried 15 to 20 cm below the surface, but it can be laid right on the ground if local conditions are such that there will be no danger of its being damaged. A grounding system consisting of 10 to 15 conductors about 0.5ℓ long is adequate for receiving antennas.

Figure X.4.4 is one possible design for an unbalanced dipole. As will be seen, the dipole is installed on a metal tower, the top of which is fitted with a metal hat which plays the role of a counterpoise. Supply to the dipole is by a cable laid out along the tower body. The cable envelope is connected to the counterpoise. It is desirable to have the radius of the counterpoise at least equal to 0.2 to 0.25λ.

Dipole elevation provides ground wave amplification. Ground wave field strength is proportional to the height at which the dipole is suspended.[1]

1. See #5 of Chapter XIII in the book Ultra-Shortwave Antennas (Svyaz'izdat, 1957) for the radiation pattern of an antenna in the vertical plane (fig.

Chapter XI

THE BROADSIDE ARRAY

#XI.1. Description and Conventional Designations

Figure XI.1.1 is the schematic of a four-stacked broadside array with eight dipoles in each stack.

As will be seen, the broadside array is made up of a number of sections which are themselves two-wire balanced lines (1-2) loaded by balanced dipoles with arm lengths of $\ell = \lambda/2$.

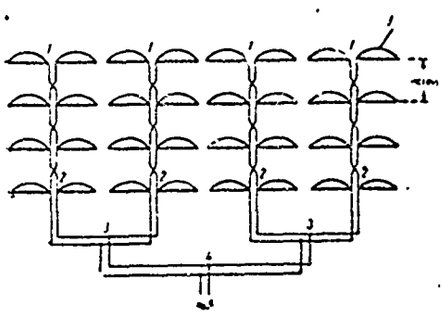

Figure XI.1.1. Schematic diagram of a broadside array.

The balanced dipoles are sections in several stacks. The line conductors are crossed in the spans between stacks. The distance between adjacent balanced dipoles in the same section equals $\lambda/2$.

The sections are connected in pairs by the distribution feeders, 2-3. These feeders will be referred to henceforth as the primary distribution feeders. These latter are, in turn, connected to each other by secondary distribution feeders, 3-4.

Figure XI.1.2 depicts a two-stacked broadside array comprising two sections.

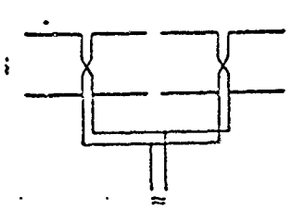

Figure XI.1.2. Schematic diagram of a two-stacked broadside array comprising two sections.

A parasitic reflector is usually installed behind the antenna and is usually a duplicate of the antenna in arrangement and design.

The broadside array is conventionally designated by the letters SG, to which is added the fraction n_1/n, designating the number of stacks (n_1) and

the number of half-wave dipoles in each stack (n).

The antenna shown in Figure XI.1.1 is conventionally designated the SG 4/8, for example.

If the antenna has a reflector the letter R is added. Thus, the broadside array with reflector comprising 4 stacks and 8 half-wave dipoles in each stack is designated SG 4/8 R.

The operating principle of the SG antenna was explained in #VII.5, that of the reflector in #IX.15.

#XI.2. Computing Reflector Current

The relationship between amplitude (m) and phase angle (ψ) for the currents flowing in reflector and antenna must be known to compute the radiation pattern, directive gain, radiation resistance, and other parameters.

In the case of the driven reflector the magnitudes of m and ψ can be arbitrary, and selected such that the optimum antenna mode is obtained. It is desirable to have m = 1 and $\psi = 90°$ when the distance between antenna and reflector is equal to $\lambda/4$.

In the case of the parasitic reflector, current amplitude and phase can be controlled by changing the reactance in the circuit. However, the range of change is limited and, moreover, so far as the parasitic reflector is concerned, the magnitudes of m and ψ are interconnected in a predetermined manner.

We can derive 2N equations from which the current in any of the dipoles in the antenna and reflector can be established (2N is the total number of dipoles in antenna and reflector) by using the coupled dipole theory explained in Chapter V.

However, in this case the determination of the currents can be very much simplified by replacing all the dipoles in the antenna and reflector with two equivalent, coupled dipoles.

In fact, the antenna consists of a system of dipoles, the currents in which have identical amplitudes and phases. Therefore, full power developed across the antenna (actual and reactive) equals

$$P = \frac{1}{2} I_I^2 [(R_1 + R_2 + \ldots + R_N) + i(X_1 + X_2 + \ldots + X_N)] = \frac{1}{2} I_I^2 [R_{II} + i X_{II}], \quad \text{(XI.2.1)}$$

where

R_1, $R_2 \ldots R_N$ and X_1, $X_2 \ldots X_N$ are the resistive and reactive radiation resistances for the first, second, etc., dipoles equated to a current loop, with the effect of all antenna dipoles and their mirror images taken into consideration;

I_I is the current flowing in the current loop of one dipole.

Formula (XI.2.1) demonstrates that all the dipoles in the antenna curtain can be considered as a single unique dipole with a total radiation resistance equal to $R_{II} + iX_{II}$ and with a current flowing in the loop equal to I_I.

Similarly, all reflector dipoles can be replaced by one equivalent dipole with radiation resistance equal to $R_{II\ II} + iX_{II\ II}$ and current flowing in the loop equal to the current flowing in one reflector dipole (I_{II}).

Here $R_{II\ II}$ and $X_{II\ II}$ are the sums of the resistive and reactive components of the radiation resistance of the reflector dipoles, established with the mutual effect of all reflector dipoles and their mirror images taken into consideration.

Replacement of the antenna and reflector dipoles by two equivalent dipoles will make it possible to use the equations for two coupled dipoles to analyze the SG antenna.

The coupling between the currents flowing in the reflector (I_{II}) and in the antenna (I_I) is established from the relationships, similar to those at (V.14.6) - (V.14.8) for two coupled dipoles,

$$I_{II} = I_I\, m e^{i\psi}, \qquad \text{(XI.2.2)}$$

$$m = \sqrt{\frac{R_{I\ II}^2 + X_{I\ II}^2}{R_{II\ II}^2 + (X_{II\ II}+X_{II\ load})^2}}, \qquad \text{(XI.2.3)}$$

$$\psi = \pi + \operatorname{arc\,tg}\frac{X_{I\ II}}{R_{I\ II}} - \operatorname{arc\,tg}\frac{X_{II\ II}+X_{II\ load}}{R_{II\ II}}, \qquad \text{(XI.2.4)}$$

where

$R_{I\ II}$ and $X_{I\ II}$ are the sums of resistive and reactive radiation resistances induced by all reflector dipoles and their mirror images in all antenna dipoles, assuming that reflector and antenna currents are the same in amplitude and coincide in phase;

$X_{II\ load}$ is the reactance inserted in the reflector and converted into current flowing in the loop. $X_{II\ load}$ is usually in the form of a segment of short-circuited line 1-2 (fig. XI.2.1).

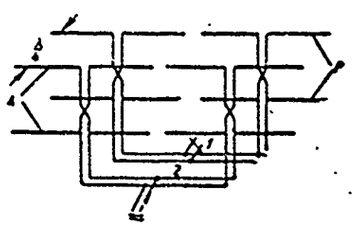

Figure XI.2.1. Schematic diagram of a two-stacked broadside array with a parasitic reflector SG 2/4 R.

A - antenna; R - reflector; 1-2 - reflector tuning stub.

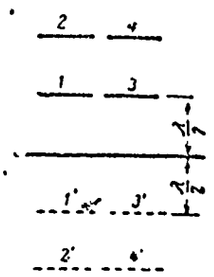

Figure XI.2.2. Schematic diagram of an SG 2/2 array and its mirror image.

If there are substantial losses in the reflector we must write $R_{II\ II} + R_{II\ loop}$ in the above formulas in place of $R_{II\ II}$, where $R_{II\ loop}$ is the resistance of the losses in the reflector equated to a current loop.

Practically speaking, $X_{II\ II}+X_{II\ load}$ can be changed within any limits by changing $X_{II\ load}$. The magnitude of $X_{II\ load}$ is selected such that the greatest gain, or the most favorable radiation pattern, is obtained.

The methods described in Chapter V are used to compute $R_{II\ II}$, $X_{II\ II}$, $R_{I\ II}$ and $X_{I\ II}$.

Example 1. Calculate the resistance of an SG 2/2 R antenna.

The circuit consists of dipoles and their mirror images, as shown in Figure XI.2.2 (the reflector dipoles are not shown).

Solution.

$$R_{II\ II} = R_1 + R_2 + R_3 + R_4.$$

Because of the symmetry with which the dipoles are positioned

$$R_1 = R_3;\ R_2 = R_4$$

$$R_{II\ II} = 2R_1 + 2R_2.$$

In turn

$$R_1 = R_{11} + R_{12} + R_{13} + R_{14} - R'_{11} - R'_{12} - R'_{13} - R'_{14},$$

$$R_2 = R_{21} + R_{22} + R_{23} + R_{24} - R'_{21} - R'_{22} - R'_{23} - R'_{24},$$

where

R_{11} and R_{22} are the radiation resistances of dipoles 1 and 2;

R'_{11} and R'_{22} are the mutual resistances between dipoles 1 and 2 and their own mirror images;

R_{12}, R_{13}, R_{14}, R'_{12}, R'_{13}, R'_{14} are the mutual radiation resistances between dipole 1 and dipoles 2, 3, and 4 and their mirror images;

R_{21}, R_{23}, R_{24}, R'_{21}, R'_{23}, R'_{24} are the mutual radiation resistances between dipole 2 and dipoles 1, 3, and 4 and their mirror images.

Own resistances of the dipoles equals

$$R_{11} = R_{22} = 73.1 \text{ ohms}.$$

The curves in the Handbook Section are used to establish the values of the other components of R_1 and R_2 (figs. H.III.6 - H.III.13).

Using these curves we obtain

$$R_1 = 73.1 + 26.4 - 12.4 - 11.8 + 1.8 + 5.8 - 1.2 - 3.8 = 77.9 \text{ ohms},$$
$$R_2 = 73.1 - 12.4 - 11.8 + 26.4 - 4.1 - 8.8 + 1.8 + 5.8 = 70 \text{ ohms},$$
$$R_{II\,II} = 2R_1 + 2R_2 = 295.8 \text{ ohms}.$$
$$R_{I\,II} = R_{1II} + R_{2II} + R_{3II} + R_{4II} - R'_{1II} - R'_{2II} - R'_{3II} - R'_{4II},$$
$$X_{I\,II} = X_{1II} + X_{2II} + X_{3II} + X_{4II} - X'_{1II} - X'_{2II} - X'_{3II} - X'_{4II}.$$

Here $R_{1\ II}$ and $X_{1\ II}$ are the sums of resistive and reactive components of the mutual resistance between dipole 1 of the antenna and all reflector dipoles.

$R_{2\ II}$, $R_{3\ II}$, $R_{4\ II}$, $X_{2\ II}$, $X_{3\ II}$, and $X_{4\ II}$ have similar values, but as applicable to dipoles 2, 3, and 4 of the antenna.

$R'_{1\ II}$ and $X'_{1\ II}$ are the sums of the resistive and reactive components of the mutual resistance between dipole 1 of the antenna and all the mirror images of the reflector dipoles.

$R'_{2\ II}$, $R'_{3\ II}$, $R'_{4\ II}$, $X'_{2\ II}$, $X'_{3\ II}$ and $X'_{4\ II}$ have similar values, but as applicable to dipoles 2, 3, and 4 of the antenna.

Because of the symmetry in the location of the dipoles,

$$R_{I\,II} = 2R_{1II} + 2R_{2II} - 2R'_{1II} - 2R'_{2II}$$

and

$$X_{I\,II} = 2X_{1II} + 2X_{2II} - 2X'_{1II} - 2X'_{2II}.$$

$R_{I\ II}$ and $X_{I\ II}$ are computed through the curves in the Handbook Section. We obtain for the SG 2/2 R antenna

$$R_{I\ II} = 58 \text{ ohms},$$

$$X_{I\ II} = -277.4 \text{ ohms}.$$

Figure XI.2.3 shows the curves for the dependence of m and φ for the SG 2/2 R antenna on $X_R = X_{II\ II} + X_{II\ load}$.

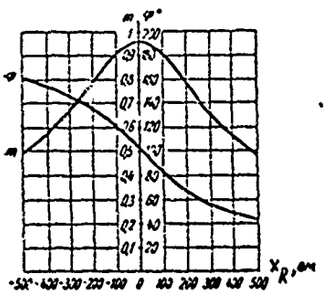

Figure XI.2.3. Dependence of m and φ for an SG 2/2 R array on reflector tuning.

As will be seen, the reflector current is only close to the antenna current in amplitude for small values of X_R. The current phase difference in this same area is close to 90°, emphasizing the fact that turning the reflector to resonance establishes a mode close to optimum.

The calculation of m and ψ for other types of antenna is made similarly.

The gain factor (ε) and the directive gain (D) for the antenna depend on m and ψ, so they depend on X_R.

So far as the SG 2/2 R antenna is concerned, maximum gain factor occurs when X_R = -40 ohms, and corresponding thereto m = 0.95 and ψ = 110°.

Table XI.2.1 lists the values of m and ψ for various versions of the SG antenna with respect to maximum gain factor and directive gain, but we must still remember that these values do not correspond to minimum radiation in the rear quadrants.

Table XI.2.1

Antenna type	m	ψ°
SG 1/2 R	0.81	120
SG 1/4 R	0.785	120
SG 2/2 R	0.95	110
SG 2/4 R	0.895	110
SG 2/8 R	0.91	110
SG 4/8 R	0.923	102
SG 6/8 R	0.87	96

#XI.3. Directional Properties

The field strength of the broadside array can be expressed through the formula[1]

$$E = \frac{120I}{r} \frac{\operatorname{ctg}\left(\frac{\pi}{2}\cos\Delta\sin\varphi\right)\sin\left(n\frac{\pi}{2}\cos\Delta\sin\varphi\right)}{\sqrt{1-\cos^2\Delta\sin^2\varphi}} \times$$

$$\times \frac{\sin\left(n_1\frac{\pi}{2}\sin\Delta\right)}{\sin\left(\frac{\pi}{2}\sin\Delta\right)} \sqrt{1+m^2+2m\cos(\psi-\alpha d_3\cos\Delta\cos\varphi)} \times$$

$$\times \sin(\alpha H_{av}\sin\Delta), \qquad \text{(XI.3.1)}$$

where

φ is the azimuth angle, read from the normal to the plane of the antenna curtain;

H_{av} is the average height at which the antenna is suspended;

1. See Appendix 4.

n_1 and n are number of stacks and number of half-wave dipoles per stack, respectively;

d_3 is the distance between antenna and reflector.

If the antenna is a stacked dipole array, and if the lower stack is at height H_1

$$H_{av} = H_1 + (n_1 - 1)\frac{\lambda}{4}. \qquad \text{(XI.3.2)}$$

Using formula (XI.3.1), we can establish the field in any direction.

It is customary to use the radiation patterns in the horizontal ($\Delta = 0$) and vertical ($\varphi = 0$) planes for the characteristics of SG antenna directional properties.

Substituting $\Delta = 0$ in formula (XI.3.1), converting, and dropping the factors not dependent on φ, we obtain the following expression for the radiation pattern in the horizontal plane

$$F(\varphi) = \frac{\operatorname{ctg}\left(\frac{\pi}{2}\sin\varphi\right)}{\cos\varphi}\sin\left(n\frac{\pi}{2}\sin\varphi\right)\times \\ \times\sqrt{1 + m^2 + 2m\cos(\psi - \alpha d_3\cos\varphi)}. \qquad \text{(XI.3.3)}$$

Figures XI.3.1 - XI.3.4 show a series of radiation patterns of SG antennas in the horizontal plane. As will be seen, the more dipoles per antenna stack, the narrower its radiation pattern in the horizontal plane. The radiation pattern in the horizontal plane is symmetrical with respect to the normal to the plane of the antenna curtain, so only half of the diagrams are shown in figures XI.3.1 - XI.3.4.

Substituting $\varphi = 0$ in formula (XI.3.1), and converting, we obtain the following expression for the radiation pattern in the vertical plane

$$F(\Delta) = \frac{E}{\frac{60I}{r}} = 2n\frac{\sin\left(n_1\frac{\pi}{2}\sin\Delta\right)}{\sin\left(\frac{\pi}{2}\sin\Delta\right)}\times \\ \times\sqrt{1 + m^2 + 2m\cos(\psi - \alpha d_3\cos\Delta)}\,\sin(\alpha H_{av}\sin\Delta). \qquad \text{(XI.3.4)}$$

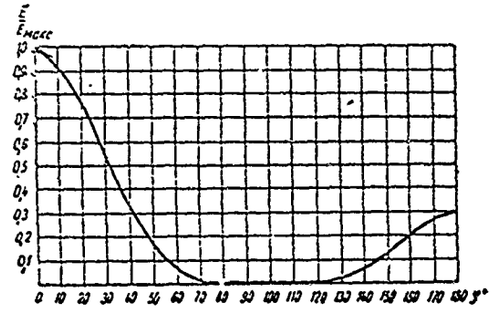

Figure XI.3.1. Radiation pattern in the horizontal plane of an SG array with two dipoles in one stack.

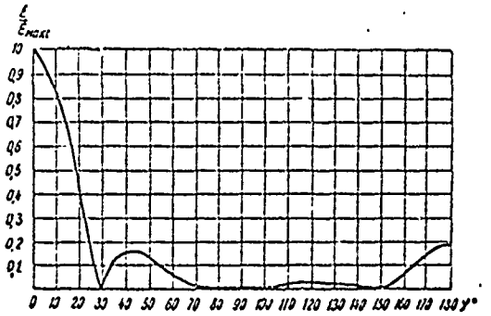

Figure XI.3.2. Radiation pattern in the horizontal plane of an SG array with four dipoles in one stack.

In the case of real ground conductivity the expression for the radiation pattern in the vertical plane becomes

$$F(\Delta) = n \frac{\sin\left(n_1 \frac{\pi}{2} \sin\Delta\right)}{\sin\left(\frac{\pi}{2}\sin\Delta\right)} \sqrt{1 + m^2 + 2m\cos(\psi - \alpha d_3 \cos\Delta)} \times$$

$$\times \sqrt{1 + |R_\perp|^2 + 2|R_\perp|\cos(\Psi_\perp - 2\pi H_{qv}\sin\Delta)}. \qquad \text{(XI.3.5)}$$

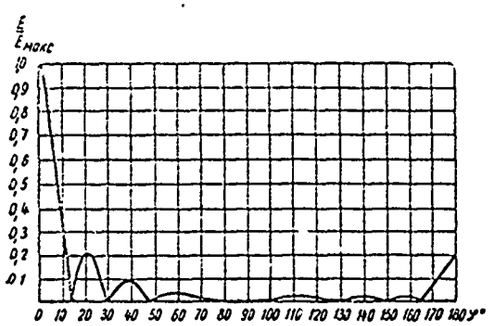

Figure XI.3.3. Radiation pattern in the horizontal plane of an SG array with eight dipoles in one stack.

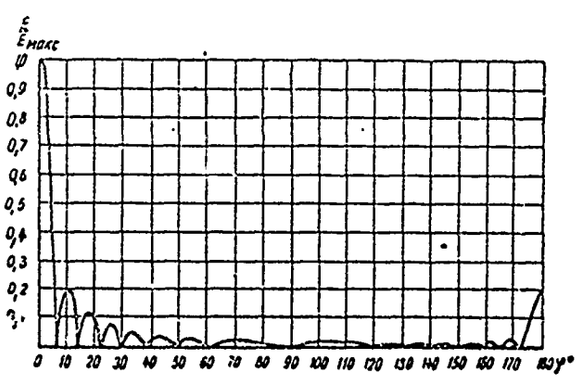

Figure XI.3.4. Radiation pattern in the horizontal plane of an SG array with sixteen dipoles in one stack.

Figures XI.3.5 - XI.3.8 show a series of radiation patterns in the vertical plane of an SG antenna. Patterns have been charted for three types of ground within the limits of the main lobe: ideal conductivity ($\gamma_v = \infty$); average conductivity ($\varepsilon_r = 8$, $\gamma_v = 0.005$); and low conductivity ($\varepsilon_r = 3$, $\gamma_v = 0.0005$).

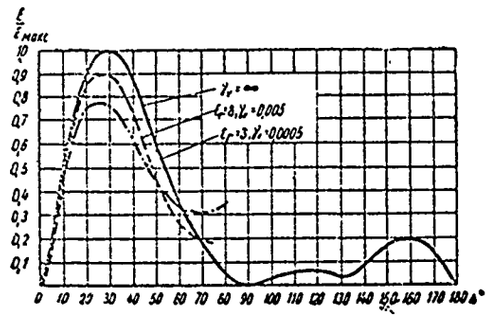

Figure XI.3.5. Radiation patterns in the vertical plane of a single-stack SG array with a reflector for ground with ideal conductivity ($\gamma_v = \infty$), for ground with average conductivity ($\varepsilon_r = 8$, $\gamma_v = 0.005$) and for ground with low conductivity ($\varepsilon_r = 3$, $\gamma_v = 0.0005$); height of suspension $H = \lambda/2$.

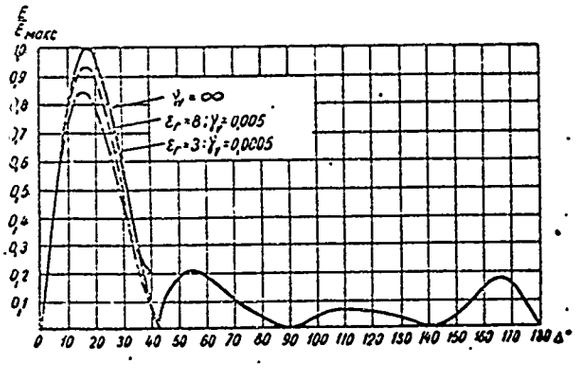

Figure XI.3.6. Radiation patterns in the vertical plane of a two-stack SG array with a reflector for ground with ideal conductivity ($\gamma_v = \infty$), for ground with average conductivity ($\varepsilon_r = 8$, $\gamma_v = 0.005$), and for ground with low conductivity ($\varepsilon_r = 3$, $\gamma_v = 0.0005$); height of suspension of lower stack $H_1 = \lambda/2$.

Laid out on the ordinate axes in figures XI.3.5 - XI.3.8 is the relationship E/E_{max}, where E_{max} is the field strength in the direction of maximum radiation for ideally conducting ground.

Accordingly, the curves for ground of average conductivity and for ground with low conductivity characterize the shape of the radiation pattern, as well as the change in the absolute magnitude of the field strength as compared with the case of ideally conducting ground.

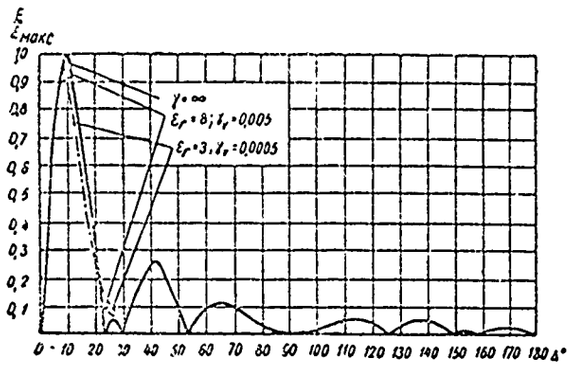

Figure XI.3.7. Radiation patterns in the vertical plane of a four-stack SG array with a reflector for ground with ideal conductivity ($\gamma_v = \infty$), for ground with average conductivity ($\varepsilon_r = 8$, $\gamma_v = 0.005$), and for ground with low conductivity ($\varepsilon_r = 3$, $\gamma_v = 0.0005$); height of suspension of lower stack $H_1 = \lambda/2$.

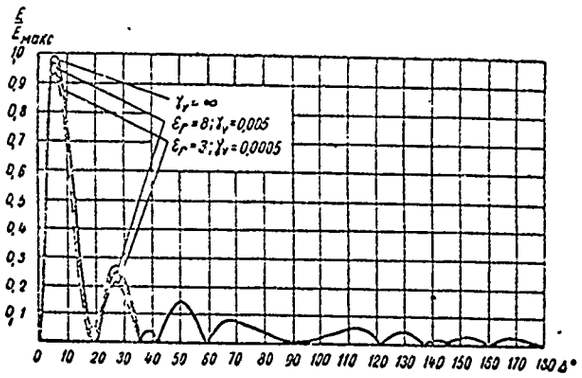

Figure XI.3.8. Radiation patterns in the vertical plane of a six-stack SG array with a reflector for ground with ideal conductivity ($\gamma_v = \infty$), for ground with average conductivity ($\varepsilon_r = 8$, $\gamma_v = 0.005$), and for ground with low conductivity ($\varepsilon_r = 3$, $\gamma_v = 0.0005$); height of suspension of lower stack $H_1 = \lambda/2$.

As will be seen from figures XI.3.5 - XI.3.8, the greater the number of stacks in the antenna, the narrower the radiation pattern in the vertical plane. Moreover, the main lobe is "pressed" toward the ground as the number of stacks is increased. Comparison of radiation patterns for various ground parameters reveals that the nature of the diagram is little dependent on soil parameters. But if the ground conductivity is reduced, the maximum beam in the diagram will be reduced, and the greater the angle of tilt of the maximum beam, the more marked is this reduction.

Radiation patterns in the vertical plane of a single-stack antenna with suspension height different from $\lambda/2$ are shown in Figure XI.3.9. Figures XI.3.10 and XI.3.11 show the radiation patterns in the vertical plane of a two-stack and four-stack antenna with lower stack suspension heights greater

than $\lambda/2$. An increase in the antenna suspension height will be accompanied by the main lobe becoming narrower and being pressed toward the ground, as well as by an increase in the pattern's side lobes.

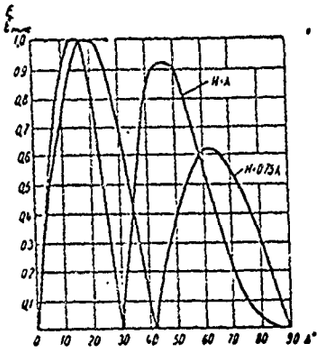

Figure XI.3.9. Radiation patterns in the vertical plane of a single-stack SG array suspended at a height different from $\lambda/2$ ($\gamma_v = \infty$).

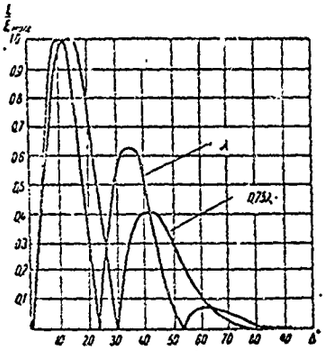

Figure XI.3.10. Radiation patterns in the vertical plane of a two-stack SG array with lower stack suspended at heights λ and 0.75 λ.

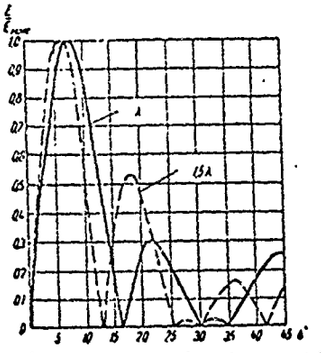

Figure XI.3.11. Radiation patterns in the vertical plane of a four-stack SG array with lower stack suspended at heights λ and 1.5 λ.

#XI.4. Radiation Resistance

The radiation resistance of an SG antenna is understood to mean the sum of the radiation resistances of all its dipoles.

In accordance with the above expounded method of replacing the dipoles of the antenna and reflector by two equivalent, single dipoles, we obtain the following expressions for the total radiation resistance of antenna and reflector

$$Z_{\Sigma A} = [R_{II} + m(R_{I\,II}\cos\psi - X_{I\,II}\sin\psi)] + \\ + i[X_{II} + m(X_{I\,II}\cos\psi + R_{I\,II}\sin\psi)]. \qquad (XI.4.1)$$

$$Z_{\Sigma R} = [R_{II\,II} + \frac{1}{m}(R_{I\,II}\cos\psi + X_{I\,II}\sin\psi)] + \\ + i[(X_{II\,II}+X_{II\,load})\frac{1}{m}(X_{I\,II}\cos\psi - R_{I\,II}\sin\psi)]. \qquad (XI.4.2)$$

Formulas (XI.4.1) and (XI.4.2) are similar to formula (V.13.7) for two conventional dipoles.

In the case of the parasitic reflector $Z_{\Sigma R} = 0$.

Since antenna and reflector are identical, $R_{I\,I} = R_{II\,II}$ and $X_{I\,I} = X_{II\,II}$.

Example 2. Calculate the resistive component of the radiation resistance ($R_{\Sigma\,A}$) for the SG 2/2 R antenna.

Solution. The resistive component of the radiation resistance of the antenna equals

Because the antenna and reflector curtains are identical

$$R_{I\,I} = R_{II\,II}.$$

The calculation of $R_{II\,II}$ for the SG 2/2 R antenna was made above (see Example 1). $R_{II\,II}$ was found to equal 295.8 ohms.

Also cited above were the results of the calculations of $R_{I\,II}$ and $X_{I\,II}$, which proved to be equal to $R_{I\,II} = 58$ ohms and $X_{I\,II} = -277.4$ ohms.

If we take the values of m and ψ corresponding to the maximum value for the gain factor, that is, m = 0.95 and $\psi = 110°$, the antenna radiation resistance will equal

$$R_{\Sigma\,A} = 295.8 + 0.95\,(58\cos 110° + 277.4\sin 110°) \approx 518 \text{ ohms}.$$

Table XI.4.1 lists the values of the resistive and reactive components of the radiation resistance for different SG antenna variants.

The values for $R_{\Sigma A}$ listed in Table XI.4.1 correspond to that mode of reflector tuning for which the maximum gain factor and directive gain are obtained.

Table XI.4.1

Antenna variant	$R_{I\ I}$, ohms	$R_{I\ II}$, ohms	$X_{I\ II}$, ohms	$R_{\Sigma A}$, ohms
SG 1/2 R	173.2	56	-129	242
SG 1/4 R	360.2	88.2	-265.6	514
SG 2/2 R	295.8	58	-277.4	518
SG 2/4 R	646.2	75.8	-586.5	1117
SG 2/8 R	1322	220	-1210	2300
SG 4/8 R	2778	268	-2274	4359
SG 6/8 R	3844.5	240.8	-3330	6705

The data listed in Table XI.4.1 are based on the assumption that the height at which the lower stack was suspended was equal to $\lambda/2$. If the suspension height is increased the radiation resistance will change somewhat because of the increase in the distance between the antenna and the mirror image. However, these changes are not substantial enough to be taken into consideration in engineering calculations. The data listed in this table can also be used for suspension heights greater than $\lambda/2$.

#XI.5. Directive Gain and Gain Factor

In accordance with what has been said in Chapter VI, the directive gain can be calculated through the formula

$$D = \frac{120F^2(\Delta)}{R_{\Sigma A}}. \qquad \text{(XI.5.1)}$$

with $F(\Delta)$ established through formula (XI.3.4) or (IX.3.5) [sic], and $R_{\Sigma A}$ from the data listed in Table XI.4.1.

The gain factor can be calculated through the formula

$$\varepsilon = D\eta/1.64, \qquad \text{(XI.5.2)}$$

where

η is the antenna efficiency.

Engineering calculations usually assume that

$$\eta = 1.$$

Table XI.5.1 lists the maximum values for D and ε for different SG antenna variants, as well as the angles of tilt for maximum beams, Δ_0.

The values for ε listed in Table XI.5.1 were calculated for ideally conducting ground. The actual values of ε, as follows from the patterns charted in figures XI.3.5 - XI.3.8, will be somewhat less; ε will decrease in proportion to the decrease in the ratio E^2/E^2_{max} when $\Delta = \Delta_0$.

The reduction in ε is greater the larger angle Δ_0.

Table XI.5.1

Antenna variant	Height at which lower stack is suspended	Directive gain, D	Gain factor, ε	Angle of tilt of maximum beam, Δ_0
SG 1/2 R	0.5λ	23	14	30°
SG 1/2 R	0.75λ	23	14	18°
SG 1/4 R	0.5λ	43	26	30°
SG 1/4 R	0.75λ	43	26	18°
SG 2/2 R	0.5λ	35	21	17°
SG 2/2 R	0.75λ	35	21	14°
SG 2/2 R	λ	35	21	12°
SG 2/4 R	0.5λ	60	37	17°
SG 2/4 R	0.75λ	60	37	14°
SG 2/4 R	λ	60	37	12°
SG 2/8 R	0.5λ	116	70.7	17°
SG 2/8 R	0.75λ	116	70.7	14°
SG 2/8 R	λ	116	70.7	12°
SG 4/4 R	0.5λ	130	80	9°
SG 4/4 R	λ	156	95	8°
SG 4/8 R	0.5λ	262	160	9°
SG 4/8 R	λ	310	190	8°
SG 6/8 R	λ	395	240	6°

#XI.6. Input Impedances

(a) Input impedance of a balanced dipole part of an antenna.

A balanced dipole has an arm length $l = \lambda/2$.

The input impedance of this dipole can be calculated through the formula

$$Z_1 = W_{in}^2/R \qquad \text{(XI.6.1)}$$

where

W_{in} is the characteristic impedance of the dipole with the resistances induced by adjacent dipoles and reflectors taken into consideration;

R is the resistive component of the radiation resistance of one balanced dipole.

The characteristic impedance of a balanced dipole can be established through the formula

$$W_{in} = W\sqrt{1 + X_{1\ ind}/\alpha W} \qquad \text{(XI.6.2)}$$

where

W is the characteristic impedance of an isolated balanced dipole

As a practical matter,

$$W_{in} \approx W,$$

$$R = 2R_{\Sigma A}/N,$$

where

$R_{\Sigma A}$ is the resistive component of the total radiation resistance of the antenna (see Table XI.4.1);

$N = nn_1$ is the total number of half-wave dipoles in the antenna.

Substituting the value for R in formula (XI.6.1),

$$Z_1 = NW_{in}^2/2R_{\Sigma A}. \qquad (XI.6.3)$$

W is on the order of 1000 ohms for dipole conductors with diameters of from 2 to 6 mm.

Formula (XI.6.1) fails to consider losses in the dipoles, but this is quite permissible because these losses in broadside arrays are usually very small.

(b) Input impedance of a section of an antenna

The input impedance of a section of an antenna is understood to mean the impedance equated to a point where the balanced dipole in the lower stack is connected into the antenna (point 2 in fig. XI.1.1).

Since the distance between dipoles in a section equals $\lambda/2$, the input impedance equals

$$Z_2 = Z_1/n_1 = W_{in}^2 n/2R_{\Sigma A}. \qquad (XI.6.4)$$

(c) Input impedance at distribution feeder branch points

The input impedance at the point where the primary distribution feeders branch (point 3 in fig. XI.1.1) is, in accordance with formula (I.9.9) equal to

$$Z_3 = \frac{W_{F1}}{2} \frac{\cos \alpha l_1 + i \frac{W_{F1}}{Z_3} \sin \alpha l_1}{\frac{W_{F1}}{Z_3} \cos \alpha l_1 + i \sin \alpha l_1}, \qquad (XI.6.5)$$

where

W_{F1} and l_1 are the characteristic impedance and length of one branch of the primary distribution feeder.

Similarly, the input impedance at the point where the secondary distribution feeders branch (point 4 in fig. XI.1.1) equals

$$Z_4 = \frac{W_{F2}}{2} \frac{\cos \alpha l_2 + i \frac{W_{F2}}{Z_3} \sin \alpha l_2}{\frac{W_{F2}}{Z_3} \cos \alpha l_2 + i \sin \alpha l_2}. \qquad (XI.6.6)$$

where

W_{F2} and l_2 are the characteristic impedance and length of one branch of the secondary distribution feeder.

If the antenna has four sections, Z_4 is the input impedance of the entire antenna.

We can calculate the input impedance at the point of feed in a similar way if the antenna has eight sections (16 dipoles) in each stack.

The lengths of the distribution feeders are often made in multiples of $\lambda/2$ in order to improve the match between the individual antenna elements. In such case the input impedance of the entire antenna equals

$$Z_A = 2Z_1/nn_1 = W_{in}^2/R_{\Sigma A}. \qquad \text{(XI.6.7)}$$

The formulas given here are also valid for calculating reflector input impedances. In the case of the parasitic reflector $R_{\Sigma R}$ should be understood to be the resistive component of the reflector's radiation resistance, calculated without regard for the effect of the antenna, which is to say

$$R_{\Sigma R} = R_{II\ II} = R_{I\ I}.$$

It must be pointed out that the formulas for input impedance given here are approximate, since they do not take into consideration differences in the radiation resistances of the individual dipoles, the effect of the shunt capacitances created by the insulators used with the antenna, the distribution feeders, etc.

#XI.7. Maximum Effective Currents, Voltages, and Maximum Field Strength Amplitudes in the Antenna

The effective current flowing in a current loop of an antenna dipole equals

$$I_A = \sqrt{\frac{P}{R_\Sigma}}, \qquad \text{(XI.7.1)}$$

where

P is the power applied to the antenna.

The maximum effective current flowing in the antenna feeder equals [formula (I.13.3)]

$$I_F = \sqrt{\frac{P}{W_F k}},$$

where

k is the traveling wave ratio on the feeder;

P is the power applied through the particular feeder; for the SG 2/8 R antenna, for example, through the primary distribution feeder one-fourth, and through the secondary distribution feeder one-half the applied power.

The traveling wave ratio on the feeder can be calculated through formula (I.7.2)

$$k = \frac{1-|p|}{1+|p|};$$

where

$|p|$ is the modulus of the reflection factor, equal to

$$|p| = \sqrt{\frac{(W_F - R_{load})^2 + X_{load}^2}{(W_F + R_{load})^2 + X_{load}^2}}, \qquad (XI.7.2)$$

where

R_{load} and X_{load} are the resistive and reactive components of the impedance of the load on the feeder.

The load impedance is Z_2 for the primary distribution feeder, Z_3 for the secondary distribution feeder, etc.

The maximum amplitude of the equivalent voltage across each of the dipoles is obtained at the generator end, and equals

$$U_{max} = I_{loop} W_{in} = \sqrt{\frac{2P}{R_\Sigma}} W_{in}, \qquad (XI.7.3)$$

where

I_{loop} is the amplitude of the current flowing in the dipole's current loop.

The maximum field strength amplitude equals

$$E_{max} = 120\, U_{max}/W_{in} d. \qquad (XI.7.4)$$

The maximum amplitudes of voltage and field strength in the distribution feeders (see XI.13) equals

$$U_{max} = \sqrt{\frac{2P_F W_F}{k}}, \qquad (XI.7.5)$$

$$E_{max} = \frac{120\, U_{max}}{W_F d}. \qquad (XI.7.6)$$

Table XI.7.1 lists the values for maximum effective current, maximum equivalent voltage, and maximum field strength for dipoles used in different antenna variants when the applied power equals 1 kw.

The compilation of Table XI.7.1 assumed that $W_{in} = 1000$ ohms, and that $d = 0{,}6$ cm, where d is the diameter of the dipole conductor.

Table XI.7.1

Antenna variant	Maximum effective current, I_A, amps	Maximum voltage amplitude, U_{max}, volts	Maximum field strength amplitude, E_{max}, volts/cm
SG 1/2 R	2.04	2880	576
SG 1/4 R	1.4	1980	396
SG 2/2 R	1.4	1980	396
SG 2/4 R	0.95	1350	270
SG 2/8 R	0.66	930	185
SG 4/8 R	0.48	680	136
SG 6/8 R	0.386	545	108

#XI.8. Waveband in Which SG Antenna can be Used

Upsetting the equality of current amplitudes and phases in the various stacks in the antenna is the primary reason why the SG antenna cannot be used on wavelengths different from those specified. As was pointed out in the foregoing, equal current amplitudes and phases in the different SG antenna stacks can be maintained because the segments of the feeder between the stack are $\lambda/2$ in length. As deviations from specified wavelengths occur the lengths of the inter-stack feeders become inappropriate, and the currents flowing in the different stacks are not the same, either in amplitude or phase. The result is distortion of the radiation pattern in the vertical plane. However, in some waveband near the specified wavelength the deterioration in directional properties is slight. The greater the number of stacks, the narrower this band.

As the calculations show, the two-stack antenna retains satisfactory directional properties and can be used without material deterioration in its parameters in the waveband 0.9 to 1.2 λ_0, where λ_0 is the specified working wavelength. The four-stack antenna can be used in the 0.95 to 1.08 λ_0 range. The single-stack antenna can be used over a broad band of wavelengths, as will be described in detail in Chapter XII on the multiple-tuned broadside array.

We should note that when the working wavelength is changed we must rebuild the reflector and the elements used to match antenna and feeder.

#XI.9. Antenna Design Formulation

(a) Antenna curtain and reflector curtain

Dipoles used in antennas and reflectors must be somewhat shorter than their nominal lengths. Shortening the dipole is equivalent to connecting a certain amount of inductive reactance in series with the dipole in order to compensate for the effect of the shunt capacitance of the insulators

and the induced reactances. The input impedance of the shortened dipole becomes resistive, and this results in an improvement in the match between the individual antenna sections. When conventional insulators are used it is recommended that dipoles be shortened 5 to 7%, as compared with their nominal lengths.

Efforts should be made to keep the shunt capacitance of the insulators as low as possible. The antenna curtain can be suspended on supports with, or without, stays (figs. XI.9.1 and XI.9.2). When a stay is used the dipoles are positioned exactly horizontal, but when the stay is not used the dipoles sag somewhat, and this sag causes distortion in the radiation pattern. This distortion is slight when the dip is small, however. A dip with an order of magnitude of 5 to 7% of the span between masts is permissible.

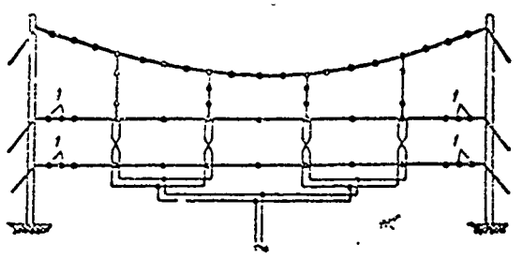

Figure XI.9.1. Suspension of an antenna curtain on supports using a stay.

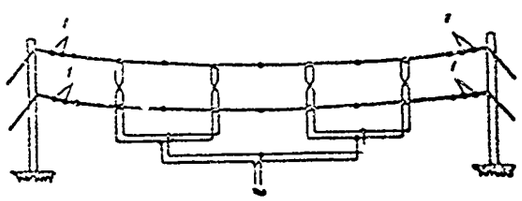

Figure XI.9.2. Suspension of an antenna curtain on supports without a stay.

If the antenna is suspended on a metal stay, the latter is usually sectioned by insulators and section lengths are made no longer than $\lambda/4$ in order to avoid the considerable effect the stay has on the directional properties of the antenna. Research on the subject has revealed the stay need not be sectioned. The effect of an unsectioned stay on the antenna gain factor is slight.

The desirable distance between the lowest point on the stay and the upper stacks of dipoles is at least $\lambda/4$.

The cable guys supporting the dipoles in the individual stacks should be sectioned by insulators in the span between the battens and the dipoles (insulators 1 in figs. XI.9.1 and XI.9.2). This is necessary in order to reduce the currents induced in the supporting cables by the antenna. Section lengths should be no longer than $\lambda/10$. The distance between the antenna supports should be selected such that there will be at least two such sections on either side.

Securing the dipoles to the vertical inter-stack feeders, which latter have been crossed, can be done by using insulators in the form of transposition blocks (fig. XI.9.3).

The reflector curtain is built like the antenna curtain.

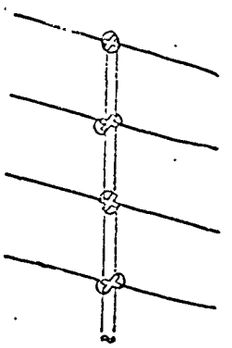

Figure XI.9.3. Securing dipoles to a vertical inter-stack feeder with transition blocks.

(b) Distribution feeders

The lengths of primary distribution feeders are selected such that the highest traveling wave ratio possible will be established on the secondary distribution feeders. The distribution system as a whole should provide the highest possible "natural" (without special tuning) traveling wave ratio on the supply feeder.

It is necessary to increase the traveling wave ratio on distribution feeders and on the supply feeder in order to reduce losses, reduce potentials, and increase the stability of the tuning of the supply feeder to the traveling wave. The smaller the traveling wave ratio on the distribution feeders, and the natural traveling wave ratio on the supply feeder, the greater will be the mismatch between feeder and antenna as atmospheric conditions (rain, frost, sleet, etc.) change.

If we are to obtain the highest possible traveling wave ratio we must select distribution feeder lengths such that there will be voltage loops (fig. XI.9.4) at the branch points.

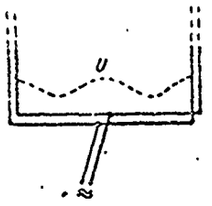

Figure XI.9.4. Choosing the lengths of distribution feeders.

Bends in distribution feeders must be made in such a way that the lengths of both conductors remain absolutely identical.

(c) Antenna supports

Supports are made of wood or metal.

There is no firm basis for giving preference to either type of support, at least not from the point of view of providing optimum electrical parameters for antennas.

The guys supporting the masts are usually broken up by insulators (sectioned) in order to reduce the currents induced in them by the antenna's electromagnetic field. Heavy currents flowing in the guys cause energy losses and radiation pattern distortion. The distance selected for the lengths of sections of guys between adjacent insulators should be no greater than $\lambda/4$.

Experimental investigations have revealed, however, that as a practical matter there are no significant losses, or any great distortion in the patterns, even when unsectioned guys are used. In the latter case however, the unsectioned guys must not be installed in front of the antenna curtain in the direction of maximum radiation. Moreover, it is necessary to measure the antenna radiation pattern and confirm the fact that the guys do not cause unusual distortion.

If unacceptable distortions are found, and are in fact caused by the guys, the necessary steps must be taken (partial sectioning, interconnecting the guys, other measures to detune the exciting guys).

The SG stacked dipole antenna is frequently suspended on free-standing metal towers.

#XI.10. SG Receiving Antenna

All of the data in the foregoing with respect to the directional properties, directive gain, gain factor, input impedance, and other parameters of the SG transmitting antenna are valid for SG receiving antennas.

The effective length of the SG receiving antenna can be computed through formula (VI.8.5).

Table XI.10.1 lists the values for effective lengths of selected variants of the SG antenna when W_F = 208 ohms and W_F = 100 ohms.

The assumption behind the table is that the supply feeder efficiency is $\eta = 1$.

Table XI.10.1

Antenna variant	Characteristic impedance of supply feeder, W_F, ohms	Effective length,, l_{eff}
SG 1/2 R	208	2λ
"	100	1.39λ
SG 1/4 R	208	2.74λ
"	100	1.9λ
SG 2/2 R	208	2.47λ
"	100	1.72λ
SG 2/4 R	208	3.24λ
"	100	2.25λ
SG 2/8 R	208	4.5λ
"	100	3.13λ
SG 4/8 R	208	6.75λ
"	100	4.7λ
SG 6/8 R	208	7.8λ
"	100	5.4λ

The compilation of Table XI.10.1 used ε values taken from Table XI.5.1 for lower stack suspension height equal to λ/2.

What was said above with respect to the design formulation of SG transmitting antennas also remains valid for SG receiving antennas. The exception is the statement concerning the possibility of using non-sectioned stays and guys on masts. When reception is involved special attention must be given to the question of eliminating distortions in the reception pattern, so the use of non-sectioned stays and guys is undesirable.

The supply feeder for the SG receiving antenna is usually a 4-wire conductor with a characteristic impedance of 208 ohms. This must be taken into consideration when designing the match between antenna and supply feeder.

#XI.11. Radiation Pattern Control in the Horizontal Plane

The antenna's radiation pattern in the horizontal plane can be controlled by shifting the point at which the supply feeder is connected to the distribution feeder. And both branches of the distribution feeder should be tuned to the traveling wave mode. Figure XI.11.1 shows the arrangement for controlling the pattern.

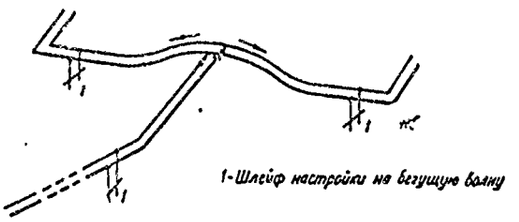

Figure XI.11.1. Schematic diagram of how the radiation pattern of the antenna is controlled in the horizontal plane.

1 - traveling wave tuning stub.

Moving the supply point to the right of center of the distribution feeder rotates the direction of maximum radiation to the left, and vice versa.

The radiation pattern in the horizontal plane in the case of unbalanced feed to the distribution feeder can be computed through the formula

$$F(\varphi) = \frac{\operatorname{ctg}\left(\frac{\pi}{2}\sin\varphi\right)}{\cos\varphi}\sin\left(\frac{n}{2}\frac{\pi}{2}\sin\varphi\right)\times \\ \times\sqrt{1+m^2+2m\cos(\psi-\alpha d_3\cos\varphi)}\times \\ \times\cos\left(\frac{\alpha D_1}{2}\sin\varphi-\frac{\alpha l_p}{2}\right), \qquad \text{(XI.11.1)}$$

where

l_p is the difference in the lengths of the branches of the distribution feeder;

D_1 is the distance between the centers of the symmetrical halves of the antenna curtain (fig. XI.11.2).

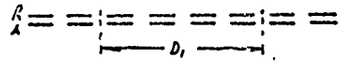

Figure XI.11.2. For formula (XI.11.1).

Chapter XII

MULTIPLE-TUNED BROADSIDE ARRAY

#XII.1. Description and Conventional Designations

The SGD [multiple-tuned broadside] array is a modified SG array designed for broadband operation.

One of the reasons why the SG array cannot be used for broadband operation is the disturbance of the equality of the currents flowing in the dipoles in the different stacks when there is a radical departure from the specified wavelength. Disturbance of the normal distribution of energy between stacks results in distortion of the radiation pattern in the vertical plane and a reduction in directive gain.

The arrangement of the SGD array is such that the distribution of energy between the stacks retains equality of currents, in phase and amplitude, regardless of the wavelength.

Figure XII.1.1 is a schematic diagram of a two-stacked SGD array. As will be seen, the emf is supplied to the center of the vertical feeder connecting both stacks. With this sort of supply arrangement the currents flowing in the upper and lower stacks are the same, regardless of the wavelength, provided the slight unbalance in energy distribution between the stacks occasioned by the ground[1] is not taken into consideration.

A second reason why the SG array cannot be used for broadband operation is the sharp change which takes place in the magnitude of the input impedance of the array with change in the wavelength, and as a consequence, the disturbance in the match between antenna and supply feeder. This difficulty can be eliminated from the SGD array by using dipoles with reduced characteristic impedances and a special system of distribution feeders.

The SGD array, like the SG array, usually has a parasitic reflector, and the distance between antenna and reflector is chosen approximately equal to 0.5 ℓ (ℓ is the length of one arm of a balanced dipole). The reflector can be tuned or untuned. The tuned reflector, as in the SG array case, is a curtain which is an exact duplicate of the antenna curtain, and is tuned by movable shorting plugs. The untuned reflector is made in the form of a flat screen, installed behind the antenna. The screen is a grid of conductors running parallel to the axes of the dipoles. The grid should be dense enough to provide the necessary weakening of the radiation in the back quadrants (see below). The author developed a short-wave antenna with an untuned reflector with rigid dipoles in 1949. Figure XII.1.2 is a schematic diagram of a two-stacked array with untuned reflector.

---

1. The first antennas using this distribution feeder arrangement were suggested by S. I. Nadenenko.

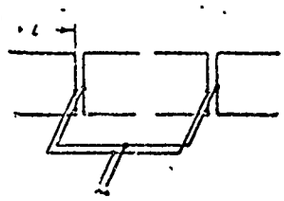

Figure XII.1.1. Schematic diagram of a two-stacked SGD array with four dipoles per stack.

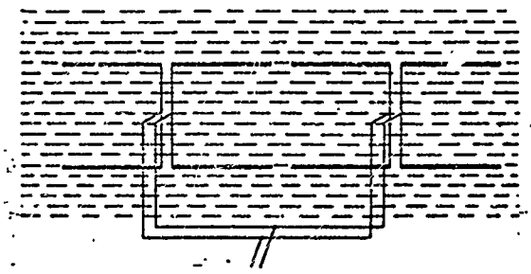

Figure XII.1.2. Schematic diagram of a two-stacked SGD array with an untuned reflector.

The conventional designations with respect to number of stacks and number of arms for the dipoles per stack in an SGD array are the same as those used for the SG array. For example, the SGD array shown in Figure XII.1.1 is conventionally designated SGD 2/4. Figures XII.1.3 and XII.1.4 show the schematics for SGD 2/8 and SGD 4/2 arrays.

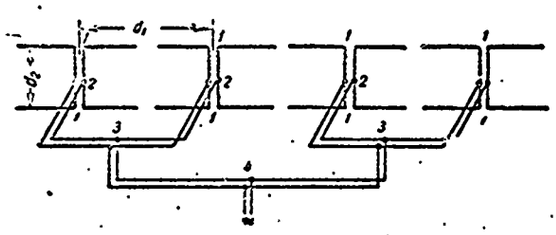

Figure XII.1.3. Schematic diagram of a two-stacked SGD array with eight dipoles per stack.

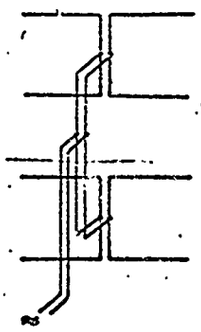

Figure XII.1.4. Schematic diagram of a four-stacked SGD array.

The use of a tuned reflector is indicated by the addition of the letters RN, and if an untuned reflector is used by the letters RA. The antenna shown in Figure XII.1.2 is conventionally designated SGD 2/4 RA.

#XII.2. Calculating the Current Flowing in the Tunable Reflector

The calculation for the ratio of the amplitude (m) to the mutual phase angle (ψ) for the currents flowing in reflector and antenna is made as in the case of the SG array.

Table XII.2.1 lists the results of computing m and ψ for certain variants of the SGDRN array. The distance between antenna and reflector was taken as equal to $0.25\lambda_0$ ($\lambda_0 = 2l$).

The values for m and ψ listed in Table XII.2.1 correspond to a maximum radiation mode in a direction normal to the plane of the antenna curtain. However, this cannot be taken as the optimum mode because it brings with it large lobes which form in the back quadrants.

Table XII.2.1

Antenna variant	Wavelengths	m	$\psi°$
SGD 1/2 RN	λ_0	0.81	120
"	$2\lambda_0$	0.82	158
SGD 1/4 RN	λ_0	0.785	120
"	$2\lambda_0$	0.827	160
SGD 2/2 RN	λ_0	0.95	110
"	$2\lambda_0$	0.905	155
SGD 2/4 RN	λ_0	0.895	110
"	$2\lambda_0$	0.85	155
SGD 2/8 RN	λ_0	0.91	110
"	$2\lambda_0$	0.745	150

#XII.3. Formulas for Calculating Radiation Patterns and Parameters of the SGDRN Array

The field strength produced by the SGDRN array in an arbitrary direction can be calculated through the formula[1]

$$E = \frac{120I}{r}\frac{\cos(\alpha l\cos\Delta\sin\varphi)-\cos\alpha l}{\sqrt{1-\cos^2\Delta\sin^2\varphi}}\frac{\sin\left(n_2\frac{\alpha d_1}{2}\cos\Delta\sin\varphi\right)}{\sin\left(\frac{\alpha d_1}{2}\cos\Delta\sin\varphi\right)}\times$$

$$\times\frac{\sin\left(n_1\frac{\alpha d_2}{2}\sin\Delta\right)}{\sin\left(\frac{\alpha d_2}{2}\sin\Delta\right)}\sqrt{1+m^2+2m\cos(\psi-\alpha d_3\cos\Delta\cos\varphi)}\times \qquad \text{(XII.3.1)}$$

$$\times\sin(\alpha H_{a\nu}\sin\Delta),$$

1. See Appendix 4.

where

I is the current flowing in the current loops of the antenna dipoles;

φ is the azimuth angle of the beam, read from the normal to the plane of the antenna curtain;

Δ is the angle of tilt of the beam;

n_1 is the number of stacks;

$n_2 = n/2$ is the number of balanced dipoles per stack, that is, the number of sections;

d_1 is the distance between the centers of two adjacent balanced dipoles;

d_2 is the distance between adjacent stacks;

d_3 is the distance between antenna and reflector;

H_{av} is the average height at which the antenna is suspended,

$$H_{av} = H_1 + \frac{(n_1 - 1)\, d_2}{2}, \qquad \text{(XII.3.2)}$$

where

H_1 is the height at which the lower stack of the antenna is suspended.

Substituting $\Delta = 0$ in formula (XII.3.1), and converting, and dropping the factors which are not dependent on φ, we obtain the following expression for the radiation pattern in the horizontal plane[1]

$$F(\varphi) = \frac{\cos(\alpha l \sin\varphi) - \cos\alpha l}{\cos\varphi} \frac{\sin\left(n_2 \frac{\alpha d_1}{2} \sin\varphi\right)}{\sin\left(\frac{\alpha d_1}{2} \sin\varphi\right)} \times$$
$$\times \sqrt{1 + m^2 + 2m\cos(\psi - \alpha d_3 \cos\varphi)}. \qquad \text{(XII.3.3)}$$

Substituting $\varphi = 0$ in formula (XII.3.1), and converting, we obtain the expression for the radiation pattern in the vertical plane

$$F(\Delta) = \frac{E}{\frac{60I}{r}} = 2n_2(1 - \cos\alpha l) \frac{\sin\left(n_1 \frac{\alpha d_2}{2} \sin\Delta\right)}{\sin\left(\frac{\alpha d_2}{2} \sin\Delta\right)} \times$$
$$\times \sqrt{1 + m^2 + 2m\cos(\psi - \alpha d_3 \cos\Delta)}\, \sin(\alpha H_{av} \sin\Delta). \qquad \text{(XII.3.4)}$$

In the case of real ground the expression for the radiation pattern in the vertical plane becomes

$$F(\Delta) = n_2(1 - \cos\alpha l) \frac{\sin\left(n_1 \frac{\alpha d_2}{2} \sin\Delta\right)}{\sin\left(\frac{\alpha d_2}{2} \sin\Delta\right)} \times$$
$$\times \sqrt{1 + m^2 + 2m\cos(\psi - \alpha d_3 \cos\Delta)} \times$$
$$\times \sqrt{1 + |R_\perp|^2 + 2|R_\perp|\cos(\Phi_\perp - 2\alpha H_{av} \sin\Delta)}. \qquad \text{(XII.3.5)}$$

1. See footnote at page 220.

The directive gain can be established through the formula

$$D = 120\frac{F^2(\Delta)}{R_{\Sigma A}}. \qquad \text{(XII.3.6)}$$

The gain factor can be established through the formula

$$\epsilon = \frac{D}{1.64}\eta \qquad \text{(XII.3.7)}$$

The radiation resistance can be established by the induced emf method. The computation for the effect of the ground can be made on the basis of the assumption that the ground has ideal conductivity.

XII.4. Formulas for Calculating Radiation Patterns, Gain Factor, and Directive Gain of the SGDRA Array

The radiation patterns in the horizontal and vertical planes can be calculated approximately by replacing the reflector with the mirror image of the antenna, that is, by replacing the reflector with an additional antenna made absolutely identical with the real antenna and located at distance $2d_3$ from it (d_3 is the distance from the antenna to the untuned reflector). Currents flowing in the mirror image are shifted 180° in phase relative to the currents flowing in the antenna.

With the introduction of the mirror image we can now calculate patterns through formulas which are identical with formulas (XII.3.1) - (XII.3.5). We need only change the factor in these formulas which takes the effect of the reflector into consideration. In formula (XII.3.1) this factor should be replaced by the factor $2\sin(\alpha d_3 \cos\varphi \cos\Delta)$, in formula (XII.3.3) by the factor $2\sin(\alpha d_3 \cos\varphi)$, and in formulas (XII.3.4) and (XII.3.5) by the factor $2\sin(\alpha d_3 \cos\Delta)$.

Accordingly, the formulas for the radiation patterns in the front half-space are in the following form:

the general formula is

$$E = \frac{240I}{r}\frac{\cos(\alpha l\cos\Delta\sin\varphi) - \cos\alpha l}{\sqrt{1-\cos^2\Delta\sin^2\varphi}}\frac{\sin\left(n_2\frac{\alpha d_1}{2}\cos\Delta\sin\varphi\right)}{\sin\left(\frac{\alpha d_1}{2}\cos\Delta\sin\varphi\right)}\times$$

$$\times\frac{\sin\left(n_1\frac{\alpha d_2}{2}\sin\Delta\right)}{\sin\left(\frac{\alpha d_2}{2}\sin\Delta\right)}\sin(\alpha d_3\cos\varphi\cos\Delta)\sin(\alpha H_{\mathrm{ant}}\sin\Delta); \qquad \text{(XII.4.1)}$$

in the horizontal plane

$$F(\varphi) = \frac{\cos(\alpha l\sin\varphi) - \cos\alpha l}{\cos\varphi}\frac{\sin\left(n_2\frac{\alpha d_1}{2}\sin\varphi\right)}{\sin\left(\frac{\alpha d_1}{2}\sin\varphi\right)}\sin(\alpha d_3\cos\varphi); \qquad \text{(XII.4.2)}$$

in the vertical plane when the ground is a perfect conductor

$$F(\Delta) = \frac{E}{\frac{60I}{r}} = 4n_2(1-\cos\alpha l)\frac{\sin\left(n_1\frac{\alpha d_2}{2}\sin\Delta\right)}{\sin\left(\frac{\alpha d_1}{2}\sin\Delta\right)}\sin(\alpha d_3\cos\Delta)\times$$
$$\times\sin(\alpha H_{a\nu}\sin\Lambda); \qquad \text{(XII.4.3)}$$

in the vertical plane when real ground is taken into consideration

$$F(\Delta) = 2n_2(1-\cos\alpha l)\frac{\sin\left(n_1\frac{\alpha d_2}{2}\sin\Delta\right)}{\sin\left(\frac{\alpha d_2}{2}\sin\Delta\right)}\sin(\alpha d_3\cos\Delta)\times$$
$$\times\sqrt{1+|R_\perp|^2+2|R_\perp|\cos(\Psi_\perp-2\alpha H_{a\nu}\sin\Delta)}. \qquad \text{(XII.4.4)}$$

The formulas obtained in this manner are accurate if the untuned reflector has an infinite expanse in the vertical and horizontal directions and is a solid, flat metal screen with infinite conductivity. It goes without saying that these formulas will only permit us to calculate the field in the front half-space. When the screen expanse is infinite and impermeability is total, the field to the rear of the screen is equal to zero.

As a practical matter, because the screen has finite dimensions, and because it is made in the form of a grid of parallel conductors, the radiation pattern charted is somewhat different than that charted for the ideal screen. Experimental and theoretical investigations have revealed, however, that when the screen dimensions and density of the grid conductors are those we recommend (see below) the real radiation pattern in the front half-space will coincide well with the radiation pattern charted on the basis of an idealized screen. Insofar as radiation in the back half-space is concerned, this too can be approximated by charting in the back half-space lobes which are identical with those in the diagram for the front half-space, but at a scale reduced by a factor established by the formula

$$\frac{\sqrt{\delta}}{2\sin(\alpha d_3\cos\varphi\cos\Delta)}. \qquad \text{(XII.4.5)}$$

The factor in (XII.4.5) takes the form

$$\frac{\sqrt{\delta}}{2\sin(\alpha d_3\cos\varphi)}. \qquad \text{(XII.4.6)}$$

when the calculation is made for the radiation pattern in the horizontal plane.

The factor in (CII.4.5) takes the form

$$\frac{\sqrt{\delta}}{2\sin(\alpha d_3 \cos\Delta)}, \qquad \text{(XII.4.7)}$$

where δ is the energy leakage power ratio, when the calculation is made for the radiation pattern in the vertical plane.

The formula for calculating δ is given below (#XII.8). We should bear in mind that δ, as established by the formula given below, is obtained for the case of a plane wave incident to the grid. In the case specified we are talking about leakage of the field created by the dipoles, and which differs substantially at the surface of the grid from the field of the plane wave. We should further note that the radiation in the back half-space is not only established by the leakage of energy through the grid, but also by the diffraction of grid energy because of the finite dimensions of the grid, something not taken into consideration when calculating radiation by the method indicated.

Nevertheless, the calculation for the field strength in the back half-space, carried out by the method described here, does enable us to obtain an approximate estimate of radiation intensity in the back quadrants. G. Z. Ayzenberg, in his monograph titled UHF Antennas, published by Svyaz'izdat in 1957, provides us with a more accurate methodology for charting the pattern of an antenna with an untuned reflector in Chapter XIV of that monograph.

The directive gain and the gain factor of SGDRA arrays can be calculated through formulas (XII.3.6) and (XII.3.7), substituting the expression at (XII.4.3) in them in place of $F(\Delta)$. The formula for the gain factor is taken as being in the following form

$$s = n_2^2 \frac{1170}{R_{\Sigma A}} (1-\cos\alpha l)^2 \frac{\sin^2\left(n_1 \frac{a d_2}{2}\sin\Delta\right)}{\sin^2\left(\frac{a d_2}{2}\sin\Delta\right)} \sin^2(\alpha d_3 \cos\Delta)\sin^2(\alpha H_{av}\sin\Delta). \qquad \text{(XII.4.8)}$$

The values for the magnitudes contained in the formula were given in #XII.3. $R_{\Sigma A}$ is calculated with the effect of the mirror image created by a parasitic reflector taken into consideration.

#XII.5. Formulas for Calculating the Horizontal Beam Width

Zero horizontal beam width of the major lobe can be established when the condition is such that the numerator of the second factor in formulas (XII.3.3) and (XII.4.2) is set equal to zero.

This condition will be satisfied upon observance of the equality

$$n_2 \frac{a d_1}{2}\sin\varphi_0 = \pi, \qquad \text{(XII.5.1)}$$

where φ_0 is the angle formed by the radius vector corresponding to the direction in which there is no radiation and the radius vector corresponding to the

direction in which maximum radiation occurs.

From (XII.5.1) we obtain the fact that zero width ($2\varphi_0$) equals

$$2\varphi_0 = 2 \arcsin \frac{\lambda}{n_2 d_1}. \qquad \text{(XII.5.2)}$$

If $\lambda/n_2 d_1 \leqslant 0.5$, then

$$2\varphi_0 \approx \frac{2\lambda}{n_2 d_1} = \frac{2\lambda}{L}, \qquad \text{(XII.5.3)}$$

where

L is the length of the antenna curtain.

The width, expressed in degrees, equals

$$2\varphi_0^\circ \approx \frac{114\lambda}{L}. \qquad \text{(XII.5.4)}$$

It is not difficult to prove that the half-power width equals

$$\varphi_{0,5}^\circ \approx 0{,}88\varphi_0. \qquad \text{(XII.5.5)}$$

By $\varphi_{0.5}$ is understood to mean the angle contained within the two radius vectors corresponding to the directions in which the field intensity is less by a factor of $\sqrt{2}$ than in the main direction (see fig. XII.6.1).

#XII.6. SGD Array Radiation Patterns and Parameters

Figures XII.6.1 - XII.6.14 show a series of design radiation patterns in the horizontal plane for a single-section ($n_2 = 1$), two-section ($n_2 = 2$), and four-section ($n_2 = 4$) SGDRA array. In the figures λ_0 designates the array's so-called principal wave, equal to 2l (shortening of l, the result of reduction in the phase velocity, not considered).

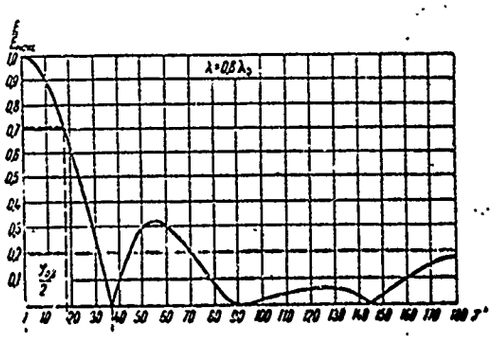

Figure XII.6.1. Radiation pattern in the horizontal plane of an SGDRA array ($n_2 = 1$).

Vertical: E/E_{max}.

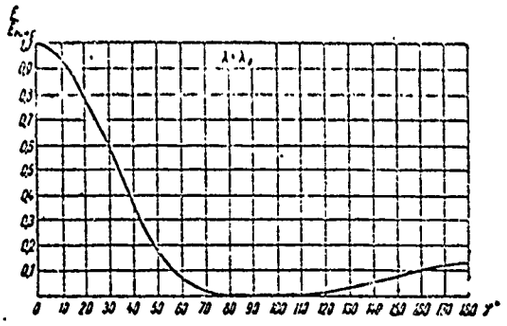

Figure XII.6.2. Radiation pattern in the horizontal plane of an SGDRA array (n_2 = 1).

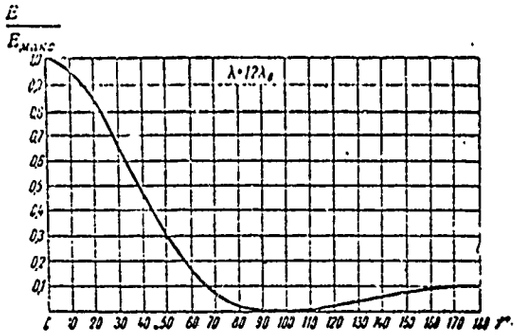

Figure XII.6.3. Radiation pattern in the horizontal plane of an SGDRA array (n_2 = 1).

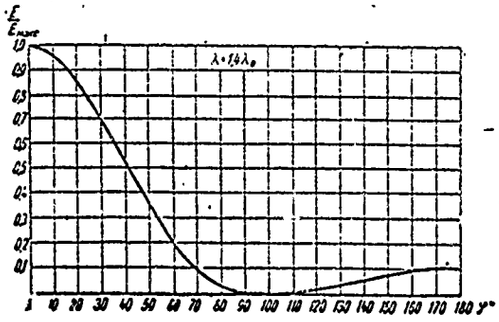

Figure XII.6.4. Radiation pattern in the horizontal plane of an SGDRA array (n_2 = 1).

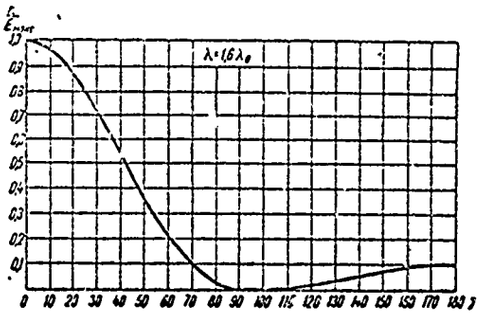

Figure XII.6.5. Radiation pattern in the horizontal plane of an SGDRA array (n_2 = 1).

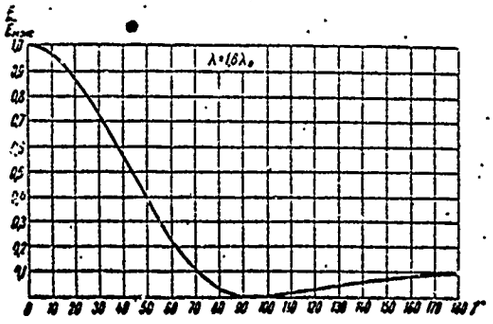

Figure XII.6.6. Radiation pattern in the horizontal plane of an SGDRA array (n_2 = 1).

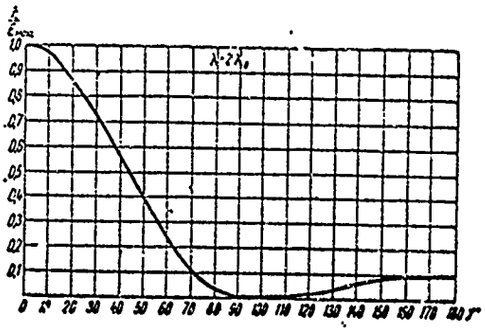

Figure XII.6.7. Radiation pattern in the horizontal plane of an SGDRA array (n_2 = 1).

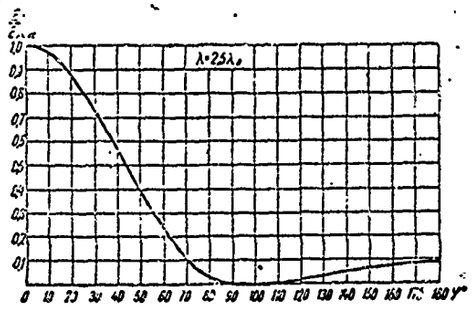

Figure XII.6.8. Radiation pattern in the horizontal plane of an SGDRA array ($n_2 = 1$).

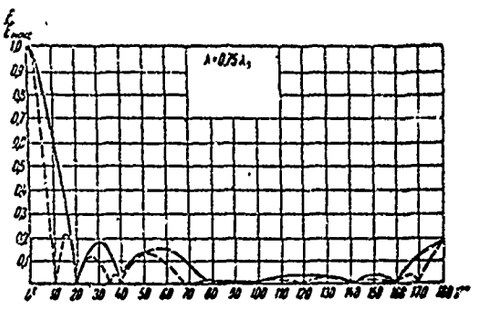

Figure XII.6.9. Radiation pattern in the horizontal plane of an SGDRA array; ——— $n_2 = 2$; ----- $n_2 = 4$.

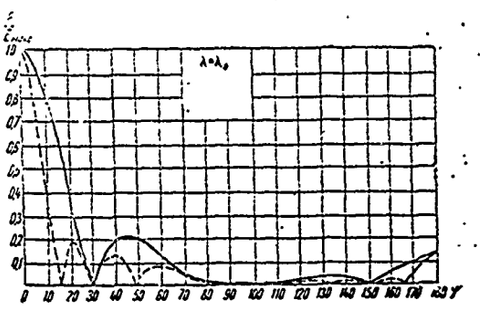

Figure XII.6.10. Radiation pattern in the horizontal plane of an SGDRA array; ——— $n_2 = 2$; ----- $n_2 = 4$.

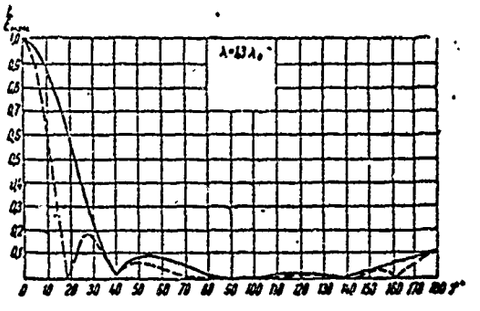

Figure XII.6.11. Radiation pattern in the horizontal plane of an SGDRA array; ——— $n_2 = 2$; ----- $n_2 = 4$.

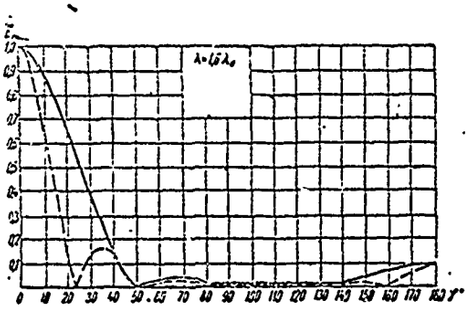

Figure XII.6.12. Radiation pattern in the horizontal plane of an SGDRA array; ——— $n_2 = 2$; ----- $n_2 = 4$.

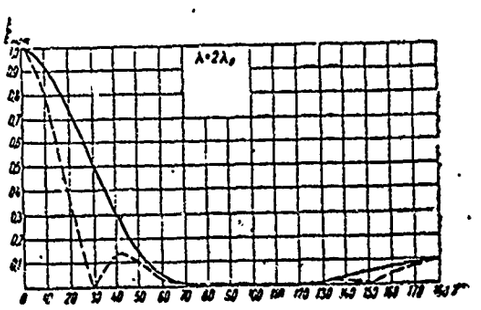

Figure XII.6.13. Radiation pattern in the horizontal plane of an SGDRA array; ——— $n_2 = 2$; ----- $n_2 = 4$.

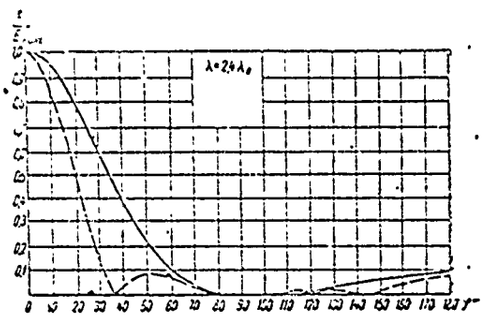

Figure XII.6.14. Radiation pattern in the horizontal plane of an SGDRA array; ——— $n_2 = 2$; ----- $n_2 = 4$.

The shape of the radiation patterns in the horizontal plane in the front half-space remains almost the same for tuned and untuned reflectors. The difference shows up in the main in some increase in the side radiation in the case of the tuned reflector, as compared with that shown for the untuned reflector. However, this difference decreases with increase in the number of sections. Figures XII.6.15 - XII.6.18 show radiation patterns in the horizontal plane for a single-section SGDRN array, charted on the assumption that the m and ψ values correspond to the maximum ε magnitude.

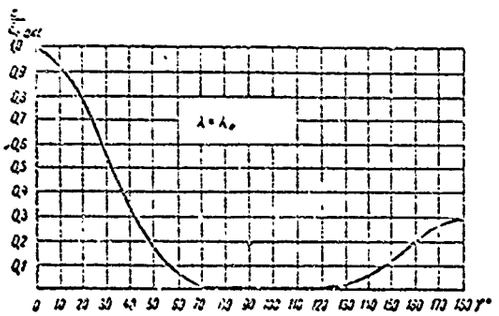

Figure XII.6.15. Radiation pattern in the horizontal plane of an SGDRN array ($n_2 = 1$).

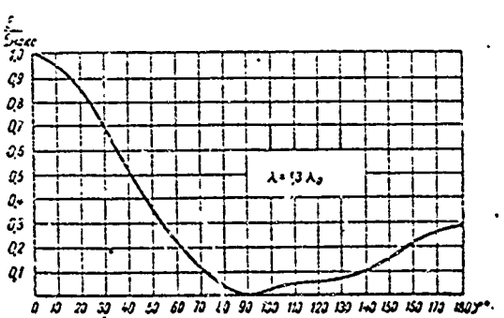

Figure XII.6.16. Radiation pattern in the horizontal plane of an SGDRN array ($n_2 = 1$).

Figures XII.6.19 - XII.6.28 show the design radiation patterns in the vertical plane of single-stacked ($n_1 = 1$) SGDRA and SGDRN antennas. Figures XII.6.29 - XII.6.42 show a series of radiation patterns in the vertical plane for two-stacked ($n_1 = 2$) and four-stacked ($n_1 = 4$) SGDRA arrays. When $n_1 \geqslant 2$, the shape of the radiation pattern in the vertical plane in the front half-space, and particularly within the limits of the major lobe, is little dependent on the type of reflector, so figures XII.6.28 - XII.6.42 are also characteristic of radiation patterns in the vertical plane of two-stacked and

four-stacked SGDRN arrays.

Radiation patterns for the SGDRA arrays were charted on the assumption that the density of the conductors in the screen was selected in accordance with the recommendations which will be given in what follows.

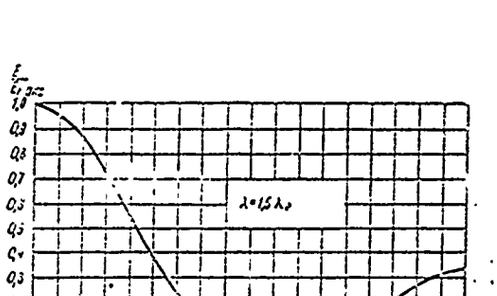

Figure XII.6.17. Radiation pattern in the horizontal plane of an SGDRN array ($n_2 = 1$).

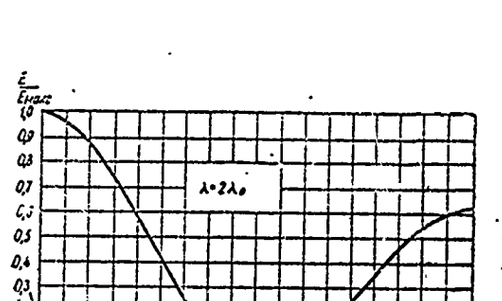

Figure XII.6.18. Radiation pattern in the horizontal plane of an SGDRN array ($n_2 = 1$).

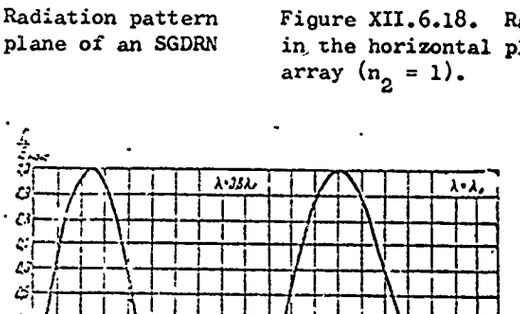

Figure XII.6.19. Radiation patterns in the vertical plane of a single-stacked SGDRA array, with antenna dipoles suspended at height $H = 0.5\ \lambda_0$.

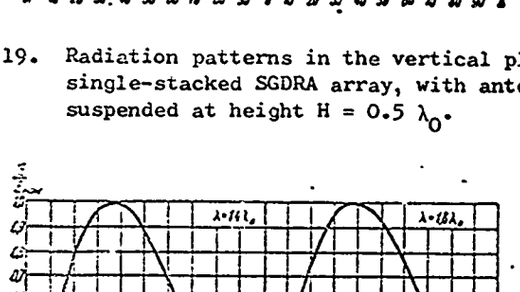

Figure XII.6.20. Radiation patterns in the vertical plane of a single-stacked SGDRA array, with antenna dipoles suspended at height $H = 0.5\ \lambda_0$.

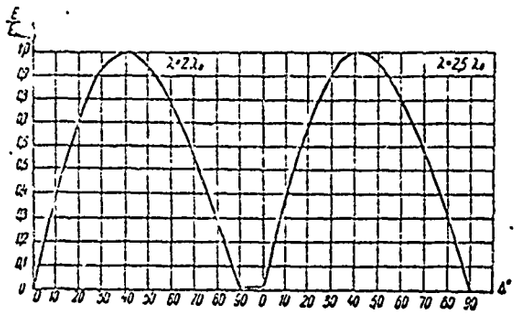

Figure XII.6.21. Radiation patterns in the vertical plane of a single-stacked SGDRA array, with antenna dipoles suspended at height H = 0.5 λ_0.

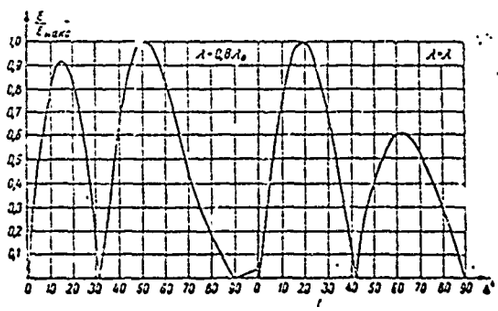

Figure XII.6.22. Radiation patterns in the vertical plane of a single-stacked SGDRA array, with antenna dipoles suspended at height H = 0.75 λ_0.

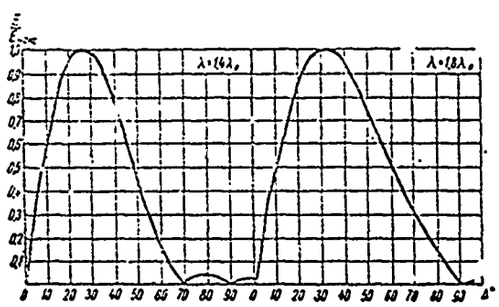

Figure XII.6.23. Radiation patterns in the vertical plane of a single-stacked SGDRA array, with antenna dipoles suspended at height H = 0.75 λ_0.

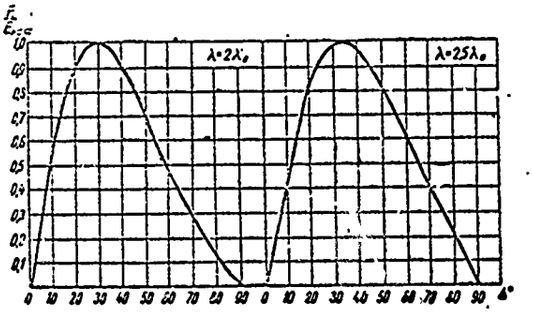

Figure XII.6.24. Radiation patterns in the vertical plane of a single-stacked SGDRA array, with antenna dipoles suspended at height H = 0.75 λ_0.

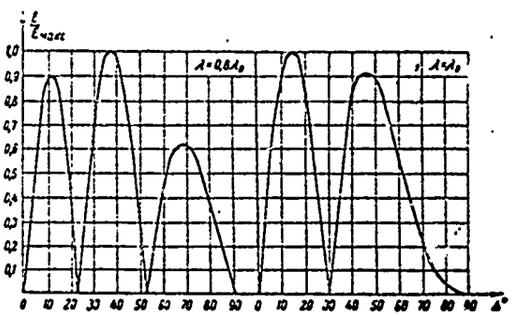

Figure XII.6.25. Radiation patterns in the vertical plane of a single-stacked SGDRA array, with antenna dipoles suspended at height H = λ_0.

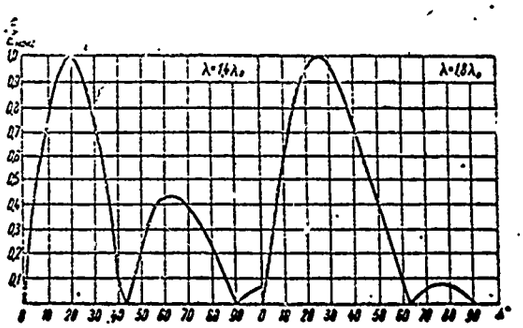

Figure XII.6.26. Radiation patterns in the vertical plane of a single-stacked SGDRA array, with antenna dipoles suspended at height H = λ_0.

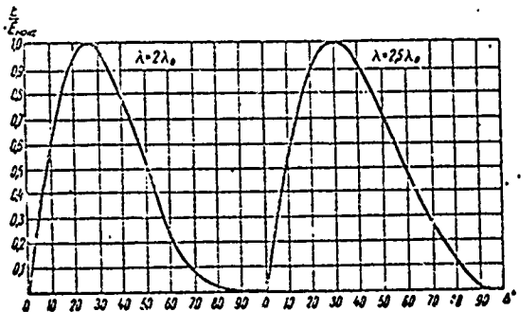

Figure XII.6.27. Radiation patterns in the vertical plane of a single-stacked SGDRA array, with antenna dipoles suspended at height $H = \lambda_0$.

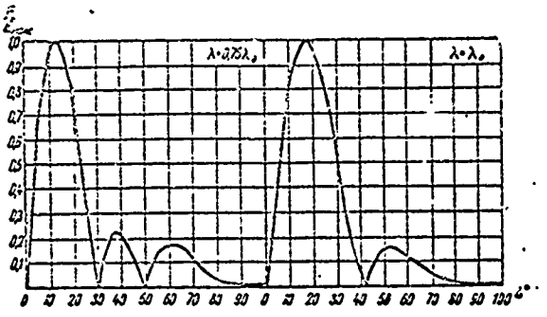

Figure XII.6.28. Radiation patterns in the vertical plane of a two-stacked SGDRA array; lower stack of array suspended at height $H_1 = 0.5\ \lambda_0$.

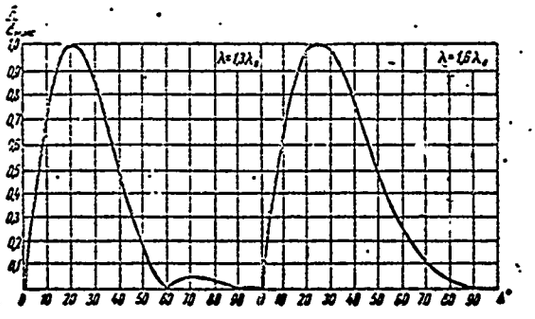

Figure XII.6.29. Radiation patterns in the vertical plane of a two-stacked SGDRA array; lower stack of array suspended at height $H_1 = 0.5\ \lambda_0$.

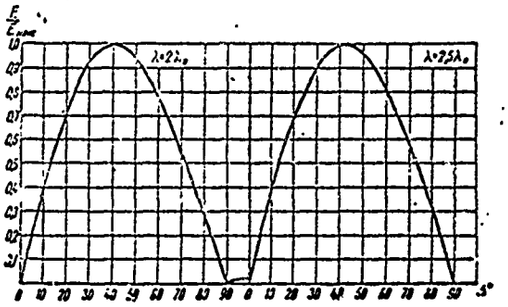

Figure XII.6.30. Radiation patterns in the vertical plane of a two-stacked SGDRA array; lower stack of array suspended at height $H_1 = 0.5\ \lambda_0$.

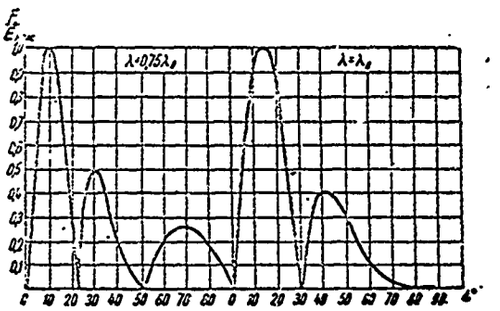

Figure XII.6.31. Radiation patterns in the vertical plane of a two-stacked SGDRA array; lower stack of array suspended at height $H_1 = 0.75\ \lambda_0$.

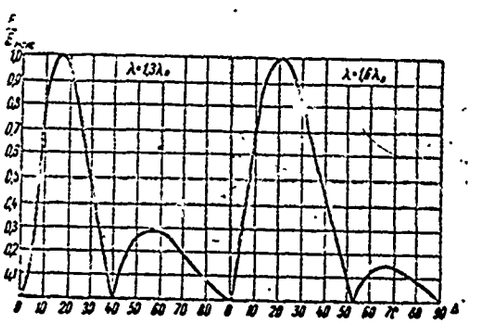

Figure XII.6.32. Radiation patterns in the vertical plane of a two-stacked SGDRA array; lower stack of array suspended at height $H_1 = 0.75\ \lambda_0$.

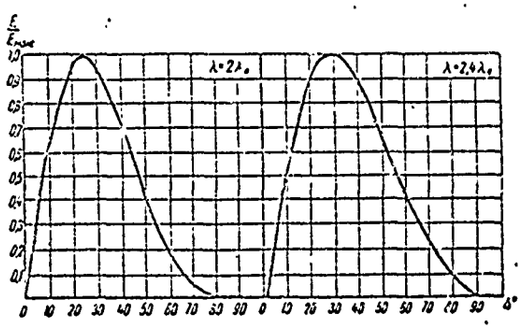

Figure XII.6.33. Radiation patterns in the vertical plane of a two-stacked SGDRA array; lower stack of array suspended at height $H_1 = 0.75\ \lambda_0$.

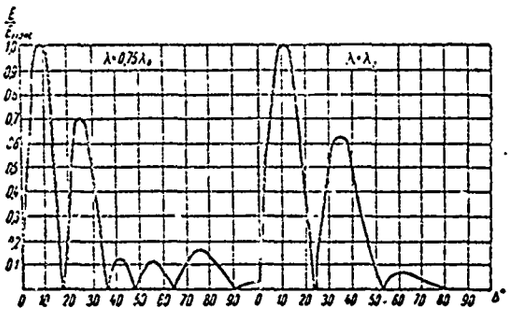

Figure XII.6.34. Radiation patterns in the vertical plane of a two-stacked SGDRA array; lower stack of array suspended at height $H_1 = \lambda_0$.

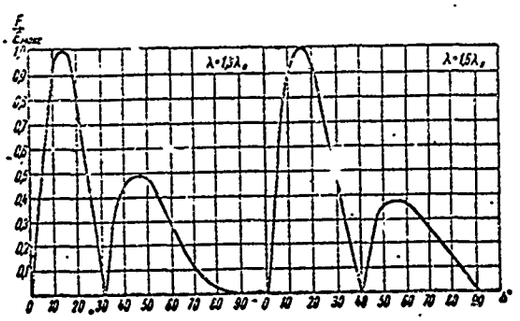

Figure XII.6.35. Radiation patterns in the vertical plane of a two-stacked SGDRA array; lower stack of array suspended at height $H_1 = \lambda_0$.

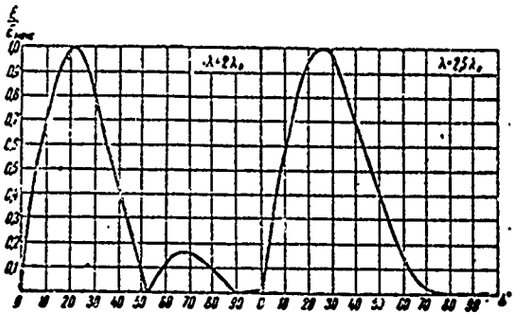

Figure XII.6.36. Radiation patterns in the vertical plane of a two-stacked SGDRA array; lower stack of array suspended at height $H_1 = \lambda_0$.

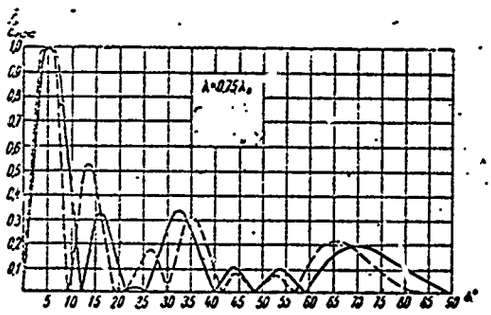

Figure XII.6.37. Radiation patterns in the vertical plane of a four-stacked SGDRA array; ——— $H_1 = \lambda_0$; ----- $H_1 = 1.5\ \lambda_0$.

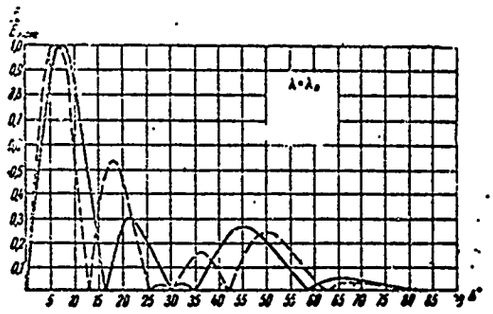

Figure XII.6.38. Radiation patterns in the vertical plane of a four-stacked SGDRA array; ——— $H_1 = \lambda_0$; ----- $H_1 = 1.5\ \lambda_0$.

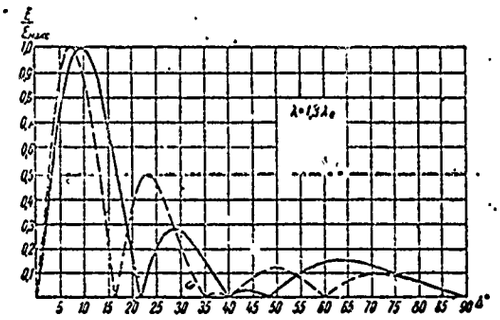

Figure XII.6.39. Radiation patterns in the vertical plane of a four-stacked SGDRA array; ——— $H_1 = \lambda_0$; ----- $H_1 = 1.5\ \lambda_0$.

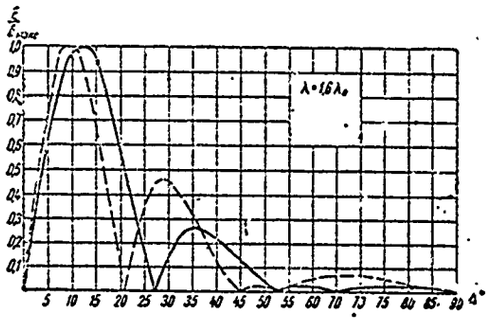

Figure XII.6.40. Radiation patterns in the vertical plane of a four-stacked SGDRA array; ——— $H_1 = \lambda_0$; ----- $H_1 = 1.5\ \lambda_0$.

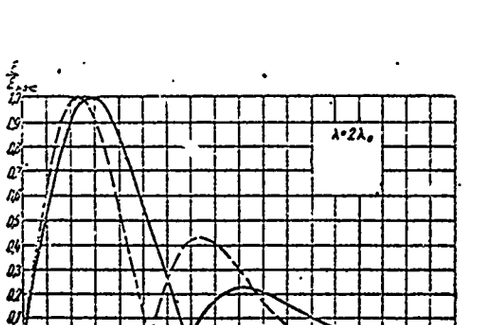

Figure XII.6.41. Radiation patterns in the vertical plane of a four-stacked SGDRA array; ——— $H_1 = \lambda_0$; ----- $H_1 = 1.5\ \lambda_0$.

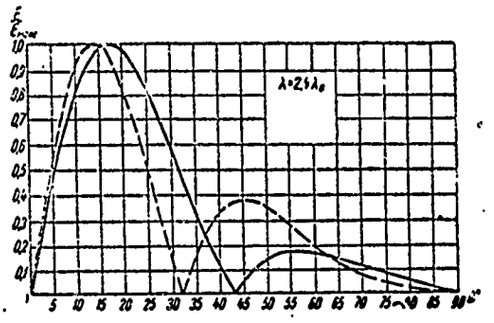

Figure XII.6.42. Radiation patterns in the vertical plane of a four-stacked SGDRA array; ——— $H_1 = \lambda_0$; ----- $H_1 = 1.5\ \lambda_0$.

Figures XII.6.43 and XII.6.44 show a series of curves which characterize the gain factors of SGD 1/2 RA and SGD 1/4 RA arrays.

The gain factor of the SGD 1/2 RN array is approximately equal to the value of the gain factor of the balanced dipole without reflector. Data on the gain factor of a balanced dipole are given in Chapter IX.

Figure XII.6.45 shows the curves which characterize the gain factor of the SGD 2/4 RA array.

The gain factor of the SGD 2/8 RA array is approximately double that of the SGD 2/4 RA array.

Investigations using decimeter models revealed that the gain factor of an SGD 2/4 RN array is 20 to 25% less than that of the SGD 2/4 RA array.

The gain factor of the SGD 2/8 RN is approximately 15% less than the gain factor of an SGD 2/8 RA antenna.

As the models showed, the gain factor of the SGD 4/4 RN array is 10 to 20% less than that of the SGD 4/4 RA array. It can be assumed that the gain factor of the SGD 4/8 RN array is approximately 10% less than the gain factor of the SGD 4/8 RA array.

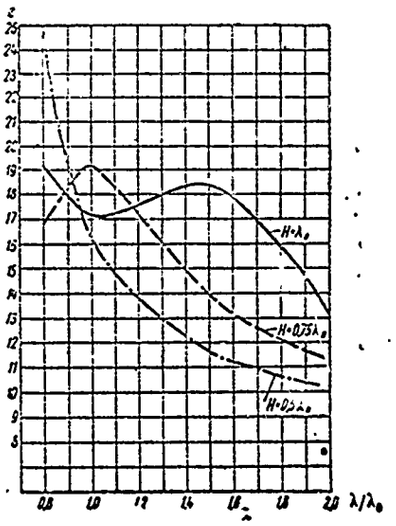

Figure XII.6.43.

Dependence of the maximum gain of an SGD 1/2 RA array on the wavelength.

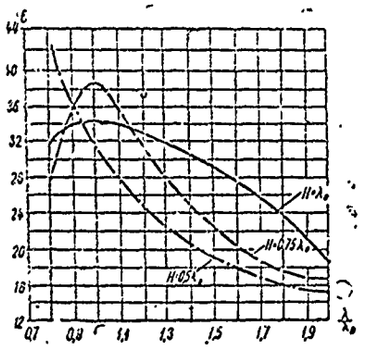

Figure XII.6.44. Dependence of the maximum gain of an SGD 1/4 RA array on the wavelength.

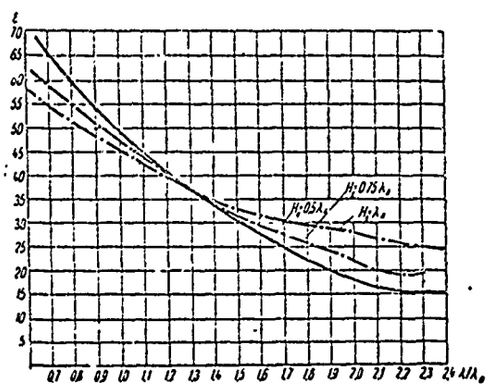

Figure XII.6.45. Dependence of the maximum gain of an SGD 2/4 RA array on the wavelength.

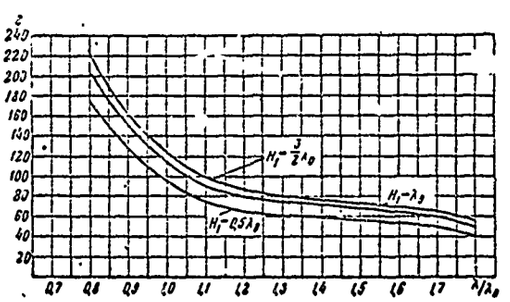

Figure XII.6.46. Dependence of the maximum gain of an SGD 4/4 RA array on the wavelength.

#XII.7. Matching the Antenna to the Supply Line. Making Dipoles and Distribution Feeders. Land in which SGD Antenna Can be Used.

The arrangement of the SGD antennas is such that they can be used over an extremely wide frequency range. As a practical matter, satisfactory directional properties can be provided starting at a wavelength of 0.75 λ_0 and on up to wavelengths of 3 λ_0 and higher. However, as the wavelength is

increased the radiation patterns in the horizontal and vertical planes expand, and the directive gain drops off accordingly. Limiting wavelengths, at which directional properties and gain factor are considered acceptable, are established by concrete conditions and specifications regarding radiation pattern shape.

In addition to directional properties, the band in which used is determined by the need to provide a good match between antenna and supply line. SGD antennas are still used for transmission, primarily, so the traveling wave ratio on the supply line must be at least 0.5 if the transmitter is to function normally and if it is to continue to do so as meteorological conditions vary. It is permissible, in extreme cases, to reduce the traveling wave ratio to 0.3 to 0.4. A high traveling wave ratio can be provided for any wavelength in the band by using the corresponding tuning elements, but their use makes antenna operation complicated because the tuning elements must be retuned when the wavelength is changed. The use of retunable elements in the SGDRA antenna is particularly undesirable. The principal advantage of the SGDRA antenna over the SGDRN antenna is the absence of reflector tuning elements. The use of tuning elements in the traveling wave mode vitiates this advantage to a considerable degree. What has been said in this regard is why it has come to be accepted to make SGD antennas in such a way that a high traveling wave ratio is obtained within the limits of a wide operating frequency range without the use of special tuning elements.

Used for the purpose are dipoles with reduced characteristic impedances and a specially selected system of distribution feeders. The distribution feeders are stepped to improve the match. Each step is equal to 0.25 λ_0. Difference combinations of dipoles and distribution feeders, for which satisfactory match with the transmission line can be obtained, are possible.

It should be emphasized that the lower the characteristic impedance of the dipoles, the better the possibility of obtaining a good match between antenna and transmission line. However, reduction in the characteristic impedance of the dipoles results in making the antenna curtain heavier. Moreover, reduction in the characteristic impedance of the dipoles requires a corresponding reduction in the characteristic impedance of the transmission lines, and this brings with it additional complexity and weight of the antenna curtain. So, what happens is an attempt to get a good match between the antenna and the transmission line without making too great a reduction in the characteristic impedances of the dipoles.

Figures XII.7.1 - XII.7.3 show one possible way in which distribution lines can be installed, as well as the magnitudes of the characteristic impedances of dipoles for SGD 1/2 RA, SGD 2/4 RA, and SGD 4/4 RA antennas.

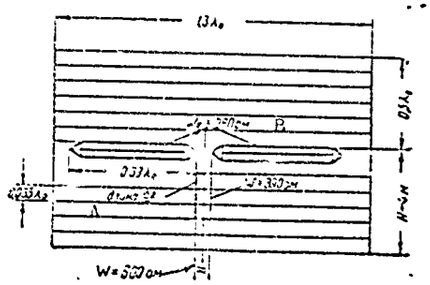

Figure XII.7.1. Schematic diagram of an SGD 1/2 RA antenna. Distance between dipoles and reflector 0.27 λ_0.

A - length; B - ohms.

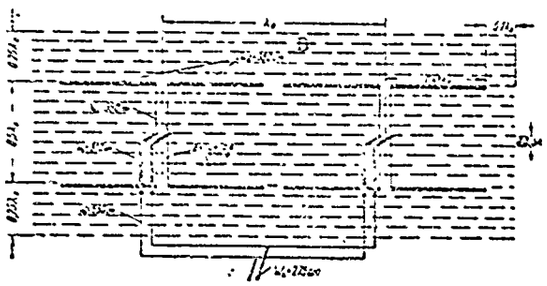

Figure XII.7.2. Schematic diagram of an SGD 2/4 RA antenna. Distance between dipoles and reflector 0.27 λ_0. Diameter of conductors 3 to 5 mm.

A - length; B - ohms.

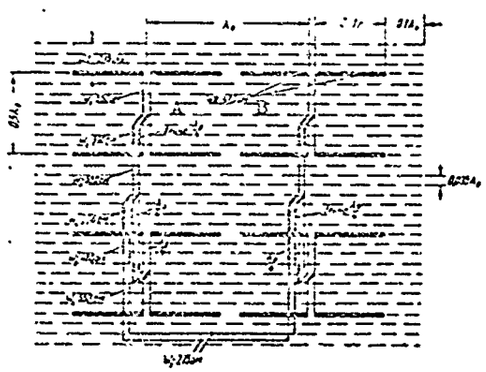

Figure XII.7.3. Schematic diagram of an SGD 4/4 RA antenna. Distance between dipoles and reflector 0.3 λ_0.

A - length; B - ohms.

The distribution lines for similar SGDRN antennas, which use dipoles with the same characteristic impedances, can be made similarly. The distribution lines for tunable reflectors are made in the same way as are the distribution lines for the corresponding antennas.

The distribution lines for the SGD 1/4 R, SGD 2/8 R, and SGD 4/8 R antennas are made with two branches, each of which is made exactly as if it were for the SGD 1/2 R, SGD 2/4 R, and SGD 4/4 R antennas, respectively. The match of these two halves with the transmission line can be provided and retained by using the corresponding exponential or step feeder transformers.

As we see from figures XII.7.1 - XII.7.3, the dipoles have characteristic impedances of 280, 350, and 470 ohms. Figure XII.7.4 shows the sketches of possible variants in making dipoles with these characteristic impedances.

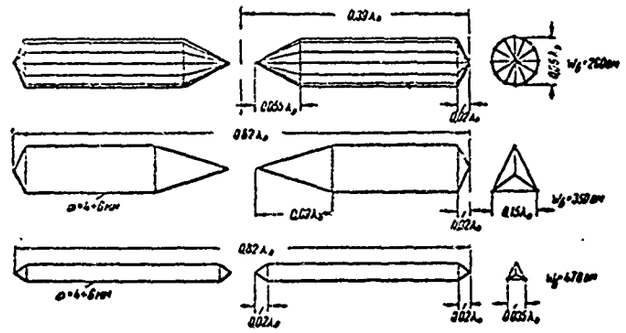

Figure XII.7.4. Sketches of possible variants using dipoles with characteristic impedances W_i equal to 280, 350, 470 ohms.

Figure XII.7.5 through XII.7.7 show the experimental curves of the relationship between the traveling wave ratio on the transmission line and the λ/λ_0 ratio, taken from decimeter models.

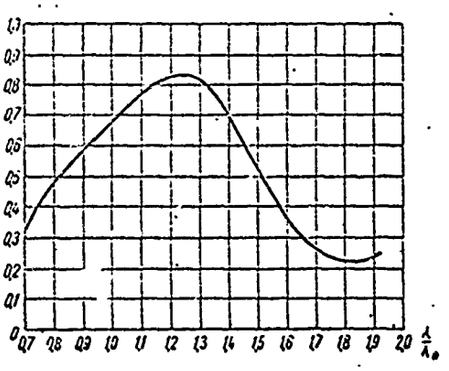

Figure XII.7.5. Experimental curve of the traveling wave ratio on the transmission line to an SGD 1/2 RA antenna made in accordance with the diagram in Figure XII.7.1.

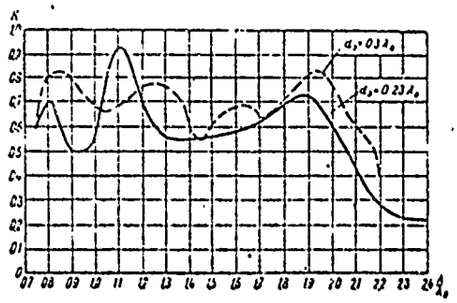

Figure XII.7.6. Experimental curve of the traveling wave ratio on the transmission line to an SGD 2/4 RA antenna made in accordance with the diagram in Figure XII.7.2.

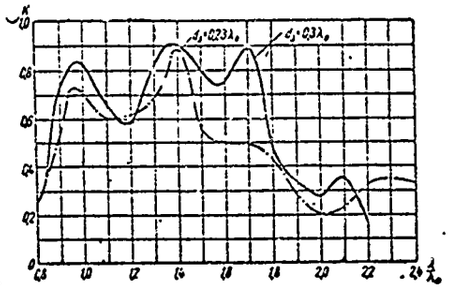

Figure XII.7.7. Experimental curve of the traveling wave ratio on the transmission line to an SGD 4/4 RA antenna.

These curves were taken for the case of untuned reflectors, but the traveling wave ratio curves for tuned reflectors are approximately the same.

The transmission line has a characteristic impedance of 275 ohms in the sketches shown for making distribution lines, the only exception being that in Figure XII.7.1. This is the characteristic impedance of a 4-wire crossed line made using a 6 mm diameter conductor and a cross section measurement for one side of the square transmission line equal to 30 cm. If it is desirable to feed the antenna over a two-wire line with a characteristic impedance of 600 ohms, we should use an exponential or step feeder transformer to make the transition from W_F = 275 ohms to W_F = 600 ohms.

These curves, showing the match between the antenna and the supply feeder, are the basis for establishing the band in which the antenna can be used. As was pointed out above, the band in which the antenna can be used is usually limited by an area in which the traveling wave ratio does not go below 0.3 to 0.5. Local conditions govern how much more precision must go into requirements for increasing the traveling wave ratio.

It must be noted that under actual conditions, because of the different variations which take place in the design formulations of dipoles, insulators, bends in distribution lines, and the like, some deviation between real values

for the traveling wave ratio and those shown in the figures is possible. For this reason, the curves shown here for the match between antenna and feeder must be taken as tentative.

The distance between dipoles and reflectors in two-stacked and four-stacked SGDRA arrays is usually taken as equal to 0.27 to 0.3 λ_0. Note that the magnitude of the distance between reflector and antenna, d_3, has a substantial effect on the match with the feeder. The average over the band is that a reduction in d_3 results in a reduction in traveling wave ratio on the feeder. The value for d_3 shown in figures XII.7.2 and XII.7.3 was chosen in order to obtain a good match. Further increase in d_3 is accompanied by deterioration in the directional properties of the antenna at the short-wave edge of the band in which the antenna is being used and, in addition, results in a heavier antenna structure.

#XII.8. Making an Untuned Reflector

As we have already pointed out above, the untuned reflector is made in the form of a flat grid of conductors paralleling the axes of the dipoles. Density of the conductors used to make the grid is selected such that the energy leakage through the grid does not exceed some predetermined magnitude.

The methodology to be used to compute energy leakage through the grid of the reflector used in the broadside array has not yet been finalized, but an approximate determination can be made if it is assumed that it will be approximately what it is in the case of normal incidence of a plane wave on a grid of infinite span. The energy of a plane wave penetrating a grid of infinite span can be established through the formula[1]

$$\delta = \frac{1}{1 + \left[\frac{\lambda}{2a} \cdot \frac{1}{\ln 2\pi \frac{r_1}{a}}\right]^2}, \qquad \text{(XII.8.1)}$$

where

δ is the ratio of the square of the field strength of the wave leaking through the grid to the square of the field strength of the incident wave;

a is the distance between adjacent conductors in the grid;

r_1 is the radius of the conductors in the grid

Assuming energy losses must not exceed 5%, and taking it that only half of the energy radiated by the antenna curtain is directed toward the grid, we obtain the following equation for finding a and r_1,

$$0{,}1 = \frac{1}{1 + \left[\frac{\lambda}{2a} \cdot \frac{1}{\ln 2\pi \frac{r_1}{a}}\right]^2}. \qquad \text{(XII.8.2)}$$

1. G. Z. Ayzenberg. Ultra-Short Wave Antennas. Svyaz'izdat, 1957, #2.XXI.

The values for a and r_1 are usually selected in such a way that the relationship at (XII.8.2) is satisfied for the shortest wavelength in the band in which the antenna is used. This requires an a equal to 0.07 λ_0, approximately. If operating conditions are such that the requirement is to devote particular attention to weakening radiation in the rear quadrants, then it is desirable to double the density of the conductors ($a \approx 0.035\ \lambda_0$).

Experimental investigations have turned up the fact that in reality the energy leakage through the grid is somewhat less than would follow from the calculation made in the manner indicated. Reflector dimensions (height and width) are selected as small as necessary, which is to say such that the gain factor provided will be as close to maximum as possible for the average for the band. Strictly speaking, every wavelength has its own optimum reflector dimensions. Dimensions are selected with the entire operating range taken into consideration.

The experimental investigations have made it possible to provide recommendations dealing with the selection of reflector dimensions, and these dimensions are shown in figure XII.7.1 through XII.7.3.

#XII.9. Suspension of Two SGDRA Arrays on Both Sides of a Reflector

SGDPA arrays can be used for operating in two opposite directions. This requires suspending two curtains, one on either side of an untuned reflector. When two such curtains are suspended all the data concerning dipoles, distribution lines, and the reflector remain as they were for one curtain suspended on one side of the reflector. The exception is the size of a (the distance between adjacent conductors in the reflector). It is desirable to reduce it somewhat in order to loosen the coupling between the antennas.

However, if a concentration of reflector conductors is such that the voltage across the supply feeder for the parasitic array is not in excess of 10% of the voltage across the supply feeder for the driven antenna and if this is considered to be adequate, then, as the research has shown, the above indicated value a($0.035\ \lambda_0$) is entirely acceptable.

The radiation patterns in the horizontal plane shown in #XII.6 were computed on the assumption that $a = 0.035\ \lambda_0$.

#XII.10. SGD Antenna Curtain Suspension

What was said above with respect to the supports and stays for the SG antenna applies equally well to the SGD antenna. If the guys and stays are sectioned, each section should be selected on the basis of the shortest wavelength in the range in which the antenna will be used. Figure XII.10.1 is a sketch of an SGD 4/4 RA array suspended on metal masts. The guys are not shown in the figure.

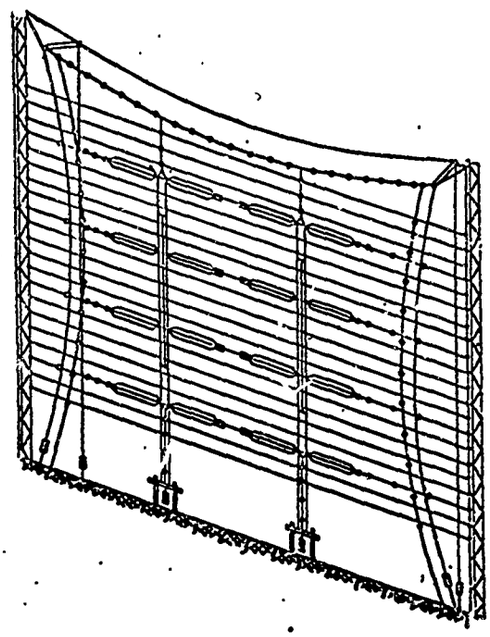

Figure XII.10.1. Sketch of an SGD 4/4 RA array (guys not shown).

It must be noted at this point that the design of the SGDRN, and particularly that of the SGDRA antenna, is not yet final.

#XII.11. SGDRA Arrays of Shunt-Fed Rigid Dipoles

The multiple-tuned shunt dipole, the feature of which is its widespread use over a wide frequency range, was described in Chapter IX. Expansion in the band can be established by making the best match with the feeder in the range of small values for the l/λ ratio (l is the length of a dipole arm). SGDRA arrays can be built using rigid multiple-tuned shunt dipoles, and it is thus possible to obtain a broader working range, within the limits of which a satisfactory match with the feeder is ensured. It is desirable to secure rigid multiple-tuned shunt dipoles directly to a metal support (fig. XII.11.1).

One possible variant in shunt dipole use is shown in Figure XII.11.2. The angle between the arms of the dipole and the shunt can be changed over broad limits, from 0° to 45°. The experimental data cited in what follows are for the case when this angle is equal to 33°.

Figure XII.11.3 is a sketch of an SGD 4/4 RA array made of rigid shunt dipoles.

Figure XII.11.4 is the experimental curve characterizing the match with the feeder for an SGD 4/4 RA antenna made in the manner described and taken

for a decimeter model. This curve was obtained for distribution and supply feeders made in accordance with the data shown in Figure XII.11.5.

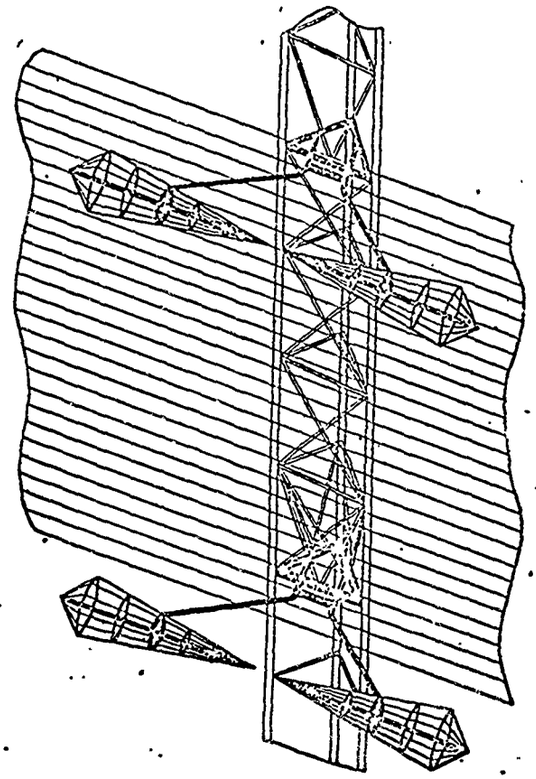

Figure XII.11.1. Securing shunt dipoles to a mast structure.

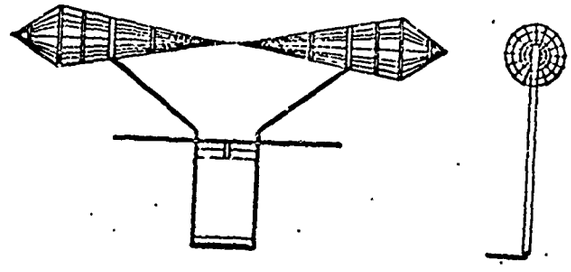

Figure XII.11.2. Variant in making a biconical shunt dipole.

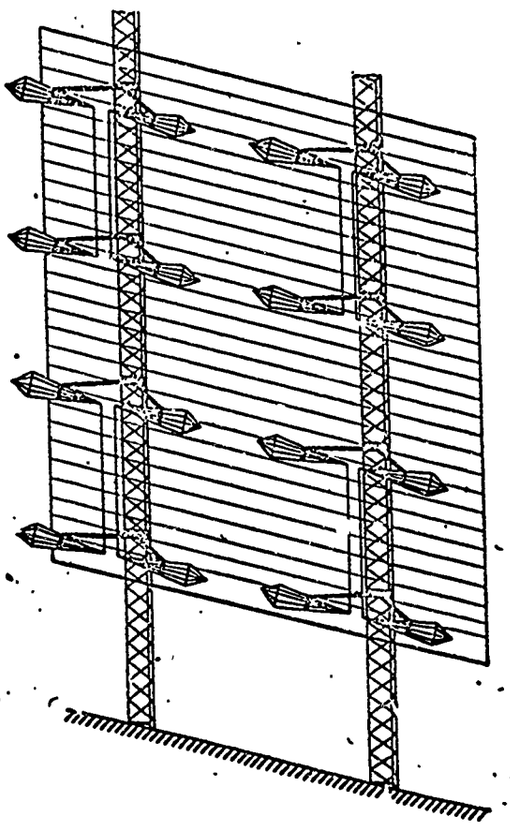

Figure XII.11.3. Sketch of an SGD 4/4 RA array using rigid shunt dipoles (guys not shown). Only primary distribution feeders are shown.

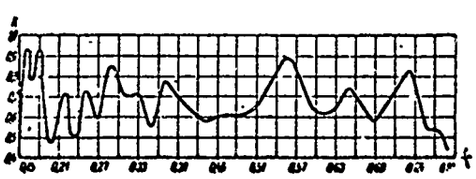

Figure XII.11.4. Experimental curve of the dependence of the traveling wave ratio on the supply feeder for an SGD 4/4 RA array of rigid dipoles on ℓ/λ.

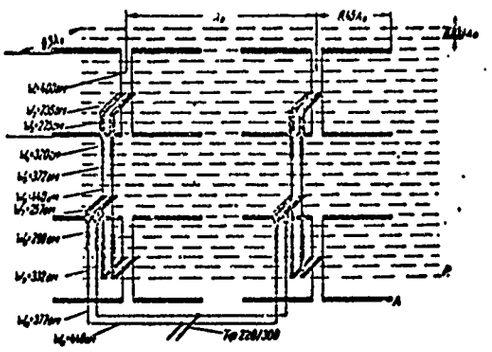

Figure XII.11.5. Schematic diagram of feed to an SGD 4/4 RA array of rigid dipoles.

#XII.12. Receiving Antennas

SGDRN arrays, and particularly the SGDRA array, can be used for reception. The actual length of an SGD receiving antenna can be calculated through formula (VI.8.5).

Receiving antennas can be made in the same way as transmitting antennas. The match between antenna and feeder, which for reception usually has a characteristic impedance of 208 ohms, can be improved by using an exponential or step feeder transformer. When the SGDRA array is used for reception it is desirable to reduce the a dimension (the distance between adjacent reflector conductors) in order to weaken the signals received from the back half-space. It is recommended that the a dimension be reduced to the magnitude 0.02 λ_0.

#XII.13. Broadside Receiving Antennas with Low Side-Lobe Levels

As is known, non-uniform distribution of current amplitudes in the antenna dipoles can result in a significant reduction in the side-lobe levels associated with broadside antennas. Side-lobe levels can be reduced if the amplitude of the currents is reduced from the central dipoles to the end dipoles. But this also bring with it some expansion in the major lobe and a reduction in the gain factor associated with that expansion. If the distribution law is properly selected the amplitudes of the current can be such that we can have a sharp reduction in the side-lobe levels for a comparatively small reduction in the gain factor.

Use of the Dolph-Chebyshev method to select the law of distribution of the currents flowing in broadside antennas will yield extremely effective results. This method makes it possible to select that amplitude distribution for a specified number of dipoles at which the side-lobe levels will not exceed the specified magnitude for the least expansion in the major lobe (for a detailed description of the Dolph-Chebyshev method see G. Z. Ayzenberg, Ultra-Short Wave Antennas. Svyaz'izdat, 1957, Chapter IX, p. 189).

Figure XII.13.1 is a schematic of an SGD $n_1/16$ (eight balanced dipoles in one stack; $n_2 = 8$) antenna . amplitudes distributed in accordance with the Dolph-Chebyshev method. The relationships between the amplitudes of the currents flowing in the dipoles are shown by the numbers in the figure. These relationships were taken from the above-indicated monograph (p. 197, Table I.IX) for an 8-element antenna and for a side-lobe level of 30 db.

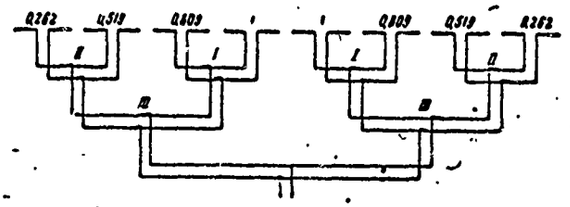

Figure XII.13.1. Schematic of the SGD $n_1/16$ R broadside array with current amplitude distributed in accordance with the Dolph-Chebyshev method. For reasons of simplicity only the dipoles in one stack have been shown. I, II, III - exponential or step transformers; coefficients of transformation characteristic impedances: I - $W_2/W_1 = 1.512$; II - $W_2/W_1 = 3.8$; III - $W_2/W_1 = 4.9$.

The radiation pattern of an antenna with a Dolph-Chebyshev current distribution can be charted through the formula

$$F(\varphi) = f_1(\varphi) f_2(\varphi) \cos(M \arccos x z_0), \qquad \text{(XII.13.1)}$$

if $|xz_0| < 1$, and through the formula

$$F(\varphi) = f_1(\varphi) f_2(\varphi) \operatorname{ch}(M \operatorname{arc\,ch} x z_0), \qquad \text{(XII.13.2)}$$

if $|xz_0| > 1$.

Here

$$x = \cos\left(\frac{\pi d}{2} \sin\varphi\right),$$

where

d is the distance between the centers of adjacent dipoles;

φ is the angle formed by the direction of the beam and the normal to the plane of the artenna,

$$z_0 = \operatorname{ch}\left(\frac{1}{M} \operatorname{arc\,ch} \frac{1}{\xi}\right), \qquad \text{(XII.13.3)}$$

ξ is the specified minimum ratio of field strength in the direction of the maximum for the major lobe to the field strength in the direction of the maximum for the side lobe;

M is the degree of the polynomial (in the case specified $M = n_2 - 1$);

$f_1(\varphi)$ is a factor which takes the directional properties of a balanced dipole into consideration [the first factor in formula (XII.4.2)];

$f_2(\varphi)$ is a factor which takes the effect of the reflector into consideration [the last factor in formula (XII.4.2)].

Figures XII.13.2 - XII.13.5 contain a series of radiation patterns charted for the case of the untuned reflector and using the formulas cited. Distance from the dipoles to the reflector was taken as equal to 0.7 l, where l is the length of one arm of the dipole.

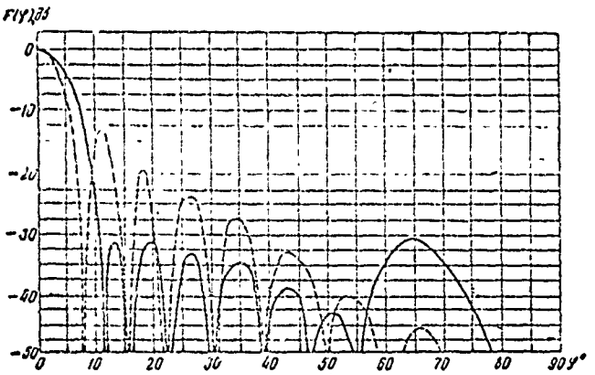

Figure XII.13.2. Radiation pattern of a broadside array consisting of 8 balanced dipoles in one stack. Current distribution among the antenna dipoles in accordance with the Dolph-Chebyshev method for $\lambda = 2l$ (l - length of a dipole arm). Distance from antenna curtain to reflector 0.7 l. Dotted lines show the radiation pattern for this same broadside array with uniform current distribution.

The relationship between the current amplitudes for these patterns is shown in Figure XII.13.1.

As will be seen, when current amplitudes are distributed according to the Dolph-Chebyshev method there will be a substantial reduction in the side-lobe level.

Current amplitudes can be Dolph-Chebyshev distributed by the corresponding selection of the characteristic impedances of the parallel distribution feeders. At the same time, we must bear in mind that the ratio of the amplitudes of currents flowing in the dipoles of parallel branches is inversely proportional to the square root of the characteristic impedances of the corresponding distribution feeders,

$$\frac{I_2}{I_1} = \sqrt{\frac{W_1}{W_2}}, \qquad \text{(XII.13.4)}$$

where

I_1 and I_2 are the currents flowing in the dipoles of two parallel branches with characteristic impedances W_1 and W_2.

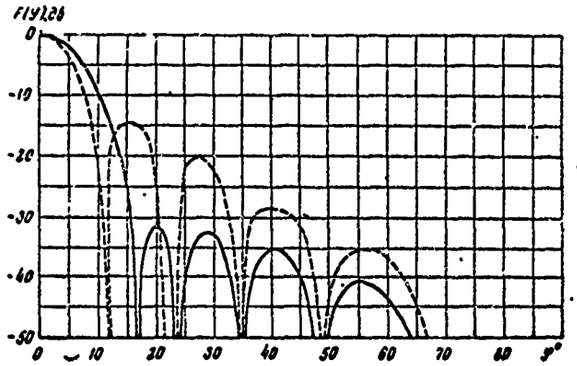

Figure XII.13.3. Radiation pattern of a broadside array consisting of 8 balanced dipoles in one stack. Current distribution among the antenna dipoles in accordance with the Dolph-Chebyshev method for $\lambda = 3l$ (l - length of a dipole arm). Distance from antenna curtain to reflector 0.7 l. Dotted lines show the radiation pattern for this same broadside array with uniform current distribution.

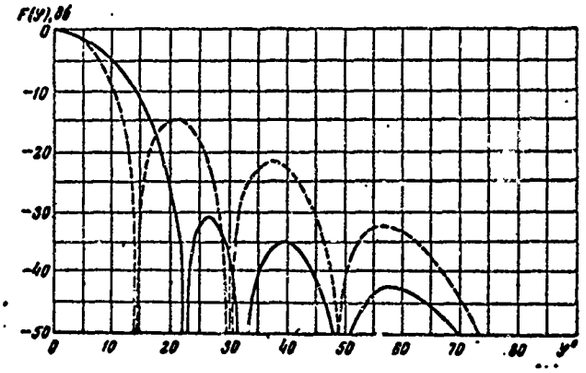

Figure XII.13.4. Radiation pattern of a broadside array consisting of 8 balanced dipoles in one stack. Current distribution among the antenna dipoles in accordance with the Dolph-Chebyshev method for $\lambda = 4l$ (l - length of a dipole arm). Distance from antenna curtain to reflector 0.7 l. Dotted lines show the radiation pattern for this same broadside array with uniform current distribution.

The proportion at (XII.13.4) is valid if the arguments for total impedances of parallel branches are identical. The necessary selection of characteristic impedances can be made using exponential or step transformation feeders.

Bear in mind that the actual relationship between dipole current amplitudes can be considerably disturbed by the mutual effect of the dipoles themselves, as well as by inaccuracies in making the dipoles and the distribution feeders. The latter results in non-identity of the arguments for the impedance of individual sections and branches of the antenna. This set of circumstances can cause the side-lobe level to increase.

Side-lobe level can also be increased by the antenna effect of distribution and supply feeders. Obviously, local terrain and construction of installations on the antenna field too have a considerable effect on side-lobe level.

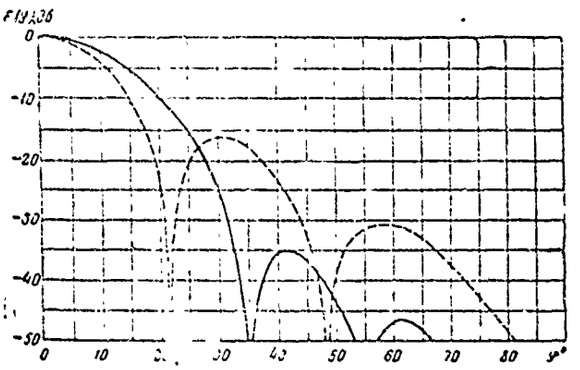

Figure XII.13.5. Radiation pattern of a broadside array consisting of 8 balanced dipoles in one stack. Current distribution among the a dipoles in accordance with the Dolph-Chebyshev method for $\lambda = 6l$ (l - length of a dipole arm). Distance from antenna curtain to reflector 0.7 l. Dotted lines show the radiation pattern for this same broadside array with uniform current distribution.

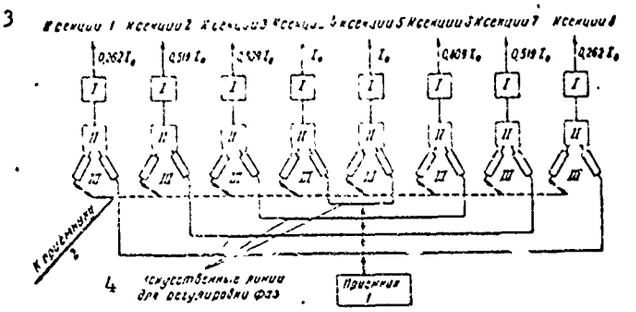

Figure XII.13.6. Schematic diagram of how a broadside array consisting of 8 sections with current distribution in accordance with the Dolph-Chebyshev method is connected to the receiver.

1 - receiver; 2 - to receiver; 3 - to sections as noted; 4 - artificial lines for phase adjustment; I - amplifier; II - attenuator; III - decoupling resistance.

We do not, at this time, have enough experience in building and using short-wave broadside antennas with low side-lobe levels. We can, however, emphasize the fact that antennas made in the manner described will have a much lower side-lobe level if they are provided with sufficiently dense untuned reflectors, and their use will result in a substantial increase in the line noise stability.

Note too that we can regulate amplitude distribution by inserting pure resistance in the corresponding branches, thus absorbing part of the energy.

The capabilities provided by antennas using the Dolph-Chebyshev current distribution arrangement can be utilized to best advantage if a system of

amplifiers, attenuators, and phase-shifters is used. Figure XII.13.6 is the schematic arrangement of such an array consisting of eight sections.

We obtain the needed distribution of current amplitudes by making the corresponding adjustments to the attenuators. The radiation patterns can be controlled by the phase-shifter system.

It is possible to use the same antenna with a number of receivers, and at the same time have each receiver set up for a specified, or adjusted direction of maximum reception. Figure XII.13.6 shows the case of parallel operation of two receivers.

It goes without saying that the arrangement described here can also be used when the number of dipoles in one stack is different from eight.

Chapter XIII

THE RHOMBIC ANTENNA

#XIII.1. Description and Conventional Designations

The rhombic antenna is in the form of a rhombus, or diamond, suspended horizontally on four supports (fig. XIII.1.1).

An emf is supplied to one of the acute angles of the rhombus, and pure resistance, equal to the characteristic impedance of the rhombus, is connected to the other acute angle. Maximum radiation is in the vertical plane passing through the apexes of the acute angles of the rhombus.

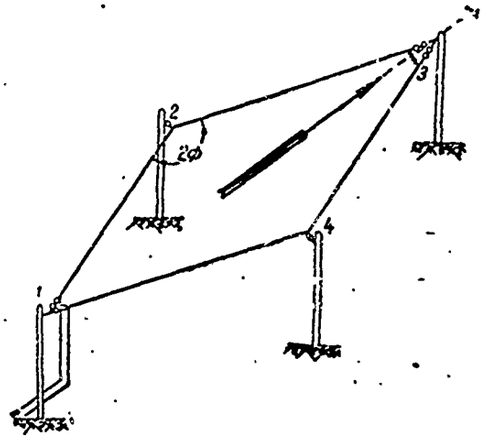

Figure XIII.1.1. Schematic diagram of a rhombic antenna.

The rhombic antenna is a multiple-tuned antenna, that is, it is included in the group of antennas suited to the task of operating over a wide frequency range.

The horizontal rhombic antenna carries the letter designation RG, to which is added the numerical expression φ/a b, the purpose of which is to designate the length of side, magnitude of the obtuse angle, and the height at which the rhombus is suspended. Here φ = 1/2 the obtuse angle of the rhombus in degrees,

$$a = \frac{l}{\lambda_0},$$

$$b = \frac{H}{\lambda_0},$$

l and H are length of side and height at which the rhombus is suspended, respectively;

λ_0 is the optimum wavelength for the rhombic antenna (the wavelength on which the antenna has optimum electrical parameters).

By way of an example, the horizontal rhombic antenna for which φ = 65°, $l = 4\lambda_0$, $H = \lambda_0$ is designated RG 65/4 1.

#XIII.2. Operating Principles

The following two requirements are imposed on the multiple-tuned antenna:

(1) constancy of input impedance over a wide frequency range and equality of that input impedance with the characteristic impedance of the transmission line;

(2) retention of satisfactory directional properties over the entire operating range.

The first requirement can only be satisfied if the antenna is made up of elements, the input impedances of which will remain constant within the limits of the entire operating range. Lines shorted by a resistor, the value of which is equal to their characteristic impedance, and the current flow in which obeys the traveling wave law, have these properties.

Chapter V included a series of radiation patterns of a conductor on which the traveling wave mode had been established (figs. V.2.1 - V.2.4). These patterns show that when the conductor is a long one the direction of maximum radiation will change little with respect to the l/λ ratio.

From what has been said, it follows that the antenna can satisfy both requirements listed if it consists of long wires which pass a traveling wave and which are properly positioned and interconnected.

The rhombic antenna is a system consisting of four long wires comprising the sides of the rhombus. The traveling wave mode is obtained by the insertion of a resistor, the value of which is equal to that of the characteristic impedance, across one of the acute angles. The characteristic impedance of the rhombic antenna is equal to double the characteristic impedance of one wire (side) of the rhombus.

The positioning of the antenna wires to form the sides of the rhombus ensure coincidence of the directions of their maximum radiation. As a matter of fact, let it be necessary to amplify the field strength in some direction lying in the plane in which the rhombus is located.

The radiation pattern of the wire passing the traveling wave current can be expressed by formula (V.2.2)

$$F(\theta) = \frac{\sin\theta}{1-\cos\theta}\sin\left[\frac{\alpha l}{2}(1-\cos\theta)\right],$$

where

θ is the angle formed by the direction of the beam and the axis of the wire.

As will be seen from formula (V.2.2), when the l/λ ratio is large, maximum radiation of the wire occurs at an angle that can be established, approximately, through the relationship

$$\sin\left[\frac{\alpha l}{2}(1-\cos\theta_0)\right] = 1, \qquad \text{(XIII.2.1)}$$

from whence

$$\alpha l(1-\cos\theta_0)=\pi \qquad \text{(XIII.2.2)}$$

and

$$\cos\theta_0=\frac{2l-\lambda}{2l}. \qquad \text{(XIII.2.3)}$$

Maximum radiation of two wires forming an angle $2\theta_0$ occurs in the direction of the bisector of this angle. Two such wires are depicted in Figure XIII.2.1. The directional properties of each of the wires in the plane in which each is positioned can be characterized by the radiation patterns (only the major lobes in the pattern are shown in fig. XIII.2.1).

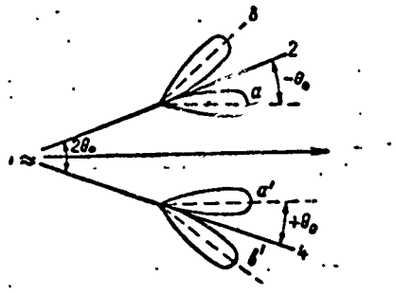

Figure XIII.2.1. Schematic diagram explaining the principle of operation of a V-antenna.

Lobe a of wire 1-2 and lobe a' of wire 1-4 are identical in shape and orientation. Let us find the relationship between the phases of the field strength vectors in the direction of the maximum beams of lobes a and a'. Let us take the clockwise direction as the positive direction for reading the angles, and let us designate the angle formed by the direction of the maximum beam of lobe a' with the axis of wire 1-4 as θ_0. Then the angle formed by the direction of the maximum beam of lobe a with the axis of wire 1-2 will equal $-\theta_0$. As follows from the formula (V.2.2), change in the sign of θ is accompanied by a change in the sign of E, that is $E(-\theta) = -E(\theta)$. Therefore, if wires 1-2 and 1-4 are fed in phase the vectors of the fields produced by them in the direction of the bisector of angle $2\theta_0$ will be opposite in phase. In the arrangement we are considering, the emf is connected between wires 1-2 and 1-4, so the current flow in them is opposite in phase, which is to say that the supply method itself is what creates a mutual phase shift of 180° in the currents flowing in wires 1-2 and 1-4. There is a corresponding mutual phase shift of 180° in the phases of vectors of the fields produced by these wires, and this shift is in the direction of the bisector. The total mutual phase shift in the vectors for the fields produced by wires 1-2 and 1-4 is 360°, equivalent to no phase shift having taken place.

The arrangement described is a V-antenna. The rhombic antenna (fig. XIII.2.2) consists of two V-antennas.

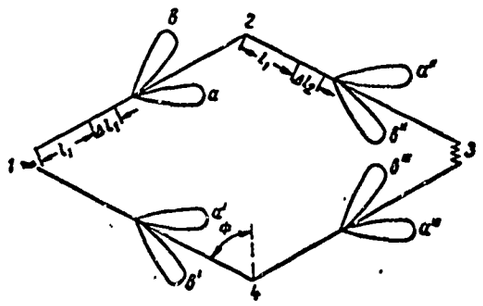

Figure XIII.2.2. Schematic diagram explaining the principle of operation of a rhombic antenna.

Let us find the relationship between the phases of the field strength vectors for the V-sections of the rhombus, 2-1-4 and 2-3-4.

Let us isolate the element Δl_1 in wire 1-2 at distance l_1 from point 1, and element Δl_2 in wire 2-3 at distance l_1 from point 2. The phase shift between the field strength vectors for elements Δl_1 and Δl_2 equals

$$\psi_{shift} = \psi_I + \psi_p + \psi_y, \qquad \text{(XIII.2.4)}$$

where

ψ_I is the phase angle, established by the shift in the phases of the currents flowing in elements Δl_1 and Δl_2;

ψ_p is the phase angle, established by the difference in the paths traveled by the beams radiated by elements Δl_1 and Δl_2;

ψ_y is the phase angle, established by the fact that the maximum beam of lobe a'' forms the angle $+\theta$, and the maximum beam of lobe a forms the angle $-\theta$, with the radiating wires, $\psi_y = \pi$.

The length of the current path from element Δl_1 to element Δl_2 equals l. Therefore

$$\psi_I = -\alpha l,$$
$$\psi_p = \alpha l \sin \Phi,$$

where

Φ is half the obtuse angle of the rhombus.

Substituting values for ψ_y, ψ_I and ψ_p in formula (XIII.2.4), and taking it that $\Phi = 90 - \theta_0$, we obtain

$$\psi_{shift} = -\alpha l + \alpha l \sin \Phi + \pi = \pi - \alpha l (1 - \sin \Phi) = \pi - \alpha l (1 - \cos \theta_0). \qquad \text{(XIII.2.5)}$$

As has already been explained, the relationship in (XIII.2.2) must be satisfied in order to obtain maximum radiation in the direction of the long diagonal of the rhombus.

Substituting (XIII.2.2) in (XIII.2.5), we obtain

$$\psi_{shift} = \pi - \pi = 0.$$

As we see, when the selection of the magnitudes of l and φ is proper, the phase shift between the field strength vectors for two symmetrically located elements of wires 1-2 and 2-3 equals zero.

It is obvious that the vector for the summed field strength for all of wire 1-2 will be in phase with the vector for the field strength for all of wire 2-3, and that the same will be true for wires 1-4 and 4-3. So all four sides of the rhombus produce in-phase fields in the direction of the long diagonal of the rhombus, and it is this latter which results in the increase in field strength in this direction.

All of the considerations cited with respect to the co-phasality of the fields produced by all four sides of a rhombic antenna can be equated to a single wave which will satisfy the relationship at (XIII.2.2). In practice, satisfactory field phase relationships can be obtained over an extremely wide frequency range. And satisfactory directional properties over a wide range should be retained as well. We note that this conclusion follows directly from the relationship at (XIII.2.3). As a matter of fact, we obtain

$$\theta_0 = \arccos\frac{2l-\lambda}{2l}. \qquad \text{(XIII.2.6)}$$

from (XIII.2.3).

Equation (XIII.2.6) demonstrates that if $l \gg \lambda$, the value of angle θ_0 needed to obtain the optimum antenna operation mode is only very slightly dependent on λ. From this we can also draw the opposite conclusion to the effect that if $l \gg \lambda$, and for a specified value of θ_0, antenna properties will change but slightly with λ.

The considerations cited here with respect to the possibility of phasing the fields produced by the sides of the rhombus refer to the case when the desirable direction of maximum radiation is in the plane in which the rhombus is located. In practice the requirement is to provide intensive radiation at some angle to the plane in which the rhombus is located. This does not, however, change the substance of the problem. We must simply understand that θ_0 is a solid angle formed by the required direction of maximum radiation and the sides of the rhombus.

#XIII.3. Directional Properties

It has been accepted that the directional properties of a horizontal rhombic antenna can be characterized by two radiation patterns, one for the normal (horizontal) component of the field strength vector, and one for the parallel component of the field strength vector.[1]

The normal component of the field strength vector is

$$E_{\perp} = \frac{30I_0}{r}\left[\frac{\cos(\Phi+\varphi)}{\sin(\Phi+\varphi)\cos\Delta + i\frac{\gamma}{\alpha}} + \frac{\cos(\Phi-\varphi)}{\sin(\Phi-\varphi)\cos\Delta + i\frac{\gamma}{\alpha}}\right]\left\{1-e^{[l\alpha\sin(\Phi+\varphi)\cos\Delta-\gamma l]}\right\}\times$$
$$\times\left\{1-e^{[l\alpha\sin(\Phi-\varphi)\cos\Delta-\gamma l]}\right\}\left[1+|R_{\perp}|e^{i(\Phi_{\perp}-2\alpha l/\sin\Delta)}\right]. \qquad \text{(XIII.3.1)}$$

The parallel component of the field strength vector is

$$E_{\parallel} = \frac{30I_0}{r}\sin\Delta\left[\frac{\sin(\Phi+\varphi)}{\sin(\Phi+\varphi)\cos\Delta + i\frac{\gamma}{\alpha}} - \frac{\sin(\Phi-\varphi)}{\sin(\Phi-\varphi)\cos\Delta + i\frac{\gamma}{\alpha}}\right]\left\{1-e^{[l\alpha\sin(\Phi+\varphi)\cos\Delta-\gamma l]}\right\}\times$$
$$\times\left\{1-e^{[l\alpha\sin(\Phi-\varphi)\cos\Delta-\gamma l]}\right\}\left[1-|R_{\parallel}|e^{i(\Phi_{\parallel}-2\alpha l/\sin\Delta)}\right], \qquad \text{(XIII.3.2)}$$

where

I_0 is the current at the point where the antenna is fed;

φ is the azimuth angle, read from the long diagonal of the rhombus (fig. XIII.3.1);

γ is the propagation factor; $\gamma = i\alpha + \beta$.

The modulus of the equivalent summed field strength vector equals[2]

$$E_{eq} = \sqrt{|E_{\perp}|^2 + |E_{\parallel}|^2}. \qquad \text{(XIII.3.3)}$$

Let us find the expressions for the radiation patterns in the vertical ($\varphi = 0$) and horizontal ($\Delta = 0$) planes.

As will be seen from formula (XIII.3.2), when $\Delta = 0$, or $\varphi = 0$,

$$E_{\parallel} = 0.$$

All that remains in these planes is the normal component of the field strength vector, and the directional properties can be characterized by formula (XIII.3.1).

Substituting $\Delta = 0$ in formula (XIII.3.1), ignoring attenuation ($\beta = 0$), dropping factors which do not depend on φ, and replacing the exponential

1. See Appendix 5.
2. See #V.5.

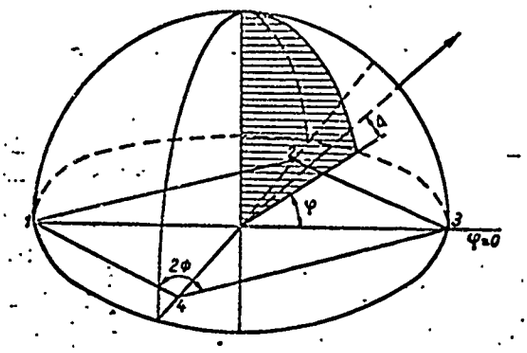

Figure XIII.3.1. Explanation of formulas (XIII.3.1) and (XIII.3.2).

functions with trigonometric functions, we obtain the following expression for the radiation pattern in the horizontal plane

$$F(\varphi)=\left[\frac{\cos(\Phi+\varphi)}{1-\sin(\Phi+\varphi)}+\frac{\cos(\Phi-\varphi)}{1-\sin(\Phi-\varphi)}\right]\times$$
$$\times\sin\left\{\frac{\alpha l}{2}\left[1-\sin(\Phi+\varphi)\right]\right\}\sin\left\{\frac{\alpha l}{2}\left[1-\sin(\Phi-\varphi)\right]\right\}. \qquad \text{(XIII.3.4)}$$

Similarly, by substituting $\varphi = 0$ in formula (XIII.3.1), we obtain the following expression for the radiation pattern in the vertical plane

$$F(\Delta)=\frac{E_1}{\frac{60\,I_0}{r}}=\frac{4\cos\Phi}{1-\sin\Phi\cos\Delta}\sin^2\left[\frac{\alpha l}{2}(1-\sin\Phi\cos\Delta)\right]\times$$
$$\times\sqrt{1+|R_\perp|^2+2|R_\perp|\cos(\Phi_\perp-2\alpha H\sin\Delta)}. \qquad \text{(XIII.3.5)}$$

In the case of ground with perfect conductivity $|R_\perp|=1$, and $\Phi_\perp=180°$, and the expression for the radiation pattern in the vertical plane becomes

$$F(\Delta)=\frac{8\cos\Phi}{1-\sin\Phi\cos\Delta}\sin^2\left[\frac{\alpha l}{2}(1-\sin\Phi\cos\Delta)\right]\sin(\alpha H\sin\Delta). \qquad \text{(XIII.3.6)}$$

#XIII.4. Attenuation Factor and Radiation Resistance

The attenuation factor, that is, the effective component of the magnitude of γ can be approximated through the formula (see #I.3)

$$\beta=\frac{R_1}{2W_r} \qquad \text{(XIII.4.1)}$$

where

W_r is the characteristic impedance of the rhombic antenna;

R_1 is the real resistance per unit length of the rhombus, assumed identical over the entire length of the antenna.

Known approximate formulas for calculating the characteristic impedances of conductors can be used to find W_r. If the sides of the rhombus are made of single wires the characteristic impedance will be about 1000 ohms, but if

each side of the rhombus consists of two divergent conductors the characteristic impedance will be about 700 ohms.

Distributed real resistance can be calculated through the formula

$$R_1 = \frac{R_r + R_{loss}}{2l} \qquad \text{(XIII.4.2)}$$

where

R_r is the resistive component of the radiation resistance of a rhombic antenna;

R_{loss} is the resistance of the losses in a rhombic antenna.

Since conductor losses at normal suspension heights for the rhombus are small, even when the effect of the ground is considered, these losses can be ignored in the computations and

$$R_1 = \frac{R_r}{2l} \qquad \text{(XIII.4.3)}$$

Calculations reveal that own radiation resistance of the sides of the rhombus is much higher than the radiation resistance induced by adjacent sides and by the mirror image. Therefore, the engineering calculations can be made on the assumption that

$$R_r \approx 4R_\Sigma, \qquad \text{(XIII.4.4)}$$

where

R_Σ is own radiation resistance of one side of a rhombic antenna.

The radiation resistance of a single conductor passing the traveling wave of current equals

$$R_c = 60\left(\ln 2\alpha l - \operatorname{ci} 2\alpha l + \frac{\sin 2\alpha l}{2\alpha l} - 0{,}423\right). \qquad \text{(XIII.4.5)}$$

Substituting the expression for R_1 from formula (XIII.4.3) in formula (XIII.4.1), and the expression for R_r from (XIII.4.4) in (XIII.4.1), we obtain

$$\beta = \frac{R_\Sigma}{lW_r}. \qquad \text{(XIII.4.6)}$$

#XIII.5. Gain Factor and Directive Gain

In accordance with the definition for gain factor, its value for the rhombic antenna can be calculated through the formula

$$s = \frac{E_r^2/P_r}{E_{\lambda/2}^2/P_{\lambda/2}} \qquad \text{(XIII.5.1)}$$

where

E_r is the strength of the field produced by the rhombic antenna;

$E_{\lambda/2}$ is the strength of the field produced by a half-wave dipole in the direction of maximum radiation;

P_r is the power applied to the rhombic antenna;

$P_{\lambda/2}$ is the power applied to the half-wave dipole.

The magnitudes included in formula (XIII.5.1) can be expressed in the following manner:

$$E_{\lambda/2} = \frac{60 I_0}{r}, \qquad \text{(XIII.5.2)}$$

$$P_r = I_0^2 W_r, \qquad \text{(XIII.5.3)}$$

$$P_{\lambda/2} = I_0^2 \cdot 73.1. \qquad \text{(XIII.5.4)}$$

Let us derive the expression for ε applicable to the vertical plane passing through the long diagonal of the rhombus ($\varphi = 0$). To do so, we will substitute the expression for E_r from formula (XIII.3.1) in formula (XIII.5.1), assuming while so doing that $\varphi = 0$. The ground will be taken as ideal conductor ($|R_\perp| = 1$, $\Phi_\perp = 180°$).

Moreover, let us replace the factor

$$1 - e^{(i\alpha l \sin\Phi\cos\Delta - \gamma)l}$$

by the approximate expression

$$e^{-\frac{\gamma l}{2}}\left[1 - e^{i\alpha\,(\sin\Phi\cos\Delta - 1)}\right],$$

which yields sufficiently accurate results in the range of the maximum value for the factor specified.

Making all the substitutions indicated, we obtain

$$\varepsilon = \frac{4680}{W_r} \cdot \frac{\cos^2\Phi\, e^{-2\gamma l}}{(1 - \sin\Phi\cos\Delta)^2} \times$$

$$\times \sin^4\left[\frac{\alpha l}{2}(1 - \sin\Phi\cos\Delta)\right] \sin^2(\alpha H \sin\Delta). \qquad \text{(XIII.5.5)}$$

Directive gain can be computed through the formula

$$D = \frac{1.64\varepsilon}{\eta}, \qquad \text{(XIII.5.6)}$$

where

η is the antenna efficiency.

#XIII.6. Efficiency

Efficiency equals

$$\eta = \frac{P_\Sigma}{P_r} = \frac{P_r - P_{term}}{P_r} \qquad \text{(XIII.6.1)}$$

where

P_Σ is the power radiated by the antenna;

P_r is the power applied to the antenna;

P_{term} is the power lost in the terminating resistor.

The magnitudes of P_r and P_{term} can be expressed in the following manner

$$P_r = I_0^2 W_r, \qquad \text{(XIII.6.2)}$$

$$P_{term} = I_0^2 e^{-4\beta l} W_r. \qquad \text{(XIII.6.3)}$$

Substituting these expressions in (XIII.6.1) we obtain

$$\eta = 1 - e^{-4\beta l}. \qquad \text{(XIII.6.4)}$$

Replacing β by its expression from formula (XIII.4.6), we obtain

$$\eta = 1 - e^{-R_r/W_r}. \qquad \text{(XIII.6.5)}$$

#XIII.7. Maximum Accommodated Power

The maximum amplitude of the voltage across the conductors of a rhombic antenna can be calculated through the formula

$$U_{max} = \sqrt{\frac{2P_r W_r}{k}} \qquad \text{(XIII.7.1)}$$

where

P_r is the input;

k is the traveling wave ratio on the conductors of the rhombus; k is usually at least 0.5 to 0.7.

With an input equal to 1 kw, and a characteristic impedance of W_r = 700 ohms, as is the case when the sides of the rhombus are made of two conductors, the maximum amplitude of the voltage equals

$$U_{max} = \sqrt{2000 \cdot 700/0.5} = 1660 \text{ volts} = 1.6 \text{ kv}.$$

Maximum field strength produced by the conductors of a single rhombic antenna equals (see formula I.13.9)

$$E_{max} = 120\, U_{max}/ndW_r \qquad \text{(XIII.7.2)}$$

where

d is the diameter of the conductors in the rhombus.

If, as is usually the case, the sides of the rhombic antenna are made up of two parallel conductors, n = 2, and W_r = 700 ohms. If the diameter of the conductors used equals 0.4 cm, and if the power is equal to 1 kw, E_{max} is about equal to 354 volts/cm.

Considering the maximum permissible field strength as equal to 7000 volts/cm, the maximum input to the rhombic antenna equals

$$P_{max} = (7000/354)^2 \approx 400 \text{ kw.}$$

The maximum voltage produced in a double rhombic antenna (see below) is approximately $\sqrt{2}$ less. The corresponding input is approximately double, and is equal to 800 kw.

The maximum input to the single rhombic antenna used in telephone work is about 200 kw, and the maximum input to the double rhombic antenna is about 400 kw (see Chapter VIII). In practice, the sides of the rhombus should be made of 0.6 cm diameter conductors in order to absolutely guarantee continuity of operation for power on the order of 400 kw in the telephone mode. It is also desirable to make the sides of the rhombus of three conductors.

#XIII.8. Selection of the Dimensions for the Rhombic Antenna. Results of Calculations for the Radiation Patterns and Parameters of the Rhombic Antenna.

The dimensions of the rhombic antenna are selected such that the strongest beams possible will be available at the reception site. Let us designate the angle of tilt of the beams reaching the reception site by Δ_0. We will use formula (XIII.3.6) to determine the optimum values of φ, l, and H.

The optimum value of angle φ can be established from the condition of a maximum for the factor

$$B = \frac{\cos\Phi}{1 - \sin\Phi\cos\Delta_0}, \qquad \text{(XIII.8.1)}$$

which is established from the equality

$$\frac{dB}{d\Phi} = 0, \qquad \text{(XIII.8.2)}$$

from which we obtain

$$\sin\varphi = \cos\Delta_0$$

and from whence

$$\varphi = 90 - \Delta_0. \qquad \text{(XIII.8.3)}$$

The optimum value for the length of side of the rhombus can be established from the condition of a maximum for the factor

$$\sin\left[\frac{\alpha l}{2}(1-\sin\Phi\cos\Delta_0)\right],$$

which reduces to solving the equation

$$\frac{l}{\lambda_0}(1-\sin\Phi\cos\Delta_0)=\frac{1}{2}.$$

Solving this equation with respect to l, we obtain

$$l=\frac{\lambda_0}{2(1-\sin\Phi\cos\Delta_0)}, \qquad \text{(XIII.8.4)}$$

where

λ_0 is the optimum wavelength, that is, the wavelength for which the dimensions of the antenna have been selected.

The optimum height at which to suspend the antenna can be established from the condition of the maximum for the factor

$$\sin(\alpha H\sin\Delta_0),$$

which reduces to solving the equation

and from whence

$$\alpha H\sin\Delta_0=\frac{\pi}{2}$$

$$H=\frac{\lambda_0}{4\sin\Delta_0}. \qquad \text{(XIII.8.5)}$$

Selection of the magnitude of Δ_0 can be made by proceeding from the characteristics of the main line (see Chapter VII). When the main line is longer than 1500 to 2000 km, Δ_0 is taken equal to 8 to 15°. If $\Delta_0 = 15°$, from equations (XIII.8.3), (XIII.8.4) and (XIII.8.5) we obtain $\Phi = 75°$, $l = 7.4\ \lambda_0$, $H = \lambda_0$.

In practice, the optimum values indicated for the magnitudes of Φ, l, and H are usually not held to in making rhombic antennas. Antennas with lengths of side equal to $7.4\ \lambda_0$ are extremely cumbersome, expensive, and require an extremely large area on which to locate them. On the other hand, the calculations show that a reduction in the length of side (l) by a factor of 1.5 to 2 as compared with its optimum value causes only a small reduction in the gain factor. Consequently, $l = 4\lambda_0$ is often selected in practice. The magnitude of Φ can be changed accordingly in order to satisfy the relationship at (XIII.8.4). Substituting $l = 4\lambda_0$ in formula (XIII.8.4) we obtain $\sin\Phi = 0.906$ and $\Phi = 65°$. Thus, the real dimensions of rhombic antennas, selected for the condition that $\Delta_0 = 15°$, are

$$\left.\begin{aligned}\Phi&=65°\\ l&=4\lambda_0\\ H&=\lambda_0\end{aligned}\right\}. \qquad \text{(XIII.8.6)}$$

If we take $\Delta_0 = 12°$ the maximum dimensions of the rhombic antenna will be equal to

$$\Phi = 78°;\ l = 11.5\lambda_0;\ \text{and } H = 1.25\ \lambda_0.$$

If the length is limited to $l = 6\ \lambda_0$, the following antenna data will be obtained

$$\left.\begin{aligned} \Phi &= 70° \\ l &= 6\lambda_0 \\ H &= 1{,}25\lambda_0 \end{aligned}\right\}. \qquad \text{(XIII.8.7)}$$

Antennas with dimensions selected in accordance with (XIII.8.6) and (XIII.8.7) are the ones most widely used.

Recommended as well for long lines (over 5000 to 7000 km) is the use of an antenna with the following dimensions

$$\left.\begin{aligned} \Phi &= 75° \\ l &= 6\lambda_0 \\ H &= 1{,}25\lambda_0 \end{aligned}\right\}. \qquad \text{(XIII.8.8)}$$

This methodology for selecting rhombic antenna dimensions will give the dependence of l, H and Φ on the optimum wavelength. In practice rhombic antennas are used over a wide frequency range, so the optimum wavelength should be selected such that satisfactory antenna parameters over the entire range of use anticipated will be provided for.

On main communication lines shorter than 1500 to 2000 km the most probable angles of tilt for beams reaching the reception site are greater than 15° (see Chapter VII). For example, if the length of the main line equals 900 km, as we see from Figure VII.2.1, the most probable angle of tilt of the beam is on the order of 30°.

In this case, if we substitute $\Delta_0 = 30°$ in formulas (XIII.8.3), (XIII.8.4) and (XIII.8.5), we obtain the following optimum dimensions for the antenna

$$\Phi = 60°;\ l = 2\lambda_0;\ \text{and } H = 0.5\ \lambda_0. \qquad \text{(XIII.8.9)}$$

In practice, because of the need to type antennas it is not convenient to select optimum dimensions for every line length, so we must use a few standardized antenna variants.

Table XIII.8.1 lists one possible rhombic antenna standardization variant for main lines of different lengths. Data for antennas for main lines shorter than 1500 km were selected through formulas (XIII.8.3), (XIII.8.4) and (XIII.8.5) in accordance with the information contained in Chapter VII with respect to the most probable angles of tilt of beams at reception sites.

Figures XIII.8.1 through XIII.8.9 show the radiation patterns in the horizontal plane of an RG 65/4 1 antenna for a normal component of the E vector.

Figures XIII.8.10 through XIII.8.26 show a series of radiation patterns in the horizontal plane of an RG 65/4 1 antenna, charted for various angles of tilt of beam, Δ, for the normal component of the electric field strength vector. The radiation patterns for the parallel component of the field strength vector are charted in these same figures, and at the same scale.

Table XIII.8.1

Length of main line, km	δ_0	l/λ_0	H/λ_0	Antenna's conventional designations	Notes
3000 and longer	75°	6	1.25	RG 75/6 1.25 or RGD 75/6 1.25	Antennas RG 70/6 1.25 and RGD 70/6 1.25 are desirable in the frequency range from 10 to 27 meters (λ_0 = 15 to 18 meters).
	70°	6	1.25	RG 70/6 1.25 or RGD 70/6 1.25	
	65°	4	1	RG 65/4 and RGD 65/4 1	
2000 - 3000	65°	4	1	RG 65/4 1 or RGD 65/4 1	Antennas RG 75/6 1.25 and RGD 75/6 1.25 are desirable in the frequency range from 10 to 30 meters (λ_0 = 25 meters).
1000 - 2000	65°	2.8	0.6	RG 65/2.8 0.6 or RGD 65/2.8 0.6	
600 - 1000	57°	1.7	0.5	RG 57/1.7 0.5 or RGD 57/1.7 0.5	
400 - 600[1]	45°	1	0.35	RG 45/1 0.35 or RGD 45/1 0.35	

1. Antennas RG 45/1 0.35 and RGD 45/1 0.35 are only recommended for reception.

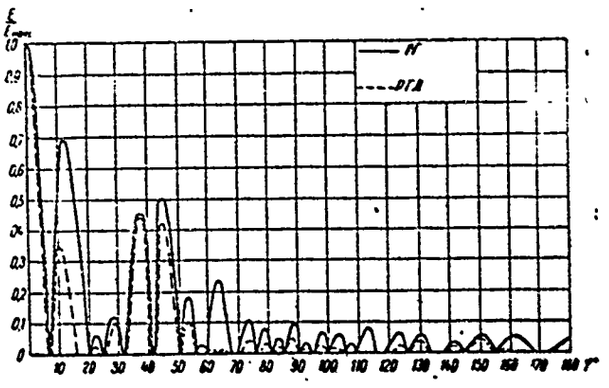

Figure XIII.8.1. Radiation patterns in the horizontal plane of RG 65/4 1 and RGD 65/4 1 antennas; $\lambda = 0.6\ \lambda_0$. —— RG; ---- RGD. Vertical: E/E_{max}.

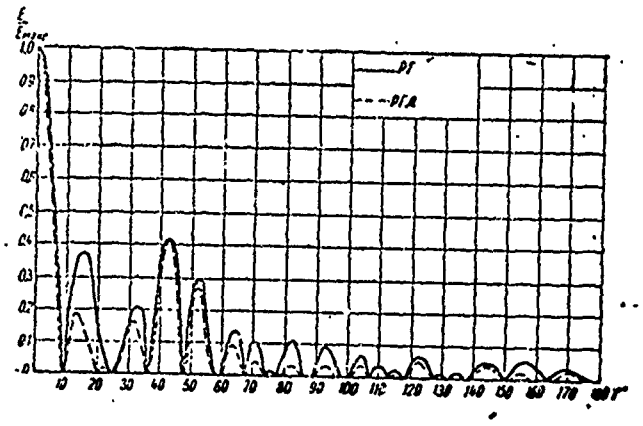

Figure XIII.8.2. Radiation patterns in the horizontal plane of RG 65/4 1 and RGD 65/4 1 antennas; $\lambda = 0.7\ \lambda_0$.

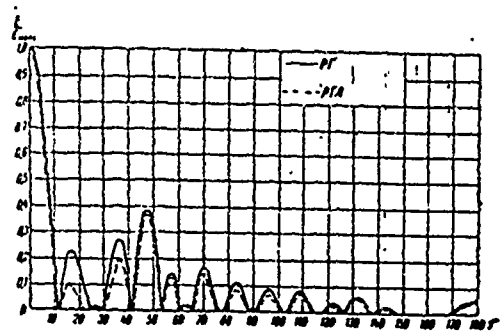

Figure XIII.8.3. Radiation patterns in the horizontal plane of RG 65/4 1 and RGD 65/4 1 antennas; $\lambda = 0.8\ \lambda_0$.

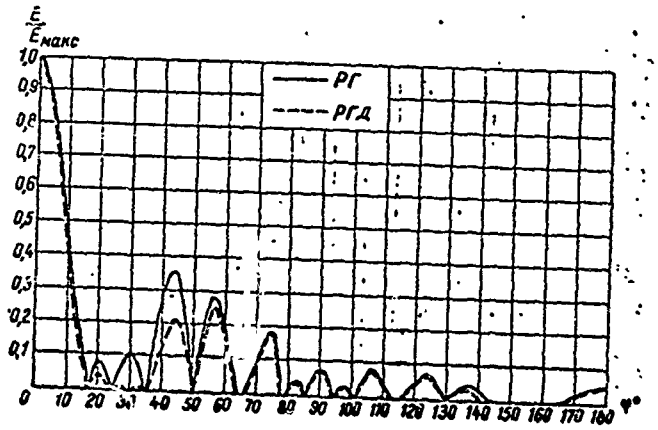

Figure XIII.8.4. Radiation patterns in the horizontal plane of RG 65/4 1 and RGD 65/4 1 antennas; $\lambda = 1.0\ \lambda_0$.

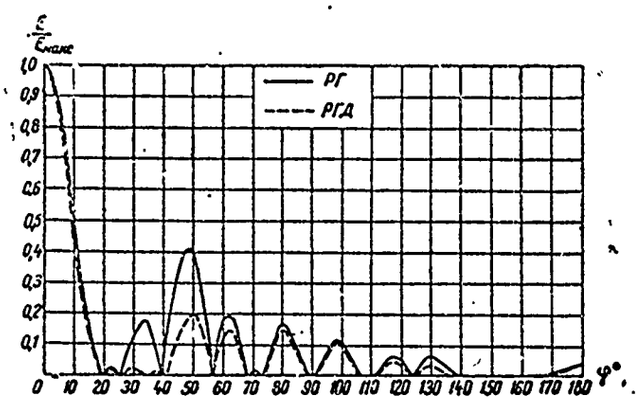

Figure XIII.8.5. Radiation patterns in the horizontal plane of RG 65/4 1 and RGD 65/4 1 antennas; $\lambda = 1.14\ \lambda_0$.

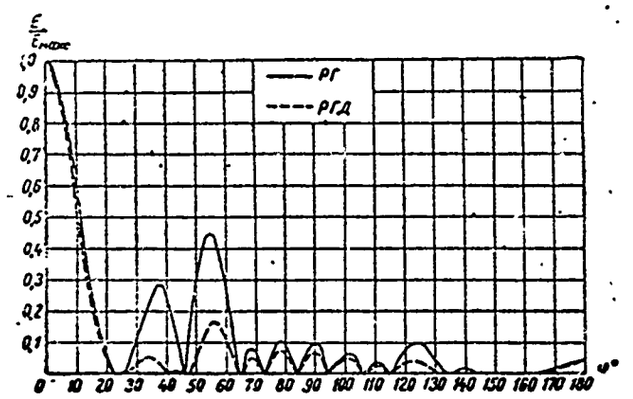

Figure XIII.8.6. Radiation patterns in the horizontal plane of RG 65/4 1 and RGD 65/4 1 antennas; $\lambda = 1.33\ \lambda_0$.

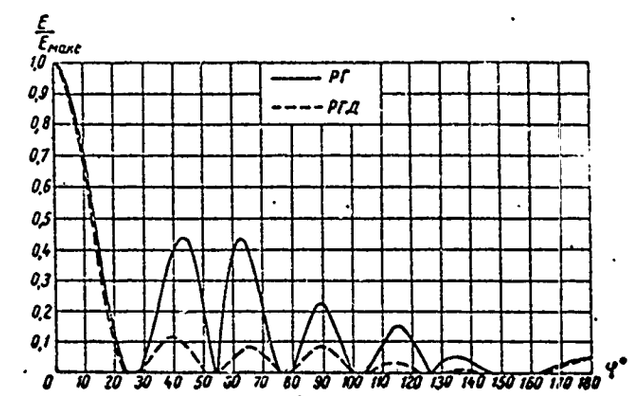

Figure XIII.8.7. Radiation patterns in the horizontal plane of RG 65/4 1 and RGD 65/4 1 antennas; $\lambda = 1.6\ \lambda_0$.

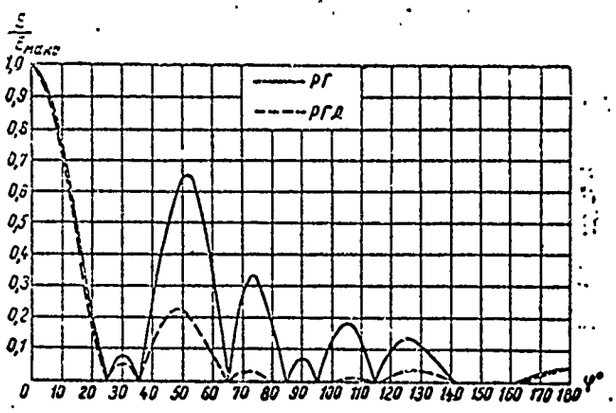

Figure XIII.8.8. Radiation patterns in the horizontal plane of RG 65/4 1 and RGD 65/4 1 antennas; $\lambda = 2\ \lambda_0$.

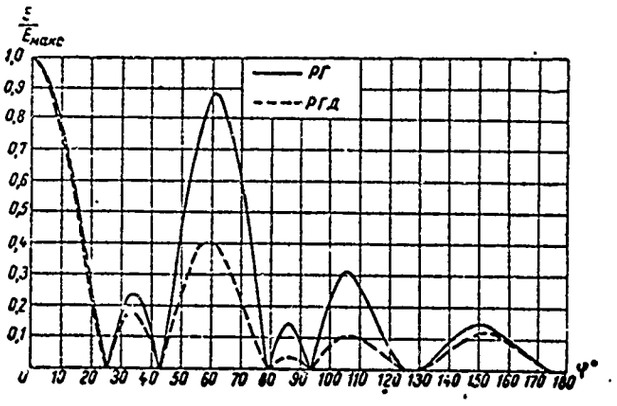

Figure XIII.8.9. Radiation patterns in the horizontal plane of RG 65/4 1 and RGD 65/4 1 antennas; $\lambda = 2.5\ \lambda_0$.

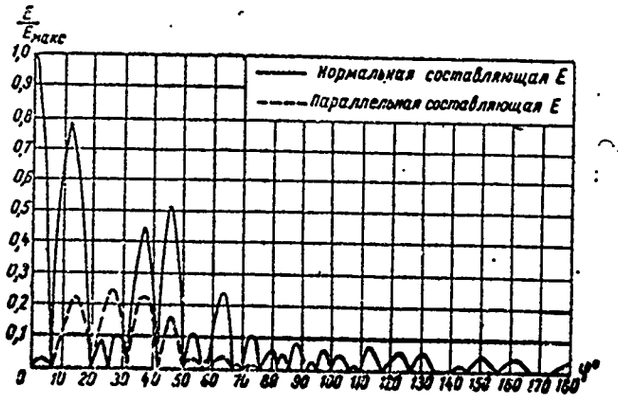

Figure XIII.8.10. Radiation patterns in the horizontal plane ($\Delta = 5°$) of an RG 65/4 1 antenna for a wavelength of $\lambda = 0.6\ \lambda_0$.

——— normal component of E; ---- parallel component of E; vertical: E/E_{max}.

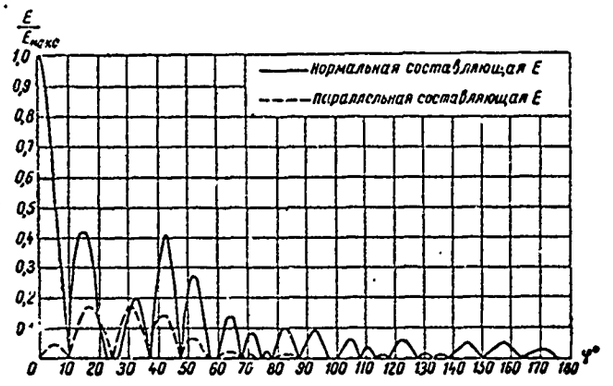

Figure XIII.8.11. Radiation patterns in the horizontal plane (Δ = 5°) of an RG 65/4 1 antenna for a wavelength of $\lambda = 0.7\ \lambda_0$.

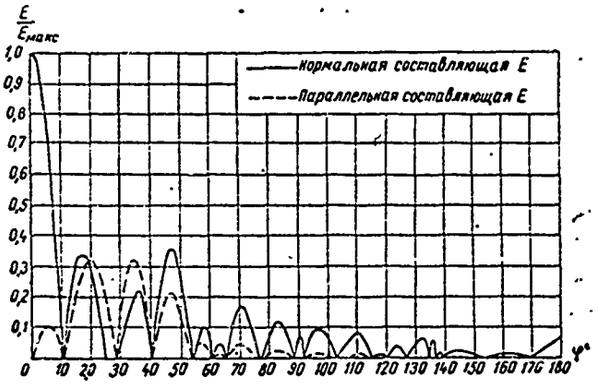

Figure XIII.8.12. Radiation patterns in the horizontal plane (Δ =19°) of an RG 65/4 1 antenna for a wavelength of $\lambda = 0.8\ \lambda_0$.

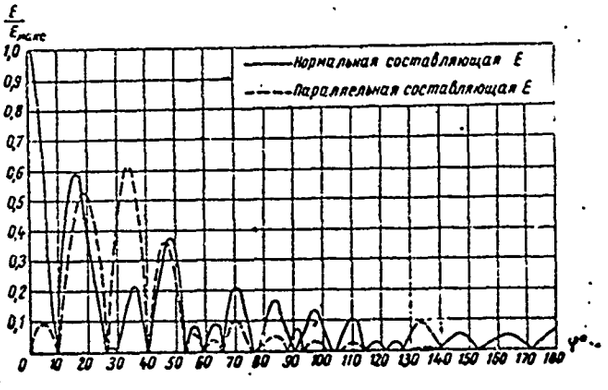

Figure XIII.8.13. Radiation patterns in the horizontal plane (Δ = 15°) of an RG 65/4 1 antenna for a wavelength of $\lambda = 0.8\ \lambda_0$.

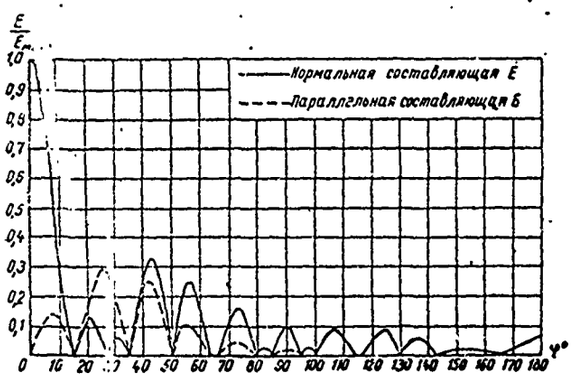

Figure XIII.8.14. Radiation patterns in the horizontal plane (Δ = 10°) of an RG 65/4 1 antenna for a wavelength of $\lambda = \lambda_0$.

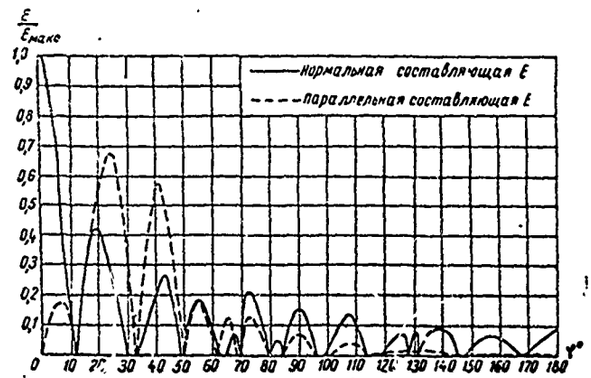

Figure XIII.8.15. Radiation patterns in the horizontal plane (Δ = 20°) of an RG 65/4 1 antenna for a wavelength of $\lambda = \lambda_0$.

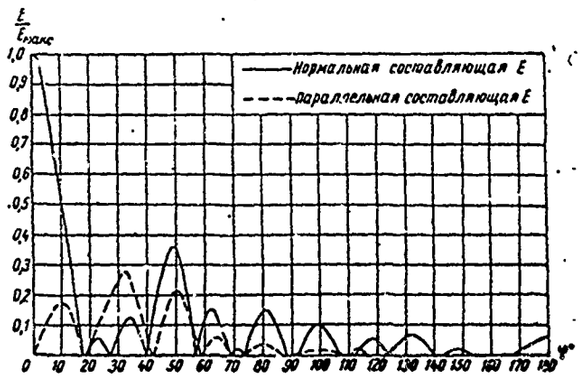

Figure XIII.8.16. Radiation patterns in the horizontal plane (Δ = 10°) of an RG 65/4 1 antenna for a wavelength of $\lambda = 1.14\ \lambda_0$.

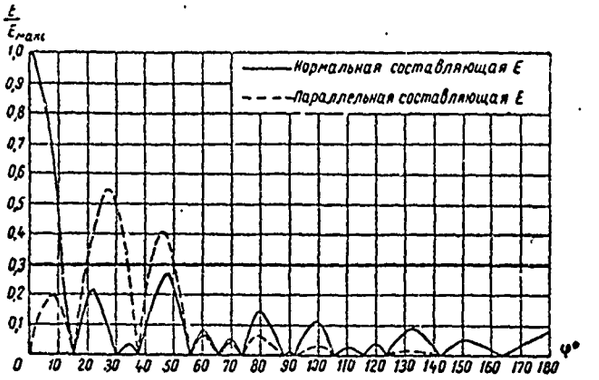

Figure XIII.8.17. Radiation patterns in the horizontal plane (Δ = 20°) of an RG 65/4 1 antenna for a wavelength of $\lambda = 1.14\ \lambda_0$.

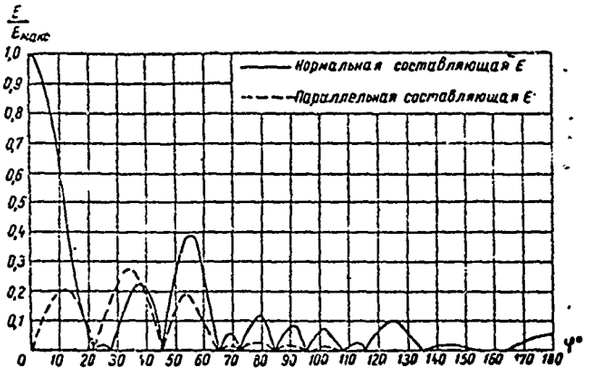

Figure XIII.8.18. Radiation patterns in the horizontal plane (Δ = 10°) of an RG 65/4 1 antenna for a wavelength of $\lambda = 1.33\ \lambda_0$.

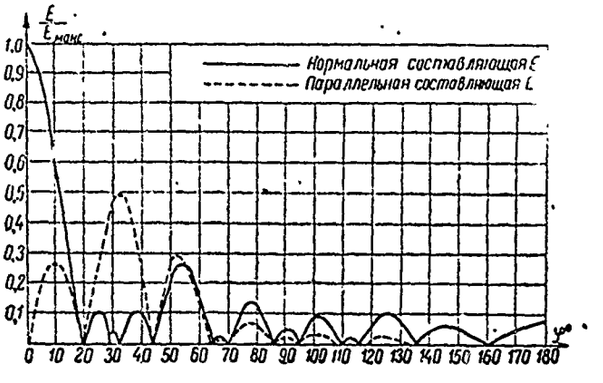

Figure XIII.8.19. Radiation patterns in the horizontal plane (Δ = 20°) of an RG 65/4 1 antenna for a wavelength of $\lambda = 1.33\ \lambda_0$.

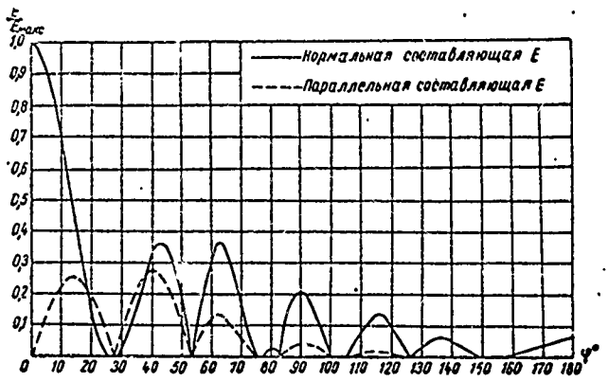

Figure XIII.8.20. Radiation patterns in the horizontal plane (Δ = 10°) of an RG 35/4 1 antenna for a wavelength of $\lambda = 1.6\ \lambda_0$.

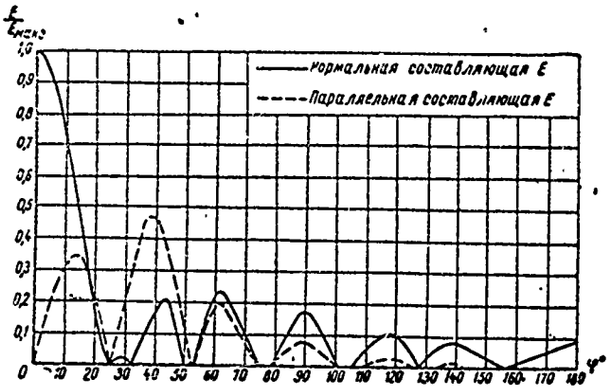

Figure XIII.8.21. Radiation patterns in the horizontal plane (Δ = 20°) of an RG 65/4 1 antenna for a wavelength of $\lambda = 1.6\ \lambda_0$.

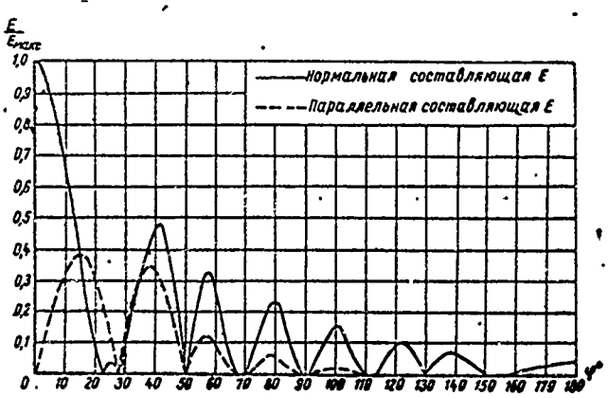

Figure XIII.8.22. Radiation patterns in the horizontal plane (Δ = 10°) of an RG 65/4 1 antenna for a wavelength of $\lambda = 2\ \lambda_0$.

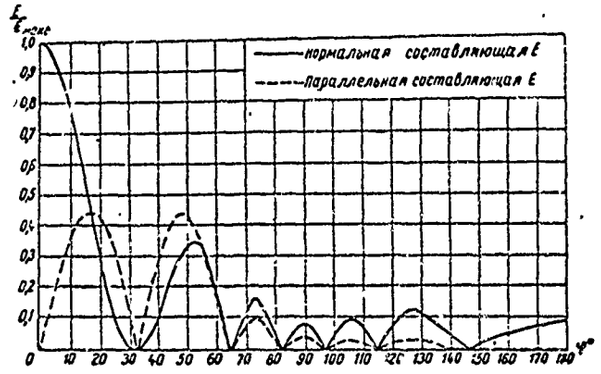

Figure XIII.8.23. Radiation patterns in the horizontal plane (Δ = 20°) of an RG 65/4 1 antenna for a wavelength of $\lambda = 2\ \lambda_0$.

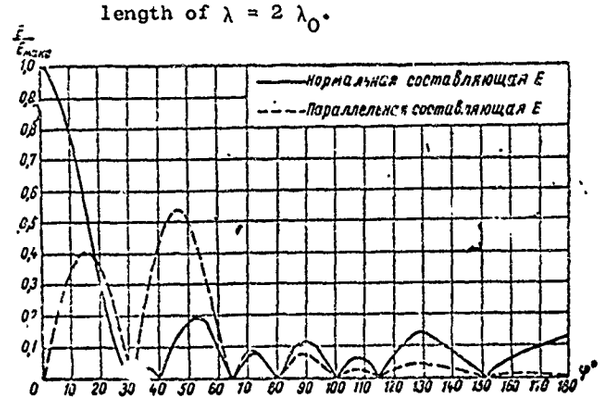

Figure XIII.8.24. Radiation patterns in the horizontal plane (Δ = 30°) of an RG 65/4 1 antenna for a wavelength of $\lambda = 2\ \lambda_0$.

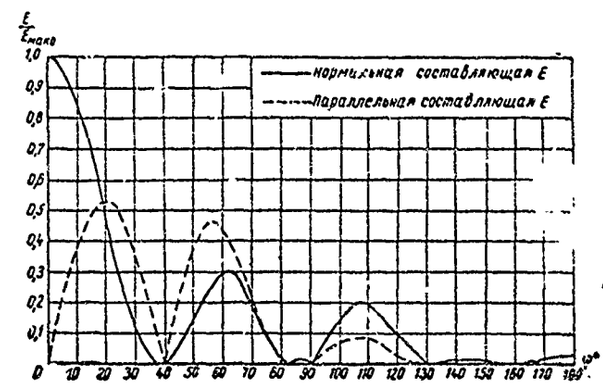

Figure XIII.8.25. Radiation patterns in the horizontal plane (Δ = 20°) of an RG 65/4 1 antenna for a wavelength of $\lambda = 2.5\ \lambda_0$.

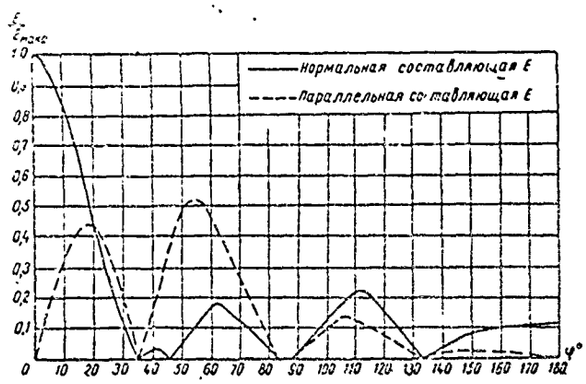

Figure XIII.8.26. Radiation patterns in the horizontal plane (Δ = 40°) of an RG 65/4 1 antenna for a wavelength of $\lambda = 2.5\ \lambda_0$.

The patterns for both field components were charted for ideally conducting ground.

As will be seen, the patterns are distinguished for the large number of side lobes, which is a characteristic feature of rhombic antennas, as well as of other antennas made using long wires, such as the V-antenna, for example.

Figures XIII.8.27 through XIII.8.35 show a series of radiation patterns in the vertical plane of an RG 65/4 1 antenna (major lobes).

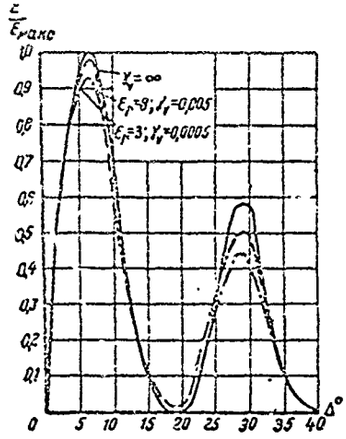

Figure XIII.8.27. Radiation patterns in the vertical plane of an RG 65/4 1 antenna for ground of ideal conductivity ($\gamma_v = \infty$), for ground of average conductivity ($\varepsilon_r = 8$; $\gamma_v = 0.005$), and ground of poor conductivity ($\varepsilon_r = 3$; $\gamma_v = 0.0005$); $\lambda = 0.6\ \lambda_0$.

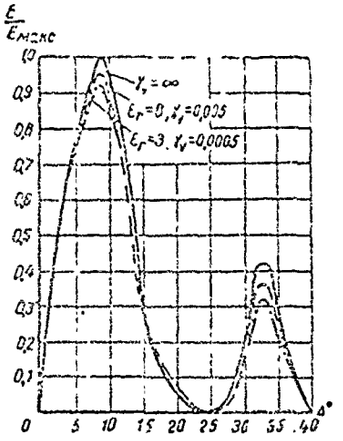

Figure XIII.8.28. Radiation patterns in the vertical plane of an RG 65/4 1 antenna for ground of ideal conductivity ($\gamma_v = \infty$), for ground of average conductivity ($\varepsilon_r = 8$; $\gamma_v = 0.005$), and ground of poor conductivity ($\varepsilon_r = 3$; $\gamma_v = 0.0005$); $\lambda = 0.7\ \lambda_0$.

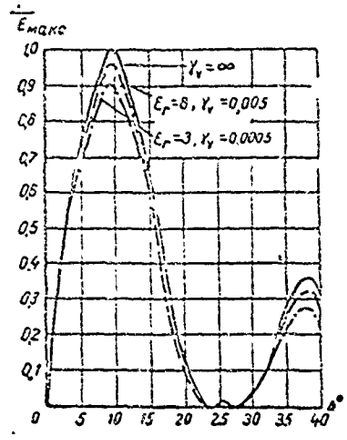

Figure XIII.8.29. Radiation patterns in the vertical plane of an RG 65/4 1 antenna for ground of ideal conductivity ($\gamma_v = \infty$), for ground of average conductivity ($\varepsilon_r = 8$; $\gamma_v = 0.005$), and ground of poor conductivity ($\varepsilon_r = 3$; $\gamma_v = 0.0005$); $\lambda = 0.8\ \lambda_0$.

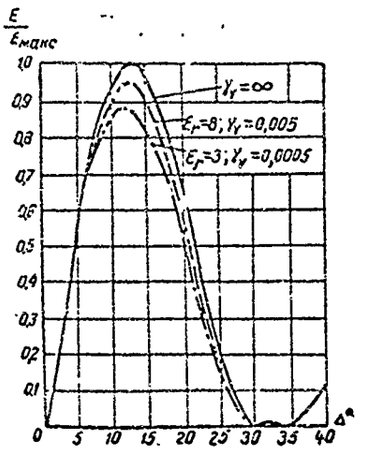

Figure XIII.8.30. Radiation patterns in the vertical plane of an RG 65/4 1 antenna for ground of ideal conductivity ($\gamma_v = \infty$), for ground of average conductivity ($\varepsilon_r = 8$; $\gamma_v = 0.005$), and ground of poor conductivity ($\varepsilon_r = 3$; $\gamma_v = 0.0005$); $\lambda = \lambda_0$.

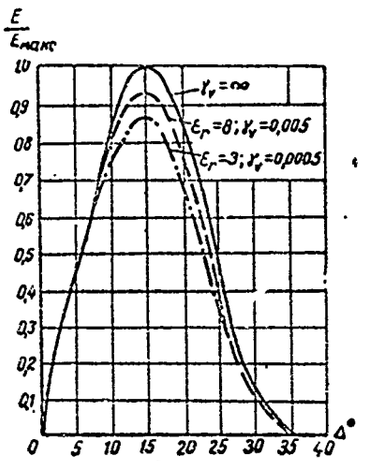

Figure XIII.8.31. Radiation patterns in the vertical plane of an RG 65/4 1 antenna for ground of ideal conductivity ($\gamma_v = \infty$), for ground of average conductivity ($\varepsilon_r = 8$; $\gamma_v = 0.005$), and ground of poor conductivity ($\varepsilon_r = 3$; $\gamma_v = 0.0005$); $\lambda = 1.14\ \lambda_0$.

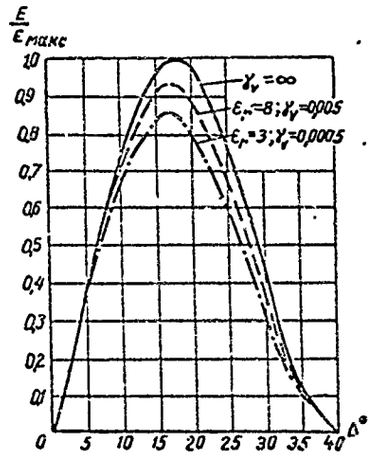

Figure XIII.8.32. Radiation patterns in the vertical plane of an RG 65/4 1 antenna for ground of ideal conductivity ($\gamma_v = \infty$), for ground of average conductivity ($\varepsilon_r = 8$; $\gamma_v = 0.005$), and ground of poor conductivity ($\varepsilon_r = 3$; $\gamma_v = 0.0005$); $\lambda = 1.33\ \lambda_0$.

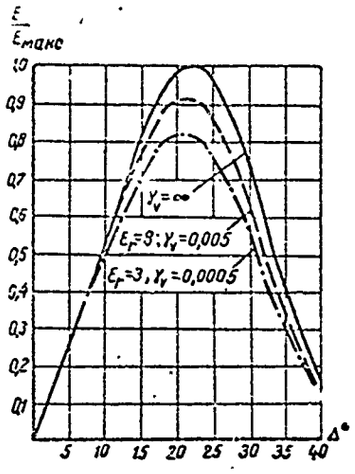

Figure XIII.8.33. Radiation patterns in the vertical plane of an RG 65/4 1 antenna for ground of ideal conductivity ($\gamma_v = \infty$), for ground of average conductivity ($\varepsilon_r = 8$; $\gamma_v = 0.005$), and ground of poor conductivity ($\varepsilon_r = 3$; $\gamma_v = 0.0005$); $\lambda = 1.6\ \lambda_0$.

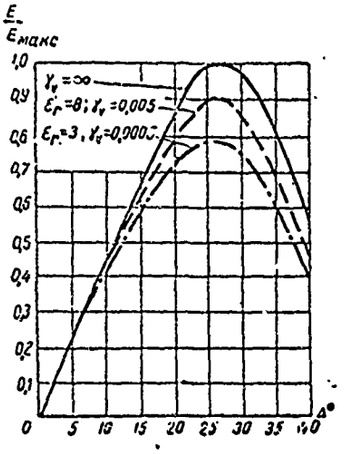

Figure XIII.8.34. Radiation patterns in the vertical plane of an RG 65/4 1 antenna for ground of ideal conductivity ($\gamma_v = \infty$), for ground of average conductivity ($\varepsilon_r = 8$; $\gamma_v = 0.005$), and ground of poor conductivity ($\varepsilon_r = 3$; $\gamma_v = 0.0005$); $\lambda = 2\ \lambda_0$.

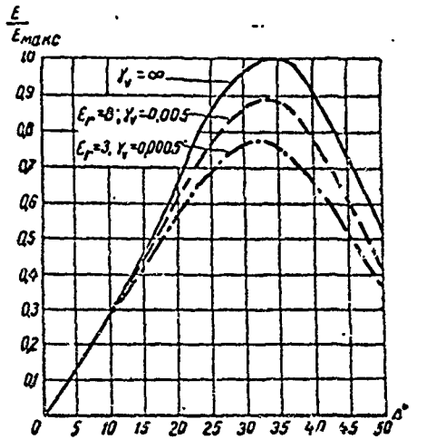

Figure XIII.8.35. Radiation patterns in the vertical plane of an RG 65/4 1 antenna for ground of ideal conductivity ($\gamma_v = \infty$), for ground of average conductivity ($\varepsilon_r = 8$; $\gamma_v = 0.005$), and ground of poor conductivity ($\varepsilon_r = 3$; $\gamma_v = 0.0005$); $\lambda = 2.5\ \lambda_0$.

Figures XIII.8.36 through XIII.8.45 are the radiation patterns in the horizontal plane of an RG 70/6 1.25 antenna.

Figures XIII.8.46 through XIII.8.55 show a series of radiation patterns in the vertical plane of an RG 70/6 1.25 antenna.

Figures XIII.8.56 through XIII.8.66 show a series of radiation patterns in the horizontal plane of an RG 75/6 1.25 antenna.

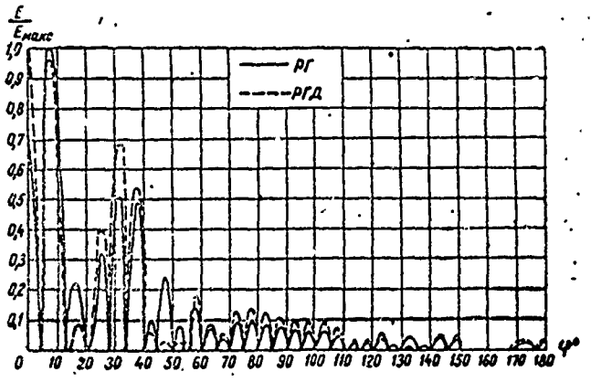

Figure XIII.8.36. Radiation patterns in the horizontal plane of RG 70/6 1.25 and RGD 70/6 1.25 antennas; $\lambda = 0.5\ \lambda_0$.
—— RG; ---- RGD; vertical: E/E_{max}.

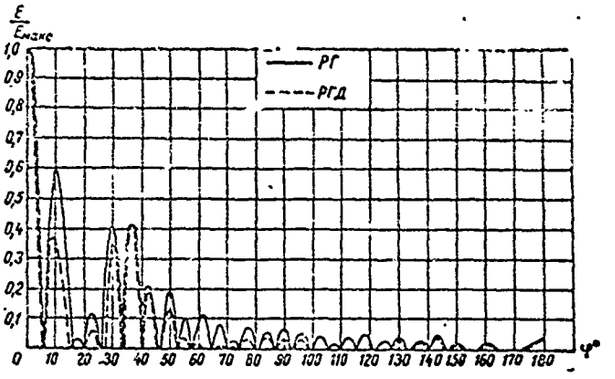

Figure XIII.8.37. Radiation patterns in the horizontal plane of RG 70/6 1.25 and RGD 70/6 1.25 antennas; $\lambda = 0.6\ \lambda_0$

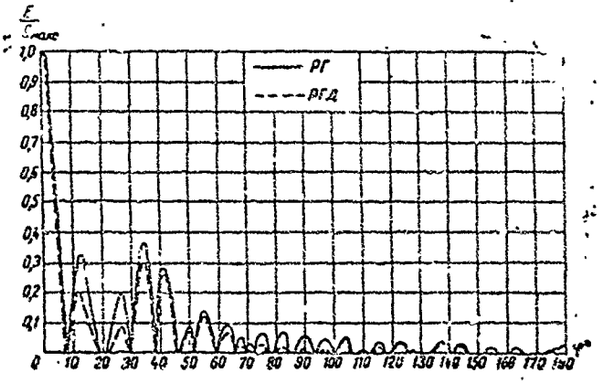

Figure XIII.8.38. Radiation patterns in the horizontal plane of RG 70/6 1.25 and RGD 70/6 1.25 antennas; $\lambda = 0.7\ \lambda_0$.

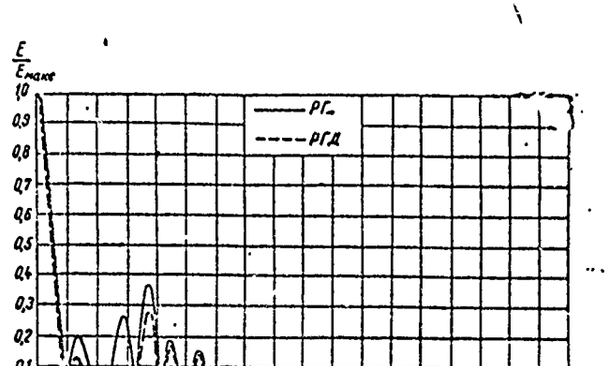

Figure XIII.8.39. Radiation patterns in the horizontal plane of RG 70/6 1.25 and RGD 70/6 1.25 antennas; $\lambda = 0.8\ \lambda_0$.

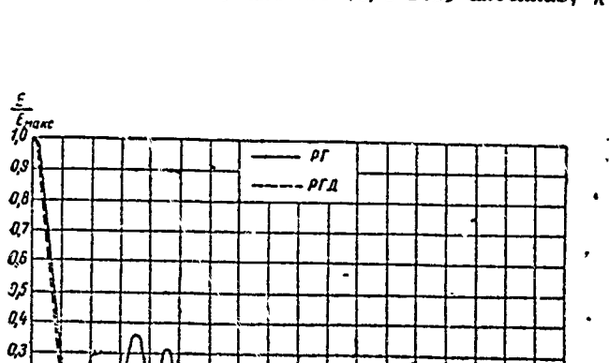

Figure XIII.8.40. Radiation patterns in the horizontal plane of RG 70/6 1.25 and RGD 70/6 1.25 antennas; $\lambda = \lambda_0$.

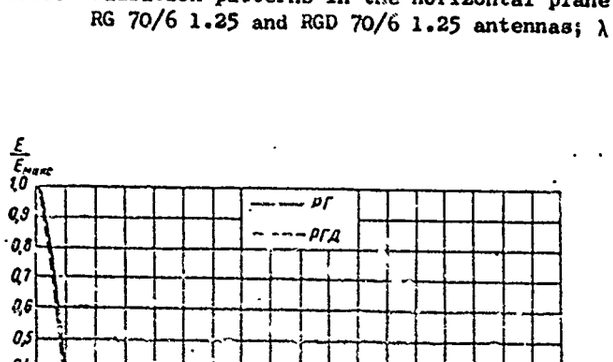

Figure XIII.8.41. Radiation patterns in the horizontal plane of RG 70/6 1.25 and RGD 70/6 1.25 antennas; $\lambda = 1.14\ \lambda_0$.

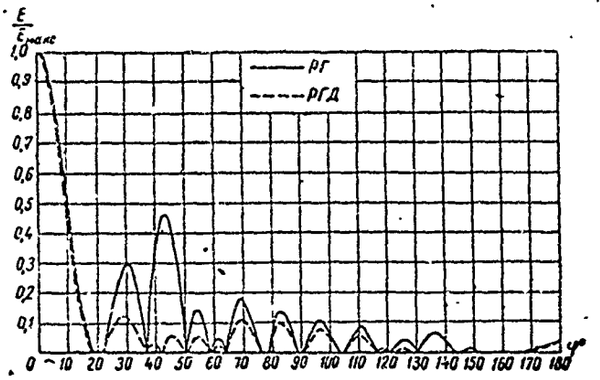

Figure XIII.8.42. Radiation patterns in the horizontal plane of RG 70/6 1.25 and RGD 70/6 1.25 antennas; $\lambda = 1.33\ \lambda_0$.

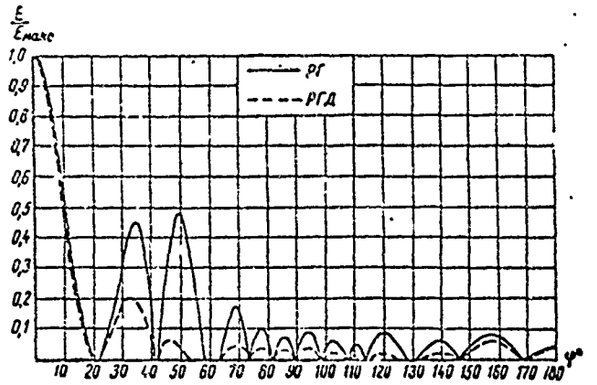

Figure XIII.8.43. Radiation patterns in the horizontal plane of RG 70/6 1.25 and RGD 70/6 1.25 antennas; $\lambda = 1.6\ \lambda_0$.

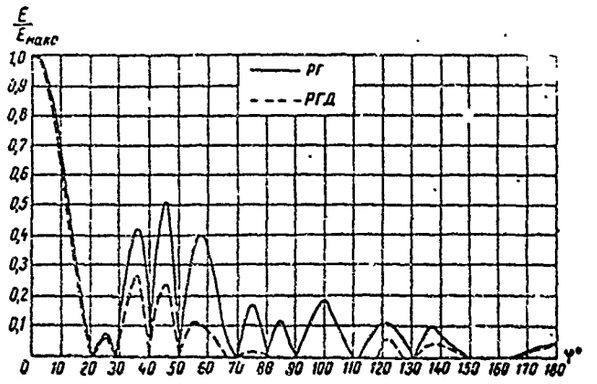

Figure XIII.8.44. Radiation patterns in the horizontal plane of RG 70/6 1.25 and RGD 70/6 1.25 antennas; $\lambda = 2\ \lambda_0$.

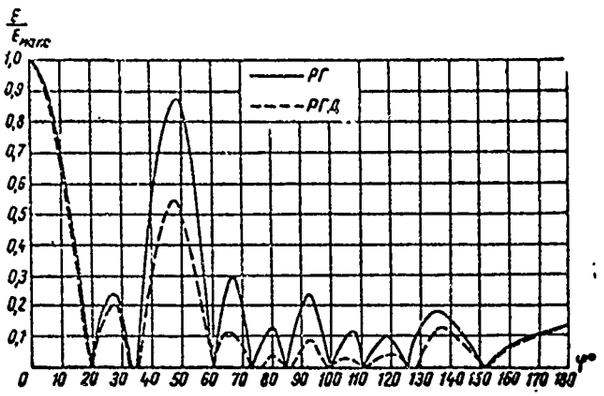

Figure XIII.8.45. Radiation patterns in the horizontal plane of RG 70/6 1.25 and RGD 70/6 1.25 antennas; $\lambda = 2.5\ \lambda_0$.

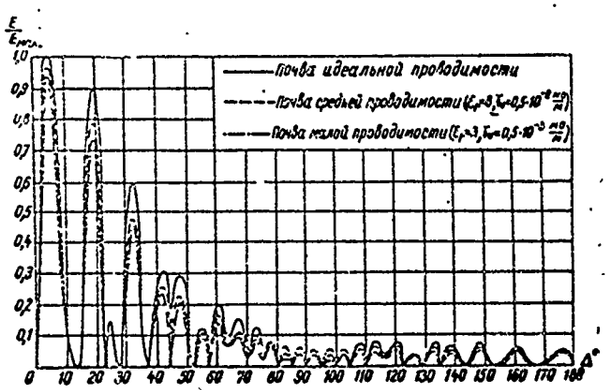

Figure XIII.8.46. Radiation patterns in the vertical plane of an RG 70/6 1.25 antenna; $\lambda = 0.5\ \lambda_0$.

——— ground of ideal conductivity; ---- ground of average conductivity; .-.-.- ground of poor conductivity; vertical: E/E_{max}.

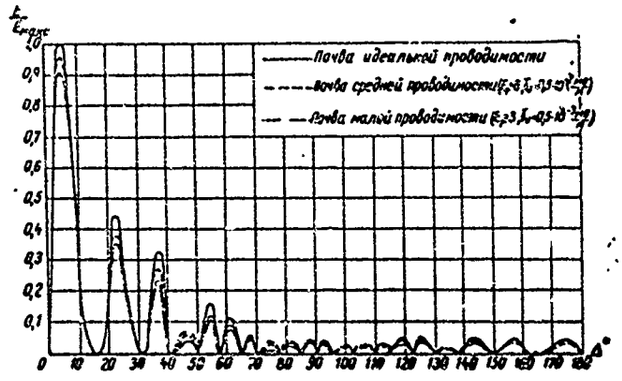

Figure XIII.8.47. Radiation patterns in the vertical plane of an RG 70/6 1.25 antenna; $\lambda = 0.6\ \lambda_0$.

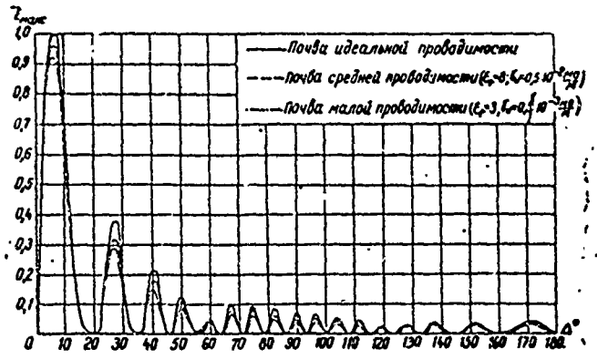

Figure XIII.8.48. Radiation patterns in the vertical plane of an RG 70/6 1.25 antenna; $\lambda = 0.7\ \lambda_0$.

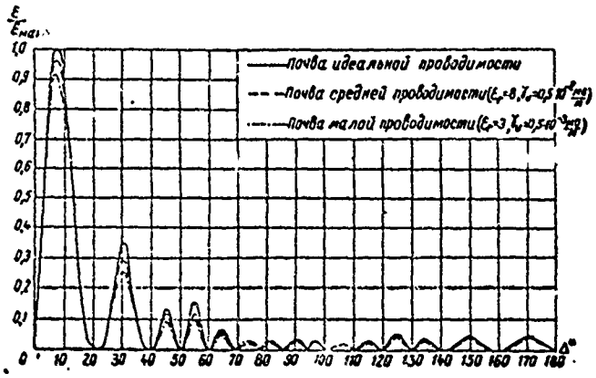

Figure XIII.8.49. Radiation patterns in the vertical plane of an RG 70/6 1.25 antenna; $\lambda = 0.8\ \lambda_0$.

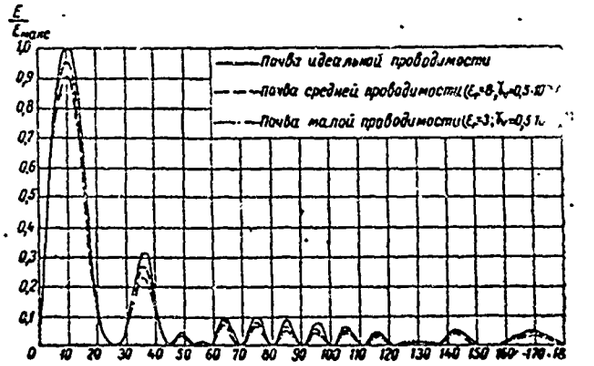

Figure XIII.8.50. Radiation patterns in the vertical plane of an RG 70/6 1.25 antenna; $\lambda = \lambda_0$.

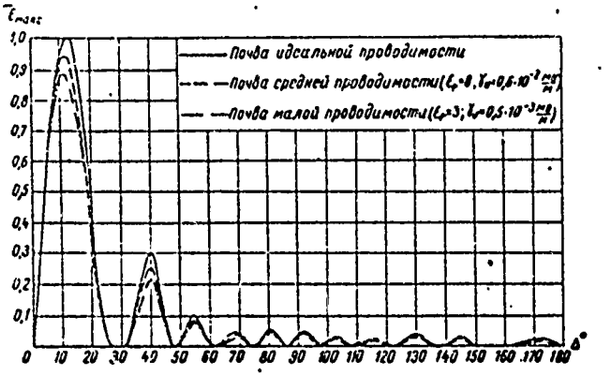

Figure XIII.8.51. Radiation patterns in the vertical plane of an RG 70/6 1.25 antenna; $\lambda = 1.125\ \lambda_0$.

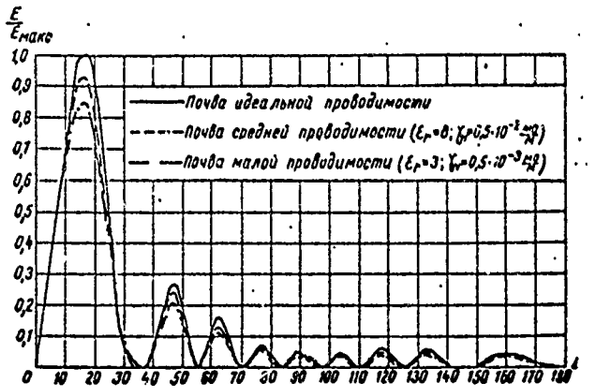

Figure XIII.8.52. Radiation patterns in the vertical plane of an RG 70/6 1.25 antenna; $\lambda = 1.33\ \lambda_0$.

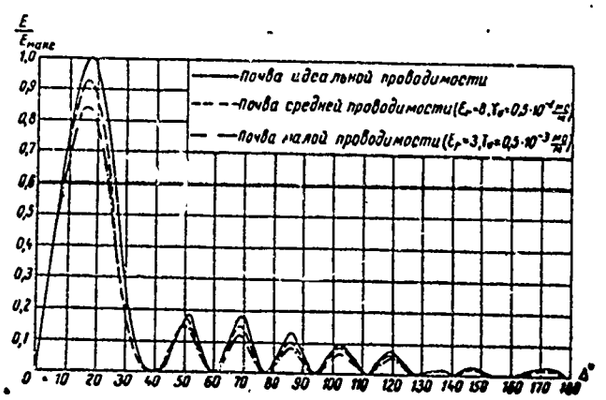

Figure XIII.8.53. Radiation patterns in the vertical plane of an RG 70/6 1.25 antenna; $\lambda = 1.6\ \lambda_0$.

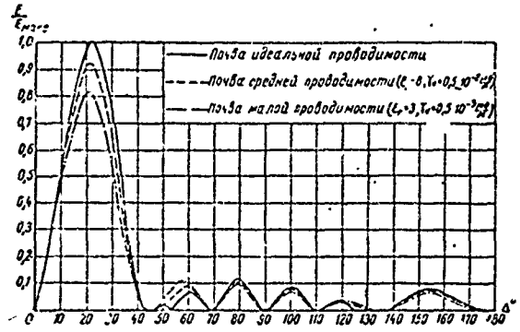

Figure XIII.8.54. Radiation patterns in the vertical plane of an RG 70/6 1.25 antenna; $\lambda = 2\ \lambda_0$.

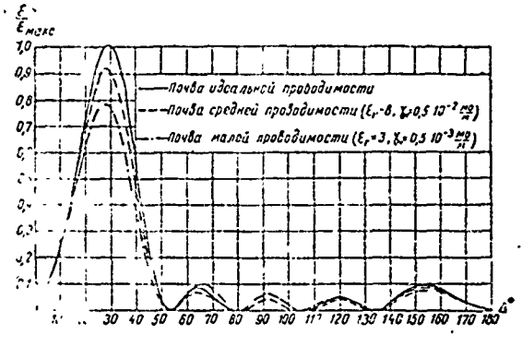

Figure XIII.8.55. Radiation patterns in the vertical plane of an RG 70/6 1.25 antenna; $\lambda = 2.5\ \lambda_0$.

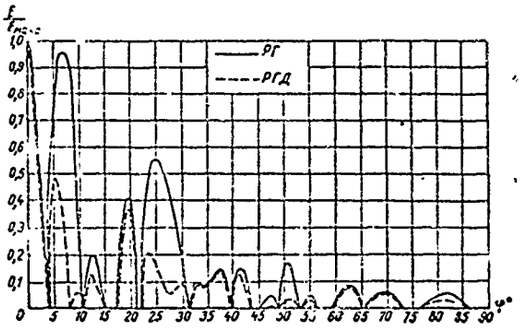

Figure XIII.8.56. Radiation patterns in the horizontal plane of RG 75/6 1.25 and RGD 75/6 1.25 antennas; $\lambda = 0.3\ \lambda_0$. ——— RG; ---- RGD; vertical: E/E_{max}.

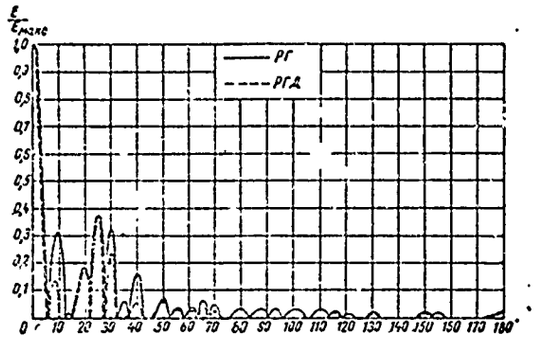

Figure XIII.8.57. Radiation patterns in the horizontal plane of RG 75/6 1.25 and RGD 75/6 1.25 antennas; $\lambda = 0.4\ \lambda_0$.

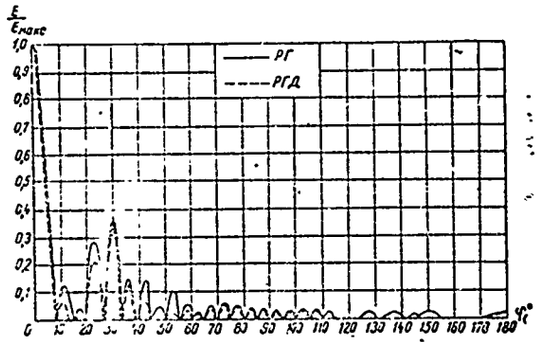

Figure XIII.8.58. Radiation patterns in the horizontal plane of RG 75/6 1.25 and RGD 75/6 1.25 antennas; $\lambda = 0.5\ \lambda_0$.

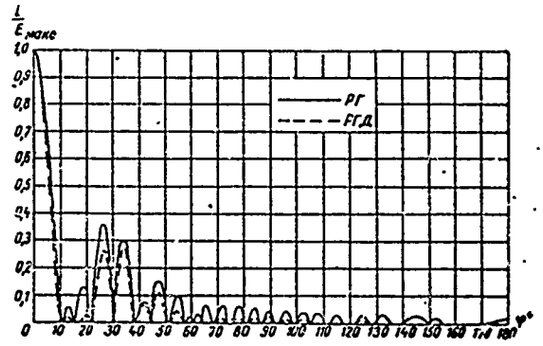

Figure XIII.8.59. Radiation patterns in the horizontal plane of RG 75/6 1.25 and RGD 75/6 1.25 antennas; $\lambda = 0.6\ \lambda_0$.

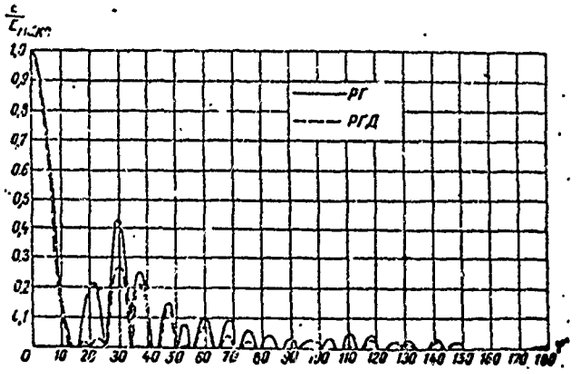

Figure XIII.8.60. Radiation patterns in the horizontal plane of RG 75/6 1.25 and RGD 75/6 1.25 antennas; $\lambda = 0.7\ \lambda_0$.

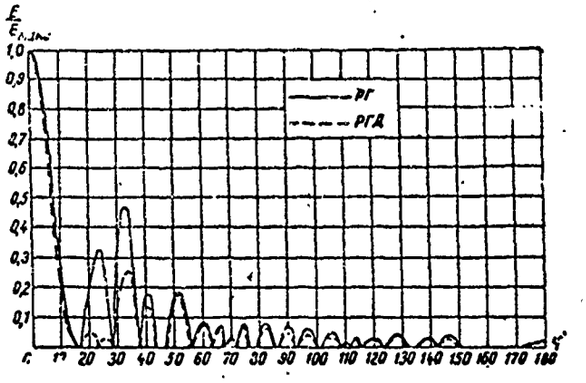

Figure XIII.8.61. Radiation patterns in the horizontal plane of RG 75/6 1.25 and RGD 75/6 1.25 antennas; $\lambda = 0.8\ \lambda_0$.

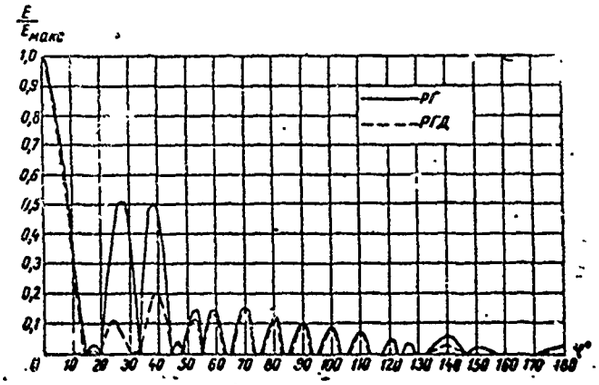

Figure XIII.8.62. Radiation patterns in the horizontal plane of RG 75/6 1.25 and RGD 75/6 1.25 antennas; $\lambda = 1.0\ \lambda_0$.

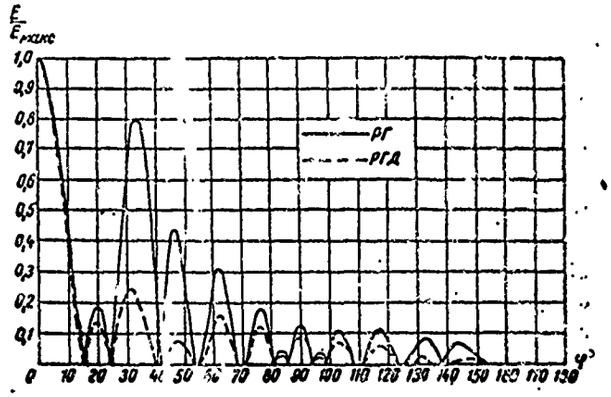

Figure XIII.8.63. Radiation patterns in the horizontal plane of RG 75/6 1.25 and RGD 75/6 1.25 antennas; $\lambda = 1.33\ \lambda_0$.

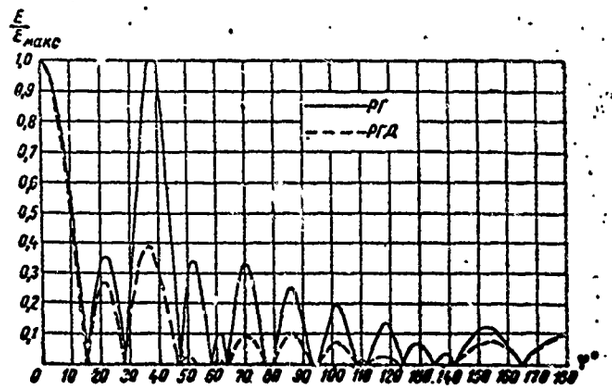

Figure XIII.8.64. Radiation patterns in the horizontal plane of RG 75/6 1.25 and RGD 75/6 1.25 antennas; $\lambda = 1.6\ \lambda_0$.

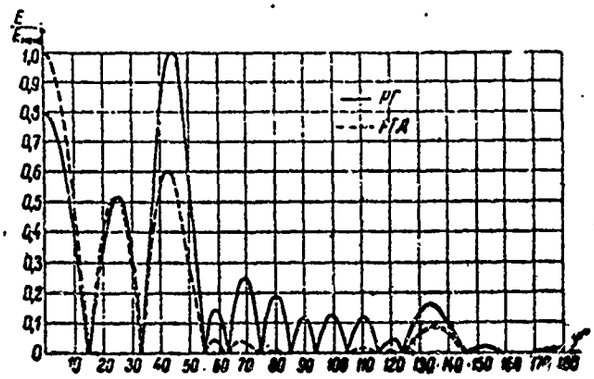

Figure XIII.8.65. Radiation patterns in the horizontal plane of RG 75/6 1.25 and RGD 75/6 1.25 antennas; $\lambda = 2\ \lambda_0$.

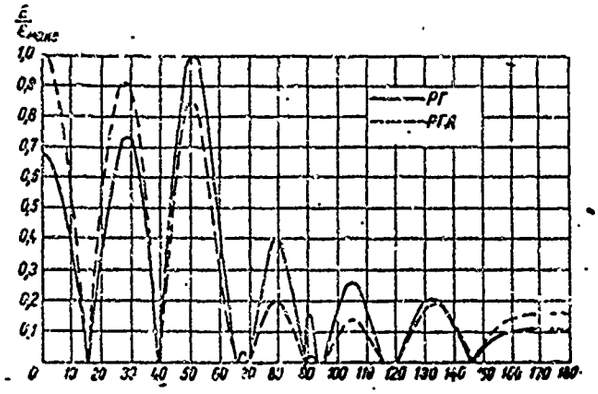

Figure XIII.8.66. Radiation patterns in the horizontal plane of RG 75/6 1.25 and RGD 75/6 1.25 antennas; $\lambda = 2.5\ \lambda_0$.

Radiation patterns in the vertical plane of an RG 75/6 1.25 antenna are shown in figures XXX.8.67 through XIII.8.77.

Figures XIII.8.78 through XIII.8.95 show a series of radiation patterns in the horizontal and vertical planes of RG 57/1.7 0.5 and RG 45/1 0.35 antennas.

No diagrams were charted for RG 65/2.8 0.6 antenna. Its pattern in the horizontal plane can be established by using the diagram for the RG 65/4 1 antenna, and it should be remembered that the optimum wave of the RG 65/2.8 0.6 antenna is 4/2.8 = 1.43 times longer than the optimum wave of the RG 65/4 1 antenna. Radiation patterns of the RG 65/2.8.0.6 in the vertical plane can be determined similarly.

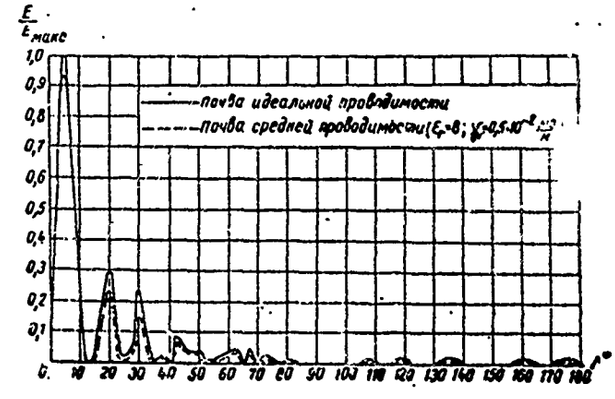

Figure XIII.8.67. Radiation patterns in the vertical plane of an RG 75/6 1.25 antenna; $\lambda = 0.4\ \lambda_0$.
—— ground of ideal conductivity; ---- ground of average conductivity ($\epsilon_r = 8$; $\gamma_v = 0.5 \cdot 10^{-2}$ mhos/m.

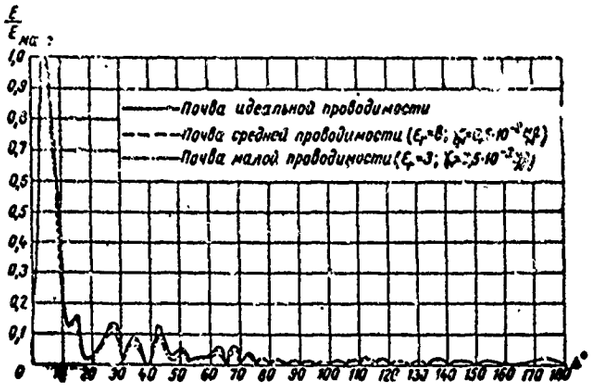

Figure XIII.8.68. Radiation patterns in the vertical plane of an RG 75/6 1.25 antenna; $\lambda = 0.5\ \lambda_0$.
—— ground of ideal conductivity; ---- ground of average conductivity ($\varepsilon_r=8$; $\gamma_v=0.5\cdot10^{-2}$ mhos/m); .-.-.- ground of poor conductivity ($\varepsilon_r=3$; $\gamma_v=0.5\cdot10^{-3}$ mhos/m). Vertical: E/E_{max}.

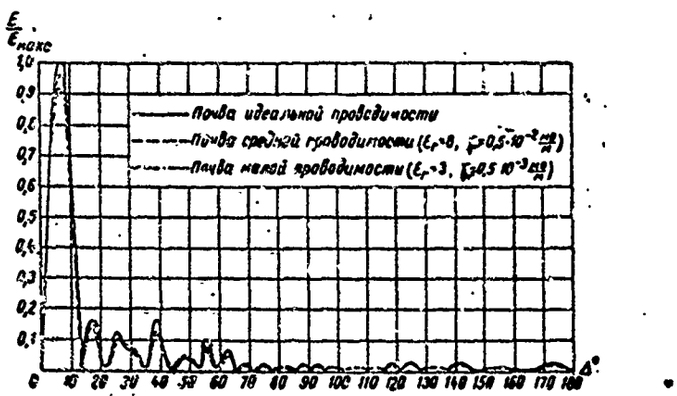

Figure XIII.8.69. Radiation patterns in the vertical plane of an RG 75/6 1.25 antenna; $\lambda = 0.6\ \lambda_0$.

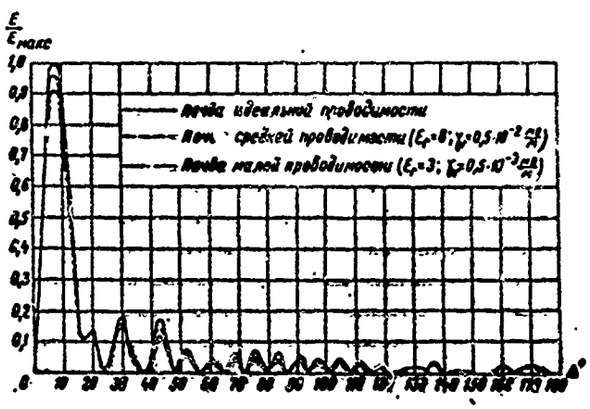

Figure XIII.8.70. Radiation patterns in the vertical plane of an RG 75/6 1.25 antenna; $\lambda = 0.7\ \lambda_0$.

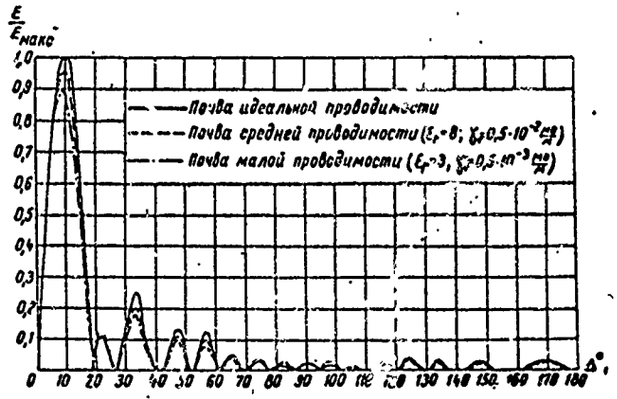

Figure XIII.8.71. Radiation patterns in the vertical plane of an RG 75/6 1.25 antenna; $\lambda = 0.8\ \lambda_0$.

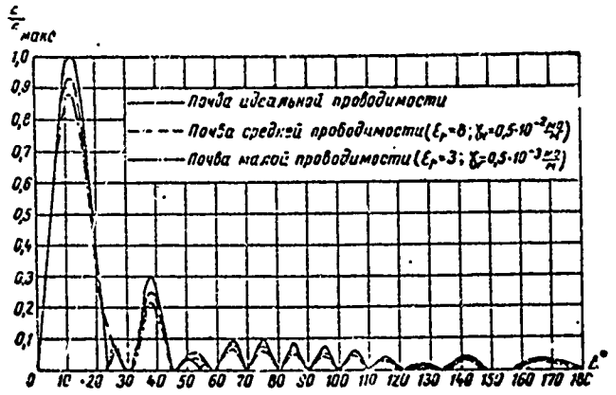

Figure XIII.8.72. Radiation patterns in the vertical plane of an RG 75/6 1.25 antenna; $\lambda = \lambda_0$.

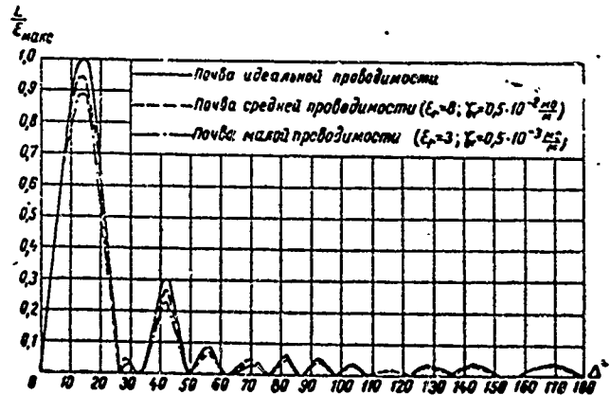

Figure XIII.8.73. Radiation patterns in the vertical plane of an RG 75/6 1.25 antenna; $\lambda = 1.125\ \lambda_0$.

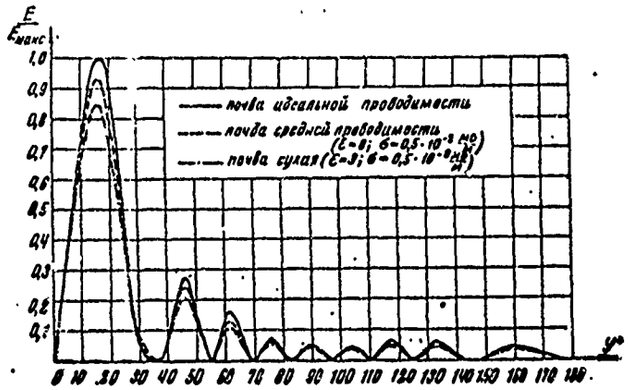

Figure XIII.8.74. Radiation patterns in the vertical plane of an RG 75/6 1.25 antenna; $\lambda = 1.32\ \lambda_0$.

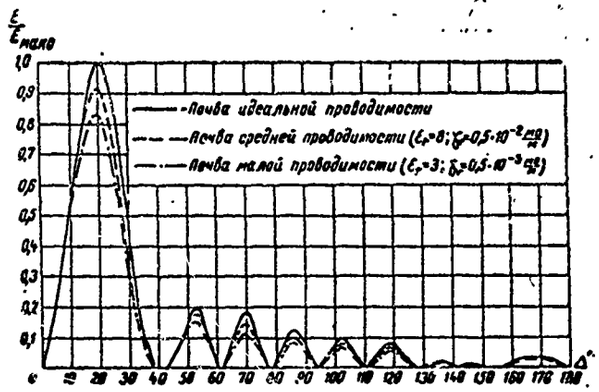

Figure XIII.8.75. Radiation patterns in the vertical plane of an RG 75/6 1.25 antenna; $\lambda = 1.6\ \lambda_0$.

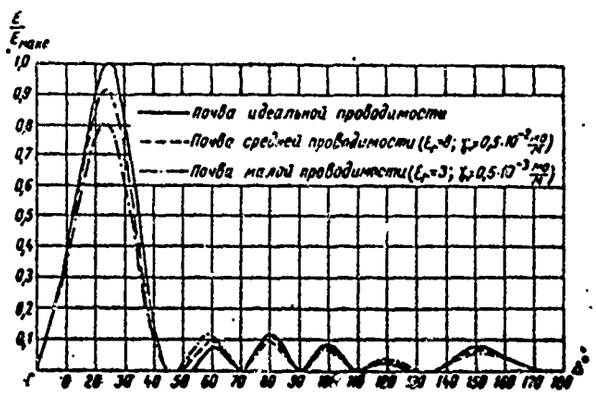

Figure XIII.8.76. Radiation patterns in the vertical plane of an RG 75/6 1.25 antenna; $\lambda = 2\ \lambda_0$.

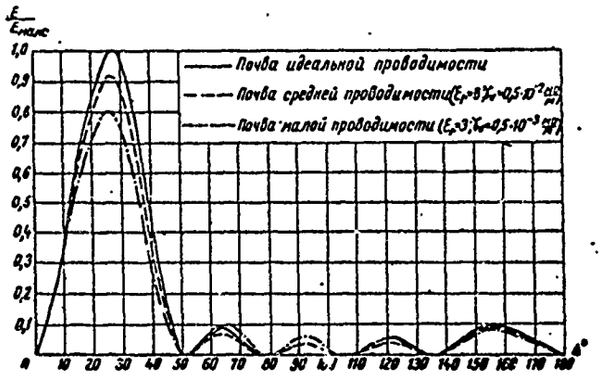

Figure XIII.8.77. Radiation patterns in the vertical plane of an RG 75/6 1.25 antenna; $\lambda = 2.5\ \lambda_0$.

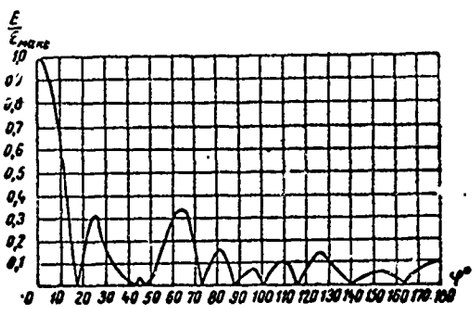

Figure XIII.8.78. Radiation pattern in the horizontal plane of an RG 57/1.7 0.5 antenna with angle of tilt $\Delta = 16°$ for a wavelength of $\lambda = 0.672\ \lambda_0$.

Vertical: E/E_{max}.

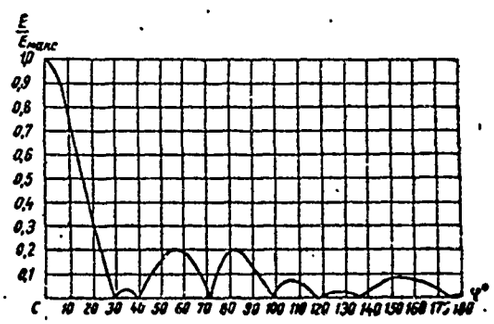

Figure XIII.8.79. Radiation pattern in the horizontal plane of an RG 57/1.7 0.5 antenna with angle of tilt $\Delta = 37°$ for a wavelength of $\lambda = \lambda_0$.

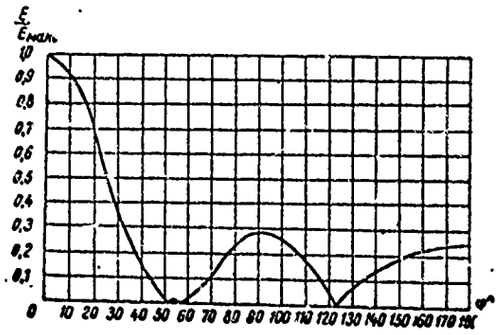

Figure XIII.8.80. Radiation pattern in the horizontal plane of an RG 57/1.7 0.5 antenna with angle of tilt $\Delta = 44°$ for a wavelength of $\lambda = 1.68\ \lambda_0$.

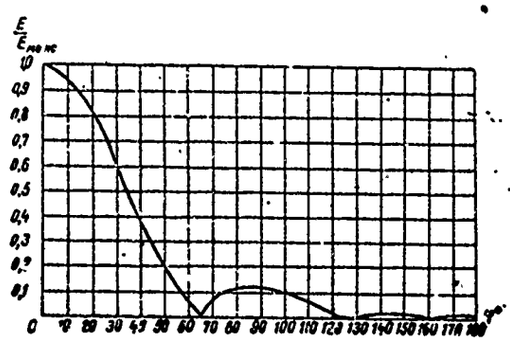

Figure XIII.8.81. Radiation pattern in the horizontal plane of an RG 57/1.7 0.5 antenna with angle of tilt $\Delta = 60°$ for a wavelength of $\lambda = 2.5\ \lambda_0$.

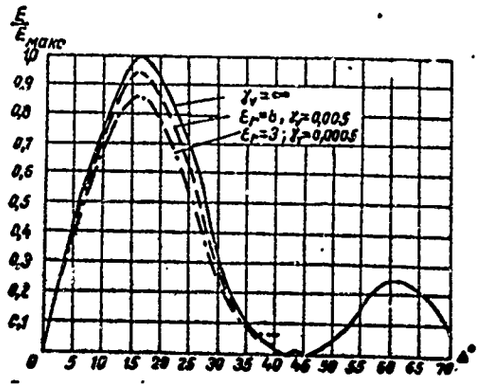

Figure XIII.8.82. Radiation patterns in the vertical plane of an RG 57/1.7 0.5 antenna for ground of ideal conductivity ($\gamma_v = \infty$), for ground of average conductivity (ε_r=6; γ_v=0.005), and for ground of poor conductivity (ε_r=3; γ_v=0.0005); $\lambda = 0.672\ \lambda_0$.

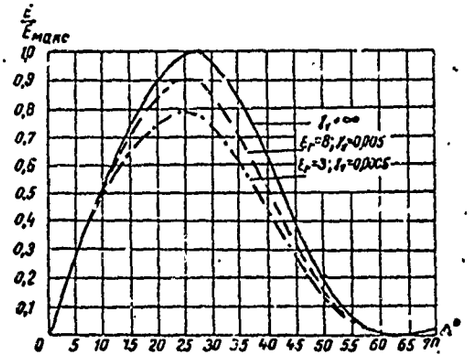

Figure XIII.8.83. Radiation patterns in the vertical plane of an RG 57/1.7 0.5 antenna for ground of ideal conductivity ($\gamma_v=\infty$), for ground of average conductivity ($\varepsilon_r=8$; $\gamma_v=0.005$), and for ground of poor conductivity ($\varepsilon_r=3$; $\gamma_v=0.0005$); $\lambda = \lambda_0$.

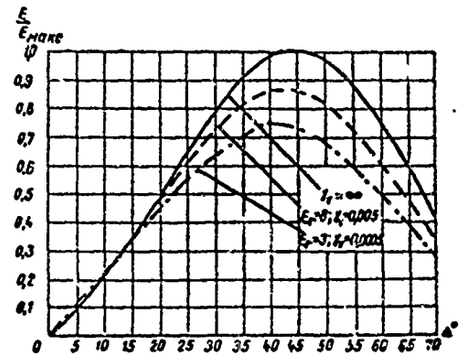

Figure XIII.8.84. Radiation patterns in the vertical plane of an RG 57/1.7 0.5 antenna for ground of ideal conductivity ($\gamma_v=\infty$), for ground of average conductivity ($\varepsilon_r=8$; $\gamma_v=0.005$), and for ground of poor conductivity ($\varepsilon_r=3$; $\gamma_v=0.0005$); $\lambda = 1.68\ \lambda_0$.

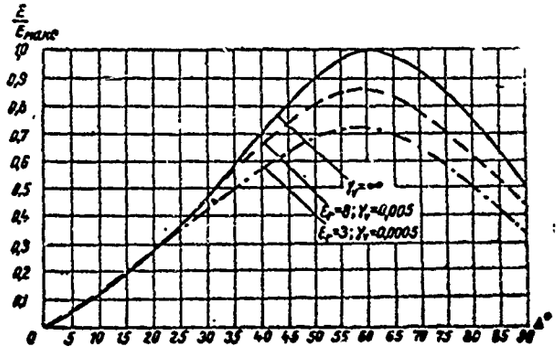

Figure XIII.8.85. Radiation patterns in the vertical plane of an RG 57/1.7 0.5 antenna for ground of ideal conductivity ($\gamma_v=\infty$), for ground of average conductivity ($\varepsilon_r=8$; $\gamma_v=0.005$), and for ground of poor conductivity ($\varepsilon_r=3$; $\gamma_v=0.0005$); $\lambda = 2.5\ \lambda_0$.

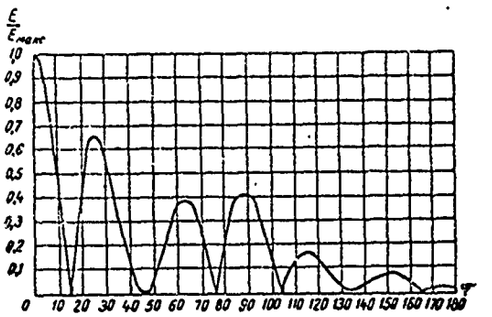

Figure XIII.8.86. Radiation pattern in the horizontal plane of an RG 45/1 0.35 antenna with angle of tilt $\Delta = 15°$ for wavelength $\lambda = 0.5\ \lambda_0$.

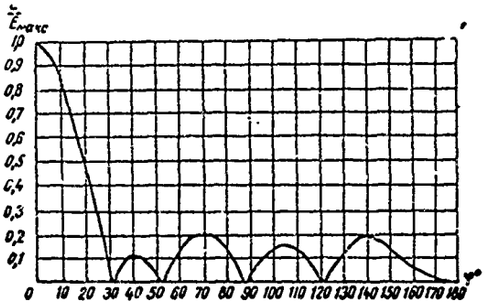

Figure XIII.8.87. Radiation pattern in the horizontal plane of an RG 45/1 0.35 antenna with angle of tilt $\Delta = 30°$ for wavelength $\lambda = 0.8\ \lambda_0$.

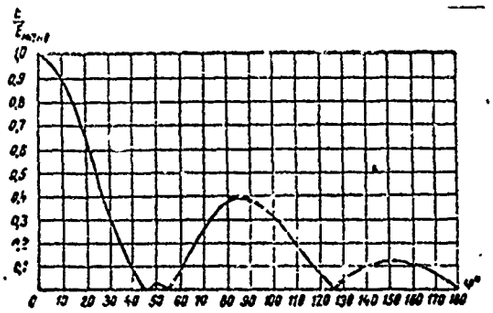

Figure XIII.8.88. Radiation pattern in the horizontal plane of an RG 45/1 0.35 antenna with angle of tilt $\Delta = 35°$ for wavelength $\lambda = \lambda_0$.

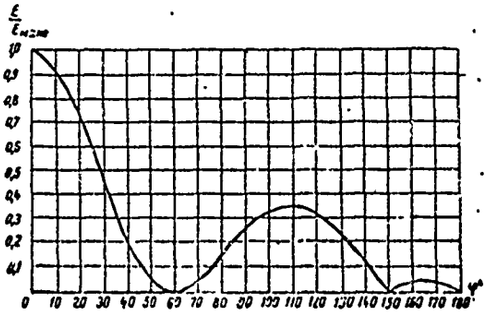

Figure XIII.8.89. Radiation pattern in the horizontal plane of an RG 45/1 0.35 antenna with angle of tilt $\Delta = 45°$ for wavelength $\lambda = 1.2\ \lambda_0$.

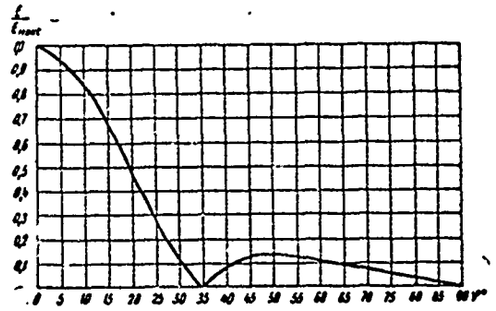

Figure XIII.8.90. Radiation pattern in the horizontal plane of an RG 45/1 0.35 antenna with angle of tilt $\Delta = 60°$ for wavelength $\lambda = 1.6\ \lambda_0$.

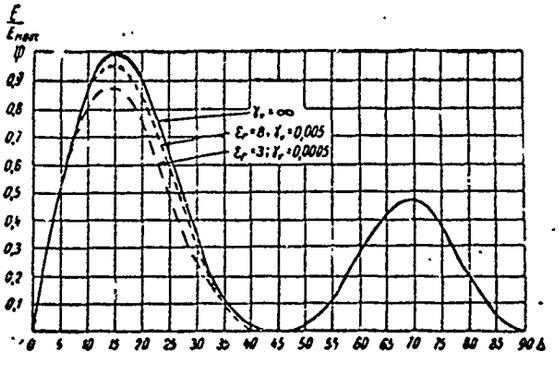

Figure XIII.8.91. Radiation patterns in the vertical plane of an RG 45/1 0.35 antenna for ground of ideal conductivity ($\gamma_v=\infty$), for ground of average conductivity ($\varepsilon_r=8$; $\gamma_v = 0.005$), and for ground of poor conductivity ($\varepsilon_r=3$; $\gamma_v=0.0005$); $\lambda = 0.5\ \lambda_0$.

Vertical: E/E_{max}.

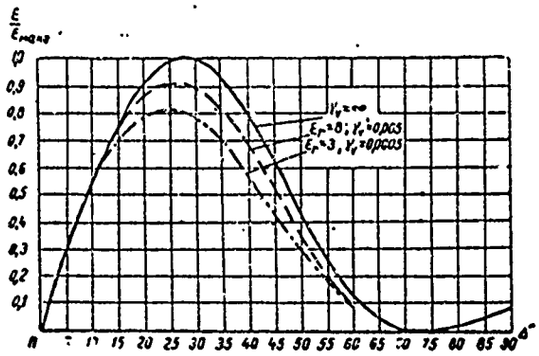

Figure XIII.8.92. Radiation patterns in the vertical plane of an RG 45/1 0.35 antenna for ground of ideal conductivity ($\gamma_v=\infty$), for ground of average conductivity ($\varepsilon_r=8$; $\gamma_v=0.005$), and for ground of poor conductivity ($\varepsilon_r=3$; $\gamma_v=0.0005$); $\lambda = 0.8\ \lambda_o$.

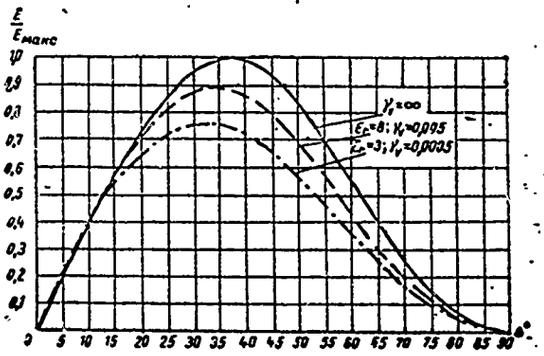

Figure XIII.8.93. Radiation patterns in the vertical plane of an RG 45/1 0.35 antenna for ground of ideal conductivity ($\gamma_v=\infty$), for ground of average conductivity ($\varepsilon_r=8$; $\gamma_v=0.005$), and for ground of poor conductivity ($\varepsilon_r=3$; $\gamma_v=0.0005$); $\lambda = \lambda_o$.

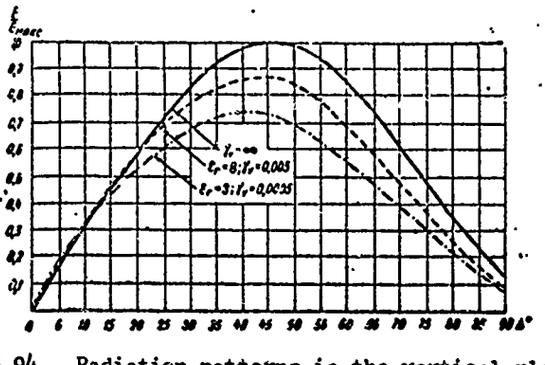

Figure XIII.8.94. Radiation patterns in the vertical plane of an RG 45/1 0.35 antenna for ground of ideal conductivity ($\gamma_v=\infty$), for ground of average conductivity ($\varepsilon_r=8$; $\gamma_v=0.005$), and for ground of poor conductivity ($\varepsilon_r=3$; $\gamma_v=0.0005$); $\lambda = 1.2\ \lambda_o$.

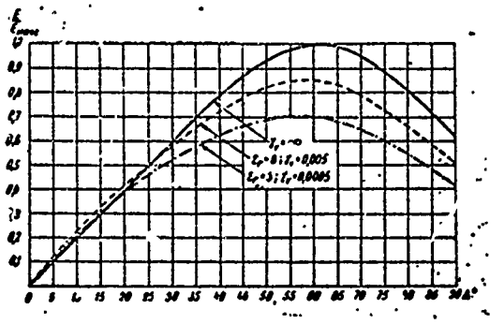

Figure XIII.8.95. Radiation patterns in the vertical plane of an RG 45/1 0.35 antenna for ground of ideal conductivity ($\gamma_v=\infty$), for ground of average conductivity ($\varepsilon_r=8$; $\gamma_v=0.005$), and for ground of poor conductivity ($\varepsilon_r=3$; $\gamma_v=0.0005$); $\lambda = 1.6\ \lambda_0$.

The radiation patterns in the vertical plane are charted for three types of ground; ideal, average, poor conductivity. The maximum field strength for ideally conducting ground was used as E_{max} in charting the patterns for the two other types of ground. Accordingly, the comparison of radiation patterns in the vertical plane for real and ideal grounds also characterizes the dependence of the absolute magnitude of the field strength on ground parameters.

So far as the RG 57/1.7 0.5 and RG 45/1 0.35 antennas are concerned, the radiation patterns in the horizontal plane are given for angles of tilt equal to the angles of tilt for the maximum beams. The reason for so doing is that these antennas are designed for operation on short main lines where angles of filt of beams at the reception site are extremely large and the radiation patterns when $\Delta = 0$ are not characteristic enough. Only the normal component of the field strength vector was considered in charting the patterns indicated.

Diagrams in the horizontal plane when $\Delta \neq 0$ were charted using formula (XIII.3.1), and it was assumed that $\gamma = i\alpha$. After these substitutions, and the corresponding conversions, the expression for the radiation patterns in the horizontal plane for a specified constant value of angle of tilt, Δ, takes the following form

$$F(\varphi) = \left[\frac{\cos(\Phi+\varphi)}{1-\sin(\Phi+\varphi)\cos\Delta_1} + \frac{\cos(\Phi-\varphi)}{1-\sin(\Phi-\varphi)\cos\Delta}\right]\times$$
$$\times \sin\left\{\frac{\alpha l}{2}\left[1-\sin(\Phi+\varphi)\cos\Delta\right]\right\}\times$$
$$\times \sin\left\{\frac{\alpha l}{2}\left[1-\sin(\Phi-\varphi)\cos\Delta\right]\right\}. \qquad \text{(XIII.8.10)}$$

Figure XIII.8.96 shows the curves characterizing the dependence of the gain factor of the RG 65/4 1 antenna on the wavelength for different values of Δ. This same figure contains the dotted charting of a curve which gives

the dependence of the gain factor in the direction of maximum radiation on the wavelength. The dotted curve is the envelope of the solid line curves. The angles of tilt for maximum beams can be established at the points of tangency of the solid and the dotted curves.

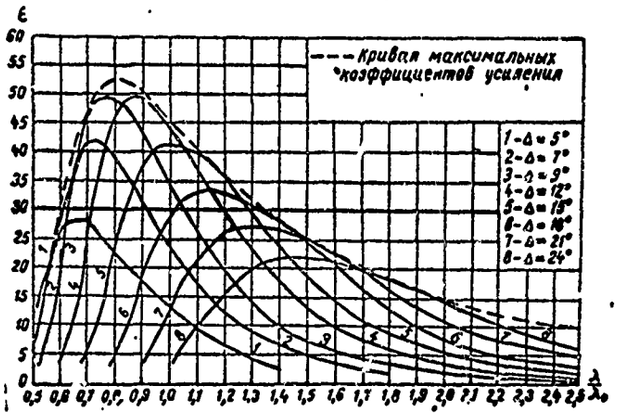

Figure XIII.8.96. Dependence of the gain factor of an RG 65/4 1 antenna on the wavelength for different angles of tilt (Δ) values; W_r = 700 ohms.

---- maximum gain curve.

Figure XIII.8.97 shows the curves characteristic of the dependence of the directive gain of the RG 65/4 1 antenna on λ/λ_0 and Δ.

Using the curves in figures XIII.8.96 and XIII.8.97, we can establish the gain factor and the directive gain of the antenna for any angles of tilt, and for any values of λ/λ_0.

Figure XIII.8.98 shows the design curve of the dependence of the efficiency of an RG 65/4 1 antenna on the wavelength. The assumption used in charting this curve was that W_r = 700 ohms.

Figures XIII.8.99 through XIII.8.110 show design curves that characterize the electrical parameters of RG 70/6 1.25, RG 75/6 1.25, RG 57/1.7 0.5, and RG 45/1 0.35 antennas.

The gain factor and directive gain are given for all antennas for the case of ideally conducting ground. Reduction in the gain factor in the case of real ground can be established by comparing the radiation patterns in the vertical plane for real and ideal ground, taking it that the gain factor is proportional to the square of the field strength.

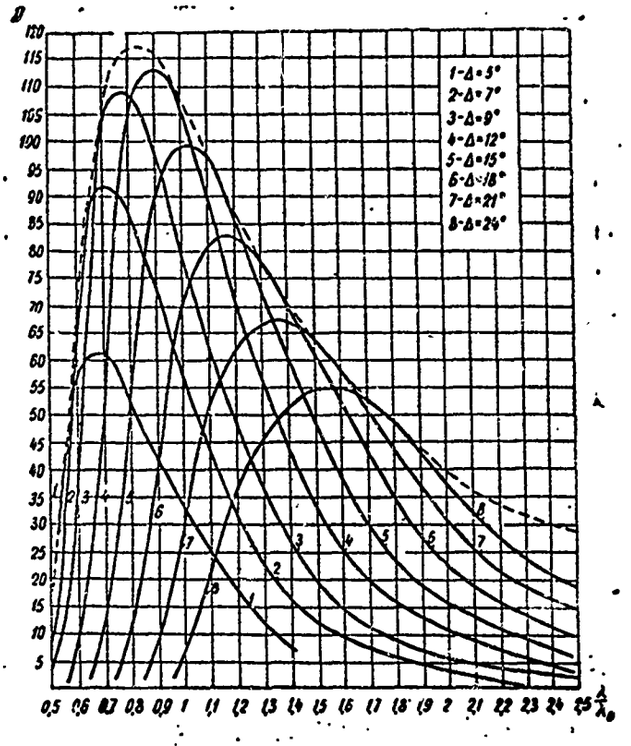

Figure XIII.8.97. Dependence of the directive gain of an RG 65/4 1 antenna on wavelength for different angles of tilt (Δ) values; W_r = 700 ohms.

----- maximum directive gain curve.

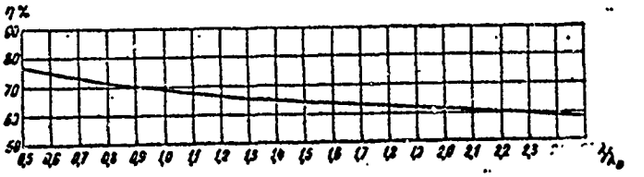

Figure XIII.8.98. Dependence of the efficiency of the RG 65/4 1 antenna on wavelength; W_r = 700 ohms.

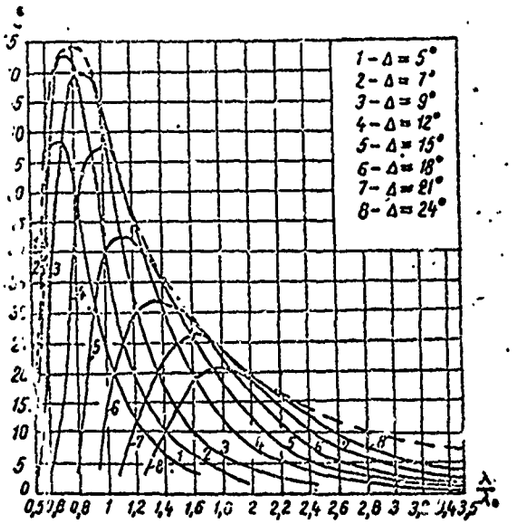

Figure XIII.8.99. Dependence of the gain factor of an RG 70/6 1.25 antenna on wavelength for different angles of tilt (Δ); W_r = 700 ohms.

----- maximum gain curve.

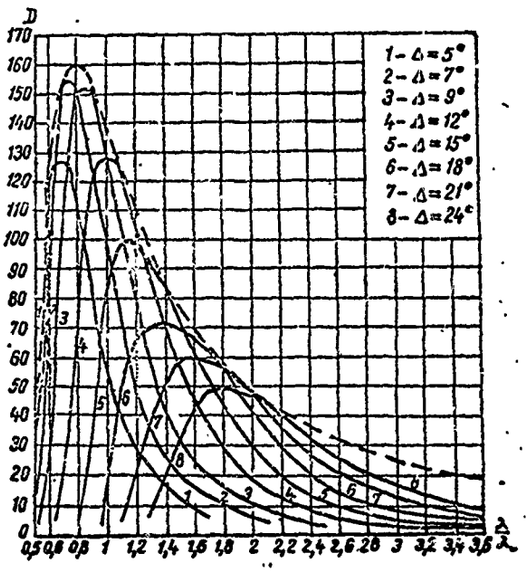

Figure XIII.8.100. Dependence of directive gain of an RG 70/6 1.25 antenna on wavelength for different angles of tilt (Δ); W_r = 700 ohms.

----- maximum directive gain curve.

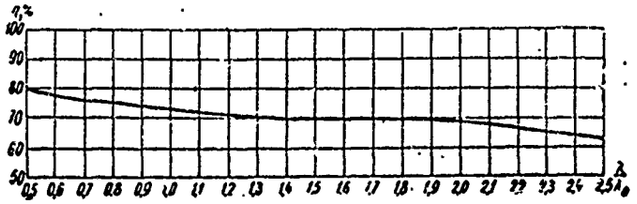

Figure XIII.8.101. Dependence of the efficiency of an RG 70/6 1.25 antenna on the wavelength; W_r = 700 ohms.

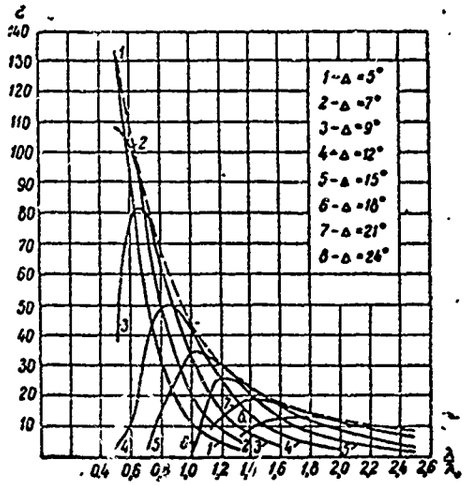

Figure XIII.8.102. Dependence of the gain factor of an RG 75/6 1.25 antenna on the wavelength for different angles of tilt (Δ); W_r = 700 ohms.

----- maximum gain curve.

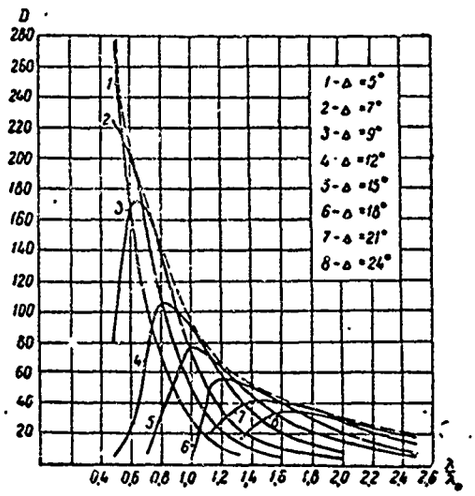

Figure XIII.8.103. Dependence of directive gain of an RG 75/6 1.25 antenna on wavelength for different angles of tilt (Δ); W_r = 700 ohms.

----- maximum directive gain curve.

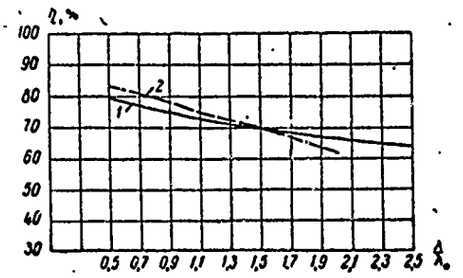

Figure XIII.8.104. Dependence of the efficiency of an RG 75/6 1.25 antenna on the wavelength; W_r = 700 ohms.

1 - designed curve; 2 - experimental curve.

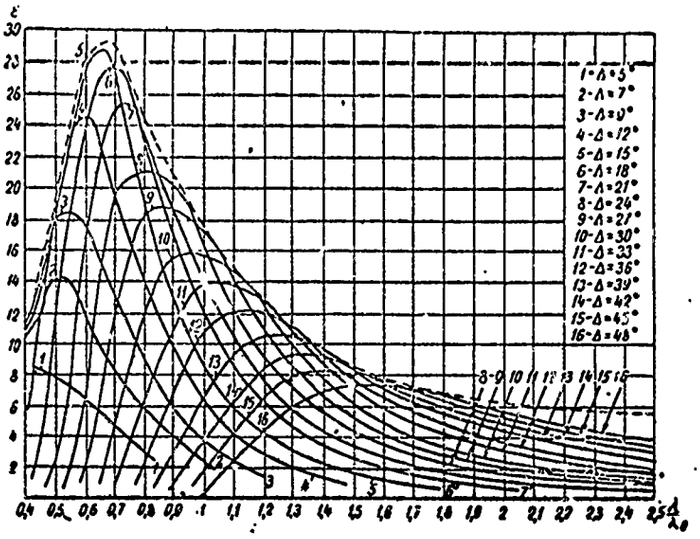

Figure XIII.8.105. Dependence of the gain factor of an RG 57/1.7 0.5 antenna on the wavelength for different angles of tilt (Δ); W_r = 700 ohms.

----- maximum gain curve.

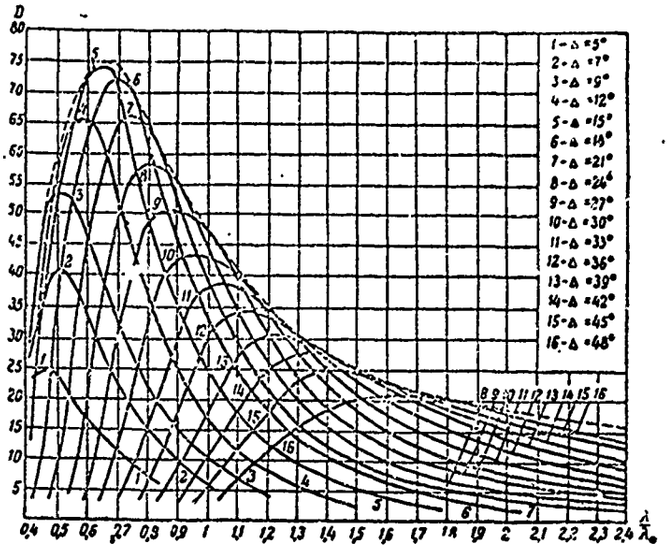

Figure XIII.8.106. Dependence of the directive gain of an RG 57/1.7 0.5 antenna on the wavelength for different angles of tilt (Δ); W_r = 700 ohms.

----- maximum directive gain curve.

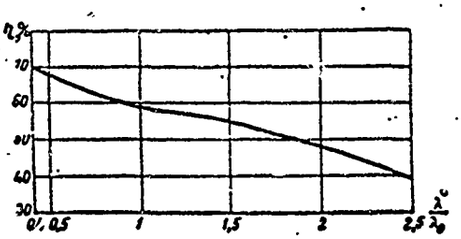

Figure XIII.8.107. Dependence of the efficiency of an RG 57/1.7 0.5 antenna on wavelength; W_r = 700 ohms.

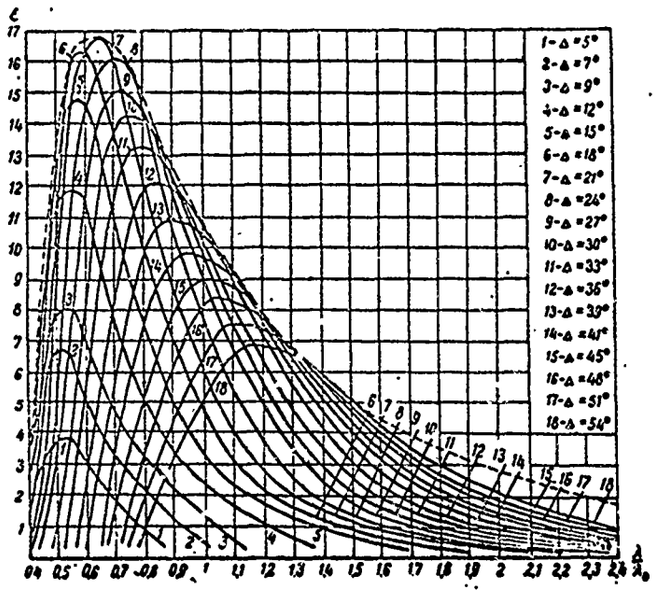

Figure XIII.8.108. Dependence of the gain factor of an RG 45/1 0.35 antenna on wavelength for different angles of tilt (Δ); W_r = 700 ohms.

----- maximum gain curve.

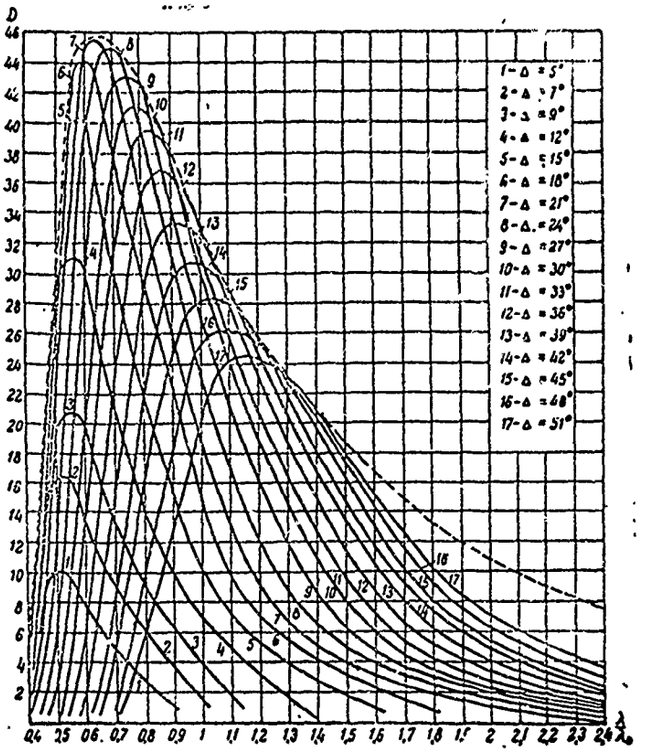

Figure XIII.8.109. Dependence of the directive gain of an RG 45/1 0.35 antenna on the wavelength for different angles of tilt (Δ); W_r = 700 ohms.

----- maximum directive gain curve.

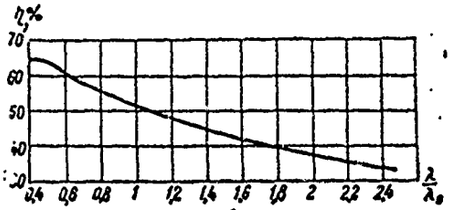

Figure XIII.8.110. Dependence of the efficiency of an R. /1 0.35 antenna on wavelength; W_r = 700 ohms.

#XIII.9. Useful Range of the Rhombic Antenna

The rhombic antenna makes a good match with transmission lines over the entire shortwave range, so the operating range is limited only by reduction in gain, and by deterioration in directional properties, as departure is made from waves close to optimum. The particular useful range depends on requirements imposed by the gain factor for the specified angles of radiation in the vertical plane.

At least two antennas are desirable in order to service the entire operating range on vital, long, communication lines.

On particularly vital lines, those using the range from 10 meters to 70 to 100 meters, it is desirable to use at least three rhombic antennas to work the three subranges so the entire range will be covered.

#XIII.10. The Double Rhombic Antenna (RGD)

The author has proposed the use of a double rhombic antenna consisting of two rhombuses, one atop the other and displaced in direction from each other along their small diagonals at distance D_1 on the order of λ_0. The double horizontal rhombic antenna is conventionally designated by the letters RGD, and its schematic is shown in Figure XIII.10.1.

The radiation pattern of the RGD antenna can be computed through the formula

$$F_2(\Delta,\varphi) = F_1(\Delta,\varphi)\cos\left(\frac{\alpha D_1}{2}\cos\Delta\sin\varphi\right), \qquad \text{(XIII.10.1)}$$

where

$F_1(\Delta,\varphi)$ is the expression for the radiation pattern of a single rhombic antenna, established through equation (XIII.3.1) through (XIII.3.3).

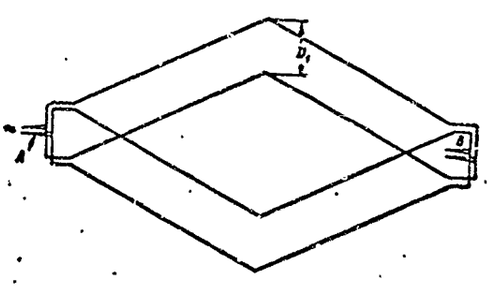

Figure XIII.10.1. Schematic diagram of a double horizontal rhombic antenna.

A - exponential four-wire line for matching antenna and supply feeder; B - exponential four-wire line for matching antenna and terminating line.

For the horizontal plane ($\Delta = 0$), formula XIII.10.1 becomes

$$F_2(\varphi) = F_1(\varphi)\cos\left(\frac{\alpha D_1}{2}\sin\varphi\right). \qquad \text{(XIII.10.2)}$$

where

$F_1(\varphi)$ can be established through equation (XIII.3.4).

The shape of the radiation pattern in the vertical plane remains the same as that of the single rhombic antenna.

The gain factor of the double rhombic antenna can be calculated through the formula

$$s = \frac{9360}{W'_r}\frac{\cos^2\Phi\, e^{-2\beta' l}}{(1-\sin\Phi\cos\Delta)^2}\sin^4\left[\frac{\alpha l}{2}(1-\sin\Phi\cos\Delta)\right]\times \\ \times \sin^2(\alpha H\sin\Delta), \qquad \text{(XIII.10.3)}$$

where

W'_r is the characteristic impedance of one rhombus in the system of the double rhombic antenna (in practice $W'_r = W_r$ is acceptable);

β' is the attenuation factor on a double rhombic antenna

$$\beta' l = \frac{R'_\Sigma}{W'_r} \approx \frac{R'_r}{4W_r}. \qquad \text{(XIII.10.4)}$$

Here R'_Σ is the radiation resistance of one side of the rhombus in the system, and R'_r is the radiation resistance of one rhombus in the system

$$R'_r = R_{r\ own} + R_{r\ in}, \qquad \text{(XIII.10.5)}$$

where

$R_{r\ own}$ is own radiation resistance of one rhombus;

$R_{r\ in}$ is the radiation resistance induced by the adjacent rhombus.

The approximate calculations can be limited to consideration of the interaction between just the parallel conductors. The radiation resistance induced by conductor 2 in conductor 1, which is parallel to it (fig. XIII.10.2) can be calculated through the formula[1]

$$R_{12} = 60\,[M_1\cos(\alpha h + \psi) + M_2\sin(\alpha h + \psi)], \qquad \text{(XIII.10}$$

where

---

1. -h must be substituted for h when calculating the resistance induced in conductor 1 in conductor 2, which is parallel to it, through formulas (XIII.10.6 through XIII.10.8).

$$M_1 = 2\mathrm{ci}\,\alpha\left(\sqrt{\rho^2+h^2}-l\right) - \mathrm{ci}\,\alpha\left[\sqrt{\rho^2+(h+l)^2}-(h+l)\right] - \\ - \mathrm{ci}\,\alpha\left[\sqrt{\rho^2+(h-l)^2}-(h-l)\right] - \frac{\sin\alpha\left(\sqrt{\rho^2+h^2}-h\right)}{\alpha\sqrt{\rho^2+h_2}} + \\ + \frac{\sin\alpha\left[\sqrt{\rho^2+(h+l)^2}-(h+l)\right]}{2\alpha\sqrt{\rho^2+(h+l)^2}} + \frac{\sin\alpha\left[\sqrt{\rho^2+(h-l)^2}-(h-l)\right]}{2\alpha\sqrt{\rho^2+(h-l)^2}}, \qquad \text{(XIII.10.7)}$$

$$M_2 = -2\mathrm{si}\,\alpha\left(\sqrt{\rho^2+h^2}-h\right) + \mathrm{si}\,\alpha\left[\sqrt{\rho^2+(h+l)^2}-(h+l)\right] + \\ + \mathrm{si}\,\alpha\left[\sqrt{\rho^2+(h-l)^2}-(h-l)\right] - \frac{\cos\alpha\left(\sqrt{\rho^2+h^2}-h\right)}{\alpha\sqrt{\rho^2+h^2}} + \\ + \frac{\cos\alpha\left[\sqrt{\rho^2+(h+l)^2}-(h+l)\right]}{2\alpha\sqrt{\rho^2+(h+l)^2}} + \frac{\cos\alpha\left[\sqrt{\rho^2+(h-l)^2}-(h-l)\right]}{2\alpha\sqrt{\rho^2+(h-l)^2}}, \qquad \text{(XIII.10.8)}$$

ψ is the phase angle by which the current flowing in conductor 1 leads the current flowing in conductor 2.

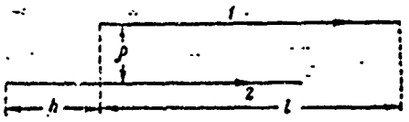

Figure XIII.10.2. Schematic diagram of the computation for the radiation resistance of a double rhombic antenna.

The efficiency of a double rhombic antenna can be computed through the formula

$$\eta = 1 - e^{-R_r'/W_r}. \qquad \text{(XIII.10.9)}$$

The directive gain can be computed through the formula

$$D = 1.64\varepsilon/\eta. \qquad \text{(XIII.10.10)}$$

Figures XIII.8.1 through XIII.8.9 use a dotted line to chart the radiation patterns of the RGD 64/4 1 antenna in the horizontal plane.

Figures XIII.10.3 through XIII.10.19 chart the radiation patterns in the horizontal plane of the RGD 65/4 1 antenna, computed for different angles of tilt of the beams for the normal (solid line) and parallel (dotted line) components of the field strength vector.

Figures XIII.8.36 through XIII.8.45 use a dotted line to chart the radiation patterns of the RGD 70/6 1.25 antenna in the horizontal plane.

Figures XIII.8.56 through XIII.8.66 use a dotted line to chart the radiation patterns of the RGD 75/6 1.25 antenna in the horizontal plane.

As will be seen from these figures, doubling the rhombic antenna results in a considerable reduction in the side lobes in the radiation patterns. The major lobe remains virtually the same as that of the single rhombic antenna.

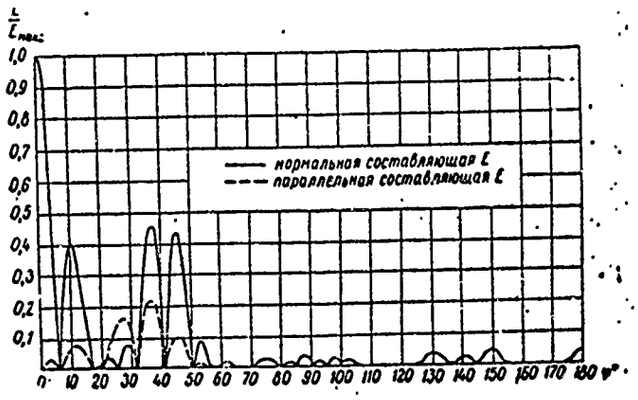

Figure XIII.10.3. Radiation patterns in the horizontal plane (Δ = 5°) of an RGD 65/4 1 antenna for wavelength $\lambda = 0.6\ \lambda_0$.

——— normal component of E;
----- parallel component of E.

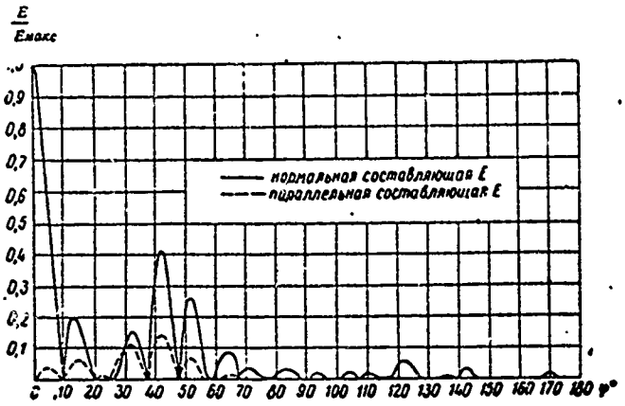

Figure XIII.10.4. Radiation patterns in the horizontal plane (Δ = 5°) of an RGD 65/4 1 antenna for wavelength $\lambda = 0.7\ \lambda_0$.

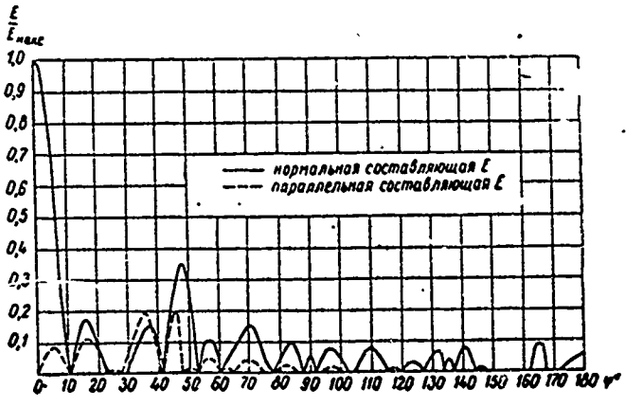

Figure XIII.10.5. Radiation patterns in the horizontal plane (Δ =10°) of an RGD 65/4 1 antenna for wavelength $\lambda = 0.8\ \lambda_0$.

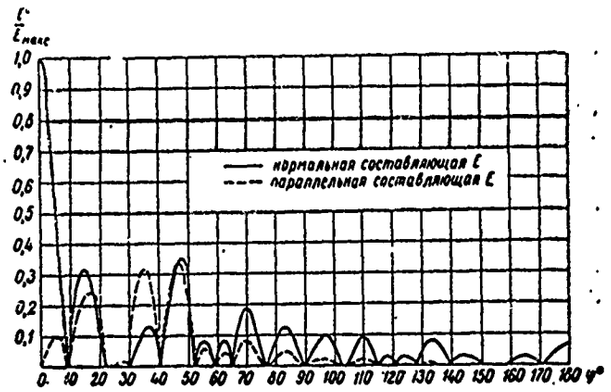

Figure XIII.10.6. Radiation patterns in the horizontal plane (Δ = 15°) of an RGD 65/4 1 antenna for wavelength $\lambda = 0.8\ \lambda_0$.

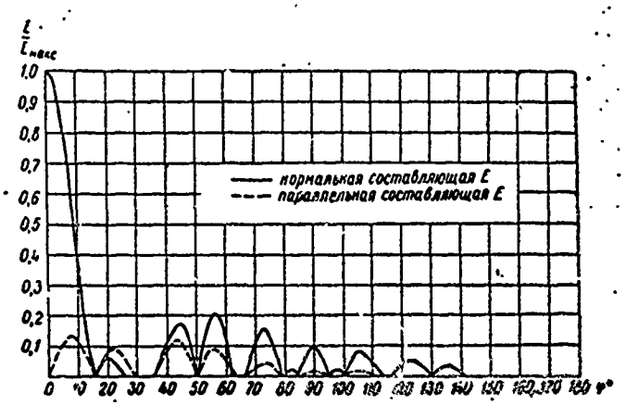

Figure XIII.10.7. Radiation pattern in the horizontal plane (Δ = 10°) of an RGD 65/4 1 antenna for wavelength $\lambda = \lambda_0$.

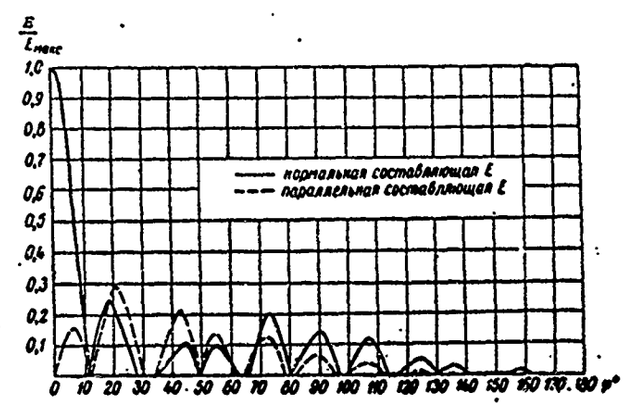

Figure XIII.10.8. Radiation patterns in the horizontal plane (Δ = 20°) of an RGD 65/4 1 antenna for wavelength $\lambda = \lambda_0$.

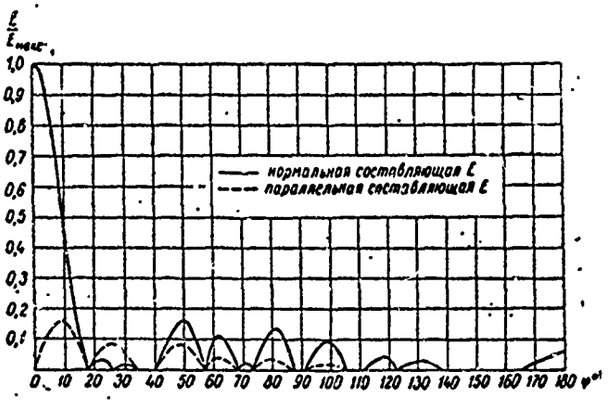

Figure XIII.10.9. Radiation patterns in the horizontal plane (Δ = 10°) of an RGD 65/4 1 antenna for wavelength $\lambda = 1.14\ \lambda_0$.

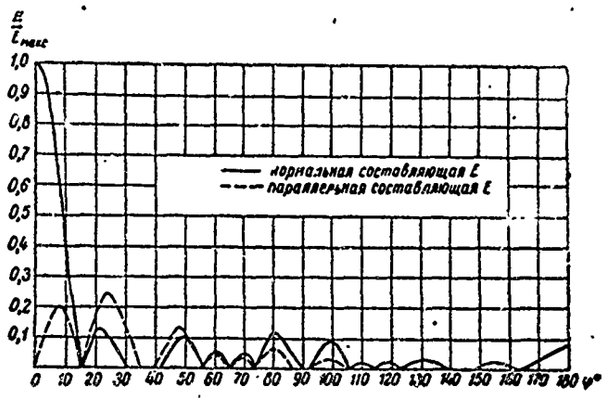

Figure XIII.10.10. Radiation patterns in the horizontal plane (Δ = 20°) of an RGD 65/4 1 antenna for wavelength $\lambda = 1.14\ \lambda_0$.

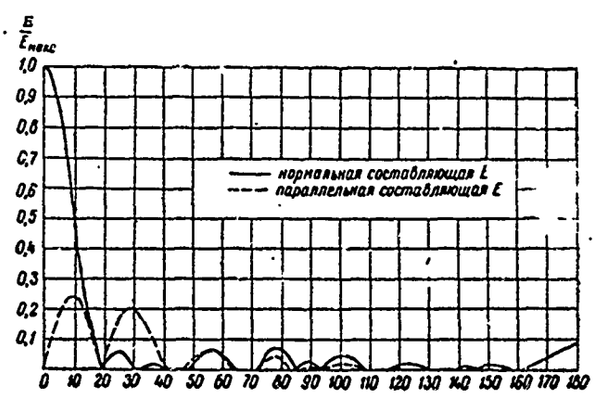

Figure XIII.10.11. Radiation patterns in the horizontal plane (Δ = 10°) of an RGD 65/4 1 antenna for wavelength $\lambda = 1.33\ \lambda_0$.

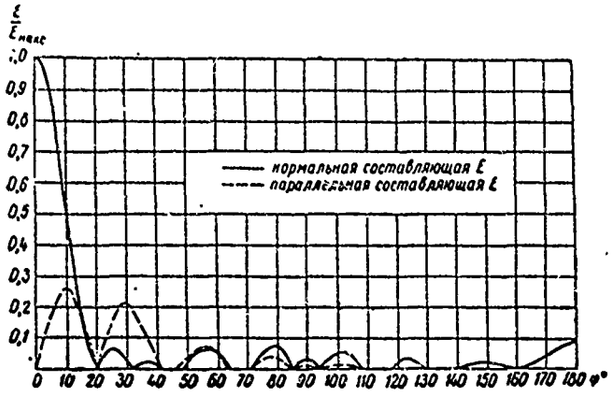

Figure XIII.10.12. Radiation patterns in the horizontal plane (Δ = 20°) of an RGD 65/4 1 antenna for wavelength $\lambda = 1.33\ \lambda_0$.

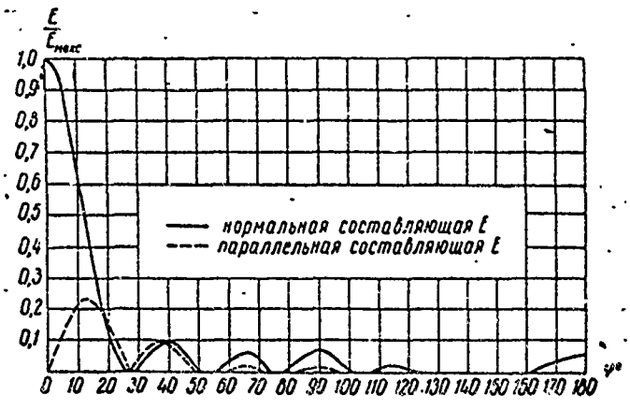

Figure XIII.10.13. Radiation patterns in the horizontal plane (Δ=10°) of an RGD 65/4 1 antenna for wavelength $\lambda = 1.6\ \lambda_0$.

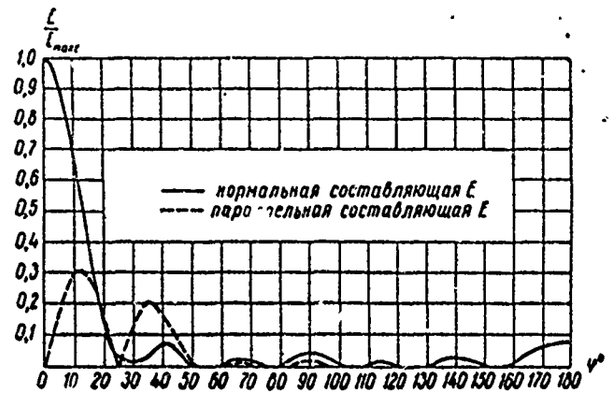

Figure XIII.10.14. Radiation patterns in the horizontal plane (Δ=20°) of an RGD 65/4 1 antenna for wavelength $\lambda = 1.6\ \lambda_0$.

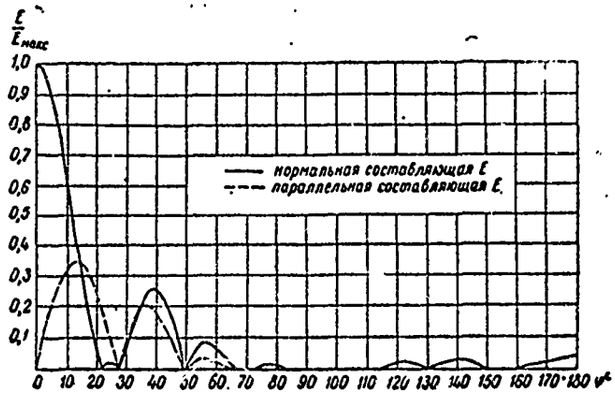

Figure XIII.10.15. Radiation patterns in the horizontal plane (Δ=10°) of an RGD 65/4 1 antenna for wavelength $\lambda = 2\lambda_0$.

Figure XIII.10.16. Radiation patterns in the horizontal plane (Δ=20°) of an RGD 65/4 1 antenna for wavelength $\lambda = 2\lambda_0$.

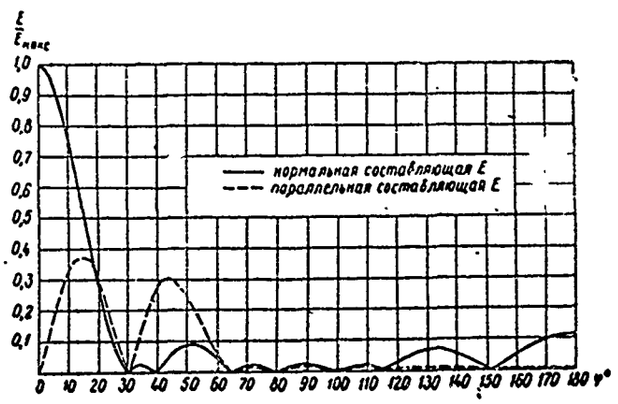

Figure XIII.10.17. Radiation patterns in the horizontal plane (Δ=30°) of an RGD 65/4 1 antenna for wavelength $\lambda = 2\lambda_0$.

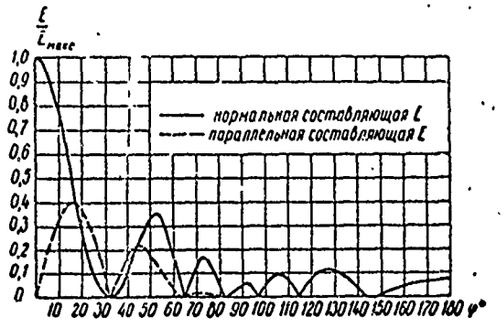

Figure XIII.10.18. Radiation patterns in the horizontal plane (Δ=20°) of an RGD 65/4 1 antenna for wavelength $\lambda = 2.5\ \lambda_0$.

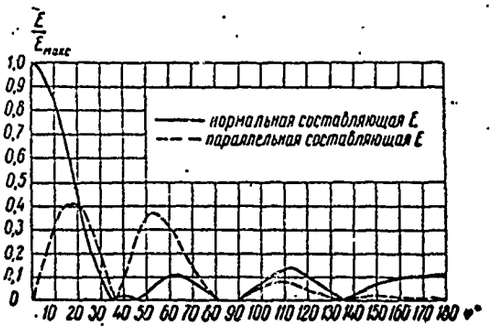

Figure XIII.10.19. Radiation patterns in the horizontal plane (Δ=40°) of an RGD 65/4 1 antenna for wavelength $\lambda = 2.5\ \lambda_0$.

Figures XIII.10.20 through XIII.10.28 chart the curves for gain factor, directive gain, and efficiency of RGD 65/4 1, RGD 70/6 1.25, and RGD 75/6 1.25 antennas.

A comparison of the curves in figures XIII.8.96 and XIII.10.20, XIII.8.99 and XIII.10.23, XIII.8.102 and XIII.10.26 reveals that the gain factor of the double rhombic antenna is 1.5 to 2 that of the gain factor of the single rhombic antenna. The increase in the gain factor of the double rhombic antenna, as compared with the single rhombic antenna, is the result of a reduction in the side lobes and an increase in efficiency.

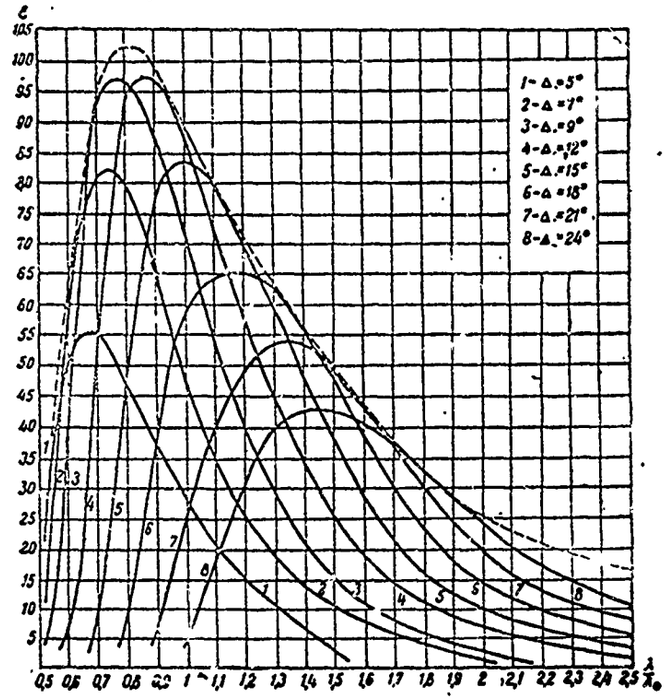

Figure XIII.10.20. Dependence of the gain of an RGD 65/4 1 antenna on the wavelength for different angles of tilt (Δ).

----- maximum gain curve.

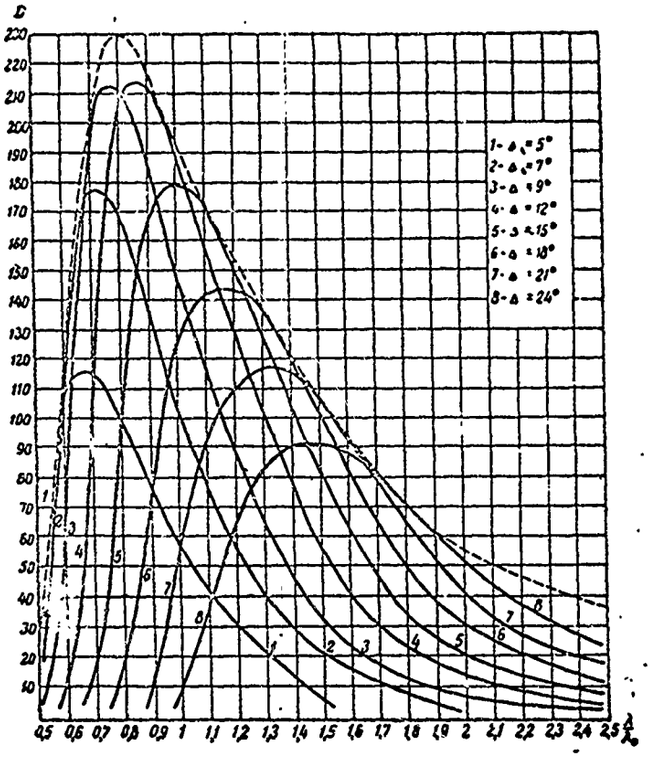

Figure XIII.10.21. Dependence of the directive gain of the RGD 65/4 1 antenna on the wavelength for different angles of tilt (Δ).

----- maximum directive gain curve.

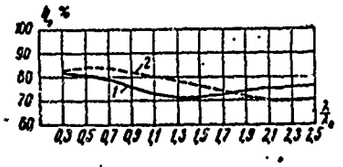

Figure XIII.10.22. Dependence of the efficiency of the RGD 65/4 1 antenna on the wavelength. W_r = 700 ohms.

1 - designed curve; 2 - experimental curve.

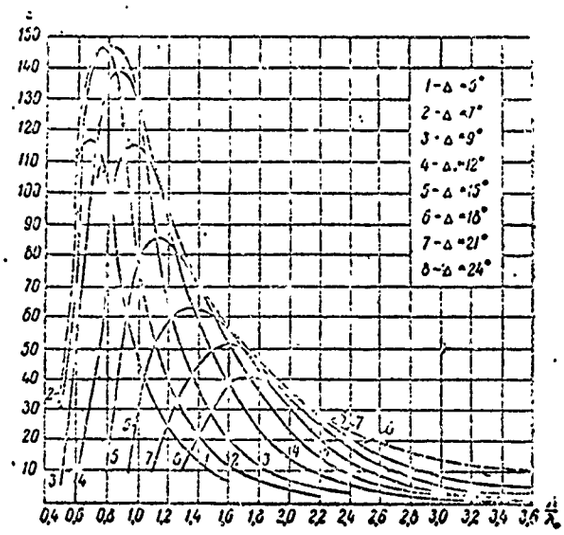

Figure XIII.10.23. Dependence of the gain of the RGD 70/6 1.5 antenna on the wavelength for different angles of tilt (Δ); W_r = 700 ohms.

----- maximum gain curve.

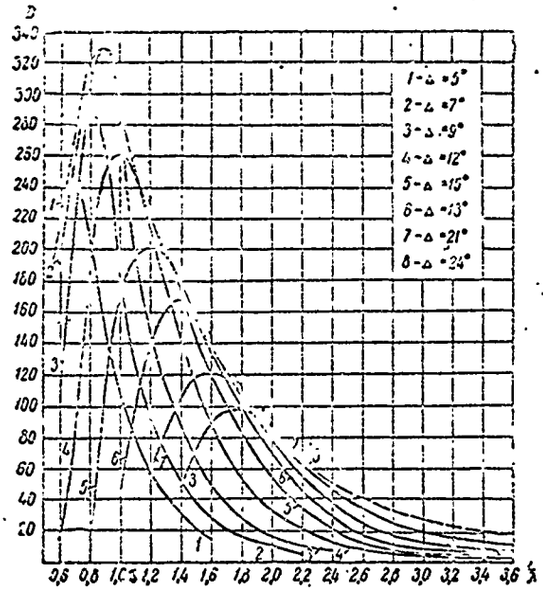

Figure XIII.10.24. Dependence of the directive gain of the RGD 70/6 antenna on the wavelength for different angles of tilt (Δ); W_r = 700 ohms.

----- maximum directive gain curve.

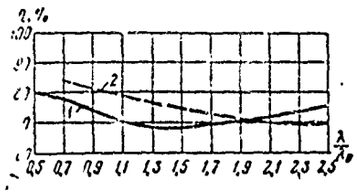

Figure XIII.10.25. Dependence of the efficiency of the RGD 70/6 1.25 antenna on the wavelength; W_r = 700 ohms.

1 - designed curve 2 - experimental curve.

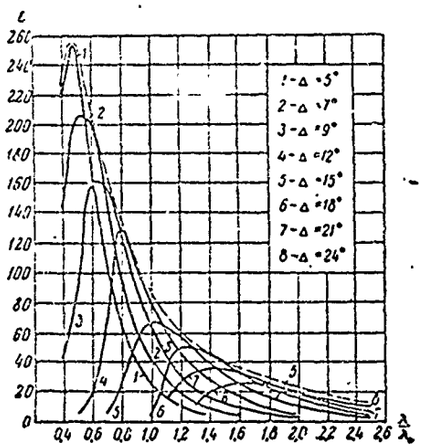

Figure XIII.10.26. Dependence of the gain of the RGD 75/6 1.25 antenna on the wavelength for different angles of tilt (Δ); W_r = 700 ohms.

----- maximum gain curve.

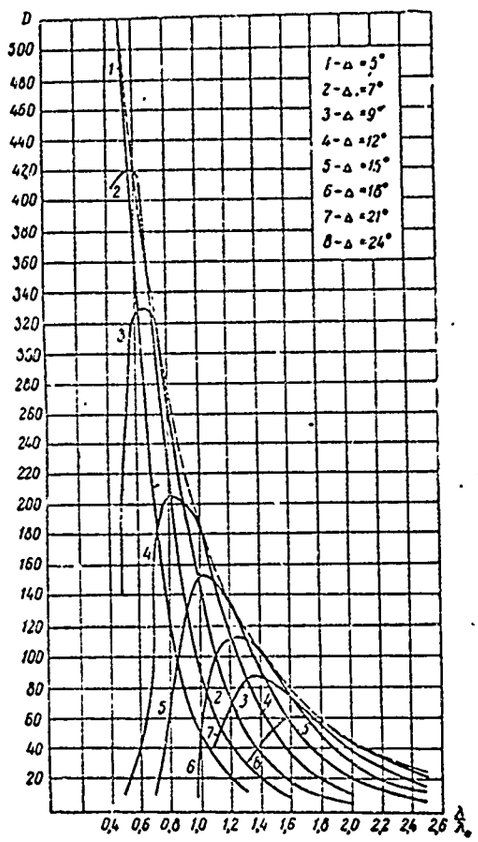

Figure XIII.10.27. Dependence of the directive gain of the RGD 75/6 1.25 antenna on the wavelength for different angles of tilt (Δ); W_r = 700 ohms.

----- maximum directive gain.

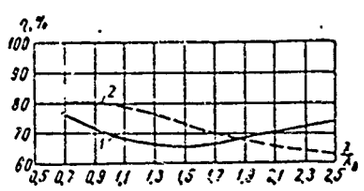

Figure XIII.10.28. Dependence of the efficiency of the RGD 75/6 1.25 antenna on wavelength; W_r = 700 ohms.

1 - designed curve; 2 - experimental curve.

#XIII.11. Two Double Rhombic Antennas

A further increase in the efficiency of rhombic antennas can be arrived at by connecting two double rhombic antennas in parallel (fig. XIII.11.1). This antenna system is designated the RGD2, to which is added numbers to show the dimensions of the rhombus.

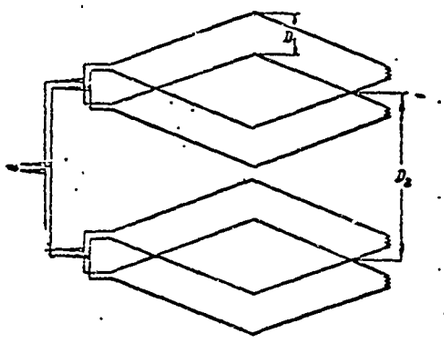

Figure XIII.11.1. Schematic diagram of the parallel connection of two double rhombic antennas.

The radiation patterns of the RGD2 antenna can be computed through the formula

$$F_4(\Delta, \varphi) = F_2(\Delta, \varphi)\cos\left(\frac{\alpha D_2}{2}\cos\Delta\sin\varphi\right), \qquad \text{(XIII.11.1)}$$

where

D_2 is the distance between the double rhombic antennas;

$F_2(\Delta,\varphi)$ is established through formula (XIII.10.1).

The radiation pattern in the horizontal plane for the angle $\Delta = 0°$ can be established through the formula

$$F_4(\varphi) = F_2(\varphi)\cos\left(\frac{\alpha D_2}{2}\sin\varphi\right). \qquad \text{(XIII.11.2)}$$

The radiation pattern in the vertical plane remains the same as it was in the case of the single rhombic antenna.

The gain factor and the directive gain of the RGD2 antenna are approximately 1.7 to 2 times those of the RGD antenna, and 2.6 to 4 times those of the RG antenna.

Figures XIII.11.2 through XIII.11.6 show a series of radiation patterns in the horizontal plane of the RGD2 65/4 1 antenna.

Two single rhombic antennas connected in parallel can also be used, and this antenna is designated the RG2.

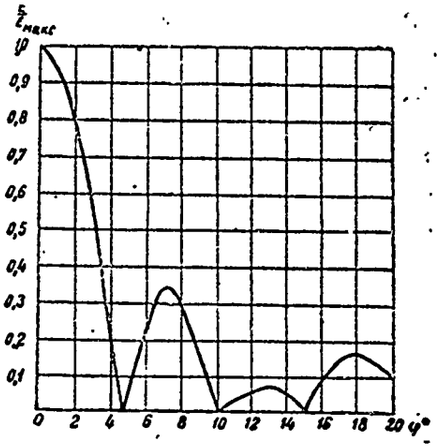

Figure XIII.11.2. Radiation pattern in the horizontal plane of an RGD2 65/4 1 antenna for wavelength $\lambda = 0.8\ \lambda_0$.

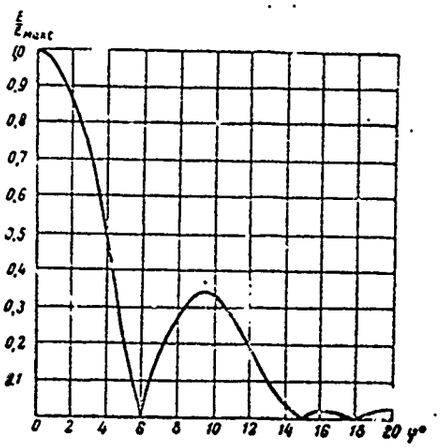

Figure XIII.11.3. Radiation pattern in the horizontal plane of an RGD2 65/4 1 antenna for wavelength $\lambda = \lambda_0$.

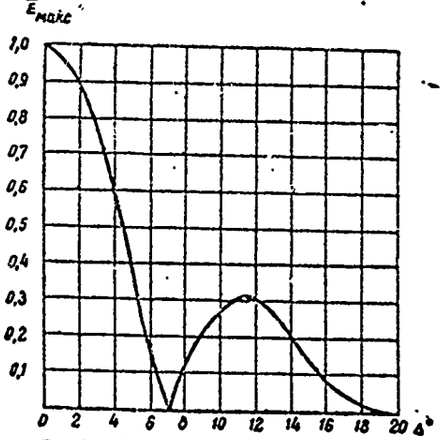

Figure XIII.11.4. Radiation pattern in the horizontal plane of an RGD2 65/4 1 antenna for wavelength $\lambda = 1.2\ \lambda_0$.

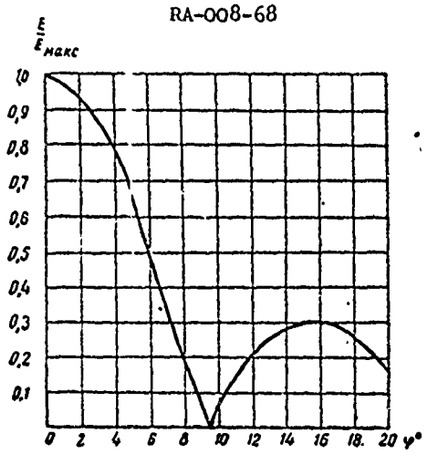

Figure XIII.11.5. Radiation pattern in the horizontal plane of an RGD2 65/4 1 antenna for wavelength $\lambda = 1.6\ \lambda_0$.

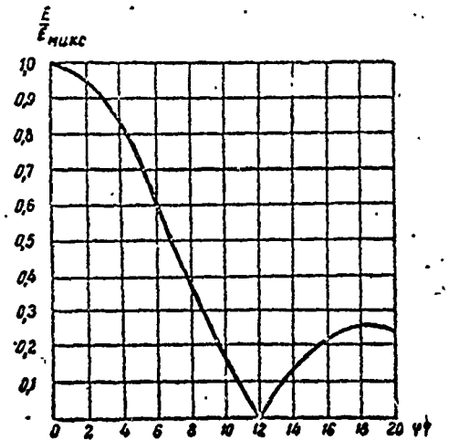

Figure XIII.11.6. Radiation pattern in the horizontal plane of an RGD2 65/4 1 antenna for wavelength $\lambda = 2\lambda_0$.

#XIII.12. Rhombic Antenna with Feedback

M. S. Neyman suggested the rhombic antenna with feedback. One version of this type of antenna is shown in Figure XIII.12.1. As we see, the antenna has no terminating resistor. The traveling wave of energy is reflected back to its input terminal after having moved down the radiating conductors of the rhombus. Given proper selection of the length of the return feeder, 3-4-1, and the relationship of the magnitudes of the characteristic impedances of the outgoing and return feeders in the system, we have a traveling wave circulating over the closed circuit 1-2-3-4-1. Analysis reveals that the following conditions are necessary, and must be adequately provided for, in order to obtain a traveling wave:

(1) total length of path 1-2-3-4-1, $L = n\lambda$ $(n = 1,2,3,\ldots)$;

(2) satisfy the relationship

$$W_1/W_r = e^{-4\beta l},$$

where

W_r is the characteristic impedance of the rhombus and return feeder;

W_1 is the characteristic impedance of the outgoing feeder, 1-2, at point 1;

$e^{-2\beta l}$ is the relationship of the voltage across the end of the rhombus to the voltage at its source in the traveling wave mode;

βl is calculated through formulas (XIII.4.6) and (XIII.10.4), presented above;

(3) no local reflections anywhere along the path over which the traveling wave is circulating.

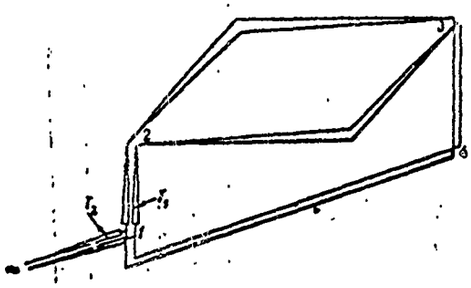

Figure XIII.12.1. Schematic diagram of a rhombic antenna with feedback. T_1 and T_2 are type TF6 225/600 and TF4 300/600 exponential transformers, respectively.

If ground, conductor, and antenna insulator losses are disregarded, and if the conditions indicated are satisfied, the efficiency equals unity.

The gain factor of an antenna with feedback, and an ideal match of all elements, equals

$$\epsilon_0 \approx \epsilon/\eta \qquad \text{(XIII.12.1)}$$

where

ϵ and η are gain factor and the efficiency of a rhombic antenna without feedback.

The actual increase in the gain factor, as demonstrated by experimental research done with rhombic antennas, is somewhat less than that obtained by calculation, obviously the result of the increase in β, primarily.

As a practical matter, however, there is no need for precise observance of condition (2) above. The magnitude of $e^{-4\beta l}$ in the range will change between 0.25 and 0.5, and if we take $W_1/W_r \approx 0.37$, good results will be obtained over the whole of the antenna's operating range.

The input impedance of an antenna with feedback equals

$$Z_{in} = W_r \frac{e^{-b}\left(1 - e^{-12\epsilon L - 4\beta l}\right)}{\left(1 + e^{-b}\right)\left(1 + e^{-12\epsilon L - 4\beta l}\right) - 4e^{-4\epsilon L - \frac{b}{2} - 2\beta l}}, \qquad \text{(XIII.12.2)}$$

where

$$e^{b} = W_r/W_1 .$$

When conditions (1) and (3) above are satisfied, the input impedance is obtained equal to

$$Z_{in} = W_r \frac{e^{-b}(1-e^{-4N})}{\left(1-e^{-2N}-\frac{b}{2}\right)^2+\left(e^{-\frac{b}{2}}-e^{-2N}\right)^2} . \qquad \text{(XIII.12.3)}$$

When conditions (1), (2), and (3), above, are satisfied,

$$Z_{in} = W_r \frac{e^{-2N}}{1-e^{-4N}} . \qquad \text{(XIII.12.4)}$$

Z_{in} is found equal to 0.57 W_r, approximately, over the entire operating range of an RG 65/4 1 antenna when conditions (1), (3), and $W_1/W_r = 0.37$ are satisfied.

Figures XIII.12.1 and XIII.12.2 show the schematic diagrams of how single and double rhombic antennas with feedback are made in practice.

Type TF4 300/600 and TF6 225/600, exponential feeder transformers, or stepped transitions, are used to satisfy the conditions necessary for a match.

Figures XIII.12.3 and XIII.12.4 show the dependence of the designed and experimental values for $\varepsilon_0/\varepsilon$ on λ/λ_0 for RG 65/4 1 and RGD 65/4 1 antennas.

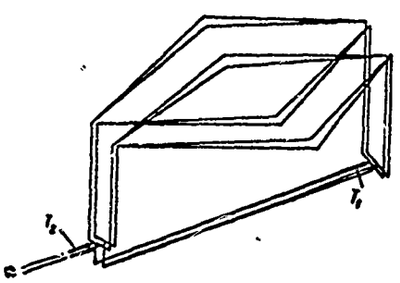

Figure XIII.12.2. Schematic diagram of a double rhombic antenna with feedback. T_1 and T_2 are type TF4 300/600 and TF6 225/600 exponential transformers, respectively.

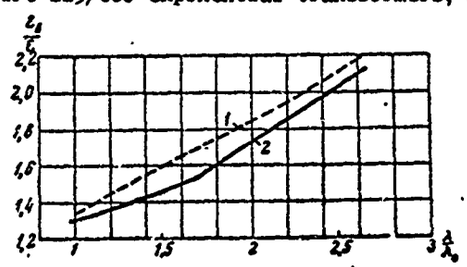

Figure XIII.12.3. Dependence of $\varepsilon_0/\varepsilon$ on λ/λ_0. 1 - designed curve; 2 - experimental curve; ε is the gain of an RG 65/4 1 antenna without feedback; ε_0 is the gain of an RG 65/4 1 antenna with feedback; λ_0 is optimum antenna wavelength.

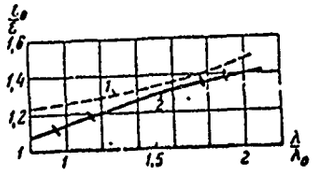

Figure XIII.12.4. Dependence of $\varepsilon_0/\varepsilon$ on λ/λ_0.

1 - designed curve; 2 - experimental curve; ε is the gain of an RGD 65/4 1 antenna without feedback; ε_0 is the gain of an RGD 65/4 1 antenna with feedback.

Figure XIII.12.5 shows the dependence of $\varepsilon_0'/\varepsilon_0$ and the traveling wave ratio (k) on the supply feeder on αl_0, where

$$l_0 = L - L_1,$$

L is the total length of the path over which the current flows for which optimum conditions prevail;

L_1 is the actual length;

ε_0' is the gain factor for the specified value of l_0;

ε_0 is the gain factor when $l_0 = 0$.

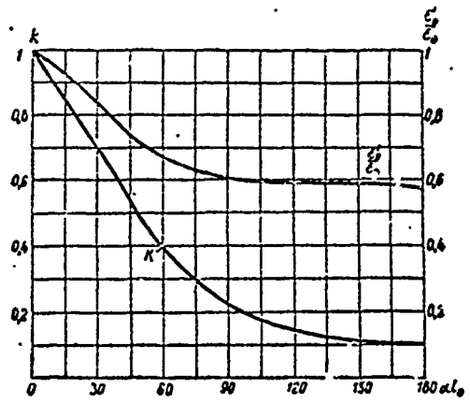

Figure XIII.12.5. Change in gain ($\varepsilon_0'/\varepsilon_0$) and traveling wave ratio (k) in the supply feeder of an RG 65/4 1 antenna with feedback for deviation in length of feedback fe[illegible] from the optimum length; l_0 is the deviation in the length of the feeder from the optimum length.

The curves in Figure XIII.12.5 characterize the criticality of tuning the rhombic antenna to the feedback.

Figure XIII.12.6 shows one of the possible convenient circuits for adjusting the length of the return feeder. The adjustment is made by changing the jumpers, 1, and the shorting plugs, K_1 and K_2. Correctness in the selection of the length of the return feeder will be established by the development of the traveling wave mode on the return feeder.

If there are two, or even three, fixed operating waves, the length of the feedback feeder can be selected such that the traveling wave mode will be

developed on all operating waves. And an increase in the gain factor will be arrived at accordingly on all operating waves as per the data in figures XIII.12.3 and XIII.12.4.

All formulas included here were derived by V. D. Kuznetsov, and he did the experimental work, the results of which are shown in figures XIII.12.3 and XIII.12.4.

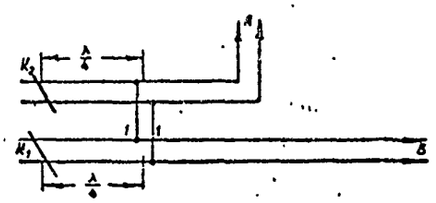

Figure XIII.12.6. Schematic diagram of feedback feeder length adjustment.

A - to input terminals of rhombus; B - to output terminals of rhombus.

#XIII.13. The Bent Rhombic Antenna

(a) Antenna arrangement

The bent rhombic antenna (RS) was proposed by V. S. Shkol'nikov and Yu. A. Mityagin. The schematic arrangement of this antenna is shown in Figure XIII.13.1, and as will be seen from this figure, the antenna has its acute and obtuse angles suspended at different heights, with the height at which the acute angles are suspended much lower than that at which the RG antenna is suspended. The reduction in the height at which the acute angles are suspended results in a considerable saving in support costs. However, this reduction in the height at which the acute angles are suspended is accompanied by a considerable deterioration in the antenna's electrical parameters. This is overcome by increasing the length of the side of the rhombus, and the height at which the obtuse angles are suspended.

Conventionally,

$$\frac{l_b}{l} \approx 1{,}5; \quad \frac{H_1}{H} \approx 0{,}5; \quad \frac{H_2}{H} \approx 1{,}25,$$

where

l_b and l are the lengths of the sides of the bent and the horizontal rhombic antennas, respectively;

H is the height at which the horizontal rhombic antenna is suspended;

H_1 and H_2 are the heights at which the acute and obtuse angles of the bent rhombic antenna are suspended, respectively.

Nevertheless, the bent rhombic antenna is very much less efficient than the horizontal rhombic antenna.

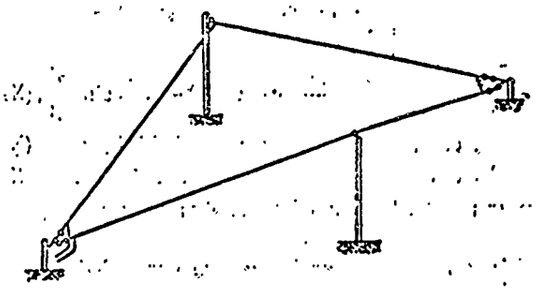

Figure XIII.13.1. Schematic diagram of the Shkol'nikov and Mityagin bent rhombic antenna.

The principal design formulas for the bent rhombic antenna follow.

(b) Radiation patterns

The radiation pattern in the horizontal plane when $\Delta = 0$ (dropping factors not dependent on φ) can be expressed through the formula

$$F(\varphi) = \left[\frac{\cos(\Phi+\varphi)}{1-\cos\Psi\sin(\Phi+\varphi)} + \frac{\cos(\Phi-\varphi)}{1-\cos\Psi\sin(\Phi-\varphi)}\right]\times \\ \times\sin\left\{\frac{\alpha l_b}{2}[1-\cos\Psi\sin(\Phi+\varphi)]\right\}\times \\ \times\sin\left\{\frac{\alpha l_b}{2}[1-\cos\Psi\sin(\Phi-\varphi)]\right\}, \tag{XIII.13.1}$$

where

Φ is half the obtuse angle between the projections of the sides of the rhombus on the horizontal plane;

φ is the azimuth angle, read from the long diameter of the rhombus;

Ψ is the angle of tilt of the sides of the rhombus to the horizontal plane.

The radiation pattern in the vertical plane ($\varphi = 0$) can be expressed through the formula

$$F(\Delta) = 4\cos\Phi\cos\Psi\left\{\frac{\sin\left[\frac{\alpha l_b}{2}(1-\cos\xi_1)\right]}{1-\cos\xi_1}\times\right. \\ \times\cos\left[\frac{\alpha l_b}{2}(1-\cos\xi_2)+\alpha H_1\sin\Delta\right]- \\ \left.-\frac{\sin\left[\frac{\alpha l_b}{2}(1-\cos\xi_2)\right]}{(1-\cos\xi_1)}\cos\left[\frac{\alpha l_b}{2}(1-\cos\xi_1)-\alpha H_1\sin\Delta\right]\right\}, \tag{XIII.13.2}$$

where

$$\cos\xi_1 = \sin\Phi\cos\Psi\cos\Delta+\sin\Psi\sin\Delta; \tag{XIII.13.3}$$

$$\cos\xi_2 = \sin\Phi\cos\Psi\cos\Delta-\sin\Psi\sin\Delta. \tag{XIII.13.4}$$

Formulas (XIII.13.1) and (XIII.13.2) are given without attenuation taken into consideration.

(c) Gain factor and directive gain. Efficiency.

The gain factor of the RS antenna is computed through the formula

$$\varepsilon = 1170\, e^{-2\beta l_c} \frac{1}{W_r} \cos^2\Phi \cos^2\Psi \times$$
$$\times \left\{ \frac{\sin\left[\frac{\alpha l_b}{2}(1-\cos\xi_1)\right]}{1-\cos\xi_1} \cos\left[\frac{\alpha l_b}{2}(1-\cos\xi_2) + \alpha H_1 \sin\Delta\right] - \right.$$
$$\left. - \frac{\sin\left[\frac{\alpha l_b}{2}(1-\cos\xi_2)\right]}{1-\cos\xi_2} \cos\left[\frac{\alpha l_b}{2}(1-\cos\xi_1) - \alpha H_1 \sin\Delta\right] \right\}^2 , \qquad \text{(XIII.13.5)}$$

where

W_r is the characteristic impedance of the RS antenna, and which remains approximately what is was for the RG antenna.

βl_b can be computed as in the case of the horizontal rhombic antenna, ignoring the mutual effect of the conductors of the rhombus and their mirror images. Available experimental data confirm the admissibility of this approximate computation.

The directive gain and efficiency are computed through formulas (XIII.5.6) and (XIII.6.5).

Figures XIII.13.2 through XIII.13.10 show a series of radiation patterns of the RS 67/6 0.5/1.25 antenna; that is, of an antenna with the following characteristics: $\Phi = 67°$, $l_b/\lambda_0 = 6$, $H_1/\lambda_0 = 0.5$, $H_2/\lambda_0 = 1.25$.

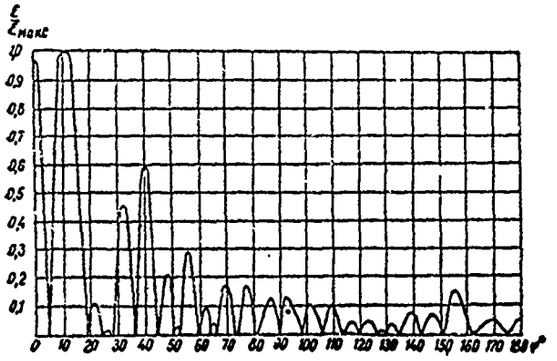

Figure XIII.13.2. Radiation pattern in the horizontal plane of an RS 67/6 0.5/1.25 antenna for a wavelength of $\lambda = 0.75\ \lambda_0$.
Vertical: E/E_{max}.

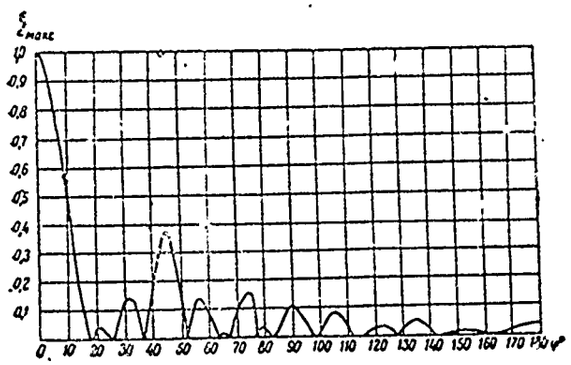

Figure XIII.13.3. Radiation pattern in the horizontal plane of an RS 67/6 0.5/1.25 antenna for a wavelength of $\lambda = 1.5\ \lambda_0$.

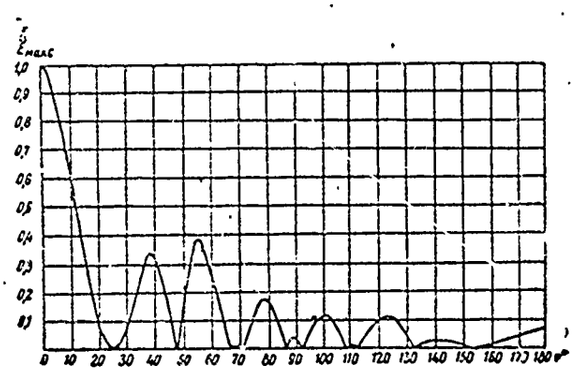

Figure XIII.13.4. Radiation pattern in the horizontal plane of an RS 67/6 0.5/1.25 antenna for a wavelength of $\lambda = 2\ \lambda_0$.

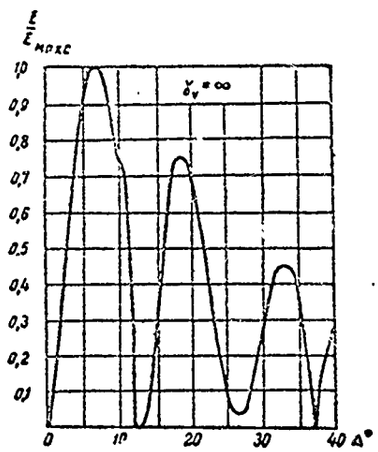

Figure XIII.13.5. Radiation pattern in the vertical plane of an RS 67/6 0.5/1.25 antenna for ground with ideal conductivity ($\gamma_v = \infty$); $\lambda = 0.75\ \lambda_0$.

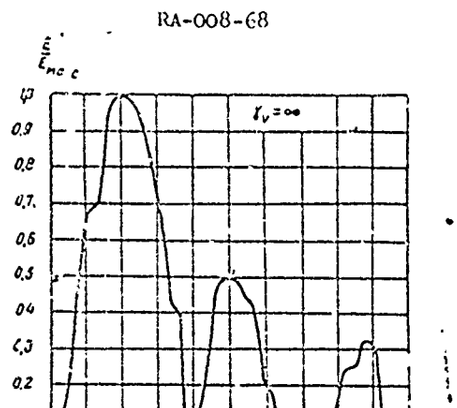

Figure XIII.13.6. Radiation pattern in the vertical plane of an RS 67/6 0.5/1.25 antenna for ground with ideal conductivity ($\gamma_v = \infty$); $\lambda = \lambda_0$.

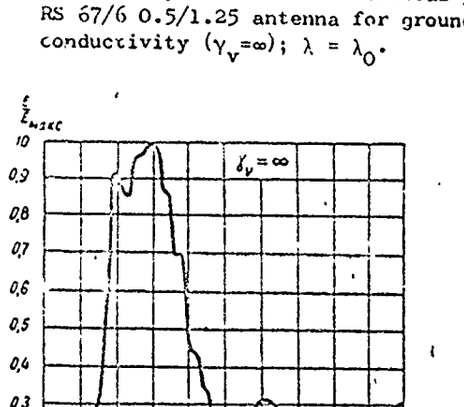

Figure XIII.13.7. Radiation pattern ir the vertical plane of an RS 67/6 0.5/1.25 antenna for ground with ideal conductivity ($\gamma_v = \infty$); $\lambda = 1.25\ \lambda_0$.

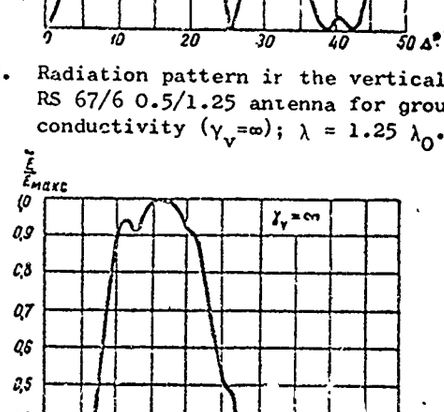

Figure XIII.13.8. Radiation pattern in the vertical plane of an RS 67/6 0.5/1.25 antenna for ground with ideal conductivity ($\gamma_v = \infty$); $\lambda = 1.5\ \lambda_0$.

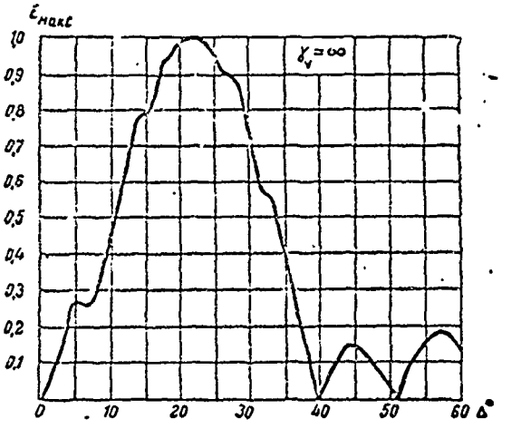

Figure XIII.13.9. Radiation pattern in the vertical plane of an RS 67/6 0.5/1.25 antenna for ground with ideal conductivity ($\gamma_v=\infty$); $\lambda = 2\ \lambda_0$.

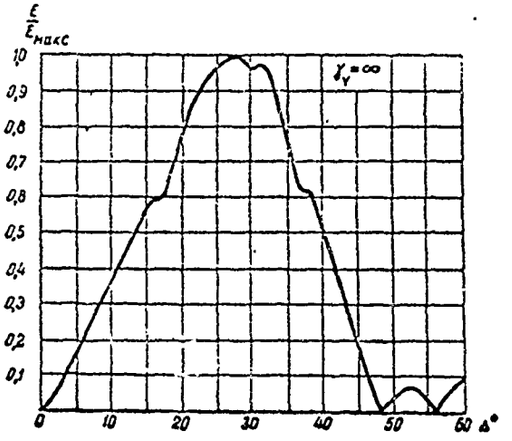

Figure XIII.13.10. Radiation pattern in the vertical plane of an RS 67/6 0.5/1.25 antenna for ground with ideal conductivity ($\gamma_v=\infty$); $\lambda = 2.5\ \lambda_0$.

Figures XIII.13.11 and XIII.13.12 show a series of curves characterizing the dependence of ε and D for the RS 67/6 0.5/1.25 antenna on λ/λ_0 and Δ.

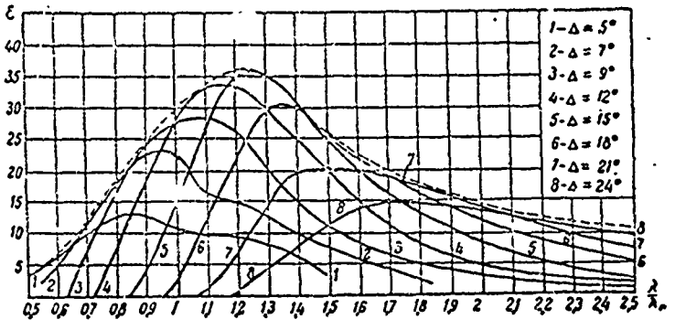

Figure XIII.13.11. Dependence of gain of an RS 67/6 0.5/1.25 antenna on wavelength for various angles of tilt (Δ).

----- maximum gain curve.

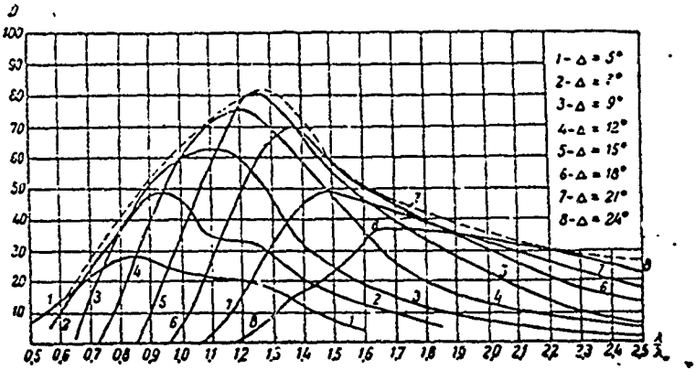

Figure XIII.13.12. Dependence of the directive gain of an RS 67/6 0.5/1.25 antenna on the wavelength for various angles of tilt (Δ).

----- maximum directive gain curve.

Radiation patterns in the vertical plane, as well as the gain factors and directive gain have all been computed for the case of ground with ideal conductivity.

Bent rhombic antennas can also be made double (RSD). In such case the separation between the doubled rhombuses is taken as equal to $\sim 0.2\ l_b$.

A complex antenna, comprising two double bent rhombic antennas (RSD2), can also be made. The relative increase in the gain factor and directive gain provided by RSD and RSD2 antennas as compared with the RS antenna, is approximately the same as that provided by the corresponding variants of horizontal rhombic antennas.

#XIII.14. Suspension of Rhombic Antennas on Common Supports

In cases of emergency, when it is necessary to string a great many rhombic antennas in a radio transmitting center and when the size of the antenna field is limited, two rhombic antennas, designed for day and night operation, can be strung over a common area on separate, or common, supports (fig. XIII.14.1).

Experimental research has developed the fact that as a result of the mutual effect, parameters of antennas strung over a common area differ from those of the same antennas installed over different areas. Fringe radiation levels are increased when two antennas are strung together.

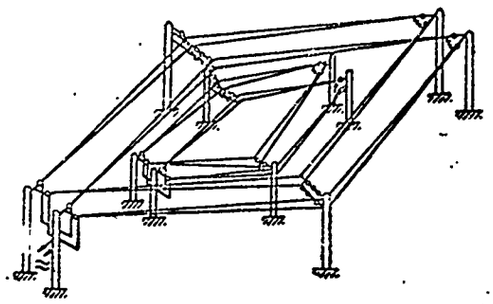

Figure XIII.14.1. Sketch of a decimeter model for testing rhombic antennas strung over a common area.

Figure XIII.14.2 shows the experimental curves characterizing the maximum reduction in the gain factor of an RG 65/4 1 antenna, computed for an optimum wave of 20 meters, when it is strung in the same area with an RG 65/4 1 antenna computed for an optimum wave of 40 meters.

Figure XIII.14.3 shows similar curves for an RGD 65/4 1 antenna.

Figure XIII.14.4 shows the curves characterizing the maximum reduction in the gain factor of an RG 70/6 1.25 antenna, computed for an optimum wave of 18 meters, when it is strung in the same area with an RG 65/4 1 antenna computed for an optimum wave of 40 meters. Figure XIII.14.5 shows similar curves for the RGD 70/6 1.25 antenna.

Maximum reduction in the gain factor for decimeter models is found as follows. A rhombic antenna with a shorter optimum wave is fed from a generator. An indicator is set up in front of the antenna at the corresponding height (Δ). The indicator is read when there is no antenna with a longer optimum wave (parasitic antenna). A parasitic antenna is then strung. A shorting plug is installed in the feeder to this antenna. The shorting plug is shifted along the feeder. The indicator reading is recorded for each position of the shorting plug, and the position of the shorting plug providing minimum indicator reading is established.

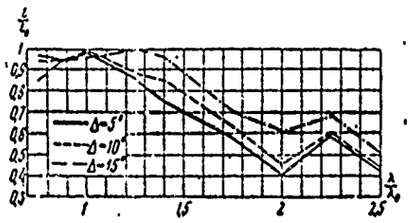

Figure XIII.14.2. Dependence of the $\varepsilon/\varepsilon_0$ ratio on the λ/λ_0 ratio. ε is the gain of an RG 65/4 1 antenna for optimum wave λ_0 (small rhombus) when strung in a common area with an RG 65/4 1 antenna for optimum wave $2\lambda_0$ (large rhombus); ε_0 is the gain of an RG 65/4 1 antenna (small rhombus) strung in a separate area.

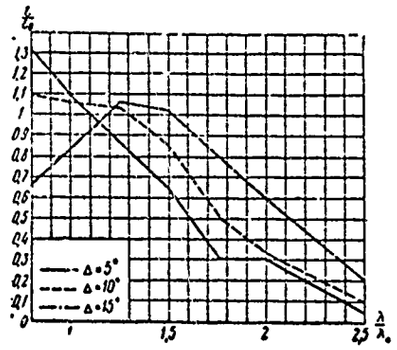

Figure XIII.14.3. Dependence of the $\varepsilon/\varepsilon_0$ ratio on the λ/λ_0 ratio. ε is the gain of an RGD 65/4 1 antenna for optimum wave λ_0 (small rhombus) when strung in a common area with an RGD 65/4 1 antenna for optimum wave $2\lambda_0$ (large rhombus); ε_0 is the gain of an RGD 65/4 1 antenna (small rhombus) strung in a separate area.

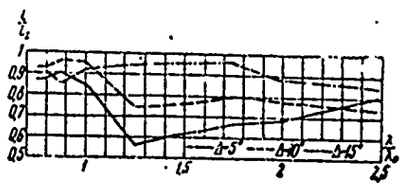

Figure XIII.14.4. Dependence of the $\varepsilon/\varepsilon_0$ ratio on the λ/λ_0 ratio. ε is the gain of an RG 70/6 1.25 antenna for optimum wave λ_0 (small rhombus) when strung in a common area with an RG 70/6 1.25 antenna for optimum wave 2.2 λ_0 (large rhombus); ε_0 is the gain of an RG 70/6 1.25 antenna (small rhombus) strung in a separate area.

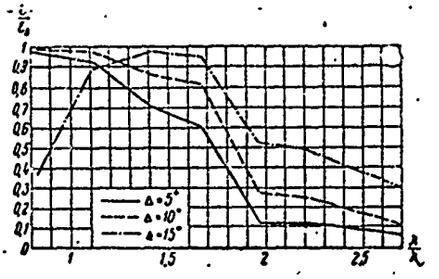

Figure XIII.14.5. Dependence of the $\varepsilon/\varepsilon_0$ ratio on the λ/λ_0 ratio. ε is the gain of an RGD 70/6 1.25 antenna for optimum wave λ_0 (small rhombus) when strung in a common area with an RGD 70/6 1.25 antenna for optimum wave 2.2 λ_0 (large rhombus); ε_0 is the gain of an RGD 70/6 1.25 antenna strung in a separate area.

The gain factor ratio, $\varepsilon/\varepsilon_0$, is established through the formula

$$\frac{\varepsilon}{\varepsilon_0} = \left(\frac{E_{min}}{E_0}\right)^2 \frac{P_0}{P}, \qquad \text{(XIII.14.1)}$$

where

E_0 is the field strength in the absence of a parasitic rhombus;

E_{min} is the minimum field strength when a parasitic rhombus is installed;

P_0 is the power fed to the antenna in the absence of the parasitic rhombus;

P is the power fed to the antenna when the parasitic rhombus is installed.

As will be seen from figures XIII.14.2 through XIII.14.5, when two rhombic antennas are strung over a common area the maximum reduction in the gain factor of a rhombic antenna is obtained at heights corresponding to the comparatively low intensity of antenna radiation. At heights corresponding to the antenna's maximum radiation the reduction in the gain factor obtained is slight. This indicates that when two antennas are suspended on common supports there is not too much distortion in the radiation patterns.

Measurements have revealed that when two antennas are strung over a common area the gain factor of the antenna with the longer optimum wave is practically unchanged.

#XIII.15. Design Formulation of Rhombic Antennas

(a) Formulation of the antenna curtain

The theoretical data presented above were derived on the assumption that the characteristic impedance of the rhombic antenna remains constant over the entire length of the antenna. This is not so in practice. Inconstancy in the characteristic impedance in turn results in inconstancy in the distance between the sides of the rhombus. The characteristic impedance

at the obtuse angles equals ~ 1000 ohms, that at the acute angles from 700 to 800 ohms.

The sides of the rhombus are made of two divergent conductors (fig. XIII.15.1), in order to equalize the characteristic impedance. The distance between them at the obtuse angles of the rhombus is equal to from 0.02 to 0.03λ. The characteristic impedance of this rhombic antenna is more uniform over the entire length, and is equal to ~700 ohms.

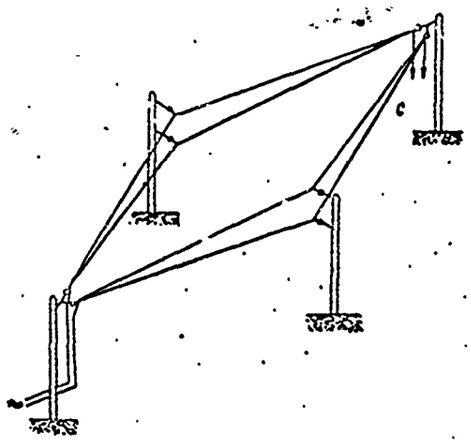

Figure XIII.15.1. Rhombic antenna, sides of which are made using two conductors.

Making the sides of the rhombus with two conductors, and thus reducing the characteristic impedance, also results in increasing the efficiency and the gain factor.

The data on efficiency and gain factor cited above refer to the rhombic antenna, the sides of which are made of two conductors. The single-conductor rhombic antenna has a gain factor 10 to 15% lower than that of the rhombic antenna made of two conductors. The directive gain is practically the same for both variants of the rhombic antenna.

(b) Terminating resistor design

The efficiency of rhombic antennas is in the 0.5 to 0.8 range. Anywhere from 50 to 20% of the power fed to the antenna will be lost in the terminating resistor. This must be taken into consideration when the type of terminating resistor used is under consideration.

Special mastic resistors can be used as the terminating resistor with low powered transmitters [P = (1-3) kw]. With high powered transmitters, and often with low powered ones, the terminating resistor will be in the form of a long steel or high-resistance alloy conductor.

The length of the dissipation line is selected such that current amplitude is attenuated to 0.2 to 0.3 its initial magnitude as it flows along the line.

The input impedance of this line is close to its characteristic impedance. The characteristic impedance of the dissipation line is usually made equal to 300, or 600 ohms. The length of lines made of steel conductors is what provides the required attenuation, equal to 300 to 500 meters. The length of the high-resistance alloy line is taken as equal to 30 to 40 meters.

The dissipation line is stretched under the rhombus, along its long diagonal. For reasons of economy in the use of support poles, the steel dissipation line is made in several loops, suspended on common poles.

The dissipation line must be made absolutely symmetrical with respect to the sides of the rhombus in order to avoid high induced currents.

The resistance per unit length of a two-conductor dissipation line can be computed through the formula

$$R_1 = \frac{11 \cdot 10^3}{r} \sqrt{\frac{\mu_r \rho}{\lambda}} \quad \text{(ohms/meter)},$$

where

r is the radius of the conductor used in the line, in mm;

μ_r is the relative permeability. At high frequencies the permeability of steel and high-resistance alloy equals $\mu_r \approx 80$;

ρ is the specific resistance (for steel $\rho = 10^{-7}$ ohms/meter, for high-resistance alloy $\rho = 8 \cdot 10^{-7}$ ohms/meter);

λ is the wavelength in meters.

The radius of the conductors used in the dissipation line is taken equal to 1 to 2 mm.

(c) Matching the rhombic antenna with the feeder and terminating resistor

The characteristic impedance of one rhombic antenna can be matched with the characteristic impedances of the feeder and the dissipation line, 600 ohms, quite well. No transitional devices are required between the single rhombic antenna and the feeder, or dissipation line.

The characteristic impedance of the double rhombic antenna is 300 to 350 ohms. Used to match it with a feeder with a characteristic impedance of 600 ohms is an exponential four-wire feeder transformer with a resistance transformation ratio of 300/600.

The type TF4 300/600 40 transformer is used for this feeder transformer in the case of the antenna with a maximum operating wave of 50 to 60 meters, while the type TF4 300/600 60 is used with antennas operating on longer waves. Step transitions (see Chapter II) can also be used.

Figures XIII.15.2, XIII.15.3, XIII.15.4 and XIII.15.5 show sketches of RG 65/4 1, RGD 65/4 1, RGD2 tr/4 and RS 67/6 0.5/1.25 antennas. Basic structural details of the antennas are indicated in the sketches.

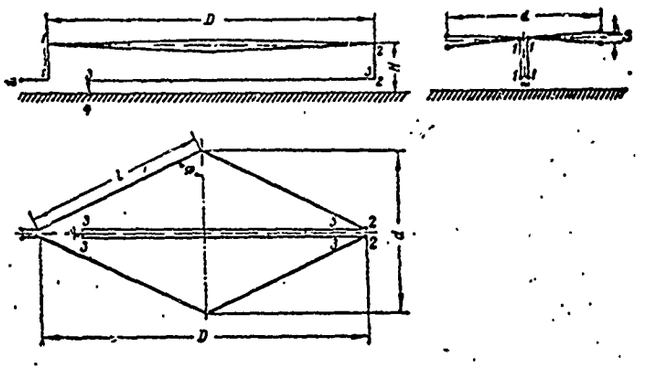

Figure XIII.15.2. Sketch of an RG 65/4 1 antenna.

Designations: H - average height at which antenna conductors are suspended; $H=\lambda_0$, $l=4\lambda_0$, $d=3.38\lambda_0$, $D=7.25\lambda_0$, S=2.5 to 3 m, $\phi=65°$; 1-1 - antenna supply feeder; 2-2 - dissipation line feeder; 3-3 - dissipation line; 4 - dissipation line ground. Antenna conductor diameter is at least 4 mm. Characteristic impedance of dissipation line approximately 600 ohms.

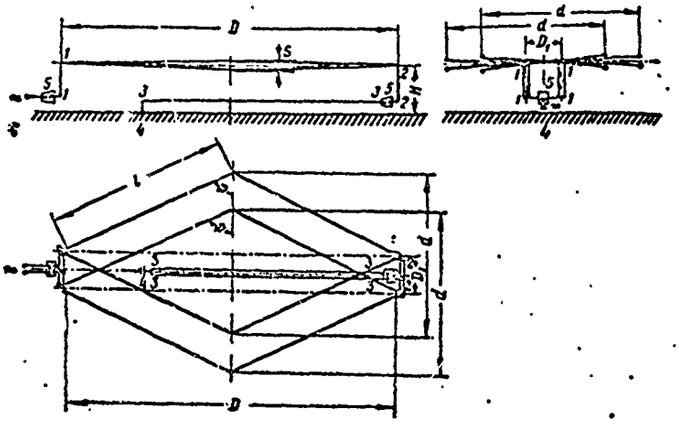

Figure XIII.15.3. Sketch of an RGD antenna.

The dimensions of RG antennas which form the RGD antenna are in accordance with the data cited in Figure XIII.15.2. Designations: $D_1=(0.8 \text{ to } 1)\lambda_0$; 1-1 - antenna supply feeder; 2-2 - dissipation line feeder; 3-3 - dissipation line; 4 - dissipation line ground; 5 - exponential feeder transformer.

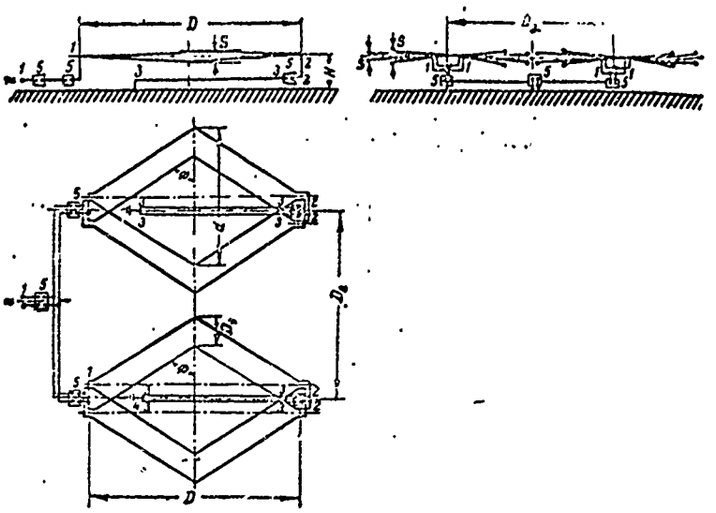

Figure XIII.15.4. Sketch of an RGD2 antenna.

The dimensions of RGD antennas which form the RDG2 antenna are in accordance with the data cited in figures XIII.15.2 and XIII.15.3. Designations: $D_2=d+(1.1 \text{ to } 1.2)D_1$; $D_1=(0.8 \text{ to } 1)\lambda_0$; 1-1 - antenna supply feeder; 2-2 - feeder to dissipation line; 3-3 - dissipation line; 4 - dissipation line ground; 5 - exponential feeder transformer.

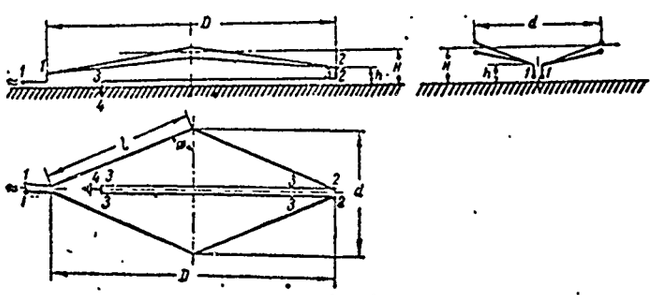

Figure XIII.15.5. Sketch of an RS 67/6 0.5/1.25 antenn

Designations: $H=1.25\ \lambda_0$; $h=0.5\ \lambda_0$; $l=\ \lambda_0$; $d=4.7\lambda_0$; $D=11.06\lambda_0$; $\phi=67°$; 1-1 - antenna supply feeder; 3-3 - dissipation line; 4 - dissipation line grou

The schematic diagrams for the formation of the RSD and RSD2 antennas from the RS antennas are simil to those for forming RGD and RGD2 antennas from RG antenna.

(d) Supports for suspending a rhombic antenna

Supports for use in suspending rhombic antennas can be wooden, or metal. When metal masts are set up at the obtuse angles they should be s 5 to 6 meters from the apex of the angle to avoid inducing high currents in

the masts. The field radiated by the induced currents interacts with the main field and can cause a marked reduction in antenna efficiency. Excitation of the supports can also cause a substantial reflection of energy at the obtuse angles of the rhombus.

The reasons cited are why it is undesirable to suspend basket cables on masts installed at the obtuse angles of the rhombus. It is also extremely undesirable to use lift cables at the obtuse angles. It is desirable to dead-end the rhombus to the mast at the obtuse angles.

#XIII.16. Rhombus Receiving Antennas

The data presented above with respect to the electrical parameters of rhombic transmitting antennas apply equally to rhombic receiving antennas.

An additional parameter, characterizing the quality of the rhombic receiving antenna is the effective length, established through the formula

$$l_{eff} = \frac{\lambda}{\pi}\sqrt{\frac{W_F}{73,1}}. \qquad \text{(XIII.16.1)}$$

Figure XIII.16.1 shows the curve for the dependence of l_{eff} on λ/λ_0 for the RG 65/4 1 antenna, computed for an optimum wave of 25 meters. The curve was plotted as applicable to the maximum gain factor and for a feeder with a characteristic impedance of 208 ohms.

The effective length can be obtained quite readily for the RG 65/4 1 antennas designed for optimum waves different from 25 meters by multiplying values for l_{eff} taken from the curve in Figure XIII.16.1 by $\lambda_0/25$.

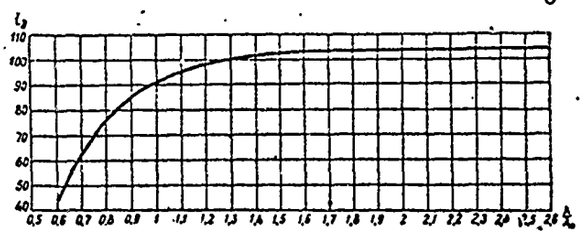

Figure XIII.16.1. Dependence of effective length of the RG 65/4 1 antenna on λ/λ_0 (λ_0 = 25 meters). Transmission line characteristic impedance W_F = 208 ohms.

Let us pause to consider some of the features involved in designing rhombic receiving antennas.

The sides of the rhombic transmitting antenna are made of two conductors in order to improve the match to the feeder and to increase the gain factor. In the case of the rhombic receiving antenna neither the increase in the gain nor improvement in the match are very substantial, so the sides of the rhombic receiving antenna can be made with one conductor. However, it is better to make the sides of the rhombus with two conductors.

The terminating resistor for the rhombic receiving antenna can be made of thin, high-ohmic wire because the currents flowing in this antenna are not very high. The wire usually used is one with a linear resistance of 400 to 600 ohms/meter, double wound to reduce the inductive component of the impedance. The terminating resistor is made as shown in Figure XIII.16.2 in order to reduce the shunt capacitance of the winding. It is better to use mastic terminating resistors with a very low reactive component of the impedance. These are ceramic tubes with a very thin conducting layer (made of graphite, for example) on the outer surface. This latter is, in turn, coated with a thin, protective lacquer coating. The terminating resistors are installed in air-tight boxes. The magnitude of the terminating resistor is taken equal to 600 to 700 ohms.

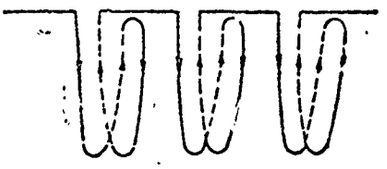

Figure XIII.16.2. Schematic diagram of the coiling of the terminating resistor of a rhombic receiving antenna.

High currents can be induced in the antenna during thunderstorms and this can cause burning of the terminating resistor. It is desirable to connect the terminating resistor to the antenna through the feeder, as shown in Figure XIII.16.3, since this makes it convenient to replace the resistor if it is burned. The characteristic impedance of this feeder should equal 600 to 700 ohms.

It is desirable to review the lightning protection provided the terminating resistor (fig. XIII.16.4). The chokes and dischargers for lightning protection can be made in the same way as are those for polyplexers and lead-ins (see Chapter XIX).

A dissipation line, which requires no special lightning protection, can be used as a dependable terminating resistor. A small diameter (1 to 1.5 mm) conductor can be used to make a dissipation line for a receiving antenna, and the length of a steel line can be cut to 120 to 150 meters. This dissipation line can be made in the form of several loops, 30 to 40 meters long, suspended on common poles. The dissipation line can also be made of high resistance alloy conductor, and when the diameter is 1 mm the line length should be on the order to 20 to 40 meters.

The characteristic impedance of the line should equal 600 to 650 ohms. The end of the dissipation line should be grounded.

The transmission line for a rhombic receiving antenna can be made of a four-wire crossed line with a characteristic impedance of 208 ohms. An

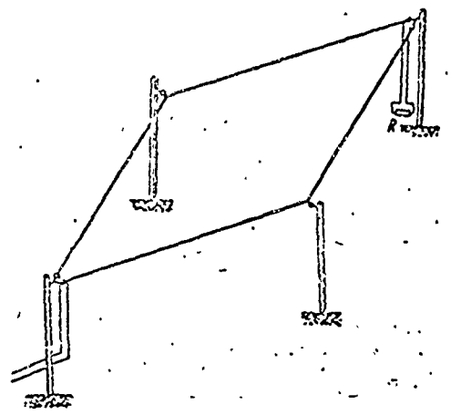

Figure XIII.16.3. Schematic diagram of how the terminating resistor (R) is inserted in a rhombic antenna at a height which can be reached from the ground.

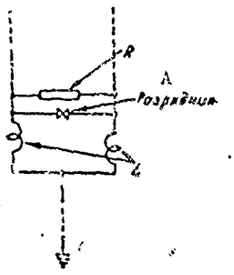

Figure XIII.16.4. Schematic diagram of the lightning protection for a terminating resistor.

R - terminating resistor; L - coil for draining off static charges. A - discharger.

exponential feeder transformer can be used to match the four-wire line to the antenna, and is usually made in two sections, a vertical and a horizontal (fig. XIII.16.5). The vertical section is a two-wire exponential transmission line, TF 700/350, of length

$$l = H - h,$$

where

H is the height at which the rhombus is suspended;

h is the height at which the transmission line is suspended.

The horizontal section is a four-wire crossed exponential transmission line, TF4P 340/208, 30 meters long. Design-wise, the TF4P exponential transmission line is a straight line continuation of the transmission line. A description, and the schematics of the TF 700/350 and TF4P 340/208 transmission lines, are given below.

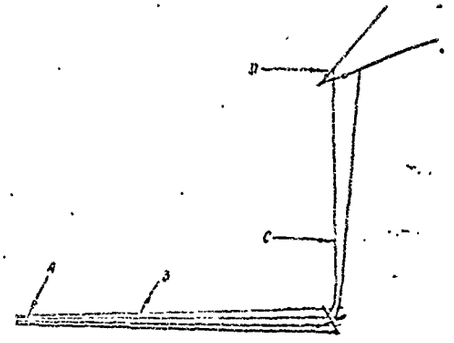

Figure XIII.16.5. Schematic diagram of the matching of a rhombic receiving antenna to a four-wire transmission.

A - four-wire transmission; B - TF4P 340/208 transmission; C - TF2 700/350 transmission; D - acute angle of the rhombus.

Double rhombic receiving antennas are connected to the transmission line through an exponential feeder, TF4P 300/208.

Step transitions can also be used to match the rhombic antenna to the transmission line.

Chapter XIV

TRAVELING WAVE ANTENNAS

#XIV.1. Description and Conventional Designations

The traveling wave antenna is a broadband antenna, and is ordinarily used for reception. Figure XIV.1.1 shows the schematic diagram of the antenna, and as will be seen is made up of balanced dipoles connected to a collection line at equal intervals through a coupler (Z_{couple}). Pure resistance, R_n, equal to the line's characteristic impedance is connected across the end of the collection line facing the correspondent being received. The other end of the collection line goes to the receiver.

The traveling wave antenna is usually suspended horizontally, 16 to 40 meters above the ground. The antenna is about 100 meters long. The number of dipoles, their length, the characteristic impedance of the collection line, as well as the resistance of the couplings, are all selected in order to satisfy the condition of obtaining the optimum parameters within the limits of the widest possible waveband. As will be shown in what follows, when pure resistance is selected for use as the coupling it is possible to use one antenna to cover the entire shortwave band.

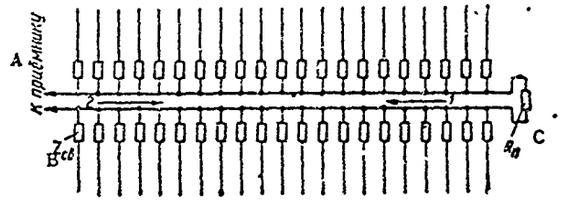

Figure XIV.1.1. Schematic diagram of a traveling wave antenna.
A - to receiver; B - coupling element, $Z_{c\phi}$;
C - pure resistance.

Two, or four, parallel connected traveling wave antennas are often used to improve directional properties. Figure XIV.1.2 is a sketch of a traveling wave antenna array comprising two identical antennas connected in parallel. A further improvement in the directional properties can be obtained by positioning several traveling wave antennas one after the other (in tandem), as shown in Figure XIV.1.3. Each of the identical antennas is connected to the receiver by its own feeder, the length of which is selected such that the emfs produced at the receiver input by the antennas are in phase, or very nearly so. This arrangement in connecting the antennas makes it possible to control the receiving pattern in the vertical plane by using phase shifters (see below).

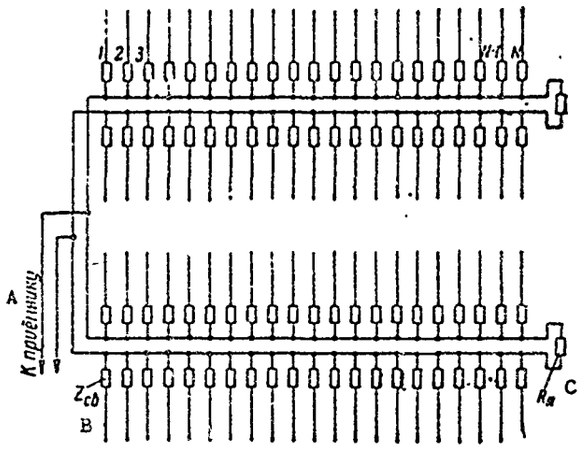

Figure XIV.1.2. Schematic diagram of a multiple traveling wave antenna.

A - to receiver; B - coupling element, Z_{co}; C - pure resistance.

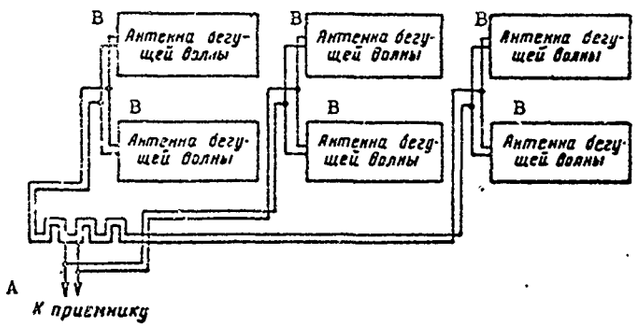

Figure XIV.1.3. Schematic diagram of a multiple traveling wave antenna with a controlled reception pattern in the vertical plane.

A - to receiver; B - traveling wave antenna.

The traveling wave antenna is designated by the letter The second letter in the antenna designator shows the nature of the decoupling resistor. If pure resistance is used for the decoupling resistors, the antenna is designated by the letters BS. If reactance is used for the decoupling resistors the designation is BYe (capacitive) or BI (inductive).

The number of traveling wave antenna connected in parallel is designated by a number following the antenna's conventional designation. For example, a traveling wave antenna array comprising two parallel connected antennas with pure resistance couplings is designated BS2. When antennas are positioned in tandem the number of antennas installed one after the other is designated a number placed in front of the antenna designation.

Corresponding numerical designations are added to the conventional designation to show the antenna's basic characteristics. The complete conventional designation for the traveling wave antenna with pure resistance couplings can be described by the following

$$\text{BS } N/\ell\ R/\ell_1\ H,$$

where

N is the number of balanced dipoles in one antenna curtain;

ℓ is length of one arm of a balanced dipole, in meters;

R is the resistance of the coupling connected in one arm of a dipole, in ohms;

ℓ_1 is the distance between adjacent dipoles, in meters;

H is the height at which the antenna is suspended, in meters.

If the antenna uses reactance for coupling the R in the conventional designation is replaced by the magnitude of the capacitance of the coupling in centimeters (the CYe antenna), or by the magnitude of the inductance in microhenries (BI antenna).

For example, BYe2 21/8 15/4.5 16 designates a traveling wave antenna comprising two parallel connected antennas with capacitance coupling, the data for which are: N = 21, ℓ = 8 meters; ℓ_1 = 4.5 meters; C_1 = 15 centimeters; H = 16 meters; where C_1 is the capacitance of the condenser connecting each arm of the dipole to the collection line.

#XIV.2. Traveling Wave Antenna Principle

Balanced dipoles receive electromagnetic energy. The emf induced in the dipoles by the incoming wave produces a voltage across the collection line.

An equivalent schematic of a traveling wave antenna can be presented as shown in Figure XIV.2.1, where the balanced dipole has been replaced by a source of emf, e, and impedances Z_d and $2Z_{co}$, where

Z_d is the input resistance of the dipole;

$2Z_{co}$ is the resistance of two series-connected couplings.

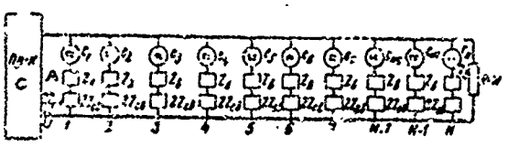

Figure XIV.2.1. Equivalent schematic diagram of a traveling wave antenna.

e - source of emf; A - Z_d, dipole input resistance; B - $2Z_{co}$, resistance of two series-connected coupling elements; C - receiver.

The summed resistance $(Z_d + 2Z_{co})$ is usually a great deal higher than the characteristic impedance of the collection line, while the distance between dipoles is small compared to the wavelength. Given these conditions, the collection line can be considered to be a line with uniformly distributed constants, that is, as a line with constant characteristic impedance.

The effect of the dipoles on the propagation factor in the first approximation can be reduced to a change in the distributed constants for the collection line. The input conductance of the dipole and coupling, equal to $1/Z_d + 2Z_{co}$, can conventionally be taken as uniformly distributed over the entire space between two adjacent dipoles, and the additional distributed conductance of the line, determined by the effect of the dipoles, is obtained equal to

$$\frac{1}{(2Z_{co} + Z_d)l_1}.$$

Since the resistances induced in the different dipoles are different, the characteristic impedance of the line changes somewhat from dipole to dipole. However, this need not be taken into consideration when explaining the antenna's operating principle, so the characteristic impedance, and the phase velocity, are taken as constant along the entire length of the antenna.

Let us consider the operation of one emf source, e_3, for example. Emf e_3 produces some voltage, U_3, across the collection line, and this voltage causes two waves of current to flow on the line, one of which is propagated toward the receiver, the other toward the terminating resistor. In accordance with the assumption made with respect to the fact that the collection line can be considered a system with constant characteristic impedance, both waves of current will not be reflected over the entire propagation path from their points of origin to the ends of the line. The wave propagated toward the terminating resistor has no effect on the receiver. Reception strength is determined by the wave directed toward the receiver input. All the other dipoles in the antenna function similarly. The total current at the receiver input is determined by the relationship of the phases of the currents which are originated by the individual emf sources.

Let us look at the case when the direction of propagation of the incoming beam coincides with the direction in which the collection line is oriented, as indicated by arrow 1 in Figure XIV.1.1. Let us now explain the relationship of the phases of the currents from two emfs, e_3 and e_6, for example. The phase angle between the currents at the receiver input from sources e_3 and e_6 equals

$$\psi = \psi_e + \psi_i,$$

where

ψ_e is the phase angle between e_3 and e_6;

ψ_i is the phase angle developed because the currents from sources e_3 and e_6 flow along paths of different lengths.

In the case specified e_6 leads e_3, and

$$\psi_e = 3\alpha l_1; \quad \psi_i = -\frac{\alpha}{k_1} 3l_1;$$

$$k_1 = \frac{v}{c},$$

where

v is the phase velocity of propagation of the electromagnetic wave along the line;

c is the speed of light.

Substituting the values for ψ_e and ψ_i, we obtain

$$\psi = 3\alpha l_1 \left(1 - \frac{1}{k_1}\right).$$

The lag between the currents from any two dipoles, the spacing between which is distance nl_1, equals

$$\psi_n = n\alpha l_1 \left(1 - \frac{1}{k_1}\right).$$

If the magnitude of k_1 is close to unity this lag is very small. Accordingly, if the phase velocity of propagation of the current along the collection line differs but slightly from the speed of light, the currents from all dipoles will be close to being in phase at the receiver input, thus providing effective reception of beams propagated in the direction of arrow 1.

The current phase relationships between the individual dipoles at the receiver input are less favorable when the directions of an incoming beam differ from that reviewed. By way of illustration, let us take a case when the direction of the incoming beam is opposite to that in the case reviewed (arrow 2 in fig. XIV.1.1). We will, in this case, look into the relationship between the current phase relationships for the third and sixth dipoles. As before, the phase angle equals

$$\psi_3 = \psi_e + \psi_i,$$

$$\psi_i = -\frac{\alpha}{k_1} 3l_1.$$

Since e_3 leads e_6 in this case,

$$\psi_e = -3\alpha l_1.$$

Total lag equals

$$\psi = -3\alpha l_1 \left(1 + \frac{1}{k_1}\right).$$

The lag between the currents for any two dipoles at distance nl_1 from each other equals $\psi_n = n\alpha l_1 (1 + 1/k_1)$.

As will be seen, very large phase angles can result. The relationship between the phases of the currents for individual dipoles will become unfavorable and the reception strength will be very much less than in the first case.

What has been said demonstrates that when the number of dipoles is sufficiently large, and when the curtain is of sufficient length, the antenna will have sharply defined directional properties if phase velocity of propagation along the line is close to the speed of light.

#XIV.3. Optimum Phase Velocity of Propagation

The phase velocity of propagation of a wave on a collection line is a highly important parameter, one with a decisive effect on the property of the traveling wave antenna. The connection between the phase velocity of propagation and the magnitude of the directive gain, D, can be characterized by the curves presented in Figure XIV.3.1 (see, for example, G. Z. Ayzenberg, Ultrashort Wave Antennas, Chapter X. Svyaz'izdat, 1957). This figure shows the dependence of the relative magnitude of the directive gain D/D_0 on the magnitude

$$A = \alpha L\left(\frac{1}{k_1} - 1\right), \qquad \text{(XIV.3.1)}$$

which characterizes the phase velocity, v, of the propagation of a wave on the collection line. In formula (XIV.3.1) L is the length of the antenna, and $k_1 = v/c$. The data presented in Figure XIV.3.1 characterize the directional properties of an antenna made up of nondirectional elements.

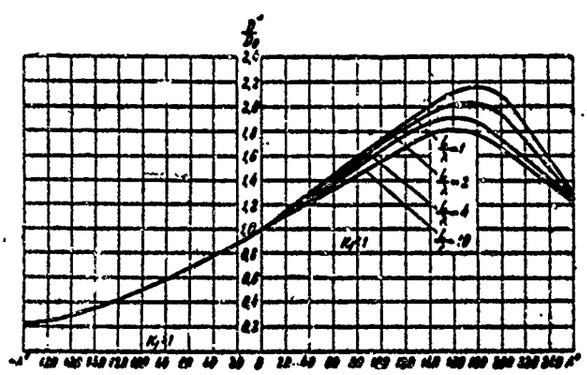

Figure XIV.3.1. Dependence of relative directive gain D/D_0 on A; D_0 is the directive gain when A = 0 (v = c).

The curves shown in Figure XIV.3.1 were calculated through the formula[1]

1. Derivation is given in G. Z. Ayzenberg, Ultrashort Wave Antennas, Svyaz'izdat, 1957.

$$D = 2\pi L \frac{1-\cos A}{A^2 I}, \qquad \text{(XIV.3.2)}$$

where

$$I = \frac{1-\cos A}{A} + \frac{1-\cos B}{B} + \mathrm{si}B - \mathrm{si}A, \qquad \text{(XIV.3.3)}$$

$$B = \alpha L \left(\frac{1}{k_1} + 1\right). \qquad \text{(XIV.3.4)}$$

The magnitude A is the lag between the currents created by the emfs induced in the first (closest to the receiver) and last dipoles at the receiver input when a wave propagated in the direction of arrow 1 (fig.XIV.1.1) is received. D_0 is the directive gain for the in-phase addition of the currents flowing in all dipoles at the receivwr input ($v = c$; $k_1 = 1$).

Positive values of A correspond to a phase velocity of propagation, v, on an antenna at less than the speed of light ($k_1 < 1$). Negative values of A correspond to a phase velocity, v, at greater than the speed of light. This phase velocity can be obtained by using an inductive coupling between the dipoles and the collection line.

Increase in directive gain with reduction in phase velocity as compared with the speed of light is the result of the narrowing of the major lobe of the reception pattern. The directive gain reaches a maximum approximately double the D_0 value when $A \approx 180°$. This mode is characterized by currents at the receiver input caused to flow by the emfs induced in the first and last dipoles that are opposite in phase. The receiving pattern of an antenna operating in this mode ($A = 180°$) has a comparatively narrow major lobe. The side lobes are somewhat larger than is the case when $k_1 = 1$. With further reduction in phase velocity the major lobe narrows even more, but the side lobe level increases to the point where there is a reduction in the directive gain.

The reduction in the directive gain when there is an increase in phase velocity with respect to the speed of light is the result of the expansion and splitting in two of the major lobe. At increased phase velocity ($k_1 > 1$) the direction of the maximum radiation from the antenna does not coincide with its axis.

By way of illustration of what has been said, Figure XIV.3.2 shows three receiving patterns charted for the case when $L = 4\lambda$ and for three values of k_1. The pattern in Figure XIV.3.2a was charted for the optimum value of k_1, established from the equality $A = 180°$, that is,

$$k_{1\ \mathrm{opt}} = \frac{2L}{2L + \lambda} \qquad \text{(XIV.3.5)}$$

which yields a magnitude $k_{1\ \mathrm{opt}} = 0.89$ when $L = 4\lambda$.

The pattern in Figure XIV.3.2b was charted for $k_1 = 1$ (v = c), while that in Figure XIV.3.2c was charted for $k_1 = 1/0.89 = 1.12$. This k_1 value corresponds to A = -180°.

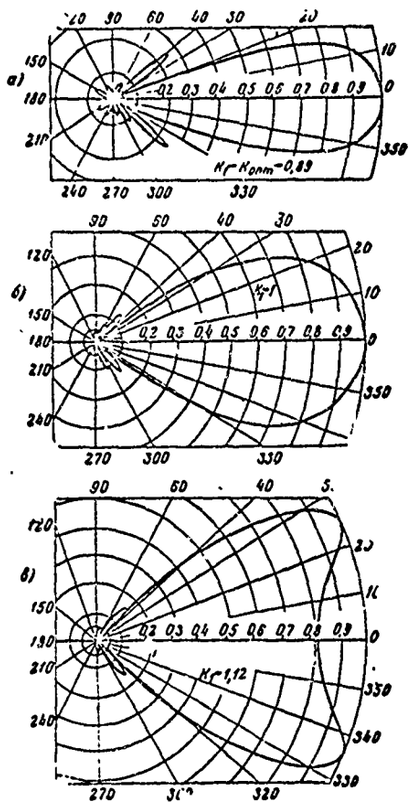

Figure XIV.3.2. Reception patterns of a traveling wave antenna for a wavelength of 4λ for different magnitudes of k_1 = v/c.

The curves shown in figures XIV.3.1 and XIV.3.2 were charted without taking the directional properties of the antenna elements into consideration. At the same time, the increase in the directive gain with decrease in the phase velocity can be limited by the growth in the side lobes. If the directional properties of the dipoles, which cause a reduction in the side lobes are taken into consideration, the optimum value of A can be increased.

Figures XIV.3.3 through XIV.3.6 show the dependence of the directive gain of a traveling wave antenna on the magnitude of A for cases when the directional properties of the antenna element can be described by the equality

$$F(\theta) = \sqrt{\cos\theta};\ F(\theta) = \cos\theta;\ F(\theta) = \cos^2\theta,$$

where θ is the angle between the axis of the antenna and the direction from which the beam is arriving. Data are cited for the cases when $L = \lambda$, $L = 2\lambda$, $L = 4\lambda$, and $L = 10\lambda$. The dependence of the directive gain on A for an antenna the elements of which are nondirective, is plotted on these curves for purposes of comparison. D_0 is the directive gain of the antenna when $k_1 = 1$ and $F(\theta) = 1$, in the curves shown in figures XIV.3.3 through XIV.3.6.

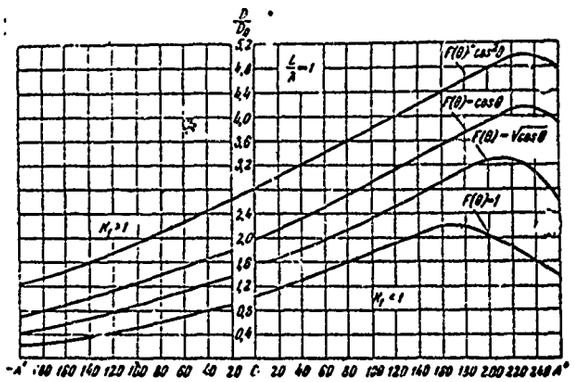

Figure XIV.3.3. Dependence of relative directive gain of a traveling wave antenna D/D_0 on A for different directional properties of antenna elements; D_0 is the directive gain of the antenna when $A = 0$ and $F(\theta) = 1$.

The curves shown in figures XIV.3.3 through XIV.3.6 were calculated through the formulas[1]

for the case when $F(\theta) = \sqrt{\cos\theta}$

$$D = 2(\alpha L)^2 \frac{1-\cos A}{A^2 I_1}, \qquad \text{(XIV.3.6)}$$

where

$$I_1 = C\left[\frac{1-\cos A}{A} + \frac{1-\cos B}{B} - 2\frac{1-\cos C}{C} - \right.$$
$$\left. - \operatorname{si} A - \operatorname{si} B + 2\operatorname{si} C\right] + \ln\frac{AB}{C^2} - \operatorname{ci} A - \operatorname{ci} B + 2\operatorname{ci} C, \qquad \text{(XIV.3.7)}$$

$$B = \alpha L\left(\frac{1}{k_1} + 1\right), \quad C = \alpha L\frac{1}{k_1}; \qquad \text{(XIV.3.8)}$$

for the case when $F(\theta) = \cos\theta$

$$D = 2(\alpha L)^2 \frac{1-\cos A}{A^2 I_2}, \qquad \text{(XIV.3.9)}$$

where

$$I_2 = \frac{2(A+\alpha L)^2}{AB} + \frac{(A+\alpha L)^2}{\alpha L}\left(\frac{\cos B}{B} - \frac{\cos A}{A} + \operatorname{si} B - \operatorname{si} A\right) -$$
$$- \frac{2(A+\alpha L)}{\alpha L}\left(\ln\frac{B}{A} - \operatorname{ci} B + \operatorname{ci} A\right) + 2 - \frac{\sin B - \sin A}{\alpha L}; \qquad \text{(XIV.3.10)}$$

1. Formulas (XIV.3.6, XIV.3.9 and XIV.3.11) were derived in G. Z. Ayzenberg's article "The Traveling Wave Antenna with Resistive Coupling Elements," in Radiotekhnika, Vol. 14, No. 6, 1959.

for the case when $F(\theta) = \cos^2\theta$

$$D = 2(\alpha L)^2 \frac{1-\cos A}{A^2 I_3}, \qquad \text{(XIV.3.11)}$$

where

$$I_3 = \frac{2(A+\alpha L)^4}{(\alpha L)^2 AB} + \frac{(A+\alpha L)^4}{(\alpha L)^3}\left(\frac{\cos B}{B} - \frac{\cos A}{A} + \operatorname{si} B - \operatorname{si} A\right) - 4\frac{(A+\alpha L)^3}{(\alpha L)^3}\left(\ln\frac{B}{A} - \operatorname{ci} B + \operatorname{ci} A\right) + 6\left(\frac{A+\alpha L}{\alpha L}\right)^2\left(2 - \frac{\sin B - \sin A}{\alpha L}\right) - \frac{4(A+\alpha L)}{(\alpha L)^2}\left(\frac{B^2-A^2}{2} - \cos B + \cos A + B\sin B - A\sin A\right) + \frac{1}{(\alpha L)^3}\left[\frac{B^3-A^3}{3} - 2B\cos B + 2A\cos A - (B^2-2)\sin B + (A^2-2)\sin A\right]. \qquad \text{(XIV.3.12)}$$

As will be seen from the curves in figures XIV.3.3 through XIV.3.6, the calculation of the directional properties of the antenna elements results in an increase in the optimum value of A, as well as to some increase in the gain as compared with the case of $F(\theta) = 1$.

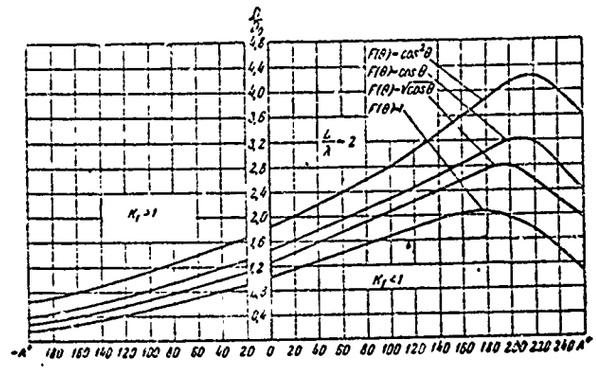

Figure XIV.3.4. Dependence of the relative directive gain of a traveling wave antenna D/D_0 on A for different directional properties of the antenna elements; D_0 is the directive gain of the antenna when $A = 0$ and $F(\theta) = 1$.

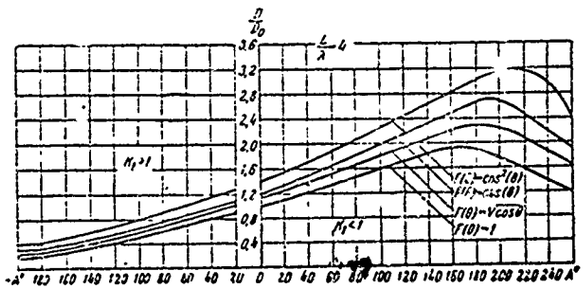

Figure XIV.3.5. Dependence of the relative directive gain of a traveling wave antenna D/D_0 on A for different directional properties of the antenna elements; D_0 is the directive gain of the antenna when $A = 0$ and $F(\theta) = 1$.

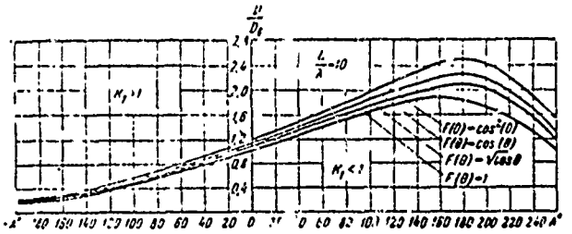

Figure XIV.3.6. Dependence of the relative directive gain of a traveling wave antenna D/D_0 on A for different directional properties of the antenna elements; D_0 is the directive gain of the antenna when A = 0 and $F(\theta) = 1$.

The data cited above are for the case when the receiving patterns of the antenna elements have axial symmetry. The reception patterns of the dipoles of a traveling wave antenna do not have axial symmetry. Nevertheless, the curves shown in figures XIV.3.3 through XIV.3.6 characterize the properties of this antenna.

The curves obtained for $F(\theta) = \sqrt{\cos\theta}$ characterize the D/D_0 ratio for a traveling wave antenna made of short dipoles in free space. The pattern of short dipoles in the principal E plane (the plane passing through the dipoles) can be established by the factor $F(\theta) = \cos\theta$, while the pattern in the principal H plane (the plane normal to the axes of the dipoles) is a circle, $F(\theta) = 1$. Property-wise, this antenna approaches that consisting of dipoles, the patterns of which have axial symmetry and can be described by the function

$$F(\theta) = \sqrt{\cos\theta}.$$

If the ground effect is taken into consideration the dipoles take on directional properties in the principal H plane as well. Antenna patterns charted with the ground effect considered do not have axial symmetry, but in some range of the H/λ ratio (H is the height of suspension above the ground) the magnitude of D/D_0 for the antenna satisfactorily characterizes the curves computed for the case $F(\theta) = \cos\theta$.

A traveling wave antenna consisting of two arrays side by side, suspended at the same height and connected in parallel, can be considered as a single traveling wave antenna made up of twin dipoles with increased directivity in the principal E plane. And if the effect of the ground is taken into consideration the directional properties of the antenna as a whole can be satisfactorily characterized by the curves for $D/D_0 = f(A)$, obtained for the case

$$F(\theta) = \cos^2\theta.$$

#XIV.4. Selection of the Coupling Elements Between Dipoles and Collection Line

The data cited demonstrate the undesirability of using an inductive coupling between the dipoles and the collection line (BI antennas) because when such coupling is used the phase velocity obtained is greater than the speed of light for virtually the entire range of the antenna.

Of the two other possible types of resistances for couplings, capacitive and resistive, the latter, as suggested by the author, is the more preferable, and the reasoning is as follows.

(1) The directive gain of traveling wave antennas decreases with increase in the wavelength, as it does in other types of antennas. It is therefore of the utmost importance to increase the directive gain at the long wave edge of the band, for it is here that the input resistances of the dipoles have a capacitive aspect, making it possible to obtain a mode close to the optimum (A = 180° to 230°). However, when a capacitive element is used for the coupling (insertion of a small capacitance in series with the dipoles), the equivalent capacitance of the dipole is extremely low and the phase velocity obtained is considerably higher than that corresponding to the optimum mode. With pure resistance as the coupling the capacitive load on the dipole provides a phase velocity close to the optimum at the long wave edge of the band.

(2) The capacitance of the coupling increases linearly as the waves are lengthened. This results in a drop in efficiency approximately proportional to the square of the wavelength, while the gain drops in proportion to the square of the wavelength. If the normal reduction in the gain, approximately proportional to the ratio $(L/\lambda)^2$,[1] is taken into consideration, antennas with capacitive coupling will show a reduction in gain over a considerable portion of the band approximately proportional to the fourth power of the wavelength.

When pure resistance is used, the coupling does not depend on the frequency, and the drop in the gain with lengthening of the waves is comparatively slow (approximately inversely proportional to λ^2; see below).

Complex impedance will provide some improvement in antenna parameters, but such improvement does not justify the complicated antenna design needed.

What has been said demonstrates the desirability of using traveling wave antennas with pure resistances for coupling (BS antennas), so our

1. The traveling wave antenna in free space has a gain proportional to the first power of the L/λ ratio. Ground effect however, causes the gain to fall approximately in proportion to $(L/\lambda)^2$ at the necessary angles of tilt.

primary attention will be given to these antennas. But since there are a great many BYe antennas in use at the present time, we will include materials on antennas of this type as well.

#XIV.5. The Calculation of Phase Velocity, v, Attenuation β_c and Characteristic Impedance W on the Collection Line.

Analysis of the formulas for calculating the phase velocity v, and attenuation β on the collection line will make it possible to select the basic dimensions of the antenna and the magnitude of the coupling element.

As was pointed out, for sufficiently short distances between dipoles their effect on collection line parameters can be reduced to a change in the line's distributed constants.

The additional admittance, Y_{add}, per unit length of collection line, created by the dipoles, can be established through the formula

$$Y_{add} = \frac{Y}{l_1} = \frac{1}{(Z_d + 2Z_{co})l_1}. \qquad (XIV.5.1)$$

The additional admittance, Y_{add}, will differ for different dipoles, but this change along the length of the antenna is not great. In formula (XIV.5.1) the impedance Z_d is some "averaged" impedance. A stricter analysis will show that taking the change in the admittance into consideration will not result in any appreciable refinement in the results.

The propagation factor on the collection line equals

$$\gamma_c = \sqrt{Z_1(Y_1 + Y_{add})}, \qquad (XIV.5.2)$$

where

Z_1 and Y_1 are the impedance and the admittance per unit length of line, established without taking the effect of the dipoles into consideration.

If losses in the collection line conductors are ignored,

$$Z_1 = i\omega L_1, \qquad Y_1 = i\omega C_1,$$

where

L_1 and C_1 are the inductance and capacitance per unit length of time.

Expression (XIV.5.2) can be written in the following form

$$\gamma_c = \sqrt{Z_1 Y_1}\sqrt{1 + Y_{add}/Y_1}. \qquad (XIV.5.3)$$

Substituting $\gamma_c = i\alpha_c + \beta_c$ and $\sqrt{Z_1 Y_1} = i\alpha$ in (XIV.5.3), we obtain

$$i\alpha_c + \beta_c = i\alpha\sqrt{1 + Y_{add}/Y_1}. \qquad (XIV.5.4)$$

The additional admittance is much less than the own admittance of the line, so

$$i\alpha_c = \beta_c \approx i\alpha\,(1 + Y_{add}/2Y_1). \qquad \text{(XIV.5.5)}$$

Taking it that

$$Y_1 = i\omega C_1 = i\frac{1}{W_0},$$

where

W_0 is the characteristic impedance of the line without taking the effect of the dipoles into consideration, and substituting this expression in (XIV.5.5), we obtain

$$\frac{\alpha_c}{\alpha} = \frac{1}{k_1} = 1 - \frac{W_0(X_d+2X_{co})}{2\alpha l_1[(R_d+2R_{co})^2+(X_d+2X_{co})^2]}, \qquad \text{(XIV.5.6)}$$

$$\beta_c = \frac{W_0(R_d+2R_{co})}{2l_1[(R_d+2R_{co})^2+(X_d+2X_{co})^2]}. \qquad \text{(XIV.5.7)}$$

In formulas (XIV.5.6) and (XIV.5.7) $Z_d = R_d + iX_d$, $Z_{co} = R_{co} + iX_{co}$.

The formula for the characteristic impedance of the line, W, with the effect of the dipoles taken into consideration, can be obtained similarly. In fact, the characteristic impedance, W, equals

$$W = \sqrt{\frac{Z_1}{Y_1+Y_{add}}} = \sqrt{\frac{Z_1}{Y_1}}\sqrt{\frac{1}{1+Y_{add}/Y_1}}. \qquad \text{(XIV.5.8)}$$

From whence

$$W = W_0\left|\frac{\alpha}{\gamma_c}\right| \approx W_0 k_1. \qquad \text{(XIV.5.9)}$$

When formulas (XIV.5.6) and (XIV.5.7) are used it must be borne in mind that the components of the input resistance of the dipole, R_d and X_d, contained in these formulas can be established as being the magnitudes of the dipole's own impedance, as well as the magnitudes of the induced resistances.

The phase velocity of the distribution of the current on the antenna, v, and the attenuation factor, β_c, must be known in order to establish the induced resistances, so the calculation for induced resistances is usually made using approximation methods. Specifically, induced resistances can be calculated on the assumption that $v = c$ and $\beta_c = 0$. It is also possible to establish initially the magnitudes of v and β_c without taking the space

coupling of the dipoles into consideration, and then compute the induced resistances in accordance with the known values of v and β_c. Then formulas (XIV.5.6) and (XIV.5.7) can be used to obtain refined values for v and β_c.

#XIV.6. Formulas for Traveling Wave Antenna Receiving Patterns

The current fed to the receiver input by the traveling wave antenna equals

$$I = \frac{2E_0}{\left(Z_d + 2Z_{c0} + \frac{W}{2}\right)\operatorname{sh}\gamma l} \cdot \frac{\cos(\pi l \cos\Delta \sin\varphi) - \cos\pi l}{\sqrt{1-\cos^2\Delta\sin^2\varphi}} \times$$

$$\times \frac{e^{N(ik_1\cos\Delta\cos\varphi-\gamma_c)l_1}-1}{e^{(ik_1\cos\Delta\cos\varphi-\gamma_c)l_1}-1} \sin(\alpha H \sin\Delta), \qquad \text{(XIV.6.1)}$$

where

E_0 is the antenna field strength;

φ is the azimuth angle of the beam, read from the axis of the collection line;

Δ is the angle of tilt of the beam, read from the plane of the ground;

γ is the current propagation factor in a balanced dipole;

γ_c is the current propagation factor in the collection line.

Formula (XIV.6.1) is derived in Appendix 6.

The antenna pattern calculation can usually assume that $\beta_c = 0$ and $\gamma_c = i\frac{\alpha}{k_1}$. So, substituting $\Delta = 0$ in (XIV.6.1), and dropping the factors not dependent on φ, we obtain the following expression for the pattern of a traveling wave antenna in the horizontal plane:

$$F(\varphi) = \frac{\cos(\pi l \sin\varphi) - \cos\pi l}{\cos\varphi} \cdot \frac{\sin\left[N\frac{\pi l_1}{2}\left(\cos\varphi - \frac{1}{k_1}\right)\right]}{\sin\left[\frac{\pi l_1}{2}\left(\cos\varphi - \frac{1}{k_1}\right)\right]}. \qquad \text{(XIV.6.2)}$$

Formula (XIV.6.2) not only characterizes the directional properties of a traveling wave antenna in the horizontal plane, ($\Delta = 0$), but also on surfaces, that make some angle Δ = constant with this plane for small values of Δ.

Substituting $\varphi = 0$ in (XIV.6.1), and dropping the factors that do not depend on Δ, we obtain the following expression for the antenna's pattern in the vertical plane:

$$F(\Delta) = \frac{\sin\left[N\frac{\alpha l_1}{2}\left(\cos\Delta - \frac{1}{k_1}\right)\right]}{\sin\left[\frac{\alpha l_1}{2}\left(\cos\Delta - \frac{1}{k_1}\right)\right]} \sin(\alpha H \sin\Delta). \qquad \text{(XIV.6.3)}$$

Formulas (XIV.6.1) and (XIV.6.3) assume ground of ideal conductivity. In the event it is necessary to calculate the real parameters of the ground,

the formula for the antenna's pattern in the vertical plane will take the form

$$F(\Delta)=\frac{\sin\left[N\frac{\alpha l_1}{2}\left(\cos\Delta-\frac{1}{k_1}\right)\right]}{\sin\left[\frac{\alpha l_1}{2}\left(\cos\Delta-\frac{1}{k_1}\right)\right]}\sqrt{1+|R_\perp|^2+2|R_\perp|\cos(\psi_\perp-2\alpha H\sin\Delta)}. \qquad \text{(XIV.6.4)}$$

When it is necessary to take the effect of attenuation on the collection line on the directional properties of the antenna into consideration, we can use the following formulas to calculate the patterns

$$F(\varphi)=\frac{\cos(\alpha l\sin\varphi)-\cos\alpha l}{\cos\varphi}\cdot\sqrt{\frac{\operatorname{ch}\beta_c Nl_1-\cos\left[\alpha Nl_1\left(\cos\varphi-\frac{1}{k_1}\right)\right]}{\operatorname{ch}\beta_c l_1-\cos\left[\alpha l_1\left(\cos\varphi-\frac{1}{k_1}\right)\right]}} \qquad \text{(XIV.6.5)}$$

and (in the case of ideally conducting ground)

$$F(\Delta)=\sqrt{\frac{\operatorname{ch}\beta_c Nl_1-\cos\left[\alpha Nl_1\left(\cos\Delta-\frac{1}{k_1}\right)\right]}{\operatorname{ch}\beta_c l_1-\cos\left[\alpha l_1\left(\cos\Delta-\frac{1}{k_1}\right)\right]}}\sin(\alpha H\sin\Delta). \qquad \text{(XIV.6.6)}$$

It should be noted that taking the attenuation into consideration does not usually result in any substantial refinement when calculating the patterns.

#XIV.7. Directive Gain, Antenna Gain, and Efficiency

(a) Antenna gain

The gain of a traveling wave antenna can be calculated through the formula

$$\varepsilon=\frac{P_A}{P_{\frac{\lambda}{2}}},$$

where

P_A is the power applied to the receiver input when reception is by a traveling wave antenna and the match of the antenna to the receiver input is optimum;

$P_{\lambda/2}$ is the power applied to the receiver input when reception is by a half-wave dipole in free space when the match of the dipole to the receiver input is optimum.

These powers can be established through the formulas

$$P_A=I^2W, \qquad \text{(XIV.7.1)}$$

$$P_{\frac{\lambda}{2}}=\frac{\lambda^2 E_0^2}{4\pi^2 73.1}, \qquad \text{(XIV.7.2)}$$

with I established through formula (XIV.6.1) for $\varphi = 0$.

Substituting the expression indicated for the current in the general formula for ε, we obtain the following expression for the gain of a

traveling wave antenna

$$\varepsilon = 292.4 \frac{W \operatorname{tg}^2 \frac{\alpha l}{2}}{\left| Z_d + 2Z_{co} + \frac{W}{2} \right|^2} \left| \frac{e^{N(1\cos\Delta - \gamma_c)l_1} - 1}{e^{(1\cos\Delta - \gamma_c)l_1} - 1} \right|^2 \sin^2(\alpha H \sin\Delta). \qquad \text{(XIV.7.3)}$$

Formula (V.18.1) can be used to calculate Z_d when establishing ε. The induced emf method can be used to calculate the radiation resistance. And the phase angle between currents flowing in the dipoles, ψ, can be established through the formula

$$\psi = \pm \frac{\alpha D_1}{k_1}, \qquad \text{(XIV.7.4)}$$

where

D_1 is the distance between the dipoles, the mutual effect of which is being calculated. The minus sign in formula (XIV.7.4) is taken when the dipole, the effect of which is being taken into consideration, is closer to the terminating resistor than is the dipole the radiation resistance of which is being calculated. The plus sign is taken if the dipole, the effect of which is being considered, is closer to the receiver.

In practice, it is sufficient to consider the effect of dipoles at distances of up to 0.75 - 1.0λ when calculating radiation resistance.

The figures obtained for the radiation resistance of all dipoles are averaged by dividing the sum of the radiation resistances of all dipoles by their number.

(b) Efficiency

As has already been pointed out above, one understands the efficiency of a receiving antenna to be the efficiency of this same antenna when it is used for transmission.

Antenna efficiency during transmission equals

$$\eta = \eta_1 \eta_2, \qquad \text{(XIV.7.5)}$$

where

η_1 is the dipole efficiency, equal to

$$\eta_1 = R_d / R_d + 2R_{co}, \qquad \text{(XIV.7.6)}$$

$$\eta_2 = P_0 - P_n / P_0. \qquad \text{(XIV.7.7)}$$

Here P_0 is the total input, and

P_n is the power expended in the termination resistor,

$$P_n = P_0 e^{-2\beta_c L}. \qquad \text{(XIV.7.8)}$$

Accordingly,

$$\eta_2 = 1 - e^{-2\beta_c L}. \qquad \text{(XIV.7.9)}$$

Substituting the expressions for η_1 and η_2 in (XIV.7.5), we obtain

$$\eta = \frac{R_d}{R_d + 2R_{co}} (1 - e^{-2\beta_c L}). \qquad \text{(XIV.7.10)}$$

In the case of the traveling wave antenna with pure reactance for the coupling (the BYe and BI antennas) formula (XIV.7.10) becomes

$$\eta = 1 - e^{-2\beta_c L}. \qquad \text{(XIV.7.11)}$$

(c) Directive gain

The directive gain of an antenna can be calculated through the formula

$$D = 1.64c/\eta \qquad \text{(XIV.7.12)}$$

or through the formula

$$D = \frac{4\pi F^2(\Delta_0, \varphi_0)}{\int_0^{2\pi} d\varphi \int_0^{\frac{\pi}{2}} F^2(\Delta, \varphi) \cos\Delta \, d\Delta}, \qquad \text{(XIV.7.13)}$$

where

$F(\Delta,\varphi)$ is an expression characterizing the space radiation pattern;

Δ_0 and φ_0 are angles which determine the direction for which the directive gain will be calculated.

The calculation of the integral in the denominator of the expression at (XIV.7.13) is very difficult, and is usually done by graphical integration. Of greater expediency is the calculation of the directive gain through formula (XIV.7.12). It is also possible to establish the value of D by comparing the receiving pattern of the traveling wave antenna with the patterns of other antennas, the directive gains of which are well known, antennas such as broadside antennas, for example. Antennas with approximately the same patterns also have approximately identical directive gains.

#XIV.8. Multiple Traveling Wave Antennas

Multiple traveling wave antennas are widely used to increase antenna gain and directive gain. Those most often used are dual antennas consisting of two parallel connected arrays (BS2 and BYe2 antennas). The schematic of a twin traveling wave antenna is shown in Figure XIV.1.2.

The gain of a twin antenna is approximately double that of a single antenna. The increase in the gain of a multiple antenna on the shortwave edge

of the band can be explained by the improvement in directional properties. At the longwave edge of the band the increase in gain is, to a considerable extent, determined by the increase in efficiency.

The receiving pattern of a twin antenna can be charted through the formula

$$F_2(\Delta, \varphi) = F_1(\Delta, \varphi) \cos\left(\frac{\pi d_1}{2} \cos\Delta \sin\varphi\right), \qquad \text{(XIV.8.1)}$$

where

d_1 is the distance between the array collection lines (in standard antennas d_1 = 25 m);

$F_1(\Delta,\varphi)$ is the pattern of a single antenna.

The pattern in the horizontal plane can be expressed through the formula

$$F_2(\varphi) = F_1(\varphi) \cos\left(\frac{\pi d_1}{2} \sin\varphi\right), \qquad \text{(XIV.8.2)}$$

with $F_1(\varphi)$ established through formula (XIV.6.2).

The pattern in the vertical plane of a twin traveling wave antenna remains the same as it would be in the case of the single antenna.

The efficiency of a twin antenna can be established approximately through the formula

$$D_t = D_s \frac{\varphi_s}{\varphi_t}, \qquad \text{(XIV.8.3)}$$

where

φ_s is the width of the pattern in the horizontal plane at half power for the single antenna;

φ_t is the corresponding width of the pattern of a twin antenna.

The gain of a twin antenna, ε_t, can be established through the formula

$$\varepsilon_t \approx 2\varepsilon_s, \qquad \text{(XIV.8.4)}$$

where

ε_s is the gain of a single antenna.

The efficiency of a twin antenna can be established through the formula

$$\eta = 1.64\varepsilon/D.$$

#XIV.9. Electrical Parameters of a Traveling Wave Antenna with Resistive Coupling Elements

(a) Selection of the dimensions and other data for the antenna

As has already been noted above, the traveling wave antenna with resistive coupling elements (the BS antenna) is the most acceptable. This

paragraph will cite data characteristic of the electrical parameters of this antenna.

The following antenna data are subject to selection:

L antenna length;

l_1 distance between dipoles;

l length of the arm of the balanced dipole;

R_{co} magnitude of the coupling resistance inserted in one arm of the dipole;

H height at which antenna is suspended;

W characteristic impedance of the collection line.

Antenna length, L, can be selected on the basis of the following considerations. As has already been pointed out, the traveling wave antenna has the best direction properties if

$$A=\alpha L\left(\frac{1}{k_1}-1\right)\approx+\pi. \qquad \text{(XIV.9.1)}$$

For fixed phase velocity, the magnitude of A is proportional to antenna length. When the antenna is very long the magnitude of A can become much larger than 180°, and this results in a sharp deterioration in directional properties. Calculations reveal that if the BS antenna is to operate over the entire shortwave band, antenna length must not exceed 80 to 150 meters. The length of a standard BS antenna is 90 meters.

The length of a dipole arm can be selected as the maximum possible in order to have a maximum increase in the antenna gain at the longwave edge of the band. However, the possibility of increasing dipole length is restricted by the need to retain satisfactory dipole directional properties at the shortwave edge of the band. If least wavelength is 12 to 13 meters, the length of the dipole arm can be taken on the order of 8 meters. At the same time, even though the dipole pattern at the shortwave edge of the band has rather large side lobes, the antenna pattern as a whole is satisfactory. Antenna data will have to be changed if it is necessary to expand the operating band, and if the shortest wave is taken as equal to 10 meters. Antenna data should approximate the following: length of dipole arm 6 to 7 meters; distance between dipoles 3.6 to 2.25 meters; and $2R_{co}$ = 500 to 800 ohms. And the antenna gain at the longwave edge of the band will be reduced by a factor of from 1.8 to 1.3 as compared with the case when the arm length is 8 meters. We have taken length l = 8 meters in calculating antenna parameters.

The characteristic impedance of the collection line determines the efficiency of the dipoles. The higher the characteristic impedance, the higher the decoupling resistance required to ensure normal phase velocity. An increase in R_{co} is accompanied by a reduction in η and a corresponding

reduction in the antenna gain. Accordingly, antenna gain will increase with reduction in W, so W is selected as low as possible without unnecessarily complicating the design of the collection line. We have selected W = 160 ohms. When the characteristic impedance of the collection line is taken at this value we can reduce the decoupling resistance, $2R_{co}$, to 400 ohms. This is the magnitude of the coupling resistance, and was taken for the standard antenna.

The characteristic impedance we have selected is readily obtainable in making a collection line in the form of a 4-conductor crossed feeder (see below).

The following considerations govern in the selection of the number of dipoles for the antenna. An increase in the number of dipoles is accompanied by a reduction in the side, and particularly in the minor lobes, and an increase in antenna gain. What must be borne in mind, however, is the fact that the greater the number of dipoles, the more the phase velocity of propagation on the collection line will differ from the speed of light. The number of dipoles can be selected in such a way that the difference between the phase velocity of propagation on the collection line (v) and the speed of light (c) will not exceed acceptable limits.

With what has been pointed out here taken into consideration, we can select the number of dipoles as between 20 and 40. The parameters of an antenna with 21 dipoles are given in what follows.[1]

The height at which the antenna is suspended, H, is established for the condition of maximum reception strength for given Δ. This yields

$$H_{opt} = \lambda/4\sin\Delta. \qquad \text{(XIV.9.2)}$$

If it is taken that the angles of tilt of incoming beams are from 7 to 15°, the most desirable height is found to be equal to λ to 2λ. Hence, the antenna has maximum efficiency at the longwave edge of the band when suspension height is 40 to 100 meters, and maximum efficiency at the shortest wavelength at a height of 15 to 25 m. Since increasing the height at which an antenna is suspended is accompanied by a sharp increase in the cost of the antenna, it becomes obvious that we can restrict the height to something on the order of 25 to 35 meters. BS antennas in use at the present time are suspended at 25 and 17 meters. Accordingly, the BS antenna has the following data:

---

1. Recent investigations have shown that if the number of dipoles is doubled and if, as a result, $2R_{co}$ is increased to 800 ohms, the change in antenna parameters will not be substantial. The level of the side lobes will fall quite a bit, however. Data on this antenna variant are not included here.

L = 90 meters, N = 21,

$2R_{co}$ = 400 ohms, t_1 = 4.5 meters,

t = 8 meters, H = 25 meters or 17 meters,

The conventional designation for the standard BS antenna is

BS 21/8 200/4.5 25

or

BS 21/8 200/4.5 17.

(b) Phase velocity and attenuation factor

Approximate formulas for establishing the phase velocity and attenuation factor in the case of the traveling wave antenna with resistive coupling elements are in the form

$$\frac{c}{v} = \frac{1}{k_1} = 1 - \frac{W_0 X_d}{2\alpha t_1[(R_d + 2R_{co})^2 + X_d^2]}, \qquad \text{(XIV.9.3)}$$

$$\beta_c = \frac{W_0(R_d+2R_{co})}{2t_1[(R_d + 2R_{co})^2 + X_d^2]}. \qquad \text{(XIV.9.4)}$$

Figures XIV.9.1 and XIV.9.2 show the dependence of $v/c = k_1$ and β_c on the wavelength for the BS 21/8 200/4.5 17 and BS 21/8 200/4.5 25 antennas. The curves were plotted with induced resistanced considered.[1]

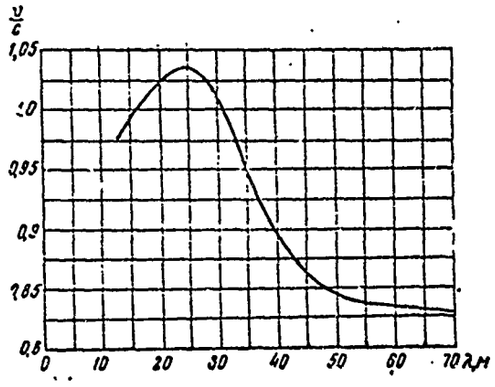

Figure XIV.9.1. Dependence of magnitude of phase velocity on the collection feeder of BS 21/8 200/4.5 17 and BS 21/8 200/4.5 25 antennas on the wavelength.

1. When the induced resistances were calculated it was assumed that phase distribution corresponded to the velocity of propagation obtained without the mutual effect of the dipoles considered.

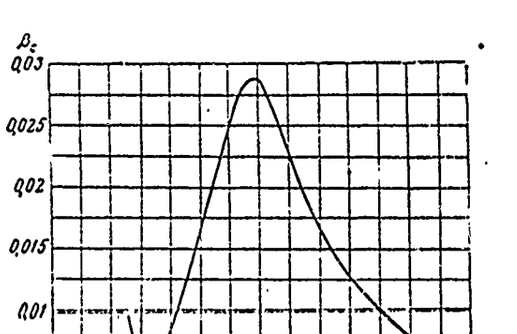

Figure XIV.9.2. Dependence of linear attenuation on the collection line of BS 21/8 200/4.5 17 and BS 21/8 200/4.5 25 antennas on the wavelength.

As will be seen from Figure XIV.9.1, the phase velocity of propagation on the BS antenna is less than the speed of light over a large part of the band. The phase velocity is somewhat greater than the speed of light over part of the band (16 to 31.5 meters). However, there is no real significance to some reduction in the antenna's directive gain in the shortwave section of the band because in this section of the band the antenna parameters have been improved by the increase in D proportional to the $1/\lambda$ ratio.

In the longwave section of the band, where maximum increase in the directive gain and in antenna gain are particularly important, the phase velocity on the antenna is close to optimum.

(c) Directional properties

Figures XIV.9.3 through XIV.9.10 show charted receiving patterns in the horizontal plane of standard BS and BS2 antennas over the entire shortwave band. Figures XIV.9.11 - XIV.9.18 show the patterns in the vertical planes of BS 21/8 200/4.5 17 and BS 21/8 200/4.5 25 antennas.

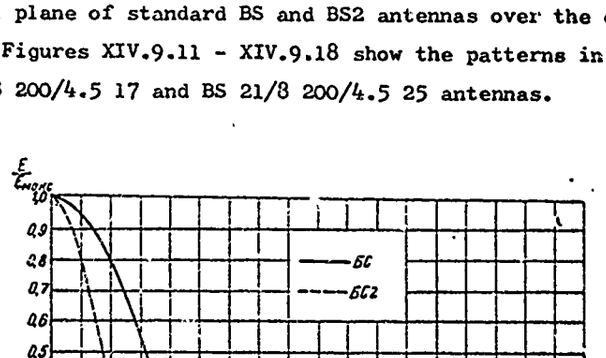

Figure XIV.9.3. Receiving patterns in the horizontal plane for BS and BS2 antennas; λ = 12.5 m.
——— BS; ----- BS2.

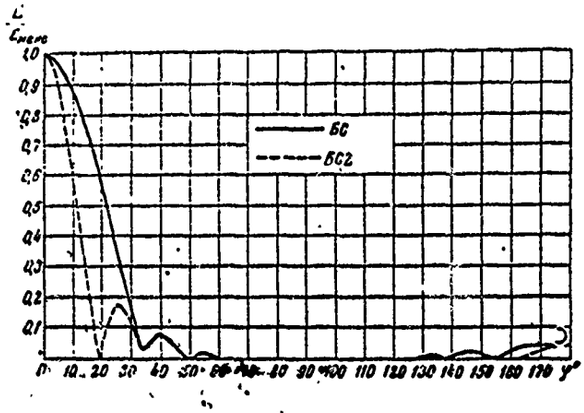

Figure XIV.9.4. Receiving patterns in the horizontal plane for BS and BS2 antennas; λ = 16 m.

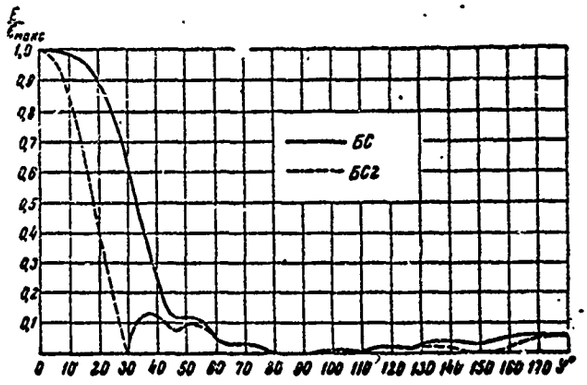

Figure XIV.9.5. Receiving patterns in the horizontal plane for BS and BS2 antennas; λ = 24 m.

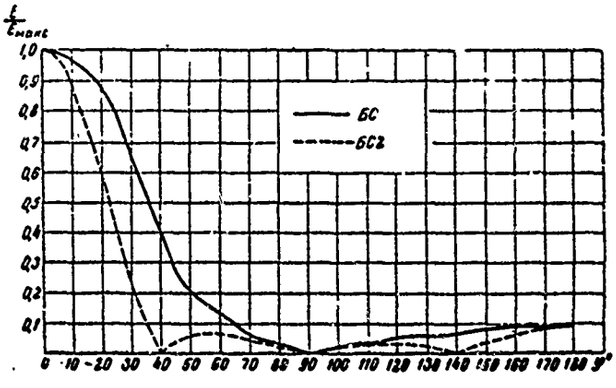

Figure XIV.9.6. Receiving patterns in the horizontal plane for BS and BS2 antennas; λ = 32 m.

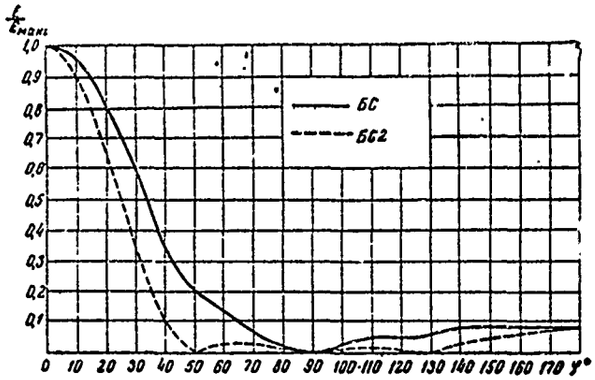

Figure XIV.9.7. Receiving patterns in the horizontal plane for BS and BS2 antennas; λ = 38.5 m.

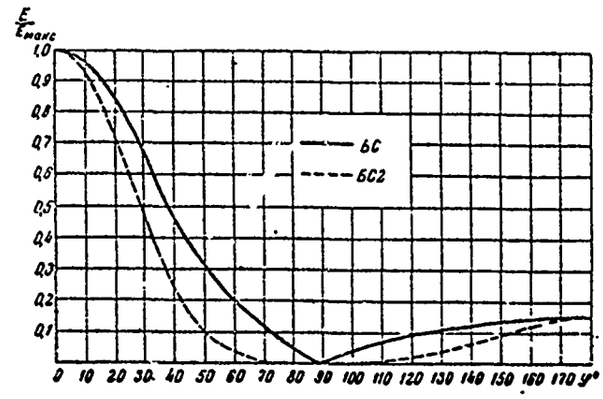

Figure XIV.9.8. Receiving patterns in the horizontal plane for BS and BS2 antennas; λ = 48 m.

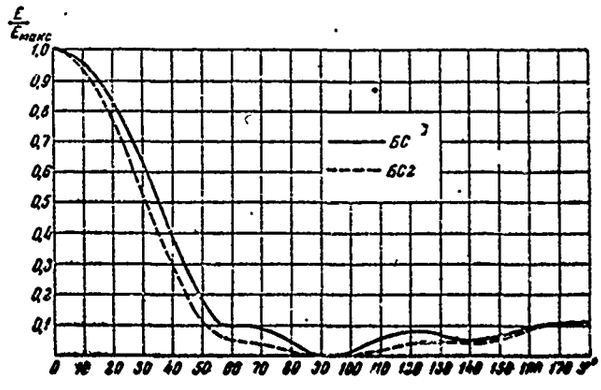

Figure XIV.9.9. Receiving patterns in the horizontal plane for BS and BS2 antennas; λ = 64 m.

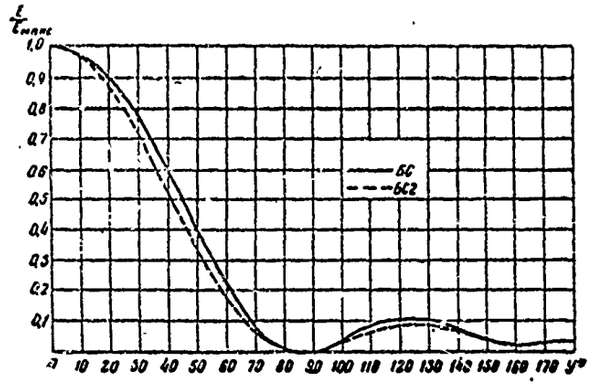

Figure XIV.9.10. Receiving patterns in the horizontal plane for BS and BS2 antennas; λ = 100 m.

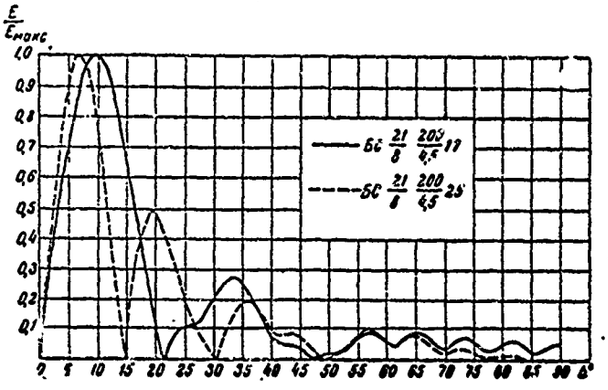

Figure XIV.9.11. Receiving patterns in the vertical plane of BS 21/8 200/4.5 17 and BS 21/8 200/4.5 25 antennas; λ = 12.5 m.

——— BS 21/8 200/4.5 17; ----- BS 21/8 200/4.5 25.

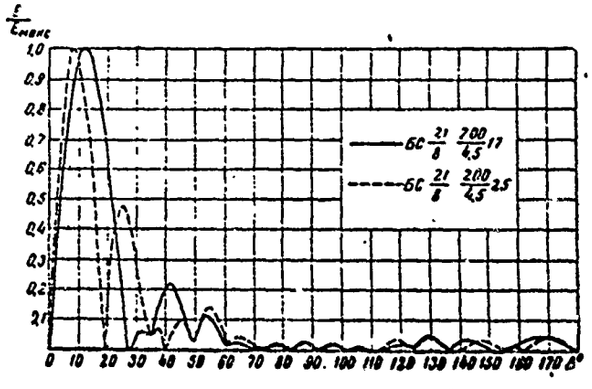

Figure XIV.9.12. Receiving patterns in the vertical plane of BS 21/8 200/4.5 17 and BS 21/8 200/4.5 25 antennas; λ = 16 m.

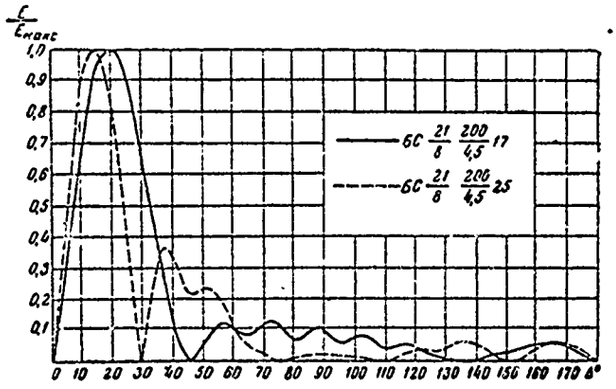

Figure XIV.9.13. Receiving patterns in the vertical plane of BS 21/8 200/4.5 17 and BS 21/8 200/4.5 25 antennas; λ = 24 m.

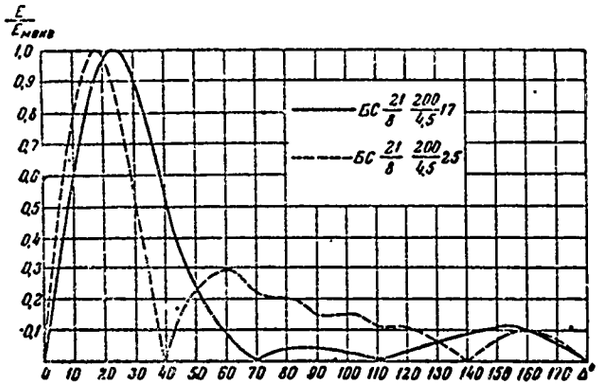

Figure XIV.9.14. Receiving patterns in the vertical plane of BS 21/8 200/4.5 17 and BS 21/8 200/4.5 25 antennas; λ = 32 m.

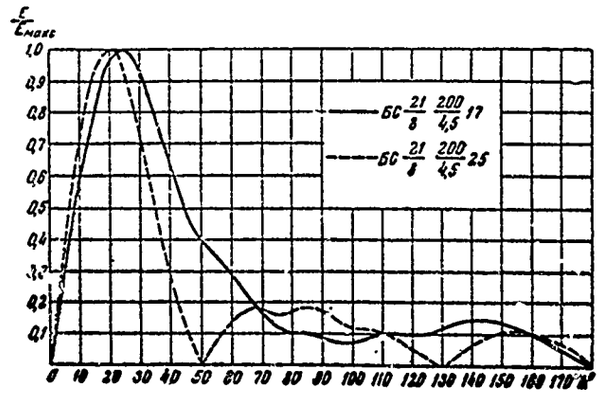

Figure XIV.9.15. Receiving patterns in the vertical plane of BS 21/8 200/4.5 17 and BS 21/8 200/4.5 25 antennas; λ = 38.5 m.

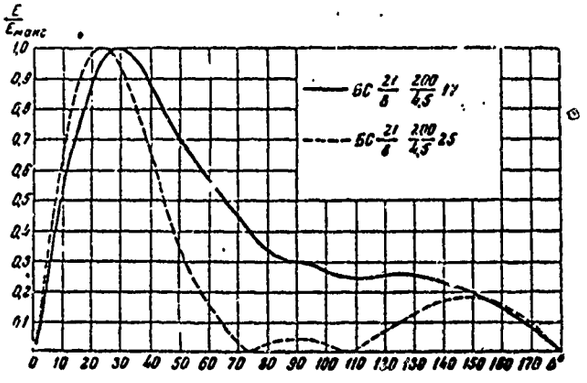

Figure XIV.9.16. Receiving patterns in the vertical plane of BS 21/8 200/4.5 17 and BS 21/8 200/4.5 25 antennas; λ = 48 m.

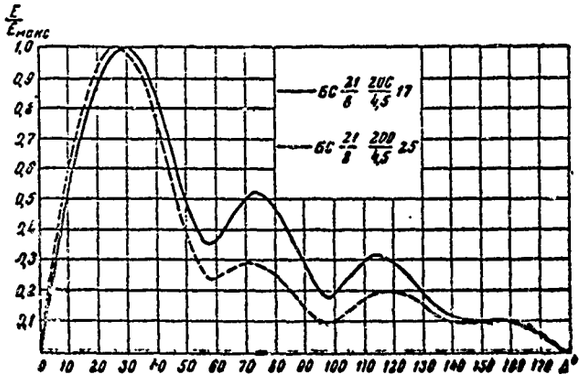

Figure XIV.9.17. Receiving patterns in the vertical plane of BS 21/8 200/4.5 17 and BS 21/8 200/4.5 25 antennas; λ = 64 m.

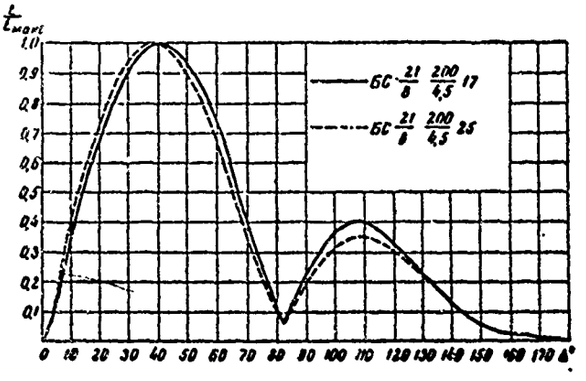

Figure XIV.9.18. Receiving patterns in the vertical plane of BS 21/8 200/4.5 17 and BS 21/8 200/4.5 25 antennas; λ = 100 m.

In order to evaluate the effect of ground parameters on the directional properties of the antenna, Figure XIV.9.19 shows the major lobes in the patterns of the BS 21/8 200/4.5 25 antenna for three wavelengths and three types of ground (ideal, average, and low conductivity).

All patterns were charted with attenuation considered.

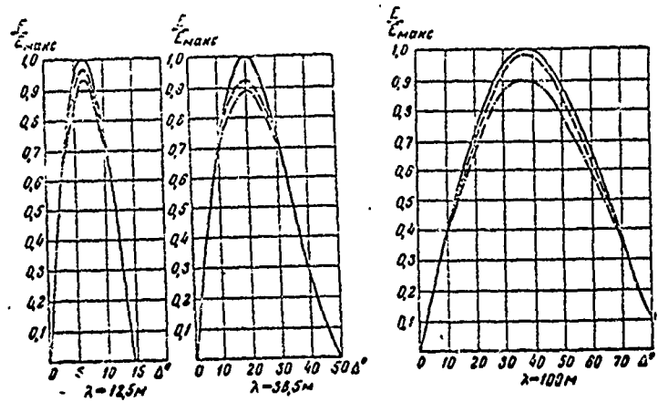

Figure XIV.9.19. Receiving patterns in the vertical plane of a BS 21/8 200/4.5 25 antenna.

——— ground of ideal conductivity;

– – – ground of average conductivity (ε_r=8; γ_v=0.005 mho/m);

-.-.- ground of low conductivity (ε_r=3; γ_v=0.0005 mho/m).

It should be noted that the series of patterns charted here will not provide completely accurate data on directional properties because the methodology used to do the charting contained a number of approximations (reflection from individual dipoles was not considered, β_c and v were approximated, and others). Nevertheless, experimental investigations have demonstrated that these patterns correctly characterize the directional properties of antennas on waves longer than 13 to 14 meters.

The data presented in figures XIV.9.3 through XIV.9.10 demonstrate that the level of the side lobes associated with the BS2 antenna are, in the majority of cases, considerably lower than 0.08 to 0.1, so the noise stability of the BS antenna is comparatively high. A comparison of patterns in the vertical plane of BS antennas suspended at heights of 17 and 25 meters reveals that at H = 25 meters the patterns in the vertical plane are improved substantially. Specifically, reception at angles of 7° to 15°, the angles at which beams on long communication lines usually arrive, is more effective.

As will be seen from the patterns, even at suspension height 25 meters the angle of maximum reception in the vertical plane at the longwave edge of the band is too high. Substantial "compression" of the major lobe in the

receiving pattern can be obtained either by raising the antenna suspension height, or by using more complex antennas, such as the 3BS2 21/8 200/4.5 25 or 3BS2 42/8 400/2.25 25.

Figure XIV.9.20 shows the dependence of the angle of tilt of direction of maximum reception for type BS 21/8 200/4.5 17 and BS 21/8 200/4.5 25 antennas on the wavelength.

Figures XIV.9.21 and XIV.9.22 show the curves that establish the dependence of the directive gain of the BS 21/8 200/4.5 17 and BS 21/8 200/4.5 25 antennas on wavelength and angle of tilt of incoming beam. The dotted lines in these figures show the values of the maximum directive gain.

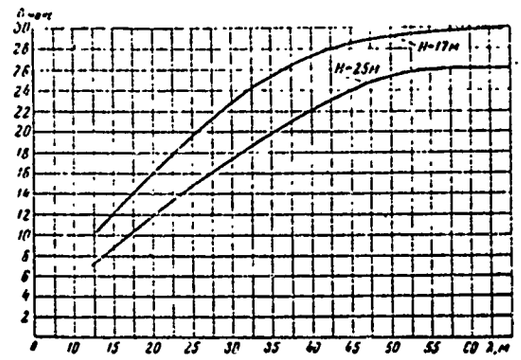

Figure XIV.9.20. Dependence of angle of tilt of direction of maximum reception of BS2 21/8 200/4.5 17 and BS2 21/8 200/4.5 25 antennas on wavelength.

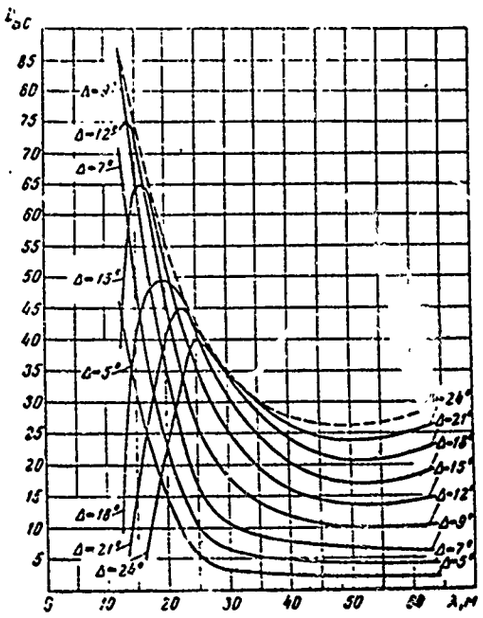

Figure XIV.9.21. Dependence of the directive gain of a BS 21/8 200/4.5 17 antenna on the wavelength and the angle of tilt of the incoming beam.
----- curve of maximum directive gain.

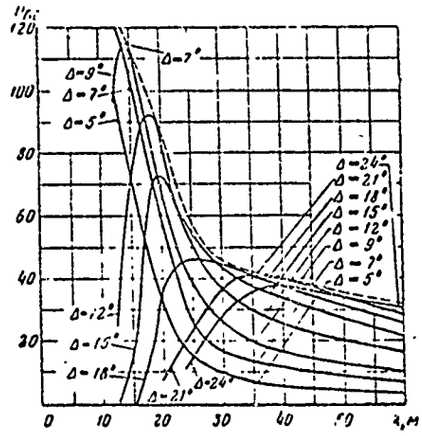

Figure XIV.9.22. Dependence of the directive gain of a BS 21/8 200/4.5 25 antenna on the wavelength and the angle of tilt of the incoming beam.

----- curve of maximum directive gain.

Figures XIV.9.23 and XIV.9.24 show similar curves for the gains of BS 21/8 200/4.5 17 and BS 21/8 200/4.5 25 antennas.

Figure XIV.9.25 shows the dependence of the efficiency of the BS 21/8 200/4.5 25 antenna, as well as the twin antenna, on the wavelength. The efficiency of the BS 21/8 200/4.5 17 antenna in the shortwave portion of the band is approximately the same as that of the antenna suspended at 25 meters. In the longwave portion of the band the efficiency of the BS 21/8 200/4.5 17 antenna is somewhat less than that of the BS 21/8 200/4.5 25 antenna, explained by the fact that at the longwave edge of the band the radiation resistance of a dipole suspended at 17 meters is markedly reduced as a result of ground effect.

Figures XIV.9.3 through XIV.9.10 use dotted lines to show the patterns in the horizontal plane of a BS2 21/8 200/4.5 twin traveling wave antenna with arrays spaced 25 meters apart.

Figures XIV.9.26 and XIV.9.27 show the curves which establish the dependence of the directive gain of the BS2 21/8 200/4.5 17 and BS2 21/8 200/4.5 25 antennas on the wavelength and angle of tilt of the incoming beam. The dotted curves in these figures show the values of the maximum directive gains.

A comparison of the data contained in figures XIV.9.21, XIV.9.22, XIV.9.26 and XIV.9.27 will show that the gain in the directive gain of the twin antenna will change from 2 at the shortwave edge of the band to 1.2 to 1.5 at the longwave edge, as compared with the single antenna.

The antenna gain of the twin antenna is twice that of the corresponding single antenna.

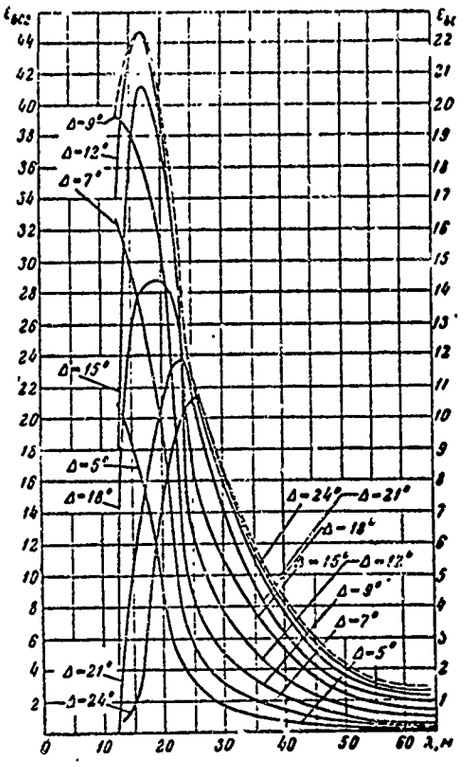

Figure XIV.9.23. Dependence of the gain of BS 21/8 200/4.5 17 and BS2 21/8 200/4.5 17 antennas on the wavelength and the angle of tilt of the incoming beam.

----- curve of maximum gain.

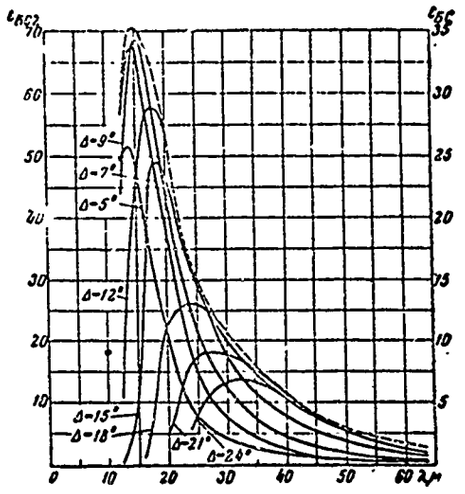

Figure XIV.9.24. Dependence of the gain of BS 21/8 200/4.5 25 and BS2 21/8 200/4.5 25 antennas on the wavelength and the angle of tilt of the incoming beam.

----- curve of maximum gain.

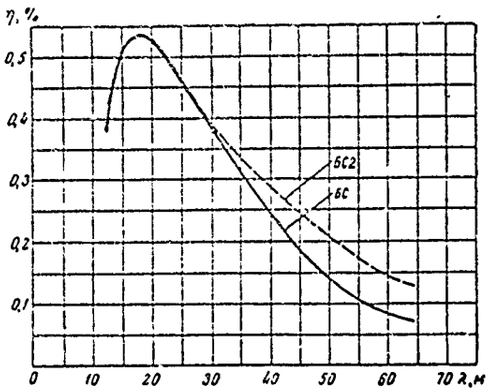

Figure XIV.9.25. Dependence of the efficiency of the BS 21/8 200/4.5 25 antenna (solid line) and the BS2 21/8 200/4.5 25 antenna (dotted line) on the wavelength.

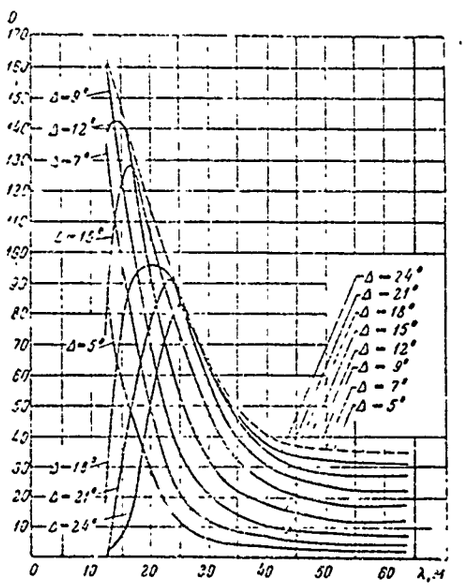

Figure XIV.9.26. Dependence of the directive gain of the BS2 21/8 200/4.5 17 antenna on the wavelength and the angle of tilt of the incoming beam.

----- curve of maximum directive gain.

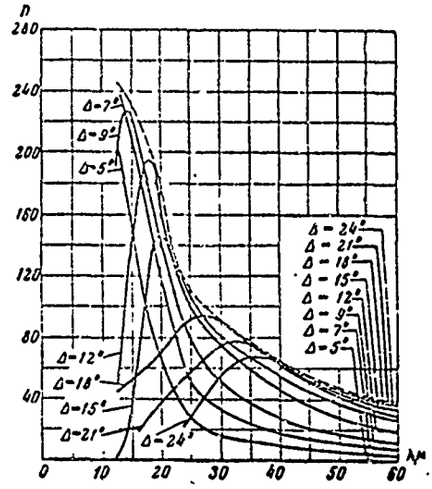

Figure XIV.9.27. Dependence of the directive gain for a BS2 21/8 200/4.5 25 antenna on the wavelength and the angle of tilt of an incoming beam.

---- curve of maximum directive gain.

#XIV.10. Traveling Wave Antennas with Controlled Receiving Patterns

As has already been pointed out above, a substantial increase in traveling wave antenna effectiveness can be arrived at by using multiple systems comprising two, three, and more BS2 antennas. The use of these antennas is desirable to improve noise resistance during reception on long communication lines.

Figure XIV.1.3 is a schematic of a multiple traveling wave antenna, the 3BS2, comprising three BS2 antennas installed in tandem and interconnected by a linear phase shifter. The lengths of the distribution lines can be selected such that the emfs induced in the receiver by the antennas are approximately in phase.

The phase shifters can control the patterns in the vertical planes of these antennas and thus ensure maximum use of antenna efficiency.

#XIV.11. Directional Properties of the 3BS2 Antenna

The multiple traveling wave antenna made up of three BS2 21/8 200/4.5 25 or BS2 21/8 200/4.5 17 antennas is designated 3BS2 21/8 200/4.5 25 or 3BS2 21/8 200/4.5 17.

The receiving patterns of a multiple traveling wave antenna made up of N BS antennas can be charted through the formula

$$F_N(\Delta, \varphi) = f_N(\Delta, \varphi) F_1(\Delta, \varphi), \qquad \text{(XIV.11.1)}$$

where

$F_1(\Delta,\varphi)$ is the pattern of the corresponding BS2 antenna;

$f_N(\Delta,\varphi)$ is a factor which takes into consideration the fact that there are N BS antennas in the system.

This factor can be established through the formula

$$f_N(\Delta,\varphi)=\frac{\sin\left\{\frac{N}{2}\left[\pi d_1(1-\cos\Delta\cos\varphi)-\psi\right]\right\}}{\sin\left\{\frac{1}{2}\left[\pi d_1(1-\cos\Delta\cos\varphi)-\psi\right]\right\}}, \qquad \text{(XIV.11.2)}$$

where

d_1 is the distance between the centers of adjacent BS antennas contained in the system (fig. XIV.1.3);

ψ is the phase angle between the emfs across adjacent antennas, created by the phase shifter.

In the case of the linear phase shifter $\psi = \alpha l_2$, where l_2 is a segment of line creating the necessary phase angle ψ. With this taken into consideration, we obtain

$$f_N(\Delta,\varphi)=\frac{\sin\left\{\frac{\pi N}{2}\left[d_1(1-\cos\Delta\cos\varphi)-l_2\right]\right\}}{\sin\left\{\frac{\pi}{2}\left[d_1(1-\cos\Delta\cos\varphi)-l_2\right]\right\}}. \qquad \text{(XIV.11.3)}$$

In the vertical plane ($\varphi = 0$) the factor $f_N(\Delta,\varphi)$ becomes

$$f_N(\Delta)=\frac{\sin\left\{\frac{\pi N}{2}\left[d_1(1-\cos\Delta)-l_2\right]\right\}}{\sin\left\{\frac{\pi}{2}\left[d_1(1-\cos\Delta)-l_2\right]\right\}}. \qquad \text{(XIV.11.4)}$$

As will be seen from formula (XIV.11.4), the minimum angle of tilt, Δ', at which $f_N(\Delta)$ can have maximum value depends on l_2 and not on the wavelength.

Actually,

$$\cos\Delta'=1-\frac{l_2}{d_1}. \qquad \text{(XIV.11.5)}$$

By changing the length l_2 we can control the values of this angle over the entire waveband.

What follows from (XIV.11.3) and (XIV.11.4) is that when positive phasing ($\psi > 0$ and $l_2 > 0$) is used angle Δ', which corresponds to the direction of maximum radiation from a multiple antenna, to a maximum for the factor $f_N(\Delta)$, is increased by comparison with the case of $\psi = 0$. Correspondingly, when negative phasing ($\psi < 0$ and $l_2 < 0$) is used, angle Δ' is decreased.

The values for lengths of segments l_2 needed to obtain the first maximum in the expression at (XIV.11.4) for various angles to the horizon are given below. They were computed through formula (XIV.11.5)

Δ'	0°	5°	10°	15°	20°	25°
l_2 (м)	0,0	0,35	1,40	3,14	5,55	8,62

Figures XIV.11.1 through XIV.11.14 show the major lobes in the patterns of 3BS2 21/8 200/4.5 17 and 3BS2 21/8 200/4.5 25 antennas in the vertical plane for phasings corresponding to the following values of ψ

$$\psi = +10°,\ \psi = 0°,\ \psi = -10° \text{ и } \psi = -20°.$$

The data contained in figures XIV.11.1 - XIV.11.14 demonstrate that use of the phase shifter makes it possible to change the angle of maximum reception in the vertical plane, within certain limits. In particular, the pattern can be "squeezed" substantially toward the horizontal. If further "squeezing" of the patterns to the ground is desired in order to obtain a corresponding increase in antenna efficiency on the longer waves in the band, we must either increase the height at which the antennas are suspended to 35 to 40 meters, or increase the number of antennas installed in tandem (6BS2 antennas, for example).

Figures XIV.11.15 through XIV.11.21 show the patterns for 3BS2 21/8 200/4.5 17 and 3BS2 21/8 200/4.5 25 antennas in the horizontal plane in the waveband for ψ = 0°.

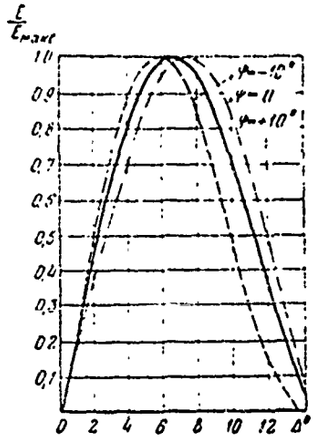

Figure XIV.11.1. The first lobes in the reception patterns in the vertical plane of a 3BS2 21/8 200/4.5 25 antenna on a wavelength of λ = 12.5 m for different angles of phasing.

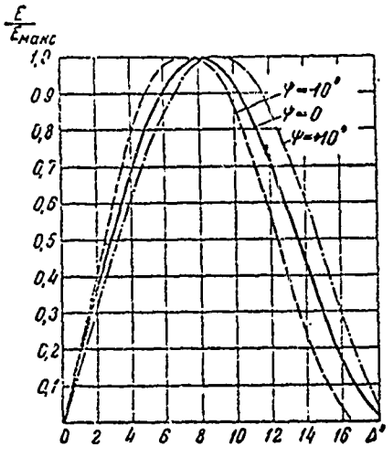

Figure XIV.11.2. The first lobes in the reception patterns in the vertical plane of a 3BS2 21/8 200/4.5 25 antenna on a wavelength of λ = 16 m for different angles of phasing.

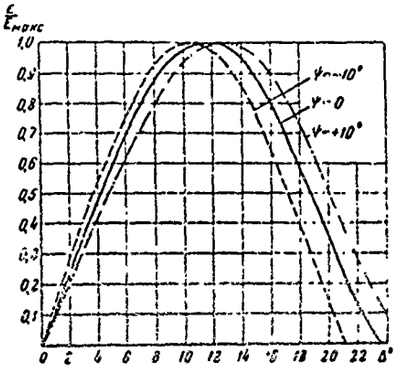

Figure XIV.11.3. The first lobes in the reception patterns in the vertical plane of a 3BS2 21/8 200/4.5 25 antenna on a wavelength of λ = 24 m for different angles of phasing.

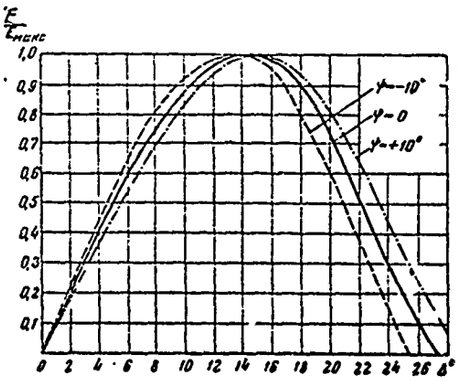

Figure XIV.11.4. The first lobes in the reception patterns in the vertical plane of a 3BS2 21/8 200/4.5 25 antenna on a wavelength of λ = 32 m for different angles of phasing.

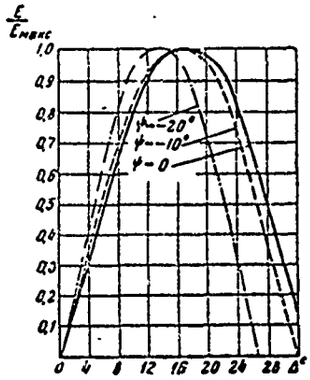

Figure XIV.11.5. The first lobes in the reception patterns in the vertical plane of a 3BS2 21/8 200/4.5 25 antenna on a wavelength of λ = 48 m for different angles of phasing.

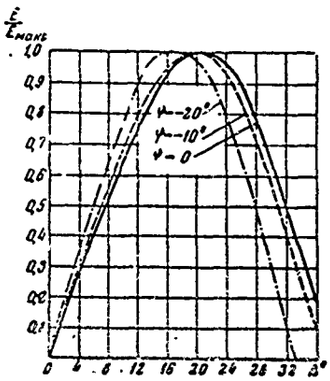

Figure XIV.11.6. The first lobes in the reception patterns in the vertical plane of a 3BS2 21/8 200/4.5 25 antenna on a wavelength of λ = 64 m for different angles of phasing.

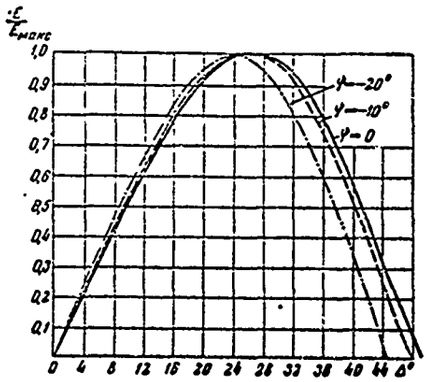

Figure XIV.11.7. The first lobes in the reception patterns in the vertical plane of a 3BS2 21/8 200/4.5 25 antenna on a wavelength of λ = 100 m for different angles of phasing.

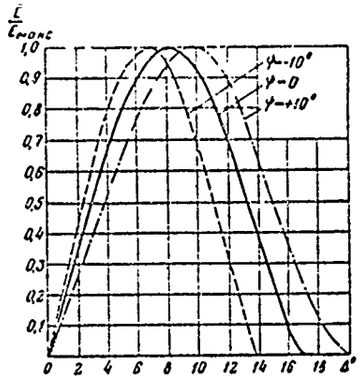

Figure XIV.11.8. The first lobes in the reception patterns in the vertical plane of a 3BS2 21/8 200/4.5 17 antenna on a wavelength of λ = 12.5 m for different angles of phasing.

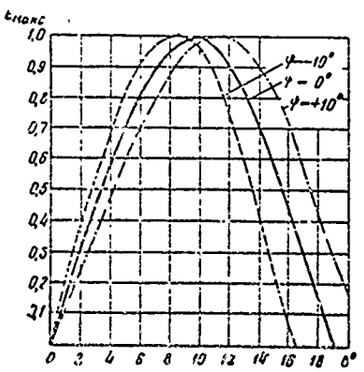

Figure XIV.11.9. The first lobes in the reception patterns in the vertical plane of a 3BS2 21/8 200/4.5 17 antenna on a wavelength of λ = 16 m for different angles of phasing.

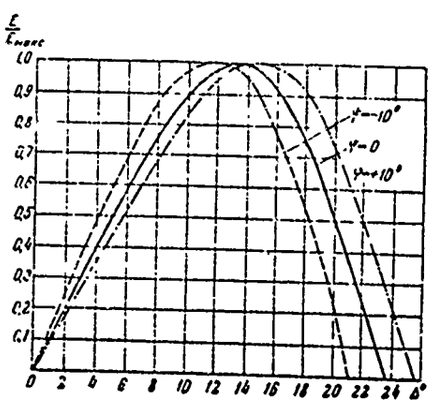

Figure XIV.11.10. The first lobes in the reception patterns in the vertical plane of a 3BS2 21/8 200/4.5 17 antenna on a wavelength of λ = 24 m for different angles of phasing.

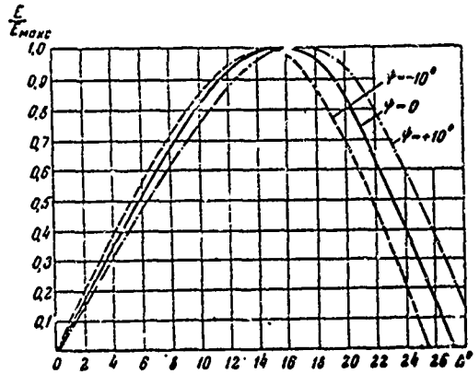

Figure XIV.11.11. The first lobes in the reception patterns in the vertical plane of a 3BS2 21/8 200/4.5 17 antenna on a wavelength of λ = 32 m for different angles of phasing.

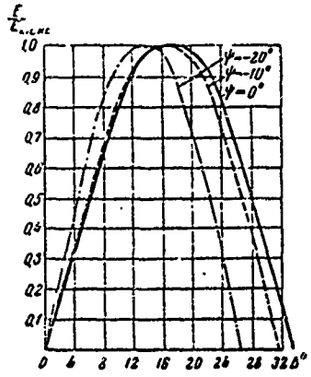

Figure XIV.11.12. The first lobes in the reception patterns in the vertical plane of a 3BS2 21/8 200/4.5 17 antenna on a wavelength of λ = 48 m for different angles of phasing.

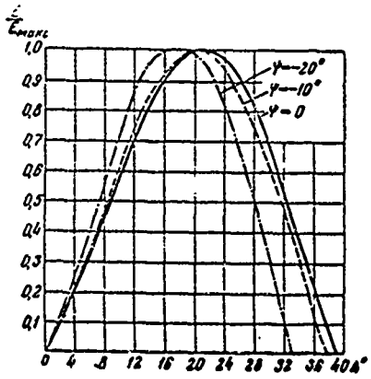

Figure XIV.11.13. The first lobes in the reception patterns in the vertical plane of a 3BS2 21/8 200/4.5 17 antenna on a wavelength of λ = 64 m for different angles of phasing.

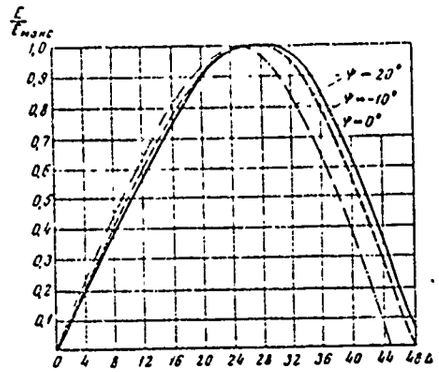

Figure XIV.11.14. The first lobes in the reception pattern in the vertical plane of a 3BS2 21/8 20/4.5 17 antenna on a wavelength of λ = 100 m for different angles of phasing.

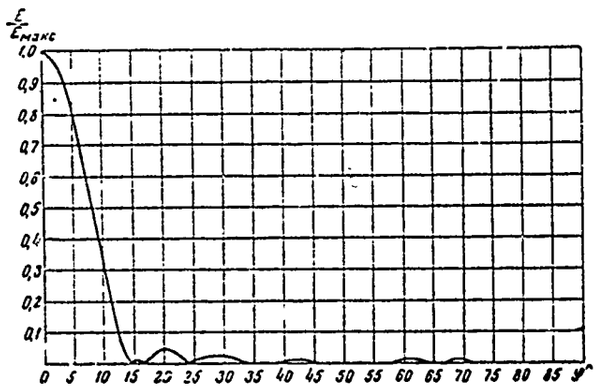

Figure XIV.11.15. Reception pattern in the horizontal plane of a 3BS2 antenna for an angle of phasing ψ = 0° on a wavelength of λ = 12.5 m.

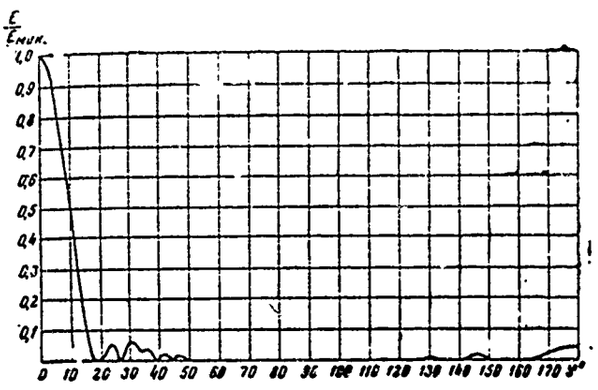

Figure XIV.11.16. Reception pattern in the horizontal plane of a 3BS2 antenna for an angle of phasing ψ = 0° on a wavelength of λ = 16 m.

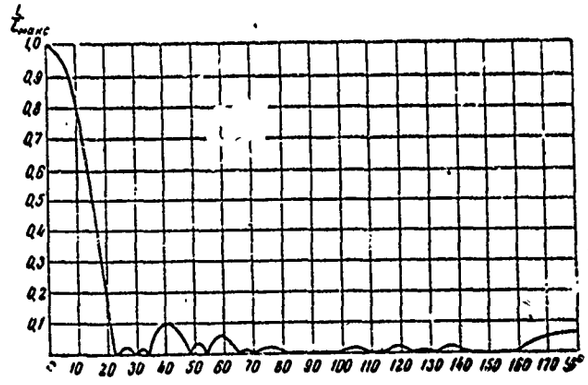

Figure XIV.11.17. Reception pattern in the horizontal plane of a 3BS2 antenna for an angle of phasing $\psi = 0°$ on a wavelength of $\lambda = 24$ m.

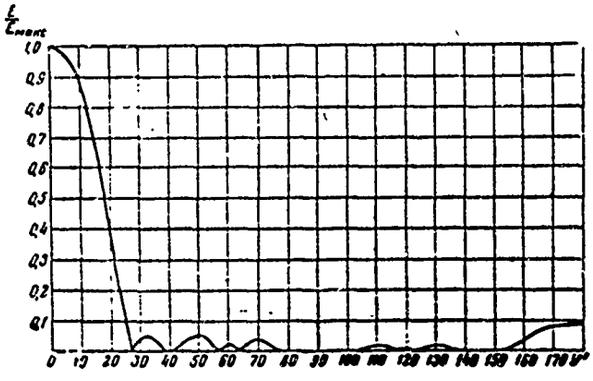

Figure XIV.11.18. Reception pattern in the horizontal plane of a 3BS2 antenna for an angle of phasing $\psi = 0°$ on a wavelength of $\lambda = 32$ m.

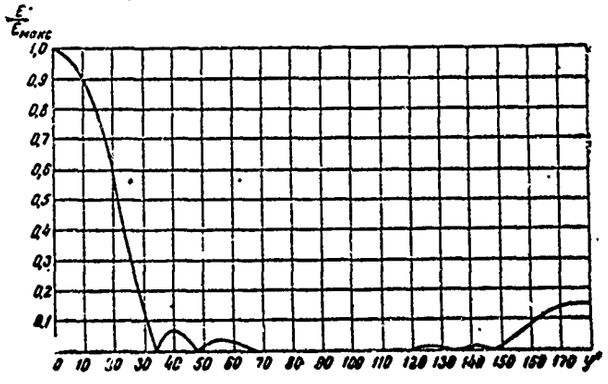

Figure XIV.11.19. Reception pattern in the horizontal plane of a 3BS2 antenna for an angle of phasing $\psi = 0°$ on a wavelength of $\lambda = 48$ m.

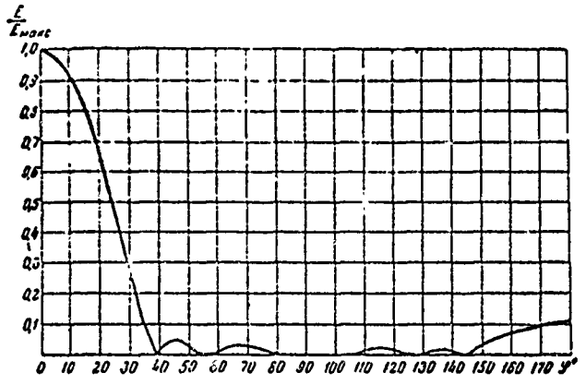

Figure XIV.11.20. Reception pattern in the horizontal plane of a 3BS2 antenna for an angle of phasing $\psi = 0°$ on a wavelength of $\lambda = 64$ m.

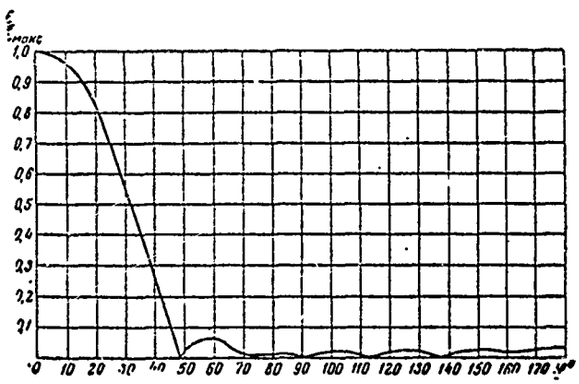

Figure XIV.11.21. Reception pattern in the horizontal plane of a 3BS2 antenna for an angle of phasing $\psi = 0°$ on a wavelength of $\lambda = 100$ m.

#XIV.12. Directive Gain, Efficiency, and Antenna Gain of the 3BS2 Antenna

(a) Directive gain

The directive gain of a multiple traveling wave antenna can be established by the method that compares patterns. Basic to this method is the fact that when there are two antennas with approximately identical side lobe levels, the directive gains will be inversely proportional to the product of the width of the pattern in the horizontal plane by the width of the pattern in the vertical plane, wherein the width of the pattern is understood to mean the angular span of the pattern at half power.

Accordingly,

$$D \approx D_s \frac{\Delta_s \cdot \varphi_s}{\Delta \cdot \varphi} \qquad \text{(XIV.12.1)}$$

In formula (XIV.12.1) D and D_s are the directive gains of the antenna under investigation and of the standard antenna, Δ, φ, Δ_s, and φ_s are the widths of the patterns in the vertical and horizontal planes of the antenna under investigation and of the standard antenna.

The BS2 antenna was used as the standard antenna in the calculation made of the directive gain of the 3BS2 antenna.

Figures XIV.12.1 and XIV.12.2 shows the curves characterizing the dependence of the directive gains for the 3BS2 21/8 200/4.5 17 and 3BS2 21/8 200/4.5 25 antennas on the wavelength when $\psi = 0°$. However, these curves will not provide the complete picture of the gain provided by the multiple 3BS2 antenna as compared with the BS2 antenna because the multiple antenna, aided by the phasing, provides maximum gain for necessary values of Δ. Analysis shows that use of the corresponding phasing will provide approximately a threefold gain in the directive gain of the 3BS2 antenna as compared with the BS2 antenna for needed values of Δ.

(b) Efficiency

The efficiency of the BS2 antenna is used as the basis for determining the efficiency of the 3BS2 multiple antenna. Change in efficiency as a result of the mutual effect of the individual BS antennas in the system is slight, so the efficiency of the 3BS2 multiple antenna can be taken as approximately equal to the efficiency of the BS2 antenna (fig. XIV.9.25).

(c) Antenna gain

The gain of a 3BS2 antenna can be established through the formula

$$\varepsilon = D\eta/1.64.$$

Figure XIV.12.3 shows the curves which characterize the dependence of the gain of the 3BS2 21/8 200/4.5 25 antenna on the wavelength.

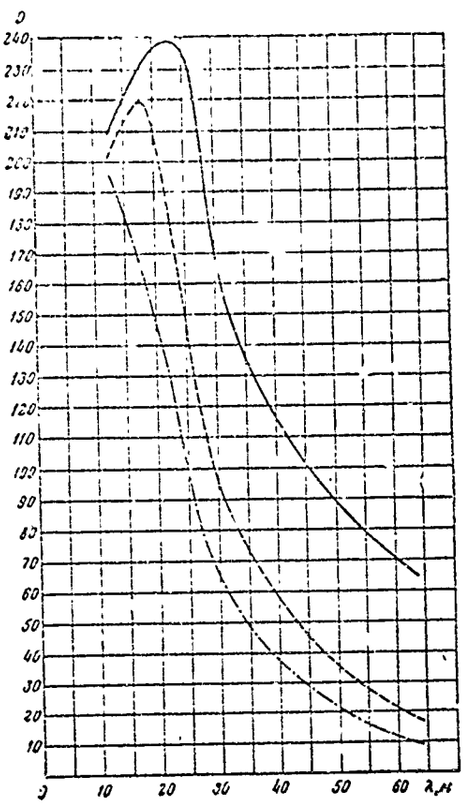

Figure XIV.12.1. Dependence of the directive gain of the 3BS2 21/8 200/4.5 17 antenna on the wavelength for different values of Δ.

——— $\Delta = \Delta_{max}$; ----- $\Delta = 9°$; -.-.- $\Delta = 7°$.

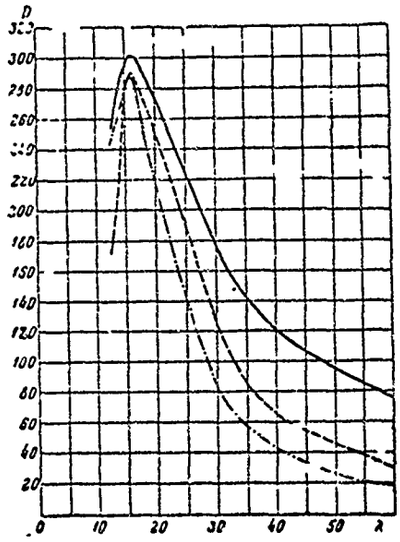

Figure XIV.12.2. Dependence of the directive gain of the 3BS2 21/8 200/4.5 25 antenna on the wavelength for different values of Δ.

——— $\Delta = \Delta_{max}$; ----- $\Delta = 9°$; -.-.- $\Delta = 7°$.

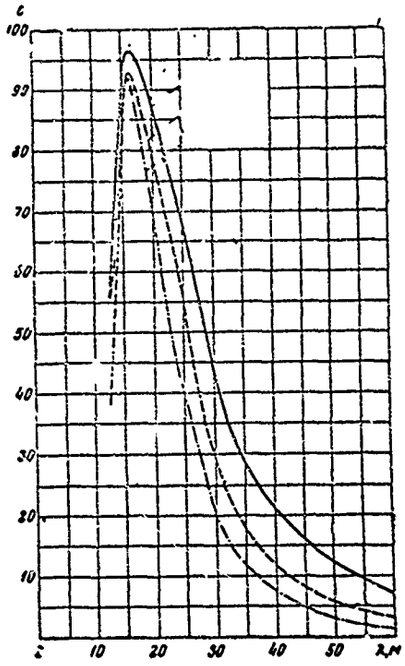

Figure XIV.12.3. Dependence of the gain of a 3BS2 21/8 200/4.5 25 antenna on the wavelength for different values of Δ.

——— $\Delta = \Delta_{max}$; ----- $\Delta = 9°$; -.-.- $\Delta = 7°$.

#XIV.13. Electrical Parameters of a Traveling Wave Antenna with Capacitive Coupling Elements

As has already been noted above, traveling wave antennas with capacitive coupling elements (BYe antennas) have very much poorer parameters than do antennas with resistive coupling elements (BS antennas). Even so, because there are a great many BYe antennas in use at the present time, it is desirable to present the basic parameters of these antennas.

Two traveling wave antennas with capacitive coupling are usually used to cover the entire shortwave band. BYe 39/4 4/2.4 16 antennas, and the corresponding BYe2 39/4 4/2.4 16 and BYe4 39/4 4/2.4 16 multiple antennas, are currently in use for the daytime waveband. The distance between multiple antenna arrays is 20 meters. BYe 24/8 15/3.96 16 and BYe2 24/8 15/3.96 16 antennas are used at night.

Figure XIV.13.1 shows the dependence of the factor k_1, which characterizes the phase velocity of propagation on the antenna, on the wavelength for the BYe 39/4 4/2.4 16 and BYe 24/8 15/3.96 16 antennas.

Figures XIV.13.2 through XIV.13.6 show the receiving patterns in the horizontal plane of the BYe 39/4 4/2.4 16 antenna. Also shown in these figures are the patterns for the BYe2 39/4 4/2.4 16 and BYe4 39/4 4/2.4 16 multiple antennas.

The patterns of the BYe 39/4 4/2.4 16 antenna in the vertical plane are shown in figures XIV.13.7 through XIV.13.11.

Figures XIV.13.12 and XIV.13.13 show the curves that establish the dependence of the directive gain and gain factor on the wavelength and angle of tilt for the BYe 39/4 4/2.4 16 antenna. The values of the maximum gain factors and directive gains are shown by dotted lines in these figures. The gains of the BYe2 39/4 4/2.4 16 and BYe4 39/4 4/2.4 16 antennas are approximately two and four times those of the single antenna. The directive gain of the BYe2 antenna is 1.5 to 2, and the directive gain of the BYe4 antenna is 2.5 to 4 times the directive gain of the single antenna.

Figure XIV.13.14 shows the curve for the dependence of the efficiency of the BYe 39/4 4/2.4 16 antenna on the wavelength.

Figures XIV.13.15 through XIV.13.29 show a series of curves characterizing the electrical parameters of BYe 24/8 15/3.96 16 and BYe2 24/8 15/3.96 16 antennas designed for operation on waves in the nighttime band.

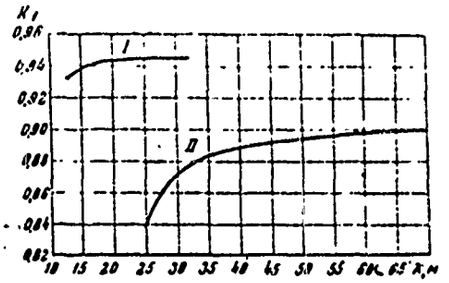

Figure XIV.13.1. Dependence of the coefficient of reduction in phase velocity (k_1) on wavelength.

I - BYe 39/4 4/2.4 16 antenna;
II - BYe 24/8 15/3.96 16 antenna.

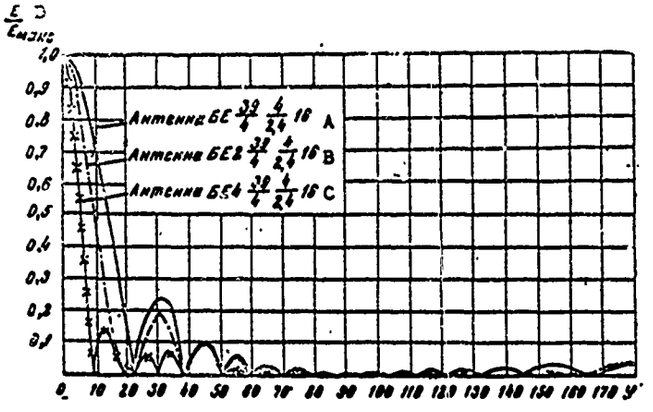

Figure XIV.13.2. Receiving patterns in the horizontal plane of BYe antennas for a wavelength of λ = 13.7 m.

A - BYe 39/4 4/2.4 16 antenna; B - BYe2 39/4 4/2.4 16 antenna; C - BYe4 39/4 4/2.4 16 antenna; D - E/E_{max}.

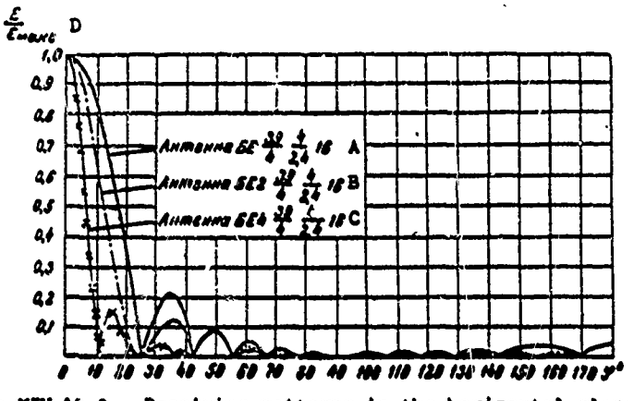

Figure XIV.13.3. Receiving patterns in the horizontal plane of BYe antennas for a wavelength of λ = 16 m.

A - BYe 39/4 4/2.4 16 antenna; B - BYe2 39/4 4/2.4 16 antenna; C - BYe4 39/4 4/2.4 16 antenna; D - E/E_{max}.

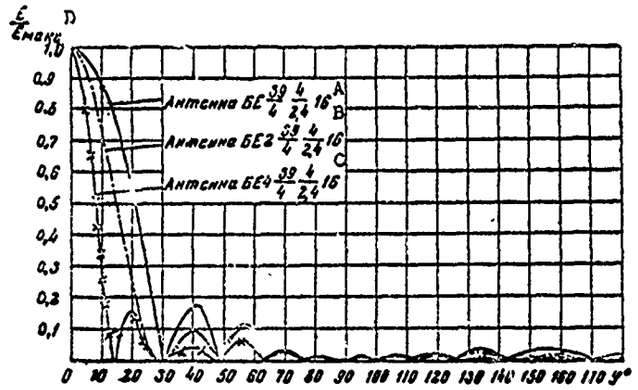

Figure XIV.13.4. Receiving patterns in the horizontal plane of BYe antennas for a wavelength of λ = 19.2 m.

A - BYe 39/4 4/2.4 16 antenna; B - BYe2 39/4 4/2.4 16 antenna; C - BYe4 39/4 4/2.4 16 antenna; D - E/E_{max}.

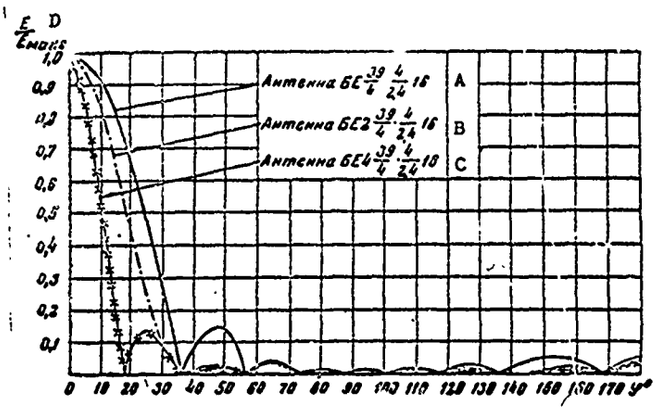

Figure XIV.13.5. Receiving patterns in the horizontal plane of BYe antennas for a wavelength of λ = 24 m.

A - BYe 39/4 4/2.4 16 antenna; B - BYe2 39/4 4/2.4 16 antenna; C - BYe4 39/4 4/2.4 16 antenna; D - E/E_{max}.

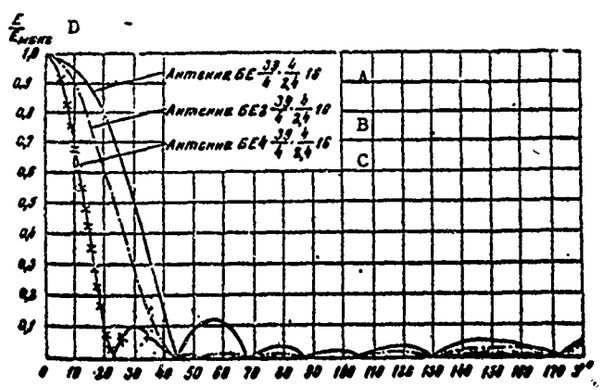

Figure XIV.13.6. Receiving patterns in the horizontal plane of BYe antennas for a wavelength of λ = 32 m.

A - BYe 39/3 3/2.4 16 antenna; B - BYe2 39/4 4/2.4 16 antenna; C - BYe4 39/4 4/2.4 16 antenna; D - E/E_{max}.

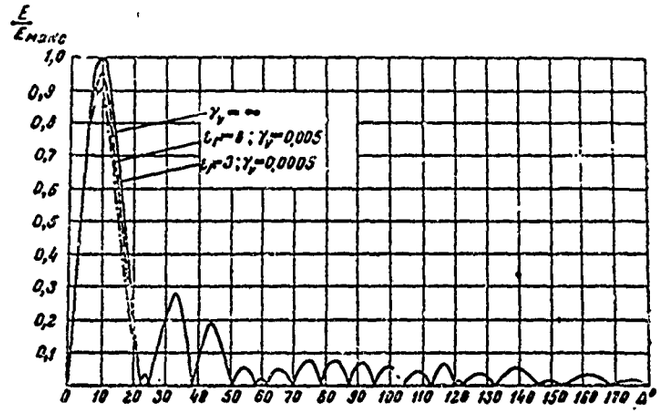

Figure XIV.13.7. Receiving patterns in the vertical plane of a BYe 39/4 4/2.4 16 antenna for ground of ideal conductivity ($\gamma_v=\infty$), ground of average conductivity ($\varepsilon_r=8$; $\gamma_v=0.005$), and ground of low conductivity ($\varepsilon_r=3$; $\gamma_v=0.0005$); $\lambda=13.7$ m.

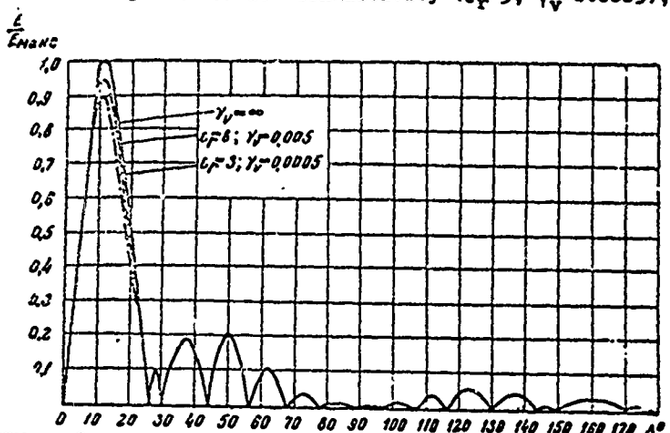

Figure XIV.13.8. Receiving patterns in the vertical plane of a BYe 39/4 4/2.4 16 antenna for ground of ideal conductivity ($\gamma_v=\infty$), ground of average conductivity ($\varepsilon_r=8$; $\gamma_v=0.005$), and ground of low conductivity ($\varepsilon_r=3$; $\gamma_v=0.0005$); $\lambda=16$ m.

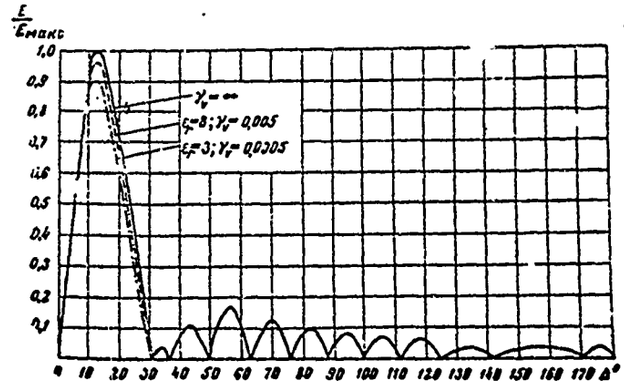

Figure XIV.13.9. Receiving patterns in the vertical plane of a BYe 39/4 4/2.4 16 antenna for ground of ideal conductivity ($\gamma_v=\infty$), ground of average conductivity ($\varepsilon_r=8$; $\gamma_v=0.005$), and ground of low conductivity ($\varepsilon_r=3$; $\gamma_v=0.0005$); $\lambda=19.2$ m.

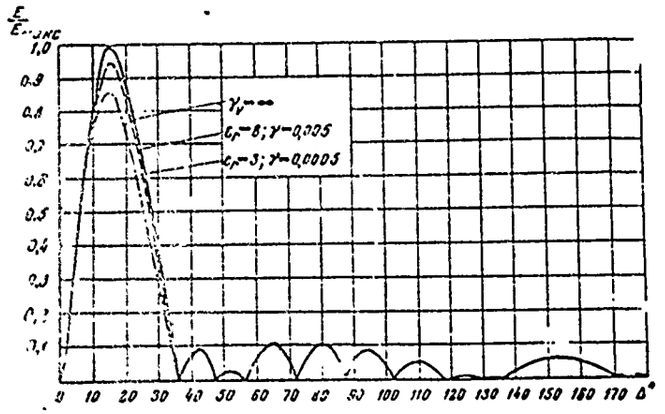

Figure XIV.13.10. Receiving patterns in the vertical plane of a BYe 39/4 4/2.4 16 antenna for ground of ideal conductivity ($\gamma_v=\infty$), ground of average conductivity ($\varepsilon_r=8$; $\gamma_v=0.005$), and ground of low conductivity ($\varepsilon_r=3$; $\gamma_v=0.0005$); $\lambda=24$ m.

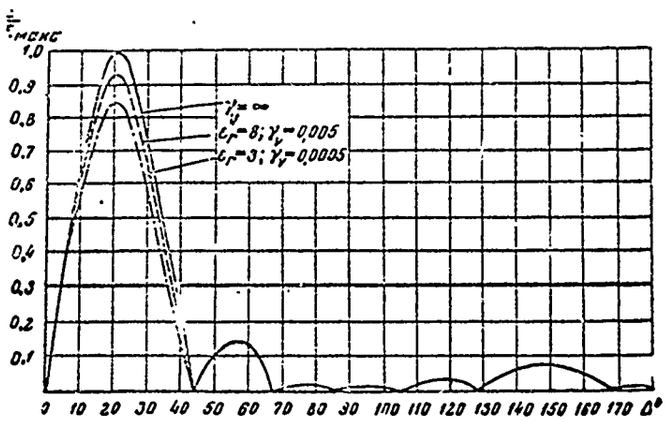

Figure XIV.13.11. Receiving patterns in the vertical plane of a BYe 39/4 4/2.4 16 antenna for ground of ideal conductivity ($\gamma_v = \infty$), ground of average conductivity ($\varepsilon_r = 8$; $\gamma_v = 0.005$), and ground of low conductivity ($\varepsilon_r = 3$; $\gamma_v = 0.0005$); $\lambda = 32$ m.

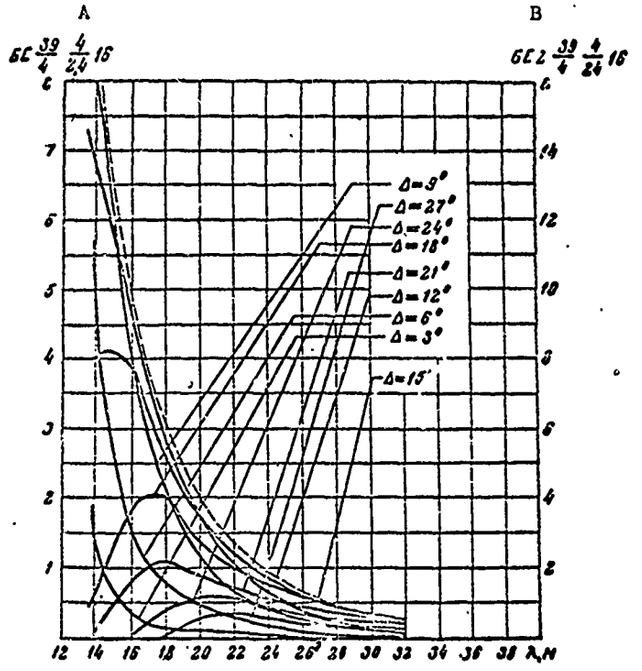

Figure XIV.13.12. Dependence of the gain (ε) of BYe 39/4 4/2.4 16 and BYe2 39/4 4/2.4 16 antennas on wavelength for different angles of tilt (Δ).

----- maximum gain curve; A - BYe 39/4 4/2.4 16; B - BYe2 39/4 4/3.4 16.

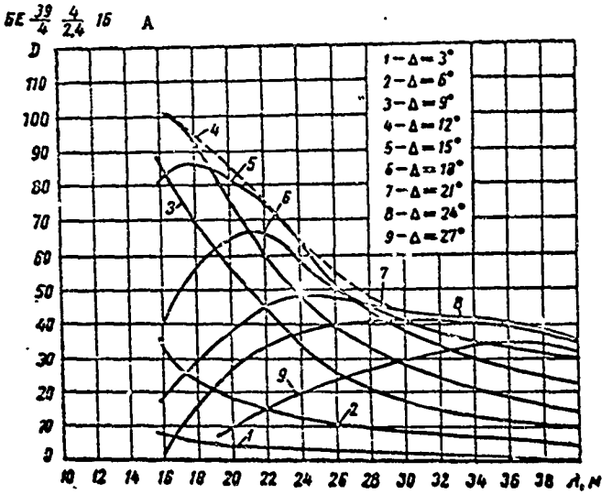

Figure XIV.13.13. Dependence of directive gain (D) of a BYe 39/4 4/2.4 16 antenna on wavelength for different angles of tilt (Δ).

----- maximum directive gain curve; A - BYe 39/4 4/2.4 16.

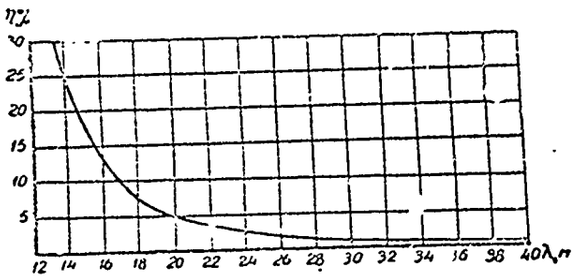

Figure XIV.13.14. Dependence of the efficiency of a BYe 39/4 4/2.4 16 antenna on the wavelength.

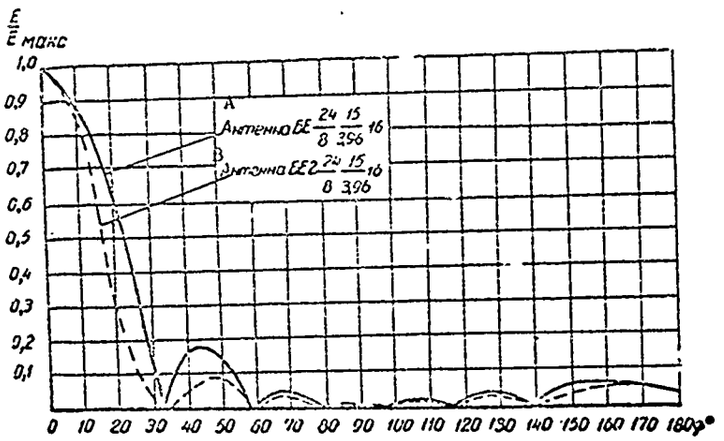

Figure XIV.13.15. Receiving patterns in the horizontal plane of BYe 24/8 15/3.96 16 and BYe2 24/8 15/3.96 16 antennas for a wavelength of λ = 30 m.

A - BYe 24/8 15/3.96 16 antenna; B - BYe2 24/8 15/3.96 16 antenna.

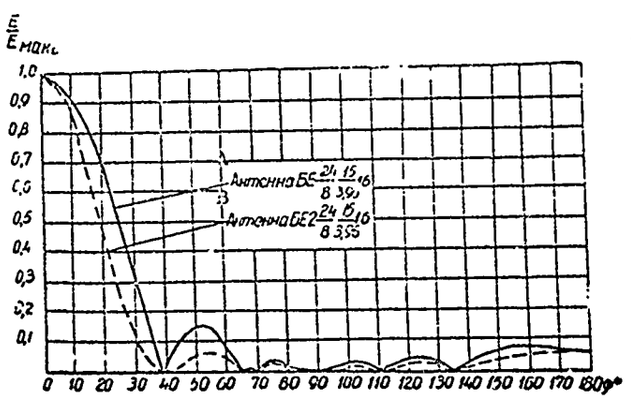

Figure XIV.13.16. Receiving patterns in the horizontal plane of BYe 24/8 15/3.96 16 and BYe2 24/8 15/3.96 16 antennas for a wavelength of λ = 35 m.

A - BYe 24/8 15/3.96 16 antenna; B - BYe2 24/8 15/3.96 16 antenna.

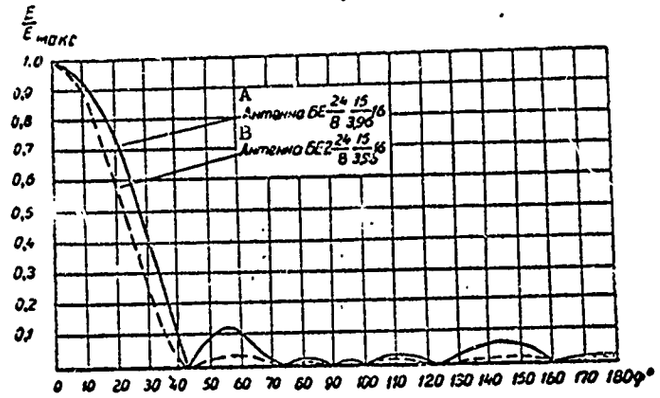

Figure XIV.13.17. Receiving patterns in the horizontal plane of BYe 24/8 15/3.96 16 and BYe2 24/8 15/3.96 16 antennas for a wavelength of λ = 40 m.

A - BYe 24/8 15/3.96 16 antenna; B - BYe2 24/8 15/3.96 16 antenna.

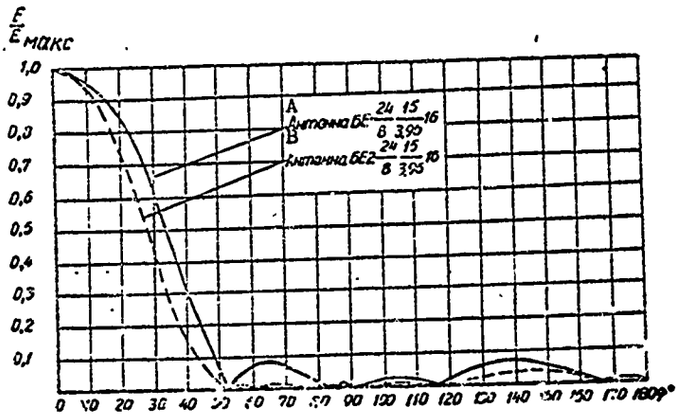

Figure XIV.13.18. Receiving patterns in the horizontal plane of BYe 24/8 15/3.96 16 and BYe2 24/8 15/3.96 16 antennas for a wavelength of λ = 50 m.

A - BYe 24/8 15/3.96 16 antenna; B - BYe2 24/8 15/3.96 16 antenna.

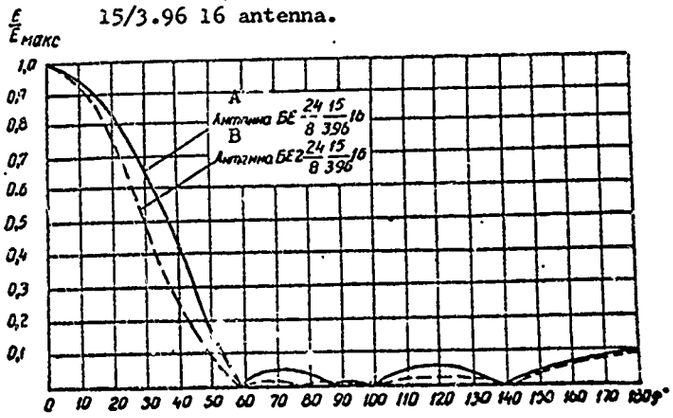

Figure XIV.13.19. Receiving patterns in the horizontal plane of BYe 24/8 15/3.96 16 and BYe2 24/8 15/3.96 16 antennas for a wavelength of λ = 60 m.

A - BYe 24/8 15/3.96 16 antenna; B - BYe2 24/8 15/3.96 16 antenna.

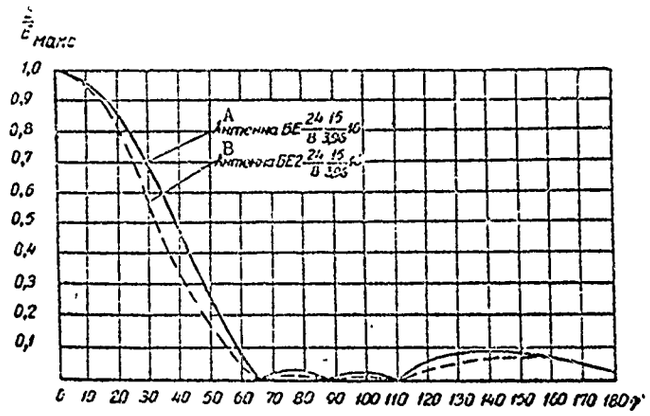

Figure XIV.13.20. Receiving patterns in the horizontal plane of BYe 24/8 15/3.96 16 and BYe2 24/8 15/3.96 16 antennas for a wavelength of λ = 70 m.

A - BYe 24/8 15/3.96 16 antenna; B - BYe2 24/8 15/3.96 16 antenna.

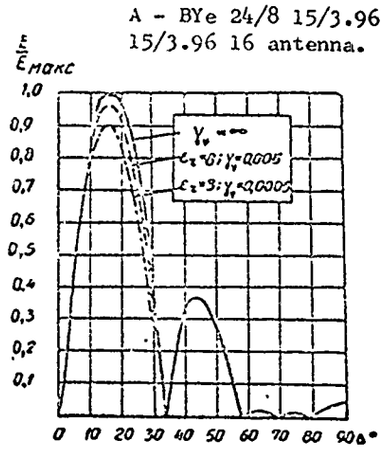

Figure XIV.13.21. Receiving patterns in the vertical plane of a BYe 24/8 15/3.96 16 antenna for ground of ideal conductivity ($\gamma_V=\infty$), ground of average conductivity ($\varepsilon_r=8$; $\gamma_V=0.005$), and ground of low conductivity ($\varepsilon_r=3$; $\gamma_V=0.0005$); λ = 30 m.

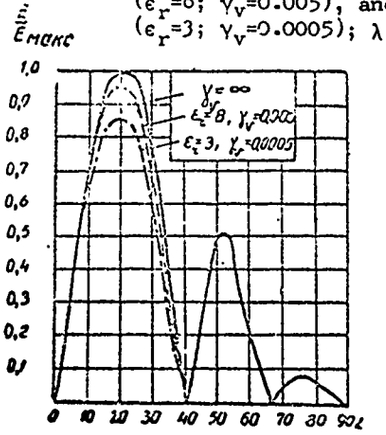

Figure XIV.13.22. Receiving patterns in the vertical plane of a BYe 24/8 15/3.96 16 antenna for ground of ideal conductivity ($\gamma_V=\infty$), ground of average conductivity ($\varepsilon_r=8$; $\gamma_V=0.005$), and ground of low conductivity ($\varepsilon_r=3$; $\gamma_V=0.0005$); λ = 35 m.

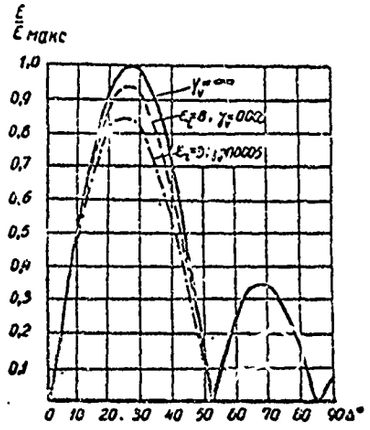

Figure XIV.13.23. Receiving patterns in the vertical plane of a BYe 24/8 15/3.96 16 antenna for ground of ideal conductivity ($\gamma_v=\infty$), ground of average conductivity ($\varepsilon_r=8$; $\gamma_v=0.005$), and ground of low conductivity ($\varepsilon_r=3$; $\gamma_v=0.0005$); λ = 50 m.

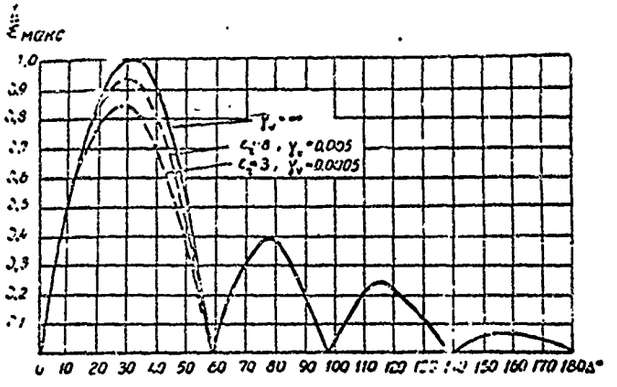

Figure XIV.13.24. Receiving patterns in the vertical plane of a BYe 24/8 15/3.96 16 antenna for ground of ideal conductivity ($\gamma_v=\infty$), ground of average conductivity ($\varepsilon_r=8$; $\gamma_v=0.005$), and ground of low conductivity ($\varepsilon_r=3$; $\gamma_v=0.0005$); λ = 60 m.

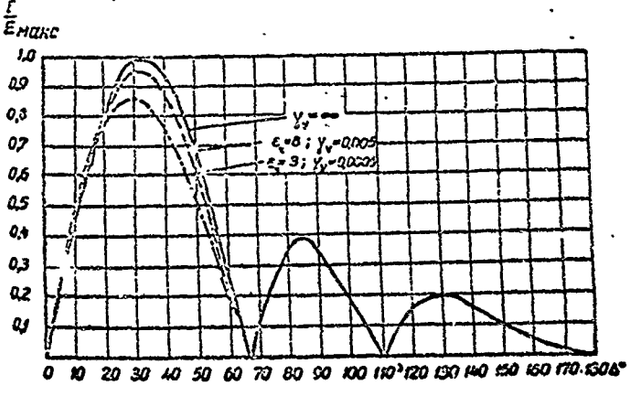

Figure XIV.13.25. Receiving patterns in the vertical plane of a BYe 24/8 15/3.96 16 antenna for ground of ideal conductivity ($\gamma_v=\infty$), ground of average conductivity ($\varepsilon_r=8$; $\gamma_v=0.005$), and ground of low conductivity ($\varepsilon_r=3$; $\gamma_v=0.0005$); λ = 70 m.

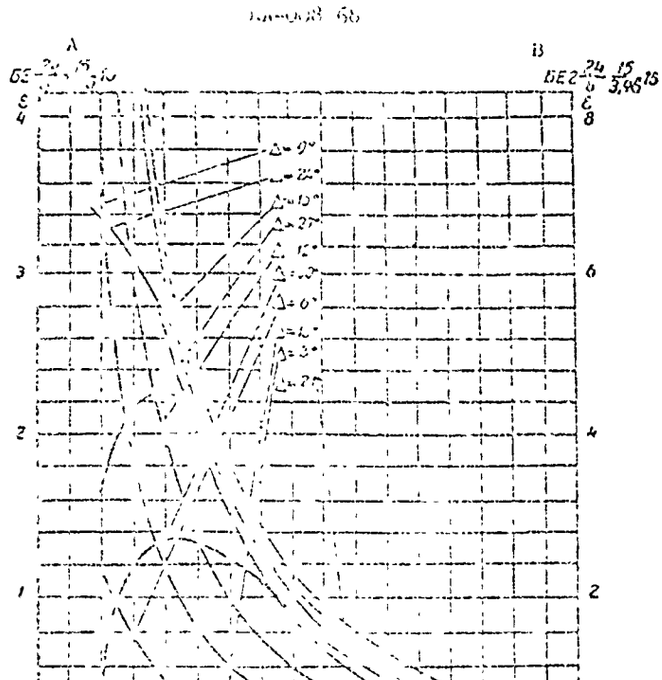

Figure XIV.13.26. Dependence of gain (g) of BYe 24/8 15/3.96 16 and BYe2 24/8 15/3.96 16 antennas on wavelength for different angles of tilt (Δ). ---- maximum gain curve.

A - BYe 24/8 15/3.96 16 antenna; B - BYe2 24/8 15/3.96 16 antenna.

Figure XIV.13.27. Dependence of directive g in (D) of a BYe 24/8 15/3.96 16 antenna on wavelength for different angles of tilt (Δ). ---- maximum directive gain curve.

A - BYe 24/8 15/3.96 16 antenna.

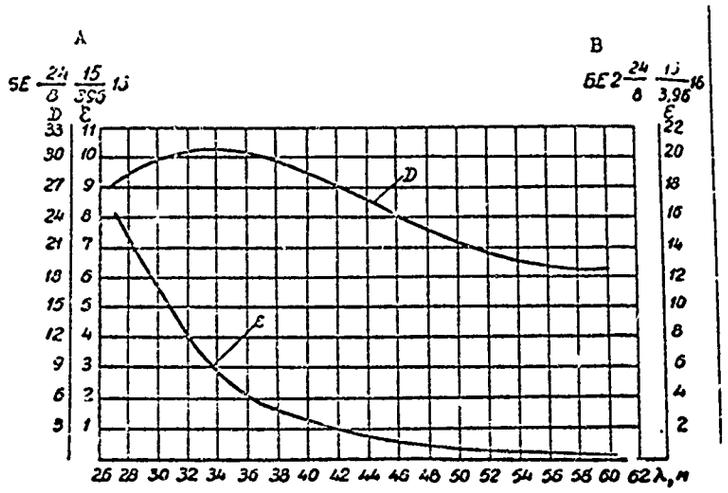

Figure XIV.13.28. Dependence of maximum directive gain (D) and gain (ε) of BYe 24/8 15/3.96 16 and BYe2 24/8 15/3.96 16 antennas on wavelength.

A - BYe 24/8 15/3.96 16 antenna; B - BYe2 24/8 15/3.96 16 antenna.

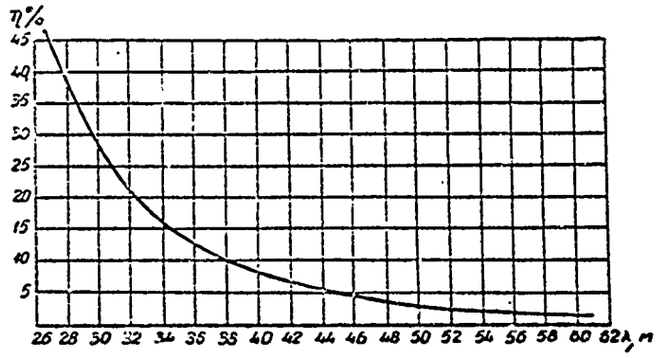

Figure XIV.13.29. Dependence of the efficiency of the BYe 24/8 15/3.96 16 antenna on the wavelength.

#XIV.14. Phasing Device for Controlling the Receiving Patterns of the 3BS2 Antenna

A linear phasing device developed by V. D. Kuznetsov can be used to control the receiving pattern in the vertical plane of a 3BS2 antenna. As will be seen from the schematic, the phasing device is an artificial balanced line, replacing the line with uniformly distributed parameters.

Antenna, 1, is connected to terminals 1-1 of the artificial line, antenna 3 to terminals 3-3, and antenna 2 to terminals 2-2. The receiver is also connected to terminals 2-2 through a conversion transformer. Moveable contacts, 2-2, slide over the artificial line.

The lengths of the feeders, and that of the artificial line, are selected such that when sliding contacts 2-2 are in the center position the emfs produced by all antennas will add in phase upon the arrival of a beam from a direction that coincides with the direction of the antennas' collection lines.

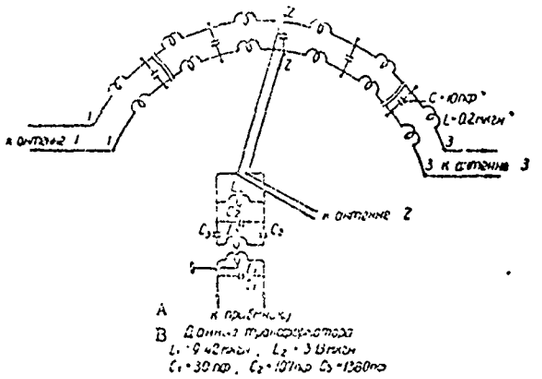

Figure XIV.14.1. Schematic diagram of phasing device.

1, 2, 3 - to antenna; A - to receiver; B - transformer data: L_1 = 9.42 microhenries; L_2 = 3.13 microhenries; C_1 = 30 pf; C_2 = 107 pf; C_3 = 1,380 pf.

When the sliding contact is moved to terminals 1-1 the phase angle between the emfs across the receiver input from antennas 1 and 2, as well as from antennas 1 and 3, will be increased, and this is equivalent to reducing the phase velocity (negative values of ψ). When the sliding contact is moved to terminals 3-3 the phase angle between the emfs across the receiver input from antennas 1 and 2 and antennas 1 and 3 will be reduced and this is equivalent to increasing the phase velocity (positive values of ψ).

The length of the artificial line is selected to provide for in-phase summing of the emfs across the receiver input at maximum required angles of elevation, and is established through the formula

$$l_s = 2D(1 - \cos \Delta_{max}) \qquad \text{(XIV.14.1)}$$

where

D is the distance between antennas. In our case D = 96 meters.

Setting the magnitude of the maximum elevation angle equal to 35°, we find

$$l_s = 35 \text{ meters.}$$

The artificial line is made up of 68 elementary cells. The equivalent length of an elementary cell is selected equal to 0.52 meter. At this length the lag between emfs across adjacent antennas produced by one cell on the shortest wave in the band λ = 12 meters, equals 31.2°. Each elementary cell is made up of two single-layer coils wound on "getinaks"* cores, and one condenser. The inductance of one coil in the cell equals 0.2 microhenry, and the cell capacitance is 10 pf.

---

* Translator's Note: A sheet material used in electrical work. Made in pressed layers consisting of several layers of paper impregnated with phenol-aldehyde, xylenol-aldehyde, phenol-aniline-aldehyde resin, or a mixture of these resins.

A conversion transformer, 60 ohms to 180 ohms, is used to match the receiver input to the output of the phasing device. The schematic and data o the elements of the transformer are shown in Figure XIV.14.1.

The necessary condition for normal operation of the 3BS2 antenna system is identity in the design and characteristics of the antennas, as well as of the feeder lines. The lengths of the feeders for all antennas up to the inputs from the phasing device should correspond to the design data following:

length of the feeder for antenna 1 equals S,

length of the feeder for antenna 2 equals $S + D + l_g/2$,

length of the feeder for antenna 3 equals S + 2D.

The possibility of equalizing the lengths of the feeders within up to 2.5 meters is envisaged in the phase shifter. A small segment of artificial line, made similar to the line for the phasing device, is inserted in the break in the feeder from antenna 2 for this purpose. Design-wise the equalizer is made in such a way that it can lengthen the feeder smoothly from 0 to 2.5 meters.

The phasing device described can also be used in the operation of the antenna system consisting of two 2BS2 antennas.

#XIV.15. Vertical Traveling Wave Antenna

There are many cases when it is necessary to substantially reduce the cost of the traveling wave antenna, as well as to shorten the time required to build it. The vertical unbalanced traveling wave antenna with resistive coupling elements (BSVN) can be recommended as an antenna meeting these specifications.

The schematic of the BSVN antenna is shown in Figure XIV.15.1a. Two parallel connected arrays (fig. XIV.15.1b) should be used to increase the efficiency of the vertical traveling wave antenna.

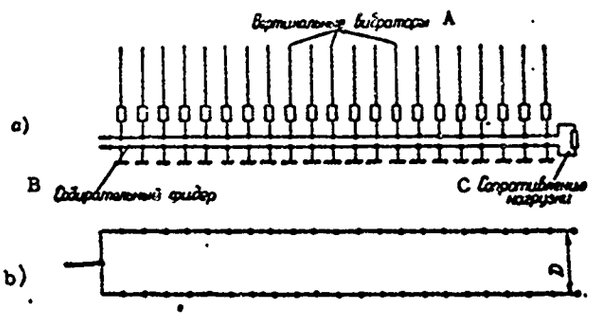

Figure XIV.15.1. Schematic diagrams of the BSVN and BSVN2 antennas.
A - vertical dipoles; B - collection feeder;
C - terminator.

The following principal parameters for one BSVN antenna array can be recommended:

(1) length of antenna array L = 90 meters;

(2) number of unbalanced dipoles in the array N = 21 to 42;

(3) length of a dipole l = 8 meters;

(4) distance between dipoles d = 2.25 to 4.5 meters.

The distance, D, between two arrays in the BSVN2 antenna can be taken as equal to 15 to 25 meters.

The collection line is an unbalanced, concentric, multiconductor feeder with a characteristic impedance of 140 ohms. The coupling resistance (R_{co}) inserted between the dipoles and the external systems of conductors making up the collection feeder, should be taken as equal to 350 to 800 ohms, and the terminating resistor is taken equal to the characteristic impedance of the collection feeder. A vertical traveling wave antenna carries the following designation

$$\text{BSVN2 } N/l \; R_{co}/d.$$

The receiving pattern in the horizontal plane of a BSVN2 antenna can be charted through the formula

$$F(\varphi) = \sqrt{\frac{\operatorname{ch}\beta_c Nd - \cos\left[\pi Nd\left(\frac{1}{k_1} - \cos\varphi\right)\right]}{\operatorname{ch}\beta_c d - \cos\left[\pi d\left(\frac{1}{k_1} - \cos\varphi\right)\right]}}\cos\left(\frac{\pi D}{2}\sin\varphi\right). \qquad \text{(XIV.15.1)}$$

The pattern in the vertical plane can be charted through the formula

$$F(\Delta) = \frac{1}{\cos\Delta}\sqrt{\frac{\operatorname{ch}\beta_c Nd - \cos\left[\pi Nd\left(\frac{1}{k_1} - \cos\Delta\right)\right]}{\operatorname{ch}\beta_c d - \cos\left[\pi d\left(\frac{1}{k_1} - \cos\Delta\right)\right]}} \times$$

$$\times \Big| \{[\cos(\pi l\sin\Delta) - \cos\pi l](1 + |R_\perp|\cos\Phi_\perp) +$$
$$+ |R_\perp|\sin\Phi_\perp [\sin(\pi l\sin\Delta) - \sin\pi l\sin\Delta]\} +$$
$$+ i\{[\sin(\pi l\sin\Delta) - \sin\pi l\sin\Delta](1 - |R_\perp|\cos\Phi_\perp +$$
$$+ |R_\perp|\sin\Phi_\perp [\cos(\pi l\sin\Delta) - \cos\pi l]\}\Big|. \qquad \text{(XIV.15.2)}$$

In formulas (XIV.15.1) and (XIV.15.2)

$|R_\parallel|$ and $\Phi_\parallel$ are the modulus and argument for the reflection factor for a parallel polarized beam;

φ is the azimuth angle, read from the axis of the antenna;

Δ is the angle of tilt of the incoming beam.

The values of k_1 and β_c for the data used here for the antenna are established from the graphics shown in figures XIV.9.1 and XIV.9.2 for the horizontal antenna.

Figure XIV.15.2 shows the charted patterns in the horizontal plane of a BSVN2 21/8 400/4.5 antenna. The calculations were made for the case when D = 25 meters. A comparison of the patterns in the horizontal plane of a vertical and of a horizontal antenna shows that the level of the side lobes is considerably higher in the case of the vertical antenna. Correspondingly, the vertical antenna has much less noise stability.

Figure XIV.15.3 shows the patterns in the vertical plane of a BSVN2 21/8 400/4.5 antenna for the same waves for moist ground ($\varepsilon_r = 25$, $\gamma_v = 10^{-2}$ mhos/m) and dry ground ($\varepsilon_r = 5$, $\gamma_v = 10^{-3}$ mhos/m).

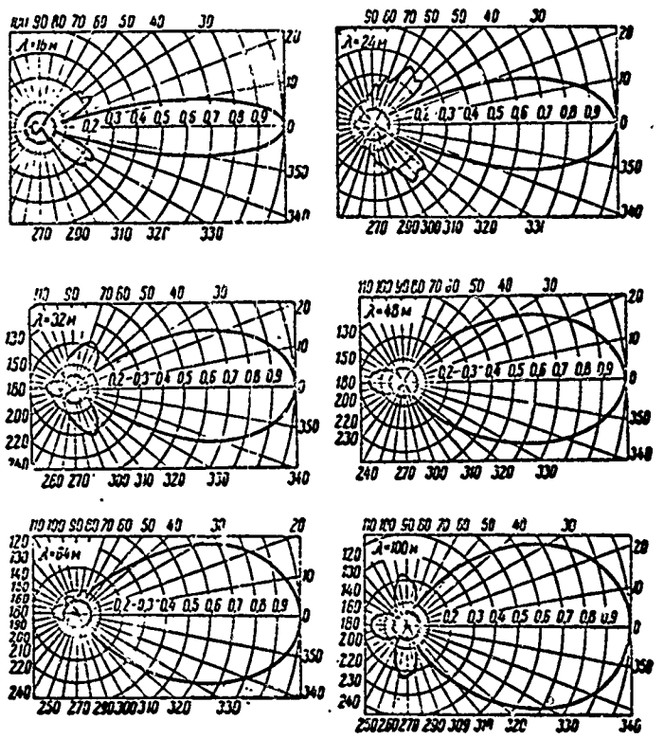

Figure XIV.15.2. Charted receiving patterns in the horizontal plane of the BSVN2 21/8 400/4.5 antenna; D = 25 m.

The directive gain can be approximated by comparing the patterns of the BSVN2 21/8 400/4.5 antenna with the patterns of the BS2 antenna.

Figure XIV.15.4 shows the dependence of the maximum directive gain of a BSVN2 21/8 400/4.5 antenna for wet soil ($\varepsilon_r = 25$, $\gamma_v = 10^{-2}$ mhos/m) and dry soil ($\varepsilon_r = 5$, $\gamma_v = 10^{-3}$ mhos/m) on the wavelength.

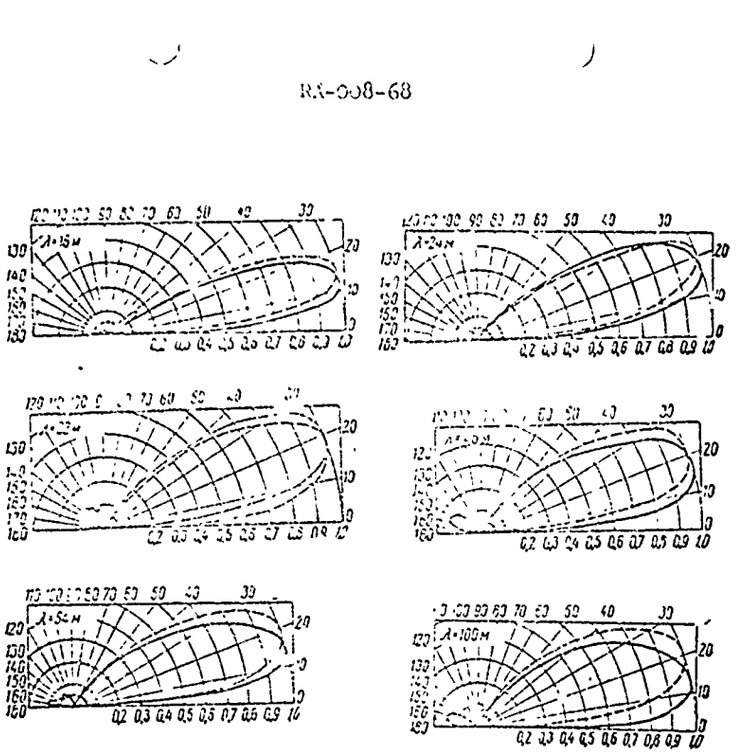

Figure XIV.15.3. Vertical plane directional patterns for the BSVN2 21/8 400/4.5 antenna.

——— wet ground (ε_r=25; γ_v=10^{-2} mhos/m);

----- dry ground (ε_r=5; γ_v =10^{-3} mhos/m).

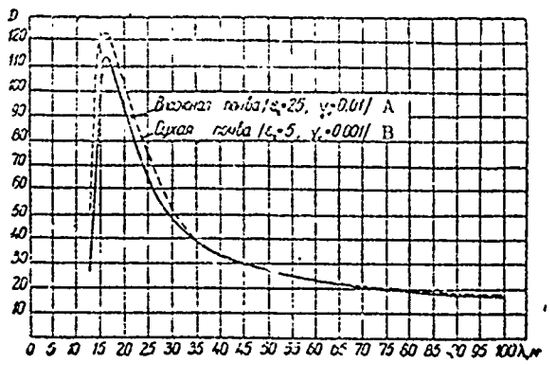

Figure XIV.15.4. Dependence of maximum directive gain of the BSVN2 21/8 400/4.5 antenna for wet and dry ground on wavelength.

A - wet ground; B - dry ground.

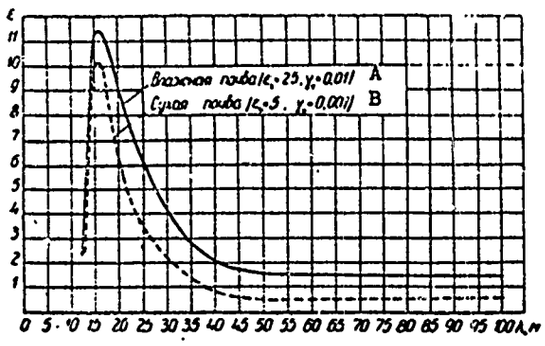

Figure XIV.15.5. Dependence of maximum gain of a BSVN2 21/8 400/4.5 antenna on wavelength for wet and dry ground.

A - wet ground; B - dry ground.

The charted values of maximum antenna gain for the BSVN antenna in the waveband are shown in Figure XIV.15.5.

In concluding this section, it should be noted that the vertical traveling wave antenna, together with the horizontal traveling wave antenna, can be used for duplex reception with separation with respect to polarization. The vertical antenna can be installed below the horizontal antenna in the same area. It is desirable to have the projections of the collection lines of the horizontal and vertical antennas on the ground coincide in order to ensure minimum mutual effect.

#XIV.16. Traveling Wave Antenna Design Formulation

(a) BS, BS2, and 3BS2 antenna formulation

The BS antenna array consists of 21 balanced dipoles. The length of the antenna array is 90 meters. The dipoles are made of hard-drawn copper, or bimetallic wire, 2 mm in diameter.

Figure XIV.16.1 shows one way in which dipoles can be connected to the collection line.

Figure XIV.16.2 shows how the coupling resistors connected between the balanced dipoles and the collection line are secured in place.

Type MLT mastic resistors, designed to dissipate 2 to 5 watts, can be used as the coupling resistors. It is desirable to use type MLT resistors, designed to dissipate 10 watts, in areas where thunderstorms occur.

The antenna array can be suspended on 4 to 6 wooden or reinforced-concrete masts by bearer cables. Insulators are inserted in the bearer cables every 3 to 4 meters. It is desirable to insulate the balanced dipoles by using stick insulators, since they have low stray capacitance.

A six-wire reduction with W =170 ohms, running to a 170 ohm terminating resistor, is connected to the end of the collection feeder directed at the correspondent.

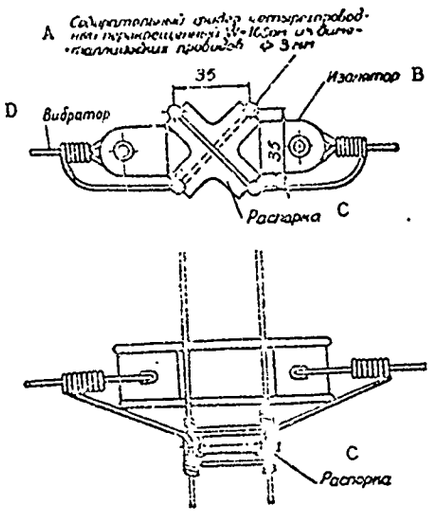

Figure XIV.16.1. Securing the dipoles to the collection line.

A - collection feeder, four-wire, crossed; W - 168 ohms of bimetallic wires, 3 mm diameter; B - insulator; C - spreader; D - dipole.

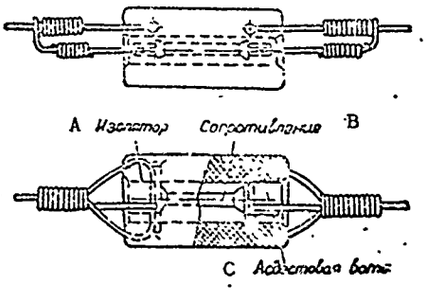

Figure XIV.16.2. Securing the coupling resistor.

A - insulator; B - resistor; C - asbestos wool.

Everything said in the foregoing with respect to making terminating resistors for rhombic receiving antennas applies with equal force to the terminating resistors for the BS antenna (see #XIII.16).

The collection line for the BS antenna is made in the form of a four-wire crossed feeder with a characteristic impedance of 168 ohms. The TF6 168/208 six-wire feeder transformer (fig. XIV.16.3) can be used to match the collection line of the BS antenna with a standard supply feeder with a characteristic impedance of 208 ohms, while TF6 168/416 transformers (fig. XIV.16.4) can be used to match the BS2 antenna with the supply feeder.

Should BS and BS2 antennas be used to operate in two opposite directions, feeder transformers TF6 168/208 (BS antenna) and TF6 168/416 (BS2 antenna) can be connected to both ends of the collection feeder. The supply feeders,

with characteristic impedance of 208 ohms, running to the service building, are connected to these transformers. Tho terminating resistors are installed in the service building.

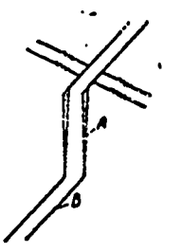

Figure XIV.16.3. Schematic diagram of the match between a BS antenna and a four-wire feeder.

A - six-wire feeder transformer TF6 168/208;
B - four-wire feeder (W = 208 ohms).

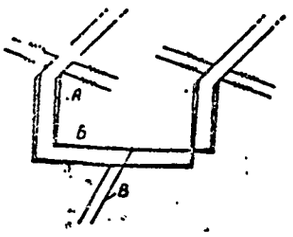

Figure XIV.16.4. Schematic diagram of the match between a BS2 antenna and a four-wire feeder.

A - vertical feeder transformer TF6 168/208;
B - horizontal feeder transformer TF6 208/416;
C - four-wire feeder (W = 208 ohms.

The BS2 antenna is suspended on 6 to 9 wooden or reinforced-concrete masts by bearer cables. A general view of a BS2 antenna suspended on nine supports is shown in Figure XIV.16.5.

The 3BS2 antenna is suspended on from 8 to 21 masts by bearer cables. A general view of a 3BS2 antenna suspended on 21 masts is shown in Figure XIV.16.6.

(b) BYe and BYe2 antenna formulation

The collection line for the BYe antenna is made in the form of a two-wire feeder of copper or bimetallic wire, 3 to 4 mm in diameter. The distance between the wires is taken equal to 8 cm.

The balanced dipoles are manufactured from hard-drawn copper or bimetallic wire, 1.5 to 2 mm in diameter.

The condensers inserted between the balanced dipoles and the collection line are made so they are at the same time collection line insulators (fig. XIV.16.7), hence the designation insulators-condensers.

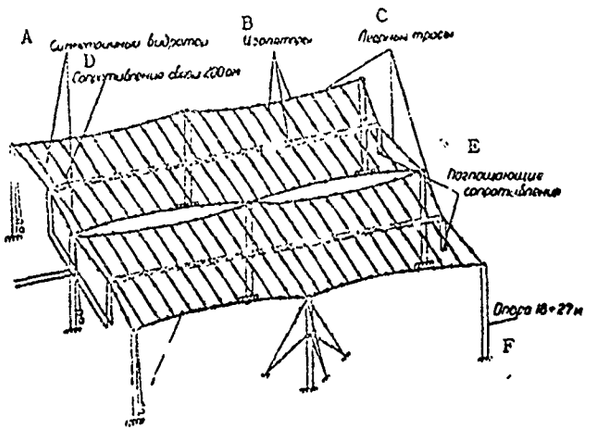

Figure XIV.16.5. General view of a BS2 antenna.

A - balanced dipole; B - insulators; C - bearer cables; D - coupling resistor 200 ohms; E - terminating resistor; F - supports, 18 to 27 meters.

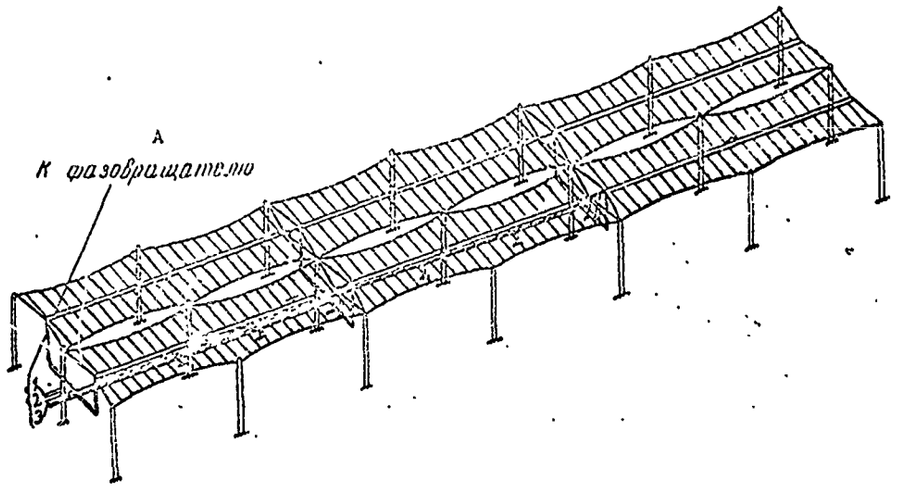

Figure XIV.16.6. General view of a 3BS2 type antenna.

A - to phase shifter.

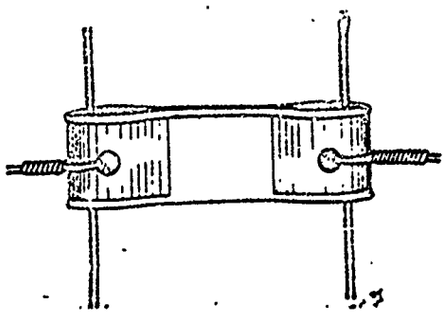

Figure XIV.16.7. Insulator-condenser for a traveling wave antenna.

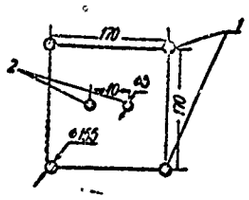

Figure XIV.16.8. Transverse cross section of a collection feeder for a BSVN antenna.

The BYe antenna array is similar to the BS antenna array.

The distribution feeder is two-wire with a characteristic impedance of 400 to 450 ohms. An exponential feeder transformer, the TF4P 400/208, is used to match the distribution feeder with the four-wire supply feeder with characteristic impedance of 208 ohms.

The distribution feeders of the BYe2 antenna also have a characteristic impedance of 400 to 450 ohms. The characteristic impedance of all antennas in the BYe2 system is about 200 ohms and can be matched well to the characteristic impedance of a four-wire feeder.

Two-wire distribution feeders are made of copper or bronze stranded conductors, 2-3 mm in diameter.

The two-wire distribution feeders are crossed every 0.5 to 1 meter to weaken antenna effect. The insulators used to make the cross are usually made of porcelain.

The terminating resistor should have a value of 400 to 450 ohms.

(c) BSVN2 antenna formulation

Each of the antenna arrays is suspended on two supports at a height of 12 to 14 meters by bearer cables. The bearer cables are broken up by insulators every 3 or 4 meters.

A cross section of the collection feeder is shown in Figure XIV.16.8. The conductors numbered 1 form the shield for the concentric feeder, while those numbered 2 form the internal conductor of the feeder. The shield conductors are interconnected by jumpers.

The shield is grounded at each dipole by stakes driven 50 to 100 cm into the ground. The use of radial grounding, consisting of 10 to 12 conductors 5 t 10 meters long is more desirable than the stakes because the loss to ground will be reduced.

Chapter XV

SINGLE-WIRE TRAVELING WAVE ANTENNA

#XV.1. Antenna Schematic and Operating Principle

The single-wire traveling wave antenna (the Beveridge antenna) is a long wire suspended not very high above the ground and loaded with pure resistance equal to the characteristic impedance of the conductor. Figure XV.1.1 is a schematic of this antenna.

So far as electrical parameters are concerned, the single-wire traveling wave antenna is not as good as the highly efficient receiving antennas (such as the BS antenna) reviewed above. However, there are many cases where the exceptional design simplicity and cheapness of the single-wire antenna make it irreplaceable.

The emf in the antenna wire is created by the horizontal component of the incident wave electric field strength vector. If the direction of the incoming signal is little different from the direction of the wire, conditions favorable for the addition of the emfs induced at individual points on the wire at the receiver input will be created. But if the direction from which the wave is arriving is substantially different from the direction of the wire, reception will be greatly weakened by the interference of the emfs induced at individual points on the wire. A more detailed description of the principle of operation of the traveling wave antenna was given in the preceding chapter.

Henceforth the single-wire traveling wave antenna will be shortened to the designation OB L/H, where L is the length of the antenna in meters, and H is the height at which the antenna is suspended above ground in meters.

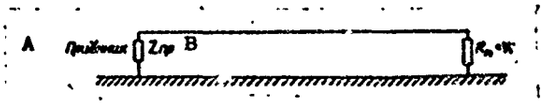

Figure XV.1.1. Schematic diagram of a single-wire traveling wave antenna.

A - receiver; B - $Z_{receiver}$.

#XV.2. Design Formulas

(a) Formulas for OB antenna radiation patterns

The single-wire traveling wave antenna can be assumed to have a parallel polarized field, as well as a normally polarized field. Without pausing to derive them, let us introduce formulas for charting the patterns of the OB antenna when receiving a parallel polarized field ($F_{\parallel}$), and when receiving a normally polarized field ($F_{\perp}$).

$$F_{\parallel}(\Delta, \varphi) = \sin\Delta\cos\varphi\left|1 - |R_{\parallel}|e^{i\Phi_{\parallel} - 12\pi H\sin\Delta}\right| \times$$

$$\times \sqrt{\frac{1 - 2e^{-\beta L}\cos\left[\alpha L\left(\frac{1}{k_1} - \cos\Delta\cos\varphi\right)\right] + e^{-2\beta L}}{\left(\frac{1}{k_1} - \cos\Delta\cos\varphi\right)^2 + \left(\frac{\beta}{\alpha}\right)^2}}, \qquad \text{(XV.2.1)}$$

$$F_{\perp}(\Delta, \varphi) = \sin\varphi\left|1 + |R_{\perp}|e^{i\Phi_{\perp} - 12\pi H\sin\Delta}\right| \times$$

$$\times \sqrt{\frac{1 - 2e^{-\beta L}\cos\left[\alpha L\left(\frac{1}{k_1} - \cos\Delta\cos\varphi\right)\right] + e^{-2\beta L}}{\left(\frac{1}{k_1} - \cos\Delta\cos\varphi\right)^2 + \left(\frac{\beta}{\alpha}\right)^2}}, \qquad \text{(XV.2.2)}$$

where

Δ is the angle of elevation;

φ is the azimuth angle;

$|R_{\parallel}|$ and $\Phi_{\parallel}$ are the modulus and argument for the parallel polarized wave reflection factor;

$|R_{\perp}|$ and $\Phi_{\perp}$ are the modulus and argument for the normally polarized wave reflection factor;

L is the length of the antenna;

H is the height at which the antenna is suspended;

β is the attenuation factor for the wave on the wire;

$$k_1 = \frac{v}{c},$$

c is the speed of light;

v is the phase velocity of propagation of the current along the wire.

Analysis of formulas (XV.2.1) and (XV.2.2) demonstrate that at low angles of elevation the antenna does not, for all practical purposes, receive the normal component of the field. Consequently, at low angles the formula for the receiving pattern of the OB antenna is established through formula (XV.2.1).

In the vertical plane the formula for the pattern becomes

$$F(\Delta) = \sin\Delta\left|1 - |R_{\parallel}|e^{i\Phi_{\parallel} - 12\pi H\sin\Delta}\right| \times$$

$$\times \sqrt{\frac{1 - 2e^{-\beta L}\cos\left[\alpha L\left(\frac{1}{k_1} - \cos\Delta\right)\right] + e^{-2\beta L}}{\left(\frac{1}{k_1} - \cos\Delta\right)^2 + \left(\frac{\beta}{\alpha}\right)^2}}. \qquad \text{(XV.2.3)}$$

(b) Propagation factor on the wire

The directional properties of the single-wire traveling wave antenna are greatly dependent on the wave propagation factor on the wire, that is, on the phase velocity, v, and the attenuation factor β. Because of the ground effect the wave propagation factor on the wire is greatly different from the wave propagation factor in free space. The phase velocity of propagation on the wire as influenced by the ground proves to be less than the speed of light. Moreover, losses in the ground produce attenuation of the current.

Analysis reveals that the parameters $1/k_1 = c/v$ and β can be established through the following equation:[1]

$$\frac{1}{k_1} - 1\frac{\beta}{\alpha} = 1 - \frac{F}{2\ln\frac{2H}{a}}. \qquad \text{(XV.2.4)}$$

Here a is the radius of the wire,

$$F = 2S^2\int_0^\infty \omega \frac{\sqrt{\omega^2+p^2}-\omega}{\varepsilon_r'\omega+\sqrt{\omega^2+p^2}} e^{-b\omega}\, d\omega,$$

where

$\varepsilon_r' = \varepsilon_r - 160\lambda\gamma_v$ is the relative complex permittivity of the soil;

$$S = |\sqrt{1-\varepsilon_r'}|,$$
$$p = \frac{\sqrt{1-\varepsilon_r'}}{|\sqrt{1-\varepsilon_r'}|}, \qquad (|p|=1),$$
$$b = 2\pi HS.$$

Figures XV.2.1 and XV.2.2 show predetermined values of $c/v - 1$ and β/α for a 2 mm diameter wire suspended at height H = 5 meters (the solid line) and at height H = 2.5 meters (the dotted line) in the 10 to 100 meter band, established by numerical integration. The curves were plotted for three grounds:

1 - low conductivity (dry): $\varepsilon_r = 3$, $\gamma_v = 0.0005$ mhos/meter;

2 - average conductivity: $\varepsilon_r = 8$; $\gamma_v = 0.005$ mhos/meter;

3 - high conductivity (wet): $\varepsilon_r = 20$, $\gamma_v = 0.05$ mhos/meter.

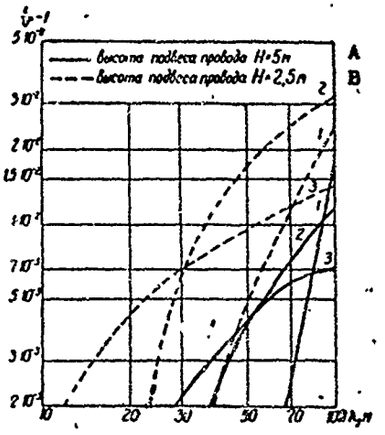

Figure XV.2.1. Dependence of the magnitude of $c/v - 1$ on λ.
Curve 1 - $\varepsilon_r = 3$; $\gamma_v = 0.0005$ mhos/m;
curve 2 - $\varepsilon_r = 8$; $\gamma_v = 0.005$ mhos/m;
curve 3 - $\varepsilon_r = 20$; $\gamma_v = 0.05$ mhos/m.
A - height at which wire suspended H = 5 m; B - height at which wire suspended H = 2.5 m.

1. G. A. Grinberg and B. E. Bonshtedt. "Fundamentals of a Precise Theory of the Wave Field of a Transmission Line," ZhTF, Issue 1, 1934.

The data shown in figures XV.2.1 and XV.2.2 demonstrate that the effect of the ground on the current propagation factor on the wire is quite significant, and that the drier the ground the stronger the effect. The effect of the ground on the propagation factor diminishes with increase in wire suspension height.

It should be noted that the formulas cited above for calculating the attenuation factor, β, are for the case of an infinitely long antenna (R_Σ=0). The attenuation factor on a wire of finite length is not only established by the losses in the ground, but also by radiation losses ($R_\Sigma \neq 0$), so that the attenuation factor β depends on antenna length. However, in the case of long antennas ($L/\lambda > 2$-3), it can be taken for engineering designs that the factor β does not depend on antenna length and that it is, for all practical purposes, equal to the attenuation factor on a wire of finite length.

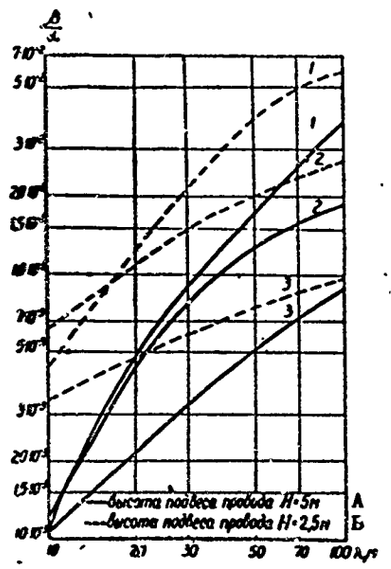

Figure XV.2.2. Dependence of the magnitude of β/α on λ.
Curve 1 - ε_r = 3; γ_v = 0.0005 mhos/m;
curve 2 - ε_r = 8; γ_v = 0.005 mhos/m;
curve 3 - ε_r = 20; γ_v = 0.05 mhos/m.
A - height at which wire suspended H = 5 m; B - height at which wire suspended H = 2.5 m.

(c) Formulas for the gain factor and the directive gain of an OB antenna

The gain factor of a single-wire traveling wave antenna, in accordance with formula (VI.3.1), equals

$$g \approx \frac{18.3}{W}\sin^2\Delta\left|1-|R_1|e^{i\Phi_1-i2\alpha H\sin\Delta}\right|^2 \times$$
$$\times \frac{1-2e^{-\alpha L}\cos\left[\alpha L\left(\frac{1}{k_1}-\cos\Delta\right)\right]+e^{-2\alpha L}}{\left(\frac{1}{k_1}-\cos\Delta\right)^2+\left(\frac{\beta}{\alpha}\right)^2} \qquad \text{(XV.2.5)}$$

where

W is the characteristic impedance of the antenna, with the real conductivity of the ground, equal to

$$W = 60 \frac{\lambda}{\pi} \ln \frac{2H}{a}. \qquad \text{(XV.2.6)}$$

taken into consideration.

The directive gain of the OB antenna can be calculated through the general formula IVI.1.6).

#XV.3. Selection of Antenna Dimensions

Antenna length is selected to provide maximum effectiveness of the antenna in the working range.

So far as the expression for the antenna gain is concerned, there is only one factor which depends on antenna length

$$g(L) \approx 1 - 2e^{-\beta L} \cos\left[\alpha L \left(\frac{1}{k_1} - \cos\Delta\right)\right] + e^{-2\beta L}. \qquad \text{(XV.3.1)}$$

The optimum antenna length is established for the condition that expression (XV.3.1) be a maximum.

We can obtain the following expression for optimum antenna length by arriving at an approximate solution to the equation $dg(L)/dL = 0$,

$$L_{opt} = \frac{\lambda}{2\left(\frac{1}{k_1} - \cos\Delta\right)}\left[1 - \frac{1}{\pi}\operatorname{arc\,tg}\frac{\beta}{\alpha\left(\frac{1}{k_1} - \cos\Delta\right)}\right]. \qquad \text{(XV.3.2)}$$

As will be seen from formula (XV.3.2) optimum antenna length depends on ground parameters, height at which the antenna is suspended, and the angle of approach of the beam.

Figure XV.3.1 shows the dependence of the optimum antenna length on the wavelength for suspension height H = 2.5 meters and ground of medium conductivity ($\varepsilon_r = 8$, $\gamma_v = 0.005$ mhos/m) at angles of arrival $\Delta = 9°$ and $\Delta = 15°$.

The data contained in this figure reveal the desirability of selecting an antenna length on the order of 300 to 400 meters. There is a sharp reduction in the antenna gain and directive gain at the shortwave edge of the band when the length is increased above 300 and 400 meters.

The antenna suspension height too is selected to obtain highest antenna efficiency over the entire band. Calculations reveal that the antenna's directive gain depends little on the suspension height, but antenna gain very definitely does. For example, the gain of a 300 meter long antenna will

increase over the band by a factor of 3 to 10 when the suspension height is increased from 1.25 meters to 5 meters. Hence, it is desirable to increase antenna suspension height, but when this is done there is a considerable increase in antenna cost, to say nothing of the intensification of the antenna effect created by the vertical wires connecting the antenna with the feeder and grounding. For these reasons antenna height is not taken as greater than 4 to 5 meters.

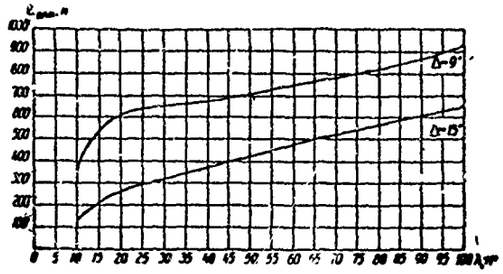

Figure XV.3.1. Dependence of the optimum length of an OB antenna on the wavelength at a suspension height of H = 2.5 meters and ground of average conductivity (ε_r=8, γ_v=0.005 mhos/m.

#XV.4. Electrical Parameters of the OB 300/2.5 Antenna

Figures XV.4.1 through XV.4.7 show the receiving patterns of the OB 300/2.5 antenna in the vertical plane in the waveband 12 to 100 meters for wet (ε_r = 20, γ_v = 0.05 mhos/meter) and dry (ε_r = 3, γ_v = 0.0005 mhos/meter) grounds, charted through formula (XV.2.3).

As will be seen from the diagrams the OB antenna has rather large side lobes in the vertical plane, and the level of the lobes is higher over wet ground than over dry.

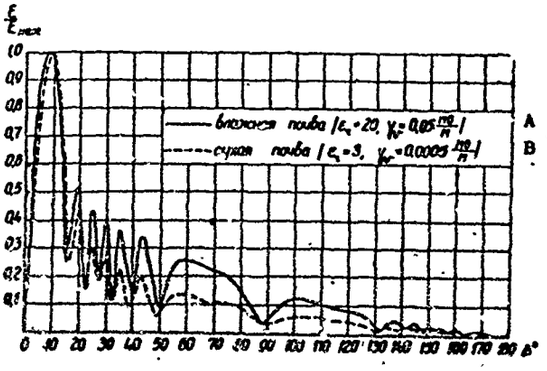

Figure XV.4.1. Receiving patterns in the vertical plane of an OB 300/2.5 antenna for a wavelength of λ = 13 m.

A - wet ground (ε_r=20, γ_v=0.05 mhos/m);
B - dry ground (ε_r=3, γ_v=0.0005 mhos/m).

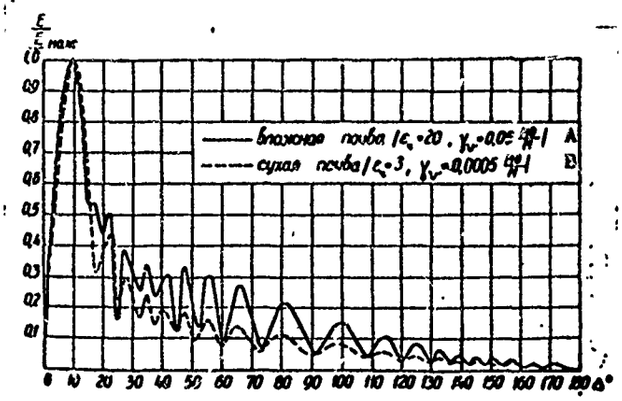

Figure XV.4.2. Receiving patterns in the vertical plane of an OB 300/2.5 antenna for a wavelength of λ = 15 m.

A - wet ground (ϵ_r=20, γ_v=0.05 mhos/m);
B - dry ground (ϵ_r=3, γ_v=0.0005 mhos/m).

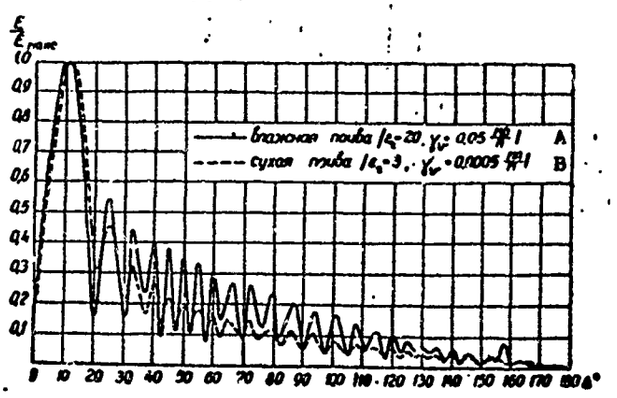

Figure XV.4.3. Receiving patterns in the vertical plane of an OB 300/2.5 antenna for a wavelength of λ = 20 m.

A - wet ground (ϵ_r=20, γ_v=0.05 mhos/m);
B - dry ground (ϵ_r=3, γ_v=0.0005 mhos/m).

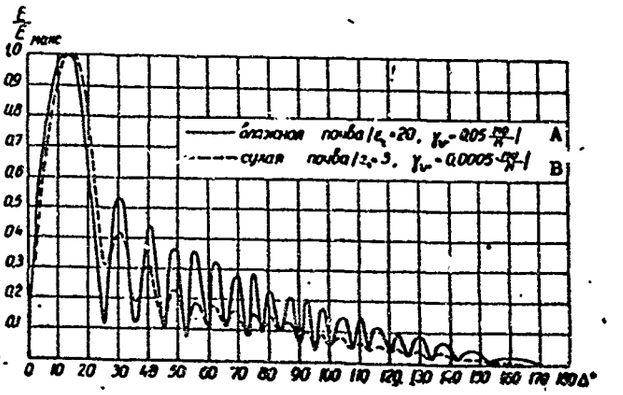

Figure XV.4.4. Receiving patterns in the vertical plane of an OB 300/2.5 antenna for a wavelength of λ = 30 m.

A - wet ground (ϵ_r=20, γ_v=0.05 mhos/m);
B - dry ground (ϵ_r=3, γ_v=0.0005 mhos/m).

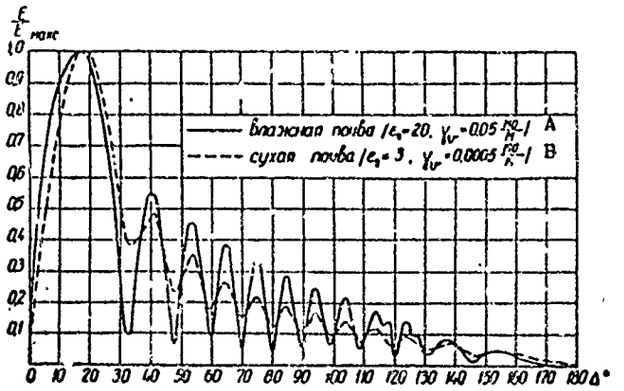

Figure XV.4.5. Receiving patterns in the vertical plane of an OB 300/2.5 antenna for a wavelength of λ = 50 m.

A - wet ground (ε_r=20, γ_v=0.05 mhos/m);
B - dry ground (ε_r=3, γ_v=0.0005 mhos/m).

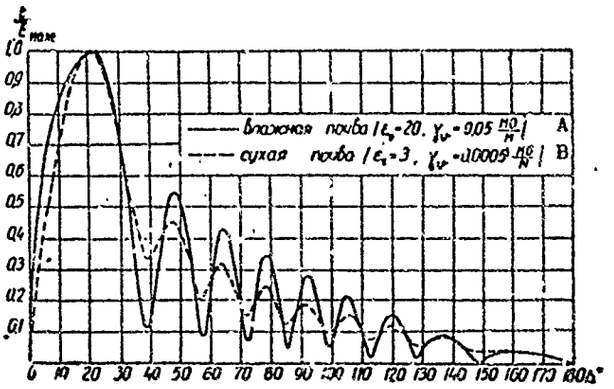

Figure XV.4.6. Receiving patterns in the vertical plane of an OB 300/2.5 antenna for a wavelength of λ = 70 m.

A - wet ground (ε_r=20, γ_v=0.05 mhos/m);
B - dry ground (ε_r=3, γ_v=0.0005 mhos/m).

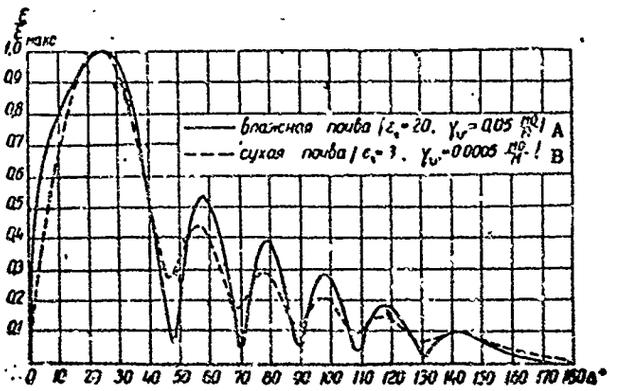

Figure XV.4.7. Receiving patterns in the vertical plane of an OB 300/2.5 antenna for a wavelength of λ = 100 m.

A - wet ground (ε_r=20, γ_v=0.05 mhos/m);
B - dry ground (ε_r=3, γ_v=0.0005 mhos/m).

Figures XV.4.8 through XV.4.14 show the receiving patterns of an OB 300/2.5 antenna over conical surfaces at elevation angles corresponding to the direction of maximum reception. The diagrams were charted for the parallel field component.

Since the patterns of the OB antenna over conical surfaces are little dependent on ground parameters, they have been shown only for wet ground.

Figure XV.4.15 shows the directive gain values for the OB 300/2.5 antenna in the waveband for wet and dry grounds. Numerical integration of formula (VI.1.6) was used to establish the directive gain values.

The data presented in Figure XV.4.15 show that the directive gain of the OB antenna has but slight dependence on ground parameters in the 30 to 100 meter waveband. At the shortwave edge of the band the directive gain of an antenna on dry ground is higher than that of an antenna on wet ground by a factor of 1.3 to 1.65.

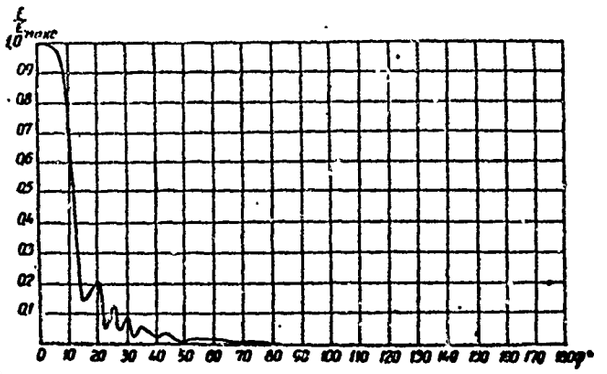

Figure XV.4.8. Receiving pattern in the horizontal plane (Δ=9°) of an OB 300/2.5 antenna on a wavelength of λ = 12 m.

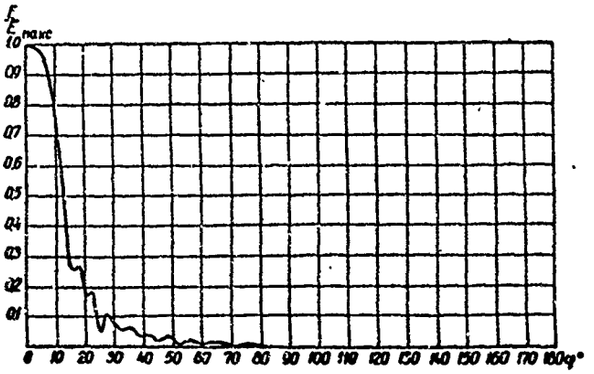

Figure XV.4.9. Receiving pattern in the horizontal plane (Δ=10°) of an OB 300/2.5 antenna on a wavelength of λ = 15 m.

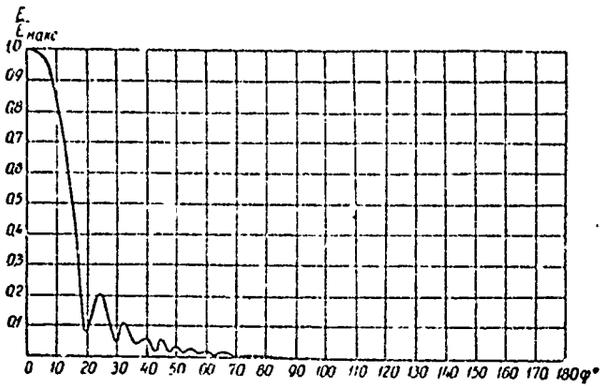

Figure XV.4.10. Receiving pattern in the horizontal plane (Δ=11°) of an OB 300/2.5 antenna on a wavelength of λ = 20 m.

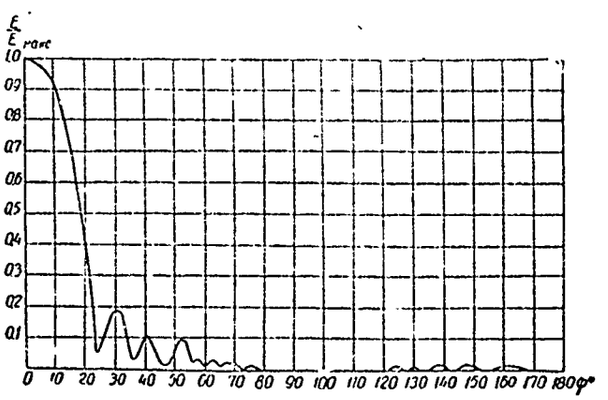

Figure XV.4.11. Receiving pattern in the horizontal plane (Δ=12°30') of an OB 300/2.5 antenna on a wavelength of λ = 30 m.

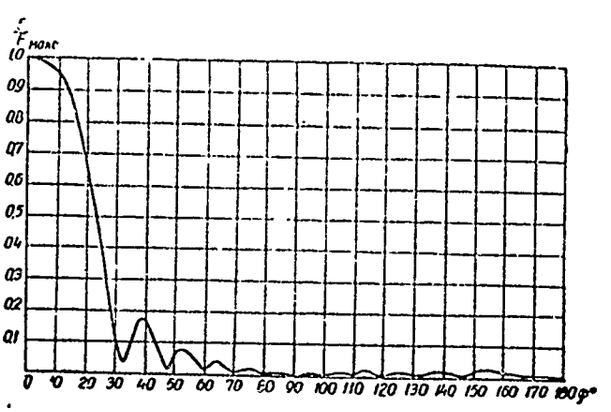

Figure XV.4.12. Receiving pattern in the horizontal plane (Δ=17°) of an OB 300/2.5 antenna on a wavelength of λ = 50 m.

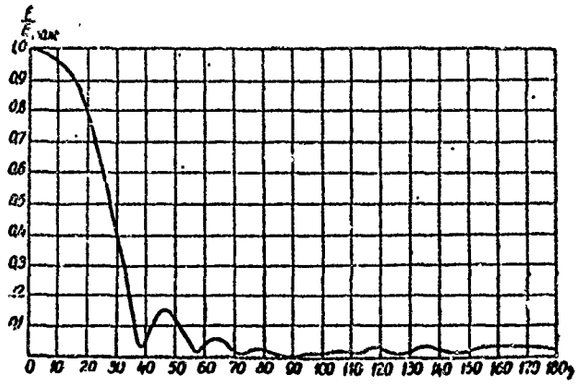

Figure XV.4.13. Receiving pattern in the horizontal plane (Δ=22°) of an OB 300/2.5 antenna on a wavelength of λ = 70 m.

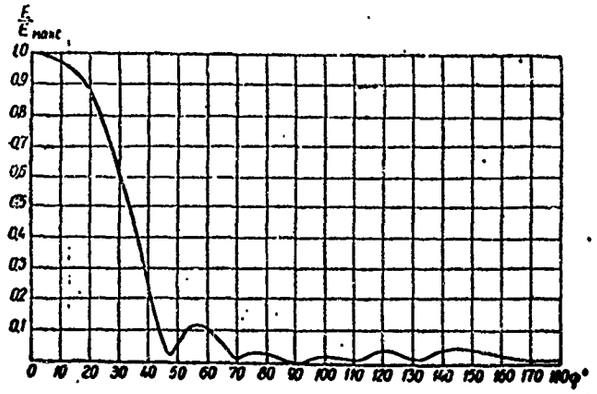

Figure XV.4.14. Receiving pattern in the horizontal plane (Δ=25°) of an OB 300/2.5 antenna on a wavelength of λ = 100 m.

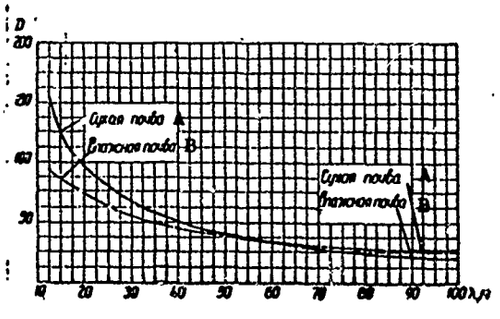

Figure XV.4.15. Dependence of the directive gain of an OB 300/2.5 antenna on the wavelength.

A - dry ground; B - wet ground.

Figure XV.4.16 shows the values of antenna gain for the OB 300/2.5 antenna in the waveband indicated in that figure. As will be seen, the OB antenna gain changes very greatly with change in ground parameters. The OB antenna gain is much lower over wet ground than it is over dry ground.

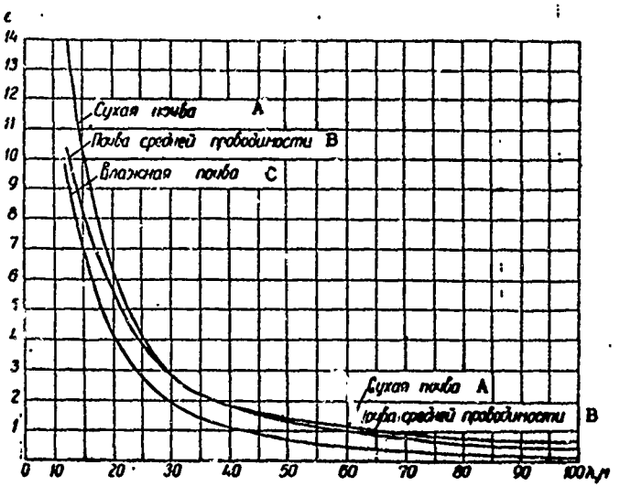

Figure XV.4.16. Dependence of the gain of an OB 300/2.5 antenna on the wavelength.

A - dry ground; B - ground of average conductivity; C - wet ground.

#XV.5. Electrical Parameters of the OB 100/2.5 Antenna

There are individual instances when it is difficult to use a 300 meter long antenna. When this is the case a shorter antenna, one approximately 100 meter long, can be used.

Figures XV.5.1 through XV.5.7 show the receiving patterns of the OB 100/2.5 antenna in the vertical plane for wet and dry ground. Figures XV.5.8 through XV.5.14 show the patterns of the OB 100/2.5 antenna over a conical surface at angles of elevation correspoding to maximum reception for wet ground.

The patterns in figures XV.5.8 through XV.5.14 were charted for the parallel field component.

The directive gain of the OB 100/2.5 antenna is less than that of the OB 300/2.5 antenna by approximately a factor of three. Figure XV.5.15 shows the change in the gain factor for the OB 100/2.5 antenna over the waveband.

Comparison of the data presented in this, as well as in the preceding paragraphs, reveals that the OB 100/2.5 antenna is very much inferior to the longer OB 300/2.5 antenna in directional properties, as well as in gain.

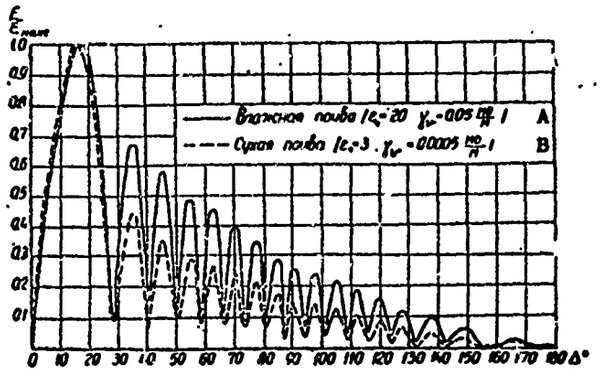

Figure XV.5.1. Receiving patterns in the vertical plane of an OB 100/2.5 antenna on a wavelength of λ = 12 m.

A - wet ground (ε_r=20, γ_v=0.05 mhos/m);
B - dry ground (ε_r=3, γ_v=0.0005 mhos/m).

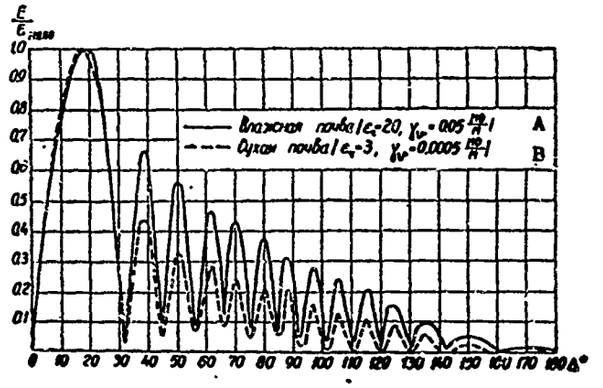

Figure XV.5.2. Receiving patterns in the vertical plane of an OB 100/2.5 antenna on a wavelength of λ = 15 m.

A - wet ground (ε_r=20, γ_v=0.05 mhos/m);
B - dry ground (ε_r=3, γ_v=0.0005 mhos/m).

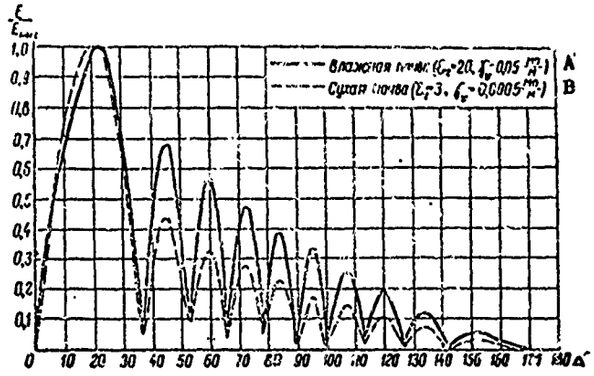

Figure XV.5.3. Receiving patterns in the vertical plane of an OB 100/2.5 antenna on a wavelength of λ = 20 m.

A - wet ground (ε_r=20, γ_v=0.05 mhos/m);
B - dry ground (ε_r=3, γ_v=0.0005 mhos/m).

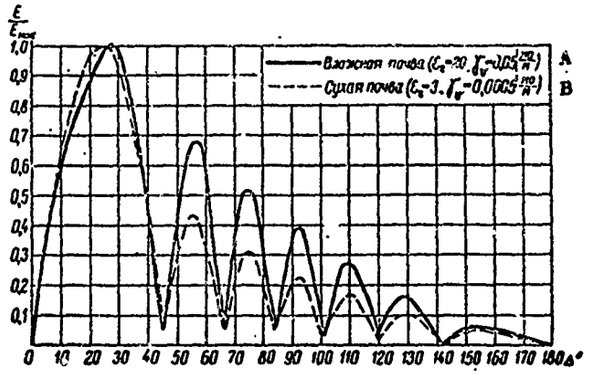

Figure XV.5.4. Receiving patterns in the vertical plane of an OB 100/2.5 antenna on a wavelength of λ = 30 m.

A - wet ground (ε_r=20, γ_v=0.05 mhos/m);
B - dry ground (ε_r=3, γ_v=0.0005 mhos/m).

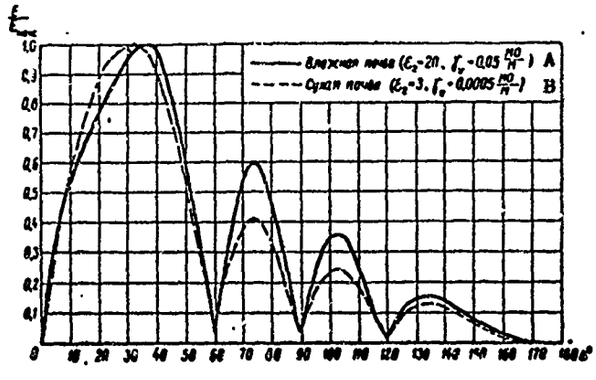

Figure XV.5.5. Receiving patterns in the vertical plane of an OB 100/2.5 antenna on a wavelength of λ = 50 m.

A - wet ground (ε_r=20, γ_v=0.05 mhos/m);
B - dry ground (ε_r=3, γ_v=0.0005 mhos/m).

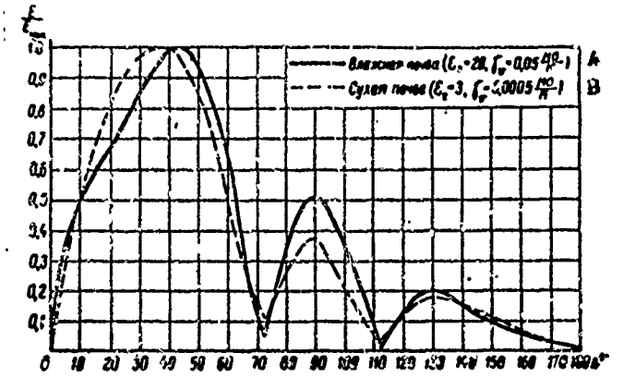

Figure XV.5.6. Receiving patterns in the vertical plane of an OB 100/2.5 antenna on a wavelength of λ = 70 m.

A - wet ground (ϵ_r=20, γ_v=0.05 mhos/m);
B - dry ground (ϵ_r=3, γ_v=0.0005 mhos/m).

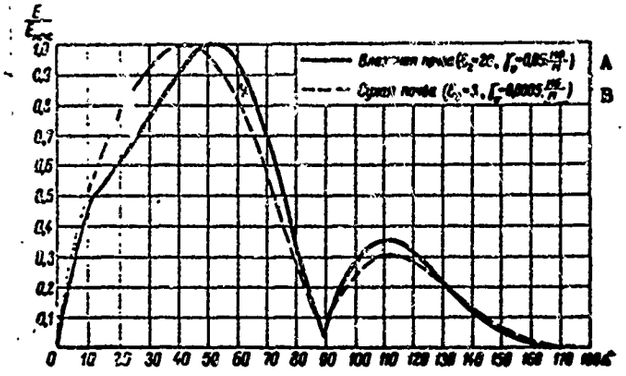

Figure XV.5.7. Receiving patterns in the vertical plane of an OB 100/2.5 antenna on a wavelength of λ = 100 m.

A - wet ground (ϵ_r=20, γ_v=0.05 mhos/m);
B - dry ground (ϵ_r=3, γ_v=0.0005 mhos/m).

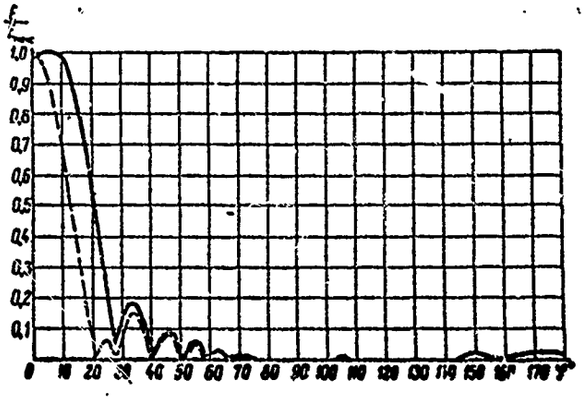

Figure XV.5.8. Receiving patterns in the horizontal plane (Δ=17.5°) of OB 100/2.5 and OB2 100/2.5 antennas on a wavelength of λ = 12 m.

——— OB antenna; - - - - - OB2 antenna.

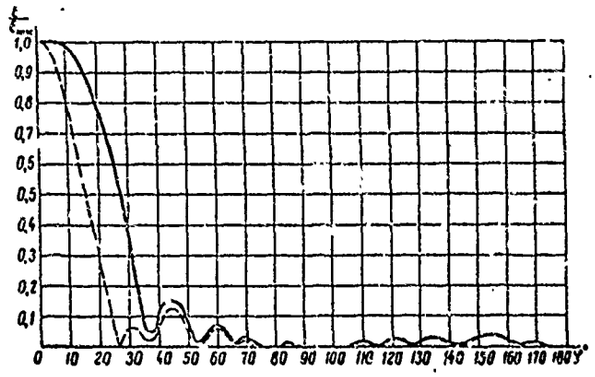

Figure XV.5.9. Receiving patterns in the horizontal plane (Δ=19°) of OB 100/2.5 and OB2 100/2.5 antennas on a wavelength of λ = 15 m.

——— OБ antenna; ----- OB2 antenna.

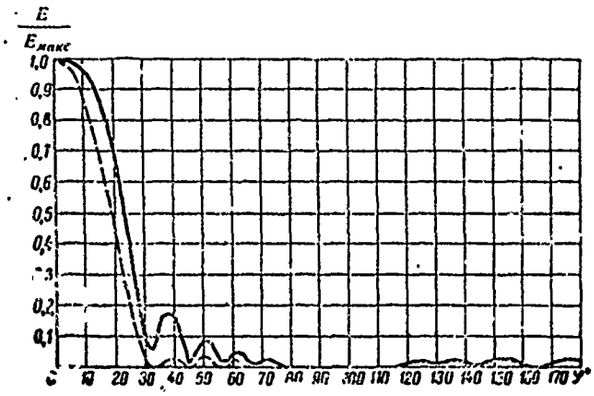

Figure XV.5.10. Receiving patterns in the horizontal plane (Δ=22°) of OB 100/2.5 and OB2 100/2.5 antennas on a wavelength of λ = 20 m.

——— OB antenna; ----- OB2 antenna.

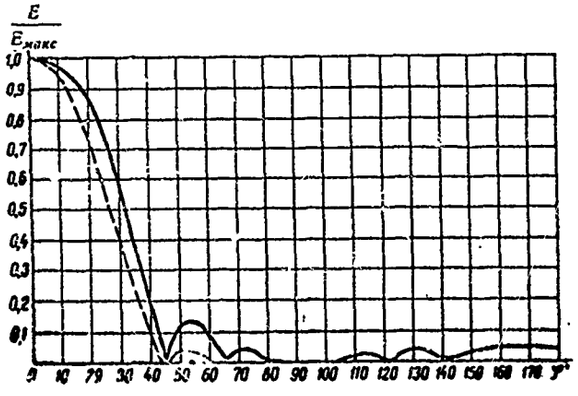

Figure XV.5.11. Receiving patterns in the horizontal plane (Δ=27.5°) of OB 100/2.5 and OB2 100/2.5 antennas on a wavelength of λ = 30 m.

——— OB antenna; ----- OB2 antenna.

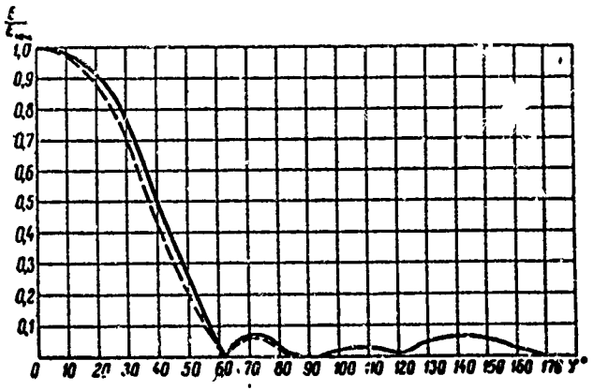

Figure XV.5.12. Receiving patterns in the horizontal plane (Δ=37°) of OB 100/2.5 and OB2 100/2.5 antennas on a wavelength of λ = 50 m.

——— OB antenna; ----- OB2 antenna.

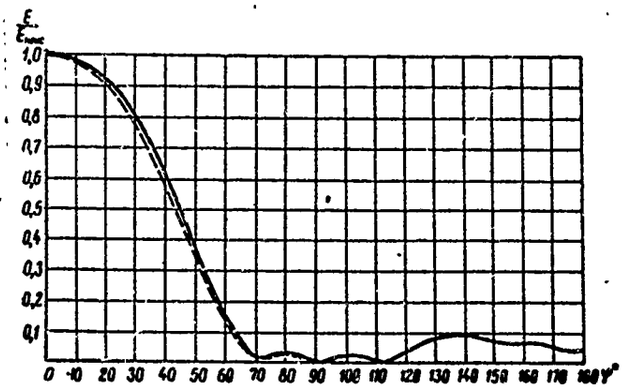

Figure XV.5.13. Receiving patterns in the horizontal plane (Δ=43°) of OB 100/2.5 and OB2 100/2.5 antennas on a wavelength of λ = 70 m.

——— OB antenna; ----- OB2 antenna.

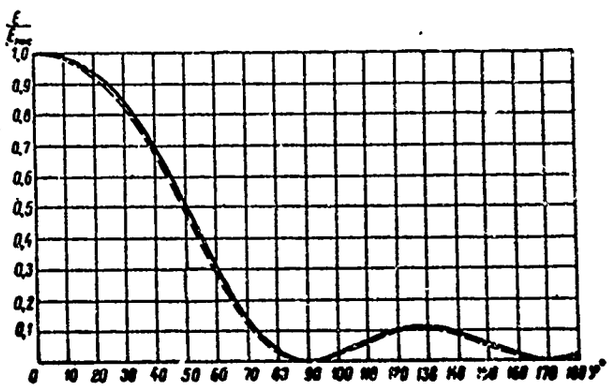

Figure XV.5.14. Receiving patterns in the horizontal plane (Δ=53°) of OB 100/2.5 and OB2 100/2.5 antennas on a wavelength of λ = 100 m.

——— OB antenna; ----- OB2 antenna.

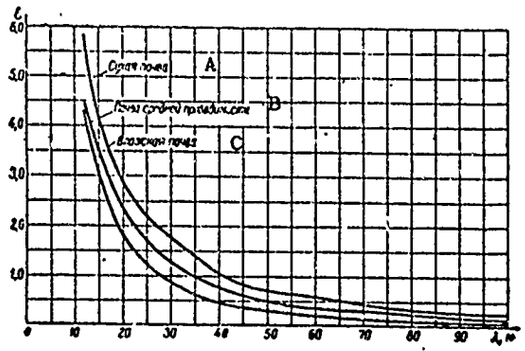

Figure XV.5.15. Dependence of the gain of the OB 100/2.5 antenna on the wavelength.

A - dry ground; B - ground of average conductivity; C - wet ground.

#XV.6. Multiple Traveling Wave Antennas

The use of multiple antennas, made up of several single OB antennas is desirable in order to increase the directive gain and the antenna gain.

The simplest way to increase efficiency is to connect two OB antennas in parallel (fig. XV.6.1). The receiving pattern in the horizontal plane of a twin antenna (the OB2 antenna) can be charted through formula (XIV.8.1).

Patterns of the OB2 300/2.5 antenna have been charted in figures XV.5.8 through XV.5.14 by the dotted lines. The distance between the antennas (d_1) was selected equal to 18 meters. The distance, d_1, should be increased when the antennas are longer, so, by way of an example, d_1 should be approximately 30 meters for the OB2 300/2.5 antenna.

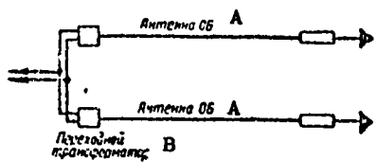

Figure XV.6.1. Schematic diagram of a multiple OB2 antenna.

A - OB antenna; B - conversion transformer.

The gain in directive gain of the OB2 100/2.5 antenna is 1.5 to 2 as compared with the OB 100/2.5 antenna in the 12 to 20 meter band when d_1 = 18 m. The gain falls off at the longwave edge of the band.

The OB2 antenna gain at this same distance between antennas increases by a factor of 1.7 to 2 over the entire 12.5 to 100 meter band.

In the case of high conductivity ground the OB2 antenna gain is considerably higher than that of the OB antenna, even when the distance between antennas is on the order of a few meters, so both wires can be suspended on

common supports. Obviously, the directive gains of both antennas will be approximately the same in this case.

It is also possible to use a multiple antenna comprising two and more OB2 antennas installed in tandem and interconnected through linear phase shifters (fig. XV.6.2).

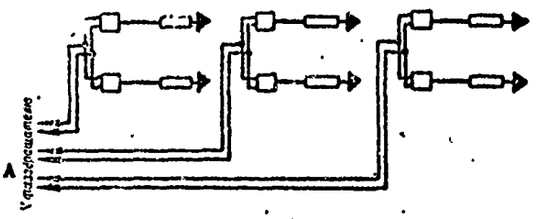

Figure XV.6.2. Schematic diagram of a multiple 3OB2 antenna.
A - to phase shifter.

#XV.7. OB Antenna Design

The OB antenna is usually made of copper or bimetallic wire 2 to 4 mm in diameter. Antenna suspension height is 2.5 to 5 meters. The terminating resistor is selected according to wire diameter, ground conductivity, and wavelength. Since the OB antenna usually works a broad band of waves it is desirable, in practice, to select the terminating resistance equal to the characteristic impedance of the antenna at the center wave in the particular band (formula XV.2.6). Characteristic impedance is ~ 500 ohms.

The antenna is usually suspended on wooden supports. Distance between supports is on the order of 20 meters.

The ground system for the terminating resistor is made of 10 to 15 radially spaced copper wires ~ 10 meters long, buried at a depth of 20 to 30 cm. The diameter of the wire used for the ground system is 2 to 3 mm.

Direct connection of the OB antenna to the receiver is permissible when the antenna is located near the service building. However, as a rule the antennas used at radio receiving centers are usually a long way from the service building. In such case the OB antenna is connected to the receiver by a four-wire standard aerial feeder.

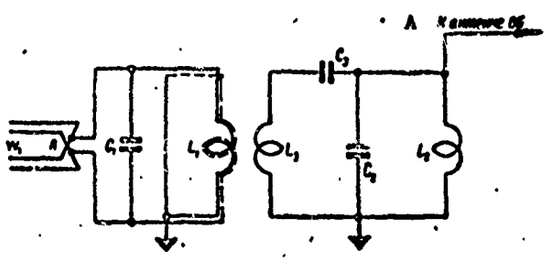

Figure XV.7.1. Schematic diagram of a transformer for making the transisiton from a four-wire feeder (A) to an OB antenna.
A - to OB antenna.

Since the OB antenna is an unbalanced system it is connected to the feeder through a conversion transformer (fig. XV.7.1). The methodology used to calculate the elements of the conversion transformer was given in Chapter XIX.

The connection of the single antenna of the OB2 antenna can be made using a twin feeder with a characteristic impedance of ~ 400 ohms (fig. XV.6.1). The trunk feeder is a standard feeder with a characteristic impedance of 208 ohms.

Chapter XVI

ANTENNAS WITH CONSTANT BEAM WIDTH OVER A BROAD WAVEBAND. ANTENNAS WITH A LOGARITHMIC PERIODIC STRUCTURE. OTHER POSSIBLE TYPES OF ANTENNAS WITH CONSTANT BEAM WIDTH

#XVI. General Remarks. Antennas with a Logarithmic Periodic Structure

The directional properties of the multiple-tuned shortwave antennas (rhombic antennas, traveling wave antennas, and others) in use until very recently undergo substantial change with change in wavelength. The width of the patterns in the horizontal and vertical planes usually narrows with shortening of the wavelength.

There are individual cases when it is necessary to have antennas with constant beam widths over a broad waveband. This is necessary, in particular, in radio broadcasting where a predetermined area must be illuminated on all operating waves. Antennas such as these must also ensure a good match with the supply feeder in the specific waveband.

One of the types of antennas with these properties is the antenna with a logarithmic periodic structure. Henceforth, for brevity's sake, we will call this type of antenna the logarithmic antenna. They are distinguished by the wide band over which they can be used, tenfold, and more. The dependence of the space radiation pattern on the wavelength is very nominal within the limits of the operating band.

Logarithmic antennas were used initially in the ultrashort wave region, but have recently come into use in the shortwave region as well. Logarithmic antennas are not yet adequately researched and there are no final, agreed designs. This is particularly true of logarithmic antennas used on short waves. Considerable difficulty is still encountered in setting up methods for making the engineering computations required for logarithmic antennas. The basic data cited in the technical literature on the subject have been obtained experimentally.

Attention here will be given primarily to variants of logarithmic antennas, the designs of which have won the greatest acceptance in the shortwave region.

#XVI.2. Schematic and Operating Principle of the Logarithmic Antenna

The schematic of the logarithmic antenna is shown in Figure XVI.2.1a. The antenna consists of two identical sections, I and II. Section II can be formed by rotating section I 180° around the axis normal to the plane of the figure and passing through the antenna supply point. The radiating elements are variable length teeth that are circles bent along an arc.

These teeth will henceforth be called the dipoles. The circular sections from which the dipoles branch play the part of the distribution lines. These lines simultaneously radiate a small part of the energy they transmit.

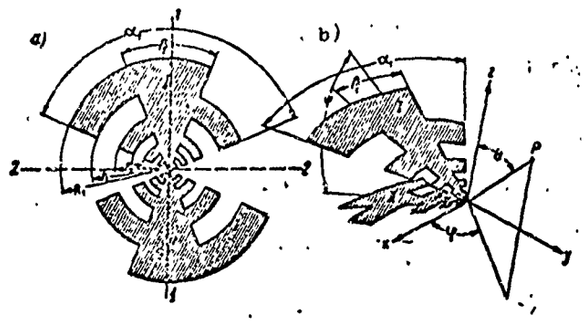

Figure XVI.2.1. Parameters and coordinates of the system for structures with round teeth.

$$\tau = \frac{R_{N+1}}{R_N}\ ;\ \sigma = \frac{r_N}{R_N}\ ;\ \alpha = 135°;\beta = 45°$$

Characteristic parameters of the logarithmic antenna are the magnitudes τ and σ, as well as angles α_1 and β_1. The relationship

$$\tau = \frac{R_{N+1}}{R_N},$$

is called the magnitude of τ. Here R_N is the distance from the point of supply to the N^{th} dipole, reading from the dipole of maximum length.

When values are assigned to α_1 and β_1 the magnitude of τ is characterized by the distance between adjacent dipoles. $\tau = 0.5$ for the antenna shown in Figure XVI.2.1. The magnitude of σ is characterized by the thickness of the radiating dipoles, and equals

$$\sigma = \frac{r_N}{R_N},$$

where

r_N and R_N are the minimum and maximum distances of the N^{th} dipole from the point of supply for the antenna.

The constancy of the magnitudes of τ and σ (the constancy of the ratios of lengths and thicknesses of adjacent dipoles) itself defines the name of the antenna; an antenna with logarithmically periodic structure.

When sections I and II are located in the same plane, as shown in Figure XVI.2.1a, the antenna's radiation pattern has two identical lobes in the positive and negative directions of axis 1-1. If, only one section of the antenna is energized in some fashion the antenna will have a unidirectional pattern. The antenna will also become unidirectional when sections I and II

are positioned at some angle ψ to each other (fig. XVI.2.1b). Maximum radiation will be obtained in the direction characterized by the angles $\varphi = \theta = 90°$, that is, in the direction of the y axis passing through the bisector of angle ψ.

The antenna dipoles need not necessarily be a circular bend. The antenna will retain its properties quite well even when the dipoles are trapezoidal (fig. XVI.2.2). Research on the logarithmic antenna has also revealed that the directional properties of the antenna do not change appreciably when it is made of continuous metal sheets, or of wire following the outline (wire logarithmic antenna), as shown in Figure XVI.2.3a.

The distribution lines are made up of three wires, but can be made of one wire as well (fig. XVI.2.3b).

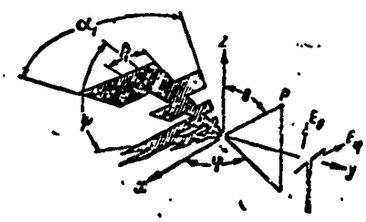

Figure XVI.2.2. Antenna with trapezoidal dipoles.

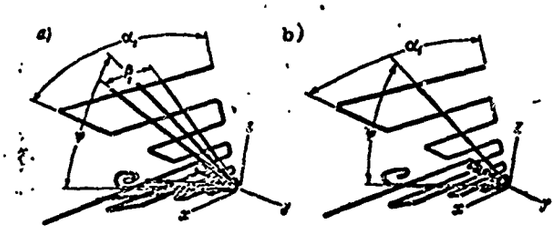

Figure XVI.2.3. Wire logarithmic antenna with trapezoidal dipoles.

A further design simplification can be arrived at by replacing the trapezoidal dipoles by triangular ones (zigzag structure), as shown in Figure XVI.2.4. Antenna variants with dipoles made of a single wire (fig. XVI.2.5) have also been investigated.

Angle ψ can change over broad limits.

V. D. Kuznetsov and V. K. Paramonov have suggested taking $\psi = 0$ (fig. XVI.2.6) in order to simplify antenna design. When $\psi = 0$, the antenna will be positioned in one plane.

The logarithmic antenna is differentiated by the high constancy of the input impedance. The traveling wave ratio is at least 0.5 to 0.7 when the characteristic impedance of the feed line is selected accordingly.

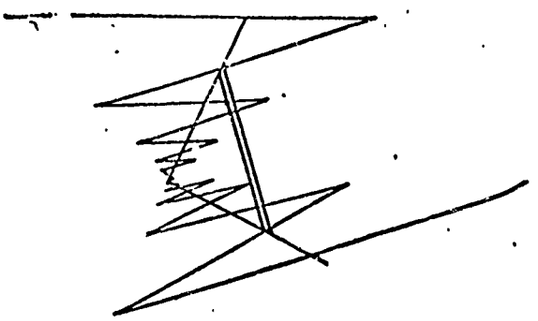

Figure XVI.2.4. Typical non-flat top zigzag wire structure.

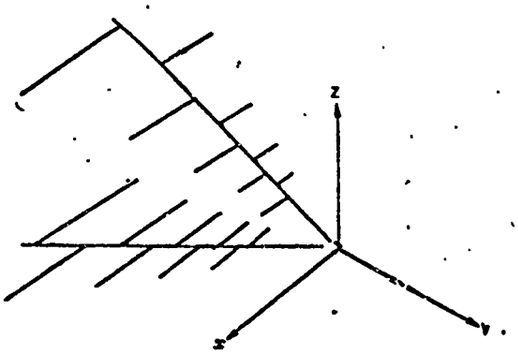

Figure XVI.2.5. Logarithmic antenna with dipoles made of a single conductor.

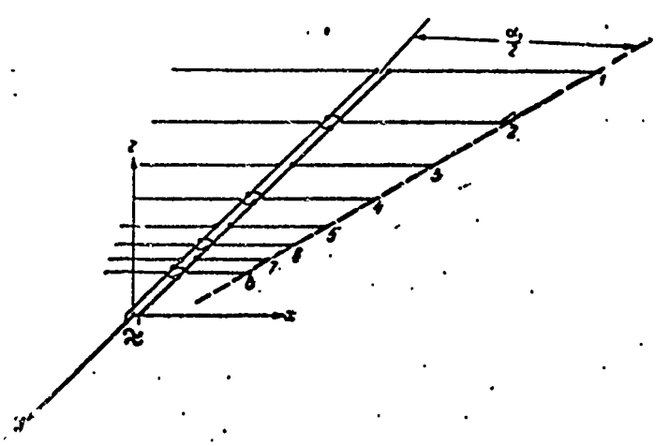

Figure XVI.2.6. Flat-top logarithmic antenna ($\psi = 0$).

So far as principle of operation is concerned, the logarithmic antenna reminds one of a director antenna consisting of one driven element, one director, and one reflector (fig. XVI.2.7).

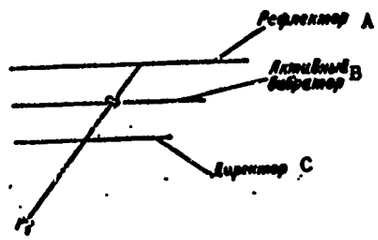

Figure XVI.2.7. Schematic diagram of a director antenna.
A - reflector; B - driven element; C - director.

As is known[1], the normal operating mode for the director antenna occurs when the dipole acting as the reflector has a reactive component of the input resistance that is inductive in nature, while the dipole acting as the director has a reactive component of the input resistance that is capacitive in nature. In the director antenna this is arrived at because the length of the reflector is somewhat longer than the resonant length (the electrical length of the dipole, $2l$, is somewhat longer than $\lambda/2$), while the director has a length shorter than the resonant length (the electrical length of the dipole, $2l$, is somewhat shorter than $\lambda/2$). In the case of these dipoles, as analysis using the induced emfs method demonstrates, the current flowing in the reflector leads the current flowing in the driven element, while the current flowing in the director lags the current flowing in the driven element. This phase relationship between the currents flowing in the driven element, the reflector, and the director, provides intense radiation in the direction r_1 (fig. XVI.2.7). In point of fact, if the point of reception is in direction r_1, because of the difference in the path of the beams, the intensity of the field created by the reflector lags the intensity of the field created by the dirven element, while that created by the director leads this field. These phase displacements compensate for the fact that the current flowing in the reflector leads the current flowing in the driven element, while the current flowing in the director lags the current flowing in the driven element.

Let us turn our attention to the schematic diagram shown in Figure XVI.2.6. The mutual arrangement of the three adjacent dipoles, 3, 4, and 5, for example, is characteristic of the director antenna. If the antenna is

---

1. See G. Z. Ayzenberg, Ultrashort Wave Antennas. Svyaz'izdat, 1957, Chapter XXIV, #1.

excited by a wave for which dipole 4 has been tuned to resonance, we have the same result as in the case of the director antenna, and dipole 3 has a length greater than the resonant length, and dipole 5 has a length less than the resonant length. This ensures the induction, thanks to the space coupling, of a current in dipole 3 that leads the current in dipole 4, and in dipole 5 a current which lags the current in dipole 4. This relationship between the phases provides maximum radiation in the y direction (fig. XVI.2.6). In the case of the logarithmic antenna there is a coupling through the twin distribution line, in addition to the space coupling. However, this coupling also ensures a lag between the currents flowing in dipoles 3, 4, and 5 favorable for the creation of maximum radiation in the y direction. In point of fact, the current flowing in dipole 3 lags the current flowing in dipole 4 because of the passage along the line over an additional path equal to the distance between these dipoles. The additional lag of the current flowing in dipole 3 relative to that in dipole 4 is the result of dipole 3 being longer than dipole 4 and, accordingly, having a positive reactive resistance. Moreover, the arms of dipole 3 are connected to the opposite wires of the twin line as compared with the identical arms of dipole 4. This results in a phase lag in the currents flowing in these dipoles of 180°. These factors are what cause the current flowing in dipole 3 to lead that flowing in dipole 4 by a good margin. Similarly, the coupling through the distribution feeder provides for the lag of the current flowing in dipole 5 relative to the current flowing in dipole 4. These considerations demonstrate that a group made up of the three dipoles, 3, 4, and 5, are identical to the director antenna, insofar as their mutual positioning and current phase relationships, established by the space coupling and the twin distribution line, are concerned.

The actual relationship between the phases of the currents flowing in the dipoles is complicated by the effect of dipoles located in front of dipole 5 and behind dipole 3. However, the practical effect of these dipoles is slight. The fact is the dipoles located ahead of dipole 5 are extremely short as compared with the working wave to which dipole 4 resonates. On the wave for which dipole 4 has a resonant length these dipoles have a high negative reactive resistance and the currents which branch in them are small. The currents flowing in the dipoles behind dipole 3 are also low because the resonant dipole, 4, and dipoles 5 and 3 which have lengths close to resonant, drew almost all the energy. Accordingly, on a wave for which dipole 4 is resonant, and in some band adjacent to this wave, the radiated field is determined by dipoles 3, 4, and 5, for the most part.

If the wave is lengthened to the point that dipole 3 is resonant, the energy will be concentrated in dipoles 2, 3, and 4, for the most part. Further lengthening of the working wave will cause dipoles 1, 2, and 3 to come into

play. And when the working wave is shortened the energy will begin to concentrate in the shorter dipoles.

This picture of how the logarithmic antenna functions holds, basically, if angle ψ is different from zero. For larger values of ψ, the space coupling between the dipoles will be reduced, naturally enough, because of the increase in the distance between the dipoles. And the role of the distribution line in setting up a definite relationship between the phases of the currents flowing in the dipoles will increase. Moreover, radiation from the distribution lines will begin to play a definite role with increase in ψ.

Moreover, if the radiation from the dipoles creates what is primarily a component of the E_φ field (normal component) (fig. XVI.2.2), radiation from the distribution feeders creates what is primarily a component of the E_θ field (parallel component). Increase in angle ψ will be accompanied by a narrowing of the pattern in the H plane (the zy plane).

This discussion of the antenna's operating principle demonstrates that the longest operating wave should be somewhat shorter than $4l_{long}$, and the shortest operating wave should be somewhat longer than $4l_{short}$ (l_{long} and l_{short} are the lengths of the arms of the longest and shortest dipoles). This can be confirmed by experimental investigations.

The operating band can be as wide as desired when the antenna is built as described. Investigation has demonstrated, however, that if the antenna contains dipoles the arms of which pick up two and more waves, these dipoles will cause a substantial deterioration in directional properties. This fact, together with the fact that the shortest operating wave is approximately equal to 4 to 5 l_{short} as indicated above (that is, $l_{short}/\lambda_{short} \approx 0.2$ to 0.25), leads to practical difficulties in using the antenna if the band is more than tenfold.

From the data presented, it follows that at small angles α_1 and the corresponding increased values of τ (smaller difference in the lengths of adjacent dipoles) a substantial role in antenna operation begins to devolve on the dipoles located closest to the three main dipoles, in front and in back of them, and that this should naturally result in some increase in antenna effectiveness. And this is what does in fact take place. It should be borne in mind, however, that a reduction in α_1 in the specified operating band requires a substantial increase in the overall length of the antenna.

The band in which the antenna can be used is not only determined by its directional properties, but also by its match to the feeder line. As was pointed out above, the logarithmic antenna too has a good match to the feeder line within the limits of the band determined by its directional properties. The wave propagated on the distribution line is only slightly reflected from the short dipoles located between the point of feed and the dipoles's radiation

on the given wave. Short dipoles have a high capacitive resistance, and only comparative weak currents branch out into them.

The main load on the distribution wires is created by some of the dipoles with lengths close to resonant length. These dipoles have active components of the input resistance of changing sign. A dipole, the length of which is longer than resonant, has a positive reactive resistance, while a dipole with a length shorter than resonant has a negative reactive component of the input resistance. At the same time, these dipoles are displaced with respect to each other by a distance close to $\lambda/2$. This results in the establishment of a condition leading to substantial mutual compensation for reflected waves.

Dipoles located further from the generator than the radiating dipoles are extremely poor reflectors of energy, practically speaking, because the energy is absorbed by the main, operating dipoles, for the most part. The characteristic impedance of the distribution line along the section from the generator to the operating dipoles is very low, and is explained by the fact that the dipoles connected into this section have a negative (capacitive) reactance, causing an increase in the distribution capacitance of the line similar to that occurring on the traveling wave antenna when the lengths of the dipole arms are shorter than $\lambda/4$. The considerable increase in the distributed capacitance created by the short dipoles leads to a reduction in the characteristic impedance to a magnitude on the order of 100 ohms.

A characteristic impedance such as this will match satisfactorily with the pure input resistance of a line with dipoles of a length close to resonant.

If the feeder line has a characteristic impedance close to that of the distribution line, the traveling wave ratio on the line will be high enough and will change little in the operating wave band.

#XVI.3. Results of Experimental Investigation of the Logarithmic Antenna on Models

Figure XVI.3.1 shows a series of experimental radiation patterns in the principal E plane (xy plane) and the principal H plane (zy plane) of a logarithmic antenna with trapezoidal dipoles with the following parameters: $\alpha_1 = 75°$; $\tau = 0.5$; $\beta_1 = 0$ (the distribution line for each half of the antenna consists of one wire of identical cross section), and $\psi = 45°$. The maximum length of a dipole is approximately $L \tan \alpha_1/2$, where L is the length of the antenna, measured from the apex (point of supply) to the end of the distribution line. The model used to produce the series of patterns in Figure XVI.3.1 had a length $L = 12.75$ cm. Maximum length of the dipole equals 12.75 tan $37°30' \approx 9.6$ cm. Correspondingly, the longest operating wave was approximately

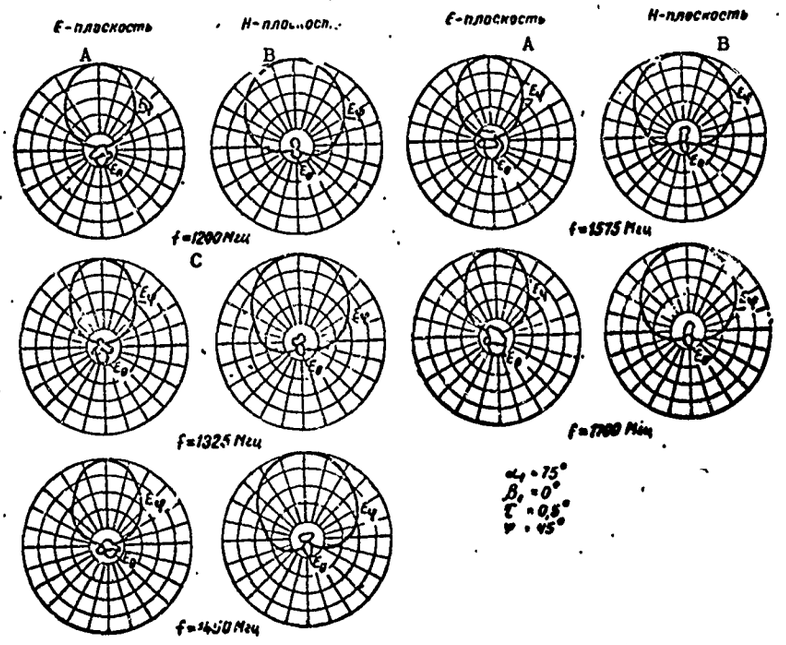

Figure XVI.3.1. Experimental radiation patterns of a non-flat top wire structure with trapezoidal dipoles. Distance from apex to the last element is 12.75 cm. Antenna elements made of 0.8 mm diameter wire.

A - principal E plane; B - principal H plane;
C - frequencies in megahertz (mh).

equal to 35 cm (f = 857 mh). Eight dipoles were included in each antenna section. The diagrams should repeat every half-cycle, because each half-cycle has its own resonant dipole (resonant tooth). Since $\tau = 0.5$, a cycle covers the bands 35 to 17.5 cm, 17.5 to 8.75 cm, 8.75 to 4.375 cm, and 4.375 to 2.187 cm.

Since, as was pointed out above, the shortest wave is approximately equal to 0.1 the longest wave, λ_{short} is approximately equal to 3.5 cm. The experimental diagrams in Figure XVI.3.1 are for frequencies corresponding to one half of the cycle for 17.5 to 35 cm (857.2 to 1714 mh). The diagrams will be repeated accurately enough at frequencies equal to those shown in the figure, multipled by $\tau^{\pm n/2}$ (in a half-cycle), where n is an integer, within the limits of those n values that correspond to the 3.5 to 35 cm band.

As will be seen from the patterns, the E_θ component is extremely small compared to the E_φ component, indicating that distribution line radiation is

not high. Maximum radiation is in the directions $\varphi = 0$ and $\theta = 0$, that is, in the direction of the semi-axis y.

Figure XVI.3.2 shows a series of experimental radiation patterns of a logarithmic antenna with trianglular dipoles (zigzag structure). The values of α_1, τ and ψ are the same as those in the preceding case. The patterns in Figure XVI.3.3 were obtained for an antenna with the following data: $\alpha_1 = 14.5°$; $\beta_1 = 0$; $\tau = 0.85$ and $\psi = 29°$. The overall view of the experimental model of this antenna is shown in Figure XVI.3.4. In this case a half-cycle encompasses the waveband in which the ratio of the longest to the shortest wave equals $\sqrt{0.85} \approx 0.92$.

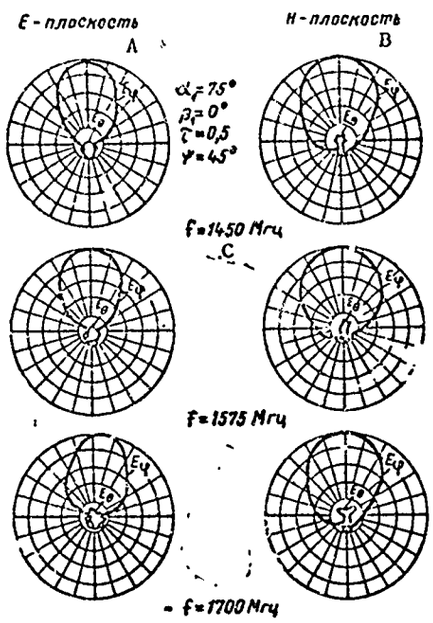

Figure XVI.3.2. Experimental radiation patterns of a wire antenna with triangular dipoles (zigzag structure).

A - principal E plane; B - principal H plane;
C - frequencies in megahertz (mh).

The patterns in Figure XVI.3.3 correspond to a half-cycle. Approximately these same patterns are obtained in the tenfold band, beginning at waves approximately equal to $4L \tan \alpha_1/2$, and ending at waves equal to $0.4L \tan \alpha_1/2$. So, in accordance with the above explanation, in this case, because of the reduction in α_1 and the increase in τ, the three main dipoles play an active part, just as do those nearest to them, and patterns obtained

are narrower. The antenna gain factor for the antenna shown in Figure XVI.3.4 is approximately 10.

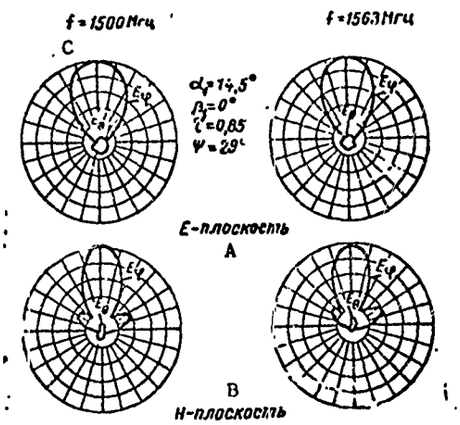

Figure XVI.3.3. Experimental radiation patterns of the antenna shown in Figure XVI.3.4.

A - principal E plane; B - principal H plane;
C - frequencies in megahertz (mh).

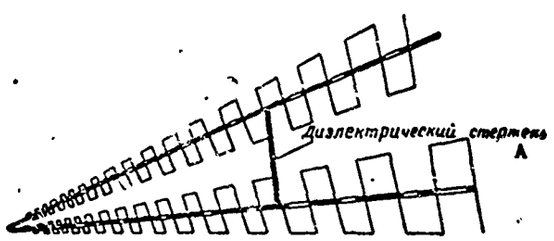

Figure XVI.3.4. Wire antenna with trapezoidal dipoles. Antenna length 2λ at a frequency of 1000 mh.

A - dielectric rod.

Table XVI.3.1 lists some of the collated data obtained experimentally on models of different variants of a logarithmic wire antenna with trapezoidal dipoles. The table was compiled for $\beta_1 = 0$.

Table XVI.3.2 lists the results of investigations of the characteristic impedance of the antenna, W_a, and the minimum values of the traveling wave ratio, k, on the feed line. As will be seen, an increase in angle ψ results in an increase in the characteristic impedance of the antenna and an improvement in the match with the supply line. The traveling wave ratio values are for the case when the characteristic impedance of the feed line equals W_a.

Figure XVI.3.5 shows the radiation patterns of an antenna with dipoles located in the same plane ($\psi = 0$). Values of α_1 and τ are as shown in the figure.

Table XVI.3.1

Порядковый номер образца (A)	Параметры (B)			Средняя ширина диаграммы в градусах (по половинной мощности) (C)		Приближ. коэф. усиления относит. полуволнового вибратора дб	Уровень боковых лепестков, дб
	s_1°	τ	ψ°	плоскость E	плоскость H		
				D	E	F	G
1	75	0,4	30	74	155	3,5	—12,4
2	75	0,4	75	72	125	4,5	—11,4
3	75	0,4	60	73	103	5,3	— 8,6
4	60	0,4	30	85	153	3,0	—12,0
5	60	0,4	45	86	112	4,2	— 8,6
6	60	0,4	60	87	87	5,3	— 7,0
7	75	0,5	30	66	126	4,9	—17,0
8	75	0,5	45	67	106	5,6	—14,9
9	75	0,5	60	68	93	6,1	—12,75
10	60	0,5	30	70	118	4,9	—17,7
11	60	0,5	45	71	95	5,8	—14,0
12	60	0,5	60	71	77	6,7	— 9,5
13	60	0,6	45	67	85	6,5	—15,8
14	60	0,707	45	64	79	7	—15,8
15	45	0,707	45	66	66	7,7	—12,3

Key: A - specimen sequence number; B - parameters; C - average width of pattern in degrees (at half power); D - principal E plane; E - principal H plane; F - approximate gain factor equated to a half-wave dipole, db; G - level of side lobes, db.

Table XVI.3.2

ψ°	W_a, ohms	k_{min}
60	120	0,7
45	110	0,69
30	105	0,67
7	65	0,55

Figure XVI.3.6 shows the patterns of a bidirectional flat top antenna ($\psi = 180°$).

We note that all the data presented in this section were obtained without regard for the effect the ground has on the radiation pattern and the gain factor.

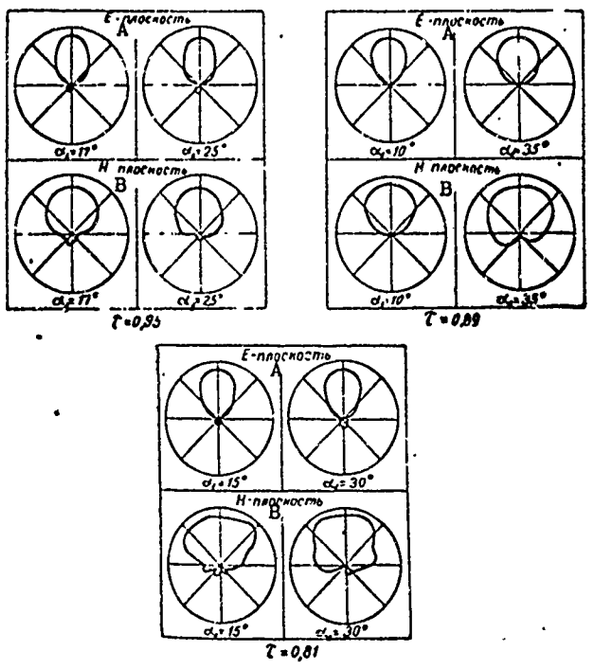

Figure XVI.3.5. Experimental radiation patterns for a flat top (ψ=0) logarithmic antenna.

A - principal E plane; B - principal H plane.

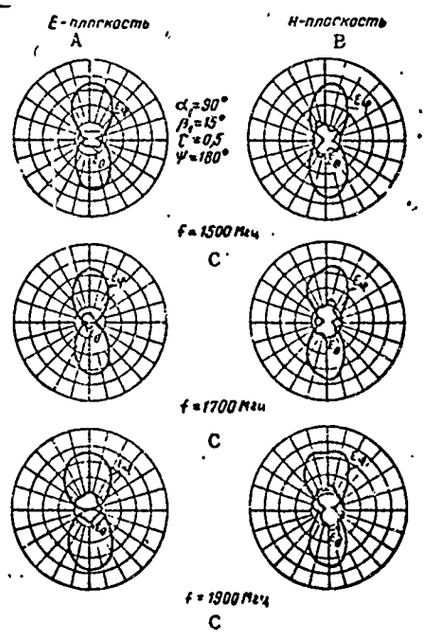

Figure XVI.3.6. Experimental radiation patterns for a flat top logarithmic antenna (ψ = 180°) with trapezoidal dipoles.

A - principal E plane; B - principal H plane;
C - frequencies in megahertz (mh).

#XVI.4. The Use of Logarithmic Antennas in the Shortwave Field

Logarithmic antennas are, obviously, finding application in the shortwave field, particularly in radio broadcasting.

The flat top, ($\psi = 0$), as well as the non-flat top variants of the logarithmic antenna can be used on these waves. The advantage of the flat top version is its design simplicity, as well as the virtually complete lack of antenna effect from the distribution feeders. The advantage of the space antenna ($\psi \neq 0$) is a higher directive gain, the result of the narrowing of the radiation pattern in the principal H plane. The space antenna has two tiers, the flat top, one. An additional advantage of the space antenna is a somewhat higher traveling wave ratio on the feeder line (see Table XVI.3.2; the increase in angle ψ is accompanied by an increase in the traveling wave ratio). Moreover, the space antenna has a higher characteristic impedance, making it easier to match it to a balanced feeder line.

The non-flat top logarithmic antenna can be suspended on supports so the bisector of angle ψ is horizontal (fig. XVI.4.1). In this case the radiation pattern in the vertical plane can be charted through the formula

$$F(\Delta) = f_1(\Delta) \sin(\alpha H \sin \Delta), \qquad \text{(XVI.4.1)}$$

where

$f_1(\Delta)$ is a function describing the radiation pattern in the principal H plane of the antenna in free space. This function can be established experimentally;

H is the height of the bisector of angle ψ above the ground; the factor $\sin(\alpha H \sin \Delta)$ takes the effect of the ground into consideration.

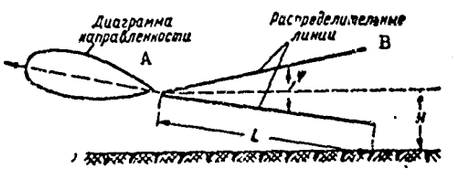

Figure XVI.4.1. A logarithmic non-flat top antenna ($\psi \neq 0$). The bisector of angle ψ is parallel to the earth's surface. Dipoles not shown.

A - radiation pattern; B - distribution lines.

There is a good deal of dependence of the radiation pattern in the vertical plane on the wavelength when the antenna bisector is oriented horizontally. Lengthening the waves expands the radiation pattern and increases the angle of maximum radiation.

Figure XVI.4.2 shows a series of radiation patterns in the vertical plane, charted through vormula XVI.4.1. And the function $f_1(\Delta)$ was established with respect to the experimental pattern in the principal H plane shown in Figure XVI.3.3. The height of H was taken as equal to $0.75\ \lambda_{long}$.

If the antenna is to have a fixed radiation pattern in the vertical plane the antenna must be suspended and tilted such that the shortest dipoles, working on the shortest waves, are closest to the ground (figs. XVI.4.3 and XVI.4.4). With the proper selection of the angles of tilt, ψ_1 and ψ_2, both sections of the antenna (fig. XVI.4.4) and the magnitudes of τ and α_1 can provide an operating mode such that the radiation pattern in the vertical plane will have the necessary shape and will remain the same over the entire band. Different combinations of the magnitudes of ψ_1 and ψ_2 and τ are possible for which the maximum radiation in the vertical plane will occur at the specified angle of tilt. Elementary considerations demonstrate that to provide maximum radiation at a specified angle of tilt requires the currents in section I of the antenna (fig. XVI.4.4) to lead the currents flowing in the corresponding dipoles in section II of the antenna by some angle γ. The phase angle γ should compensate for the difference in the path of the beams of identical elements in sections I and II of the antenna in the direction of maximum radiation (Δ_0).

The radiation pattern of a tilted logarithmic antenna can be expressed through the formula

$$E \sim A\left[f(\Delta, \psi_1)\, e^{i[\tau - \alpha d(\cos\psi_1 - \cos\psi_2)\cos\Delta]} + f(\Delta, \psi_2)\right], \qquad \text{(XVI.4.2)}$$

where

$f(\Delta,\psi_1)$ and $f(\Delta,\psi_2)$ are radiation patterns of sections I and II, with their mirror images taken into consideration.

The factor when $f(\Delta,\psi_1)$ takes into consideration the phase angle between the fields of the identical elements in sections I and II of the antenna, determined by the difference in the path of the beams and the phase angle γ. The difference in the path equals $\alpha d(\cos\psi_1 - \cos\psi_2)\cos\Delta$, where

d is the distance from the antenna origin (supply point) to the excited element (fig. XVI.4.4).

The function $f(\Delta,\psi_1)$ can be expressed as follows:

$$f(\Delta, \psi_1) = f_1(\Delta)\, e^{i\alpha d \sin\psi_1 \sin\Delta} - f_{1m}(\Delta)\, e^{-i\alpha d \sin\psi_1 \sin\Delta}, \qquad \text{(XVI.4.3)}$$

where

$f_1(\Delta)$ is a function expressing the radiation pattern of section I (without the effect of the ground taken into consideration).

$f_{1\,m}(\Delta)$ is a function expressing the radiation pattern of the mirror image of section I.

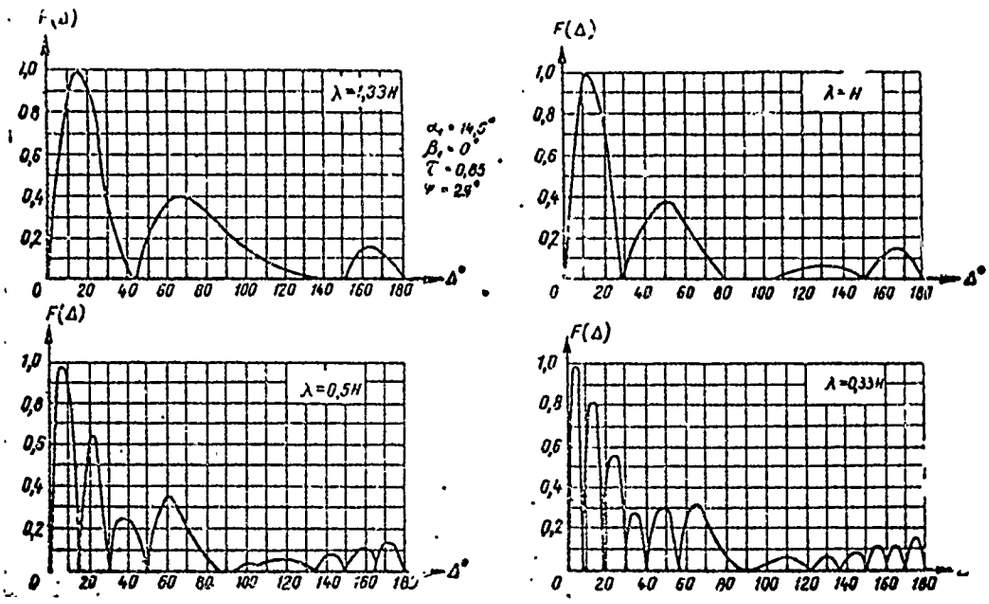

Figure XVI.4.2. Radiation patterns in the vertical plane of a non-flat top logarithmic antenna. The bisector of angle ψ is parallel to the earth's surface.

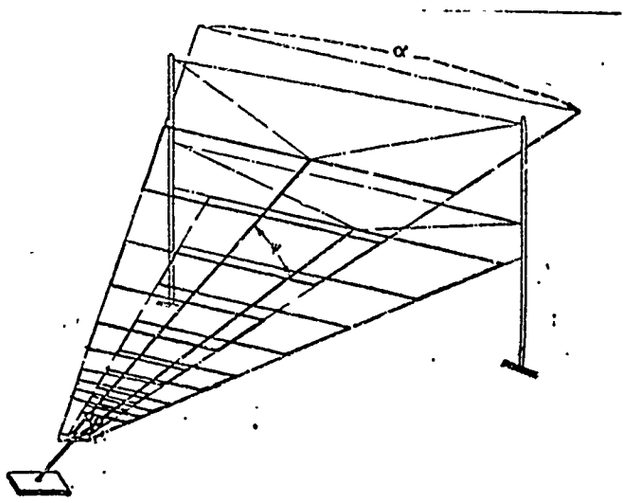

Figure XVI.4.3. Non-flat top logarithmic antenna suspended at an angle.

-.-.-. wire ropes supporting the antenna. The insulators supporting the wire ropes not shown.

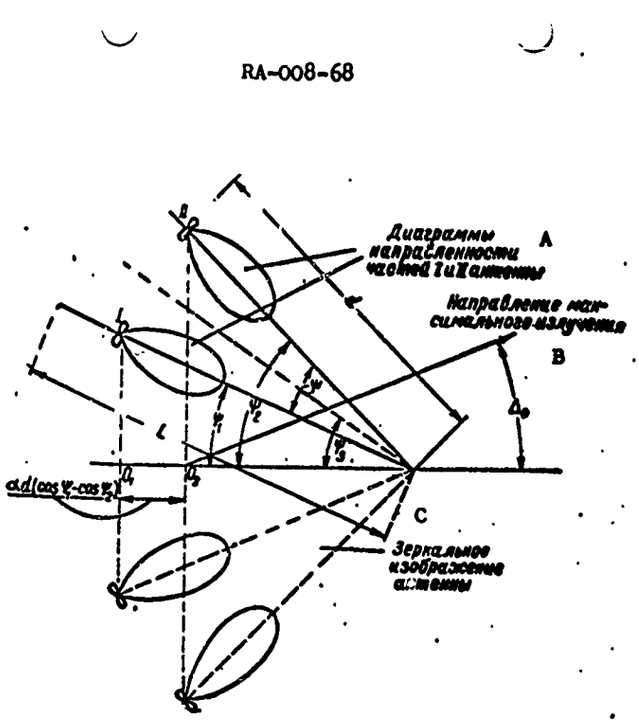

Figure XVI.4.4. Schematic representation of a tilted non-flat top logarithmic antenna.

A - radiation patterns of sections I and II of the antenna; B - direction of maximum radiation; C - mirror image of the antenna.

The radiation patterns described by expressions $f_1(\Delta)$ and $f_{1\,m}(\Delta)$ are the same, but turned by an angle $2\psi_1$, with respect to each other. The factors $e^{i\alpha d \sin\psi_1 \sin\Delta}$ and $e^{-i\alpha d \sin\psi_1 \sin\Delta}$ take into consideration the phase angle between the fields created by section I of the antenna and its mirror image. The phase angle can be read relative to the phase center (point O_1 in fig. XVI.4.4).

The function $f(\Delta,\psi_2)$ can be expressed in a manner similar to that used to express $f(\Delta,\psi_1)$, but ψ_1 is replaced by ψ_2.

The expression for $f_1(\Delta)$, or the corresponding expression for element II, can be established experimentally. Specifically, this can be done by moving the radiation pattern in the principal H plane of a flat top antenna by an angle $\psi = 180°$. The pattern thus obtained is bidirectional, but each half of this pattern makes it possible to judge the nature of $f(\Delta)$ within the limits of the major lobe.

Figure XVI.4.5 shows a series of curves that characterize the width of the radiation pattern in the principal H plane and in the principal E plane of one section of the antenna in accordance with angle α_1 for different values of τ. As will be seen from the curves, by selecting the corresponding values of α_1 and τ, it is possible to change the width of the pattern in the principal H plane over broad limits for comparatively small changes in the width of the pattern in the principal E plane.

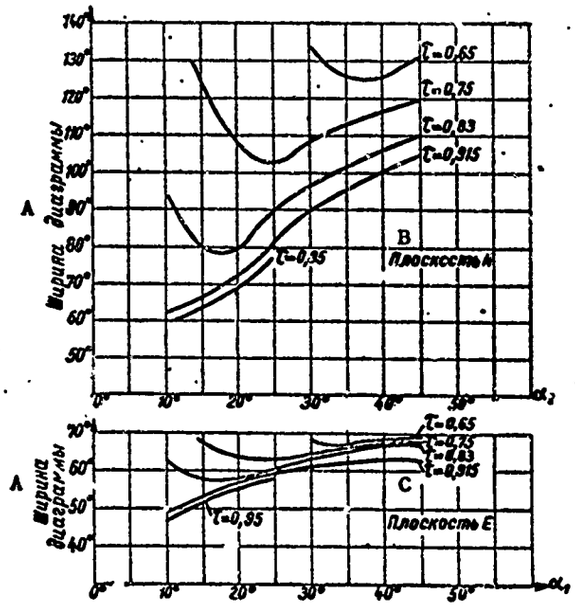

Figure XVI.4.5. Curves depicting the width of the pattern of one section of the antenna (I or II) in the principal E and H planes (without ground effect taken into consideration).

A - pattern width; B - principal H plane; C - principal E plane).

We will not pause here to discuss the methods used in selecting the magnitudes of α_1, τ, L, ψ_1 and ψ_2, but will limit ourselves instead to citing the results of computations and the experimental data for a series of antennas that provide maximum radiation at specified angles of tilt. The computations revealed the desirability of establishing the dependence between the magnitudes of τ and α_1 shown in Table XVI.4.1.[1]

Table XVI.4.1

τ	α_1
0,83	10°
0,8	14°
0,75	19°; 24°; 30°
0,65	37°; 45°

1. Cm. R. H. Du Hamel and D. C. Berry. "A new concept in high frequency antenna design." I.R.E. National Convent. Rec. P. I. V. 7. March 1959.

Established as a result of the computations and the experimental investigation were the desirable values for the magnitudes of α_1, ψ_1, ψ_2, and γ for which maximum radiation will be obtained at angles of tilt of 40°, 24° and 16°.

The radiation patterns of the antennas with maximum radiation at the indicated angles are shown in figures XVI.4.6 through XVI.4.8. These also show the corresponding values for the magnitudes of α_1, ψ_1, ψ_2 and γ. The shapes of the diagrams shown hold for an approximately tenfold band. A pattern of the shape shown in Figure XVI.4.6 is good for communications over distances between 200 and 800 km; Figure XVI.4.7 for communications over distances between 800 and 1600 km; and Figure XVI.4.8 for communications over distances between 1350 and 2500 km.

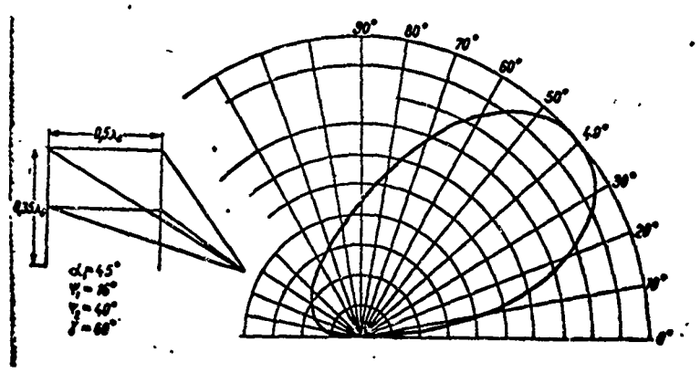

Figure XVI.4.6. Radiation pattern in the vertical plane of a tilted non-flat top logarithmic antenna; λ_{long} - the longest wave in the antenna's band.

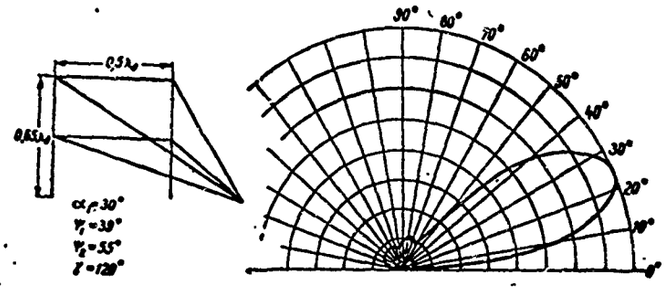

Figure XVI.4.7. Radiation pattern in the vertical plane of a tilted non-flat top logarithmic antenna; λ_{long} - the longest wave in the antenna's band.

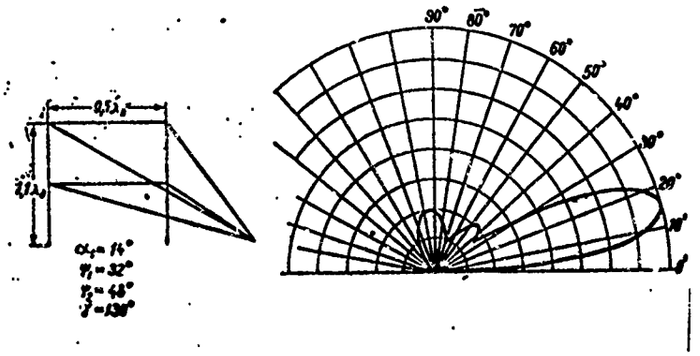

Figure XVI.4.8. Radiation pattern in the vertical plane of a tilted non-flat top logarithmic antenna.

The first pattern corresponds to an antenna gain of ~ 9.5 db, the second ~ 12.5, and the third ~ 14 db, as compared with the half-wave dipole in free space.

Let us pause to consider the question of selecting the magnitude of γ. As was pointed out above, the purpose of the phase angle γ between the current flowing in sections I and II is to compensate for the difference in beam paths, equal to $2\pi d/\lambda\ (\cos\psi_1 - \cos\psi_2)$.

The magnitude of d is approximately equal to the distance from the antenna source to the dipole resonant to the specified wave. The d/λ ratio is approximately the same for all waves in the operating band because with lengthening of the wave will come an increase in the distance from the resonant dipoles to the antenna source (supply point).

The magnitude of d/λ is a function of α_1 (fig. XVI.4.9). Analysis and experimental investigations reveal that the magnitude of γ at which the difference in beam paths is completely compensated for by $[2\pi/\lambda \cdot d(\cos\psi_1 - \cos\psi_2) = \gamma]$ is not optimum. This is so in all cases when the dipoles are located along the line of maximum radiation. The optimum value of γ is somewhat larger than the magnitude of $2\pi/\lambda \cdot d(\cos\psi_1 - \cos\psi_2)$. It can be selected experimentally, or by computation.

The phase angle between the points in sections I and II can change when making an experimental selection of the magnitude of γ by using the schematic shown in Figure XVI.4.10. Selecting the length of a loop, we can provide the corresponding lead for the current flowing in section I with respect to the current flowing in section II.

The loop can be selected by controlling the antenna gain factor, or by controlling the shape of the antenna radiation pattern.

The diagram shown in Figure XVI.4.10 can provide the necessary value for γ within the limits of a comparatively narrow band, because the magnitude of γ is approximately equal to

$$\frac{2\pi}{\lambda} t_n,$$

where

t_n is the length of the loop.

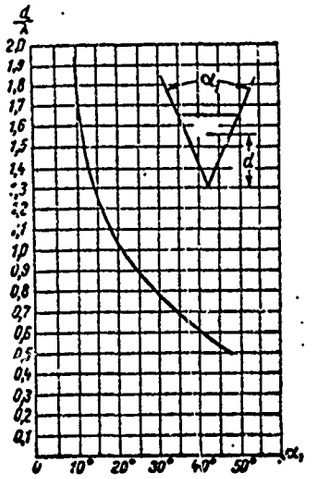

Figure XVI.4.9. Dependence of the distance of the phase center (d) on angle α_1 for a single-element antenna.

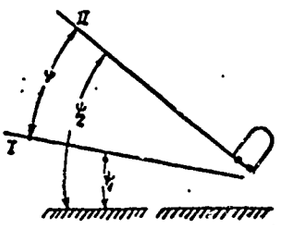

Figure XVI.4.10. Schematic diagram of the phase displacement of antenna sections I and II.

The magnitude of γ changes with change in the wavelength. The diagram in Figure XVI.4.10 can be used to achieve the optimum regime on the center wave in the band, so that satisfactory, but not optimum, conditions prevail over the entire band.

It is possible, however, to ensure a virtually identical and optimum value of γ on all waves as follows. It is known that if an indicator is set up at a long distance from a logarithmic antenna in the direction of maximum radiation, and if the phase angle between the field strength at the indicator and the current at the antenna origin is recorded, this phase angle will change with change in the wavelength. If the ratio of the magnitude of the distance from the field indicator to the antenna origin to the wave length is kept constant, shortening the wavelength of the logarithmic antenna by one cycle will cause the field phase to lag 360°. In other words, a 360° lag

in phase will result. Dependence of phase on wavelength within the limits of a cycle is almost linear.

So it follows that if we multiply the dimensions of all elements in the structure by the magnitude of τ, the field intensity at the reception site will lead by 360°. If the requirement is to lead by 90° we must multiply the dimensions of all elements in the structure by the magnitude $\tau^{90/360} = \tau^{1/4}$.

So, in order to provide the proper phase relation between the fields of sections I and II we must multiply all the dimensions of the elements in section I by $\tau^{\gamma/360}$. As a practical matter, wire diameters cannot be changed.

Investigations have demonstrated that when the phase shift is made in the manner indicated, the magnitude of γ will not change more than ±15° within the limits of a cycle.

#XVI.5. Other Possible Arrangements of Antennas with Constant Width Radiation Patterns

Rhombic and broadside antennas, and generally speaking, practically any type of directional antenna can be used as the basis for obtaining radiation patterns in the horizontal plane with little change in width within the limits of an extremely broad waveband. This is done by making the antenna system of two directional antennas with their directions of maximum radiation turned with respect to each other. Figure XVI.5.1 is the schematic diagram of an antenna such as this. It comprises two rhombuses.

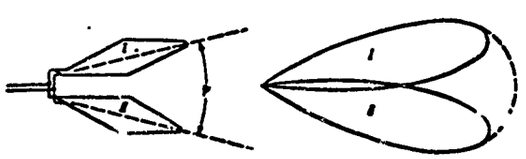

Figure XVI.5.1. Schematic diagram of a multiple rhombic antenna with a radiation pattern in the horizontal plane with little change in width.

With proper selection of angle ψ, and of the parameters of the rhombic antennas, the result is a radiation pattern in the horizontal plane that changes little over a broad waveband. The rhombic antennas can be single, as well as twin.

Broadside antennas will yield the same results. By way of an example, Figure XVI.5.2 shows a four-section broadside antenna. The left half of the antenna (I), has a pattern turned to the left because the feeding

point, 1, is shifted to the right. The right half of the antenna (II), the feeding point of which is shifted to the left, has a pattern turned to the right. The summed pattern, the result of adding two partial patterns, has a width that changes little within the operating band of the antenna.

An eight-section broadside antenna can be used similarly.

Shortwave traveling wave antennas set up for the schematic shown in Figure XVI.5.1 can also be used as the basis for an antenna system with a pattern in the horizontal plane, the width of which will change but little.

A characteristic feature, and a substantial shortcoming, of all such antennas is poor utilization of their potentials. Thus, only three, or a few more, dipoles operate on each operating wave in the logarithmic antenna. The rest (shorter and longer) are not used.

The gain factor of the antenna made in accordance with the schematic shown in Figure XVI.5.1 is less than that of an antenna comprising two cophasally excited rhombuses with identical directions of maximum radiation by a factor of three to four.

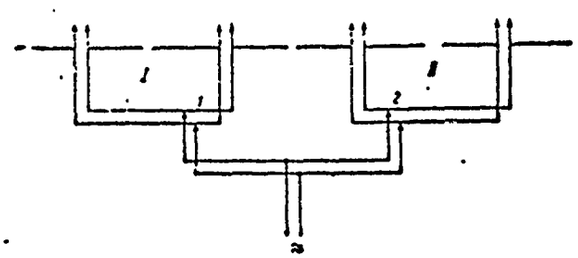

Figure XVI.5.2. Schematic diagram of a broadside antenna with a radiation pattern in the horizontal plane which changes little in width.

The feeding point for the primary distribution feeders of the broadside antenna can be selected such that on the longest wave in the band the antenna gain factor obtained will be only slightly lower than that if all sections were fed in phase. However, shortening the operating wave will result in an antenna gain for the antenna made according to the schematic in Figure XVI.5.2 that will increase approximately in proportion to the first power of the ratio λ_{long}/λ (because of the compression of the radiation pattern in the vertical plane). The gain factor of the conventional broadside antenna in which all sections are excited in phase increases approximately in proportion to $(\lambda_{long}/\lambda)^2$, because of the narrowing of the radiation pattern in the horizontal and vertical planes. Here λ_{long} is the maximum length of the wave in the antenna's working band, and λ is the antenna's operating wave.

We should note that the antennas described in this section are not as good as the logarithmic antenna because they cannot maintain a constant

radiation pattern in the vertical plane. Moreover, these antennas have less of an operating band. Yet the shortcomings noted are not always significant. There are many cases where antennas with constant pattern widths in the horizontal plane described here can prove more acceptable than the logarithmic antenna.

Chapter XVII

COMPARATIVE NOISE STABILITY OF RECEIVING ANTENNAS

#XVII.1. Approximate Calculation of emf Directive Gain

Reception quality can be established through the relationship

$$x = e_s/e_r \qquad \text{(XVII.1.1)}$$

where

e_s is the useful signal emf across the receiver input;

e_r is emf across the receiver input produced by unwanted signals.

As was pointed out above (#VI.10), in practice the relative noise stability, δ_{av}, of two receiving antennas, can, in most cases, be characterized by the relationship

$$\delta_{av} = x_1/x_2 = D_{emf\ 1}/D_{emf\ 2} \qquad \text{(XVII.1.2)}$$

where

x_1 and x_2 are average operational values of the x factor for antennas 1 and 2;

$D_{emf\ 1}$ and $D_{emf\ 2}$ are the emf directive gains for antennas 1 and 2.

The emf directive gain can be established through the formula

$$D_{emf} = \frac{4\pi |F(\varphi_0, \Delta_0)|}{\int_0^{2\pi} \int_0^{+\frac{\pi}{2}} |F(\varphi, \Delta)| \cos\Delta \, d\Delta \, d\varphi}, \qquad \text{(XVII.1.3)}$$

where

$F(\varphi,\Delta)$ is a function which establishes the receiving pattern;

φ, Δ are the current angular coordinates;

$F(\varphi_0,\Delta_0)$ is the value of $F(\varphi,\Delta)$ for the direction in which D_{emf} is being established.

It is convenient to establish the relative noise stability of antennas by using a non-directional (isotropic) antenna ($D_{emf\ 2}=1$) as the standard. Then

$$\delta_{av} = D_{emf\ 1}. \qquad \text{(XVII.1.4)}$$

Substituting the expression for D_{emf} in (XVII.1.4), and normalizing the receiving pattern with respect to $|F(\varphi_0,\Delta_0)|$, we obtain

$$\delta_{av} = \frac{4\pi}{\int_0^{2\pi} \int_0^{\frac{\pi}{2}} |F_1(\varphi, \Delta)| \cos\Delta \, d\Delta \, d\varphi}, \qquad \text{(XVII.1.5)}$$

where

$$|F_1(\varphi, \Delta)| = \frac{|F(\varphi, \Delta)|}{|F(\varphi_0, \Delta_0)|}.$$

The receiving pattern is usually symmetrical with respect to the direction $\varphi = 0$, so formula (XVII.1.5) can be rewritten

$$\delta_{av} = \frac{2\pi}{\int_0^{\pi}\int_0^{\frac{\pi}{2}} |F_1(\varphi, \Delta)| \cos\Delta \, d\Delta \, d\varphi} \quad \text{(XVII.1.6)}$$

Accordingly, the integral

$$A = \int_0^{\pi}\int_0^{\frac{\pi}{2}} |F_1(\varphi, \Delta)| \cos\Delta \, d\Delta \, d\varphi. \quad \text{(XVII.1.7)}$$

must be calculated in order to establish the noise stability factor, δ_{av}.

Mathematical difficulties associated with the need to integrate the function $|F_1(\varphi,\Delta)|$ are encountered in establishing the magnitude of A in final form, even for comparatively simple antennas. Practically, the computation can be made by numerical integration, but there is an unusual amount of computational effort involved. This is why the approximate solution to the expression for A has been introduced. The following simplifications have been made in order to make the computations less arduous.

1. Integration with respect to the variable Δ has been limited to the range of angles from 0° to 50 or 60°. The basis for this simplification is the low probability of arrival of noise at angles higher than 50 to 60° in the shortwave region. Unwanted signals at these high angles can be generated in the main stations working on short mainlines, but these stations usually work on longer waves. Also to be borne in mind is the fact that the basic types of shortwave antennas have extremely weak reception at high angles relative to the horizon ($\Delta >$ 50 to 60°), so the exclusion of the range of angles $\Delta >$ 50 to 60° from the integration will cause no marked change in the magnitude of A. We have settled on limits of integration from 0° to 60°.

2. The limitation imposed on the limits of integration of the range of angles 0 to 60° permits the assumption that in the sector of angles from Δ_1 to Δ_2 the patterns in the horizontal plane have the same shape as the pattern in the horizontal plane when $\Delta = \Delta_{max}$ without the errors in the assumption being too great. Here Δ_1 and Δ_2 are the minimum and maximum angles limiting the major lobe of the pattern of the antenna in the vertical plane, while Δ_{max} is the elevation corresponding to the direction of maximum reception. In the sectors 0° to Δ_1 and Δ_2 to 60° it can be taken that the patterns in the horizontal plane are identical with the patterns in the sector Δ_1 to Δ_2, and differ from them only by the absence of a major lobe.

It has been accepted that the patterns of the first type occur in the sector of angles corresponding to the width of the pattern in the vertical plane at half power.

With these simplifications in mind, the computation for A can be carried out through the following formula

$$A = \int_{\Delta_1}^{\Delta_2} \cos\Delta\, d\Delta \int_0^{\pi} |F_1^{(1)}(\varphi)|\, d\varphi + \int_0^{\Delta_1} \cos\Delta\, d\Delta \int_0^{\pi} |F_1^{(2)}(\varphi)|\, d\varphi + \int_{\Delta_2}^{\frac{\pi}{3}} \cos\Delta\, d\Delta \int_0^{\pi} |F_1^{(2)}(\varphi)|\, d\varphi, \qquad \text{(XVII.1.8)}$$

where

$F_1^{(1)}(\varphi)$ is an expression establishing the pattern of the antenna in the horizontal plane when $\Delta = \Delta_{max}$;

$F_1^{(2)}(\varphi)$ is an expression establishing the pattern in the horizontal plane for values of Δ lying in the sectors 0° to Δ_1 and Δ_2 to 60°.

Integrating, we obtain

$$A = (\sin\Delta_2 - \sin\Delta_1) \int_0^{\pi} |F_1^{(1)}(\varphi)|\, d\varphi + \left(\frac{\sqrt{3}}{2} - \sin\Delta_2 + \sin\Delta_1\right) \times \int_0^{\pi} |F_1^{(2)}(\varphi)|\, d\varphi. \qquad \text{(XVII.1.9)}$$

Accordingly, the relative noise stability of an antenna can be established through the formula

$$\delta_{av} = \frac{2\pi}{(\sin\Delta_2 - \sin\Delta_1) \int_0^{\pi} |F_1^{(1)}(\varphi)|\, d\varphi + \left(\frac{\sqrt{3}}{2} - \sin\Delta_2 + \sin\Delta_1\right) \int_0^{\pi} |F_1^{(2)}(\varphi)|\, d\varphi}. \qquad \text{(XVII.1.10)}$$

#XVII.2. Results of the Calculation

The approximation method discussed was used to establish the noise stability of the basic types of shortwave receiving antennas. Figure XVII.2.1 shows the curves of the dependence of the magnitude of $D_{emf\ 1}$ for the direction of maximum reception for the traveling wave antennas BS2 21/8 200/4.5 17, BS2 21/8 200/4.5 25, and 3BS2 21/8 200/4.5 25 on the wavelength. The 3BS2 antenna has the greatest noise stability. The magnitude of $D_{emf\ 1}$ for this antenna is 4 to 6 db higher than that of $D_{emf\ 1}$ for the BS2 antenna suspended at a height of 17 meters, and 3 to 5 db higher than that of $D_{emf\ 1}$ for the BS2 antenna suspended at a height of 25 meters.

Figure XVII.2.2 shows similar curves for the rhombic antennas RG 65/4 1, RGD 65/4 1 and RG 70/6 1.25, also with respect to the wavelength. As will be seen from this figure, the magnitude of $D_{emf\ 1}$ for the twin antenna (RGD) is 2 to 5 db higher than that for the single antenna.

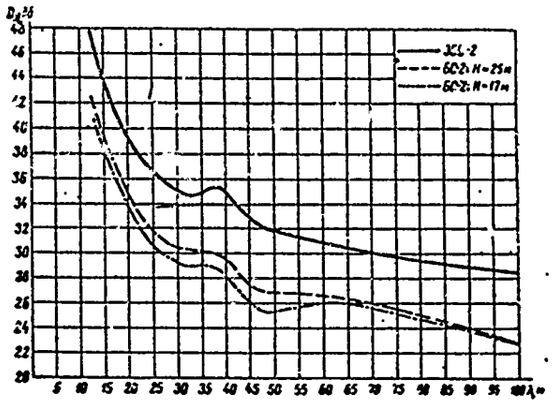

Figure XVII.2.1. Dependence of the computed values of emf directive gain of 3BS2 21/8 200/4.5 25, BS2 21/8 200/4.5 25, and BS2 21/8 200/4.5 17 antennas.

——— 3BS2; ---- BS2, H = 25 m; -.-.- BS2, H = 17 m.

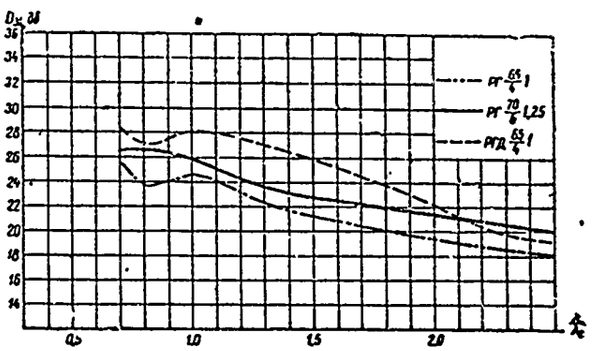

Figure XVII.2.2. Dependence of the computed values of emf directive gain of RGD 65/4 1, RG 70/6 1.25, and RG 65/4 1 antennas.

—.— RG 65/4 1; ——— RG 70/6 1.25; ---- RGD 65/4 1.

A comparison between Figure XVII.2.1 and XVII.2.2 reveals that the BS2 antenna suspended at heights of 17 and 25 meters, and this is particularly true of the 3BS2 antenna, has a substantially greater noise stability than do the rhombic antennas.

The data cited here are only a very approximate approach to the absolute values of the magnitudes of δ_{av} and $D_{emf\ 1}$ for traveling wave and rhombic antennas. In addition to the errors introduced by the inaccuracy of the methodology used for the calculation, there are large errors resulting from the fact that the antenna effect of the feeder, and the leakage of the single-cycle wave in the receiver, were not taken into consideration in the calculation. These latter errors are mostly reflected in the region of large values of $D_{emf\ 1}$.

However, experimental investigations have revealed that the curves shown are satisfactory for use in characterizing the relative noise stability of BS2 and rhombic antennas.

Chapter XVIII

METHODS OF COPING WITH SIGNAL FADING IN RADIO RECEPTION

#XVIII.1. Reception by Spaced Antennas

It has been established that the fluctuations in field intensity at points at considerable distances from each other are out of synchronism because the beams incident at these points are reflected from regions of the ionosphere at considerable distances from each other. Because the ionosphere is not sufficiently homogeneous, because of the rotation of the plane of polarization of the beams, and because of the change in the phase of the field resulting from change in the height of the reflecting layer, the fluctuations in field intensity at diverse points are not in synchronism.

If there are two or more beams with different angles of tilt at the reception point, the nonsynchronism in fluctuations in field intensity is also the result of nonidentity in the components of the phase velocity of propagation of these beams along the ground surface (v_g). This component increases with increase in angle Δ, and equals

$$v_g = c/\cos \Delta,$$

where

c is the speed of light (fig. XVIII.1.1).

In the case of two beams, the change in the field intensity in the direction of propagation because of nonidentity in phase velocities can be described by the formula

$$E = E_1\sqrt{1 + m^2 + 2m\cos[\alpha z(\cos\Delta_2 - \cos\Delta_1) + (\psi_2 - \psi_1)]}. \qquad \text{(XVIII.1.1)}$$

where

$$m = E_1/E_2;$$

E_1 and E_2 are the amplitudes of the field strength vectors for the first and second beams;

Δ_1 and Δ_2 are the angles of tilt of the first and second beams;

z is a current coordinate on an axis extended along the ground surface in the direction in which the beams are propagated;

ψ_1 and ψ_2 are the phase angles of the vectors E_1 and E_2.

Angles ψ_1 and ψ_2 are determined by the length of the path, change in phase during passage through the ionosphere, and other factors.

If $E_1 = E_2 = E_0$, the summed field intensity in the z direction will change in accordance with the law that has

$$E = 2E_0 \cos\left\{\frac{1}{2}\left[\alpha z(\cos\Delta_2 - \cos\Delta_1) + (\psi_2 - \psi_1)\right]\right\}. \qquad \text{(XVIII.1.2)}$$

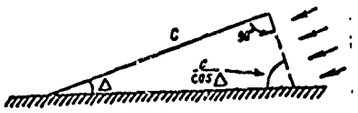

Figure XVIII.1.1. Determination of the phase velocity, v_{ground}, for a tilted beam.

As will be seen, standing waves of field intensity form along the ground surface. Field intensity loops are obtained at points z_{loop}, established through the relationship

$$\frac{1}{2}\left[\alpha z_{loop}(\cos\Delta_2 - \cos\Delta_1) + (\psi_2 - \psi_1)\right] = n\pi, \qquad \text{(XVIII.1.3)}$$

where n = 0, 1, 2, 3, ..., from whence

$$z_{loop} = \lambda \frac{n - \frac{\psi_2 - \psi_1}{2\pi}}{\cos\Delta_2 - \cos\Delta_1}. \qquad \text{(XVIII.1.4)}$$

Field intensity nodes are obtained at points z_{node}, established through the relationship

$$\frac{1}{2}\left[\alpha z_{node}(\cos\Delta_2 - \cos\Delta_1) + (\psi_2 - \psi_1)\right] = (2n+1)\frac{\pi}{2}, \qquad \text{(XVIII.1.5)}$$

from whence

$$z_{node} = \lambda \frac{0{,}5(2n+1) - \frac{\psi_2 - \psi_1}{2\pi}}{\cos\Delta_2 - \cos\Delta_1}. \qquad \text{(XVIII.1.6)}$$

The distance between a field intensity loop and a field intensity node equals

$$d = z_{node} - z_{loop} = \frac{\lambda}{2}\frac{1}{\cos\Delta_2 - \cos\Delta_1}. \qquad \text{(XVIII.1.7)}$$

Example. λ = 20 meters, Δ_1 = 20° and Δ_2 = 10°. The distance between a loop and the nearest field intensity node equals

$$d = \frac{\lambda}{2}\frac{1}{\cos\Delta_2 - \cos\Delta_1} = \frac{20}{2}\cdot\frac{1}{0{,}985 - 0{,}940} \approx 223 \text{ meters}.$$

Changes in ψ_1 and ψ_2 were not taken into consideration in the derivation of formula (XVIII.1.7). Actually, ψ_1 and ψ_2 are constantly changing because of the complex structure of the beams, so the field intensity loops and nodes are constantly shifted along the z axis.

And if there are several beams with different amplitudes present at the reception site the distribution of field intensity maxima and minima will be even more complicated.

It must be pointed out that as a practical matter the distribution of the field over the ground is a complex one, even when there is only one beam. As a matter of fact, the "beam" concept is very conditional indeed. Practically speaking, because of the "roughness" and nonuniformity of the ionosphere the "beam" is a bundle of homogeneous beams with dissimilar trajectories, albeit differing but slightly, and thus with somewhat different angles of tilt as a result.

A schematic of spaced reception is shown in Figure XVIII.1.2, with three antennas set up on the territory of the field. The separation between the centers of the antennas is made at least 300 to 400 meters. There is a separate feeder for each of the receivers, and the signals at the outputs of the receivers add. The probability of the minima of the signals from the individual receivers coinciding in time is very slight because of nonsynchronism in the fluctuations in field intensity at the individual antennas. Specifically, the probability of deep, short-term signal minima coinciding is remote. Thanks to spaced reception, the time during which deep signal minima occur is reduced considerably, and this is equivalent to increasing transmitter power.

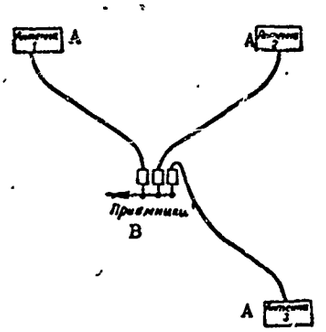

Figure XVIII.1.2. Schematic diagram of spaced reception.
A - antenna; B - receiver.

Lines longer than 2500 to 3000 km usually use three spaced antennas (triplex reception). Duplex reception, that is reception using two spaced antennas, is used on shorter lines.

On the basis of the considerations discussed here with respect to the reasons for the fluctuation in field intensity, it is desirable, when using duplex reception, to separate the antennas so they will be simultaneously

placed along the direction of beam propagation and normal to that direction.

Available experimental data reveal that in telegraph work triplex reception, when compared with simplex reception, has the effect of increasing transmitter power from 9 to 16 times. In the case of duplex reception the gain is equivalent to increasing transmitter power 5 to 8 times.

#XVIII.2. Reception with an Antenna Using a Differently Polarized Field

We know that the field intensity vector is constantly rotating at the reception site, the result of the features associated with the propagation of waves reflected from the ionosphere. Hence it is possible to have intensive reception by an antenna receiving a field with different polarizations; specifically, by an antenna receiving a normally polarized field and by an antenna receiving a parallel polarized field. Since the normal and the parallel components of the field will fade heterogeneously, this is one way to reduce signal fading.

Experimental investigations have thus far shown that the use of polarized duplex reception has an effect close to that provided by duplex reception by spaced antennas.

The simplest arrangement of an antenna system for polarized duplex reception, suggested by V. N. Gusev and B. D. Lyubomirov, is shown in Figure XVIII.2.1. It is made up of one vertical, and one horizontal, dipole. The antenna reflector is made in the form of a grid.

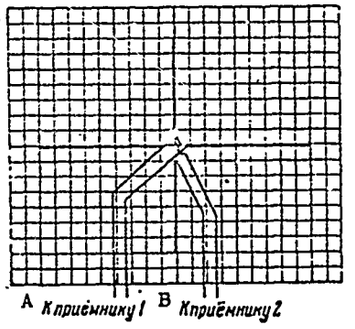

Figure XVIII.2.1. Schematic diagram of an antenna system for polarized duplex reception.

A - to receiver 1; B - to receiver 2.

Polarized duplex reception is particularly desirable in cases when the site is not largeenough to take two spaced antennas.

A system consisting of a BS2 horizontal traveling wave antenna, under which is an unbalanced BSVN2 vertical traveling wave antenna, is one convenient variant of an antenna system for polarized duplex reception.

More complex antenna systems, made up of horizontal and vertical dipoles, can also be used for polarized duplex reception.

N. I. Chistyakov has suggested the use of two unbalanced traveling wave antennas with tilted dipoles (fig. XVIII.2.2) for polarized duplex reception. Antenna geometry, including the number and length of the dipoles, is the same as that of the conventional BSVN antenna. Antennas can be duplex (BSVN-2) or simplex (BSVN), depending on conditions.

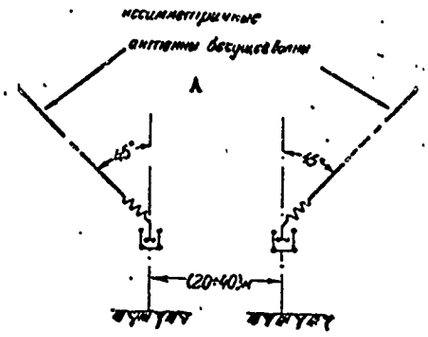

Figure XVIII.2.2. Schematic diagram of an antenna system for polarized duplex reception suggested by N. I. Chistyakov.

A - unbalanced traveling wave antennas.

#XVIII.3. Antenna with Controlled Receiving Pattern

Spaced reception reduces the depth of fading, but does not provide effective relief against selective fading and echoing.

As we have already pointed out (Chapter VII), selective fading occurs as a result of the summing of the beams, which have quite a bit of difference in the paths they travel, at the reception site.

There is usually a definite connection between the time of arrival of the beam and the angle of tilt. The smaller the angle, the shorter the beam path, and the sooner it will arrive at the reception site. But it also follows that selective fading can be lessened by using receiving antennas with narrow receiving patterns in the vertical plane which make it possible to single out one beam, or bundles of beams, incoming in the narrow sector of the angles of tilt. The use of a narrow pattern is desirable when the angle of tilt of the maximum beam in the pattern can be controlled in accordance with change in the angles of tilt of incoming beams.

A general view of one variant of an antenna system with a narrow controlled reception pattern is shown in Figure XVIII.3.1. It contains 16 rhombic antennas in a single line in the direction to the correspondent connected to a receiver that can make an in-phase addition of the emfs from all antennas. The antennas brought into the receiver is shown in Figure XVIII.3.2.

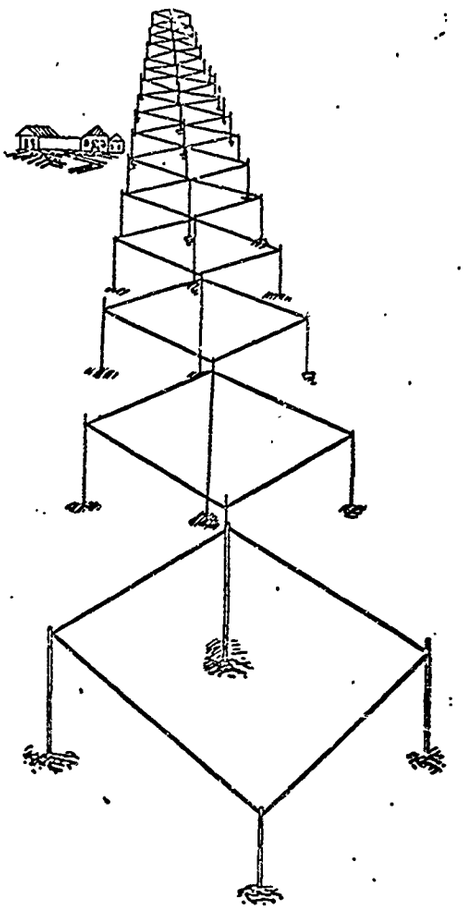

Figure XVIII.3.1. General view of an antenna system with a controlled radiation pattern.

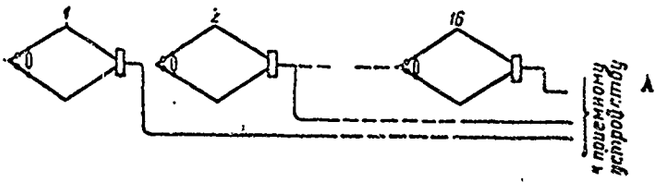

Figure XVIII.3.2. Schematic diagram of antenna supplies to receiver.

A - to receiver.

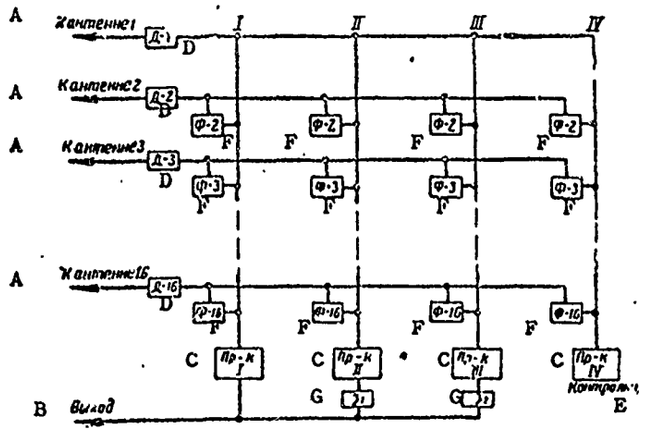

Figure XVIII.3.3. Block schematic of a receiver for an antenna system with controlled reception pattern.

A - to antenna; B - output; C - receiver; D - detector; E - monitor; F - phase shifter; G - delay line.

Figure XVIII.3.3 is a schematic of how the receiver system functions. As will be seen, the signal from each of the antennas is fed into a detector, D. The output is the IF current distributed over four branches. The outputs of the detectors to each of the branches are connected to a common bus through a phase shifter, F. The in-phase addition of the emfs from all antennas can be obtained by the corresponding adjustment of the phase shifter. The emf applied to each of the branches is fed into the individual receiver.

The receiving pattern in the vertical plane of each of the branches can be described by the formula

$$F(\Delta) = f_1(\Delta)\frac{\sin\left\{\frac{N}{2}\left|\psi - \alpha d\left(\frac{1}{k_1} - \cos\Delta\right)\right|\right\}}{\sin\left\{\frac{1}{2}\left|\psi - \alpha d\left(\frac{1}{k_1} - \cos\Delta\right)\right|\right\}}. \qquad \text{(XVIII.3.1)}$$

where

$f_1(\Delta)$ is a factor characterizing the pattern of a single rhombic antenna;

N is the number of rhombic antennas in the antenna system;

ψ is the phase angle between the emfs across two adjacent antennas, produced by the phase shifter;

d is the distance between the centers of two adjacent rhombuses;

$k_1 = v_{cable}/c$; where v_{cable} is the phase velocity of propagation of the waves on the cable connecting the antenna and receiver.

The cable is laid along the direction of the long diagonals of the rhombuses and the difference in the lengths of the cables conducting the emfs from two adjacent antennas is equal to the distance between the centers of these antennas.

As will be seen from formula (XVIII.3.1), the angle of tilt at which maximum reception is obtained depends on the magnitude of ψ. The value of this angle can be controlled by changing ψ.

The receiving pattern of the antenna system is quite acute. Figure XVIII.3.4 shows the pattern in the vertical plane, charted for the following conditions:

the antenna system is made up of RG 65/4 1 rhombic antennas;

number of rhombuses N = 16;

length of one side of the rhombus l = 100 meters;

length of the optimum wave for the rhombus λ_0 = 25 meters;

k_1 = 0.95.

The pattern was charted for ψ = 40°. The dotted line is the pattern for ψ = -80°.

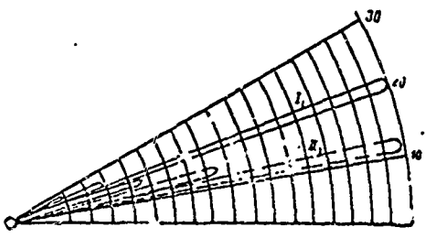

Figure XVIII.3.4. Reception pattern in the vertical plane of an antenna system with controlled pattern.

I - phase shifter tuning: ψ = 40°;
II - phase shifter tuning: ψ = -80°.

The narrow, controlled pattern makes it possible to tune to receive just one of the incoming beams in each branch. Reception is as follows. Each of the branches I, II, and III is tuned by its own individual system of phase shifters to receive one of the incoming beams, and the separate branches are tuned to different beams. Signals from each of the incoming beams pass through own individual receivers, after which they are added.

The output of the receiver in branch I, which is receiving a beam with maximum angle of tilt arriving at the reception point later than the other beams, is connected directly to the collection bus. The output of the receiver in branch II, tuned to receive a beam with a smaller angle of tilt incoming at the reception point at some time, τ, earlier than the beam being received by branch I, is connected through the delay line d_1. Delay line d_1 is a system of circuits forming an artificial, adjustable signal time

delay which compensates for the lead in travel along the route. Similarly, the output of the receiver in branch III, which receives a beam with minimum angle of tilt, is connected through delay line d_2, which compensates for the lead time in the arrival of this beam. Thus, the addition of the signals in the collection line takes place as if all three beams had arrived simultaneously.

The tuning of branches I, II, and III for maximum reception of one of the beams can be controlled by a special system that automatically changes the positions of the phase shifters with changes in the angles of tilt of the incoming beams. If there are only two strong beams at the reception site, reception is by two of the branches.

Branch IV is used to monitor the field structure at the reception site.

Reception in each of the branches of just one bundle of beams with slightly different paths results in a sharp reduction in selective fading. However, non-selective fading in each of the branches, caused by the complex structure of the beam and the rotation of the plane of polarization, is not eliminated. Weakening of non-selective fading occurs when signals from two or three branches are added, for this is the equivalent of duplex, or triplex, spaced reception.

The reception system described, along with weakening of selective and general fading, provides an increase in the directive gain in each of the branches by a factor of N compared with reception by just one rhombus.

Operating experience demonstrates that a reception system with a controlled receiving pattern has a positive, reliable effect only when clearly defined bundles of beams with predetermined angles of tilt are present at the reception site.

This system will not be reliable in its effects if a scattered field is present at the reception site. A scattered field, with no clearly defined beams, is often observed on long lines when there is poor passage of radio waves.

The noise stability of an antenna with a controlled receiving pattern can be improved substantially by the use of twin-rhombic antennas, or, and this is more desirable, twin traveling wave antennas.

Chapter XIX

FEEDERS. SWITCHING FOR ANTENNAS AND FEEDERS.

#XIX.1. Requirements Imposed on Transmitting Antenna Feeders

The basic requirement imposed on the transmitting antenna feeder is that of reducing to a minimum energy losses in the feeder. Two types of losses occur in the feeder: losses due to heating of the conductors, the insulators, and surrounding objects; and losses due to radiation. Heat loss can be reduced by using high conductivity conductors (copper, bimetal), special high-frequency insulators, and by keeping the open feeder away from the ground and surrounding objects.

Radiation losses are reduced by using symmetrical feeders, with two, or more, conductors located close to each other and carrying opposite phase waves, or by using shielded feeders. These measures simultaneously reduce energy losses to surrounding objects.

Definite requirements are also imposed on the dielectric strength of a feeder. The characteristic impedance and the diameter of the conductors in the feeder must be selected such that the possibility of torch emanation is precluded. The insulators used with the feeder must have a dielectric strength such as to preclude the possibility of their breaking down and being destroyed as a result of overheating.

Finally, reliable mechanical strength, and convenience in replacement, as well as in making repairs to damaged parts of the feeder (insulators, conductors, brackets, and the like), must all be provided for.

#XIX.2. Types of Transmitting Antenna Feeders. Design Data and Electrical Parameters.

(a) General remarks

Two-wire and four-wire aerial feeders, and coaxial lines are used as transmitting antenna feeders. Aerial feeders, because of their simplicity, have been used to advantage.

Only open aerial lines will be reviewed here. Information on coaxial lines can be obtained in the special literature on the subject.

(b) Two-wire aerial feeder

The two-wire aerial feeder is usually made of bimetallic or hard-drawn copper wire. Wire diameter will vary between 3 and 6 mm, depending on the length of the feeder and the transmitting power. The distance between wires is 20 to 40 cm.

The feeder is secured to wooden or reinforced concrete supports installed 20 to 30 meters apart.

Strict equidistant spacing of supports must be avoided in order to do away with the possibility of intensifying the effect of reflection occasioned by the shunt capacitance of the insulators. If the antenna is designed for operation on just one wave it is sufficient to ensure nonmultiplicity in the length of the span between supports with respect to one-quarter the length of this wave.

The height at which the feeder is suspended is selected as at least 3.0 meters to avoid any interference when moving about on the antenna field territory. Always to be borne in mind is that serious burns can result from coming into contact with an operating feeder. Clearance for trucks must be assured where freders cross roads.

Special feeder insulators are used to secure the feeder to the supports. Their design is such that the conductor can hang freely in them. Insulator shape and size depend on the computation made to reduce to a minimum the shunt capacitance between the conductors. Block and stick insulators are used in practice.

Feeders must be run from transmitter to antenna by as straight a line as possible to reduce reflections at bends.

The ends of the feeder are dead-ended at the last supports, but quite often special devices are used to regulate the tension on the feeder. Figures XIX.2.1 and XIX.2.2 show variants in the designs used to secure feeders to intermediate and end supports.

The characteristic impedance of the two-wire feeder is established through formula (H.IV.17) or (H.IV.20) in the Handbook Section.

The dependence of the characteristic impedance of the feeder on the D/d ratio, where D and d are the distance between wires and their diameter, computed through formula (H.IV.20), is shown in Figure XIX.2.3.

Formula (H.IV.15) can be used to compute the pure resistance per unit length of a two-wire copper feeder (R_1). Figure XIX.2.4 shows the curves of the dependence of R_1 on the wavelength for copper two-wire feeders for different values of d.

If we ignore the conductivity of the insulation, and this is permissible when dealing with feeders with high-quality insulators, the attenuation per unit length of a two-wire feeder can be established through the formula

$$\beta = R_1/2W \qquad \text{(XIX.2.1)}$$

Feeder efficiency in the general case can be expressed through formula (I.14.1). The efficiency of a feeder with a traveling wave ratio of 1 can be computed through formula (I.14.4).

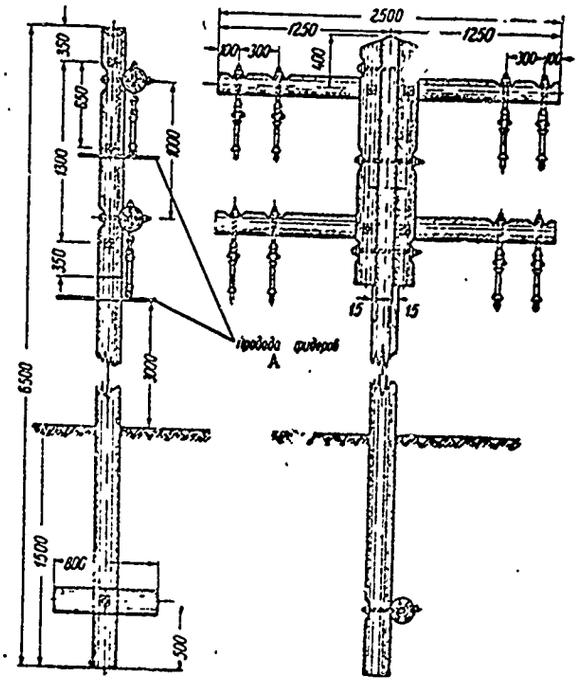

Figure XIX.2.1. Variant in the design for securing four two-wire feeders to the end support (stick insulators).

A - feeder conductors.

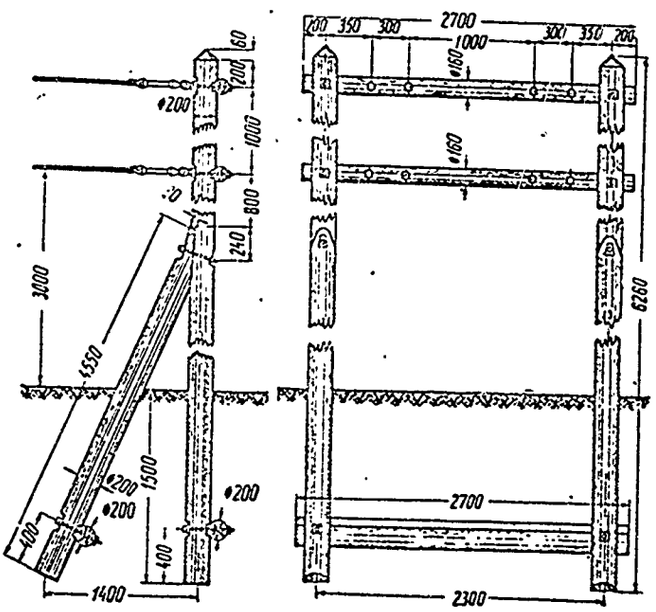

Figure XIX.2.2a. Variant in the design for securing four two-wire feeders to the end support (stick insulators).

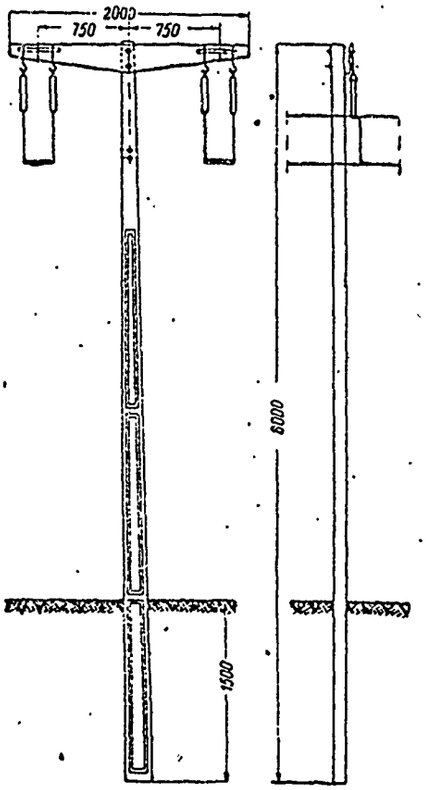

Figure XIX.2.2b. Variant in the design for securing a four-wire feeder to a reinforced concrete support.

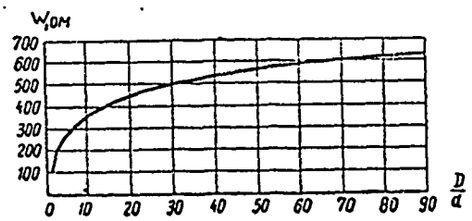

Figure XIX.2.3. Dependence of the characteristic impedance of a two-wire feeder on the D/d ratio; D - distance between conductor axes; d - conductor diameter.

Using formulas (I.14.1) and (I.14.4), we obtain

$$\eta = \eta_0 \frac{1-|p|^2}{1-|p|^2 r_0^2}, \qquad \text{(XIX.2.2)}$$

where

η_0 is the efficiency for a traveling wave ratio equal to 1;

$|p|$ is the modulus of the reflection factor.

Figures XIX.2.5 through XIX.2.7 show a series of curves that characterize the dependence of the efficiency η_0 on the line length l, the wavelength λ, and the wire diameter d. The curves were plotted through the use of formula I.14.4, that is, for the case of k = 1.

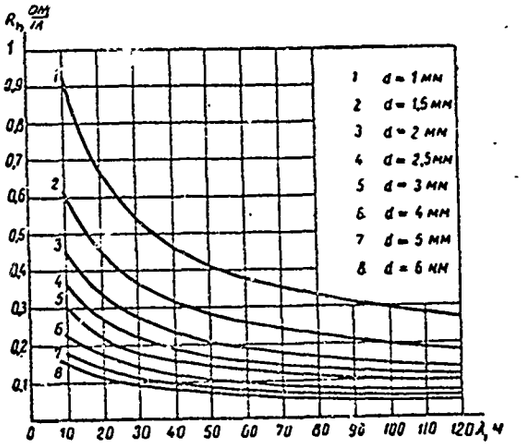

Figure XIX.2.4. Pure linear resistance of a two-wire copper feeder for various conductor diameters.

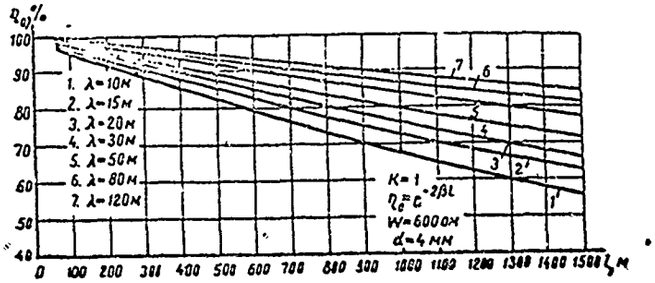

Figure XIX.2.5. Dependence of the efficiency of a two-wire feeder on its length for various wavelengths and a traveling wave ratio, k, equal to unity.

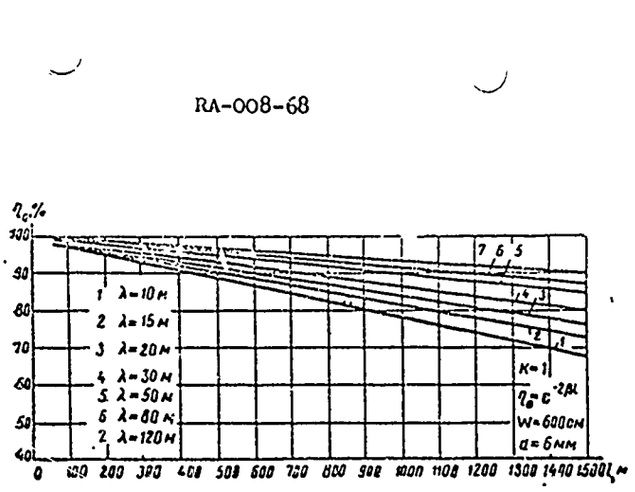

Figure XIX.2.6. Dependence of the efficiency of a two-wire feeder on its length for various wavelengths and a traveling wave ratio, k, equal to unity.

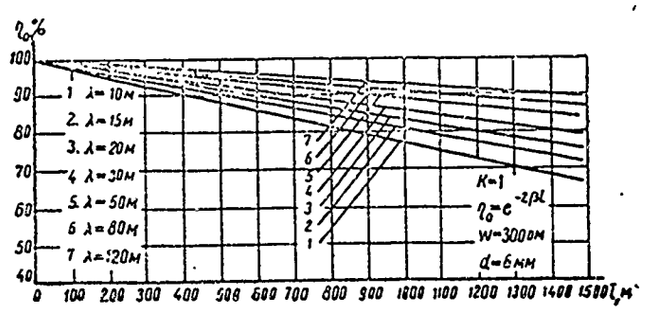

Figure XIX.2.7. Dependence of the efficiency of a four-wire feeder on its length for various wavelengths and a traveling wave ratio, k, equal to unity.

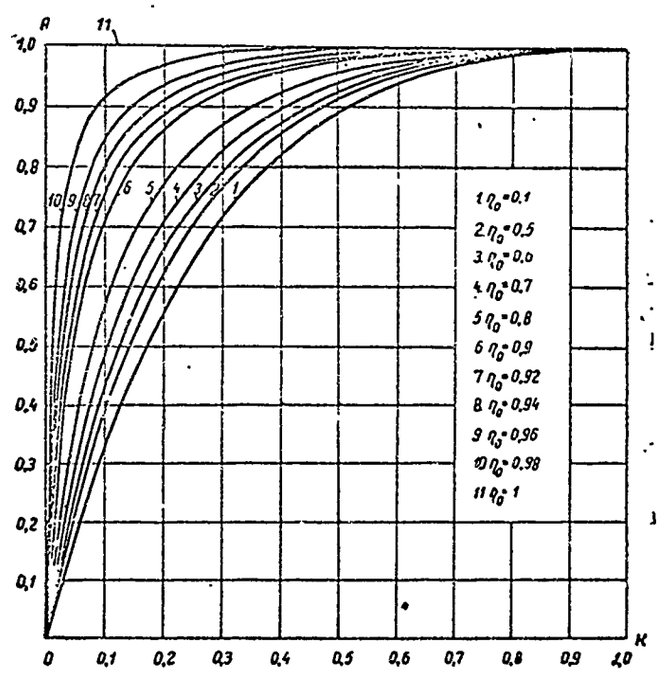

Figure XIX.2.8. Dependence of the factor A on the traveling wave ratio. A is a correction factor for computing the efficiency when k ≠ 1.

Figure XIX.2.8 shows the values for the magnitude of

$$A = \frac{1-|\rho|^2}{1-|\rho|^2 e^{-4\beta l}} \approx \frac{1-|\rho|^2}{1-|\rho|^2 r_0^2}, \qquad \text{(XIX.2.3)}$$

This yields a correction factor for use in computing the efficiency of the feeder when the traveling wave ratio is different from 1.

Formulas I.13.2 and I.13.9 can be used to establish the maximum voltage and the field strength produced by the feeder. Maximum permissible powers are established through formulas VIII.1.1 and VIII.1.2. The dielectric strength of the insulators used with aerial feeders can be established from the data contained in Chapter VIII.

(c) Four-wire aerial feeder

The four-wire aerial feeder can be used to advantage to feed antennas excited by powerful transmitters to reduce the field strength on the conductors. Wire diameters here are the same as those for the two-wire feeder. Distance between wires is on the order of 25 to 40 cm. Suspension height and distance between feeder supports can be selected as in the case of the two-wire feeders.

Block or stick insulators are used to string the feeder. A variant in using stick insulators to secure a feeder to intermediate and end supports is shown in Figure XIX.2.9, as well as in XIX.2.10. The feeder wires are made up to be rectangular in cross section (fig. XIX.2.11). Wires 1 and 4, and wires 2 and 3, are interconnected by jumpers at the beginning and end of the feeder and at each of the intermediate supports. It is also recommended that jumpers be installed between the in-phase power leads every 2 to 3 meters in order to prevent the appearance of asymmetry on the line.

The characteristic impedance of a four-wire feeder is

$$W = 60 \ln\left(\frac{\sqrt{D_1^2 + D_2^2}}{D_2}\,\frac{2D_1}{d}\right). \qquad \text{(XIX.2.3)}$$

In the special case when $D_1 = D_2 = D$

$$W = 60 \ln \frac{2\sqrt{2}D}{d}. \qquad \text{(XIX.2.4)}$$

The dependence of the characteristic impedance of the feeder on the D/d ratio, computed through formula (XIX.2.4), is shown in Figure XIX.2.12. As will be seen, the characteristic impedance of the four-wire feeder is less than that of the two-wire feeder by a factor of 1.6 to 1.8. Correspondingly, the maximum power that can be handled by the four-wire feeder is greater than that handled by a two-wire feeder by a factor of 2.5 to 2.2 (see formula VIII.1.1).

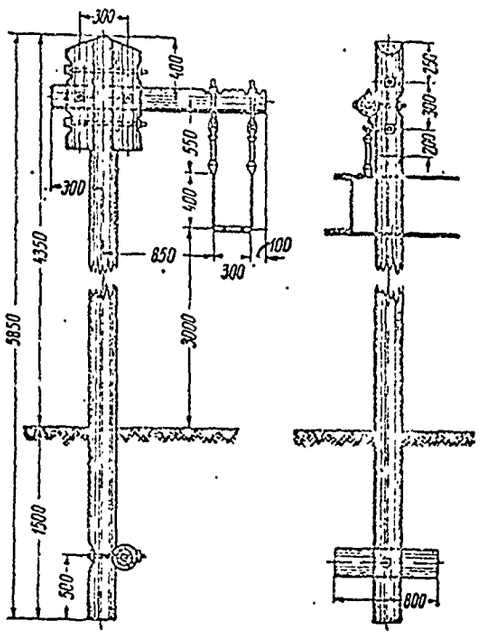

Figure XIX.2.9. Variant in the design for securing a four-wire feeder to an intermediate support.

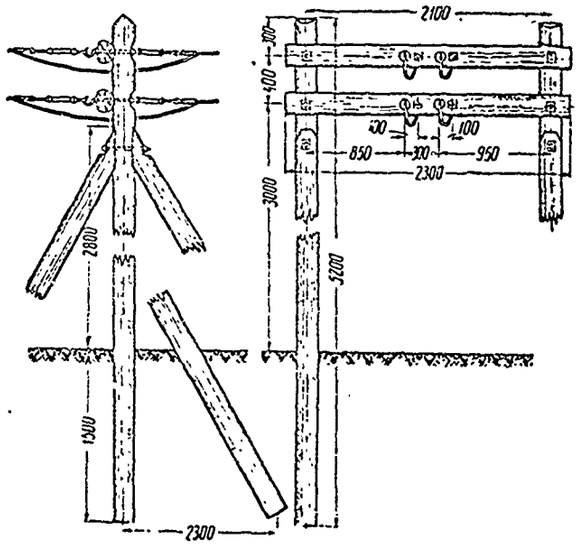

Figure XIX.2.10. Variant in the design for securing a four-wire feeder to an end support.

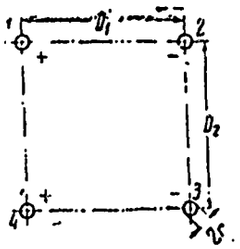

Figure XIX.2.11. Schematic diagram of the cross section of a four-wire feeder.

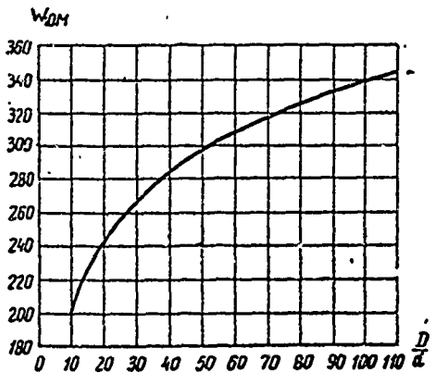

Figure XIX.2.12. Dependence of the characteristic impedance of a four-wire feeder on the D/d ratio. The feeder conductor is located at the apexes of the angles of a square with side D.

The attenuation factor for the four-wire feeder is equal to

$$\beta = R_1/2W,$$

where R_1 is the resistance per one meter of one wire, if losses in the insulators are ignored.

Efficiency is established through formulas (I.14.1) and (I.14.4).

(d) Six-wire aerial feeder

The use of a six-wire feeder (fig. XIX.2.13) to reduce the characteristic impedance can be desirable in certain cases.

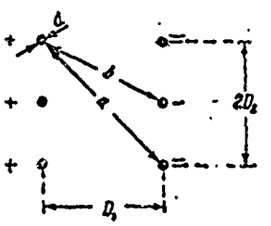

Figure XIX.2.13. Transverse cross section of a six-wire feeder.

The characteristic impedance of this feeder is

$$W = 120 \frac{\ln \frac{D_1 a}{d D_2} + \ln \frac{b}{D_2} \cdot \frac{\ln \frac{D_1 D_2 a}{d b^2}}{\ln \frac{2 D_1 D_2}{d b}}}{2 + \frac{\ln \frac{D_1 D_2 a}{d b^2}}{\ln \frac{2 D_1 D_2 a}{d b}}}. \qquad \text{(XIX.2.5)}$$

If $D_1 = 2D_2 = D$, then

$$W = 120 \frac{\ln \frac{2\sqrt{2}D}{d} + 0{,}81 \frac{\ln \frac{0{,}566D}{d}}{\ln \frac{0{,}894D}{d}}}{2 + \frac{\ln \frac{0{,}566D}{d}}{\ln \frac{0{,}894D}{d}}}. \qquad \text{(XIX.2.6)}$$

The attenuation factor can be established, approximately, through the formula

$$\beta = R_1/3W, \qquad \text{(XIX.2.7)}$$

where R_1 is the resistance per unit length of one wire.

Formulas (XIX.2.5) and (XIX.2.6) do not take nonuniformity in the distribution of current flowing in the wires into consideration.

#XIX.3. Receiving Antenna Feeders. Design Data and Electrical Parameters.

(a) Requirements imposed on receiving antenna feeders

The basic requirement imposed on the receiving feeder is that there be no reception of electromagnetic energy (no antenna effect). Reception of electromagnetic energy by a feeder causes distortion of the antenna receiving pattern and this, in turn, can reduce antenna gain and increase noise reception intensity.

Reduction in the receiving effect can be achieved by the use of symmetrical aerial feeders, or shielded symmetrical and asymmetrical cables.

The highest possible feeder efficiency should also be provided, but in the case of reception feeder efficiency is not as great an influence as it is in the case of transmission.

The same requirements in regard to shunt capacitance of insulators, mechanical strength, convenience in making repairs and replacing damaged sections noted for transmitting feeders apply to those used for reception.

(b) Types of receiving antenna feeders

In the reception field the most widely used feeder is the four-wire crossed aerial feeder, as well as symmetrical and coaxial cables. The symmetrical and coaxial cables practically eliminate antenna effect when the corresponding transition to the antenna is made.

On vital lines equipped with highly directional receiving antennas, such as the 3BS2 for example, it is extremely desirable to use symmetrical and coaxial cables to obtain the best use of their space selectivity.

It should be borne in mind that widely used crossed four-wire aerial feeders have a marked antenna effect because of the penetration of single-cycle waves into the receiver input circuit. These waves will form as a result of the feeder picking up electromagnetic energy, just like the Beveridge antenna, which is made up of several parallel wires. The space waves propagated along the feeder axis induce particularly intensive single-sycle waves.

The use of static shields between the feeder coil and the receiver input circuit will not completely eliminate the peretration of single-cycle waves.

Two-wire aerial feeders can only be used to connect the curtains in multiple antennas and as short jumpers for connecting individual feeders with each other.

(c) Aerial crossed four-wire and multiwire feeders

The four-wire aerial feeder is usually made of bimetallic wires with a diameter d = 1.5 mm, positioned at the corners of a square with side D = 35 mm. The crossed wires are connected together at the source and terminus of the feeder to form a single electrical conductor.

Special porcelain insulators are used to suspend the feeder on wooden, or reinforced concrete supports 2.5 to 4 meters high. The distance between supports is selected on the order of 10 meters. The wires are strung so they slide freely in the insulator, and can be readily removed from it.

The feeder is strung in a straight line, or with smooth bends, made on a large radius. It is desirable to make the angle of the turn taken around any one upright no larger than 18 to 20°.

The end of the feeder is secured to the end supports by blocks and a counterweight so the feeder is held taut. The weight used is on the order of 60 kg.

Several feeders are often strung on the same supports, but when this is done the distance between individual feeders should be at least 0.75 m in order to eliminate the substantial mutual effect close spacing can have.

Figures XIX.3.1 and XIX.3.2 show variants in the manner in which a feeder can be secured on wooden intermediate and end supports.

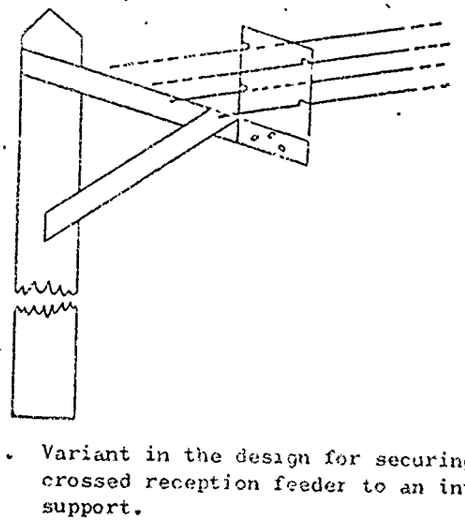

Figure XIX.3.1. Variant in the design for securing a four-wire crossed reception feeder to an intermediate support.

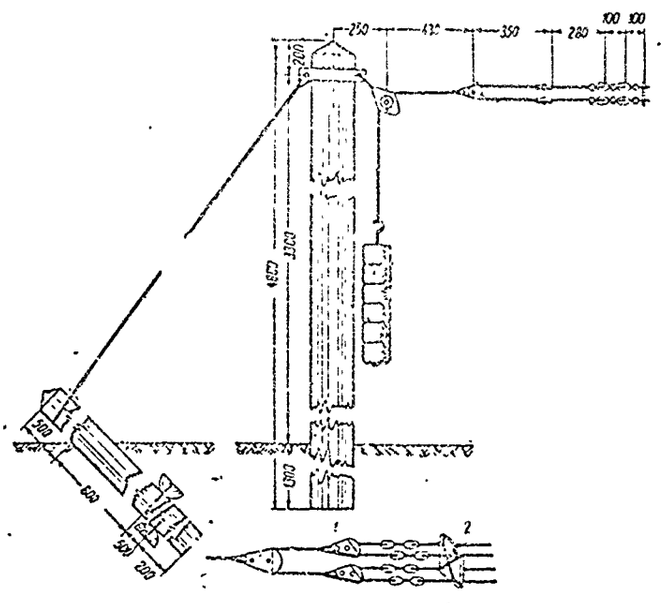

Figure XIX.3.2. Variant in the design for securing a four-wire crossed reception feeder to an end support.

1 - block; 2 - spacer insulator.

The characteristic impedance of a crossed four-wire feeder can be established through the formula

$$W = 60 \ln\left(\frac{2D_1}{d}\frac{D_2}{\sqrt{D_1^2+D_2^2}}\right), \qquad \text{(XIX.3.1)}$$

where

D_1 and D_2 are the sides of a rectangle at the apexes of which the conductors are located;

d is the diameter of the wires used for the feeder.

In the special case of $D_1 = D_2 = D$

$$W = 60 \ln \frac{\sqrt{2}D}{d}. \qquad \text{(XIX.3.2)}$$

The characteristic impedance of a feeder with $D_1 = D_2 = 35$ mm, and d = 1.5 mm, is W = 208 ohms.

The attenuation factor and efficiency of the feeder are established through the same formulas used for the purpose for the four-wire transmitting feeder.

Figure XIX.3.3 shows curves that characterize the efficiency of a four-wire receiving feeder in the traveling wave mode. The correction factor for the case when the traveling wave ratio does not equal 1 can be established by using the curves shown in Figure XIX.2.8.

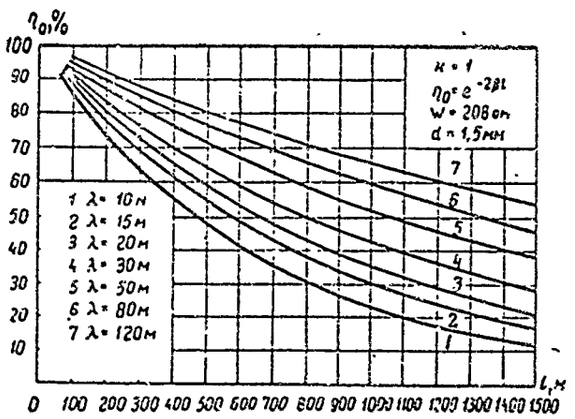

Figure XIX.3.3. Dependence of the efficiency of a crossed four-wire feeder on its length for various wavelengths and a traveling wave ratio, k, equal to unity.

There are individual cases when it can be necessary to use crossed multiwire feeders in order to reduce the characteristic impedance or to reduce antenna effect.

Figure XIX.3.4 shows the positioning of the conductors of a six-wire crossed feeder. Crossed feeders made up of a great many conductors can be formed similarly.

The characteristic impedance of a crossed feeder made up of n conductors, formed into a cylinder, can be established through the formula

$$W = \frac{240}{n} \ln \frac{8R}{nd}, \qquad \text{(XIX.3.3)}$$

where

n is the total number of conductors in both symmetrical halves of the feeder.

The attenuation factor can be established through the formula

$$\beta = 2R_1/nW, \qquad \text{(XIX.3.4)}$$

where

R_1 is the resistance per unit length of one conductor.

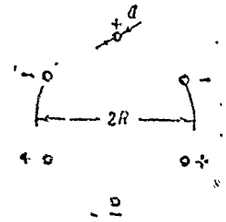

Figure XIX.3.4. Transverse cross section of a crossed six-wire feeder.

(d) Two-wire aerial feeder

As has been indicated above, the two-wire aerial feeder is seldom used as an independent feed system for reception, and then only when the antenna is located near the service building.

The two-wire feeder can be used as a jumper to connect individual sections of four-wire feeders, for the lead-in into receiver rooms, and for distribution feeders for antennas.

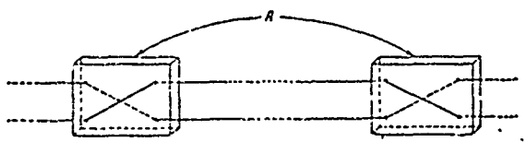

Figure XIX.3.5. Crossed two-wire feeder.
A - insulator.

The characteristic impedance of the two-wire feeder is selected in accordance with the point at which it is connected into the circuit.

The two-wire feeder is crossed at predetermined intervals (fig. XIX.3.5) to reduce the antenna effect. These intervals in distribution feeders are about one meter apart, and in jumpers made of wires located close to each other and suspended without tension, a few tens of centimeters apart.

The insulators used at the points where the feeders are crossed should have as low a shunt capacitance as possible.

#XIX.4. Transmitter Antenna Switching[1]

(a) General considerations

Modern shortwave radio transmitting centers usually have a great many transmitters and, correspondingly, quite a few antennas. It is virtually impossible to connect the antennas to the transmitters because each transmitter operates on different waves and in different directions. Hence the need to switch the transmitters to the different antennas.

It is in the radio centers that the switching must be done to change the direction of maximum radiation from the antennas, and, in particular, to reverse and switch the antennas to change the shape of the radiation pattern.

The general requirements imposed on all types of antenna switching are simplicity of the device used, speed and convenience in switching, minimum energy reflection, and minimum mutual effect between feeders.

The operational nature of the work that goes on in the radio center, the requirement that the number of operators be reduced, and that the transition be made to completely automated equipment without operators, all impose the requirement that devices used for antenna switching be made with remote controls, the while striving to design the simplest of automation arrangements.

It is desirable to have as few switching points as possible between transmitter and antenna to antenna switching will not cause heavy reflections on the line.

It is also necessary that the switching elements be simple in design and that the sections of the line containing the switching elements be as similar as possible to the other sections of the line. It is taken that an antenna switching system ought not reduce the traveling wave ratio by more than 10 to 20%.

Any switching element is part of the line, so switches, like feeder lines, can be symmetrical and asymmetrical. Symmetrical switches are sometimes made up of two asymmetrical switches.

Experience with switching lines carrying industrial, or low frequencies, cannot be borrowed to build circuits for switching transmitting antennas because in high frequency circuits even a small section of an idle line connected into a circuit can cause reflection of a considerable amount of energy. Antenna switching should be planned to there is no possibility of simultaneously connecting more than one antenna to one transmitter, more than one transmitter to one antenna, or a transmitter to another transmitter.

The quality of an antenna switching arrangement is judged by the number of connections to one switching circuit; the more connections, the worse the switching arrangement. The ideal is an arrangement in which the switching circuit has but one connection to each wire in the feeder.

---

1. #XIX.4 was written by M. A. Shkud.

The quality of the switching system can also be judged by the completeness with which all necessary connections are made. The total number of possible connections must be taken to mean the product of number of transmitters by number of antennas. The most complete switching system is one that can switch any antenna to any transmitter. If the switching system is such that only some of these connections can be made, the lower the percentage of total number of connections, the greater the limitation imposed on the system, and the lower its operational capacity.

The number of connections needed will depend on the ratio center's operating schedule. There are many cases when there is no need to complicate the antenna switching system, to plan a great many connections that will see little use. If the operations of a radio center are planned such that one transmitter, or individual groups of transmitters, are connected to a predetermined, limited number of antennas, this will result in correspondingly simplifying the antenna switching. And it is mandatory as well to plan on the possibility of replacing each transmitter by another in case of emergency, or when planned repairs must be made.

Operations in radio communication centers often are such that transmitters are sending in the same directions almost around the clock, and the only time that switching takes place is when waves are shifted. When transmitters are used for short sessions, and consequently are switching in different directions quite often, an antenna switching system with heavy limitations can cause a sharp reduction in the station's operating capacity, and even result in a considerable curtailment in transmitter use. Selection of the number of connections in the antenna switching system has a very material effect indeed on operating conditions. If this selection is to be the proper one note must be made of operation conditions, for only in this way can the required number of switchings per day per transmitter be arrived at.

The following general conclusion can be drawn. If the number of daily connections required for all transmitters is a small percentage of the total number of connections possible, it is desirable to build simple systems for group switching. But if the number of connections per day is 25 to 30% the total number, taking seasonal changes and the nature of the traffic load into consideration, it is rational to use a system that will provide access to the total number of connections possible; that is, a system that will connect any transmitter to any antenna.

(b) Antenna switching arrangements

Antenna switching systems can be made using small capacity, conventional switches, or special antenna switches of different capacities. Antenna switching systems containing simple switches with capacities of 1x2, 1x3, 1x4, and 1x5 are widely used. These switches are remotely controlled,

so the switching system is quite convenient in operation. Simple switches are usually installed outside the building, in the feeder approach. Installation of a system such as this is extremely simple. Switches for installation inside the building are also available. In this latter case energy propagation must take place over shielded feeders.

A variant of the 1x3 switch for an outside installation is shown in Figure XIX.4.1. A variant of the 1x4 capacity switch for an inside installation is shown in Figure XIX.4.2.

Figure XIX.4.3 is a schematic diagram of antenna switching for a large radio center with 16 transmitters and 34 antennas. The number of connections possible in this radio center is 544. The switching is based on the use of simple transfer switches and is built in four groups of four transmitters. The connections in each group are made by 1x2, 1x3, and 1x4 transfer switches. In addition to the switching provided for connecting the transmitter to the antenna it will use, the circuitry is such that the transmitters can be switched to dummy antennas for tuning and for substituting transmitters in adjacent groups.

As will be seen from the diagram, group switching by low capacity transfer switches makes it possible to build a system with adequately high capacity. But systems such as these cannot provide the high degree of operational capacity it is possible to obtain using special antenna switches.

There are various principles on which the construction of special antenna changeover switches can be based, and the main ones will be reviewed.

There are several types of antenna changeover switches functioning on the principle of a crossbar connection. In these switches the transmitter bus bars are on one shaft, and the antenna bus bars are on a perpendicular shaft, but in another plane. The positions at which the bus bars intersect have switching elements installed for the purpose of connecting antenna and transmitter at such positions, and to disconnect the bus bars so that the idle end on the other side of the connected position is open. These switches resemble the plate-type (Swiss) switch used in telephone-telegraph engineering, but they differ from them in that they have no idle ends. The different switches of this type in use differ in the operating principles designed into the switching element. Some are quite complicated because one operation must change the four circuits connected to them.

Figure XIX.4.4 shows the schematic diagram of a crossbar antenna transfer switch for connecting three transmitters to 13 antennas. The connecting feeders are shown as single wires in order to simplify the diagram.

As will be seen from this schematic, switches of this type can, in principle, have any capacity. A substantial shortcoming in these switches is the great number of switching elements cut into the switching circuit, equal at a maximum to n + m - 1 (n is the number of transmitters, m is the number of antennas).

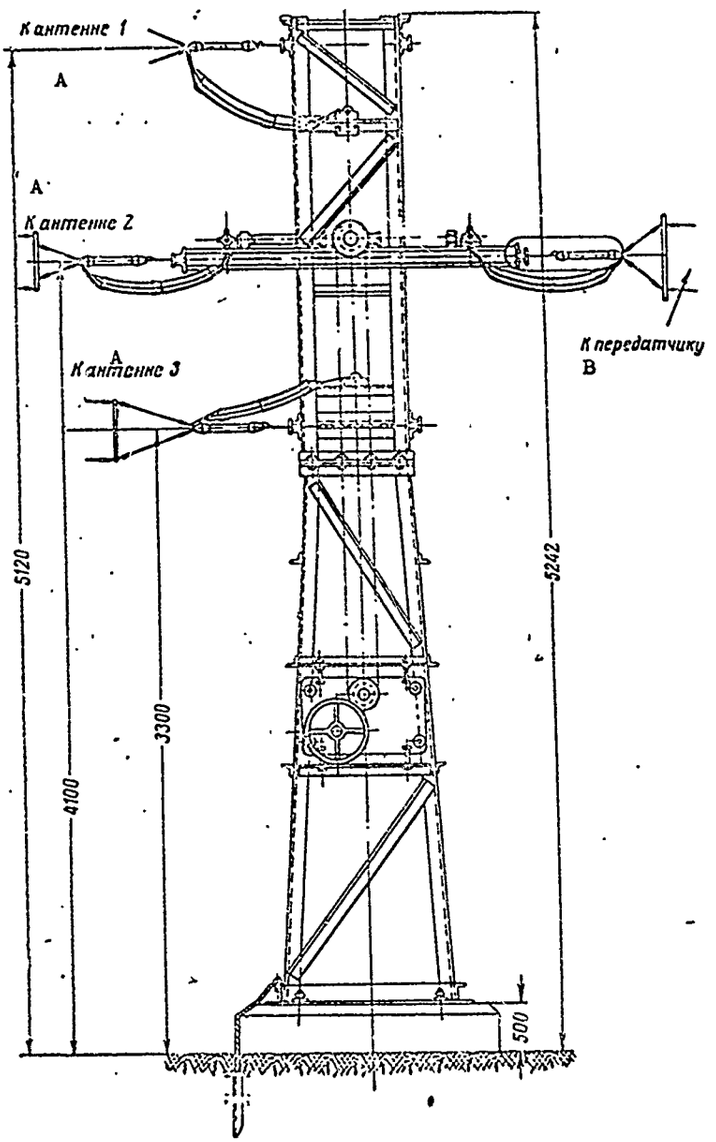

Figure XIX.4.1. Switch for a 1x3 outside installation with remote control.

A - to antenna; B - to transmitter.

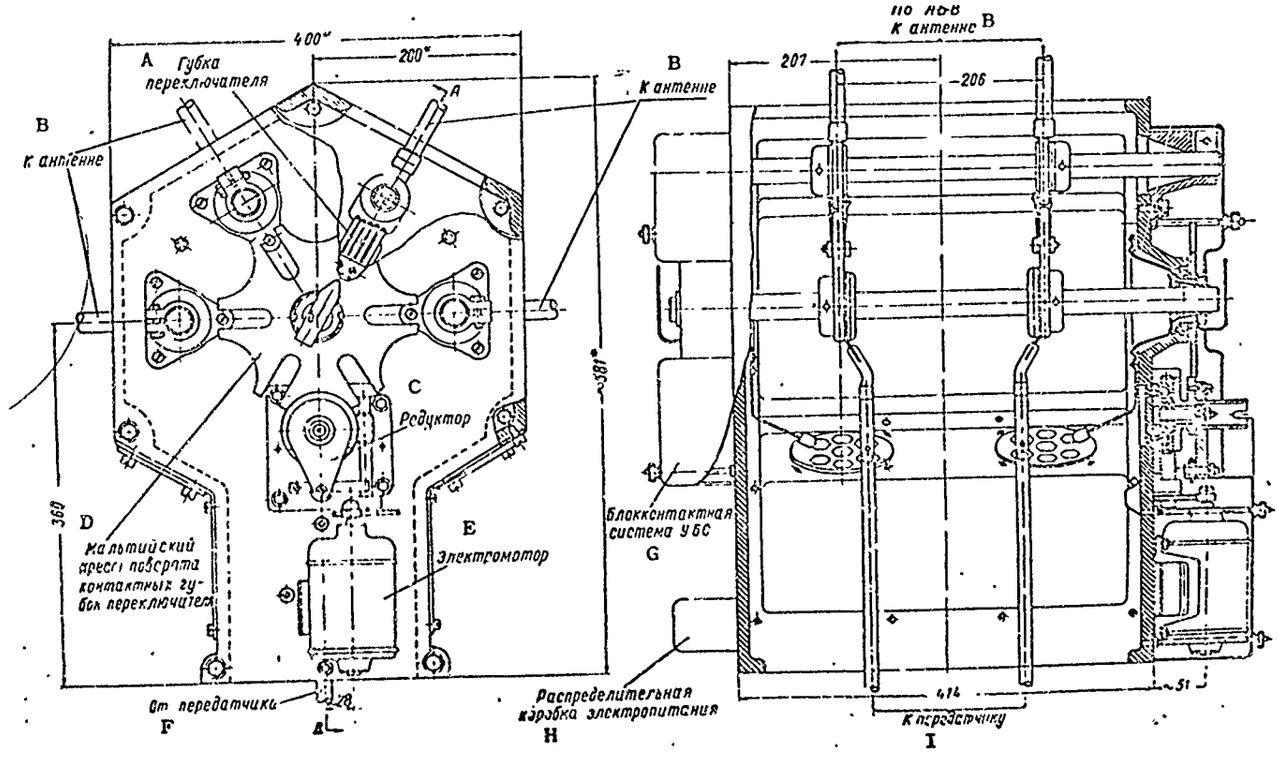

Figure XIX.4.2. Switch with a 1x4 capacity for an inside installation.

A - switch blade; B - to antenna; C - reduction; D - star wheel for turning the switch contact blades; E - electric motor; F - from transmitter; G - UBS interlock contact system; H - electrical supply distribution box; I - to transmitter.

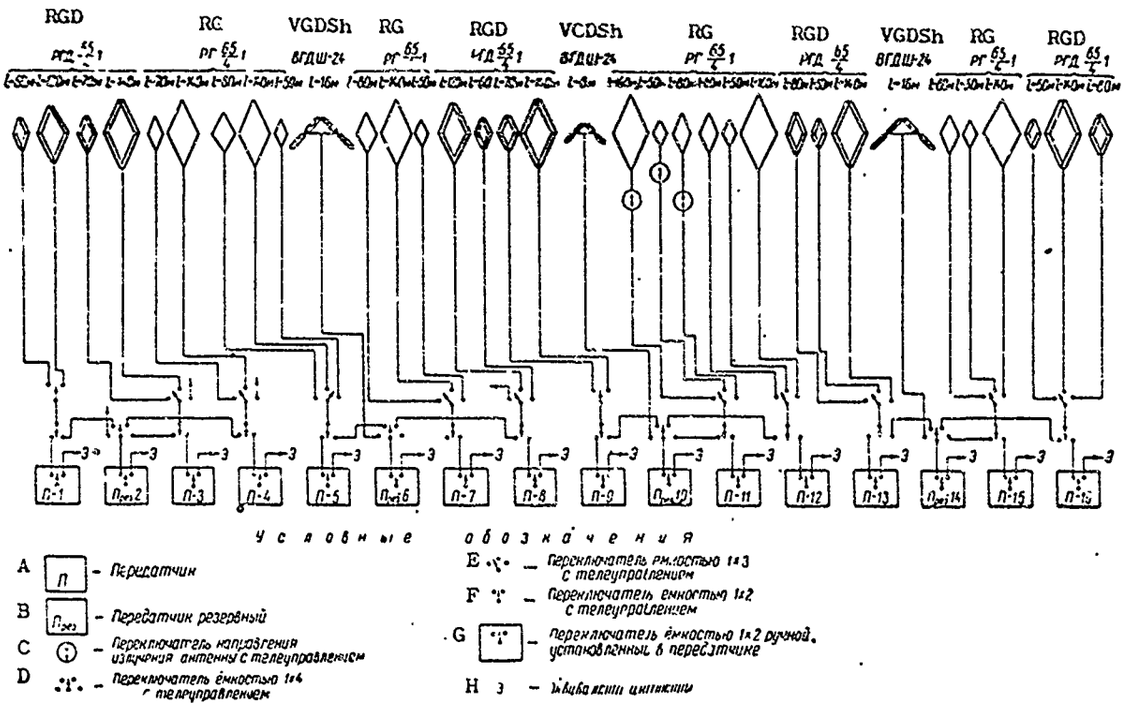

Figure XIX.4.3. Schematic diagram of antenna switching in a large radio center.

Conventional symbols: A - transmitter; B - standby transmitter; C - switch for controlling antenna radiation by remote control; D - switch, 1x4 capacity with remote control; E - switch, 1x3 capacity with remote control; F - switch, 1x2 capacity with remote control; G - switch, manual, 1x2 capacity, installed at transmitter; H - dummy antennas.

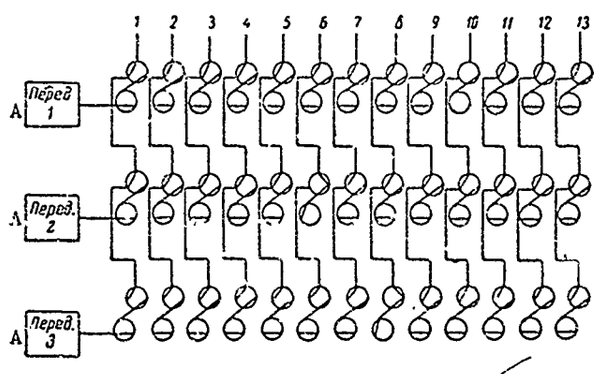

Figure XIX.4.4. Schematic diagram of a crossbar antenna changeover switch for operating three transmitters on 13 antennas.

A - transmitter.

In the case of the high capacity antenna changeover switch, it is necessary to introduce a second stage of switching and set the switches up in groups in order to reduce the number of switches cut into the switching circuit. For example, if the requirement is to switch six transmitters to 30 antennas, the maximum number of switches in the switching circuit is 35. But if the first stage has each transmitter serviced by a 1x3 capacity switch, and if the circuitry is made up into three groups of 6x10 capacity switches, there will be no more than 16 connections in the circuit. This breakdown into groups is sometimes necessary for convenience in laying out the antenna feeders, which are usually run to the building from different sides.

The schematic diagram of a switching element for a crossbar switch is shown in Figure XIX.4.5. In this diagram the solid line indicates the position of the switch when the transmitter is connected to the antenna, and the dotted line the position when the transmitter and antenna bus bars are directly connected. As will be seen from the diagram, this switching can be done by using a switching element made up of two 1x2 switches, one connected to the transmitter bus bar, the other to the antenna bus bar, and jumpered (5) together. It is desirable to locate the 1x2 switches as close to each other as possible, so a simple connection can be made to one common drive, and in order to keep the jumper (5) short and without complicated bends.

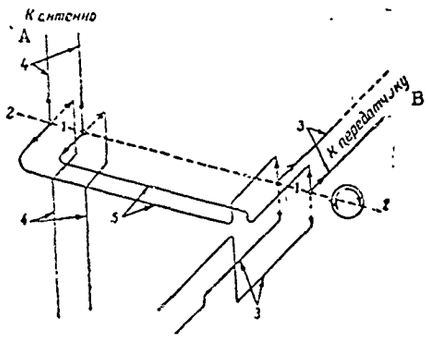

Figure XIX.4.5. Schematic diagram of a switch for an antenna changeover switch made in accordance with the diagram in Figure XIX.4.4.

1 - two-pole knife switch; 2 - switch shaft; 3 - transmitter bus bar; 4 - antenna bus bar; 5 - jumper; A - to antenna; B - to transmitter.

The crossbar switch manufactured by "Tesla," the Czechoslovakian firm, has a capacity of six transmitters on 30 antennas (6x30), and is made up of two 6x15 switches. Each transmitter is connected to these switches by a 1x2 switch.

The 6x15 switches are assembled from 1x2 switches, the diagram as shown in Figure XIX.4.4. Design-wise, this switch is made so the switches are sections of bus bar from one switching point to the other. The transmitter bus bars are located on the peripheries of a cylindrical surface, one above the other. The antenna bus bars are located on uprights on a coaxial cylindrical surface somewhat larger in diameter. The motor-drive simultaneously switches the antenna switch and the transmitter switch. The changeover switch is located in a round building, the diameter of which is in excess of . meters.

This changeover switch has n(m+1), that is, 186 switches. Maximum connection is made through 21 switches and 42 knife contacts. The changeover switch is made of open feeders and this can result in marked coupling originating between feeders. Half of the switch must be completely cut out in order to make repairs to any element.

The switching element in the Shandorin changeover switch differs in that it has two separate elements, one making the connection to the bus bars "directly" (when no connection is required), the other connecting the transmitter to antenna when this is necessary (figs. XIX.4.6 and XIX.4.7).

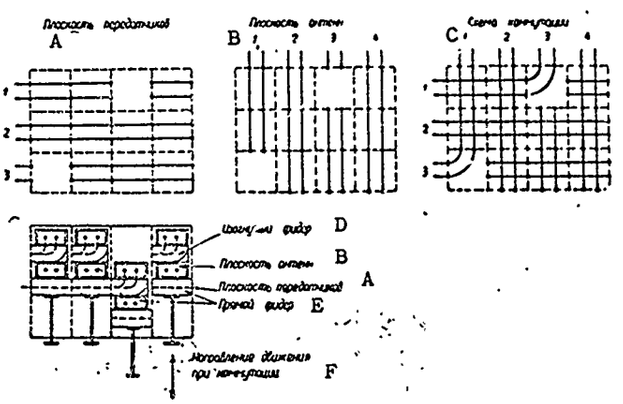

Figure XIX.4.6. Schematic diagram of the Shandorin changeover switch.

A - plane of transmitters; B - plane of antennas; C - switching schematic; D - bent feeder; E - direct feeder; F - direction of movement during switching.

Elements are shifted during switching by moving them forward. As will be seen from Figure XIX.4.6, the element "directly" connected has two straight sections of the feeder that move like knife blades into fixed contacts, forming continuous bus bars for antennas and transmitters. The element for making the transmitter-antenna connection is a bent section of feeder that connects the antenna bus and the transmitter bus. This element is behind the

antenna bus bars when in the cut-out position, and when cut in can be advanced and assumes a position in the plane of the bus bars of antennas and transmitters. At the same time, the element making the direct connection between bus bars moves and assumes a position in front of the transmitter bus bars. A changeover switch of this design provides good decoupling of circuits. Lines can be made uniform. The number of contacts is double that found in the circuit using 1x2 switches.

The crossbar changeover switch can be manufactured with telescoping bus bars. The bus bars are not cut, however, but extend into the connection, where the contact is made with knife-like, or other, devices on the ends of the bus bars. This switch will have one or two contacts for each conductor, and this is one great advantage of the switch. However, automation is difficult.

This type of switch is desirable when power is low, when overall size can be kept small, so the bus bars only have to move short distances.

From the foregoing, it will be seen that crossbar type antenna changeover switches have a great many switch points, and hence a very complex automation and signal system. There are a great many contact points in the line. Also extremely difficult is how to resolve questions concerned with servicing and safety in these switches.

Rotating switches provide the least number of contacts in a connection circuit for a minimum number of switching elements in antenna changeover switches.

The changeover switches can have quite high capacities, so can be made in several stages, using low capacity switches, or can be made with very few stages using high capacity switches.

In the first case each transmitter, and each antenna, can be cut in through that number of stages providing that number of directions at the output of the last stage, a multiple field, in other words, equal to the product of the number of transmitters by the number of antennas (n x m). Any transmitter can be connected to any antenna.

For example, if 4 transmitters must be switched to 16 antennas, the first stage of 1x4 switches can be cut in on each transmitter, after which a second stage, also made up of 1x4 switches can now be inserted in each of the 16 directions obtained, so a multiple field of transmitters in 64 directions is the result. It is enough to cut in one stage of 1x4 siwtches on each antenna and obtain a multiple field, also made up of 64 directions, from 16 antennas. Both multiple fields are interconnected by jumpers so each transmitter can be switched to any of the 16 antennas.

When it is necessary to switch 8 transmitters to 16 antennas, one 1x2 stage on the antenna side is sufficient, and there will be 128 directions in each multiple field.

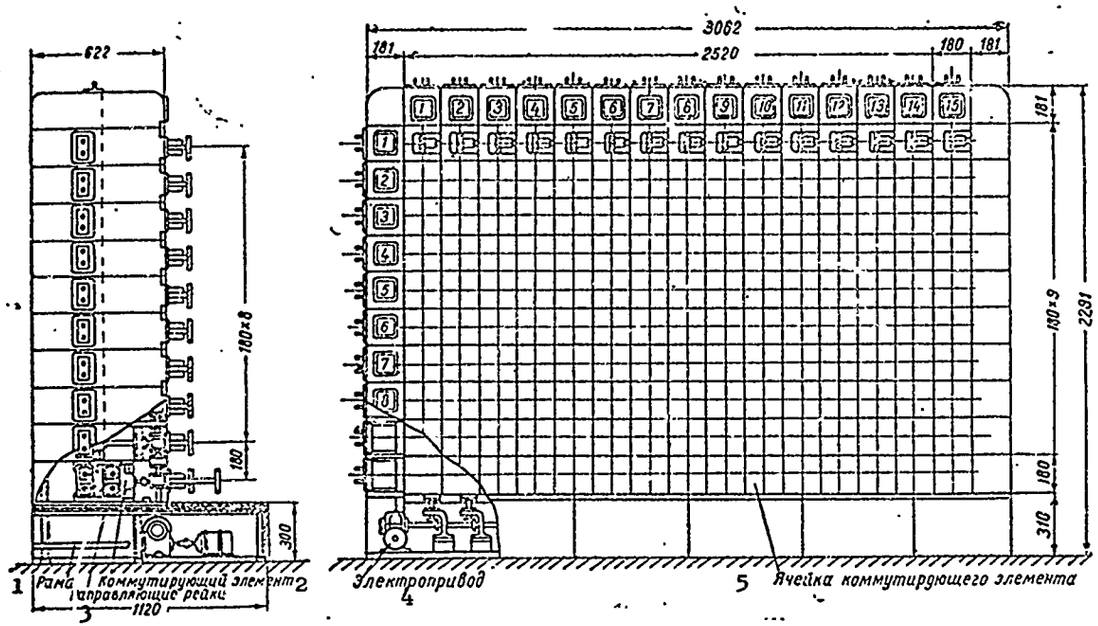

Figure XIX.4.7. General view of the Shandorin crossbar changeover switch.

1 - frame; 2 - switching element; 3 - guide racks; 4 - electric drive; 5 - switching element cell.

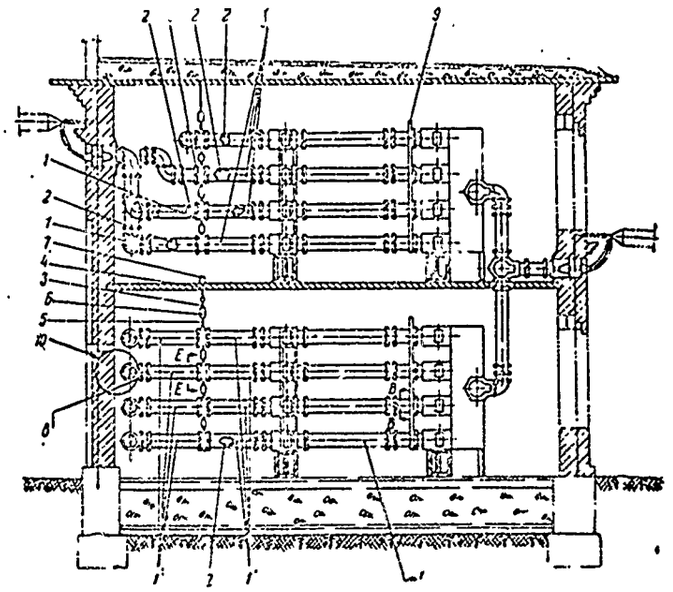

Figure XIX.4.8a. Cut of the Yakovlev changeover switch.

1 - two-wire feeder to screen; 2 - feeder; 3-7 - fastener parts; 8 - flange; 9 - fastener; 10 - feeder in section.

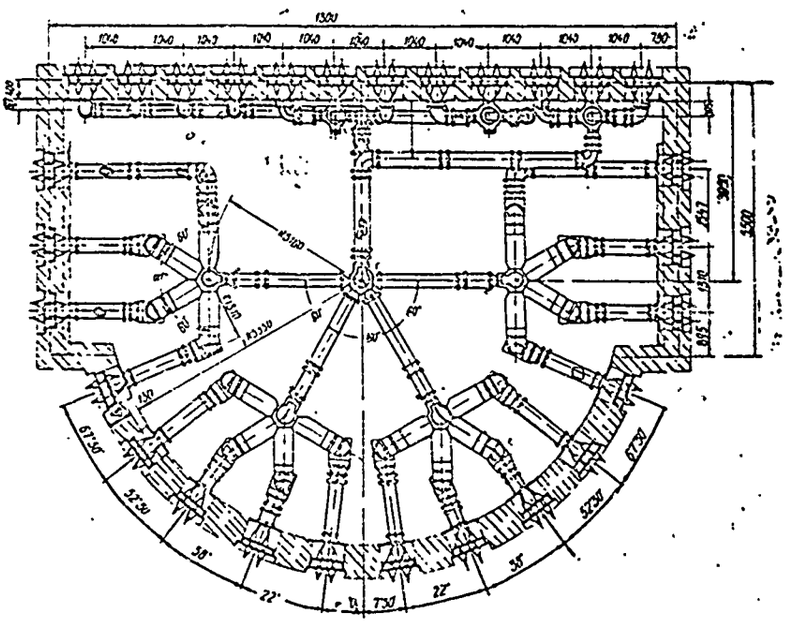

Figure XIX.4.8b. Plan view of the Yakovlev changeover switch.

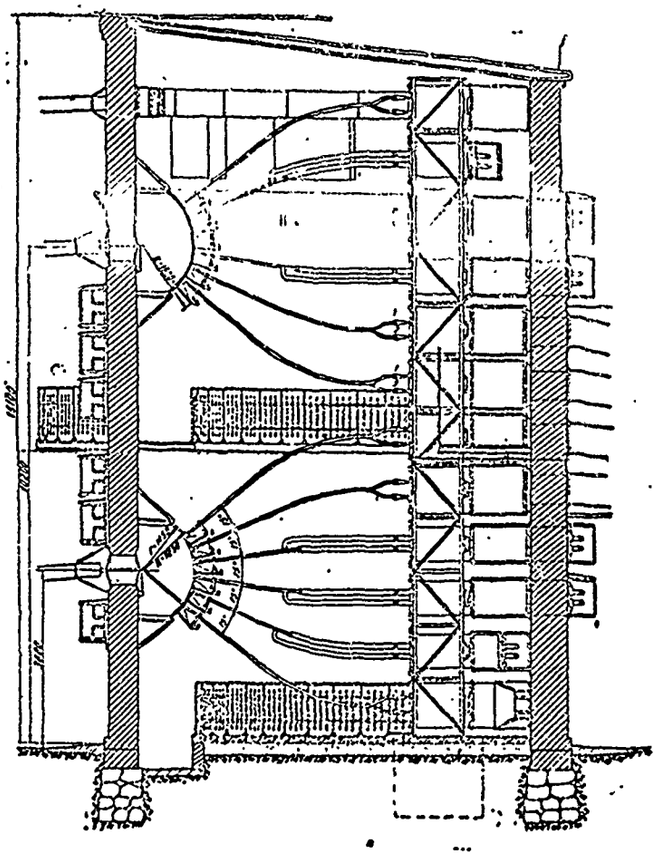

Figure XIX.4.9a. Cut of the Shkud changeover switch.

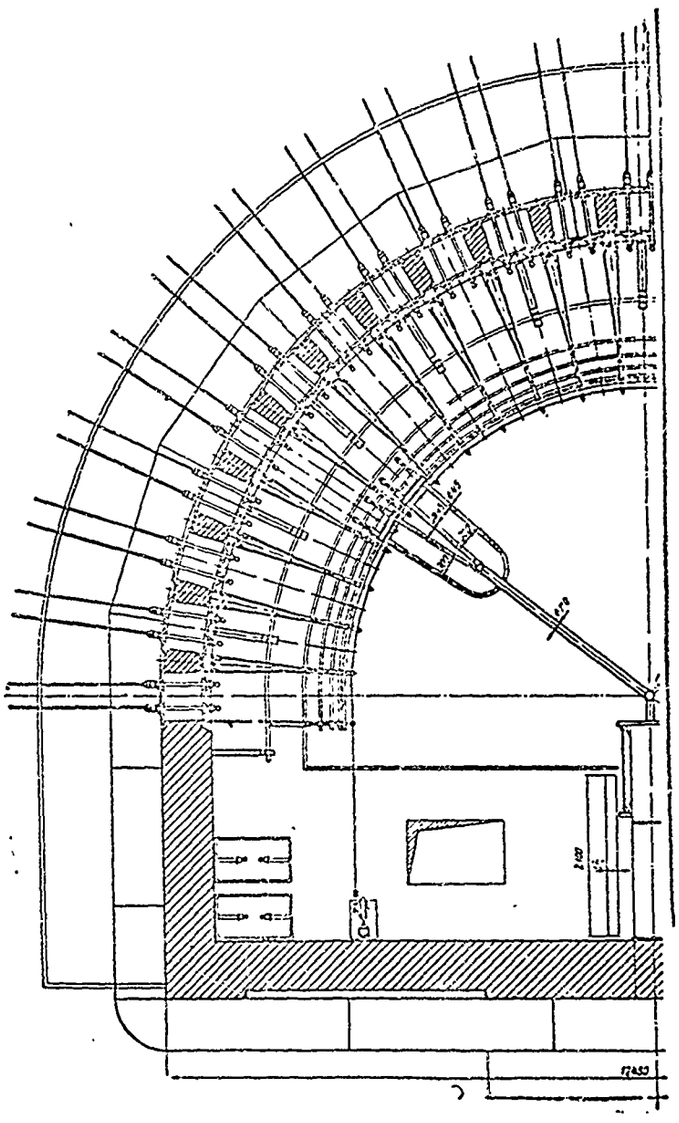

Figure XIX.4.9b. Plan view of the Shkud changeover switch.

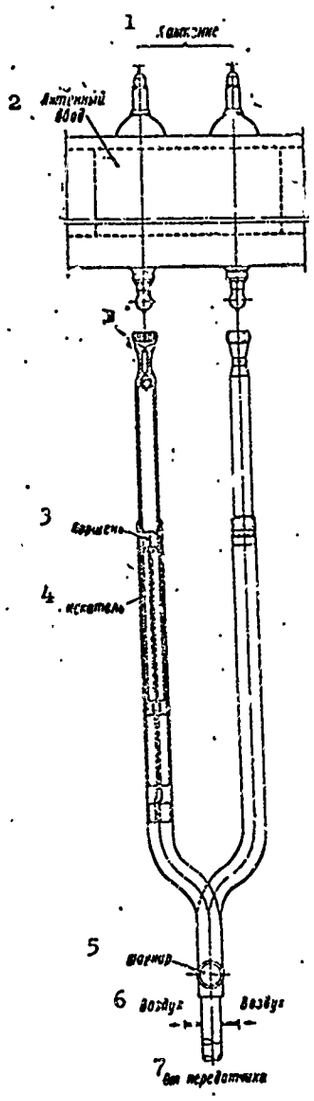

Figure XIX.4.10. Finder switch.

1 - to antenna; 2 - antenna input; 3 - piston; 4 - finder; 5 - hinge; 6 - air; 7 - from transmitter.

If it is necessary to switch 10 transmitters to 40-antennas, we can do so by inserting in the transmitter side two 1x4 and 1x10 or 1x5 and 1x8 stages, or three 1x2, 1x4, and 1x5 stages, and two 1x2 and 1x5 stages on the antenna side.

In these circuits the number of contacts in any connection equals the number of stages, and will not be in excess of 5 or 6, even at high capacities, and the number of controlled switches equals an + bm (a is the number of stages in the field of transmitters; b is the number of stages in the field of antennas). Thus, in a 10 x 40 switch the number of switches equals 100 in the case of four stages, and 110 in the case of five stages. A crossbar changeover switch would require 400 switches to arrive at this same capacity.

As will be seen from the description given, the basic number of switches equates to a multiple field of antennas, so it is rational to have few stages in this field. For example, if two 1x4 and 1x10 stages are built into the field of transmitters, and one 1x10 stage is built into the antenna field, each connection will have three contacts and 60 switches will be required.

Design-wise, it is desirable to put these changeover switches together from switches that can be assembled in one unit. Figure XIX.4.8 shows an 8x16 capacity changeover switch assembled from 1x4 and 1x2 switches. The switch was suggested by Yakovlev and is now produced by industry. The switches used in this changeover switch are two-wire, completely shielded, and of a design such that the elements can be fastened to each other, thus making it possible to readily assemble changeover switches of necessary capacity.

A changeover switch based on rotating switching elements is quite compact when made up of xoaxial elements and coaxial cables are used as feeders to the switch. Ryabov and Pakhomov have suggested a 6x12 capacity switch such as this.

Figures XIX.4.9a and XIX.4.9b show the design, consisting of two 6x25 capacity changeover switches proposed by Shkud, for use with aerial feeders with a characteristic impedance of 300 ohms, and for power ratings up to 150 kw. The antenna lead-ins are on a semicircle with a radius of about 5 m. Fixed contacts, which make the connections, are affixed to the lead-in insulators. Finder switches (fig. XIX.4.10) for transmitters are stacked, three above, and three below the line of antennas (see fig. XIX.4.9a). The axes of rotation of the finders are in the center of a circle of antenna lead-ins. Each finder has two tubes, their axes of rotation in the center of the changeover switch, positioned one above the other. At some distance from the axis of rotation, the tubes turn and align themselves horizontally into a linear section that makes contact at the antenna lead-ins.

So no one finder will interfere with the other finders, and so it will be able to turn freely, the linear section can be telescoped to shorten it as the finder moves from antenna to antenna. An outstanding reature of the Shkud changeover switch is that there is only one contact in the connection circuit. The finder is rotated by a motor drive, and telescoping is by pneumatic drives that are the tubes themselves. The outer tube is the drive cylinder, the inner the piston, which has soft packing for this purpose.

The changeover switches reviewed do not exhaust all the available types of such switches, but do give an idea of the principles involved in building antenna switching.

As we indicated above, there are, in the antenna switching system used in radio centers, in addition to switching transmitters to different antennas, arrangements for reversing antennas, and arrangements for turning and changing antenna patterns.

Antenna reversal is usually done by chaing the point at which the transmitter is cut in, by chainging the load resistance, or the transmitter and the tuning stub. Used for the purpose are external switches with four pairs of fixed contacts, positioned at the corners of two squares, and two pairs of blades which, when rotated, can be positioned at two opposite sides of a square (see fig. XIX.7.7). This switch has two positions; one position connects one pair of sides, the second position the other pair of sides. A similar type of switch is often used for the mutual replacement of transmitters. Two transmitters are cut into their own switching circuitry through the switch, and if one of them breaks down the other transmitter can be used to operate with any of the antenna groups.

The phasing of half the antennas must be changed in order to rotate the radiation patterns of broadside antennas. This is often done by using a 1x3 capacity antenna switch.

When the switch i in its center position both halves of the antenna are fed in phase, but if the switch is set to either of its extreme positions one of the halves of the antenna is cut in directly, while the other half is cut in through a stub, shifting the phase, the magnitude of the shift being selected in accordance with the length of stub selected.

(c) Feeder lead-ins

Feeders for transmitting antennas are dead-ended at the ends of the feeder supports at the service building. The feeders are usually lead from the supports to special brackets installed in the building wall. Jumpers are used to connect the feeders to the lead-ins.

Feeders are sometimes lead into the building through the upper half of a window in the transmitter room. Window glass, with holes drilled in it, and through which brass rods which connect the outside section of the feeder

with the inside section (fig. XIX.4.11) are inserted, is the insulator in this case. Characteristic impedance of the feeder must remain unchanged, whatever the lead-in used.

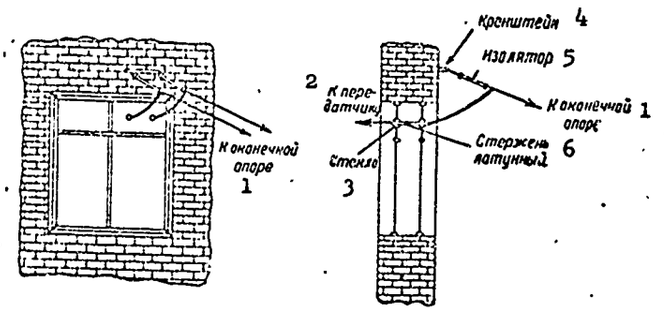

Figure XIX.4.11. Two-wire feeder lead-in through building window.

1 - to end support; 2 - to transmitter; 3 - glass; 4 - bracket; 5 - insulator; 6 - brass rod.

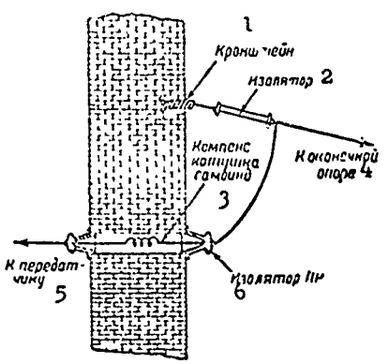

Figure XIX.4.12. Feeder lead-in through building wall.

1 - bracket; 2 - insulator; 3 - self-induction compensating coil; 4 - to end support; 5 - to transmitter; 6 - PR insulator.

Feeder lead-ins can also be brought in through the wall, in which case there are special openings and porcelain insulators, type PR (fig. XIX.4.12), on either side of the wall. Lead-in runs laid on a wall should be in metal tubing to avoid substantial losses. Lead-ins of this type insert a great deal of additional capacitance in the feeder, causing a substantial reflection of energy. An induction coil is inserted in the lead-in wire to compensate for this additional capacitance. The coil is chosen with about 4 to 5 microhenries of inductance, and should be selected more precisely on the spot. The correctness with which the coils for the lead-ins are selected can be

monitored by measuring the traveling wave ratio on the section of feeder between the transmitter and the lead-in, and comparing it with the traveling wave ratio on the external section of the feeder.

Lead-ins are often made of coaxial, or of two-wire shielded cables, in addition to the aerial feeder lead-ins.

#XIX.5. Lead-ins and Switching for Feeders for Receiving Antennas

Aerial feeders, and shielded cables, can be used for lead-ins, for the runs inside the station, and for switching in receiving radio centers. Shielded cables have been used advantageously for lead-ins in recent years.

The aerial feeder lead-in usually passes through the upper window pane, and the glass has through-bolts inserted in it for the purpose. Small segments of a two-wire crossed feeder are used to connect the four-wire feeder to the bolts. Bolt diameters and the distance between the bolts must be selected such that the characteristic impedance of the line segment formed by the bolts equals the characteristic impedance of the four-wire feeder. The characteristic impedance of the two-wire segment of the feeder must also be made equal to the characteristic impedance of the four-wire feeder, insofar as possible.

Figure XIX.5.1 shows a variant in fastening a four-wire feeder directly to the wall of the service building. In many cases the four-wire feeder terminates at the last upright installed close to the window. This, however, makes the building facade more massive and lengthens the two-wire insert. The latter is undesirable because it makes it difficult to make a two-wire line with a characteristic impedance equal to the characteristic impedance of the four-wire feeder. The section of line connecting the feeder to the lead-in too is sometimes made four-wire.

Lightning arrestors are installed on the service building at the feeder lead-in site. One side of the arrestor is connected to each of the through-bolts, the other to the grounding bus (fig. XIX.5.2). The feeders are run from the through-bolts to the antenna changeover switch.

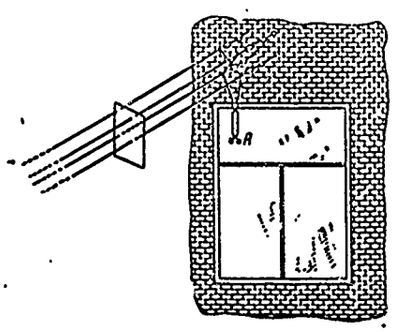

Figure XIX.5.1. Variant for securing a four-wire receiver feeder to a building wall.

A - through-bolts.

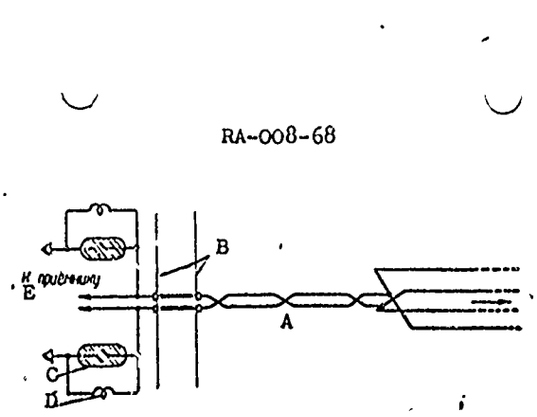

Figure XIX.5.2. Schematic diagram of the lead-in and lightning protection for a receiving antenna.

A - feeder to antenna; B - window glass; C - discharger; D - choke; E - to receiver.

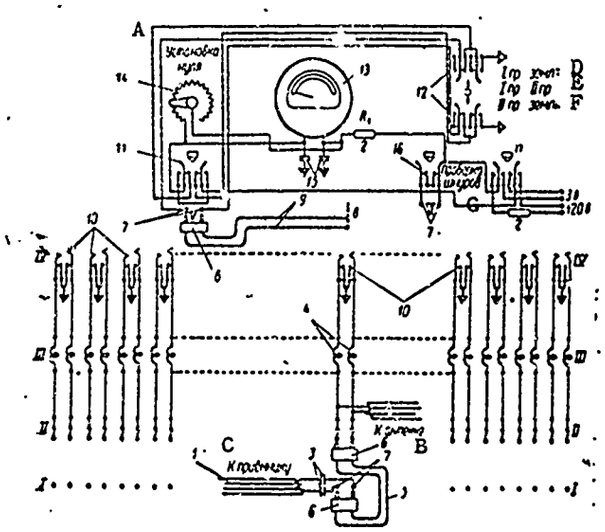

Figure XIX.5.3. Variant schematic diagram of air feeder changeover switch.

1 - four-wide feeder; 2 - resistor; 3 - constant capacitance condenser C ≈ 2000 cm; 4 - HF choke; 5 - two-wire cord; 6 - wall plug with spring prongs; 7 - telephone jacks; 8 - two-wire telephone plug; 9 - cord, two-wire, telephone; 10 - telephone plug jack, two-wire; 11 - pushbutton, six-spring, with index; 12 - key, three-way, 12-spring; 13 - galvanometer, double scale; 14 - galvanometer potentiometer; 15 - constant capacitance C ≈ 10,000 cm; 16 - pushbutton, four-spring. A - zero set; B - to antenna; C - to receiver; D - I conductor-ground; E - I conductor-II conductor; F - II conductor-ground; G - check of cords.

Figure XIX.5.3 shows a variant in the schematic arrangement of the switch for aerial feeders with auxiliary devices for measuring terminating resistances and insulation. The feeders from the receivers are led to a system of telephone jacks, I-I, and the feeders from the antenna lead-ins are led to a system of telephone jacks, II-II.

System II-II has three pairs of jacks for each antenna, the purpose of which is to make it possible to connect two, or three, receivers to one antenna.

Switching is done by two-wire cords terminating in two-pronged plugs.

The characteristic impedance of the cords is selected close to that of the four-wire feeder. A pair of HF chokes, 4, are connected to the jack for each antenna. The other ends of the chokes are wired to the telephone jack system, IV-IV. When the jack is not in use the other ends of the chokes are grounded and serve to leak static charges that build up on the antenna to ground. In order to avoid a substantial reaction of the chokes, 4, on the feeder, their impedance must be considerably greater than the characteristic impedance of the feeder. #XIX.8. contains data on these chokes.

Any antenna can be connected through telephone jacks, IV-IV, by cord 9 to the ohmmeter installed on the changeover switch. When plug 8 is inserted in any of the jacks in IV, the chokes connected to the jack are disconnected from ground. The chokes now decouple the HF channel from the ohmmeter circuit.

The ohmmeter consists of a galvanometer, 13, multiplier R_1, and batteries. The current in the ohmmeter circuit flows through a six-spring pushbutton, 11, and a three-way, 12-spring key, 12. The position of right pushbutton 11 and key 12 shown in Figure XIX.5.3 is that when galvanometer 13 is operating in the circuit for measuring small resistances (ohmmeter circuit).

A high-voltage battery, cut in by pressing the right pushbutton, 11, is used to measure the insulation. Key 12 is set in the center position shown in Figure XIX.5.3 to measure leakage between conductors.

To measure leakage of conductors to ground, key 12 is set as shown in Figure XIX.5.3; I conductor-ground, or II conductor-ground. Each of these positions corresponds to a measurement of leakage to ground from one of the antenna conductors. Shunt resistance 14 is used to zero the galvanometer. To set zero the internal circuit of the galvanometer is shorted by pressing left pushbutton 11.

Four-spring pushbutton 16 is used to check the changeover switch cords. One end of the cord is inserted in jack V of the ohmmeter circuit, the other end in jack VI.

When pushbutton 16 is pressed the conductors at the other end of the cord are opened and the insulation between the conductors is checked by the ohmmeter. When pushbutton 16 is released the conductors at the end of the cord are shorted and the ohmmeter now checks for continuity, or poor contacts in the cord.

Intra-station four-wire feeders running from the changeover switch to the antenna lead ins, or to the receiver, are usually made of 0.5 mm diameter wire. Correspondingly, the distance between wires is reduced to

1.2 cm. Reducing the distance between wires of four-wire feeders makes it possible to bring the feeders within a few centimeters of each other without danger of marked mutual effect between them.

Aerial lead-ins and intra-station switching are inconvenient because they encumber and spoil the overall appearance of the equipment room. Moreover, the two-wire cords used to switch antennas in the case of open, intra-station runs, upset somewhat the match between feeders and receivers.

So, in recent years, the intra-station switching and lead-ins are made with two-conductor double-ended cables, or HF coaxial cable.

In the latter case a special transformer is required to make the transition from the double-ended four-conductor feeder to the single-ended coaxial cable. The transformer must provide for transition to the coaxial cable without upsetting the balance of the four-conductor feeder, as well as provide a good match of characteristic impedance of the four-conductor feeder with the characteristic impedance of the coaxial cable converted through the transformer. And, at the same time, symmetry and the match of the characteristic impedances, must be ensured over the entire operating band.

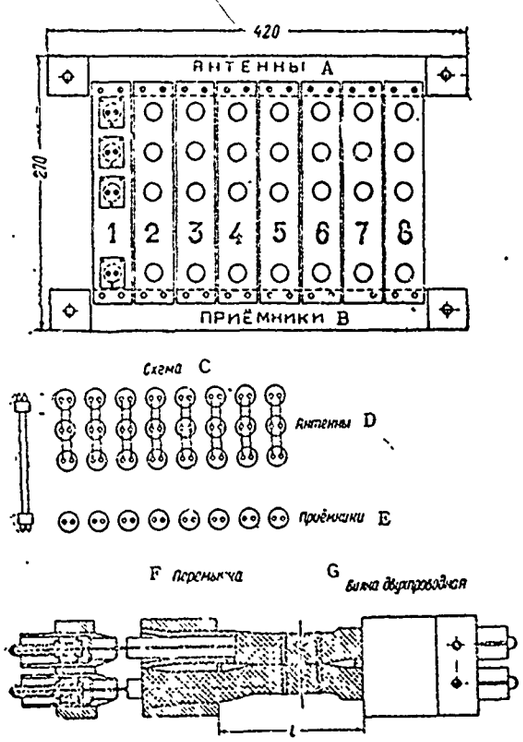

Figure XIX.5.4. Low capacity antenna changeover switch made of double-ended shielded lines.

A - antennas; B - receivers; C - schematic diagram; D - antennas; E - receivers; F - jumper; G - two-wire plug.

When a coaxial cable is used the switching is done by either flexible coaxial shielded sections of cable, or by a stacked changeover switch arrangement. The latter has preferential distribution. Figure XIX.5.4 shows the external view and the schematic of a low-capacity antenna changeover switch of double-ended shielded lines.

Devices providing protection against lightning are installed in the circuit of an aerial four-conductor feeder. There is no way to install clils to leak off static charges.

#XIX.6. Transformer for the Transition from a Four-Wire Feeder to a Coaxial Cable

(a) Transformer schematic

Described here is the transformer developed by V. D. Kuznetsov, and analyzed by V. D. Kuznetsov and L. S. Tartakovskiy. The schematic of the transformer is shown in Figure XIX.6.1.

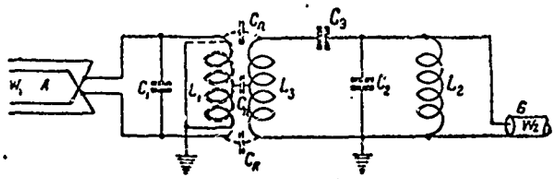

Figure XIX.6.1. Schematic diagram of a transformer for the transition from four-wire feeder A to coaxial cable B.

The transformer will function over a wide range of frequencies only when there is strong (close to unity) inductive coupling between coils L_1 and L_3. However, in such case there is also an increase in the capacitive coupling between the coils, and this leads to the establishment of a single-cycle wave from the open four-wire feeder in the coaxial cable. In order to avoid this, coil L_1, as shown in Figure XIX.6.1, is made in two sections, wound alternately, with the center point grounded (one of the coil sections is shown by a dotted line). In this case the single-cycle wave travels through two identical halves of coil L_1, which are strongly coupled to each other and wound in opposite directions. The toral inductance of coil L_1 is therefore negligibly small for the single-cycle wave. Correspondingly, for the single-cycle wave on coil L_1 there is established a voltage node and the distributed shunt capacitances C_n between coils L_1 and L_3 have very little effect on circuit operation.

Thus, it is possible to create a strong inductive coupling between coils L_1 and L_3 without causing any great coupling between them through capacitance C_n for a single-cycle wave. Practically speaking, coil L_3 can be wound directly on coil L_1.

(b) Analysis of transformer operation

We have shown the transformer circuitry, consisting of the two halves shown in Figure XIX.6.2, for purposes of convenience.

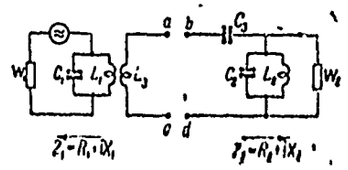

Figure XIX.6.2. Equivalent transformer circuit.

Let the impedance at terminals ac equal $Z_1 = R_1 + iX_1$, and the impedance at terminals bd equal $Z_2 = R_2 + iX_2$.

The optimum output of energy from the primary circuit to the secondary circuit occurs when

$$R_1 = R_2, \qquad \text{(XIX.6.1)}$$

$$X_1 + X_2 = 0. \qquad \text{(XIX.6.2)}$$

Analysis reveals that the equality at (XIX.6.1) can be satisfied when the following relationships are observed

$$\frac{L_1}{L_2} = \frac{L_3K^2}{L_1} = \frac{C_1}{C_2} = \frac{W_2}{W_1} = M, \qquad \text{(XIX.6.3)}$$

where

K is the coupling factor between coils L_1 and L_3;

M is the resistance transformation ratio.

It is impossible to observe the equality at (XIX.6.2) over the entire operating band. As a practical matter, all that can be discussed is the creation of a regime in which the magnitude $X_1 + X_2$ has minimum values in the operating wave band. As a result of the analysis of the transformer circuit it was made clear that the minimum value of $X_1 + X_2$ is obtained in the case of equality between the resonant frequencies of circuits L_1C_1 and L_2C_2 and the resonant frequency of the circuit formed from the stray inductance of coil L_3, equal to $L_3(1 - K^2)$, and capacitance C_3.

Thus, the following relationship should be realized

$$\frac{1}{\sqrt{L_1C_1}} = \frac{1}{\sqrt{L_2C_2}} = \frac{1}{\sqrt{L_3(1-K^2)C_3}} = \omega_0. \qquad \text{(XIX.6.4)}$$

Hereafter we will call ω_0 the transformer's natural frequency, and, correspondingly, $\lambda_0 = 2\pi \cdot 3 \cdot 10^8/\omega_0$ the transformer's natural wave.

Let us introduce the designations

$$\rho_1 = \omega_0 L_1 = \frac{1}{\omega_0 C_1} = \sqrt{\frac{L_1}{C_1}} \quad \text{— to describe the input circuit,}$$

$\rho_2 = \omega_0 L_2 = \frac{1}{\omega_0 C_2} = \sqrt{\frac{L_2}{C_2}}$ — to describe the output circuit.

From formula (XIX.6.3) it follows that

$$W_1/\rho_1 = W_2/\rho_2 . \qquad \text{(XIX.6.5)}$$

Let us designate $W_1/\rho_1 = W_2/\rho_2$ in terms of b.

From formulas (XIX.6.3) and (XIX.6.5), it follows that

$$M = W_2/W_1 = \rho_2/\rho_1 . \qquad \text{(XIX.6.6)}$$

Upon observance of the equalities at (XIX.6.3) and (XIX.6.4), the following expressions for $R = R_1 = R_2$ and $X = X_1 + X_2$ are obtained

$$R = \frac{W_2}{1 + b^2 \Delta^2}, \qquad \text{(XIX.6.7)}$$

$$X = \frac{[2K^2 b^2 - (1 - K^2)]\,\Delta - (1 - K^2) b^2 \Delta^3)\, W_2}{(1 + b^2 \Delta^2)\, bK^2}, \qquad \text{(XIX.6.8)}$$

where

Δ is the generalized detuning, equal to

$$\Delta = \frac{\omega_0}{\omega} - \frac{\omega}{\omega_0} = \frac{\lambda}{\lambda_0} - \frac{\lambda_0}{\lambda} .$$

Let us designate by P_{max} the power fed to the coaxial cable, given the condition of an ideal match between primary and secondary circuits, that is, given observance of the equalities at (XIX.6.1) and (XIX.6.2). The ratio of the power delivered when the match to the maximum power is not ideal, something not difficult to prove, equals

$$\frac{P}{P_{max}} = \frac{4\left(\frac{R_2}{R_1}\right)}{\left(1 + \frac{R_2}{R_1}\right)^2 + \left(\frac{X_1 + X_2}{R_1}\right)^2} . \qquad \text{(XIX.6.9)}$$

In the case of equality of the pure resistances of the primary and secondary circuits ($R_1 = R_2 = R$)

$$\frac{P}{P_{max}} = \frac{4}{4 + \left(\frac{X}{R}\right)^2} , \qquad \text{(XIX.6.10)}$$

where $X = X_1 + X_2$.

Substituting the values for X and R from formulas (XIX.6.7) and (XIX.6.8) in formula (XIX.6.10), we can determine the change in the P/P_{max} ratio in the band.

Knowing P/P_{max} it is not difficult to determine the traveling wave ratio on a four-wire feeder. In fact, if the losses in the transformer are ignored, the P/P_{max} ratio, computed through formula (XIX.6.10), will, at the

same time, characterize the energy output from the four-wire feeder to the transformer,

$$P_f/P_{f\ max},$$

where

$P_{f\ max}$ is the optimum energy output from the four-wire feeder to the transformer; that is, the output when the traveling wave ratio, k, equals unity;

P_f is the output energy for a real value of k.

As is known, the dependence between the traveling wave ratio on the feeder and the output energy in the resistance of the feeder load (in this case a transformer and the coaxial cable connected to it) can be expressed by the formula

$$P_f/P_{f\ max} = 4k/(1+k)^2 \qquad \text{(XIX.6.11)}$$

Equating the right sides of equations (XIX.6.10) and (XIX.6.11) to each other, we obtain

$$\frac{1}{1+\left(\frac{X}{R}\right)^2} = \frac{4k}{(1+k)^2}, \qquad \text{(XIX.6.12)}$$

From formula (XIX.6.12) we obtain

$$k = \left(1+\frac{a^2}{2}\right) - \sqrt{a^2+\frac{a^4}{4}}, \qquad \text{(XIX.6.13)}$$

where

$$a = X/R. \qquad \text{(XIX.6.14)}$$

Figure XIX.6.3 shows the curves for $k = f_1(\lambda)$ and $a = f_2(\lambda)$, plotted with a logarithmic scale on the axis of abscissas. The k values, computed through formula (XIX.6.13) equate to the case when the traveling wave mode is present on the coaxial cable, so its input resistance equals W_2.

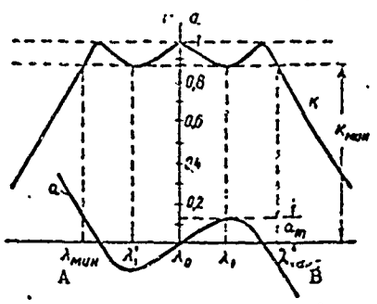

Figure XIX.6.3. Transformer curves made using the schematic diagram in Figure XIX.6.1.

A - minimum; B - maximum.

If the traveling wave ratio on the coaxial cable has some value k_f, the traveling wave ratio on the four-wire feeder can change between kk_f to k/k_f as limits if $k < k_f$, or from kk_f to k_f/k if $k_f < k$, where k is the traveling wave ratio computed through formula (XIX.6.13).

The $k = f_1(\lambda)$ and $a = f_2(\lambda)$ curves are symmetrical with respect to the transformer's natural wave, λ_0. It therefore follows that when designing the transformer its natural wave, equal to

$$\lambda_0 = \sqrt{\lambda_{min} \cdot \lambda_{max}},$$

where

λ_{min} and λ_{max} are minimum and maximum waves in the specified operating band for the transformer,

must be assumed.

It is also desirable to select transformer parameters such that on the λ_{min} and λ_{max} waves the traveling wave ratio is that of waves λ_1' and λ_1 (fig. XIX.6.3), because in this case the greatest values of k in the specified operating range will be obtained. This condition must be satisfied in order that the absolute values of a be the same on the λ_{min}, λ_1', λ_1, and λ_{max} waves.

By utilizing formula (XIX.6.13), and assigning the minimum permissible value to k in the operating band, we can select the data for the transformer. As a matter of fact, by assigning the minimum permissible value to the traveling wave ratio, k_{min}, we can establish the maximum value for a corresponding to it, and we can designate that value as a_{max}. It therefore follows from formula (XIX.6.13) that

$$a_{max} = 1 - k_{min}\sqrt{k_{min}}.$$

The dependence between transformer data and the magnitude of a can be established through formulas (XIX.6.7), (XIX.6.8) and (XIX.6.14). Substituting the values for R and $X = X_1 + X_2$ from formulas (XIX.6.7) and (XIX.6.8) in the expression for a, we obtain

$$a = p\Delta - q\Delta^3, \qquad \text{(XIX.6.15)}$$

where

$$p = 2b - \frac{c}{b}, \qquad \text{(XIX.6.16)}$$

$$q = bc, \qquad \text{(XIX.6.17)}$$

$$c = \frac{1 - K^2}{K^2}. \qquad \text{(XIX.6.18)}$$

Note that the coefficients p and q do not depend on the wavelength.

Let us designate the value of Δ when $\lambda = \lambda_1$ by Δ_1, and the value of Δ when $\lambda = \lambda_{max}$ by Δ_{max}.

Δ_1 can be established from the condition that

$$da/d\lambda = 0. \qquad \text{(XIX.6.19)}$$

From this condition we find

$$\Delta_1 = \sqrt{\frac{p}{3q}}. \qquad \text{(XIX.6.20)}$$

Taking $\lambda_0 = \sqrt{\lambda_{min}\lambda_{max}}$, we obtain

$$\Delta_{max} = \frac{\lambda_{max}}{\lambda_0} - \frac{\lambda_0}{\lambda_{max}} = \sqrt{F} - \sqrt{\frac{1}{F}},$$

where

$F = \lambda_{max}/\lambda_{min}$ is the operating band overlap.

Taking formulas (XIX.6.20) and (XIX.6.15) into consideration, we obtain the following equations

$$\sqrt{\frac{4p^3}{27q}} = a_{max}, \qquad \text{(XIX.6.21)}$$

$$p\Delta_{max} - q\Delta^3_{max} = -a_{max}. \qquad \text{(XIX.6.22)}$$

Solving equations (XIX.6.21) and (XIX.6.22) for p and q, we obtain

$$p = \frac{3a_{max}}{\Delta_{max}}, \qquad \text{(XIX.6.23)}$$

$$q = \frac{4a_{max}}{\Delta^3_{max}}. \qquad \text{(XIX.6.24)}$$

Moreover, from formulas (XIX.6.16) through (XIX.6.18) we can find

$$b = \frac{a_{max}}{\Delta_{max}}\left(0{,}5 + \operatorname{ch}\frac{\varphi}{3}\right), \qquad \text{(XIX.6.25)}$$

where

$$\varphi = \operatorname{Arch}\left(1 + \frac{8}{a^2_{max}}\right),$$

$$c = \frac{q}{b}, \qquad \text{(XIX.6.26)}$$

$$K = \frac{1}{\sqrt{1+c}}, \qquad \text{(XIX.6.27)}$$

(c) Example of transformer calculation

Magnitudes specified are as follows.

Transformer operating band:

$$\lambda_{min} = 14 \text{ m}, \quad \lambda_{max} = 70 \text{ m}.$$

Characteristic impedance:

$$W_1 = 208 \text{ ohms}, \quad W_2 = 70 \text{ ohms}.$$

The minimum permissible value of the traveling wave ratio on the four-wire feeder is

$$k_{min} = 0.88.$$

Transformer parameters are:

(1) operating band overlap

$$F = \lambda_{max}/\lambda_{min} = 70/14 = 5;$$

(2) maximum value of the generalized detuning of the circuits

$$\Delta_{max} = \sqrt{F} - \sqrt{\frac{1}{F}} = \sqrt{5} - \sqrt{\frac{1}{5}} = 1{,}789.$$

(3) maximum absolute value of the magnitude a

$$a_{max} = 1 - k_{min}/\sqrt{k_{min}} = 1 - 0.88/\sqrt{0.88} = 0.128;$$

(4) the coefficients p and q are

$$p = 3a_{max}/\Delta_{max} = 3 \cdot 0.128/1.789 = 0.215$$

$$q = 4a_{max}/\Delta^3_{max} = 4 \cdot 0.128/1.789^3 = 0.0895;$$

(5) the magnitude b is

$$\operatorname{ch}\varphi = 1 + \frac{8}{a^2_{max}} = 1 + \frac{8}{0{,}128^2} = 482{,}6,$$

from whence $\varphi = 6.84$, and

$$b = \frac{a_{max}}{\Delta_{max}}\left(0{,}5 + \operatorname{ch}\frac{\varphi}{3}\right) = \frac{0{,}128}{1{,}789}\left(0{,}5 + \operatorname{ch}\frac{6{,}84}{3}\right) = 0{,}394.$$

(6) the coefficient of coupling between coils L_1 and L_3 is

$$c = \frac{q}{b} = \frac{0{,}0895}{0{,}394} = 0{,}227,$$

$$K = \frac{1}{\sqrt{1+c}} = \frac{1}{\sqrt{1+0{,}227}} = 0{,}903.$$

(7) the resistance transformation ratio is

$$M = \frac{W_2}{W_1} = \frac{70}{208} = 0{,}337.$$

(8) characteristics of the transformer circuits are

$$\rho_1 = W_1/b = 208/0.394 = 525 \text{ ohms}, \quad \rho_2 = \rho_1 M = 525 \cdot 0.337 = 177.5 \text{ ohms};$$

(9) the natural wave and the transformer's natural frequency are

$$\lambda_0 = \sqrt{\lambda_{min}\lambda_{max}} = \sqrt{14 \cdot 70} = 31.3 \text{ meters},$$

$$\omega_0 = 2 \cdot 3.14 \cdot 3 \cdot 10^8/\lambda_0 = 1884 \cdot 10^6/31.3 \approx 60 \cdot 10^6 \text{ 1/seconds}.$$

The elements of the transformer's circuits are

$$L_1 = \rho_1 \cdot 10^6/\omega_0 = 525 \cdot 10^6/60 \cdot 10^6 = 8.75 \text{ microhenries};$$

$$C_1 = 10^{12}/\omega_0\rho_1 = 10^{12}/60 \cdot 10^6 \cdot 525 = 31.8 \text{ picofarads};$$

$$L_2 = L_1 M = 8.75 \cdot 0.337 = 2.94 \text{ microhenries};$$

$$C_2 = C_1/M = 31.8/0.337 = 94.2 \text{ picofarads};$$

$$L_3 = L_2/K^2 = 2.94/0.903^2 = 3.62 \text{ microhenries};$$

$$C_3 = C_2 \cdot K^2/1-K^2 = 94.2 \cdot 0.903^2/1-0.903^2 = 414 \text{ picofarads}.$$

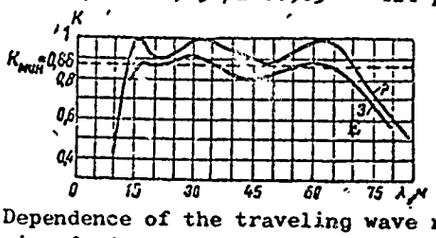

Figure XIX.6.4. Dependence of the traveling wave ratio, k, on a four-wire feeder connected to a coaxial cable through the transformer made in accordance with the schematic diagram in Figure XIX.6.1. on the wavelength.

E - experimental curve; P - design curve.

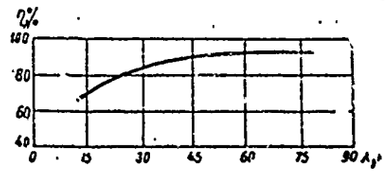

Figure XIX.6.5. Experimental transformer efficiency curve for the transformer made in accordance with the schematic diagram in Figure XIX.6.1.

Figures XIX.6.4 and XIX.6.5 show the results of an experimental investigation of one model transformer. The experimental values of k (fig. XIX.6.4) are somewhat less than the designed values, explained by the losses and stray capacitances that were not taken into consideration in the computations.

#XIX.7. Multiple Use of Antennas and Feeders

(a) Operation of two transmitters on one antenna

Operating conditions in modern radio transmitting centers are such that all too frequently the development of radio communications is limited by the limitations of the antenna field territory. Under these conditions, one of the methods whereby area can be saved is to use one antenna for operating two transmitters. Economic considerations can also cause this step to be taken. Figure XIX.7.1 shows the schematic of the operation of two transmitters on one antenna when each of the transmitters has one operating wave (λ_1 and λ_2).

The principal element in the circuit is the combination stub suggested by S. I. Hadenenko. The stub is short-circuited at both ends of a two-wire line connected to the feeder (fig. XIX.7.2). Total stub length equals an integer of the half-waves for one of the transmitters. Let us designate this transmitter's wave λ_1. The stub is connected to the feeder in such a way that the length of one of its sections equals half the operating wave of the second transmitter (λ_2).

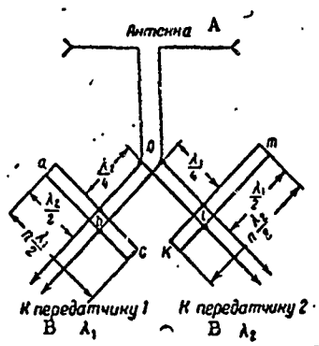

Figure XIX.7.1. Schematic diagram of the operation of two transmitters on one antenna with one operating wave at each transmitter.

A - antenna; B - to transmitter.

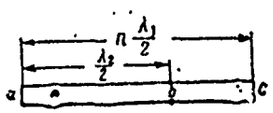

Figure XIX.7.2. Combination stub for the schematic diagram in Figure XIX.7.1.

b - point of connection of combination stub to supply feeder.

Under these conditions the stub is an infinitely high resistance on wave λ_1 and a short circuit on wave λ_2, if attenuation is neglected.

The circuit in Figure XIX.7.1 functions as follows.

When transmitter 1 is operating on wave λ_1 stub abc, with length n $\lambda_1/2$, has high resistance and passes this wave, with no marked effect on it. Segment lm of stub klm, the length of which equals $\lambda_1/2$, shorts the feeder to the second transmitter. Since stub klm is cut in at distance $\lambda_1/4$ from the branch point O, wave λ_1 reaches the antenna without having been reflected at this point. When transmitter 2 is operating on wave λ_2, the picture is similar because the length of stub klm equals n $\lambda_2/2$, and the segment ab, of length $\lambda_2/2$ of stub abc is connected at distance $\lambda_2/4$ from branch point O. Thus, simultaneous operation of two transmitters on one antenna can be had without substantial mutual effect between them.

The impedance of combination stub abc on wave λ_1 equals

$$Z_{stub} = 2\frac{W^2}{R_1 l}\sin^2 \alpha l_1, \qquad \text{(XIX.7.1)}$$

where

W is the characteristic impedance of the stub;

R_1 is the resistance per unit length of the stub;

l is the total length of the stub;

l_1 is the length of any of the component segments of a combination stub.

A similar expression can be obtained for stub klm when operating on wave λ_2.

The less the difference between the lengths of waves λ_1 and λ_2, the smaller the factor $\sin^2 \alpha l_1$, and, consequently, the less Z_{stub}.

Since $W \gg R_1 l$, the impedance of the stub on wave λ_1 is obtained as many times that of the characteristic impedance, even when the difference between λ_1 and λ_2 is small. Practically speaking, it is sufficient if the lengths of waves λ_1 and λ_2 differ from each other by 8 to 10%. If special, large diameter conductors with small losses are used, the system can be tuned, even when the difference in the lengths of waves λ_1 and λ_2 is equal to 5% and less.

Figure XIX.7.3 shows the schematic diagram of the operation of two transmitters with two opwerating waves on one antenna. The basic element in the circuit is the combination stub shown in Figure XIX.7.4.

As will be seen, an additional stub has been connected to the combination stub abc, of length n $\lambda_1/2$ shown in Figure XIX.7.4, at distance $\lambda_{1/2}$ from point c. When attenuation is low this stub has no effect on the mode of operation on waves λ_1 and λ_2; that is, the impedance of stub abc does not change on these waves at point b. If attenuation is not taken into consideration, it is possible, by selecting the length of the additional stub de, to obtain an impedance of the combination stub at point b equal to infinity on wave λ_3. Actually, if the constant reactance is connected in parallel

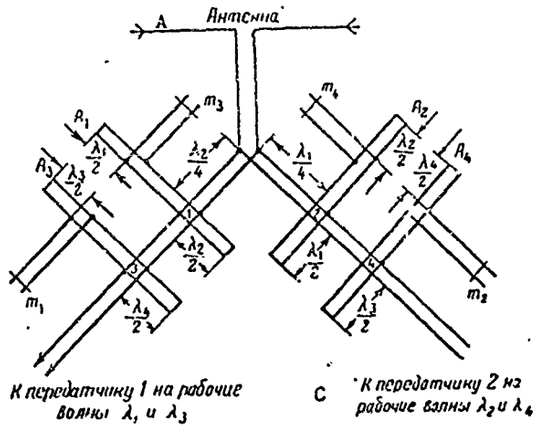

Figure XIX.7.3. Schematic diagram of the operation of two transmitters on one antenna with two operating waves at each transmitter.

A - antenna; B - to transmitter 1 on operating waves λ_1 and λ_3; C - to transmitter 2 on operating waves λ_2 and λ_4.

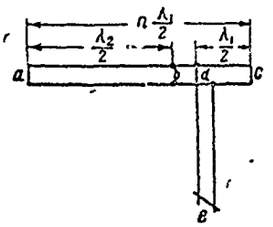

Figure XIX.7.4. Combination stub for the schematic diagram in Figure XIX.7.3.

with the reactance, the magnitude of which can be changed from minus infinity to plus infinity, the total impedance of this combination will change within any limits, and can, in particular, take a value equal to infinity. The length of the additional stub, de, needed for so doing can be established by computation. The impedance of the section of line ab at point b on wave λ_3 equals

$$Z_1 = i W \operatorname{tg}\left[\frac{2\pi}{\lambda_3}(ab)\right]. \qquad \text{(XIX.7.2)}$$

In order for the impedance of the combination stub at point b on wave λ_3 to be equal to infinity, it is necessary for the impedance of section bd at point b to be equal Z_1. The impedance of stub bd at point b equals

$$Z = W \frac{\cos\left[\frac{2\pi}{\lambda_3}(bd)\right] + i\frac{W}{Z_2}\sin\left[\frac{2\pi}{\lambda_3}(bd)\right]}{\frac{W}{Z_2}\cos\left[\frac{2\pi}{\lambda_3}(bd)\right] + i\sin\left[\frac{2\pi}{\lambda_3}(bd)\right]}, \qquad \text{(XIX.7.3)}$$

where

Z_2 is the input impedance of the two parallel connected stubs, de and dc. It can be established through formula (XIX.7.3) as

$$Z_2 = W \frac{\cos\left[\frac{2\pi}{\lambda_3}(bd)\right] - i\frac{W}{Z_1'}\sin\left[\frac{2\pi}{\lambda_3}(bd)\right]}{\frac{W}{Z_1'}\cos\left[\frac{2\pi}{\lambda_3}(bd)\right] - i\sin\left[\frac{2\pi}{\lambda_3}(bd)\right]}. \qquad \text{(XIX.7.4)}$$

The impedance of the segment of line dc equals

$$Z_3 = iW\,\mathrm{tg}\left[\frac{2\pi}{\lambda_3}(dc)\right]. \qquad \text{(XIX.7.5)}$$

The needed impedance Z_4 of the section de, and consequently, its length, can be established from the relationship

$$Z_2 = \frac{Z_3 Z_4}{Z_3 + Z_4}, \qquad \text{(XIX.7.6)}$$

from whence

$$Z_4 = \frac{Z_2 Z_3}{Z_3 - Z_2}. \qquad \text{(XIX.7.7)}$$

Let us now turn our attention to Figure XIX.7.3. Transmitter 1 is operating on waves λ_1 and λ_3, while transmitter 2 is operating on waves λ_2 and λ_4. The circuit functions as follows.

Combination stub A_1 is taken with length $n\,\lambda_1/2$, and is connected to the feeder for transmitter 1 at distance $\lambda_2/4$ from the branch point. The position of bridge m_3 on the additional stub is selected such that wave λ_3 is passed freely by stub A_1. The length of combination stub A_3 equals $n\,\lambda_3/2$. It is connected to the feeder at a distance from stub A_1 such that on wave λ_4 the impedance of the feeder for transmitter 1 equals infinity at the branch point. This can obviously be achieved because on wave λ_4 combination stub A_1 has a finite impedance, while the impedance of the section of the feeder 1-3 on wave λ_4 at point 1 can be that desired by selecting the length of 1-3. The position of bridge m_1 is selected such that it provides for free passage of wave λ_1 through the combination stub A_3.

Stubs A_2 and A_4 are set up in precisely this way. The length of stub A_2 is taken equal to $n\,\lambda_2/2$, while the position of bridge m_4 is selected such that wave λ_4 is passed freely by the stub. The length of stub A_4 is selected equal to $n\,\lambda_4/2$, and the position of bridge m_2 is selected to wave λ_2 passes freely.

Thus, when transmitter 1 is operating on wave λ_1 or λ_3, stubs A_1 and A_3 have a high impedance and pass these waves freely, while stubs A_2 and A_4 short-circuit the feeder to transmitter 2 and provide adequately high impedance of this feeder at the branch point.

When transmitter 2 is operating on waves λ_2 or λ_4 the picture is reversed, and now stubs A_2 and A_4 pass these waves while stubs A_1 and A_3 short the feeder to transmitter 1 and provide a sufficiently high impedance of this feeder at the branch point.

Consideration of the losses in the stubs imposes definite conditions on the relationships existing between wavelengths λ_1, λ_2, λ_3, λ_4, which can be developed in each concrete case by introducing the attenuation factor in formulas (XIX.7.2) through (XIX.7.7).

An experimental setting of the positions occupied by the bridges of stubs A_1, A_2, A_3, and A_4 can be made by using an ammeter inserted in the combination stub near the point where it is connected to the feeder. By moving bridge m, one finds the position of minimum reading for the corresponding wave on the ammeter.

The points at which stubs A_3 and A_4 are connected can be established experimentally in this same way. And the effort is made to obtain a current minimum for the feeder for transmitter 1 when operating on transmitter 2 waves, and a current minimum for the feeder for transmitter 2 when operating on transmitter 1 waves.

What should be borne in mind is that when two transmitters are working on one antenna at the same time the maximum amplitude of field intensity produced at some point on the antenna is equal to the arithmetical sum of the amplitudes of the field intensities produced at this point by each of the transmitters.

(b) Use of one antenna for operations in two directions

The combination stub shown in Figure XIX.7.3 can be used for the simultaneous operation of two transmitters on one antenna in different directions.

Figure XIX.7.5 is an example of a circuit for using a rhombic antenna for simultaneous operation in two directions.

When transmitter 1 is operating on waves λ_1 and λ_3 combination stubs A and D pass these waves, but stubs B and C form a short circuit. When transmitter 2 is operating on waves λ_2 and λ_4 on the other hand, stubs B and C pass these waves, while stubs A and D make the short circuit.

Rhombic antennas are often used for operations at different times in two opposite directions. In such case resort is usually had to switching, as shown schematically in figures XIX.7.6 and XIX.7.7.

Rotating the direction of maximum radiation 180° is readily accomplished with the SG and SGD antennas by connecting the supply feeder to the reflector, and connecting the elements for tuning the reflector to the antenna.

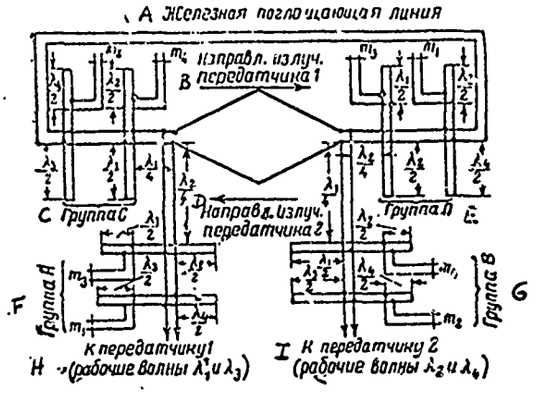

Figure XIX.7.5. Schematic diagram of the use of a rhombic antenna for simultaneous operation in two directions.

A - iron dissipation line; B - direction of radiation from transmitter 1; C - group C; D - direction of radiation from transmitter 2; E - group D; F - group A; G - group B; H - to transmitter 1 (working waves λ_1 and λ_3); I - to transmitter 2 (working waves λ_2 and λ_4).

Figure XIX.7.6. Schematic diagram of the use of a rhombic antenna for operating in two directions at different times.

A - direction B; B - dissipation line; C - direction A; D - to transmitter.

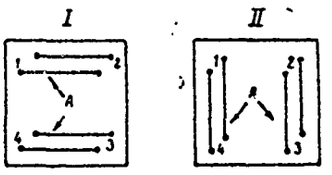

Figure XIX.7.7. Schematic diagram of switching for Figure XIX.7.6.

A - jumpers; I - position of jumpers when operating in direction B; II - position of jumpers when operating in direction A.

(c) Use of one feeder for operation on two antennas

In some cases the use of one feeder for operation on two antennas is of interest. We will limit ourselves here to mention of the simplest circuit used when each antenna is operating on one fixed wave.

The circuit is shown in Figure XIX.7.8. Combination stub A_1, described above, is selected with length $n\,\lambda_1/2$ (n is an integer), and is suspended on the feeder to antenna 1 at distance $\lambda_2/4$ from the branch point. Combination

stub A_2 is taken with length $n\,\lambda_2/2$ and is suspended on the feeder to antenna 2 at distance $\lambda_1/4$ from the branch point. When operation is on wave λ_1 stub A_1 has extremely high impedance and freely passes this wave, while stub A_2, because one of its segments has length $\lambda_1/2$, shorts the feeder to antenna 2, and, at the same time, gives this feeder extremely high impedance at branch points. The picture is the reverse when operation is on wave λ_2. Thus, when operation of the transmitter is on wave λ_1 antenna 1 is excited, and when the transmitter is operating on wave λ_2 antenna 2 is excited.

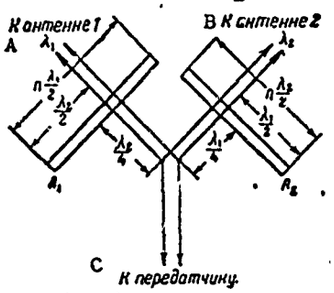

Figure XIX.7.8. Schematic diagram of the operation of one feeder for two antennas.

A - to antenna 1; B - to antenna 2; C - to transmitter.

(d) Parallel operation of receivers on one antenna

Wideband antenna amplifiers (ShAU) are usually used for multiple use of receiving antennas. The use of an amplifier makes it possible to connect a great many receivers in parallel to one antenna through decoupling resistors, thanks to which the mutual effect of the input circuits of the receivers is minimum.

However, there are still individual cases when parallel operation of several receivers on one antenna is done without the amplifiers. It must be remembered that the use of antenna amplifiers results in some deterioration in the receiving channel. As a matter of fact, even the best quality amplifiers will develop combination frequencies, as well as the phenomenon known as cross modulation. We must point out that the latter can have a substantial effect only in special cases when the receiving antenna is within the field produced by powerful shortwave transmitters.

The development of combination frequencies and the possibility of the development of cross modulation results in a reduction in reception noise stability. In no case can what has been pointed out be the basis for refusing to use antenna amplifiers, but is, nevertheless, the basis for the appearance of a definite interest in the parallel operation of receivers without amplifiers, because in individual cases this type of operation can prove to be desirable. In what follows we have presented an analysis of parallel operation of receivers without amplifiers taken from the writings of A. A. Pistol'kors. This analysis has in mind receivers in which the inputs are in the form of

oscillating circuits, inductively coupled to the feeder running to the change-over switch. Circuit parameters and coupling factors are selected such that when the receiver is tuned to the incoming wave its input resistance will be equal to the characteristic impedance of the feeder. In the case of complete match between characteristic impedance and antenna impedance, the power produced at the receiver input will equal

$$P_1 = e^2/4W, \qquad \text{(XIX.7.8)}$$

where

e is the effective value of the antenna emf equated to the receiver input;

W is the characteristic impedance of the feeder.

Let there now be a second receiver, for operation on another wave (fig. XIX.7.9a), which we will connect in parallel to the receiver we have tuned as discussed.

In the general case, the input resistance of the second receiver on the operating wave of the first receiver is complex. Let us designate this resistance, recomputed for the points at which the feeders branch, by $Z_1 = R_1 + iX_1$. The power separable at the input to the first receiver is reduced, the result of the effect caused by the second receiver. Using the equivalent circuit for the parallel connection of the two receivers (fig. XIX.7.9b), we can find the following expression for the reduced power

$$P_r = \frac{e^2 (R_1^2 + X_1^2) W}{(W^2 + 2WR_1)^2 + (2WX_1)^2}. \qquad \text{(XIX.7.9)}$$

Then the relationship is

$$\frac{P_r}{P_1} = \frac{4W^2 (R_1^2 + X_1^2)}{(W^2 + 2WR_1)^2 + (2WX_1)^2}. \qquad \text{(XIX.7.10)}$$

Designating $p = R_1/W$ and $q = X_1/W$, we obtain

$$\frac{P_r}{P_1} = \frac{p^2 + q^2}{(0{,}5 + p)^2 + q^2}. \qquad \text{(XIX.7.11)}$$

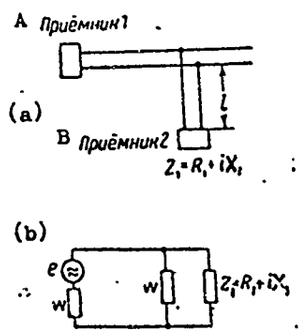

Figure XIX.7.9. (a) Analysis of the parallel operation of receivers; (b) equivalent circuit showing the operation of two receivers on one antenna. A - receiver 1; B - receiver 2.

Let us consider the two extreme cases, when (1) $q \ll p$ and (2) $q \gg p$. The first case will obviously occur when the receivers are operating on the same, or extremely close, frequencies. We can then put $p = 1$, and the reduction in power at the input of the receivers will equal $P_2/P_1 = 0.45$. When three receivers are connected in parallel $p = 0.5$, and then $P_2/P_1 = 0.25$. We can similarly compute the reduction in power for any number of receivers operating in parallel.

The second case takes place during the operation of receivers on different frequencies when the input resistance of the second receiver on the operating wave of the first receiver can be taken as purely reactive. This case of parallel operation of receivers is the one prevailing in practice. Depending on the relationship of the frequencies and the lengths of the feeders connecting the receivers to the changeover switch, reactance X_1, and consequently $q = X_1/W$, can take every possible value. The magnitude of P_2/P_1 will, at the same time, change from 0 to 1.

The input resistance of the interference receiver, when there is a considerable detuning of the receivers, can be established by the impedance of coupling coil L. Designating the length of line equivalent to this coil by l_{eq}, we receive the following equation for q

$$q = \tan [\alpha(l+l_{eq})], \qquad \text{(XIX.7.12)}$$

where

l_{eq} is established from the expression

$$\tan \alpha l_{eq} = \omega L/W. \qquad \text{(XIX.7.13)}$$

So, knowing the inductance of the coupling coil for the interference receiver, the length of the connection feeder, and the wavelength on which the receiver is operating, we can, through formulas (XIX.7.11) through (XIX.7.13) establish the reduction in power at the receiver input.

The task of establishing the mutual effect of the receiver inputs can be simplified considerably if it is assumed that the feeders running from the receivers to the changeover switch have the same lengths, and that the inductances of the receiver coupling coils are equal to each other. In this case the reduction in power can be established through the formula

$$\frac{P_2}{P_1} = \frac{q^2}{0{,}25(n-1)^2+q^2}, \qquad \text{(XIX.7.14)}$$

where

q is established through formula (XIX.7.12);

n is the number of receivers connected in parallel.

The dependence of reduction in power on the ratio $l+l_{eq}/\lambda$ for a series of values of n is shown in Figure XIX.7.10.

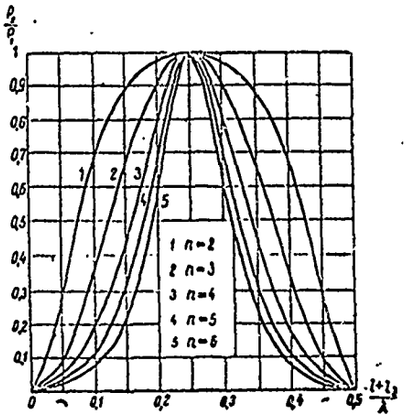

Figure XIX.7.10 Dependence of reduction in power on the $l+l_{eq}/\lambda$ ratio.

The curves shown provide a means for finding that band of waves in which parallel operation of the receivers is possible.

Let us consider an example. Let the length, l, of a feeder connecting a receiver to a changeover switch equal 5 meters. We will assume the inductance of each of the coupling coils at the receiver inputs equals 2 microhenries. Using formula (XIX.7.13), we can establish the fact that the length, l_{eq}, will remain approximately the same on all waves in the shortwave band and will equal $\sim$ 2.5 meters.

On waves satisfying the ratio $l+l_{eq}/\lambda = n/4$, where n = 1, 3, 5, ..., the mutual effect will be least. In the case specified this ratio can be satisfied on a wave equal to 30 meters.

Let the reduction in power be to the magnitude $P_2 = 0.25\ P_1$, which is acceptable. Then the band of waves within the limits of which it will be possible to have parallel operation of the receivers will equal

when n = 2 λ = 167 to 16.5 meters;
when n = 3 λ = 94 to 18.0 meters;
when n = 4 λ = 65 to 19.5 meters;
when n = 5 λ = 55.5 to 20.5 meters;
when n = 6 λ = 48.5 to 21.8 meters.

Thus, when the number of receivers connected in parallel is increased, the band of waves within the limits of which these receivers can operate is reduced. Practically speaking, it can be taken that the use of one receiving antenna for the parallel operation of three or four receivers is permissible. Any further increase in the number of receivers is not recommended.

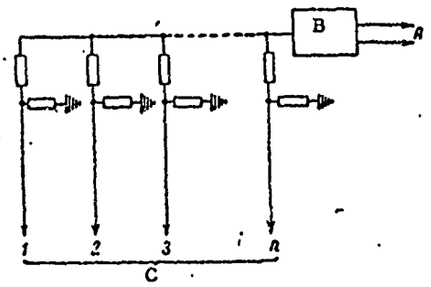

Figure XIX.7.11. Schematic diagram of the operation of an antenna with an amplifier.

A - feeder to antenna; Б - multiple-tuned amplifier; C - feeders to receivers.

If the need to use one antenna for a greater number of receivers is an urgent one, the multiple-tuned antenna amplifier should be used. The schematic of the operation of an antenna with an amplifier is shown in Figure XIX.7.11. As will be seen, the emf is fed from the antenna to the amplifier. The receivers are connected to the amplifier through decoupling resistors. The power amplification provided by the amplifier should cover the losses due to the branching of the energy over n channels (n is the number of receivers), as well as the losses in the decoupling resistors.

The amplfifiers usually amplify a signal by 20 to 30 db. The number of parallel connected receivers can be increased to 10 to 20. The decoupling resistors, and the number of parallel connected receivers, can be selected such that the gain in signal strength is at least 2 to 3 db, with the gain factor for the amplifier, and the losses associated with the parallel operation of the receivers, taken into consideration. At the same time, there is no reduction in receiver sensitivity, practically speaking, because the receivers are working in parallel. The match between the input resistance of the amplifier and the feeder should be a good one. In the properly designed amplifier the reflection factor for the input will not be in excess of 0.15 ($k \geqslant 0.73$).

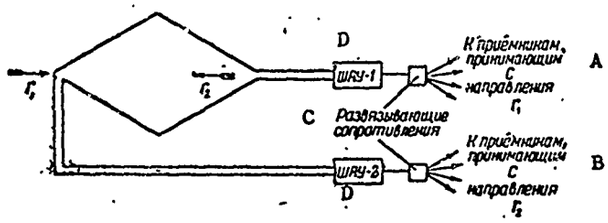

Figure XIX.7.12. Schematic diagram of the use of a rhombic antenna for operating in two opposite directions.

A - to receiver receiving from direction r_1; B - to receiver receiving from direction r_2; C - decoupling resistors; D - ShAU (wideband antenna amplifier).

A good match between amplifier input and feeder is particularly important when the amplifier is used with rhombic antennas or traveling wave antennas for simultaneous operation in two opposite directions (fig. XIX.7.12).

The input of the ShAU-2 amplifier is the terminating resistance for receivers used in direction r_1, while the input of the ShAU-1 amplifier is the terminating resistance for receivers used in direction r_2. A poor match between amplifier input and feeder will result in amplification of noise reception from the rear half-space.

#XIX.8. Lightning Protection for Antennas

Lightning protection for transmitting antennas is provided by grounding the antenna, or the feeder. A point with zero potential is chosen for grounding in order to avoid the effect of grounding on the operating mode of the antenna installation. This point is the mid-point of the bridge in the stubs for tuning the reflector and the feeder (fig. XIX.8.1) in all tuned antennas.

In those cases when operation occurs on a fixed wave, a two-wire closed-end line $\lambda/4$ long, the center point of the bridge of which is grounded, can be used to ground any antenna.

The ends of the dissipation line (fig. XIX.8.2) can be grounded in rhombic antennas.

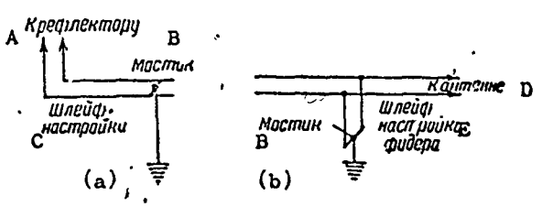

Figure XIX.8.1. Schematic diagram of the grounding of a tuned antenna. (a) reflector ground; (b) supply feeder ground.

A - to reflector; B - bridge; C - tuning stub; D - to antenna; E - stub for tuning feeder.

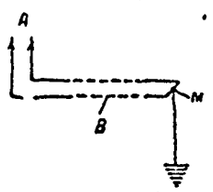

Figure XIX.8.2. Schematic diagram of grounding of dissipation line.

A - to antenna; B - dissipation line; M - bridge.

The center point of the shunt in shunt dipoles is grounded.

In addition to permanently made grounds, switches, installed in the feeder lead-ins to the transmitter building, can be used. These switches disconnect the feeder from the transmitter output and ground the feeder when the antenna is not in use.

Lightning arrestors, installed in the lead-ins of feeders into the receiver buildings, or right on the antenna changeover switch panels, are used with receiving antennas, and these are in addition to the methods already described.

The arrestors are dischargers, one end of which is connected to the feeder conductors, the other end to ground. Chokes, connected in parallel, are used to leak off the static charges which pile up in the antenna system. The choke impedance should be 5 to 10 times greater than the feeder's characteristic impedance over the entire operating band.

Figure XIX.5.2 shows the schematic of the lightning protection provided for a receiving antenna. The data on one variant of the induction coils is as follows:

number of turns n = 100;

wire diameter d = 0.4 to 0.5 mm;

coil diameter D = 12 mm;

length of coil ℓ = 60 mm, wound continuously, with copper wire PEShO, inductance L = 22 microhenries.

The lightning arrestors are gas-filled dischargers, RA-350.

#XIX.9. Exponential Feeder Transformers

There are a number of cases when the input resistance of shortwave multiple-tuned antennas differs considerably from the characteristic impedance of the supply feeders. For example, the input resistance of a rhombic receiving antenna is approximately 700 ohms, whereas the characteristic impedance of the supply feeder for this antenna is 208 ohms. In such cases, exponential and step feeder transformers (see Chapter II) are used to match the antenna with the feeder.

Feeder transformers are also used for matching individual elements of distribution feeders of complex multiple-tuned antennas. Let us pause to consider the arrangement of exponential feeder transformers.

Exponential feeder transformers are lines, the characteristic impedance of which changes in accordance with an exponential law, that is, in accordance with the e^{bz} law (fig. XIX.9.1), where b is a constant (positive, or negative). Chapter II contains an explanation of the theory of these lines.

The characteristic impedance of a feeder transformer is made equal to the load resistance at one end, and to the characteristic impedance of the

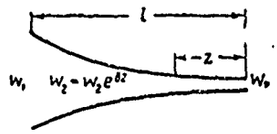

Figure XIX.9.1. Principal schematic diagram of an exponential feeder transformer.

feeder connected to it at the other end. To obtain a good match over a wide band of waves, the length of the feeder transformer should be at least some magnitude, l, established through formula (II.5.5).

By assigning the necessary values to the reflection factor, p, we can establish b and l.

Figure XIX.9.2 shows the schematic of a two-wire feeder transformer with a transformation factor $W_1/W_2 = 700/350 = 2$, designated the TF2 700/350. The dimensions shown in Figure XIX.9.2 are in millimeters.

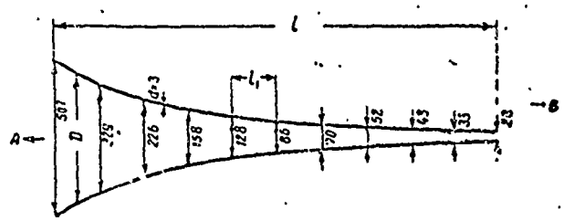

Figure XIX.9.2. Exponential feeder transformer TF2 700/350.
A ends - to system with high characteristic impedance;
B ends - to system with low characteristic impedance.

The TF2 700/350 transformer is used to match a single rhombic receiving antenna with a feeder, and is made of 3 mm diameter copper wire. The transformer is positioned vertically, and is at the same time a downlead. The distances between the wires, shown in Figure XIX.9.2, are maintained by spreaders made of insulating material.

Transformer length is established by the height at which the antenna is suspended. When it is desirable to have the length of the transformer longer than antenna height it can be located horizontally, in part, on the feeder supports.

Figure XIX.9.3 shows a four-wire crossed feeder transformer with transformation ratio of $W_1/W_2 = 340/208 = 1.6$, designated the TF4P 340/208.

The transformer is usually made of bimetallic wire with diameter d = 1.5 mm, and designwise is a straight line extension of the standard receiving feeder with a characteristic impedance of 208 ohms.

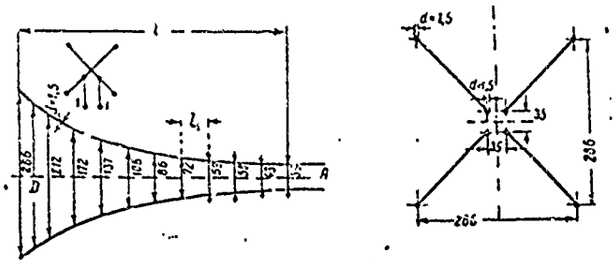

Figure XIX.9.3. (a) Exponential feeder transformer TF4P 340/208.
A ends - to standard four-wire receiver feeder;
1-1 - supply.

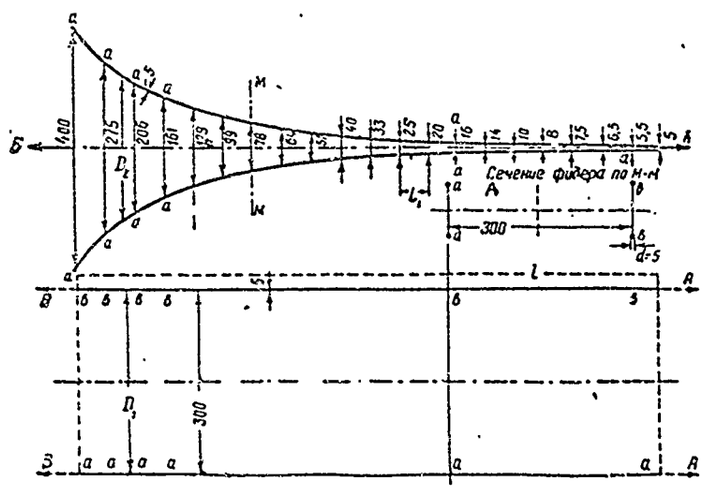

Figure XIX.9.4. Exponential feeder transformer TF4 300/600.
a-a - metallic jumper; A ends - to system with high characteristic impedance; B ends - to system with low characteristic impedance; A - feeder cross section through M-M.

The length of a feeder transformer is selected according to the maximum wave in the operating band in accordance with formula (II.5.5). The distances between spreaders t_1 is selected as 2 to 3 meters. The transformer is positioned horizontally on conventional feeder supports.

The TF4P transformer, in combination with the above-described TF2 transformer, matches the input resistance of a single rhombic receiving antenna with the characteristic impedance of a standard four-wire receiving feeder. With some shortening on the high characteristic impedance side it can also be used to match the input resistance of a twin rhombic receiving antenna, or of a traveling wave antenna, with the receiving feeder (see chapters XIII and XIV).

Figure XIX.9.4 shows a four-wire feeder transformer with a transformation ratio W_1/W_2 = 300/600, designated the TF4 300/600. The transformer is positioned horizontally on feeder supports. Each pair of conductors in the same vertical plane is connected by metal jumpers. The distance between the two planes formed in this manner is kept constant and equal to 300 to 400 mm.

The TF4 300/600 transformer can be used to match a twin rhombic transmitting antenna and a multiple-tuned balanced transmitting dipole with a twin-conductor feeder (see chapters IX and XIII).

The use of a line with smoothly changing characteristic impedance for matching multiple-tuned antennas was first suggested and realized by the author in 1931.

In concluding this section, we should note that the step feeder transformers described in Chapter II are much shorter than exponential feeder transformers for a specified band of waves and a specified maximum value for the reflection factor.

Chapter XX

TUNING AND TESTING ANTENNAS

#XX.1. Measuring Instruments

(a) Measuring loop

This paragraph will review a measuring instrument widely used in practice to tune and test shortwave antennas. Primary attention will be given to a simple instrument made right in the radio centers.

A so-called measuring loop, a two-conductor line $\lambda/4$ long (fig. XX.1.1) short-circuited on one end, is used to measure feeder potentials and voltages. A high-frequency ammeter is inserted in the short-circuited end of the loop, and its readings are proportional to the voltage applied to the loop across points a and b.

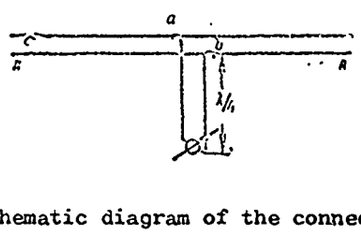

Figure XX.1.1. Schematic diagram of the connection of a measuring loop for measuring voltage.
A-A - feeder.

The input resistance of the measuring loop, that is, the resistance at points ab (see formula I.12.3), equals

$$R_{ab} = W^2_{loop}/R_{amm} + 0.5\ R_{loop}, \qquad (XX.1.1)$$

where

W_{loop} is the characteristic impedance of the loop;
R_{amm} is ammeter resistance,

$$R_{loop} = R_l l,$$

where

R_l is the resistance per unit length of the loop;
l is the length of the loop.

The characteristic impedance of the loop is on the order of hundreds of ohms, while the resistance of the instrument and loop conductors is on the order of units of ohms. Consequently, the input resistance of the loop is extremely high (on the order of tens of thousands of ohms), a condition necessary in order to measure voltage.

The voltage across the feeders measured by the loop (the difference in potentials between the feeder conductors) can be established through the formula

$$U = IW_{loop} \qquad (XX.1.2)$$

where

I is the current read on the ammeter inserted in the loop.

The loop is connected to the feeder as shown in Figure XX.1.1, in order to measure the voltage.

The measuring loop can also be used to measure conductor potential. One terminal of the loop (fig. XX.1.2) is touched to the conductor. The ammeter reading in this case is proportional to twice the conductor potential because a potential equal in magnitude, and opposite in sign to the conductor potential is automatically established at the second terminal of the loop (terminal b). Thus, the conductor potential can be established through the formula

$$V = 1/2\ IW_{loop}. \qquad (XX.1.3)$$

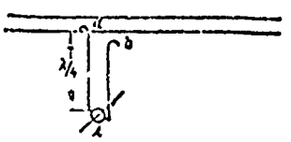

Figure XX.1.2. Schematic diagram of the connection of a measuring loop for measuring conductor potential.

When out of phase and in-phase waves are present on the feeder the measuring loop can establish the potential of each of these waves, as well as the phase displacement between them. The conductor potential, and the potential difference between them, is measured for this purpose.

The sought-for potentials can be established through the formulas

$$V_{out} = 1/2\ I_{12}W_{loop}, \qquad (XX.1.4)$$

$$V_{in} = \sqrt{\frac{1}{2}(I_1^2 + I_2^2 - 2I_{12}^2)}\quad W_{loop}/2, \qquad (XX.1.5)$$

$$\cos\varphi = \frac{I_1^2 - I_2^2}{4I_{12}} \frac{1}{\sqrt{\frac{1}{2}(I_1^2 + I_2^2 - 2I_{12}^2)}}, \qquad (XX.1.6)$$

where

V_{out} is the out of phase wave potential;

V_{in} is the in-phase wave potential;

φ is the phase angle between the out of phase and in-phase waves;

I_1 is the ammeter reading when the loop is connected to conductor 1;

I_2 is the ammeter reading when the loop is connected to conductor 2;

I_{12} is the ammeter reading when the loop is connected to both conductors simultaneously.

If only the out of phase wave is present on the feeder (and this is customarily what is attempted) all three measurements will be the same, that is, $I_1 = I_2 = I_{12}$.

The measuring loop used for measurements on transmitting antenna feeders can be made of copper wire, or of stranded conductors, 2 to 4 mm in diameter. The distance between the loop conductors is 100 to 400 mm. Spreaders, made of an insulating material and installed 1 to 2 meters apart, are used to keep constant the distance between the conductors.

The loop terminals are in the form of hooks connected to an insulator, and these are used to connect the loop to the line conductors. The insulator can be mounted on a wooden holder 1.5 to 3 meters long. The ammeters are mounted on the wooden holders, or on some other insulating material. One loop design is shown in Figure XX.1.3.

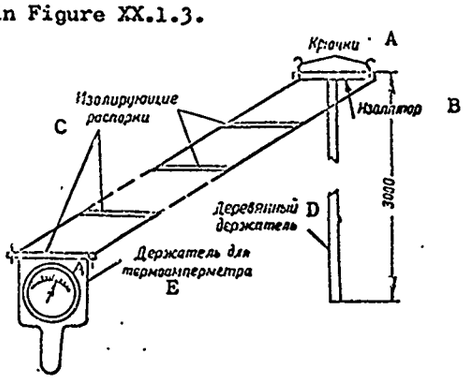

Figure XX.1.3. Variant in the design of a measuring loop.

A - hooks; B - insulator; C - insulating spreader; D - woodon holdor; E - holdor for thermocouple ammeter.

The measuring loop used for taking measurements on receiver feeders and antennas is also usually made of a two-wire copper or bimetallic conductor 1.5 mm in diameter.

The distance between conductors is 4 to 5 cm. The terminals are four hooks. The hooks, located crosswise, are interconnected. During measurements the hooks are attached to all four feeder conductors, with the result that the distance between feeder conductors is retained. A general view of the measuring loop for a four-wire receiving feeder is shown in Figure XX.1.4.

(b) Milliammeter with series-connected capacitances

A thermal milliammeter, or a thermocouple milliammeter, inserted between the feeder conductors through a low-capacity condenser (fig. XX.1.5) can also be used to measure the voltage across feeders.

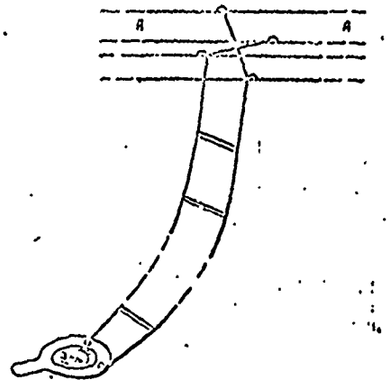

Figure XX.1.4. Schematic diagram of the connection of a measuring loop to a four-wire crossed feeder.

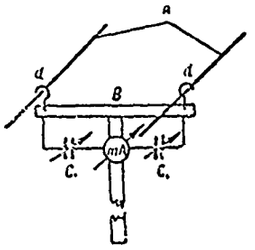

Figure XX.1.5. Thermocouple milliammeter with series-connected capacitances (C_1) for measuring the voltage across a two-conductor feeder, A.

The capacitances of condensers C_1 are selected such that the instrument resistance is much greater than the equivalent resistance of the feeder at the measurement site. The maximum equivalent resistance of the feeder is obtained at a voltage loop, and equals W/k. In practice the capacitance of condensers C_1 should be on the order of unity, or tenths of a picofarad.

The instrument described can also be used to obtain conductor potential readings. When potential is measured the instrument is connected to the conductor as shown in Figure XX.1.6. What has to be remembered, however, is that instrument readings are proportional to the conductor potential being measured only if its capacitance coupling with the other feeder conductor can be neglected.

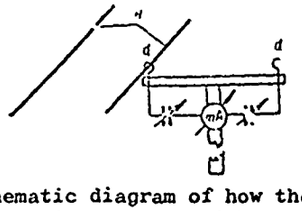

Figure XX.1.6. Schematic diagram of how the potential on a conductor is measured with the meter sketched in Figure XX.1.5.

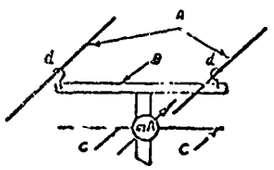

Figure XX.1.7. Thermocouple milliammeter with cat whiskers (C) for measuring the difference in potentials on a two-conductor feeder, A. B - insulator.

It is convenient to use a milliammeter with series-connected condensers to make measurements in the region of the longest waves in the shortwave band, where the use of a measuring loop is inconvenient because of its extreme length.

A second type of voltage measurement instrument is shown in Figure XX.1.7. The coupling with the feeder is through a capacitance between cat whiskers C and the feeder conductors A.

(c) The resonant circuit

An instrument consisting of an LC tank and a thermocouple milliammeter (fig. XX.1.8), can be used to measure conductor potentials. A lead with a hook, used to connect the instrument to the feeder, is connected to tank output a, through a small capacitance, C_1, on the order of a few tenths of a picofarad. The tank output, b, is connected to metal shield A, to which the tank is connected. Note should be made of the fact that maximum instrument resistance is obtained when the tank is tuned to resonance with a wave somewhat longer than the operating wave.

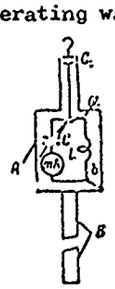

Figure XX.1.8. Measuring circuit with tuned LC circuit for measuring potentials on conductors.
A - shield; B - holder.

The tank is a step-up current transformer for the current flowing in the linear chain of the instrument, so low response current measuring devices can be used.

Instrument readings are proportional to the potential difference established between the points of measurement on conductor and shield.

The shield is a box measuring about 10 x 15 x 20 cm. The lead connecting tank, capacitance, C_1, and hook is a part of the shield and is in the form of a tube about 1 meter long.

(d) Instruments for measuring the current flowing in conductors

The current flowing in antennas and feeders can be measured by connecting a thermocouple ammeter in the conductor. This method is only suitable for measuring the current at individual points however, because the conductors must be cut to insert the meter.

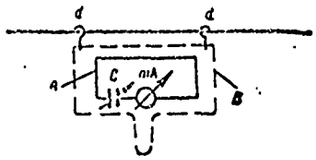

Figure XX.1.9. First variant of a circuit for measuring the current flowing in a conductor.
A - wire loop; B - holder.

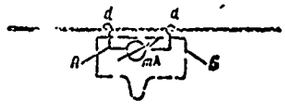

Figure XX.1.10. Second variant of a circuit for measuring the current flowing in a conductor.
A - wire with hooks; B - holder.

Small loops (fig. XX.1.9) are used to measure current distribution on conductors. The loop is mounted on a holder made of a dielectric and is hung on the conductor by the hooks connected to it.

A variable condenser can be inserted in the loop circuit to increase response, and is used to tune the loop to the operating wave.

Instrument readings are proportional to the current flowing in the conductor over section dd. The length of section dd must be taken as extremely small compared with the wavelength.

Another circuit used to measure current distribution is shown in Figure XX.1.10. In this circuit the milliammeter is connected directly into the conductor by the cat whisker and hooks. The necessary response of the milliammeter can be established through the relationship

$$I_{conn} = Z_f/Z_{conn} \cdot I_f, \qquad (XX.1.7)$$

where

I_f is the current flowing in the conductor;

Z_f is the impedance of the conductor over section dd;

Z_{conn} is the impedance of the milliammeter and the cat whisker connected to it.

(e) Electric field intensity indicator

A special device which measures electric field intensity near antennas, not only in relative, but in absolute magnitudes as well, is used to measure electric field intensity when tuning shortwave antennas. It is not the task of this book to describe this device, but we have included a description of a simple field intensity indicator in what follows since it is used in transmitting stations for different types of checks made to determine if antennas are operating properly.

This electric field intensity indicator usually consists of a balanced dipole 2 to 3 meters long connected to a tank with a thermocouple and galvanometer (fig. XX.1.11). If greater response is required of the instrument a detector, or a cathode voltmeter can be used instead of the thermocouple.

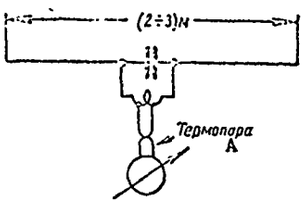

Figure XX.1.11. Electrical field intensity indicator.
A - thermocouple.

It is desirable to tune the tank to a wave somewhat different from the operating wave in order to increase the stability of readings taken by the portable instrument.

The indicator's dipole is positioned horizontally when measuring the field strength of horizontal antennas, and is positioned vertically when measuring the field strength of vertical antennas.

(f) Measurement of the traveling wave ratio

Measurement of the traveling wave ratio, k, on a feeder is made by one of the voltage indicators described above. The following relationship is used for the purpose:

$$k = U_{node}/U_{loop},$$

where

U_{node} is the voltage measured at a voltage node;

U_{loop} is the voltage measured at a voltage loop.

If there is a sharply defined standing wave on the feeders, and measurement of the voltages at the node and loop using the same instrument is difficult, the following relationship can be used to determine k:

$$k = \frac{\sin az}{\sqrt{\left(\frac{U_z}{U_{node}}\right)^2 - \cos^2 az}}, \qquad \text{(XX.1.8)}$$

where

U_z is the voltage measured at distance z from the node.

The traveling wave ratio can also be measured by using the reflectometer suggested by Pistol'kors and Neyman. The reflectometer operating principle is explained by the circuitry sketched in Figure XX.1.12. The principal part of the circuit is the small piece of line terminated at both ends by resistances equal to its characteristic impedance. In series with the resistances at each end of the line are thermocouple milliammeters, or thermocouples with galvanometers. The instrument is set up parallel to the supply feeder and in direct proximity to it.

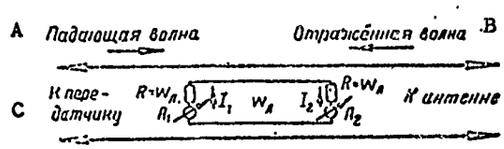

Figure XX.1.12. Schematic diagram of a reflectometer for measuring the traveling wave ratio on a feeder.

A - incident wave; B - reflected wave; C - to transmitter; D - to antenna.

Current I_1, read on milliammeter A_1 which is connected into the transmitter side, is proportional to the incident wave current on the supply feeder, while current I_2, read on milliammeter A_2 connected into the antenna side, is proportional to the reflected wave (see Appendix 8). When the mode on the feeder is that of the traveling wave, current I_2 equals zero.

$I_1 = I_2$ for the pure standing wave.

The traveling wave ratio on the feeder is established through the relationship

$$k = \frac{1-|\rho|}{1+|\rho|},$$

where $|\rho| = \frac{I_2}{I_1}$.

(g) Power measurement

Feeder power can be found by measuring the voltage at the node (U_{node}) and at the loop (U_{loop}),

$$P_f = U_{node} U_{loop} / W_f. \qquad (XX.1.9)$$

U_{node} and U_{loop} can be measured by a measuring loop. Feeder power can also be found by using the instrument developed by B. G. Strausov, and which is similar to the reflectometer described above. Actually, the readings of instrument A_1 (fig. XX.1.12) is proportional to the incident wave current

flowing in the feeder, while the readings of instrument A_2 are proportional to the reflected wave current flowing in the feeder.

Thus, the feeder power can be found through the formula

$$P_f = A(I_1^2 - I_2^2),$$

where

I_1 and I_2 are the current readings from instruments A_1 and A_2;
AI_1^2 is the incident wave power;
AI_2^2 is the reflected wave power;
A is the proportionality factor, fixed when the measuring device is calibrated.

(h) Local oscillators

Low power local oscillators (up to 1 or 2 watts) can be used for receiving antenna excitation during measurements. Local oscillator output must be balanced if it is connected to a balanced feeder. The output can be balanced by making the local oscillator in the form of a push-pull circuit. The coupling to the feeder can be by autotransformer, or by induction. In the latter case an electrostatic shield must be installed between the output circuit of the local oscillator and the feeder coil. The output stage of the local oscillator can be single-cycle when an electrostatic shield is used.

As the antenna is tuned the load on the local oscillator changes, and this can cause instability in its frequency and output. This can be avoided by tuning with minimum coupling between local oscillator and feeder.

#XX.2. Tuning and Testing Antennas. Tuning a Feeder to a Traveling Wave.

(a) Tuning and testing a balanced horizontal dipole.

General remarks. Antennas are tuned and tested prior to being put into operation, as well as periodically during operation and after repair and adjustment.

An external inspection of antenna and feeders is made prior to the electrical check and tuning. Checked at the same time is proper connection of individual antenna elements to each other, insulation, and other items.

Tuning and testing a balanced horizontal dipole involves checking the insulation, checking and adjusting balance, tuning the reflector, and tuning the feeder to the traveling wave.

In the case of a multiple-tuned balanced dipole, where special tuning of the feeder to the traveling wave is not required, the match of antenna to feeder is checked.

Insulation check. A megohmmeter is used to check insulation. Leakage resistance of each conductor to ground and leakage resistance between the conductors can be checked in this way.

Antenna and feeder insulation can be considered satisfactory if the leakage resistance between conductors, or from each conductor to ground, is at least equal to the permissible leakage resistance for one insulator (or group of insulators), divided by the total number of insulators (or groups of insulators) installed in the feeder and antenna.

It is desirable to make an insulation check not only during dry weather, but when it is raining as well. Standards for leakage per insulator, or group of insulators, should be specified in each individual case.

Balance check. Antenna systems are balance checked on operating waves, and in the case of multiple-tuned dipoles on the extreme waves in the band. A measuring loop one-quarter the operating wave in length is used to measure feeder potential. The loop is first connected to one feeder conductor by a hook, then to the second conductor, and then both hooks are connected to both feeder conductors. All three measurements are made on the same feeder section. If the meter reads the same for all three measurements the feeder and antenna are in balance. These measurements are made at two points $\lambda/4$ apart.

If the meter readings taken during this procedure differ, the feeder is carrying an out of phase, as well as an in-phase wave. Presence of an in-phase wave indicates an unbalance in the antenna system, or at the transmitter output.

To ascertain just where the unbalance is (in the transmitter, or on the antenna) cross the feeder conductors at the points where they are connected to the transmitter output circuit. If the difference in indicator readings remains the same, but the readings on the first and second conductors are reversed, the unbalance is at the transmitter output.

If the unbalance remains unchanged the unbalance is in the antenna system.

In this latter case the nature of the unbalance must be established. This is done by checking the distribution of potentials along each feeder conductor and establishing the unbalance factor through the formula

$$\delta = \frac{V_1 - V_2}{V_1 + V_2},$$

where

V_1 is the potential of one conductor at the potential loop

V_2 is the potential of the second conductor at this same section.

Let us take the following example in order to clarify the principle involved in the unbalance. The transmitter power, and its coupling with the feeder, is reduced. A short-circuiting bridge (fig. XX.2.1) is used to short the feeder near the antenna, and once again an unbalance check is made. If the unbalance disappears, the antenna is at fault. Causes of unbalance can

include damage to insulators, different lengths in the balanced halves of the antenna, etc. If the unbalance does not disappear, moving the short-circuiter along the feeder can readily establish the site of the unbalance.

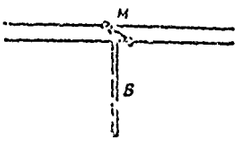

Figure XX.2.1. Bridge (M) for short-circuiting a two-conductor feeder. B - bridge holder.

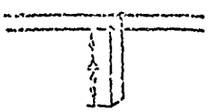

Figure XX.2.2. Loop for eliminating unbalance.

Feeder potential is checked once again when the causes of the unbalance have been eliminated. The antenna and feeder can be considered to be adequately balanced if the unbalance factor is not in excess of 10 to 15%.

The unbalance caused by an unbalance at the transmitter output can be weakened substantially when the operation is on one fixed wave by using a $\lambda/4$ long short-circuiter at the end of the line connected to the feeder in the immediate vicinity of the transmitter (fig. XX.2.2). This line has an extremely high resistance with respect to an out of phase wave, and an extremely low resistance with respect to an in-phase wave.

The balance of an antenna system can also be checked by using the measuring devices described above for measuring potential and current. These devices can be used to plot the curves of potential, or current, distributions on either of the feeder conductors and in this way establish the degree of unbalance.

Tuning the reflector and tuning the feeder to the traveling wave. Tuning the reflector and tuning to the traveling wave on a feeder for a balanced horizontal dipole is no different from similar tuning done for the SG antenna, as will be described in what follows. The traveling wave ratio on the operating waves should be checked in the case of the multiple-tuned balanced dipole. Ordinarily the match of feeder to multiple-tuned dipole can be considered satisfactory if the traveling wave ratio on the operating waves is at least 0.5. There are individual cases when it is permissible to reduce the traveling wave ratio to 0.3 to 0.4.

(b) Tuning and testing the broadside array (SG)

Procedure for tuning and testing the SG antenna. The following is the procedure used to tune and test the SG antenna. Check the antenna insulation. Check the reflector insulation. Check the feeder insulation. Check the switching used for the distribution feeders to the antenna and reflector. Check the antenna system balance. Check the balance of the distribution feeders to the antenna and reflectors. Tune the reflector. Tune the feeder to the traveling wave. The final stage can be the pattern measurement.

Insulation check. Insulation is checked in a manner similar to that used to check the insulation of a balanced dipole. The insulation of the antenna, together with the supply feeder and reflector should be checked.

Switching check. This check involves a determination of proper interconnection of the distribution feeders. It must be ascertained that all right-hand conductors of the downleads from each section are connected to one feeder conductor (or to the loop for tuning the reflector), and that all the left-hand conductors are connected to the other supply feeder conductor (or to the loop for tuning the reflector). Figure XX.2.3 shows examples of correct, and incorrect, ways to connect distribution feeders.

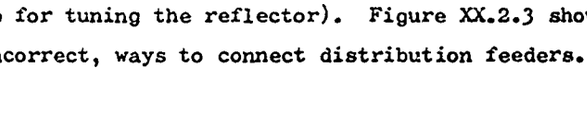

Figure XX.2.3. Connecting distribution feeders. (a) correct; (b) incorrect.

Balance check. Antenna system balance is checked in the same way that the balanced dipole is checked. A balance check should be made not only of the supply feeder conductors, but also of the conductors in the loop for tuning the reflector.

Balancing the supply from the distribution feeders involves providing uniform distribution of the power developed across the antenna to all sections. Equality between voltages (or currents) across the distribution feeders branching from a common point can be used as the criterion that the uniformity with which power is distributed is adequate. Described in what follows is the methodology used for balancing, as applicable to an antenna consisting of four sections (fig. XX.2.4).

First, either half of the antenna, the left-hand side, for example, is balanced. Then the voltage across feeders 1 and 2 at a distance $\lambda/4$ from branch point a is measured by a measuring loop.

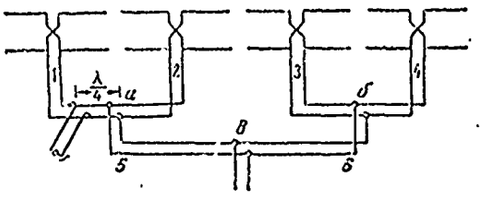

Figure XX.2.4. Schematic diagram of how measurements are made when balancing antenna feed.

If the voltages across feeders 1 and 2 are not the same, the branch point a is moved so as to change the relationship between the lengths of these feeders, and once again the voltages at distances $\lambda/4$ from the new point a position are measured. This procedure is followed until the voltages across feeders 1 and 2 are the same. This same procedure is followed with the second half of the antenna where, by moving point b, the voltages across feeders 3 and 4 are balanced.

The whole array is balanced when the individual sections have been balanced. This involves connecting the measuring loop alternately to feeders 5 and 6 at a distance of $\lambda/4$ from branch point c, and then, by moving this point, balancing the voltages across feeders 5 and 6.

Reflector distribution feeders are balanced similarly. If balancing proves to be difficult because needle deflections are slight when the voltages are measured, the readings can be amplified by tuning the reflector to resonance. This latter procedure is carried out by moving the short-circuiting bridge of the loop used to tune the reflector.

Evaluation of the degree of unbalance is made with respect to the magnitude of the unbalance factor for the distribution feeders, and this equals

$$\delta = \frac{U_1 - U_2}{U_1 + U_2},$$

where

U_1 and U_2 are the voltages across two balanced points on the distribution feeders at a distance $\lambda/4$ from their supply point.

Distribution feeders can be considered to be adequately balanced if the unbalance factor, δ, is not in excess of 5 to 15%.

SG receiving antennas are balanced in the same way as are transmitting antennas. Local oscillators are used to feed receiving antennas.

Reflector tuning. Tuning the reflector of an SG transmitting antenna is with respect to maximum radiation in the outgoing direction, or with respect to minimum radiation in the return direction, depending on which is the most important in each concrete case. Considering the crowded condition existing in the ether, tuning is usually done with respect to the minimum radiation in the return direction.

The reflector is tuned by setting up a field strength indicator at a distance equal to 5 to 10 λ in the outgoing (or return) direction. By moving the short-circuiting bridge, m (fig. XX.2.5), find the location corresponding to the maximum (or minimum) reading on the field strength indicator. A permanent bridge is installed at this point in place of the tuning loop.

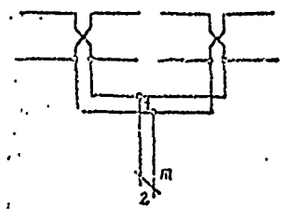

Figure XX.2.5. Reflector tuning diagram.
1-2 - tuning loop; m - bridge.

Tuning the reflector to maximum radiation in the outgoing direction closely coincides with its tuning to resonance, and this can sometimes be used for coarse-tuning the reflector. When this is the procedure a thermoammeter is connected into bridge m. Moving the bridge, find the location corresponding to the maximum reading on the thermoammeter, thus showing that the reflector is tuned to resonance.

A permanent bridge is installed at the point in the loop found in this manner.

This second method for tuning the reflector is not recommended.

The reflector for the 5G receiving antenna is tuned to the minimum reception on the reflector side. A local oscillator with a balanced horizontal dipole, similar to the dipole used with the field strength indicator, is installed at a distance 5 to 10 λ from the antenna in the direction opposite to the direction of maximum reception. Moving bridge m along the reflector tuning loop, find the position at which minimum readings occur on the voltage indicator, which is connected across the antenna supply feeder, at the receiver output.

This requires that the reactance of the loop for the reflector be variable within required limits, and that its length, 1-2, be no shorter than λ/2 (fig. XX.2.5).

Tuning the feeder to the traveling wave. The Tatarinov method. The feeder is tuned to the traveling wave after the reflector is tuned. Tuning the transmitting antenna feeder to the traveling wave has the following advantages:

(1) feeder efficiency is increased;

(2) voltage across the feeder is reduced;

(3) the impedance at the feeder's input terminals can be predetermined and made equal to its characteristic impedance, thus simplifying the matching of the output stage of the transmitter to the feeder.

The feeder must be loaded with resistance equal to its characteristic impedance, W_f, in order to establish the traveling wave regime. In the general case the input impedance of the SG antenna does not equal the characteristic impedance of the supply feeder. An adapter, which transforms antenna impedance into impedance equal to W_f, is used to establish the traveling wave regime. During the first years of use of the SG antenna the adapter was made in the form of very complicated transformers consisting of circuits with lumped constants. Later on these transformers were replaced by more convenient and simpler circuits for use in tuning to the traveling wave suggested by V. V. Tatarinov. The Tatarinov circuit replaces the complicated adapter with a reactance, X, connected across the line at some predetermined location (fig. XX.2.6). The idea behind Tatarinov's circuit is that the equivalent impedance of the feeder at an arbitrary point at distance z_1 from the voltage loop is equal to

$$Z_{eq} = W_f \frac{k - i\,0{,}5(1-k^2)\sin 2\alpha z_1}{k^2\cos^2\alpha z_1 + \sin^2\alpha z_1}, \qquad \text{(XX.2.1)}$$

where

k is the traveling wave ratio on the feeder.

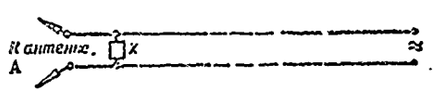

Figure XX.2.6. Schematic of how a feeder is tuned to the traveling wave by the Tatarinov method.

A - to antenna; X - reactance.

The equivalent admittance of the feeder equals

$$Y_{eq} = 1/Z_{eq}.$$

Substituting the expression for Z_{eq}, and converting, we obtain

$$Y_{eq} = G + iB \qquad \text{(XX.2.2)}$$

where

$$G = \frac{1}{W_f}\,\frac{k}{\cos^2\alpha z_1 + k^2\sin^2\alpha z_1}, \qquad \text{(XX.2.3)}$$

$$B = \frac{1}{W_f}\,\frac{0{,}5(1-k^2)\sin 2\alpha z_1}{\cos^2\alpha z_1 + k^2\sin^2\alpha z_1}, \qquad \text{(XX.2.4)}$$

with G and B the resistive and reactive components of the equivalent admittance.

The formulas cited indicate that a feeder with an antenna connected to it can be replaced by the equivalent circuit shown in Figure XX.2.7.

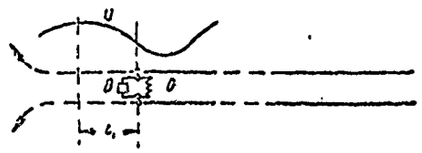

Figure XX.2.7. Equivalent circuit for a feeder with antenna connected to it.

Analysis of formula (XX.2.3) discloses that for certain predetermined z_1 values the component $G = 1/W_f$. If a multiplier reactance X, established through the ratio $1/X = -B$, is connected to the feeder at some one of these points, the reactive component of the equivalent impedance at this point will equal zero and the equivalent impedance of the line will equal $1/G = W_f$. A traveling wave will be established on the feeder on the section between the point of supply and the point at which reactance X is connected. Thus, in order to set up a traveling wave regime on the line it is sufficient to connect to it reactance X at some distance z_1 from the voltage loop, with X and z_1 established through the equations

$$G = \frac{1}{W_f}, \qquad \text{(XX.2.5)}$$

$$\frac{1}{X} = -B. \qquad \text{(XX.2.6)}$$

Substituting the values for G and B from formulas (XX.2.3) and (XX.2.4) in (XX.2.5) and (XX.2.6), we obtain

$$\operatorname{ctg} \alpha z_1 = \pm \sqrt{k}, \qquad \text{(XX.2.7)}$$

$$X = \pm W_f \frac{\sqrt{k}}{1-k}. \qquad \text{(XX.2.8)}$$

From the two possible solutions for z_1 and X, that one is chosen which carries the plus sign because then X is inductive, and this is more favorable, practically speaking.

S. I. Nadenenko suggested making inductance X in the form of a short-circuited stub. The resistance of the short-circuited stub, losses disregarded, equals

$$X = W_{stub} \tan \alpha l_{stub}, \qquad \text{(XX.2.9)}$$

where

W_{stub} and l_{stub} are the characteristic impedance and length of the stub.

Selecting l_{stub}, we can obtain a value for X which will satisfy the equality ac. (XX.2.6). The needed value for l_{stub} is established from the condition that

$$W_{stub} \tan \alpha l_{stub} = W_f \sqrt{k}/1-k, \qquad (XX.2.10)$$

from whence

$$l_{stub} = \lambda/2\pi \cdot \text{arc tan } (W_f/W_{stub} \cdot \sqrt{k}/1-1). \qquad (XX.2.11)$$

If

$$W_f = W_{stub},$$

then

$$l_{stub} = \lambda/2\pi \text{ arc tan } (\sqrt{k}/1-1). \qquad (XX.2.12)$$

The curves for the dependencies of z_1/λ and l_{stub}/λ on k are shown in Figure XX.2.8.

The circuit for tuning a feeder to the traveling wave by using the stub is shown in Figure XX.2.9.

Tuning is in the following sequence. A measuring loop, or other instrument, is used to establish the voltage at the node, U_{node}, and at the loop, U_{loop}. The ratio of these magnitudes equals the natural traveling wave ratio on the feeder, $k = U_{node}/U_{loop}$.

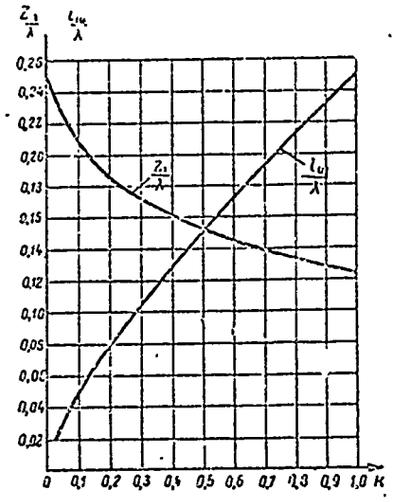

Figure XX.2.8. Dependence of z_1/λ and l_{stub}/λ on the traveling wave ratio.

l_{stub} is the length of the stub used to tune to the traveling wave; z_1 is the distance from the voltage loop to the point where the stub is connected.

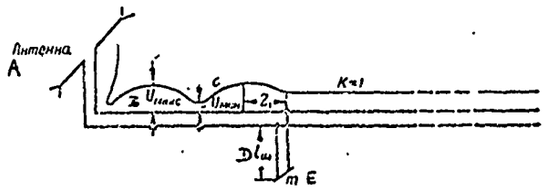

Figure XX.2.9. Schematic diagram of how a feeder is tuned to a traveling wave by using a short-circuited stub.

A - antenna; B - U_{max}; C - U_{min}; D - l_{stub}; E - bridge.

Using formulas (XX.2.7) and (XX.2.11), or the curves in Figure XX.2.8, the point where the connection is made (z_1), and the length of the stub, l_{stub}, are established.

A stub of length l_{stub} is then connected to the line (fig. XX.2.9). Because of inaccuracies in measuring the natural traveling wave ratio, the values for z_1 and l_{stub} found through computations usually do not provide a sufficiently high value for the traveling wave ratio. Final adjustment of the magnitudes of z_1 and l_{stub} is made experimentally after the stub is connected, with the stub moved to right or left, and the bridge, m, moved up or down, and measuring the magnitude of k each time. Adjustment continues until such time as k is high enough. A traveling wave ratio on the order of 0.8 to 0.9 can be considered as quite adequate.

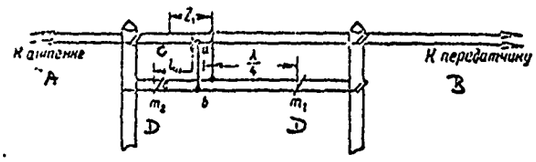

Figure XX.2.10. Variant in the design of a stub for tuning a feeder to a traveling wave.

A - to antenna; B - to transmitter; C - l_{stub}; D - bridge.

Figure XX.2.10 shows one type of stub for tuning a feeder to the traveling wave. A twin line, connected to the feeder by two jumpers, a and b, is stretched between the two poles carrying the feeder at a distance of 0.75 to 1.2 meters from the feeder. Movable bridges are installed in the line on both sides of these jumpers. Bridge m_1, which is at a distance equal to $\lambda/4$ from the jumpers, is used to prevent the right branch of the twin line, which has a higher resistance at b points, from affecting the tuning. Thus, a quarter-wave line replaces the insulators, which would be to the right of point b of the jumpers, ab.

Bridge m_2 is installed at some distance from the jumpers such that the total length of abc is equal to l_{stub}. Moving the jumpers, ab, and the bridges m_1 and m_2, along the feeder, we can choose the necessary magnitudes of z_1 and l_{stub}.

It is desirable to use the section closest to the antenna to tune the feeder so the traveling wave will be established on the longer section of the feeder. A local oscillator is used to tune the SG receiving antenna feeder, and no difference exists between this procedure and that used to tune the SG transmitting antenna feeder. Figure XX.2.11 shows how a stub for tuning the traveling wave on a four-wire receiving feeder is connected. Formula XX.2.11 is used to compute the magnitude of l_{stub}.

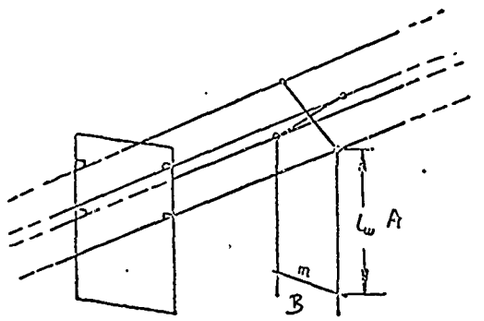

Figure XX.2.11. Schematic diagram of how a four-wire feeder is tuned to a traveling wave.

A - l_{stub}; B - bridge.

Tuning to the traveling wave regime by inserting a line segment with a characteristic impedance different from the characteristic impedance of the feeder. One of the methods used to tune to the traveling wave regime is to insert a line segment with a characteristic impedance different from that of the feeder (fig. XX.2.12). This insert transforms impedance Z_2 at point I into impedance Z_1 at point II.

If the length of the insert with characteristic impedance different from that of the feeder equals $\lambda/4$, the transformation of the impedance by this insert can, in accordance with (I.9.9), be established through the formula

$$Z_{eq} = W_2^2/Z_2, \qquad \text{(XX.2.13)}$$

where

Z_2 is the equivalent impedance of the line ahead of the insert (at points ab, fig, XX.2.12);

Z_{eq} is the equivalent impedance of the line after the insert (at points cd);

W_2 is the characteristic impedance of the insert.

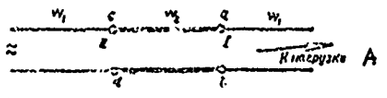

Figure XX.2.12. Matching insert. A - to load.

The insert with length $\lambda/4$ with increased characteristic impedance $W_2 > W_1$, must be inserted in such a way that points ab are at a voltage loop. In this case $Z_2 = W_1/k$.

And

$$Z_{eq} = R_{eq} = W_2^2 k/W_1 \qquad (XX.2.14)$$

$R_{eq} = W_1$ must prevail in order for the traveling wave ratio after the insert to equal unity. If this condition is to be met, and as follows from formula (XX.2.14), W_2 must equal

$$W_2 = W_1/\sqrt{k} \quad . \qquad (XX.2.15)$$

If the insert has a reduced characteristic impedance ($W_2 < W_1$), it must be inserted in such a way that the points ab are at a voltage node. And in order to provide the traveling wave regime the equality

$$W_2 = W_1\sqrt{k} \qquad (XX.2.16)$$

must be satisfied.

A significant increase in the traveling wave ratio can be obtained even when the length of the insert is different from $\lambda/4$ if the point where the insert is installed, and its length, are selected accordingly.

Inserts with increased characteristic impedance can be made quite conveniently in four-wire uncrossed feeders by drawing single-phase conductors together (fig. XX.2.13a).

It is convenient to install an insert with reduced characteristic impedance (fig. XX.2.13b) in a twin line.

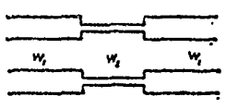

(a)

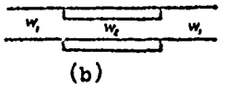

(b)

Figure XX.2.13. Matching inserts in a four-wire non-crossed feeder and in a twin feeder. a - insert with increased characteristic impedance; b - insert with reduced

#XX.3. Tuning and Testing SG and SGD Antennas on Two Operating Waves

(a) General remarks

There are a number of cases when it is necessary to provide for the simultaneous tuning of the same SG or SGD antenna to two operating waves. The SG antenna can, as was pointed out above, be used in some band. If two operating waves are needed within the limits of the operating band, the antenna can be tuned to these waves in the appropriate manner.

The SGDRN antennas are usually made in such a way that no special tuning is required in order to obtain a satisfactory match. But there are individual cases when it can be desirable to tune the antennas so a traveling wave ratio close to unity will be provided on both operating waves, while simultaneously tuning the reflector to these two operating waves.

Given below is the methodology for tuning SG and SGDRN antennas to two fixed operating waves, one which can be used as well for tuning SGDRA antennas, if for some reason it is necessary to provide a traveling wave ratio close to unity on two operating waves.

The antenna is checked and tuned on each of the two fixed waves in the same way as one fixed wave is checked and tuned. The check is made of the insulator, the switching of the distribution feeders, the balance of the antenna system, and the balancing of the distribution feeders, is done in the same way as for the SG antenna.

It is desirable to check the balance of the antenna system on the shorter of the operating waves. Balancing of the distribution feeders is done on one wave and checked on the second. If the balance of the distribution feeders on the second wave is inadequate, it is desirable to select the points for the branching of the distribution feeders such that approximately identical unbalance factors, δ, are obtained on both operating waves. The final decision with respect to the correctness of the antenna feed can be made on the basis of the radiation pattern.

(b) Reflector tuning

It is convenient to tune the reflector initially on the shorter of the operating waves, which we will designate λ_1. The methodology used for tuning is that used to tune the reflector of the SG antenna. The result of tuning to wave λ_1 is finding the point at which bridge m_1 must be installed, so as to ensure the optimum reflector regime on this wave. Then a short-circuited line of length $\lambda_1/2$ (fig. XX.3.1) is installed in place of the bridge. This serves to act as a short-circuiter on wave λ_1. Once this line is in place the reflector is tuned to the second wave (λ_2).

Short-circuiting bridge m_2 is then shifted to the other section of the tuning stub and secured in place at the point corresponding to the minimum radiation in the return direction, or to the maximum radiation in the outgoing direction. Section 1-2 must be no shorter than $\lambda_2/2$ in order to be certain that it will be possible to tune the reflector to wave λ_2.

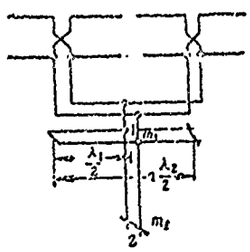

Figure XX.3.1. Schematic diagram for tuning the reflector of SGD and SG antennas to two waves. m - bridge.

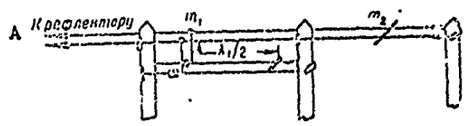

Figure XX.3.2. Design of the circuit shown in Figure XX.3.1. A - to reflector; m - bridge.

How the reflector will tune to wave λ_2 will depend on how it was tuned to wave λ_1. If it is desirable to tune to both waves independently, this can be done by adding an additional short-circuited stub to the $\lambda_1/2$ stub, so that the total length of both stubs will equal n $\lambda_2/2$. In Figure XX.3.1 the booster stub is shown by the broken line.

Another design for tuning a reflector to two waves is shown in Figure XX.3.2. The additional stub, which is for decoupling tuning to waves λ_1 and λ_2, is not shown in Figure XX.3.2.

(c) Tuning the feeder to the traveling wave

Tuning is done in such a way that the traveling wave regime is obtained on both operating waves, λ_1 and λ_2. Combination stubs which, while tuning the feeder to the traveling wave on one wave, offer extremely high impedance to the second wave and pass it without changing the regime on the feeder, are used for this purpose.

Different types of combination stub circuits, and methods for using them, are possible. One such is shown in Figure XX.3.3. When this one is used tuning of the feeder to the traveling wave is done first on the longer wave, λ_2. Tuning is by the method described above for tuning the SG antenna. A simple short-circuited line, with length $l_{stub\ 2}$, is used as the tuning stub.

What must be attempted here is to connect the stub $l_{stub\ 2}$ at a point where the reactive component of the equivalent admittance for the feeder on wave λ_1 is capacitive in nature. This makes it necessary to connect the stub for tuning to wave λ_2 in the section between the loop and the first voltage node of wave λ_1 following the loop. The rading is made from the voltage loop to the transmitter. In this case stub $l_{stub\ 2}$ can increase the traveling wave ratio on wave λ_1 somewhat.

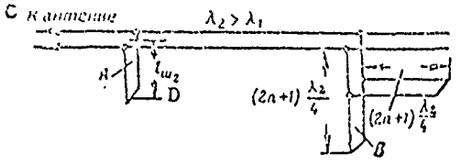

Figure XX.3.3. One version of the arrangement for tuning a two-wire feeder to a traveling wave when operating on two waves.

A - stub for tuning feeder to wave λ_2; B - combination stub for tuning feeder to wave λ_1; C - to antenna; D - $l_{stub\ 2}$.

The feeder is tuned to wave λ_1 after it has been tuned to wave λ_2. A simple stub is used for the initial tuning. Establishing point z_1 and length $l_{stub\ 1}$, for the stub, it is then replaced by a combination stub which consists of two lines each of length $(2n + 1)\lambda_2/4$, where n = 0, 1, 2, ... (fig. XX.3.3). The input impedance of this combination of two lines on wave λ_2 is extremely high, so connecting it to the feeder has no effect on the feeder regime on this wave.

At the same time, by selecting the point at which one line is connected to the other, the input impedance of this system on wave λ_1 can be made equal to the input impedance of the simple stub of length $l_{stub\ 1}$, thus providing for tuning to wave λ_1.

Selection of the necessary lengths for the elements of the combination stub is by computation, and then these are refined experimentally.

Thus, when the transmitter is operating on wave λ_2, the combination stub passes this wave, causing no change in feeder regime, and the simple stub $l_{stub\ 2}$ sets up a traveling wave on the feeder.

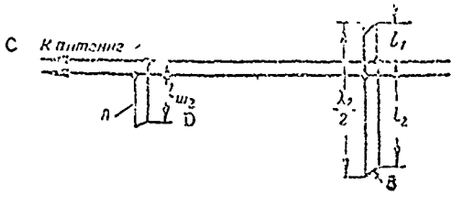

Figure XX.3.4. Second version of the arrangement for tuning a two-wire feeder to a traveling wave when operating on two waves.

A - stub for tuning feeder to wave λ_2; B - combination stub for tuning feeder to wave λ_1; C - to antenna; D - $l_{stub\ 2}$.

Another combination stub arrangement is shown in Figure XX.3.4. The total length of this combination stub $(l_1 + l_2)$ should be equal to $\lambda_2/2$. Regardless of the ratios of l_1/l_2 (with the exception of those close to zero,

or to infinity), the combination stub offers extremely great impedance to wave λ_2 and passes it without reflection. We can, so far as wave λ_1 is concerned, by selecting the l_1/l_2 ratio, obtain an impedance equal to the impedance of a simple stub of length $l_{stub\ 1}$, and thus tune the feeder to the traveling wave.

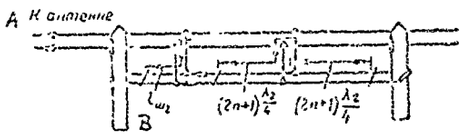

Figure XX.3.5. Design for the arrangement in Figure XX.3.3.
A - to antenna; B - $l_{stub\ 2}$.

Desigrs for the arrangements in figures XX.3.3 and XX.3.4 are shown in figures XX.3.5 and XX.3.6.

The arrangements shown for tuning the SG antenna to two waves feature the fact that tuning to wave λ_1 depends on tuning to wave λ_2. As a practical matter, and particularly when one, or both operating waves change from time to time, it is convenient to have independent tuning. The combination stub shown in Figure XX.3.4 can be used for this purpose on wave λ_1 as well as wave λ_2. Figure XX.3.7. shows an arrangement for independent tuning to two waves.

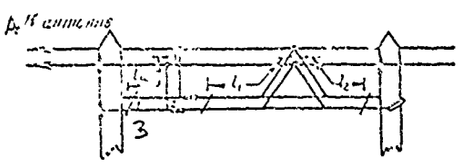

Figure XX.3.6. Design for the arrangement in Figure XX.3.4.
A - to antenna; B - $l_{stub\ 2}$.

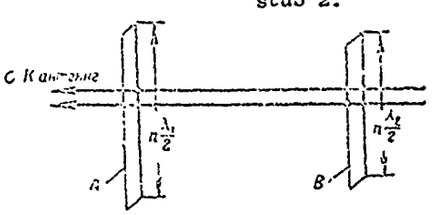

Figure XX.3.7. Schematic diagram of independent tuning of a feeder to two waves.

A - combination stub for tuning the feeder to wave λ_2;
B - combination stub for tuning the feeder to wave λ_1;
C - to antenna.

In the special case when $\lambda_2 = 2\lambda_1$, the most convenient arrangement to use for independent tuning is that shown in Figure XX.3.8. As will be seen, two short-circuiting stubs with lengths $\lambda_1/2 = \lambda_2/4$ are used to tune to wave λ_1. These stubs offer extremely high impedance to wave λ_2 and have no

noticeable effect on the feeders. When operating on wave λ_1 stub 2'4' causes a short circuit to occur at point 2', and this causes the combination stub as a whole to act like a segment with length $l_{stub\ 1}$ needed to tune to wave λ_1.

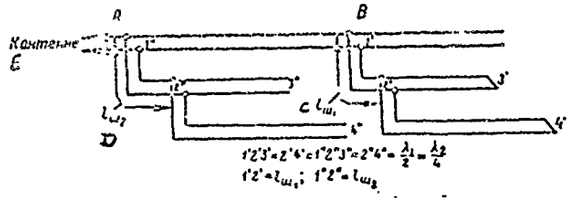

Figure XX.3.8. Variant of the arrangement for independent tuning of a feeder to two short waves ($\lambda_2=2\lambda_1$).

A - combination stub for tuning to wave λ_1; B - combination stub for tuning to wave λ_2; C - length of the stub needed to tune the feeder to the traveling wave regime when operating on wave λ_1; D - length of the stub needed to tune the feeder to the traveling wave regime when operating on wave λ_2; E - to antenna.

The tuning to wave λ_2 is done by the open-ended stubs with length $\lambda_1/2 = \lambda_2/4$. These stubs have extremely high impedance for wave λ_1, so have no noticeable effect on the feeders. When operating on wave λ_2 stub 2"4" causes a short circuit at point 2", and at the same time provides the equivalent of the entire combination stub to the short-circuiting segment of length $l_{stub\ 2}$ needed to tune to wave λ_2.

#XX.4. Testing and Tuning SGDRN and SGDRA Antennas

The check made of insulation and balance of the antenna system, as well as supply balance is made as in the case of the SG antenna. It must be borne in mind that the proper supply distribution must be made to correspond to the same length of current path from the point of branching to the dipoles, or to the next distribution feeder.

Tuning the reflector for the SGDRN antenna in accordance with conditions is done on one, or on two waves (see #XX.3).

Normally, SGDRN and SGDRA antenna feeders are not tuned to the traveling wave regime because they have an adequately satisfactory normal match with the supply line. When the antennas are put into service they should be checked for the traveling wave ratio on at least three or four waves, and should be checked, in particular, on the proposed operating waves. If the measured values of the traveling wave ratio are substantially lower than those suggested on the antenna's name plate a careful check should be made as to the correctness of the dimensions of the antenna array. One reason for a reduction in the traveling wave ratio can be incorrect feeder bends. Identity

in the lengths of the feeder conductors must be provided for at the sites of bends, and the characteristic impedances must be retained intact.

#XX.5. Testing the Rhombic Antenna and the Traveling Wave Antenna

The rhombic antenna and the traveling wave antenna operate over a band of waves and require no special tuning. Prior to being put into service, and periodically during operation, they are tested to check the correctness of the distribution feeder connections, insulation, supply balance of the distribution feeders (in a multiple antenna). Also checked is antenna system balance, the match of antenna and feeder, and the magnitudes of the terminator and decoupling resistors, which are measured by an ohmmeter.

It is desirable to check antenna system balance, as well as the supply balance for the distribution feeders running from the supply feeder and the dissipation line, at least on two waves. The supply points are set up in the geometric center of the distribution feeders.

It is desirable to check the match of antenna and feeder on at least two or three waves in the operating band for the antenna. The match of antenna and feeder can be considered satisfactory if the traveling wave ratio for the operating band is at least 0.6 to 0.7.

Correctness of supply line lengths must be carefully checked when 3BS2 antennas are put into service. The required relationship between the lengths of the feeders for adjacent BS2 antennas in the 3BS2 antenna complex (see Chapter XIV) must be observed with an accuracy of within 0.5 meter.

The check of supply line lengths must consider the complete path traveled by the current, beginning at the point of connection to the collection line and ending at the phase shifter terminals. The correctness of the connections of feeders to the phase shifter must also be checked very carefully (to make sure there is no 180° phase rotation as a result of crossing the feeder conductors).

#XX.6. Pattern measurement

Radiation patterns in the vertical and horizontal planes provide a representation of the correctness of tuning, and an overall picture of radiation from the antennas, as well as making it possible to reveal indirect radiation from conductors adjacent to the antenna, if such is taking place.

Pattern measurement in the horizontal plane is made on the earth's surface, or at some angle to the horizon.

The radiation pattern is measured from an aircraft or a helicopter at a distance from the earth's surface. The field intensity indicator described above is usually used to measure the pattern at the earth's surface. The indicator is moved around the antenna in a circle, the center of which coincides with the center of the antenna. The radius of the circle should be

at least six to ten times a maximum linear dimension of the antenna (width, length, height). It is desirable that the area round the antenna within the limits of this radius be level and free of installations of various types. Efforts should be made to keep the height at which the indicator is set up at the different points the same. Field intensity is measured every 3° to 5°. Measurements should be made at points distant from structures, feeders, protrusions, depressions, and installations of various types.

If terrain conditions are such that the indicator must be set up at different distances from the center of the antenna, reducing the data from the measurements to the same distance is done by taking into consideration the fact that the field strength of a ground wave is inversely proportional to the square of the distance.

The constancy of the power radiated by an antenna is monitored either by using a second, fixed, field intensity indicator, usually located in the direction of maximum radiation, or by a voltage or current indicator in the antenna.

The readings of both indicators are recorded simultaneously and the ratio of the readings from the fixed indicator to the readings of the mobile one is taken. The effect of change in transmitter power on the results of the measurements is excluded.

It is more desirable to measure the pattern from an aircraft, or from a helicopter, because then it is possible to obtain a picture of the radiation distribution at angles of elevation corresponding to the beams prevailing at the reception site.

It is most convenient to measure the pattern of a receiving antenna by moving a local oscillator with a dipole around it and measuring the emf across the receiver input connected to the supply feeder. The emf at the receiver input is measured by comparison, using a standard signal generator.

#XX.7. Measuring Feeder Efficiency

The efficiency of a feeder is measured by establishing the voltages at nodes and loops at the origin and termination of the feeder. The efficiency is established through the formula

$$\eta = U'_{node} U'_{loop} / U_{node} U_{loop}, \qquad (XX.7.1)$$

where

U'_{node} and U'_{loop} are the voltages at the node and loop at the termination of the feeder;

U_{node} and U_{loop} are voltages at the node and loop at the origin of the feeder.

Two voltage indicators are needed to make the measurements, one as a monitor, connected at some point on the feeder, and fixed in place, the other for measuring at the voltage nodes and loops.

If transmitter power changes during the measurements, formula (XX.7.1) is used and the ratio of the readings from the mobile voltage indicator to the readings from the fixed voltage indicator is substituted in it.

Attention must be given to the identity of distances between feeder conductors at all measurement points, otherwise the measurement results can be distorted because of lack of identity in feeder characteristic impedance at measurement points.

The efficiency measured in this way characterizes feeder losses for the prevailing traveling wave ratio. Formula XIX.2.2, or the curves shown in Figure XIX.2.8, can be used to establish the efficiency when the traveling wave ratio equals unity.

The efficiency can also be established by measuring the traveling wave ratio on a short-circuited, or open-ended, feeder. The attenuation factor on the feeder is established through formulas (I.8.2) or (I.8.3), using the traveling wave ratio value found. The efficiency can be established through formulas (I.14.2) or (I.14.3), using the magnitude of β found.

APPENDICES

Appendix 1

Derivation of an approximation formula for the characteristic impedance of a uniform line

$$\rho = \sqrt{\frac{iL_1\omega + R_1}{iC_1\omega + G_1}}.$$

Ignoring G_1, and converting, we obtain

$$\rho = \sqrt{\frac{L_1}{C_1}}\sqrt{1 - i\frac{R_1}{L_1\omega}} = W\sqrt{1 - i\frac{R_1}{L_1\omega}}, \qquad (A.1.1)$$

and since $R_1 \ll L_1\omega$,

$$\rho \approx W\left(1 - i\frac{R_1}{2L_1\omega}\right). \qquad (A.1.2)$$

As is known, for a uniform line $L_1C_1 = 1/c^2$, from whence

$$C_1 = \frac{1}{L_1c^2}, \qquad (A.1.3)$$
$$W = \sqrt{\frac{L_1}{C_1}}.$$

Substituting for C_1 its expression from (A.1.3), we obtain

$$W = L_1c. \qquad (A.1.4)$$

Substituting $\omega = \alpha c$ in formula (A.1.2), and taking formula (A.1.4) into consideration, we obtain

$$\rho \approx W\left(1 - i\frac{R_1}{2W\alpha}\right), \qquad (A.1.5)$$

and since

$$\frac{R_1}{2W} = \beta,$$

then

$$\rho \approx W\left(1 - i\frac{\beta}{\alpha}\right). \qquad (A.1.6)$$

Appendix 2

Derivation of the traveling wave ratio formula

The minimum voltage across a line is obtained at the point where $U_{incident}$ and $U_{reflected}$ are opposite in phase

$$U_{minimum} = |U_{in}| - |U_{re}|. \qquad (A.2.1)$$

The maximum voltage is obtained at the point where U_{in} and U_{re} coincide in phase

$$U_{maximum} = |U_{in}| + |U_{re}|. \qquad (A.2.2)$$

Substituting the values for U_{min} and U_{max} in the expression for k, we obtain

$$k = \frac{U_{min}}{U_{max}} = \frac{|U_{in}| - |U_{re}|}{|U_{in}| + |U_{re}|} = \frac{1 - |U_{re}|/|U_{in}|}{1 + |U_{re}|/|U_{in}|} = \frac{1 - |p|}{1 + |p|} \qquad (A.2.3)$$

Appendix 3

Derivation of the formula for transmission line efficiency

Let us designate the line output power by P_1, and the power reaching the load by P_2. Then

$$\eta = P_2/P_1. \qquad (A.3.1)$$

P_1 equals the difference in the powers of the incident and reflected waves at the point of application of the emf, that is, at the beginning of the line

$$P_1 = P_{1\,in} - P_{1\,re}, \qquad (A.3.2)$$

$$P_{1\,in} = I_{1\,in}^2 W,$$

$$P_{1\,re} = I_{1\,re}^2 W,$$

$I_{1\,in}$ and $I_{1\,re}$ are the currents in the incident and reflected waves at the point of application of the emf.

$$P_1 = (I_{1\,in}^2 - I_{1\,re}^2)W. \qquad (A.3.3)$$

Similarly, the output power at the termination equals

$$P_2 = (I_{2\,in}^2 - I_{2\,re}^2)W. \qquad (A.3.4)$$

$I_{2\,in}$ and $I_{2\,re}$ are the currents in the incident and reflected waves at the termination.

Substituting the expressions for P_1 and P_2 in formula (A.3.1), we obtain.

$$\eta = I_{2\,in}^2 - I_{2\,re}^2 / I_{1\,in}^2 - I_{1\,re}^2 \qquad (A.3.5)$$

We note that

$$\left.\begin{aligned} I_{1\,in} &= I_{2\,in} e^{\beta l} \\ I_{1\,re} &= I_{2\,re} e^{-\beta l} \end{aligned}\right\} \qquad (A.3.6)$$

Substituting formula (A.3.6) in (A.3.5), we obtain

$$\eta = \frac{I_{2in}^2 - I_{2re}^2}{I_{2in}^2 e^{2\beta l} - I_{2re}^2 e^{-2\beta l}} = e^{-2\beta l} \frac{1 - \left(\frac{I_{2re}}{I_{2in}}\right)^2}{1 - \left(\frac{I_{2re}}{I_{2in}}\right)^2 e^{-4\beta l}} = \qquad (A.3.7)$$

$$= e^{-2\beta l} \frac{1 - |p|^2}{1 - |p|^2 e^{-4\beta l}}.$$

Appendix 4

Derivation of the radiation pattern formulas for SG and SGD antennas

In its general form, the radiation pattern for the SG and SGD antennas can be expressed in the following manner

$$E = f_1(i) \cdot f_2(n_2) \cdot f_3(n_1) \cdot f_4(g) \cdot f_5(r), \qquad (A.4.1)$$

where

$f_1(i)$ is a factor which takes into consideration the directional properties of a balanced dipole, which is the basic element of an antenna;

$f_2(n_2)$ is a factor which takes into consideration the presence of n_2 balanced dipoles in each of the antenna tiers;

$f_3(n_1)$ is a factor which takes into consideration the fact that there are n_1 tiers in the antenna;

$f_4(g)$ is a factor which takes the ground effect into consideration;

$f_5(r)$ is a factor which takes the effect of the reflector into consideration.

Let us find the expressions for the individual factors.

(1) the factor $f_1(i)$

The field strength for a balanced dipole equals

$$E = f_1(l) = \frac{60I}{r} \cdot \frac{\cos(\alpha l \cos\theta) - \cos\alpha l}{\sin\theta}.$$

θ is the angle formed by the direction of the beam and the dipole axis.

(2) the factor $f_2(n_2)$

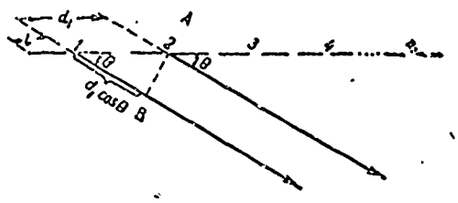

Figure A.4.1.

Let there be n_2 balanced dipoles located in one line (fig. A.4.1). The total field strength for all balanced dipoles equals

$$E_l = E_1 + E_2 \ldots + E_{n_2}. \qquad (A.4.2)$$

Let us assume the amplitudes and phases of the currents in all balanced dipoles to be identical, as is the case for SG and SGD antennas. Accordingly, the amplitudes of the field strength vectors (E_1, E_2, ..., E_{n_2}) are equal to each other, and the phase shift between them can only be determined by the difference in the path of the beams.

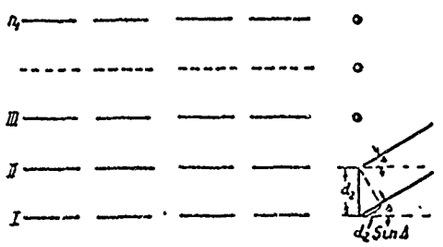

Figure A.4.2.

As will be seen from Figure A.4.1, the difference in the paths of the beams from dipoles 1 and 2 equals

$$d_1 \cos\theta,$$

where

d_1 is the distance between the centers of two adjacent balanced dipoles.

The phase shift between E_1 and E_2 equals

$$\psi_2 = \alpha d_1 \cos\theta \qquad \text{(A.4.3)}$$

and

$$E_2 = E_1 e^{j\alpha d_1 \cos\theta}. \qquad \text{(A.4.4)}$$

Similarly,

$$E_3 = E_2 e^{j\alpha d_1 \cos\theta} = E_1 e^{j2\alpha d_1 \cos\theta}, \qquad \text{(A.4.5)}$$

$$E_4 = E_1 e^{j3\alpha d_1 \cos\theta}, \qquad \text{(A.4.6)}$$

. . . . . .

$$E_{n_2} = E_1 e^{j(n_2-1)\alpha d_1 \cos\theta}. \qquad \text{(A.4.7)}$$

The summed field for all n_2 dipoles equals

$$E_\Sigma = E_1 \left[1 + e^{j\alpha d_1 \cos\theta} + e^{j2\alpha d_1 \cos\theta} + \ldots + e^{j(n_2-1)\alpha d_1 \cos\theta}\right]. \qquad \text{(A.4.8)}$$

The right side of the equality at (A.4.8) is the sum of the terms of a geometric progression of the type

$$S = q + qa + qa^2 + qa^3 + \ldots + qa^{n-1}.$$

As is known

$$S = q\,\frac{a^n - 1}{a - 1},$$

In this case,

$$q = E_1;\ a = e^{j\alpha d_1 \cos\theta}.$$

As a result, we obtain

$$E_I = E_1 \frac{e^{jn_2\alpha d_1\cos\theta} - 1}{e^{j\alpha d_1\cos\theta} - 1} = E_1 f_2(n_2), \tag{A.4.9}$$

where

$$f_2(n_2) = \frac{e^{jn_2\alpha d_1\cos\theta} - 1}{e^{j\alpha d_1\cos\theta} - 1}. \tag{A.4.10}$$

(3) the factor $f_3(n_1)$

Figure A.4.2 contains the sketches of an antenna array consisting of n_1 tiers in two projections.

The summed field for all tiers equals

$$E_\Sigma = E_I + E_{II} + \ldots + E_{n_1}. \tag{A.4.11}$$

Let us assume that the currents flowing in the dipoles in all tiers are the same in magnitude and in phase. Then the amplitudes of E_I, E_{II} ... E_{n1} will be equal to each other, and the phase shift between them can only be determined by the difference in the paths of the respective beams.

The difference in the paths of the beams from the dipoles located in the first and second tiers equals

$$d_2 \sin\Delta,$$

where

d_2 is the distance between the antenna tiers.

The phase shift between E_{II} and E_I equals

$$\psi_{II} = \alpha d_2 \sin\Delta. \tag{A.4.12}$$

Thus,

$$E_{II} = E_I\, e^{j\alpha d_2\sin\Delta}. \tag{A.4.13}$$

Similarly,

$$E_{III} = E_{II}\, e^{j\alpha d_2\sin\Delta} = E_I\, e^{j2\alpha d_2\sin\Delta}, \tag{A.4.14}$$

$$E_{IV} = E_I\, e^{j3\alpha d_2\sin\Delta}. \tag{A.4.15}$$

. . . . . .

$$E_{n_1} = E_I\, e^{j(n_1-1)\alpha d_2\sin\Delta}. \tag{A.4.16}$$

The summed field strengths for all n_1 tiers equal

$$E_\Sigma = E_I\left[1 + e^{j\alpha d_2\sin\Delta} + e^{j2\alpha d_2\sin\Delta} + \ldots + e^{j(n_1-1)\alpha d_2\sin\Delta}\right] =$$

$$= E_I \frac{e^{jn_1\alpha d_2\sin\Delta} - 1}{e^{j\alpha d_2\sin\Delta} - 1} = E_I \cdot f_2(n_1), \tag{A.4.17}$$

from whence

$$f_{3(n_1)} = \frac{e^{jn_1 \alpha d_2 \sin\Delta} - 1}{e^{j\alpha d_2 \sin\Delta} - 1}. \qquad (A.4.18)$$

(4) the factor $f_4(g)$

The influence of the mirror image on t` field strength of a horizontal dipole and ideally conducting ground can be determined by the factor $(1 - e^{-i2\alpha H \sin\Delta})$, where H is the height at which the dipole is suspended.

In our case we are discussing a multitiered, cophasally fed system, so H should be understood to mean the average height at which the antenna dipoles are suspended (H_{av})

$$H_{av} = H_1 + (n_1 - 1)d_2/2 , \qquad (A.4.19)$$

where

H_1 is the height at which the lower tier of the antenna is suspended.

Accordingly, the factor $f_4(g)$ can be expressed by the formula

$$f_4(g) = 1 - e^{-i2\alpha H_{av} \sin\Delta}. \qquad (A.4.20)$$

(5) the factor $f_5(r)$

As explained above, the influence of the reflector on the field strength of a balanced dipole can be expressed by the factor

$$\sqrt{1 + m^2 + 2m\cos(\psi - \alpha d_3 \cos\varphi \cos\Delta)},$$

where d_3 is the distance between the antenna and the reflector.

The SG and SGD antennas we are considering have an identically located dipole at the reflector for every dipole in the antenna. Therefore, the influence of the entire reflector on the antenna must be characterized by the same mathematical formula as that used in the case of the antenna consisting of one dipole and a reflector.

Accordingly,

$$f_5(r) = \sqrt{1 + m^2 + 2m\cos(\psi - \alpha d_3 \cos\varphi \cos\Delta)}. \qquad (A.4.21)$$

(6) the complete formula for the radiation patterns propagated by SG and SGD antennas.

Substutiting the expressions for $f_1(i)$, $f_2(n_2)$, $f_3(n_1)$, $f_4(g)$ and $f_5(r)$ in (A.4.1), we obtain

$$E = \frac{60I}{r} \frac{\cos(\alpha l' \cos\theta) - \cos\alpha l}{\sin\theta} \frac{e^{jn_1 \alpha d_1 \cos\theta} - 1}{e^{j\alpha d_1 \cos\theta} - 1} \frac{e^{jn_1 \alpha d_2 \sin\Delta} - 1}{e^{j\alpha d_2 \sin\Delta} - 1} \times$$
$$\times (1 - e^{-i2\alpha H_{av} \sin\Delta}) \sqrt{1 + m^2 + 2m\cos(\psi - \alpha d_3 \cos\varphi \cos\Delta)}. \qquad (A.4.22)$$

By using Euler's formulas, which yield the dependence between the indexes and the trigonometric functions, it is not difficult to prove the equality

$$e^{\pm i\psi} - 1 = i\,2\sin\frac{\psi}{2}\,e^{\pm i\frac{\psi}{2}}. \qquad (A.4.23)$$

Using this formula, and taking it that

$$\cos\theta = \cos(90^\circ - \varphi)\cos\Delta = \sin\varphi\cos\Delta, \qquad \sin\theta = \sqrt{1-\cos^2\theta} = \sqrt{1-\sin^2\varphi\cdot\cos^2\Delta},$$

we obtain the following expression for the modulus of the vector for field strength

$$E = \frac{120I}{r}\,\frac{\cos(\alpha l\sin\varphi\cos\Delta) - \cos\alpha l}{\sqrt{1-\sin^2\varphi\cdot\cos^2\Delta}}\,\frac{\sin\left(n_2\frac{\alpha d_1}{2}\sin\varphi\cdot\cos\Delta\right)}{\sin\left(\frac{\alpha d_1}{2}\sin\varphi\cdot\cos\Delta\right)}\times$$

$$\times\,\frac{\sin\left(n_1\frac{\alpha d_2}{2}\sin\Delta\right)}{\sin\left(\frac{\alpha d_2}{2}\sin\Delta\right)}\sin(\alpha H_{0\nu}\sin\Delta)\sqrt{1+m^2+2m\cos(\psi-\alpha d_2\cos\varphi\cos\Delta)}. \qquad (A.4.24)$$

Formula (A.4.24) is suitable for computing the radiation patterns for SG and SGD antennas on any wavelength, given the condition of the cophasal nature of the feed to all the balanced dipoles in the antennas.

In the SG antenna

$$d_1 = \lambda$$

$$d_2 = l = \frac{\lambda}{2},$$

from whence

$$\alpha d_1 = 2\pi,$$

$$\alpha d_2 = \alpha l = \pi. \qquad (A.4.25)$$

Substituting formula (A.4.25) in (A.4.24) and converting, we obtain

$$E = \frac{120I}{r}\,2\,\frac{\cos^2\left(\frac{\pi}{2}\sin\varphi\cos\Delta\right)}{\sqrt{1-\sin^2\varphi\cos^2\Delta}}\,\frac{\sin(n_2\pi\sin\varphi\cos\Delta)}{\sin(\pi\sin\varphi\cos\Delta)}\,\frac{\sin\left(n_1\frac{\pi}{2}\sin\Delta\right)}{\sin\left(\frac{\pi}{2}\sin\Delta\right)}\times$$

$$\times\sin(\alpha H_{0\nu}\sin\Delta)\sqrt{1+m^2+2m\cos(\psi-\alpha d_2\cos\varphi\cos\Delta)}. \qquad (A.4.26)$$

Substituting in formula (A.4.26)

$$n_2 = n/2,$$

where

n is the number of half-wave dipoles in one tier, and

$$\sin(\pi\sin\varphi\cos\Delta) = 2\sin\left(\frac{\pi}{2}\sin\varphi\cos\Delta\right)\cos\left(\frac{\pi}{2}\sin\varphi\cos\Delta\right),$$

we reduce it to the following form

$$E = \frac{120I}{r}\,\frac{\operatorname{ctg}\left(\frac{\pi}{2}\sin\varphi\cos\Delta\right)\sin\left(n\frac{\pi}{2}\sin\varphi\cos\Delta\right)\sin\left(n_1\frac{\pi}{2}\sin\Delta\right)}{\sqrt{1-\sin^2\varphi\cos^2\Delta}\cdot\sin\left(\frac{\pi}{2}\sin\Delta\right)}\times$$

$$\times\sin(\alpha H_{0\nu}\sin\Delta)\sqrt{1+m^2+2m\cos(\psi-\alpha d_2\cos\varphi\cos\Delta)}. \qquad (A.4.27)$$

Appendix 5

Derivation of the radiation pattern formula for a rhombic antenna

#A.5.1. The field strength created by the separate sides of a rhombic antenna

Let us take an arbitrary direction which has azimuth angle φ, read from the long diagonal of the rhombus, and an angle of tilt Δ, read from the horizontal plane (fig. A.5.1).

Let us introduce the notations:

l is the length of a side of rhe thombus;

θ_1 is the angle formed by the direction of the beam and sides 1-2 and 4-3 of the rhombus;

θ_2 is the angle formed by the direction of the beam and sides 2-3 and 1-4 of the rhombus;

I_0 is the current flowing at the origin of side 1-2;

I_{01} is the current flowing at the origin of side 2-3;

γ is the propagation factor on the conductors of the rhombus.

The field strength created by a rhombic antenna equals

$$E = E_{12} + E_{23} + E_{43} + E_{14}. \qquad (A.5.1)$$

where E_{12}, E_{23}, E_{43} and E_{14} are the field strengths created by sides 1-2, 2-3, 4-3, and 1-4.

In accordance with formula (V.2.1), and discarding the factor i, we obtain

$$E_{12} = \frac{60\pi}{r\lambda} I_0 \sin\theta_1 \frac{e^{(i\alpha\cos\theta_1-\gamma)l}-1}{i\alpha\cos\theta_1-\gamma}, \qquad (A.5.2)$$

$$E_{23} = \frac{60\pi}{r\lambda} I_{01} \sin\theta_2 \frac{e^{(i\alpha\cos\theta_2-\gamma)l}-1}{i\alpha\cos\theta_2-\gamma} e^{i\psi_1}, \qquad (A.5.3)$$

$$E_{43} = -\frac{60\pi}{r\lambda} I_{01} \sin\theta_1 \frac{e^{(i\alpha\cos\theta_1-\gamma)l}-1}{i\alpha\cos\theta_1-\gamma} e^{i\psi_2}, \qquad (A.5.4)$$

$$E_{14} = -\frac{60\pi}{r\lambda} I_0 \sin\theta_2 \frac{e^{(i\alpha\cos\theta_2-\gamma)l}-1}{i\alpha\cos\theta_2-\gamma}. \qquad (A.5.5)$$

where

ψ_1 is the component of the phase shift angle between the field strength vectors for sides 2-3 and 1-4, determined by the difference in the beam paths;

ψ_2 is the component of the phase shift angle between the field strength vectors for sides 4-3 and 1-2, determined by the difference in the beam paths.

The minus signs in the right-hand sides of equations (A.5.4) and (A.5.5) take into consideration the opposite phases of the currents flowing in sides 1-4 and 4-3 relative to the currents flowing in sides 1-2 and 2-3.

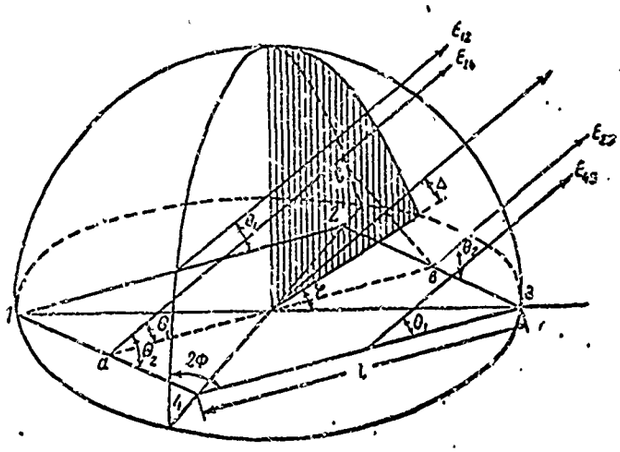

Figure 5.1.

The magnitude of ψ_1 can be determined by the difference in the beam paths from identically located points on sides 1-4 and 2-3, say points a and b. The difference in beam paths from point a, located in side 1-4, and point b, located in side 2-4, is equal to the segment ac. The length of this segment equals $l \cos \theta_i$. Accordingly,

$$\psi_1 = \alpha l \cos \theta_1. \qquad \text{(A.5.6)}$$

similarly,

$$\psi_2 = \alpha l \cos \theta_2, \qquad \text{(A.5.7)}$$

$$I_{01} = I_0 e^{-\gamma l}. \qquad \text{(A.5.8)}$$

Let us express angles θ_1 and θ_2 in terms of the angle of tilt Δ and the azimuth angle φ (fig. A.5.2):

$$\left.\begin{aligned} \cos \theta_1 &= \cos \varphi_1 \cos \Delta \\ \cos \theta_2 &= \cos \varphi_2 \cos \Delta \end{aligned}\right\}, \qquad \text{(A.5.9)}$$

where

φ_1 is the azimuth angle of the beam, read from the direction of sides 1-2 and 4-3;

φ_2 is the azimuth angle of the beam, read from the direction of sides 2-3 and 1-4.

As will be seen from Figure A.5.2,

$$\left.\begin{aligned}\varphi_1 &= \varphi - \varphi_0\\ \varphi_2 &= \varphi + \varphi_0\end{aligned}\right\}, \tag{A.5.10}$$

where

$$\varphi_0 = 90^\circ - \Phi, \tag{A.5.11}$$

from whence

$$\left.\begin{aligned}\varphi_1 &= \varphi + \Phi - 90^\circ\\ \varphi_2 &= \varphi - \Psi + 90^\circ\end{aligned}\right\}. \tag{A.5.12}$$

Substituting formulas (A.5.12) in (A.5.9), we obtain

$$\left.\begin{aligned}\cos\theta_1 &= \cos(\varphi + \Phi - 90^\circ)\cos\Delta = \sin(\varphi + \Phi)\cos\Delta\\ \cos\theta_2 &= \cos(\varphi - \Phi + 90^\circ)\cos\Delta = \sin(\Phi - \varphi)\cos\Delta\end{aligned}\right\} \tag{A.5.13}$$

Substituting the expressions for $\cos\theta_1$ and $\cos\theta_2$ in formulas (A.5.6) and (A.5.7), we obtain

$$\psi_1 = \alpha l \sin(\Phi + \varphi)\cos\Delta. \tag{A.5.14}$$

$$\psi_2 = \alpha l \sin(\Phi - \varphi)\cos\Delta. \tag{A.5.15}$$

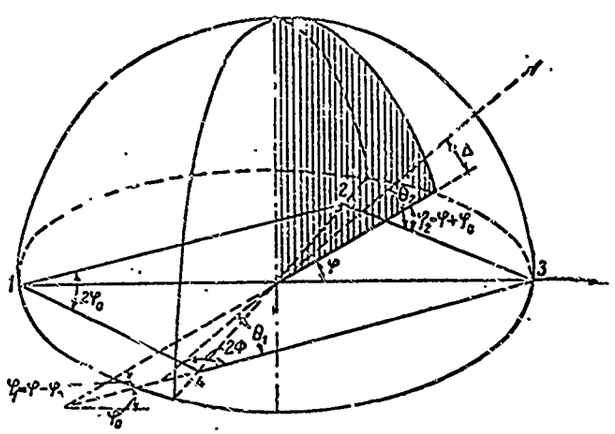

Figure A.5.2.

Substituting the expressions for ψ_1, ψ_2, I_{01}, $\cos\theta_1$ and $\cos\theta_2$ in formulas (A.5.2 - A.5.5), we obtain

$$E_{12} = \frac{60\pi}{r\lambda} I_0 \sin\theta_1 \frac{e^{[i\alpha l\sin(\Phi+\varphi)\cos\Delta-\gamma]l}-1}{i\alpha\sin(\Phi+\varphi)\cos\Delta-\gamma}. \tag{A.5.16}$$

$$E_{23} = \frac{60\pi}{r\lambda} I_0 \sin\theta_2 \frac{e^{[i\alpha l\sin(\Phi-\varphi)\cos\Delta-\gamma]l}-1}{i\alpha\sin(\Phi-\varphi)\cos\Delta-\gamma} e^{[i\alpha l\sin(\Phi+\varphi)\cos\Delta-\gamma]l}, \tag{A.5.17}$$

$$E_{43} = -\frac{60\pi}{r\lambda} I_0 \sin\theta_1 \frac{e^{[i\alpha l\sin(\Phi+\varphi)\cos\Delta-\gamma]l}-1}{i\alpha\sin(\Phi+\varphi)\cos\Delta-\gamma} e^{[i\alpha l\sin(\Phi-\varphi)\cos\Delta-\gamma]l}, \tag{A.5.18}$$

$$E_{14} = -\frac{60\pi}{r\lambda} I_0 \sin\theta_2 \frac{e^{[i\alpha l\sin(\Phi-\varphi)\cos\Delta-\gamma]l}-1}{i\alpha\sin(\Phi-\varphi)\cos\Delta-\gamma}. \tag{A.5.19}$$

#A.5.2. Determining the normal and parallel components of the field strength vector for a rhombic antenna

Let us designate the normal and parallel components of the field strength vector by $E_{\perp}$ and $E_{\parallel}$ (fig. A.5.3). Let us express $E_{\perp}$ and $E_{\parallel}$ by E (E is the modulus of the composite field strength vector).

Let us designate segment ab by E_0 and segment ac by E_1.

Figure A.5.3 makes it apparent that the following relationships exist between the $E_{\perp}$, E_0, and E moduli,

$$E_{\perp} = E_0 \sin \varphi, \tag{A.5.20}$$

$$E = E_0 \sin \theta, \tag{A.5.21}$$

from whence

$$E_0 = \frac{E}{\sin \theta}. \tag{A.5.22}$$

Substituting the expression for E_0 from formula (A.5.22) in formula (A.5.20), we obtain

$$E_{\perp} = E \frac{\sin \varphi}{\sin \theta}. \tag{A.5.23}$$

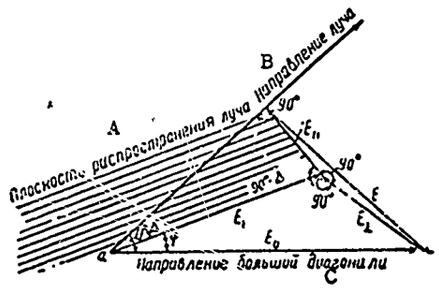

Figure A.5.3.

A - plane of beam propagation; B - direction of beam;
C - direction of long diagonal.

From Figure A.5.3 we also find that

$$E_1 = E_1 \sin \Delta, \tag{A.5.24}$$

$$E_1 = E_0 \cos \varphi = E \frac{\cos \varphi}{\sin \theta}. \tag{A.5.25}$$

Substituting the expression for E_1 from formula (A.5.25) in formula (A.5.24), we obtain

$$E_1 = E \frac{\cos \varphi}{\sin \theta} \sin \Delta. \tag{A.5.26}$$

Using expressions (A.5.25) and (A.5.26), we obtain the angles Δ, φ_1 and θ_1 formed by the beam for side 1-2,

$$E_{12\perp} = E_{12} \frac{\sin \varphi_1}{\sin \theta_1}, \tag{A.5.27}$$

$$E_{12\parallel} = E_{12} \frac{\cos \varphi_1}{\sin \theta_1} \sin \Delta, \tag{A.5.28}$$

and angles Δ, φ_2 and θ_2 formed by the beam for side 2-3,

$$E_{23\perp} = E_{23}\frac{\sin\varphi_2}{\sin\theta_2}, \tag{A.5.29}$$

$$E_{23\parallel} = E_{23}\frac{\cos\varphi_2}{\sin\theta_2}\sin\Delta, \tag{A.5.30}$$

For side 4-3

$$E_{43\perp} = E_{43}\frac{\sin\varphi_1}{\sin\theta_1}, \tag{A.5.31}$$

$$E_{43\parallel} = E_{43}\frac{\cos\varphi_1}{\sin\theta_1}\sin\Delta. \tag{A.5.32}$$

For side 1-4

$$E_{14\perp} = E_{14}\frac{\sin\varphi_2}{\sin\theta_2}, \tag{A.5.33}$$

$$E_{14\parallel} = E_{14}\frac{\cos\varphi_2}{\sin\theta_2}\sin\Delta. \tag{A.5.34}$$

The summed normal component of the field for all four sides of the rhombus equals

$$E_\perp = E_{12\perp} + E_{23\perp} + E_{43\perp} + E_{14\perp}. \tag{A.5.35}$$

The summed parallel component of the field for all four sides of the rhombus equals

$$E_\parallel = E_{12\parallel} + E_{23\parallel} + E_{43\parallel} + E_{14\parallel}. \tag{A.5.36}$$

Substituting in formulas (A.5.35) and (A.5.36) in place of

$$E_{12\perp},\ E_{23\perp},\ E_{43\perp},\ E_{14\perp} \text{ и } E_{12\parallel},\ E_{23\parallel},\ E_{43\parallel},\ E_{14\parallel}$$

their expressions from formulas (A.5.27 - A.5.34), in place of E_{12}, E_{23}, E_{43} and E_{14} their expressions from formulas (A.5.16 - A.5.19), in place of φ_1 and φ_2 their expressions from formula (A.5.12), and making the corresponding conversions, we obtain the following expressions for the normal and parallel components of the field strength vector for a rhombic antenna

$$E_\perp = i\frac{30I_0}{r}\left[\frac{\cos(\Phi+\varphi)}{\sin(\Phi+\varphi)\cos\Delta + i\frac{\gamma}{\alpha}} + \frac{\cos(\Phi-\varphi)}{\sin(\Phi-\varphi)\cos\Delta + i\frac{\gamma}{\alpha}}\right]\times$$
$$\times\left\{1 - e^{[l\alpha\sin(\Phi+\varphi)\cos\Delta-\gamma]l}\right\}\left\{1 - e^{[l\alpha\sin(\Phi-\varphi)\cos\Delta-\gamma]l}\right\}. \tag{A.5.37}$$

$$E_\parallel = -i\frac{30I_0}{r}\sin\Delta\left[\frac{\sin(\Phi+\varphi)}{\sin(\Phi+\varphi)\cos\Delta + i\frac{\gamma}{\alpha}} - \frac{\sin(\Phi-\varphi)}{\sin(\Phi-\varphi)\cos\Delta + i\frac{\gamma}{\alpha}}\right]\times$$
$$\times\left\{1 - e^{[l\alpha\sin(\Phi+\varphi)\cos\Delta-\gamma]l}\right\}\left\{1 - e^{[l\alpha\sin(\Phi-\varphi)\cos\Delta-\gamma]l}\right\}. \tag{A.5.38}$$

Formulas (A.5.37) and (A.5.38) yield the expressions for the field strength of a rhombic antenna without the influence of the ground being taken into consideration.

If this influence is taken into consideration, the formulas for the normal and parallel components of the field strength vector will take the following form

$$E_{\perp} = i\frac{30I_0}{r}\left[\frac{\cos(\Phi+\varphi)}{\sin(\Phi+\varphi)\cos\Delta+i\frac{\gamma}{\alpha}}+\frac{\cos(\Phi-\varphi)}{\sin(\Phi-\varphi)\cos\Delta+i\frac{\gamma}{\alpha}}\right]\times$$
$$\times\left\{1-e^{(l\alpha\sin(\Phi+\varphi)\cos\Delta-\gamma)l}\right\}\left\{1-e^{(l\alpha\sin(\Phi-\varphi)\cos\Delta-\gamma)l}\right\}\times \quad \text{(A.5.39)}$$
$$\times\left[1+|R_{\perp}|e^{i(\Phi_{\perp}-2\alpha l/\sin\Delta)}\right],$$

$$E_{\parallel} = -i\frac{30I_0}{r}\sin\Delta\left[\frac{\sin(\Phi+\varphi)}{\sin(\Phi+\varphi)\cos\Delta+i\frac{\gamma}{\alpha}}-\frac{\sin(\Phi-\varphi)}{\sin(\Phi-\varphi)\cos\Delta+i\frac{\gamma}{\alpha}}\right]\times$$
$$\times\left\{1-e^{(l\alpha\sin(\Phi+\varphi)\cos\Delta-\gamma)l}\right\}\left\{1-e^{(l\alpha\sin(\Phi-\varphi)\cos\Delta-\gamma)l}\right\}\times\left[1-|R_{\parallel}|e^{i(\Phi_{\parallel}-2\alpha l/\sin\Delta)}\right]. \quad \text{(A.5.40)}$$

where

$|R_{\perp}|$ is the modulus of the coefficient of reflection normal for the polarized wave;

$|R_{\parallel}|$ is the modulus of the coefficient of reflection parallel for the polarized wave;

$\Phi_{\perp}$ and $\Phi_{\parallel}$ are the arguments for the coefficients of reflection normal and parallel for the polarized waves.

Appendix 6

Derivation of the radiation pattern formula for the traveling wave antenna

In its general form the traveling wave antenna radiation pattern formula can be written

$$I_c = f_1(t)f_2(c)f_3(g), \qquad (A.6.1)$$

where

I_c is the current flowing at the receiver input;

$f_1(t)$ is a factor which characterizes the directional properties and receptivity of one dipole in a traveling wave antenna;

$f_2(c)$ is a factor which characterizes the summation of the currents flowing in the individual dipoles at the receiver input;

$f_3(g)$ is a factor which characterizes the influence of the ground on receptivity.

(1) the factor $f_1(t)$.

The equivalent circuit for a traveling wave antenna has the form shown in Figure A.6.1.

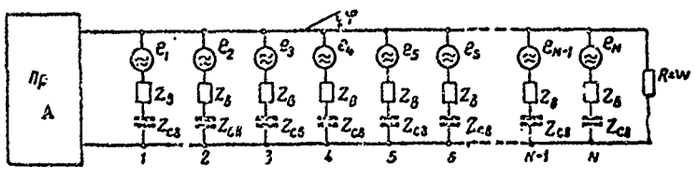

Figure A.6.1.

A - receiver.

It has already been pointed out in Chapter XIV that if the summed impedance $Z_{in} + Z_{coupling}$ is sufficiently great as compared with the characteristic impedance of the collection line, and, moreover, if the distance between adjacent dipoles is short as compared with the wavelength, then the collection line can be considered to be a line with uniformly distributed constants. Since the conditions pointed out are in fact observed, it will be assumed in the course of analyzing the operation of a single balanced dipole that the dipole is operating in a line which has a constant characteristic impedance. The corresponding equivalent schematic diagram of the operation of a single dipole is shown in Figure A.6.2.

Figures A.6.1 and A.6.2 show the equivalent circuits for the case when condensers are used as decoupling resistors. The equivalent circuits are of a type similar to those of other types of decoupling resistors.

In order to simplify what has been said, let us assume that the receiver input impedance is equal to the characteristic impedance of the collection line.

The equivalent circuit in Figure A.6.2 can be replaced by the simpler circuit shown in Figure A.6.3.

In Figure A.6.3 resistor R_1 is equivalent to the left side of the collection line, while resistor R_2 is equivalent to the right side of the collection line.

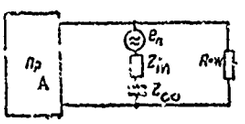

Figure A.6.2.

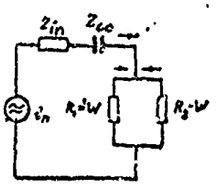

Figure A.6.3.

A - receiver.

The current flowing from the point where the n^{th} dipole is connected to the receiver equals

$$I_n = \frac{1}{2}\frac{e_n}{Z_{in} + Z_{co} + \frac{W}{2}}, \qquad \text{(A.6.2)}$$

$$e_n = \frac{E_0 \lambda}{\pi}\frac{1}{\operatorname{sh}\gamma l}\frac{\cos(\alpha l\cos\theta) - \cos\alpha l}{\sin\theta}, \qquad \text{(A.6.3)}$$

where

γ is the propagation factor for the electromagnetic wave on a balanced dipole;

E_0 is the field strength at the center of the balanced dipole;

θ is the angle formed by the incoming beam and the axis of the dipole.

Substituting formula (A.6.3) in (A.6.2), we obtain

$$I_n = f_1(l) = \frac{E_0}{\alpha\left(Z_{in} + Z_{co} + \frac{W}{2}\right)}\frac{1}{\operatorname{sh}\gamma l}\frac{\cos(\alpha l\cos\theta) - \cos\alpha l}{\sin\theta}. \qquad \text{(A.6.4)}$$

Angle θ can be expressed by the azimuth angle and the angle of tilt (fig. A.6.4)

$$\cos\theta = \cos\Psi\cdot\cos\Delta, \qquad \text{(A.6.5)}$$

where

Ψ is the azimuth angle of the incoming beam, read from the axis of the dipole;

Δ is the angle of tilt of the incoming beam.

Let φ be the azimuth angle of the incoming beam, read from the direction of the collection line. Then $\Psi = 90 - \varphi$.

Substituting this value for Ψ in (A.6.5), we obtain

$$\left.\begin{aligned} \cos\theta &= \cos(90-\varphi)\cos\Delta = \sin\varphi\cos\Delta \\ \sin\theta &= \sqrt{1-\cos^2\theta} = \sqrt{1-\sin^2\varphi\cos^2\Delta} \end{aligned}\right\}. \qquad \text{(A.6.6)}$$

Substituting the expressions for $\cos\theta$ and $\sin\theta$ in formula (A.6.4), we obtain

$$f_1(l) = \frac{E_0}{\alpha\left(Z_{in}+Z_{co}+\frac{W}{2}\right)}\,\frac{1}{\operatorname{sh}\gamma l}\,\frac{\cos(\alpha l\sin\varphi\cos\Delta)-\cos\alpha l}{\sqrt{1-\sin^2\varphi\cos^2\Delta}} \qquad \text{(A.6.7)}$$

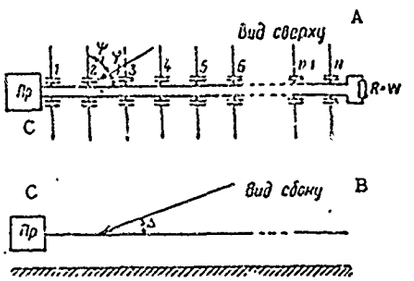

Figure A.6.4.

A - top view; B - side view; C - receiver.

(2) the factor $f_2(c)$

Formula (A.6.7) will yield an expression for the current caused to flow by the emf across a single balanced dipole, and moreover, the formula will yield the current flowing in the collection line at the point where the particular balanced dipole is connected.

Let us find the expression for the current caused to flow by the emf across a single balanced dipole at the receiver input. Let us assume, for purposes of simplicity of explanation, that the receiver is connected directly to the end of the collection line. The expression for the current at the receiver input should take into consideration the change in the phase and the amplitude of the current during the propagation process from the point at which the dipole is connected to the receiver input.

Moreover, the phase of the emf induced by the wave should be taken into consideration.

The change in amplitude and phase as the current is propagated along the collection line can be computed by multiplying the right-hand side of equation (A.6.7) by the factor

$$e^{-\gamma_c(n-1)l_1}, \qquad \text{(A.6.7)}$$

where

γ_c is the propagation factor on the collection line;

n is the dipole ordinal number;

$(n-1)l_1$ is the distance on the collection line from the point at which the n^{th} dipole is connected to the receiver input.

The propagation factor consists of a real and an imaginary part

$$\gamma_c = \beta_c + i\,\frac{\alpha}{k_1},$$

where

$$\alpha = \frac{2\pi}{\lambda}, \quad k_1 = \frac{v}{c},$$

v is the rate of propagation on the collection line;

c is the rate of propagation of radio waves in free space;

β_c is the attenuation factor for the collection line.

Change in the phase of the emf induced in the dipoles is determined by the change in the phase of the field strength.

Let us take the phase of the field strength vector at the center of the first dipole as zero. Then the phase angle for the field strength vector at the center of the n^{th} dipole equals

$$\psi = \alpha(n-1)l_1 \cos x, \tag{A.6.8}$$

where

x is the angle formed by the direction of the beam and the collection line.

Thus, the field strength at the center of the n^{th} dipole equals

$$E_n = E_0 e^{i\alpha(n-1)l_1 \cos x}. \tag{A.6.9}$$

Angle x can be expressed in terms of the azimuth angle and the angle of tilt as

$$\cos x = \cos\varphi \cos\Delta. \tag{A.6.10}$$

Substituting the expression for cos x in formula (A.6.9), we obtain

$$E_n = E_0 e^{i\alpha(n-1)l_1 \cos\varphi \cos\Delta}. \tag{A.6.11}$$

The current from the n^{th} dipole at the receiver input equals

$$I_n = f_1(l)\, e^{(n-1)(i\alpha\cos\varphi\cos\Delta - \gamma_c)l_1}. \tag{A.6.12}$$

The summed current from all N dipoles at the receiver input equals

$$I = f_1(l) \sum_{n=1}^{N} I_n = f_1(l) \sum_{n=1}^{N} e^{(n-1)(i\alpha\cos\varphi\cos\Delta - \gamma_c)l_1}. \tag{A.6.13}$$

The expression containing the symbol Σ is the sum of the terms of a geometric progression of the type

$$S = 1 + q + q^2 + \ldots + q^{N-1}. \qquad \text{(A.6.14)}$$

As we know, this sum equals

$$S = \frac{q^N - 1}{q - 1}. \qquad \text{(A.6.15)}$$

In the case which has been specified

$$q = e^{(i2\cos\varphi\cos\lambda - \gamma_c)l_1}.$$

Using the relationship at (A.6.15), we obtain

$$I = I_1(l)\,\frac{e^{N(i2\cos\varphi\cos\lambda - \gamma_c)l_1} - 1}{e^{(i2\cos\varphi\cos\lambda - \gamma_c)l_1} - 1}. \qquad \text{(A.6.16)}$$

The factor characterizing the summation of the currents from the individual dipoles at the receiver input can be expressed by the formula

$$I_2(c) = \frac{e^{N(i2\cos\varphi\cos\lambda - \gamma_c)l_1} - 1}{e^{(i2\cos\varphi\cos\lambda - \gamma_c)l_1} - 1}. \qquad \text{(A.6.17)}$$

(3) the factor $f_3(g)$

The influence of ideally conducting ground on the radiation pattern of a horizontal antenna can be defined by the factor

$$f_3(g) = 2\sin(\alpha\, H\, \sin\Delta), \qquad \text{(A.6.18)}$$

where

H is the height at which the antenna is suspended.

(4) the complete formula for the space radiation pattern for a traveling wave antenna

This formula has the following form

$$I_c = \frac{2E_0}{2\left(Z_{in} + Z_{re} + \frac{W}{2}\right)}\,\frac{1}{\sin\gamma l}\,\frac{\cos(\alpha l \sin\varphi\cos\Delta) - \cos\alpha l}{\sqrt{1 - \sin^2\varphi\cos^2\Delta}} \times$$

$$\times\,\frac{e^{N(i2\cos\varphi\cos\lambda - \gamma_c)l_1} - 1}{e^{(i2\cos\varphi\cos\lambda - \gamma_c)l_1} - 1}\sin(\alpha H \sin\Delta). \qquad \text{(A.6.19)}$$

Appendix 7

Derivation of the basic formulas for making the calculations for a rhombic antenna with feedback

The following relationship shouldbe found at the point of feed

$$U_1 + U_2 e^{-i\psi - 2\beta l - \frac{b}{2}} = U_1 e^{-i\psi - 2\beta l + \frac{b}{2}} + U_2, \qquad (A.7.1)$$

where

U_1 is the incident wave voltage outgoing from the point of feed to transmission line 1-2:

U_2 is the incident wave voltage outgoing from the point of feed to transmission line 1-3 (Fig. XIII.12.1);

$$\psi = \alpha L,$$

$e^{b/2}$ is the coefficient of transformation of the voltage across an exponential transmission line

$$e^b = W_p / W_1,$$

W_p and W_1 are the maximum and minimum characteristic impedances of an exponential transmission line.

From formula (A.7.1)

$$\left|\frac{U_2}{U_1}\right| = \left|\frac{1 - e^{-i\alpha L - 2\beta l + \frac{b}{2}}}{1 - e^{-i\alpha L - 2\beta l - \frac{b}{2}}}\right|. \qquad (A.7.2)$$

Optimum conditions prevail when $U_2 = 0$. From (A.7.2) it follows that $U_2 = 0$ for the conditions

$$(1)\ \alpha L = n2\pi \text{ or } L = n\lambda; \qquad (2)\ 2\beta l = 1/2\, b. \qquad (A.7.3)$$

$(n = 1, 2, 3 \ldots)$

The antenna input impedance equals

$$Z_{in} = \frac{U}{I_1 - I_2} =$$

$$= \frac{U_1 + U_2 e^{-i\alpha L - 2\beta l - \frac{b}{2}}}{\frac{U_1}{W_p e^{-b}} + \frac{U_2}{W_p} - \frac{U_1}{W_p} e^{-i\alpha L - 2\beta l + \frac{b}{2}} - \frac{U_2}{W_p e^{-b}} e^{-i\alpha L - 2\beta l - \frac{b}{2}}}, \qquad (A.7.4)$$

where

I_1 are the wave currents outflowing in lines 1-2 and 1-4;

I_2 are these same wave currents returning to point 1 after flowing around the entire current circulating path.

After conversion, formula (A.7.4) can be given in the form

$$Z_{in} = W_p \frac{e^{-b}\left(1 - e^{-12\alpha L - 4\beta L}\right)}{\left(1 + e^{-b}\right)\left(1 + e^{-12\alpha L - 4\beta L}\right) - 4e^{-4\alpha L - 2\beta L - \frac{b}{2}}}. \qquad \text{(A.7.5)}$$

Appendix 8

Analysis of reflectometer operation

Let there be only a traveling wave on the transmission line, and let there be no losses in that line. Then the current flowing in the transmission line and the voltage across the transmission line will only change in phase, remaining fixed in amplitude, and the electrical lines of force moving from one conductor to the other will be normal to the axis of the line. Let us place a long line segment ad-bc between the transmission line conductors and hook up impedances Z_1 and Z_2 (fig. A.8.1) to the ends of the segment. We select the dimensions of this line such that its coupling to the transmission line is so loose that no considerable change in the characteristic impedance of the transmission line will be noted. An emf will only be induced in the line along sides ad and bc. Then, if we designate the emf induced in side ad by $e_{1\ incident}$, the emf induced in side bc will be equal to

$$e_{2\ in} = e_{1\ in} e^{-i\alpha l}. \qquad (A.8.1)$$

The current flowing in impedance Z_1 equals

$$I_1 = e_{1\ in} - e'_{2\ in}/Z_1 + Z'_2 \qquad (A.8.2)$$

where

$e'_{2\ in}$ is the emf induced in side bc and converted in side ad;

Z'_2 is impedance Z_2 converted at the ad terminals;

$$e'_{2\ in} = e_{1\ in} e^{-i\alpha l}/\cos\alpha l + i \cdot Z_2/W_{line} \sin\alpha l \qquad (A.8.3)$$

$$Z'_2 = W_\ell \frac{\cos\alpha l + i \frac{W_\ell}{Z_2} \sin\alpha l}{\frac{W_\ell}{Z_2} \cos\alpha l + i \sin\alpha l}, \qquad (A.8.4)$$

where

$W_{l(ine)}$ is the characteristic impedance of the measuring line.

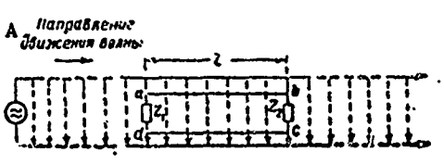

Figure A.8.1.

A - wave movement.

Substituting the expression for $e_{2\ in}$ in (A.8.2), we obtain

$$I_1 = \frac{e_{1\ in}}{Z_1 + Z_2}\left(1 - \frac{e^{-i\alpha l}}{\cos\alpha l + i\frac{Z_2}{W_\ell}\sin\alpha l}\right). \qquad (A.8.5)$$

And, similarly, we obtain

$$I_2 = \frac{e_{1\ in}}{Z_1 + Z_2}\left(\frac{1}{\cos\alpha l + i\frac{Z_1}{W_\ell}\sin\alpha l} - e^{-i\alpha l}\right). \qquad (A.8.6)$$

As will be seen from formulas (A.8.5) and (A.8.6), if it is assumed that $Z_1 = Z_2 = W_1$, then

$$\left.\begin{aligned} I_1 &= \frac{e_{1\ in}}{2W_\ell}(1 - e^{-i2\alpha l}) \\ I_2 &= 0 \end{aligned}\right\}. \qquad (A.8.7)$$

Accordingly, only current I_1 creates an incident wave.

If, on the transmission line, in addition to the incident wave there is also a reflected wave, then in addition to the $e_{1\ in}$ and $e_{2\ in}$ emfs, there will be yet another pair of emfs across the measuring line, $e_{1\ reflected}$ and $e_{2\ reflected}$. And in a manner similar to that in the foregoing, it is readily proven that as a result of the $e_{1\ reflected}$ and $e_{2\ reflected}$ when $Z_2 = Z_1 = W_{line}$ a current

$$I_2 = e_{1\ refl}/2Z_1\ (1 - e^{-i2\alpha l}) \qquad (A.8.8)$$

will flow in impedance Z_2

The $e_{1\ reflected}$ and $e_{2\ reflected}$ emfs will cause no current to flow in impedance Z_1 since

$e_{1\ incident}$ is proportional to the incident wave current flowing in the transmission line;

$e_{1\ reflected}$ is proportional to the reflected wave current flowing in the transmission line.

HANDBOOK SECTION

H.I. Formulas for computing the direction (azimuth) and length of radio communication lines

The direction of a line can be characterized by its azimuth, that is, by the angle formed by the arc of a great circle and the northerly direction of the meridian passing through the point from which the direction is to be determined. The azimuth is read clockwise. Figure H.I.1 shows the azimuths, α, of points a, b, c, and c, located in different directions from point A. Azimuth is read from 0° to 360°.

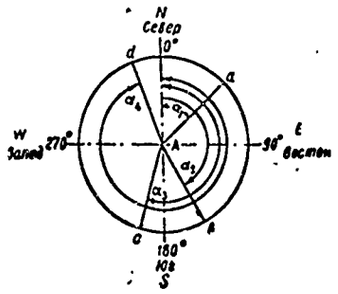

Figure H.I.1.

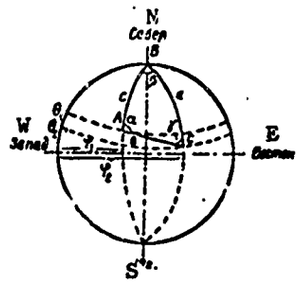

Figure H.I.2.

Let us use the cosine formula for a triangle to determine the direction (azimuth) and the length of a line connecting points A and C (fig. H.I.2)

$$\begin{aligned}\cos a &= \cos b \cos c + \sin b \sin c \cos \alpha \\ \cos b &= \cos a \cos c + \sin a \sin c \cos \beta \\ \cos c &= \cos a \cos b + \sin a \sin b \cos \gamma\end{aligned} \qquad \text{(H.I.1)}$$

as well as the sine formula

$$\frac{\sin \alpha}{\sin a} = \frac{\sin \beta}{\sin b} = \frac{\sin \gamma}{\sin c}, \qquad \text{(H.I.2)}$$

where

a, b, c, and α, β, γ are the sides and the angles of a specific triangle, ABC, formed by the arcs of great circles passing through points A and C and the north pole, B.

The sides and the angles of triangle ABC are expressed in degrees, and are associated with the geographic latitudes and longitudes of points A and C by the following relationships

$$\begin{aligned}a &= 90° - \theta_2, \\ c &= 90° - \theta_1, \\ \beta &= \varphi_2 - \varphi_1.\end{aligned} \qquad \text{(H.I.3)}$$

where

φ_1 and φ_2 are the longitudes of points A and C;

θ_1 and θ_2 are the latitudes of points A and C.

The formulas at (H.I.3) are algebraic in nature, which is to say that when they are used the signs of the latitudes and the longitudes must be taken into consideration. We will take it as convention to read north latitude, N, and east longitude, E, as positive, and south latitude, S, and west longitude, W, as negative.

The direction (azimuth) of the line is determined through formulas (H.I.1) through (H.I.3).

The distance between points A and C can be found through

$$d = 2\pi Rb/360 = 6.28 \cdot 6370/360\ b = 111b\ (km), \quad (H.I.4)$$

where

R is the radius of the earth (R = 6370 km);

b is the angular distance between points A and C, expressed in degrees.

Example 1. Point A is Moscow. Point C is Kuybyshev. Find the azimuth and the length of the line between Moscow and Kuybyshev.

The geographic coordinates (latitude and longitude) of Moscow and Kuybyshev are

Name of point	Latitude	Longitude
Moscow	θ_1 = 55°44'45" N	φ_1 = 37°17'30" E
Kuybyshev	θ_2 = 53°10'30" N	φ_2 = 49°45'30" E

In accordance with (H.I.3)

$$c = 90° - \theta_1 = 90° - 55°44'45'' = 34°15'15''$$
$$a = 90° - \theta_2 = 90° - 53°10'30'' = 36°49'30''$$
$$\beta = \varphi_2 - \varphi_1 = 49°45'30'' - 37°17'30'' = 12°28'.$$

In accordance with (H.I.1)

$$\cos b = \cos c \cos a + \sin c \sin a \cos \beta = \cos 34°15'15'' \cos 36°49'30'' + \\ + \sin 34°15'15'' \sin 36°49'30'' \cos 12°28' = 0,9911,$$

from whence

$$b = 7°39' = 7.65°.$$

In accordance with (H.I.4)

$$d = 111b = 111 \cdot 7.65° = 849 \text{ km}.$$

The azimuth of the line between Moscow and Kuybyshev can be determined from the relationship

$$\sin \alpha = \frac{\sin a \cdot \sin \beta}{\sin b} = \frac{0,5993 \cdot 0,2159}{0,1331} = 0,969,$$

from whence α can have two values

$$\alpha_1 = 75°42' \text{ or } \alpha_2 = 180 - 75°42' = 104°18'.$$

Since Kuybyshev is located to the southeast of Moscow, as will be seen from Figure H.I.2 the angle formed by the Moscow-Kuybyshev line and the northerly direction of the meridian is obtuse, so

$$\alpha = \alpha_2 = 104°18'.$$

Example 2. Point A is New York. Point C is Moscow. Find the azimuth and the length of the line between Moscow and New York.

The geographic latitudes and longitudes are

Name of point	Latitude	Longitude
New York	$\theta_1 = 40°41'55''$ N	$\varphi_1 = 73°58'21''$ W
Moscow	$\theta_2 = 55°44'45''$ N	$\varphi_2 = 37°17'30''$ E

$$c = 90° - \theta_1 = 90° - 40°41'55'' = 49°18'05'',$$
$$a = 90° - \theta_2 = 90° - 55°44'45'' = 34°15'15'',$$
$$\beta = \varphi_2 - \varphi_1 = 37°17'30'' - (-73°58'21'') = 111°15'51'',$$
$$\cos b = \cos c \cos a + \sin c \sin a \cos\beta = 0{,}6521 \cdot 0{,}8266 + + 0{,}7581 \cdot 0{,}5628\,(-0{,}3654) = 0{,}3832,$$

from whence

$$b = 67°28' = 67.467°$$
$$d = 111b = 111 \cdot 67.467 = 7492 \text{ km}$$

The direction (azimuth) from Moscow to New York, γ, is determined from the relationship

$$\sin\gamma = \frac{\sin c \cdot \sin\beta}{\sin b} = \frac{\sin 49°18'05'' \cdot \sin 111°15'51''}{\sin 67°28'} = \frac{0{,}7581 \cdot 0{,}9319}{0{,}9237} = 0{,}764,$$

from whence

$$\gamma = 49°49'.$$

New York is to the west of Moscow, so the azimuth of the line Moscow-New York equals

$$\gamma' = 360° - \gamma = 360° - 49°49' = 310°11'.$$

H.II. Formula and graphic for use in computing the angle of tilt of a beam to the horizon

The formula for computing the angle of tilt of a beam to the horizon is in the form

$$\operatorname{tg}\Delta = \frac{\beta - (1+\beta)(1-\cos\nu)}{(1+\beta)\sin\nu}, \qquad \text{(H.II.1)}$$

where

$$\beta = \frac{H}{R}, \qquad \nu = \frac{d \cdot 360}{2R2\pi},$$

and

H is the height of the reflecting layer, in km;

R is the earth's radius (R = 6370 km);

d is the length of the wave jump, measured in kilometers; that is, the distance between two adjacent points of reflection from the earth, measured along an arc of a great circle on the earth.

Figure H.II.1 contains the curves providing the dependence between the angle of tilt, Δ, the height of the reflecting layer, H, and the length of the wave jump, d.

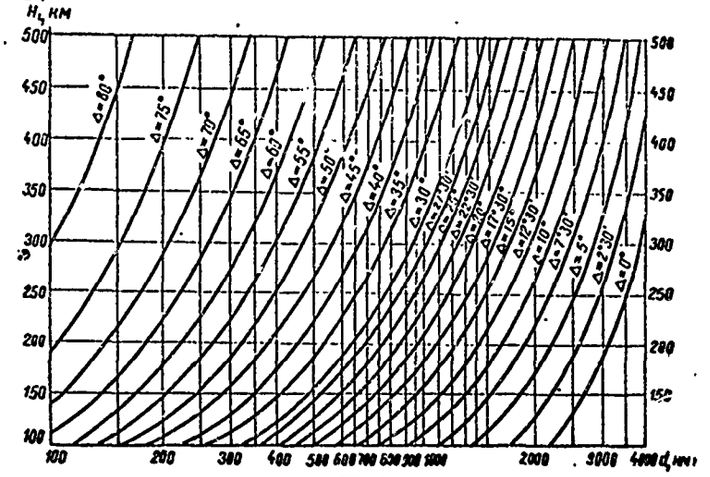

H.II.1.

H.III. Graphics for computing the mutual impedances of parallel balanced dipoles

#H.III.1. Auxiliary functions of f(δ,u) for computing the mutual impedances of balanced dipoles[1]

(a) General expressions for the functions and their properties

As was pointed out in #V.12, the functions of f(δ,u) can be expressed by the formulas

$$\left.\begin{aligned} f_1(\delta, u) &= \mathrm{si}\left(\sqrt{u^2+\delta^2}+u\right)+\mathrm{si}\left(\sqrt{u^2+\delta^2}-u\right)\\ f_2(\delta, u) &= \mathrm{si}\left(\sqrt{u^2+\delta^2}+u\right)-\mathrm{si}\left(\sqrt{u^2+\delta^2}-u\right)\\ f_3(\delta, u) &= \mathrm{ci}\left(\sqrt{u^2+\delta^2}+u\right)+\mathrm{ci}\left(\sqrt{u^2+\delta^2}-u\right)\\ f_4(\delta, u) &= \mathrm{ci}\left(\sqrt{u^2+\delta^2}+u\right)-\mathrm{ci}\left(\sqrt{u^2+\delta^2}-u\right) \end{aligned}\right\} \qquad \text{(H.III.1)}$$

where

$$\delta = \alpha d = 2\pi \cdot d/\lambda.$$

1. Graphics for the functions of f(δ,u) were compiled by L. S. Tartakovskiy.

In the mutual impedance expressions the variable u takes the value

$$2\pi\frac{H_1}{\lambda},\ 2\pi\left(\frac{H_1}{\lambda}\pm\frac{l}{\lambda}\right),\ 2\pi\left(\frac{H_1}{\lambda}\pm 2\frac{l}{\lambda}\right).$$

Figures H.III.1 - H.III.4 are the graphics of the dependence of the functions of $f(\delta,u)$ on $y = u/2\pi$. The graphics were constructed for various values of $d' = d/\lambda = \delta/2\pi$ and for values of $y = u/2\pi$, changing in the range from 0 to 5.25.

From (H.III.1) we see that all four functions are even with respect to the variable δ, that is

$$f(-\delta,u) = f(\delta,u).$$

The functions $f_1(\delta,u)$ and $f_3(\delta,u)$ are even with respect to the variable u, and the functions $f_2(\delta,u)$ and $f_4(\delta,u)$ are odd. That is,

$$f_1(\delta,-u)=f_1(\delta,u);\ f_3(\delta,-u)=f_3(\delta,u);$$
$$f_2(\delta,-u)=-f_2(\delta,u);\ f_4(\delta,-u)=-f_4(\delta,u).$$

Consequently, for negative values of δ and u, the functions of $f(\delta,u)$ can be determined from the data on these same functions for positive values of δ or u.

Figures H.III.1 - H.III.4 contain the values for the functions of $f(\delta,u)$ for positive values of δ and u.

(b) Special expressions and limiting values for the functions of $f(\delta,u)$

Table H.III.1 contains a summary of expressions, or values, which use functions of $f(\delta,u)$ when one, or both arguments vanish.

Table H.III.1

	$\delta=0$ $u\neq 0$	$\delta\neq 0$ $u=0$	$\delta=0$ $u=0$
$f_1(\delta,u)$	$\mathrm{si}\,2u$	$2\mathrm{si}\,\delta$	0
$f_2(\delta,u)$	$\mathrm{si}\,2u$	0	0
$f_3(\delta,u)$	$-\infty$	$2\mathrm{ci}\,\delta$	$-\infty$
$f_4(\delta,u)$	∞	0	$2Ar\,\mathrm{sh}\frac{u}{\delta}=$ $=2\ln\left[\sqrt{\left(\frac{u}{\delta}\right)^2+1}+\frac{u}{\delta}\right]$

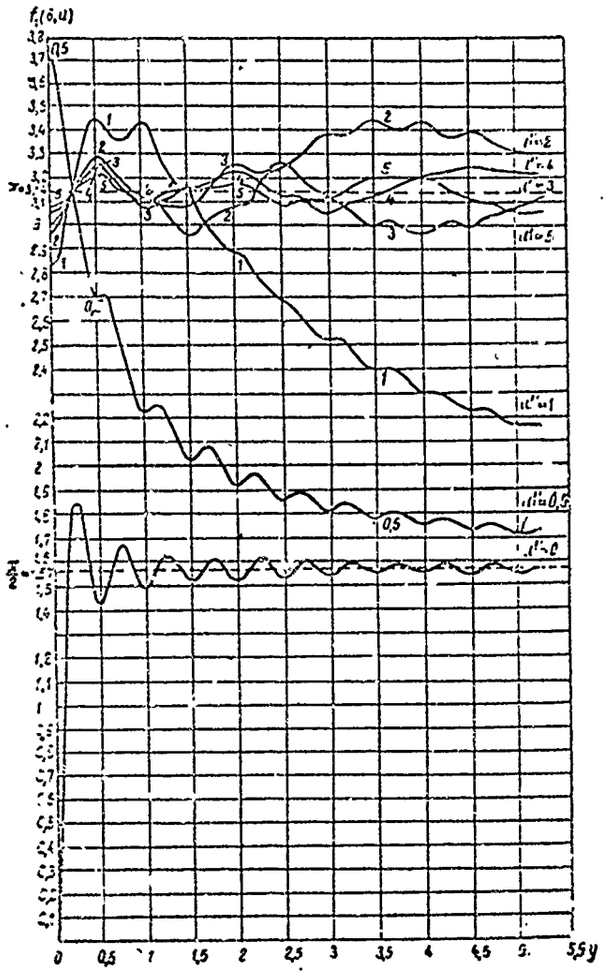

Figure H.III.1.

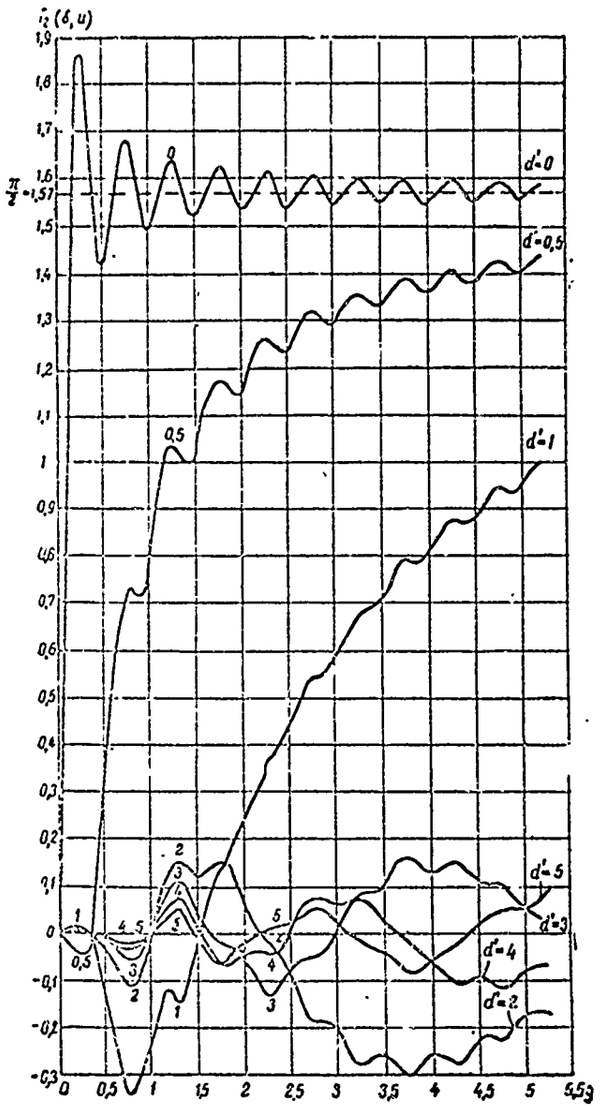

Figure H.III.2.

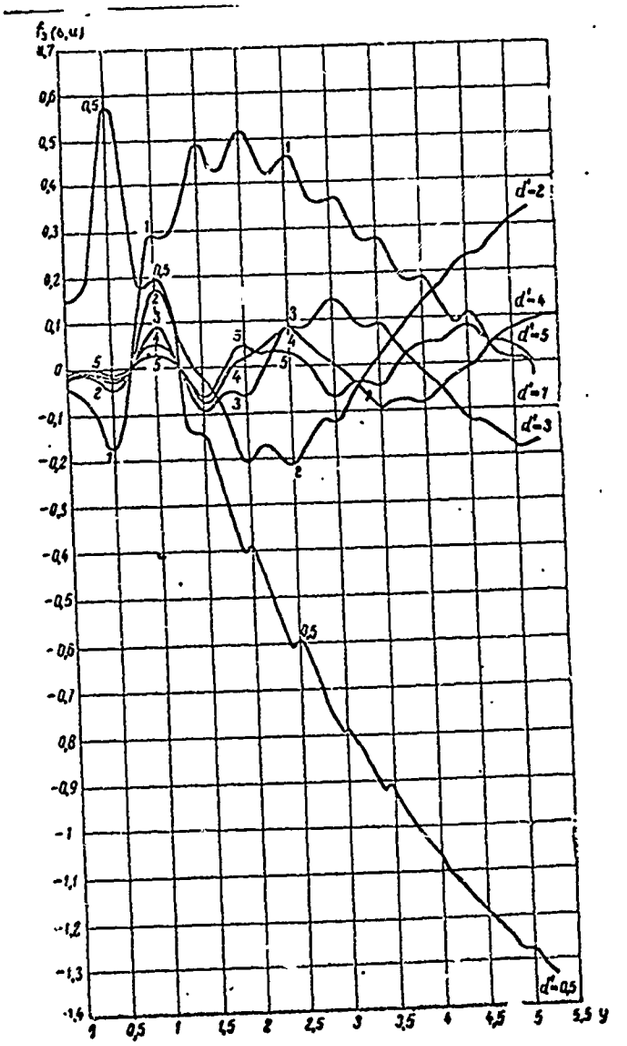

Figure H.III.3.

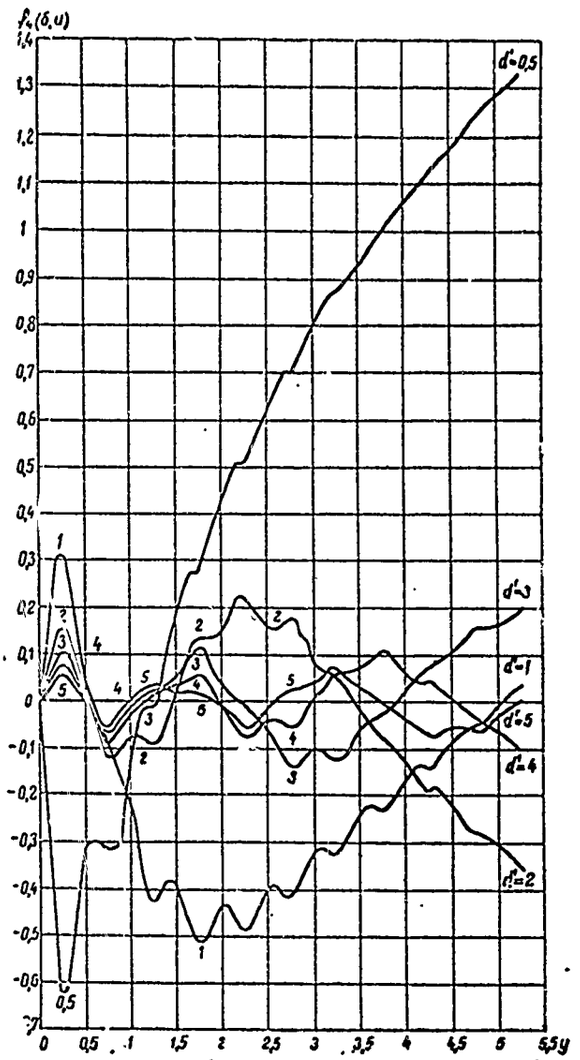

Figure H.III.4.

Example. Find R_{12} and X_{12}, given the following conditions

$$l = 0.625\lambda, \quad H_1 = 0.5\lambda, \quad d = \lambda,$$

from whence

$$p = al = 2\pi \frac{l}{\lambda} = 2\pi\, 0{,}625$$

$$q = a H_1 = 2\pi \frac{H_1}{\lambda} = 2\pi\, 0{,}5$$

$$\delta = a d = 2\pi \frac{d}{\lambda} = 2\pi$$

$$q + p = 2\pi\ 1{,}125$$

$$q - p = -2\pi\, 0{,}125$$

$$q + 2p = 2\pi\ 1{,}75$$

$$q - 2p = -2\pi\, 0{,}75$$

$$\sin q = \sin 2\pi\ 0{,}5 = \sin 180^\circ = 0, \quad \cos q = -1,$$

$$\sin (q + 2p) = \sin 2\pi\ 1{,}75 = \sin 630^\circ = -1, \quad \cos (q + 2p) = 0,$$

$$\sin (q - 2p) = \sin (-2\pi\ 0{,}75) = \sin (-270^\circ) = 1, \quad \cos (q - 2p) = 0.$$

Utilizing the curves in Figures H.III.1 through H.III.4, and taking the evenness of the functions of $f_1(\delta,u)$ and $f_3(\delta,u)$ and the oddness of the functions $f_2(\delta,u)$ and $f_4(\delta,u)$ into consideration, we obtain

$f_1(\delta, q) = f_1(2\pi, 2\pi\ 0{,}5) = 3{,}445$ $f_3(\delta, q) = f_3(2\pi, 2\pi\ 0{,}5) = -0{,}178$
$f_1(\delta, q+p) = f_1(2\pi, 2\pi\ 1{,}125) = 3{,}330$ $f_3(\delta, q+p) = f_3(2\pi, 2\pi\ 1{,}125) = 0{,}289$
$f_1(\delta, q-p) = f_1(2\pi, -2\pi\ 0{,}125) = 2{,}920$ $f_3(\delta, q-p) = f_3(2\pi, -2\pi\ 0{,}125) = -0{,}059$
$f_1(\delta, q+2p) = f_1(2\pi, 2\pi\ 1{,}75) = 3$ $f_3(\delta, q+2p) = f_3(2\pi, 2\pi\ 1{,}75) = 0{,}427$
$f_1(\delta, q-2p) = f_1(2\pi, -2\pi\ 0{,}75) = 3{,}344$ $f_3(\delta, q-2p) = f_3(2\pi, -2\pi\ 0{,}75) = 0{,}068$
$f_2(\delta, q) = f_2(2\pi, 2\pi\ 0{,}5) = -0{,}149$ $f_4(\delta, q) = f_4(2\pi, 2\pi\ 0{,}5) = 0{,}062$
$f_2(\delta, q+p) = f_2(2\pi, 2\pi\ 1{,}125) = -0{,}137$ $f_4(\delta, q+p) = f_4(2\pi, 2\pi\ 1{,}125) = -0{,}370$
$f_2(\delta, q-p) = f_2(2\pi, -2\pi, 0{,}125) = -0{,}005$ $f_4(\delta, q-p) = f_4(2\pi, -2\pi\ 0{,}125) = -0{,}22$
$f_2(\delta, q+2p) = f_2(2\pi, 2\pi\ 1{,}75) = 0{,}137$ $f_4(\delta, q+2p) = f_4(2\pi, 2\pi\ 1{,}75) = -0{,}511$
$f_2(\delta, q-2p) = f_2(2\pi, -2\pi\ 0{,}75) = 0{,}360$ $f_4(\delta, q-2p) = f_4(2\pi, -2\pi\ 0{,}75) = 0{,}090$

Substituting the values obtained for the functions in the expressions for the coefficients K, L, M. and N, we find

$K_1 = -0{,}312$ $L_1 = -1{,}172$
$K_2 = 0{,}262$ $L_2 = -0{,}329$
$K_3 = 0{,}221$ $L_3 = 0{,}003$
$M_1 = 1{,}428$ $N_1 = -3{,}280$
$M_2 = 0{,}291$ $N_2 = 0{,}215$
$M_3 = 0{,}582$ $N_3 = -0{,}949.$

Substituting the numerical values obtained in formulas (V.12.5) and (V.12.6), we obtain

$$R_{12} = 16.95 \text{ ohms} \quad \text{and} \quad X_{12} = 52.75 \text{ ohms}.$$

#H.III.2. Graphics of the mutual impedance of parallel balanced dipoles

Figures H.III.6 - H.III.21 contain the graphics for the active, R_{12}, and reactive, X_{12}, components of the mutual impedance, equated to the current loop for two parallel half-wave dipoles (fig. H.III.5). These graphics have been taken from V. V. Tatarinov.

Figures H.III.23 - H.III.38 contain the graphics for the active, R_{12}, and reactive, X_{12}, components of the mutual impedance of two identical parallel balanced dipoles when there is no mutual displacement along the direction of their axes (fig. H.III.22). The values of the components of the mutual impedance are equated to the current loop.

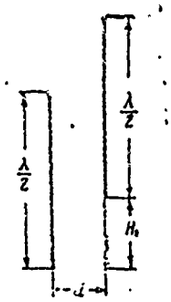

Figure H.III.5.

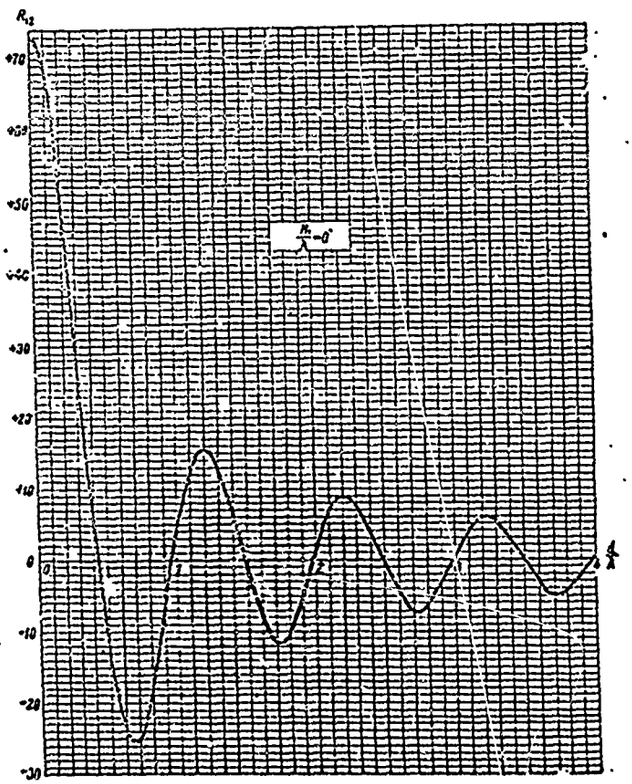

Figure H.III.6.

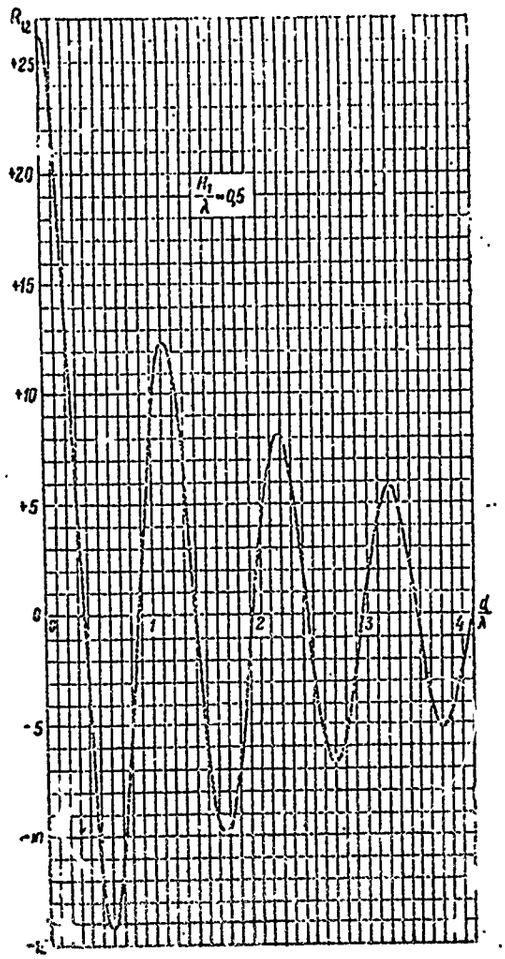

Figure H.III. 7.

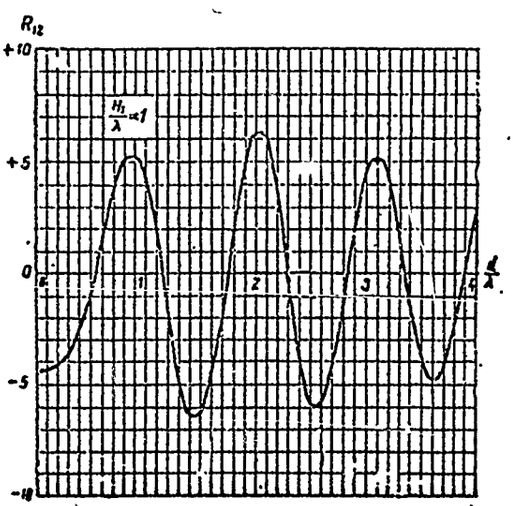

Figure H.III.8.

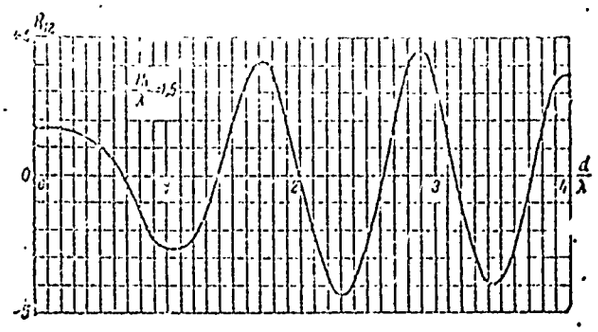

Figure H.III.9.

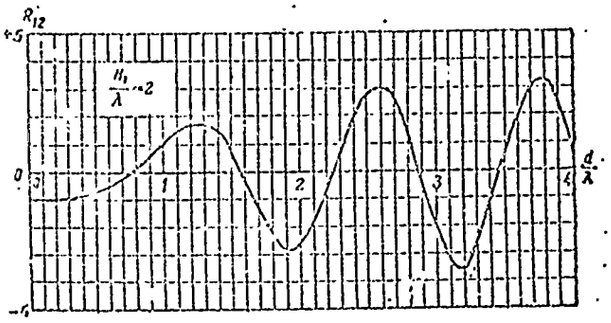

Figure H.III.10.

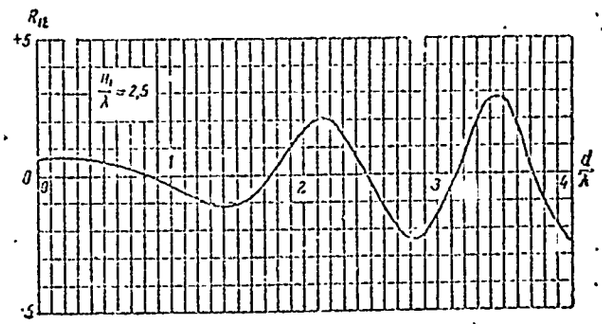

Figure H.III.11.

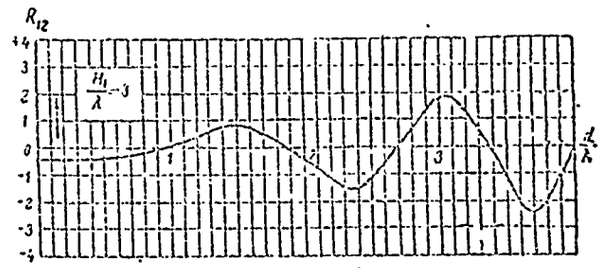

Figure H.III.12.

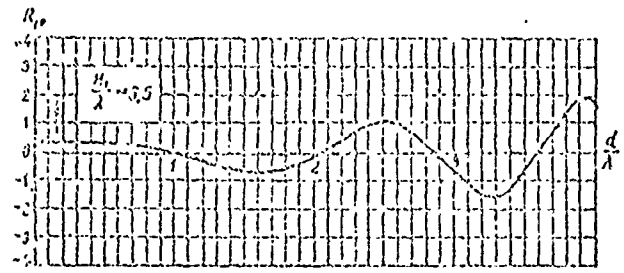

Figure II.III.13.

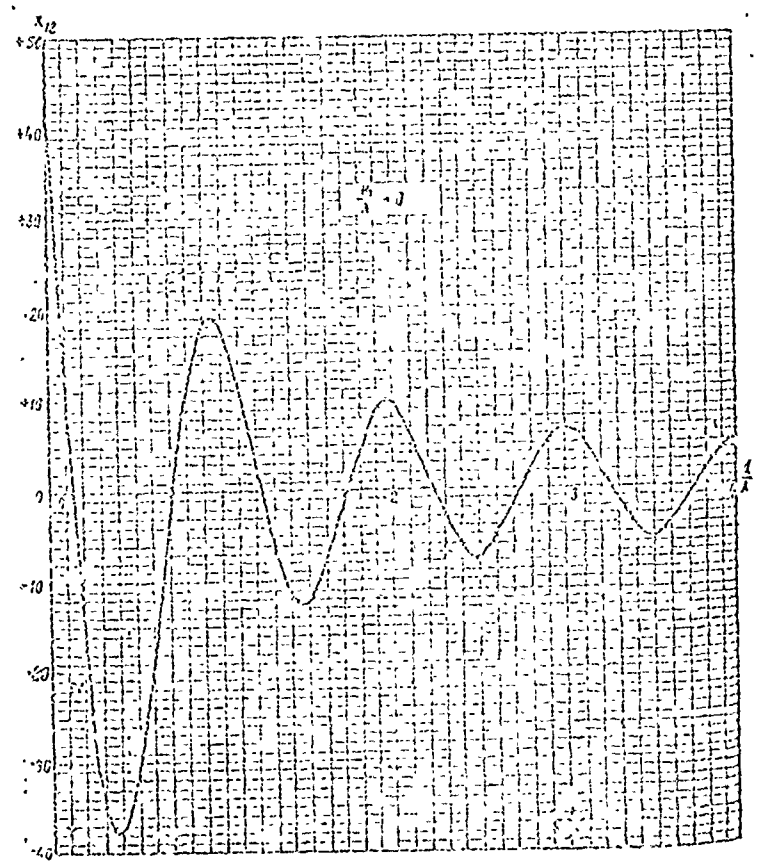

Figure II.III.14.

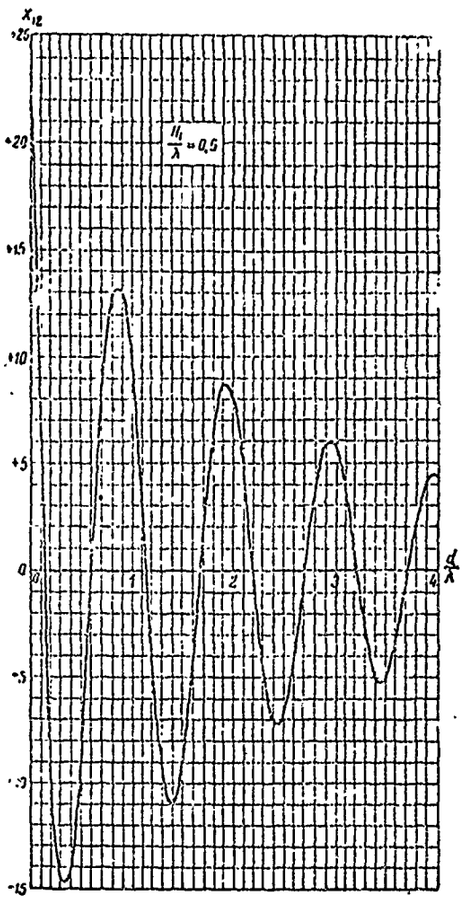

Figure H.III.15.

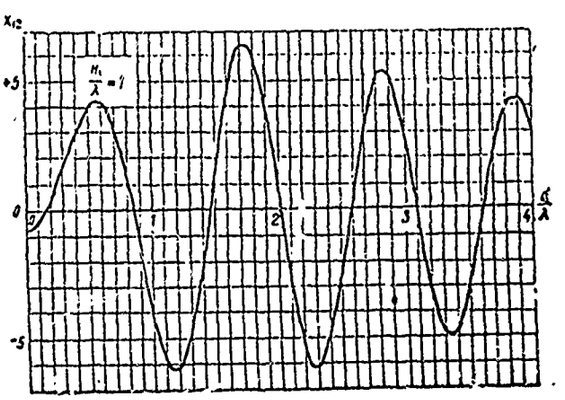

Figure H.III.16.

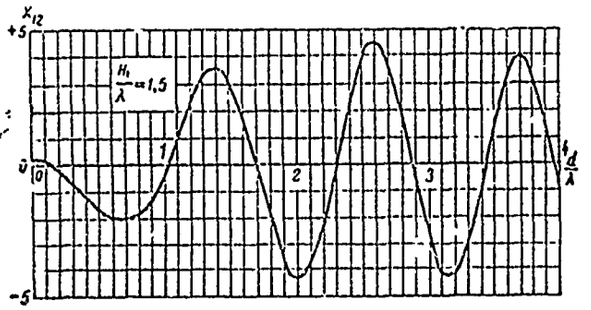

Figure H.III.17.

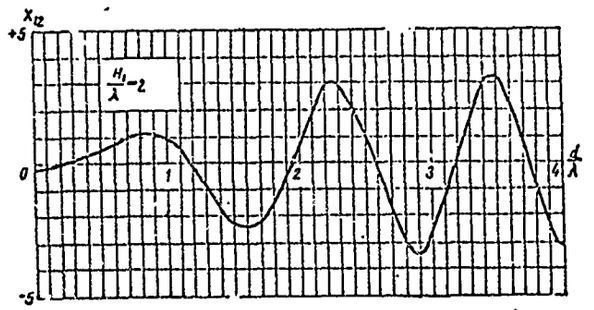

Figure H.III.18.

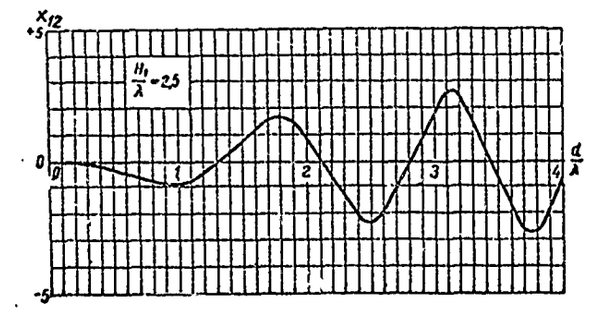

Figure H.III.19.

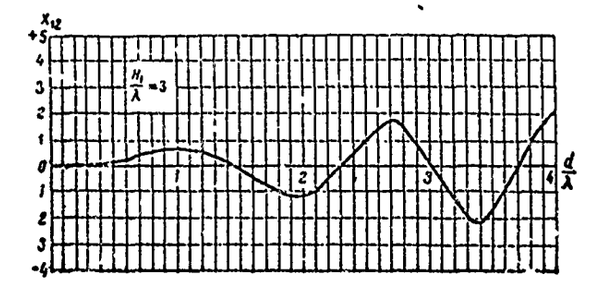

Figure H.III.20.

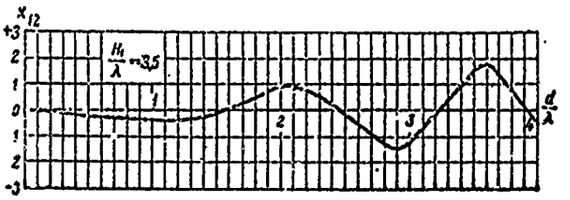

Figure H.III.21.

Figure H.III.22.

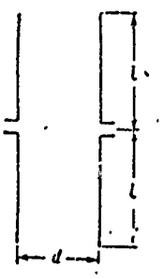

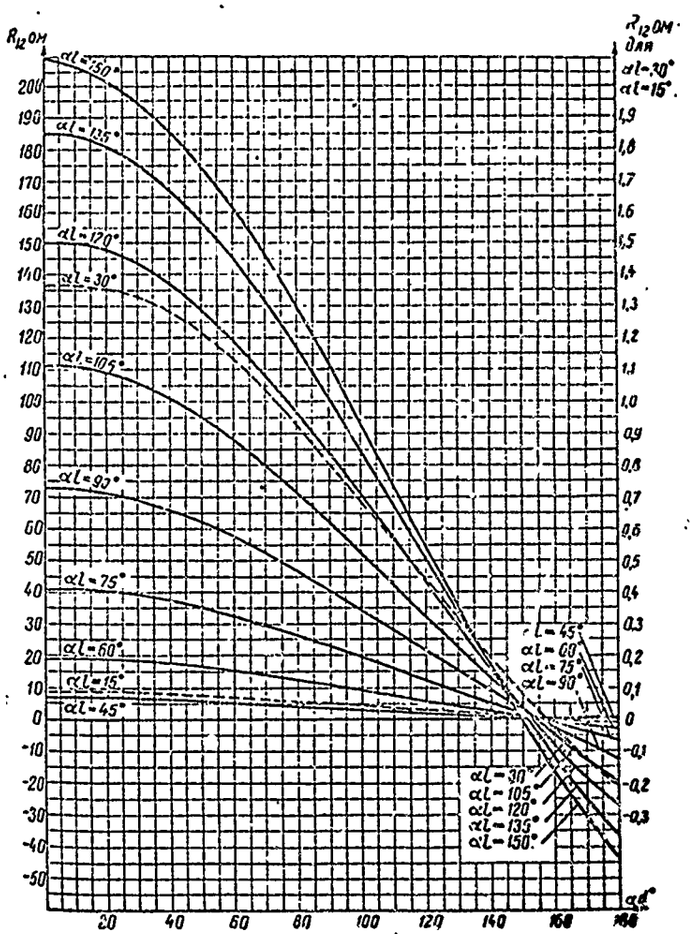

Figure H.III.23.

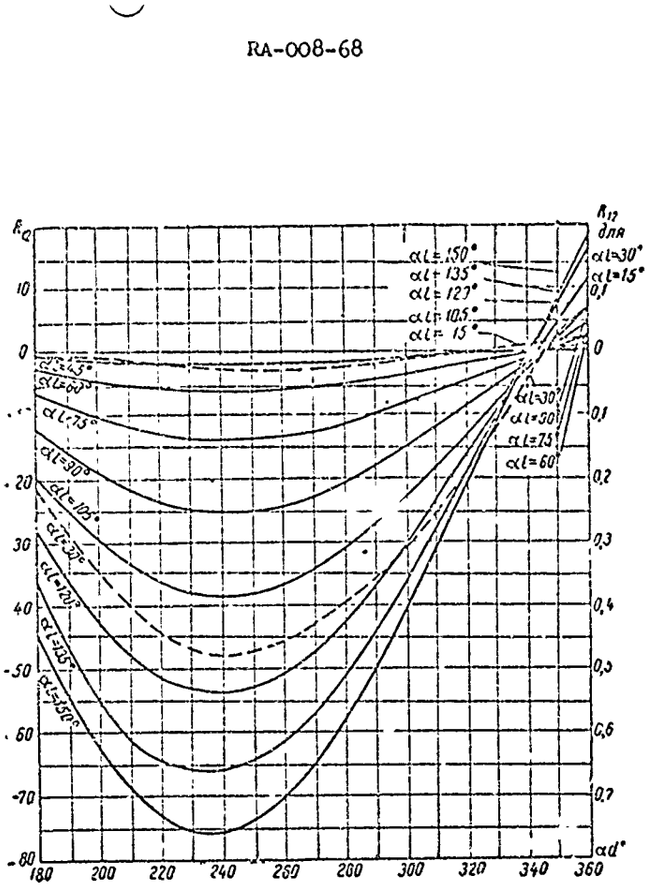

Figure H.III.24.

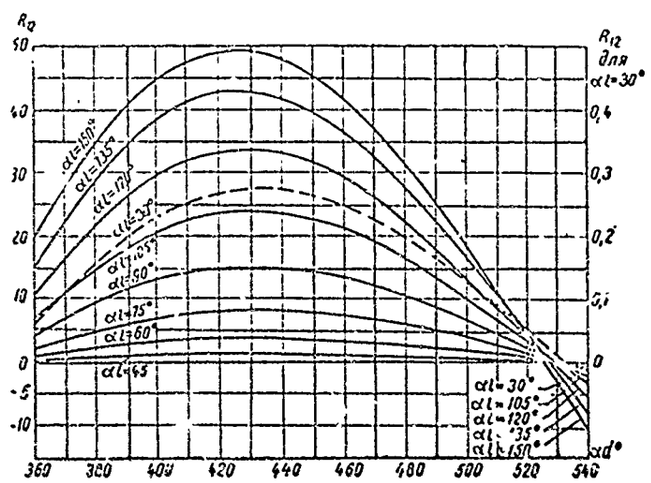

Figure H.III.25.

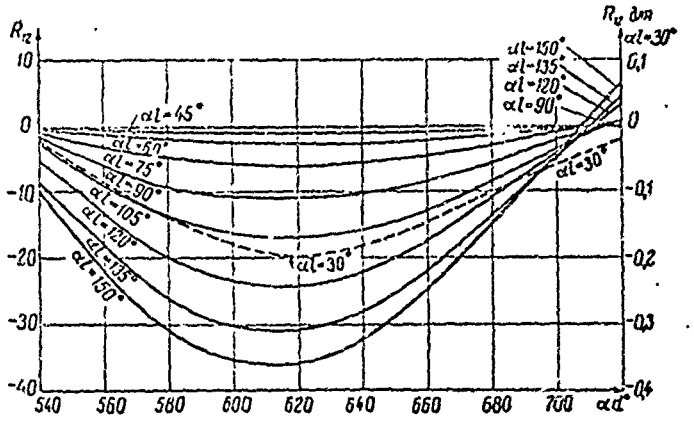

Figure H.III.26.

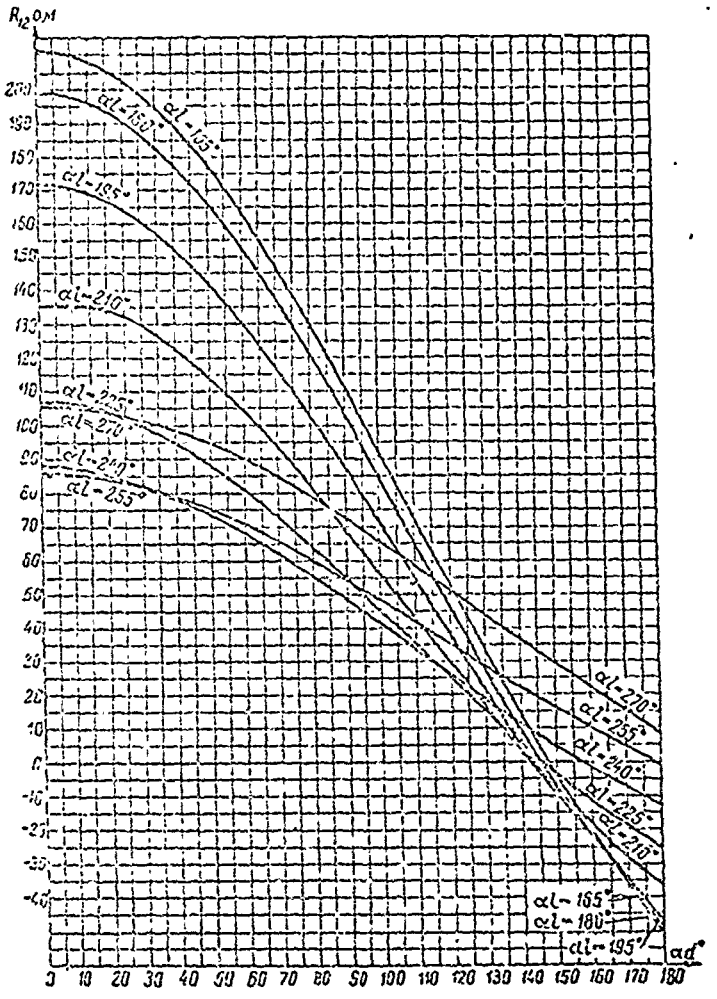

Figure H.III.27.

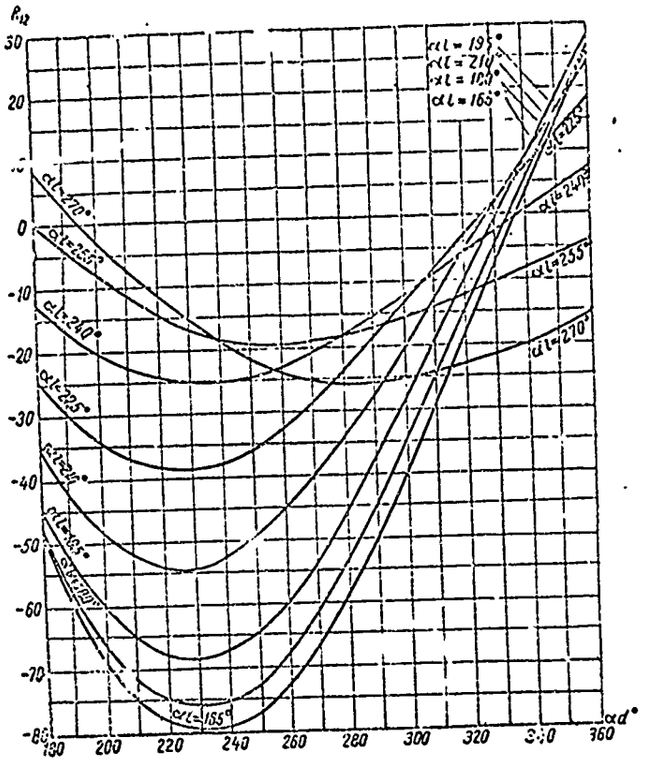

Figure H.III.28.

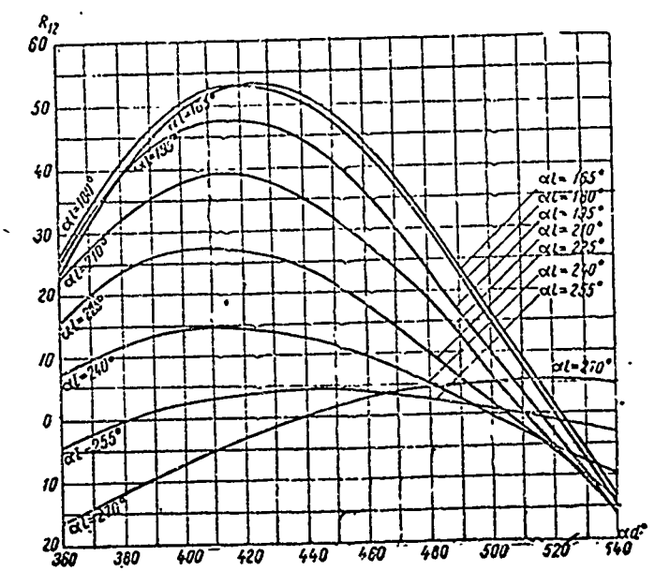

Figure H.III.29.

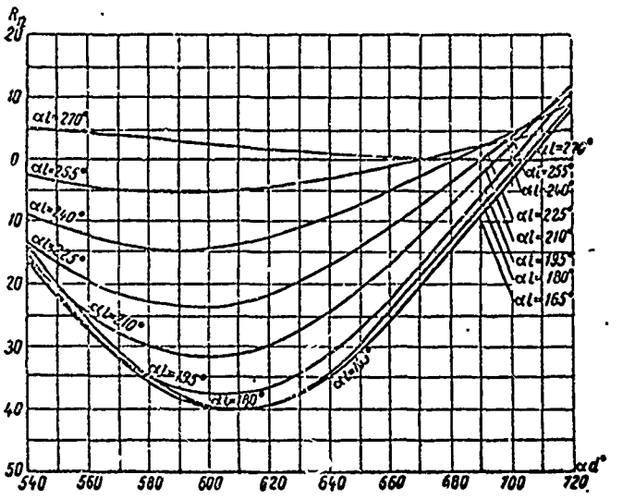

Figure H.III.30.

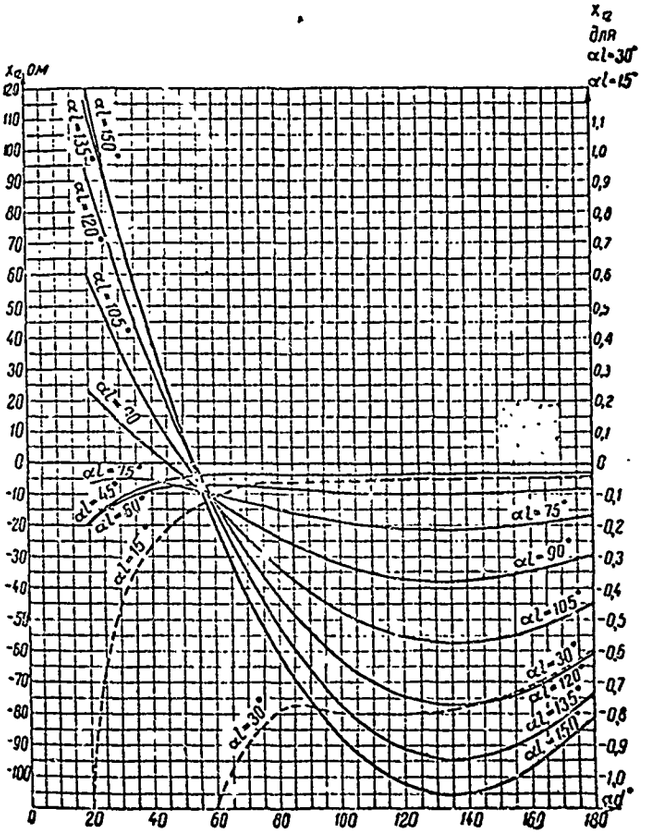

Figure H.III.31.

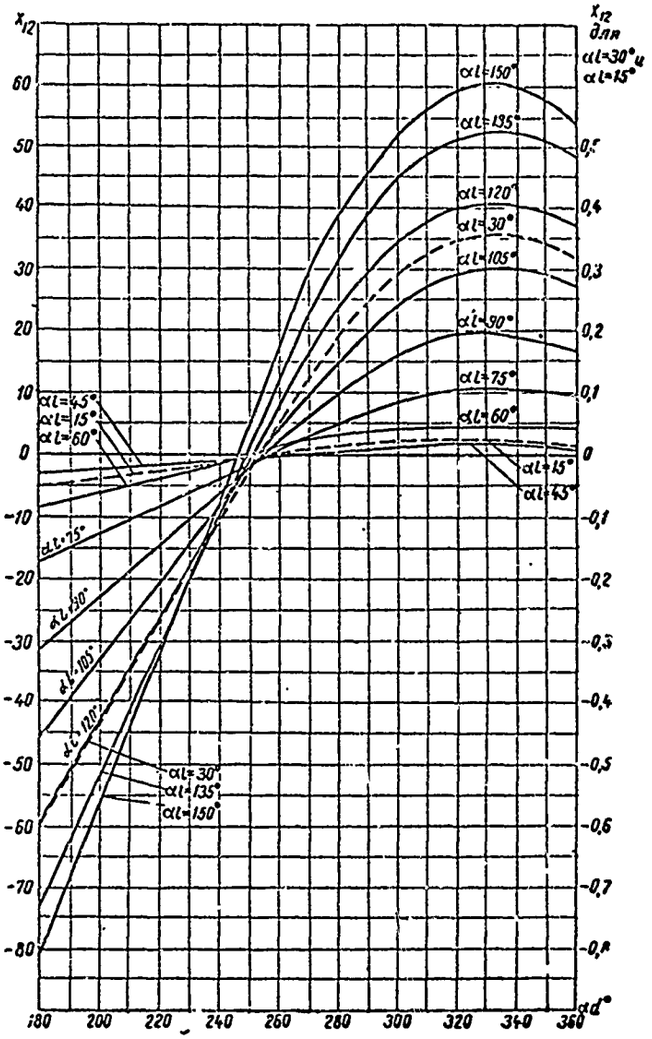

Figure H.III.32.

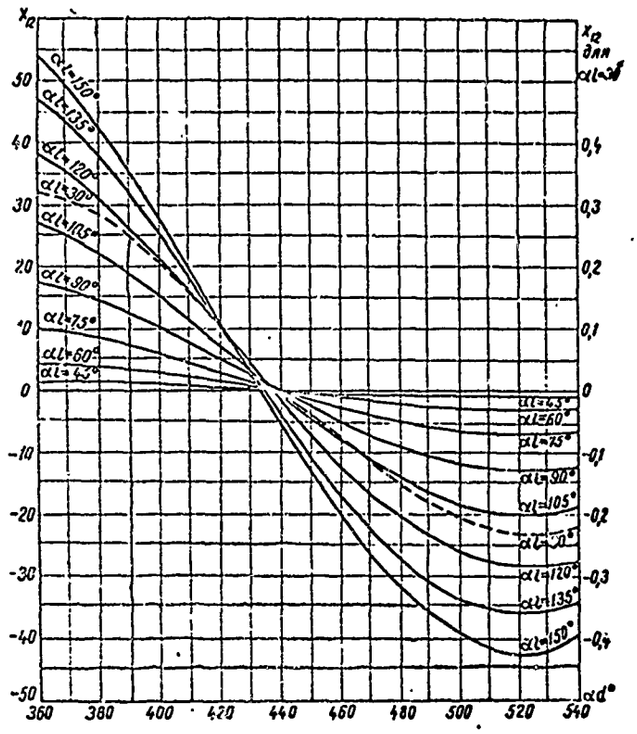

Figure H.III.33.

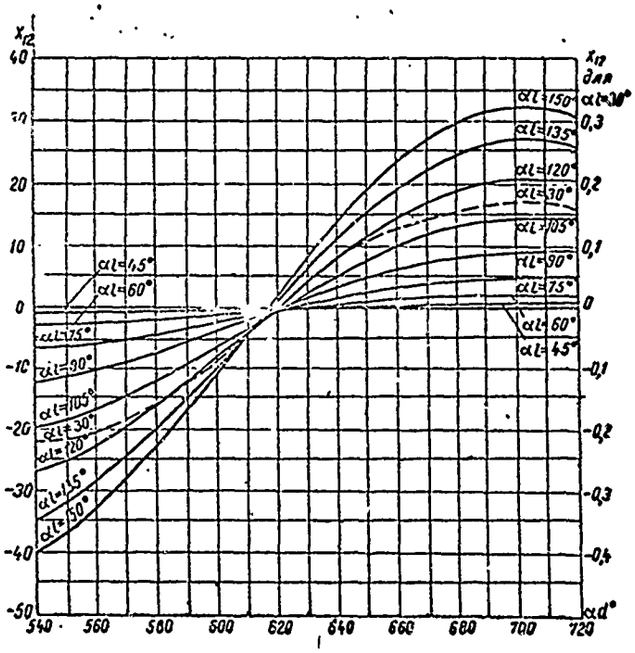

Figure H.III.34.

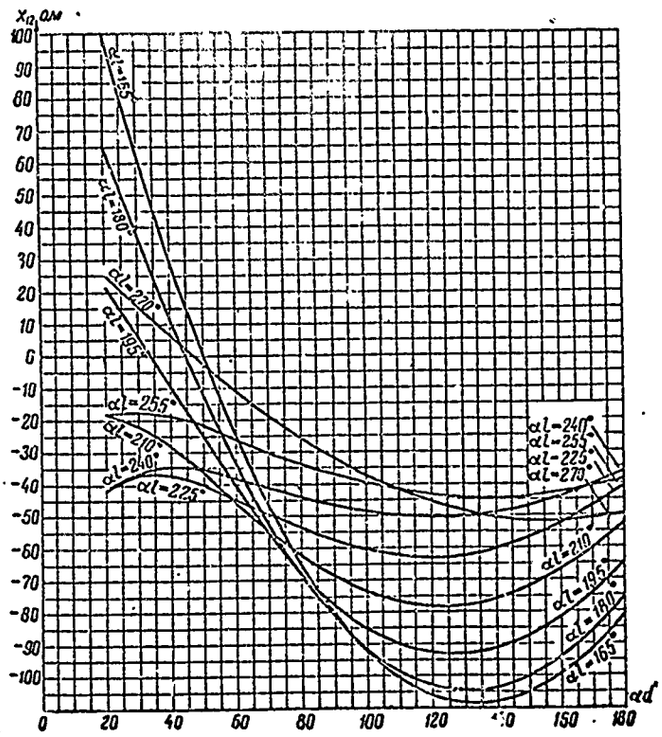

Figure H.III.35.

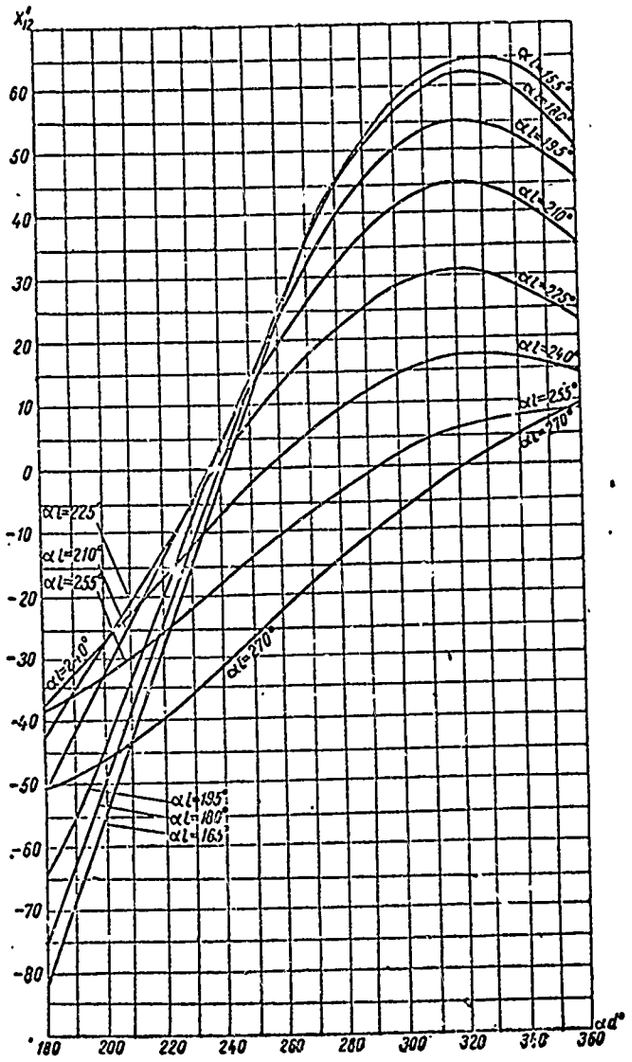

Figure H.III.36.

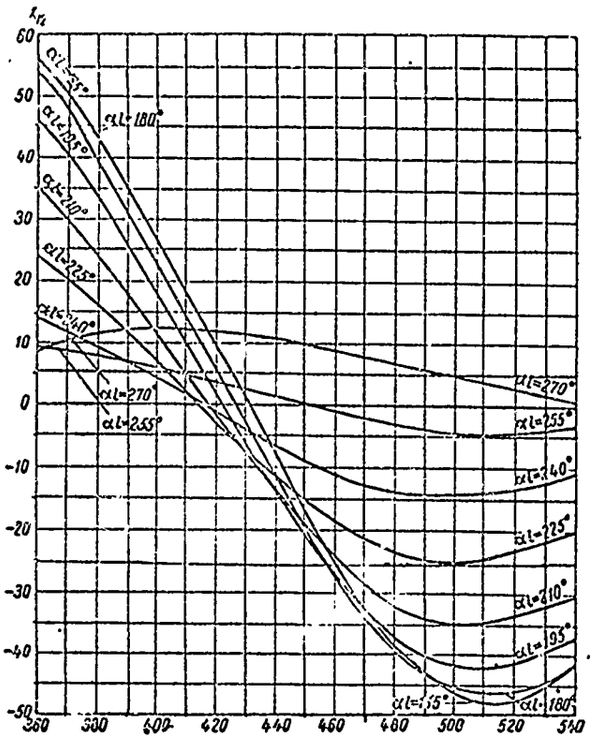

Figure H.III.37.

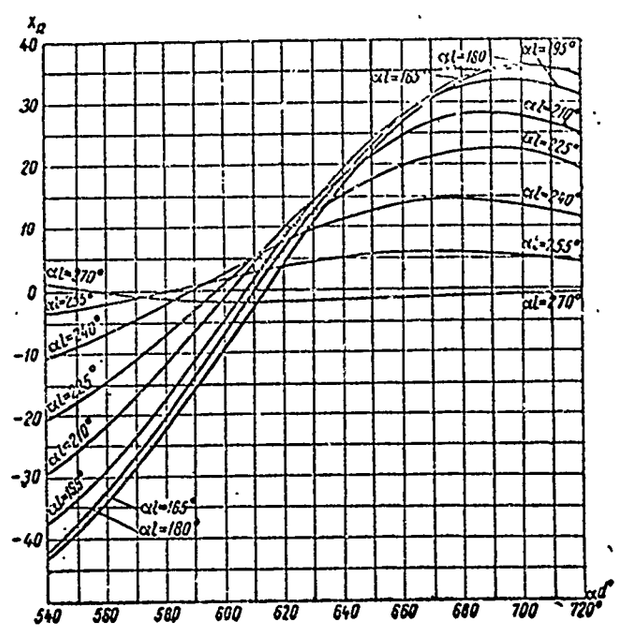

Figure H.III.38.

H.IV. Formulas for computing the distributed constants and characteristic impedances of transmission lines

#H.IV.1. The relationships between L_1, C_1 and W

As was explained in Chapter I, the characteristic impedance of a line at high frequencies can be taken equal to

$$W = \sqrt{\frac{L_1}{C_1}}, \qquad \text{(H.IV.1)}$$

where

L_1 and C_1 are the inductance and capacitance per unit length of the line.

In formula (H.IV.1) L_1, C_1, and W are measured in practical units; henries per meter (h/m), farads per meter (f/m), and ohms. Accordingly, W equals

$$W = \sqrt{L_1(\text{h/m})/C_1(\text{f/m})}, \text{ ohms} \qquad \text{(H.IV.2)}$$

If L_1 and C_1 are measured in absolute units, centimeters of inductance, and centimeters of capacitance per centimeter length, the characteristic impedance can be expressed through the formula

$$W = 30\sqrt{L_1(\text{cm/cm}) \,/\, C_1(\text{cm/cm})}, \text{ ohms} \qquad \text{(H.IV.3)}$$

If the line is in free space, or in air, the electrical parameters of which are virtually the same as the free space parameters, then

$$L_1(\text{h/m})C_1(\text{f/m}) = 1/9\cdot10^{16}(\text{sec}^2/\text{m}^2) \qquad \text{(H.IV.4)}$$

or

$$L_1(\text{cm/cm})C_1(\text{cm/cm}) = 1 . \qquad \text{(H.IV.5)}$$

Substituting (H.IV.4) in (H.IV.2) and (H.IV.5) in (H.IV.3), we obtain the fact that the characteristic impedance equals

$$W = 1/3\cdot10^{8}C_1\ (\text{f/m}) = 3\cdot10^{8}L_1(\text{h/m}), \text{ ohms} \qquad \text{(H.IV.6)}$$

or

$$W = 30/C_1(\text{cm/cm}) = 30\ L_1(\text{cm/cm}), \text{ ohms} \qquad \text{(H.IV.7)}$$

Given below are the formulas for computing the distributed constants per unit length; capacitance C_1, inductance L_1, pure resistance R_1, and the characteristic impedance W.

The formulas are given for a number of the most frequently used types of lines.

#H.IV.2. Formulas for computing L_1, C_1, R_1, and W

(a) A long horizontal conductor suspended close to the ground

The capacitance per unit length of the line (conductor) is

$$C_1 = \frac{1}{9\cdot10^9\cdot 2\ln\frac{4H}{d}}\left(\frac{f}{m}\right) = \frac{1}{2\ln\frac{4H}{d}}\left(\frac{cm}{cm}\right), \qquad \text{(H.IV.8)}$$

where

H is the height at which the conductor is suspended;

d is the diameter of the conductor;

H and d are measured in the same units.

The inductance per unit length of line is

$$L_1 = \frac{1}{10^9}\,2\ln\frac{4H}{d}\left(\frac{h}{m}\right) = 2\ln\frac{4H}{d}\left(\frac{cm}{cm}\right). \qquad \text{(H.IV.9)}$$

The pure resistance per unit line of a copper conductor (ground effect not considered) is

$$R_1 = \frac{1.18}{d\sqrt{\lambda}}, \frac{ohms}{m} = \frac{1.18\cdot10^{-3}}{d\sqrt{\lambda}}, \frac{ohms}{cm}, \qquad \text{(H.IV.10)}$$

where

d is the diameter of the conductor, in mm;

λ is the wavelength in meters.

The pure resistance per unit length of a conductor made of any material is

$$R_1 = \frac{11\cdot10^3}{d}\sqrt{\frac{\mu_r\rho}{\lambda}}, \frac{ohms}{m}, \qquad \text{(H.IV.11)}$$

where

d is the diameter of the conductor in mm;

λ is the wavelength in meters;

ρ is the specific resistance of the material of which the conductor is made (ohms/meter);

μ_r is the relative permeability of the material of which the conductor is made.

Given below are the values of ρ and μ_r for various metals.

Metals	ρ (ohms/m) at 20°C	μ_r
Copper, cold drawn	$0.177 \cdot 10^{-7}$	1
Copper, annealed	$0.1725 \cdot 10^{-7}$	1
Aluminum, industrial, cold drawn	$0.282 \cdot 10^{-7}$	1
Zinc, traces of iron	$0.575 \cdot 10^{-7}$	1
Iron 99, 98% pure	$1 \cdot 10^{-7}$	80
Steel	1 to $2 \cdot 10^{-7}$	80
Steel, manganese	$7.15 \cdot 10^{-7}$	80

The μ_r values are given for high frequencies.

The characteristic impedance of the line is

$$W = 60 \ln 4H/d \text{ ohms} \qquad \text{(H.IV.12)}$$

Formulas (H.IV.8) through (H.IV.11) do not consider ground conductivity characteristics other than ideal.

(b) A two-conductor line

The capacitance per unit length of the line is

$$C_1 = \frac{1}{9 \cdot 10^9} \cdot \frac{1}{4 \ln \left[\frac{D}{d} + \sqrt{\left(\frac{D}{d}\right)^2 - 1} \right]} \cdot \frac{f}{m} = \frac{1}{4 \ln \left[\frac{D}{d} + \sqrt{\left(\frac{D}{d}\right)^2 - 1} \right]} \cdot \frac{cm}{cm}, \qquad \text{(H.IV.13)}$$

where

D is the distance between the conductors;

d is the conductor diameter;

D and d are measured in the same units.

The inductance per unit length of line is

$$L_1 = \frac{1}{10^9} 4 \ln \left[\frac{D}{d} + \sqrt{\left(\frac{D}{d}\right)^2 - 1} \right] \cdot \frac{h}{m} = 4 \ln \left[\frac{D}{d} + \sqrt{\left(\frac{D}{d}\right)^2 - 1} \right] \cdot \frac{cm}{cm}. \qquad \text{(H.IV.14)}$$

The pure resistance per unit length of a copper wire line is

$$R_1 = \frac{2,96}{d \sqrt{\lambda}} \left(\frac{ohms}{m}\right) = \frac{29,6 \cdot 10^{-3}}{d \sqrt{\lambda}} \left(\frac{ohms}{cm}\right), \qquad \text{(H.IV.15)}$$

where

d is the conductor diameter in mm;

λ is the wavelength in meters.

The pure resistance per unit length of a line of any metal is

$$R_1 = \frac{22 \cdot 10^3}{d} \sqrt{\frac{\mu \rho}{\lambda}} \cdot \frac{ohms}{m}. \qquad \text{(H.IV.16)}$$

The characteristic impedance of the line is

$$W = 120 \ln \left[\frac{D}{d} + \sqrt{\left(\frac{D}{d}\right)^2 - 1} \right], \ ohms \qquad \text{(H.IV.17)}$$

If the distance between the conductors, D, is very much greater than their diameter, d, formulas (H.IV.14), (H.IV.14), and (H.IV.17) can be simplified and will be in the form

$$C_1 = \frac{1}{9 \cdot 10^9} \cdot \frac{1}{4 \ln \frac{2D}{d}} \left(\frac{f}{m}\right) = \frac{1}{4 \ln \frac{2D}{d}} \left(\frac{cm}{cm}\right), \qquad \text{(H.IV.18)}$$

$$L_1 = \frac{1}{10^7} 4 \ln \frac{2D}{d} \left(\frac{h}{m}\right) = 4 \ln \frac{2D}{d} \left(\frac{cm}{cm}\right), \qquad \text{(H.IV.19)}$$

$$W = 120 \ln \frac{2D}{d}, \ ohms \qquad \text{(H.IV.20)}$$

(c) A coaxial line

The capacitance per unit length of line is

$$C_1 = \frac{1}{9 \cdot 10^9} \cdot \frac{1}{2 \ln \frac{d_1}{d_2}} \left(\frac{f}{m}\right) = \frac{1}{2 \ln \frac{d_1}{d_2}} \left(\frac{cm}{cm}\right), \qquad \text{(H.IV.21)}$$

where

d_1 is the inside diameter of the shield;

d_2 is the diameter of the internal conductor.

The inductance per unit length of line is

$$L_1 = \frac{1}{10^7} 2 \ln \frac{d_1}{d_2} \left(\frac{h}{m}\right) = 2 \ln \frac{d_1}{d_2} \left(\frac{cm}{cm}\right). \qquad \text{(H.IV.22)}$$

The pure resistance per unit length of a copper line is

$$R_1 = \left(\frac{1}{d_1} + \frac{1}{d_2}\right) \frac{1,48}{\sqrt{\lambda}} \cdot \frac{ohms}{m} = \left(\frac{1}{d_1} + \frac{1}{d_2}\right) \frac{14,8 \cdot 10^{-3}}{\sqrt{\lambda}} \cdot \frac{ohms}{cm}. \qquad \text{(H.IV.23)}$$

The characteristic impedance of the line is

$$W = 60 \ln \frac{d_1}{d_2}, \ ohms \qquad \text{(H.IV.24)}$$

Formulas (H.IV.21) through (H.IV.24) are given without taking the effect of the dielectric insulating the internal conductor from the shield into consideration. The calculation for the effect of the dielectric on the distributed capacitance is made by multiplying the right-hand side of equation (H.IV.21) by the magnitude

The effect of the dielectric on the characteristic impedance can be taken into consideration by multiplying the right-hand side of equation (H.IV.24) by $\frac{1}{\sqrt{1+a(\varepsilon_r-1)}}$.

The phase velocity is obtained as equal to

$$v = \frac{c}{\sqrt{1+a(\varepsilon_r-1)}}. \qquad \text{(H.IV.25)}$$

Here ε_r is the relative dielectrical permeability; that is, the ratio of the dielectrical permeability of the insulating dielectric to the dielectrical permeability of air.

a is the fill factor; that is, the ratio of the volume of the inner space of the cable filled by the dielectric to the total volume of the inner space in the cable.

#H.IV.3. Formulas for computing the characteristic impedance of selected types of transmission lines

(a) Two-wire unbalanced transmission line operating on a single-cycle wave (fig. H.IV.1).

The characteristic impedance can be found through the formula

$$W = 30 \ln \frac{4H}{d} \sqrt{1+\left(\frac{2H}{D}\right)^2}, \text{ ohms}. \qquad \text{(H.IV.26)}$$

If H ⩾ D, then

$$W = 60 \ln \frac{2H}{\sqrt{\frac{d}{2} D}}, \text{ ohms}.$$

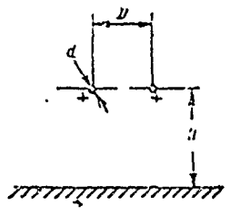

Figure H.IV.1.

(b) Three-wire unbalanced transmission line operating on a single-cycle wave (fig. H.IV.2) H ⩾ D

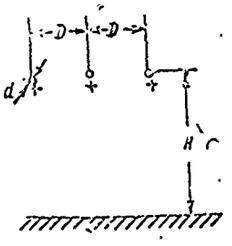

Figure H.IV.2.

$$W = 60 \frac{\ln \frac{4H^2}{dD} + \ln \frac{2H}{D} \cdot \frac{\ln \frac{D}{d}}{\ln \frac{2D}{d}}}{2 + \frac{\ln \frac{D}{d}}{\ln \frac{2D}{d}}}, \text{ ohms} \qquad \text{(H.IV.27)}$$

(c) Transmission line made up of n conductors located on the surface of a cylinder (fig. H.IV.3) $H \gg 2R$

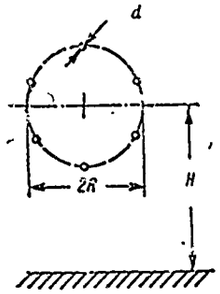

Figure H.IV.3.

$$W = 60 \ln \frac{2H}{R \sqrt[n]{\frac{nd}{2R}}}, \text{ ohms} \qquad \text{(H.IV.28)}$$

(d) Three-wire unbalanced transmission line (fig. H.IV.4).

The characteristic impedance of the upper conductor when the lower conductors are grounded equals

$$W_3 = 60 \left(\ln \frac{4H}{d_2} - \frac{\ln^2 \frac{2H}{D_2}}{\ln \frac{2H}{\sqrt{\frac{d_1}{2} D_1}}} \right), \text{ ohms} \qquad \text{(H.IV.29)}$$

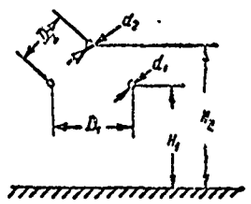

Figure H.IV.4.

The characteristic impedance of the two lower conductors when the upper conductor is grounded equals

$$W_1 = 60 \left(\ln \frac{2H}{\sqrt{\frac{d_1}{2} D_1}} - \frac{\ln^2 \frac{2H}{D_2}}{\ln \frac{4H}{d_2}} \right), \text{ ohms} \qquad \text{(H.IV.30)}$$

The mutual characteristic impedance is

$$W_{12} = 60 \left[\frac{\ln \frac{4H}{d_2} \ln \frac{2H}{\sqrt{\frac{d_1}{2} D_1}}}{\ln \frac{2H}{D_2}} - \ln \frac{2H}{D_2} \right], \text{ ohms} \qquad \text{(H.IV.31)}$$

The characteristic impedance when the wave is of the opposite phase equals

$$W_{opp} = 60 \ln \frac{2D_2^2}{d_2 \sqrt{\frac{d_1}{2} D_1}}, \text{ ohms} \qquad \text{(H.IV.32)}$$

The ratio of the current flowing to ground to the current flowing in conductor 2 at conductor potential (symbol blurred in text) equal to zero is

$$\frac{I_3}{I_2} = 1 - \frac{\ln \frac{2H}{D_2}}{\ln \frac{2H}{\sqrt{D_1 \frac{d_1}{2}}}}. \qquad \text{(H.IV.33)}$$

Formulas (H.IV.29) - (H.IV.33) are based on the assumption that $H_1 \gg D_1$ and $H_1 \gg D_2$, and that, accordingly, $H_1 \approx H_2 \approx H$.
In these formulas

$$H = H_1 + H_2/2.$$

(e) Single-wire transmission line surrounded by n shielded conductors located on the surface of a cylinder (fig. H.IV.5).

Figure H.IV.5.

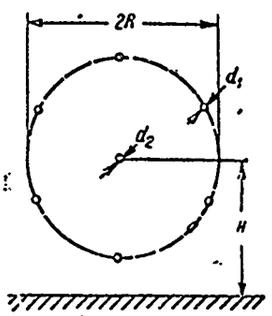

The characteristic impedance of the inner conductor when the outer conductors are grounded equals

$$W_2 = 60 \left(\ln \frac{4H}{d_2} - \frac{\ln^2 \frac{2H}{R}}{\ln \frac{2H}{R \sqrt[n]{\frac{nd_1}{2R}}}} \right), \text{ ohms} \qquad \text{(H.IV.34)}$$

The characteristic impedance of the outer conductors when the inner conductor is grounded equals

$$W_1 = 60 \left(\ln \frac{2H}{R \sqrt[n]{\frac{nd_1}{2R}}} - \frac{\ln^2 \frac{2H}{R}}{\ln \frac{4H}{d_2}} \right), \text{ ohms} \qquad \text{(H.IV.35)}$$

The mutual characteristic impedance equals

$$W_{12} = 60 \frac{\ln \frac{4H}{d_2} \ln \frac{2H}{R\sqrt[n]{\frac{nd_1}{2R}}} - \ln^2 \frac{2H}{R}}{\ln \frac{2H}{R}}, \text{ ohms} \qquad \text{(H.IV.36)}$$

The characteristic impedance for a wave of opposite phase equals

$$W_{opp} = 60 \ln \frac{2R}{d_2 \sqrt[n]{\frac{nd_1}{2R}}}, \text{ ohms} \qquad \text{(H.IV.37)}$$

$$\frac{I_2}{I_1} = 1 - \frac{\ln \frac{2H}{R}}{\ln \frac{2H}{R\sqrt[n]{\frac{nd_1}{2R}}}}. \qquad \text{(H.IV.38)}$$

(f) A multi-conductor line made up of n_2 conductors located on the surface of a cylinder surrounded by n_1 shielded conductors (fig. H.IV.6).

The characteristic impedance of the inner conductors when the outer conductors are grounded is

$$W_2 = 60 \left(\ln \frac{2H}{R_2 \sqrt[n_2]{\frac{n_2 d_2}{2R_2}}} - \frac{\ln^2 \frac{2H}{R_1}}{\ln \frac{2H}{R_1 \sqrt[n_1]{\frac{n_1 d_1}{2R_1}}}} \right), \text{ ohms} \qquad \text{(H.IV.39)}$$

The characteristic impedance of the outer conductors when the inner conductors are grounded equals

$$W_1 = 60 \left(\ln \frac{2H}{R_1 \sqrt[n_1]{\frac{n_1 d_1}{2R_1}}} - \frac{\ln^2 \frac{2H}{R_1}}{\ln \frac{2H}{R_2 \sqrt[n_2]{\frac{n_2 d_2}{2R_2}}}} \right), \text{ ohms} \qquad \text{(H.IV.40)}$$

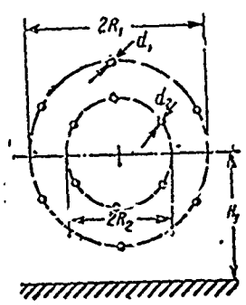

Figure H.IV.6.

The mutual characteristic impedance equals

$$W_{12} = \frac{\ln\frac{2H}{R_1\sqrt[n_1]{\frac{n_1 d_1}{2R_1}}}\ln\frac{2H}{R_2\sqrt[n_2]{\frac{n_2 d_2}{2R_2}}} - \ln^2\frac{2H}{R_1}}{\ln\frac{2H}{R_1}}, \text{ ohms} \qquad \text{(H.IV.41)}$$

The characteristic impedance for a wave with the opposite phase is

$$W_{opp} = 60\ln\frac{R_1}{R_2\sqrt[n_2]{\frac{n_2 d_2}{2R_2}}\sqrt[n_1]{\frac{n_1 d_1}{2R_1}}}, \text{ ohms} \qquad \text{(H.IV.42)}$$

$$\frac{I_2}{I_1} = 1 - \frac{\ln\frac{2H}{R_1}}{\ln\frac{2H}{R_1\sqrt[n_1]{\frac{n_1 d_1}{2R_1}}}}, \qquad \text{(H.IV.43)}$$

where

n_1 is the number of conductors in the shield;

n_2 is the number of inner conductors.

(g) A multi-conductor uncrossed balanced transmission line (fig. H.IV.7).

$$W \approx \frac{120}{n}\ln\frac{2\sqrt{n}D}{d}, \text{ ohms} \qquad \text{(H.IV.44)}$$

n is the number of conductors passing the in-phase current.

(h) Flat balanced transmission line (fig. H.IV.18). a ⩾ d.

$$W = 30\left[4\ln\left(1+\frac{D}{a}\right) + 8\frac{D}{a+D} - 2\left(\frac{D}{a+D}\right)^2\right], \text{ ohms} \qquad \text{(H.IV.45)}$$

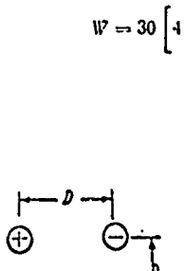

Figure H.IV.7.

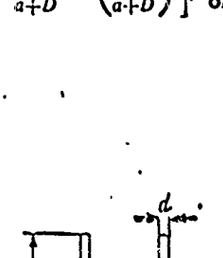

Figure H.IV.8.

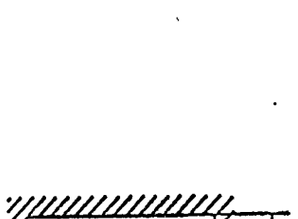

Figure H.IV.9.

(i) Conductor in a shield with a square cross section (fig. H.IV.9) D/d > 2.

$$W = 60\ln\frac{1{,}078D}{d}, \text{ ohms} \qquad \text{(H.IV.46)}$$

(j) Two-wire line in a shield with a rectangular cross section (fig. H.IV.10).

$$W = 120 \ln \frac{\operatorname{th}\left(\frac{\pi}{a} r_1\right) \operatorname{th}\left(\frac{\pi}{2a} D\right)}{\operatorname{th}\left(\frac{\pi}{4a} d\right) \operatorname{th}\left(\frac{\pi}{2a} b\right)}, \text{ ohms} \qquad \text{(H.IV.47)}$$

(k) Two-wire line in a shield with a cricular cross section (fig. H.IV.11).

$$W = 120 \operatorname{arch}\left(\frac{l}{d} \frac{D^2 - l^2 + d^2}{D^2 + l^2 - d^2}\right), \text{ ohms} \qquad \text{(H.IV.48)}$$

when D/d > 4,

$$W = 120 \ln\left(\frac{2l}{d} \frac{D^2 - l^2}{D^2 + l^2}\right), \text{ ohms} \qquad \text{(H.IV.49)}$$

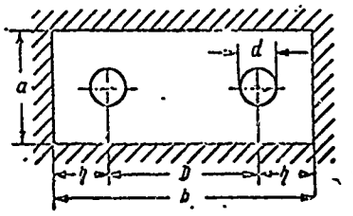

Figure H.IV.10.

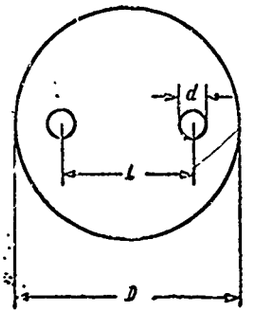

Figure H.IV.11.

Formulas (H.IV.26) through (H.IV.43), cited in this paragraph, are from an unpublished work by V. D. Kuznetsov.

H.V. Materials for making shortwave antennas

#H.V.1. Conductors

Tables H.V.1, H.V.2, and H.V.3 contain basic data on conductors used in shortwave antennas.

Table H.V.1

Basic data on materials for antenna conductors.

№№ пп. A	Характеристика материалов Б	Единица измерения C	D Проволока: медная твёрдотянутая E	бронзовая F	биметаллическая G	стальная H	алюминиевая твёрдотянутая I
1	Удельный вес .	$\frac{g}{см^3}$	8,89	8,89	8,3	7,85	2,7
2	Коэффициент температурного линейного расширения α	—	$17 \cdot 10^{-6}$	$18 \cdot 10^{-6}$	$12 \cdot 10^{-6}$	$12 \cdot 10^{-6}$	$23 \cdot 10^{-6}$
3	Модуль упругости E	$\frac{kg}{мм^2}$	13 000	13 000	19 000 —20 000	20 000	6 300
4	Предел прочности	»	42—43	70	75	37	16—17
5	Предел упругости σ	»	28—35	40	29	29	11—12
6	Коэффициент упругого удлинения β	—	$77 \cdot 10^{-6}$	$77 \cdot 10^{-6}$	$52,5 \cdot 10^{-6}$	$50 \cdot 10^{-6}$	$159 \cdot 10^{-6}$
7	Сопротивление постоянному току 1 *км* длины при 1 *кв. мм* поперечного сечения при температуре + 20°Ц, *ом* .		17,84	40,62	[1]	$\frac{138}{146}$	29,5
8	Температурный коэффициент изменения электрического сопротивления постоянному току на 1°Ц		0,00393	0,00152	0,0041	0,00455	—

1. depends on conductor diameter.

Key: A - No.; B - Characteristics of materials; C - Units of measurement; D - Wire; E - Copper, hard drawn; F - Bronze; G - Bimetallic; H - Steel; I - Aluminum, hard drawn. 1 - specific weight; 2 - temperature coefficient of linear expansion, α; 3 - modulus of elasticity, E; 4 - yield strength; 5 - elastic limit, σ; 6 - coefficient of elastic elongation, β; 7 - DC resistance of 1 km of length at 1 kv/mm of transverse cross section at +20°C, ohms; 8 - temperature coefficient of change in the electrical resistance to DC per 1°C.

Table H.V.2

Basic data on solid conductors used in antenna installations

№ пп	Наименования проводов	Диаметр провода, мм	Сечение, мм²	Электрическое сопротивление 1 км провода при 20°Ц, ом	Вес 1 км провода, кг	Вес проволоки в бухте не менее, кг	№№ стандартов
A	B	C	D	E	F	G	H
1	Проволока сплошная медная твёрдотянутая «МС»	1,5	1,77	10,08	15,71	10	OST NKTP-2797
		2,5	4,91	3,63	43,64	25	
		3,0	7,07	2,52	62,84	35	
		3,5	9,61	1,82	85,60	48	
		4,0	12,57	1,42	111,71	50	
2	Проволока сплошная отожжённая «ММ», мягкая, медная	1	0,78	—	6,98	15	GOST-2112—46
		2	3,14	—	27,93	20	
		3	7,07	—	62,84	40	
		4	12,57	—	111,71	60.	
3	Проволока биметаллическая	1,5	1,77	28,5	15	10	GOST-3822—47 eff. 8/1/48
		2.	3,14	20	26,5	15	
		3,0	7,07	6,7	59,5	25	
		4,0	12,57	3,8	106	40	
		6,0	28,20	2	—	40	
4	Проволока стальная обыкновенная с содержанием меди менее 0,2%	1,5	1,77	78,1	13,9	10	GOST-1668—46
		2,0	3,14	43,9	24,7	20	
		2,5	4,91	28,1	38,5	20	
		3,0	7,07	19,5	55,5	25	
		4,0	12,57	11.0	98,6	40	
		5	19,63	7,0	154	50	
		6	28,27	4.9	222	50	
5	Проволока стальная перевязочная и спаечная	1,0	0,78	—	6,17	5	OST-11458—39
		1,4	1,54	—	12,1	10	
		2,0	3,14	—	24,7	15	
		2,5	4,91	—	38,5	20	
6	Проволока алюминиевая круглая «АТ»	2	3,14	9,4	8,5	15	OST-7567
		3	7,07	4,2	19,1	15	
		4	12,57	2,4	34	20	
		4,5	15,90	1,9	42,7	20	
7	Проволока алюминиевая мягкая «АМ»	1	0,78	37,6	2,12	—	OST-7567
		2	3,14	9,4	8,5	—	
		3	7,07	4,2	19,1	—	
		4	12,57	2,4	34	—	
		4,5	15,90	1,9	42,7	—	
8	Альдрей	4	12,57	2,65	34	—	
9	Провод изолированный с резиновой изоляцией ПР-380	10 наружн. диаметр	11 номинальное сечение				
		3,0	1,0	—	20	—	
		3,7	2,5	—	35	—	
		4,6	6,0	—	70	—	

Key: A - No.; B - conductor designation; C - conductor diameter, mm; D - cross section, mm^2; E - electrical resistance of 1 km of conductor at 20°C, ohms; F - weight of 1 km of conductor, kg; G - weight of wire in a coil, at least, kg; H - no. of standard.

1 - wire, solid, copper, hard drawn, "MS"; 2 - wire solid, annealed, "MM," soft, copper; 3 - wire bimetallic; 4 - wire, steel, ordinary, with a copper content of at least 0.2%; 5 - wire steel, wrapped and tinned; 6 - wire, aluminum, round "AT"; 7 - wire, aluminum, soft "AM"; 8 - aldrey (an aluminum magnesium alloy); 9 - conductor insulated with PR-380 rubber insulation; 10 - OD; 11 - designed cross section.

Table H.V.3

Basic data on stranded conductors used in antenna installation

№ пп. A	Наименование проводов B	Номинальное сечение провода, мм² C	Диаметр отдельных проволок, мм D	Число проволок E	Диаметр провода, мм F	Электрическое сопротивление 1 км провода при 20° Ц, ом G	Временное сопротивление разрыву кг/мм² H	Вес 1 км, кг I	№№ стандартов J
1	Провод медный антенный нормальный ПА	1,5	0,52	7	1,6	12,65	35		VTUZ-271—43
		2,5	0,67	7	2,0	7,6	35		
		4,0	0,85	7	2,6	4,76	35		
		6,0	1,03	7	3,1	3,17	35		
		10	1,03	12	4,3	1,90	35		
		16	1,03	19	5,2	1,18	35		
2	Провод медный антенный гибкий ПАГ	1,5	0,15	7×12	1,6	12,61	35		VTUZ-271—43
		2,5	0,20	7×12	2,0	7,6	35		
		4	0,32	7×7	2,6	4,76	35		
		6	0,39	7×7	3,1	9,17	35		
		10	0,51	7×7	4,3	1,90	35		
3	Провод медный антенный плетёный ПАП	1,5	0,34	16	2	12,45	40		VTUZ-271—43
4	Провод бронзовый ПАБМ	1,5	0,2	7×7	1,8	—	54	15	OST-EL-2—40
		2,5	0,26	7×7	2,3	—	56	25	
		4,0	0,32	7×7	2,9	—	65	40	
		10	0,51	7×7	4,6	—	65	100	
		25	0,49	7×19	7,4	—	65	250	
5	Провод бронзовый ПАБО	4	0,32	7×7	2,9	—*)	75	40	OST-EL-2—40
		10	0,51	7×7	4,6	—	75	100	
		25	0,49	7×19	7,4	—	75	250	
6	Провод алюминиевый	16	—	7	5,1	1,96	16	44	GOST-339—41
		35	—	7	7,5	0,91	16	95	
		70	—	7	10,6	0,45	16	190	
		120	—	19	14,0	0,27	16	323	
7	Провод сталеалюминиевый	50	8 стальн. 1,1 ал.	11 стальн. 7 ал. 6	9,8	—	—	190	
		70	9 3,25 стальн. 1,3 ал.	12 стальн. 7 ал. 6	11,6	—	—	264	
		95	10 3,83 стальн. 1,8 ал. 2,08	13 стальн. 7 ал. 28	13,5	—	—	386	

*) See Table H.IV.1.

Key: A - No.; B - conductor designation; C - rated cross section of the conductor, mm^2; D - diameter of individual wires, mm; E - number of wires; F - wire diameter, mm; G - electrical resistance of 1 km of conductor at 20°C, ohms; H - critical tensile strength, kg/mm^2; I - weight of 1 km, kg; J - no. of standard.

1 - conductor, copper, antenna, normal, PA; 2 - conductor, copper, antenna, flexible, PAG; 3 - conductor, copper, antenna, braided, PAP; 4 - conductor, bronze, PABM; 5 - conductor, bronze, PABO; 6 - conductor, aluminum; 7 - conductor, steel-aluminum; 8 - steel 1.1, aluminum 3.25; 9 - steel 1.3, aluminum 3.83; 10-steel 1.8, aluminum 2.08; 11 - steel 7, aluminum 6; 12 - steel 7, aluminum 6; 13 - steel 7, aluminum 28.

#H.V.2. Insulators

(a) Antenna insulators

Insulators, stick, armored, with slotted head (fig. H.V.1a, Table H.V.4). Material - steatite.

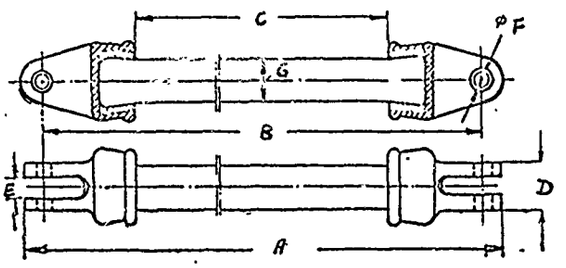

Figure H.V.1a.

Table H.V.4

No	Type insulator	Dimensions, mm A	B	C	D	E	F	G	Weight, kg
1	IPA-750	$345^{\pm 7}$	$315^{\pm 7}$	200	28	12	13	25	0,65
2	IPA-1,5т	$351^{\pm 7}$	$321^{\pm 7}$	200	42	12	13	30	1,15
3	IPA-2,5т	$382^{\pm 7}$	$340^{\pm 7}$	200	44	12	18	38	2,0
4	IPA-2,5т	$482^{\pm 9}$	$440^{\pm 9}$	$300^{\pm 9}$	44	12	18	38	2,1
5	IPA-4,5т	$426^{\pm 10}$	$370^{\pm 10}$	$196^{\pm 6}$	48	12	18	42	2,7
6	IPA-4,5т	$526^{\pm 9}$	$470^{\pm 9}$	$296^{\pm 9}$	48	12	18	42	3,1

Insulators, stick, armored, with slotted head (fig. H.V.1b, Table H.V.5). Material, steatite.

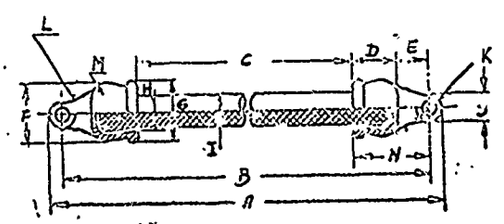

Figure H.V.1b.

Table H.V.5

No.	Type insulator	Dimensions, mm A	B	C	D	E	F	G	H	I	J	K	L	M	N
1	IPA-750	455	430	300	37	28	48	44	31	25	25	13	50	7	65
2	IPA-1,5т	465	440	300	42	20	56	52	38	30	25	13	45	8	70
3	IPA-1,5т	569	$539^{\pm 16}$	$394^{\pm 12}$						30		13			
4	IPA-750	$359^{\pm 8}$	329	194	37	30,5	48	48	40	25	30	13	0	7	67,5
5	IPA-750	488	453	304			—	66		30		17			
6	IPA-1,5т	$369^{\pm 8}$	339	196	42	30,5	56	52	—	30	30	13	0	8	72,5
7	IPA-2,5т	$506^{\pm 12}$	$464^{\pm 12}$	296	47	37	68	65	60	30	42	18	0	10	84
8	IPA-2,5т	$406^{\pm 8,5}$	364	196	47	37	68	65	60	38	42	18	0	10	84
9	IPA-4,5т	$384^{\pm 9}$	$352^{\pm 9}$	196								18			
10	IPA-4,5т	$484^{\pm 12}$	$452^{\pm 12}$	296						42		18			
11	IPA-$\frac{300}{1,5}$	465	440	300	42	28	56	52	38	30	25	13	45	8	70
12	IPA-$\frac{300}{0,75}$	$455^{\pm 10}$	430	300	37	28	48	44	31	25	25	13	50	7	65
13	IPA $\frac{300}{4,5}$	520	480	300	65	25	88	80	75	50	40	18	40	12	99

Insulator, +--shaped, armored (fig. H.V.1c, Table H.V.6).
Material - steatite.

Table H.V.6

A Размеры, мм A	a_1	a_2	a_3	a_4	a_5	D	d_1	d_2	d_3	B Испыт. напряж., кв	C Разрушающая нагрузка растяж., кг	D Вес, кг
369	339	194	369	339	194	56	30	30	13	70	750	3,6
406	364	196	370	328	168	68	38	42	13	70	1500	5,3

Key: A - dimensions, mm; B - test voltage, kv; C - destruction load, tensile, kg; D - weight, kg.

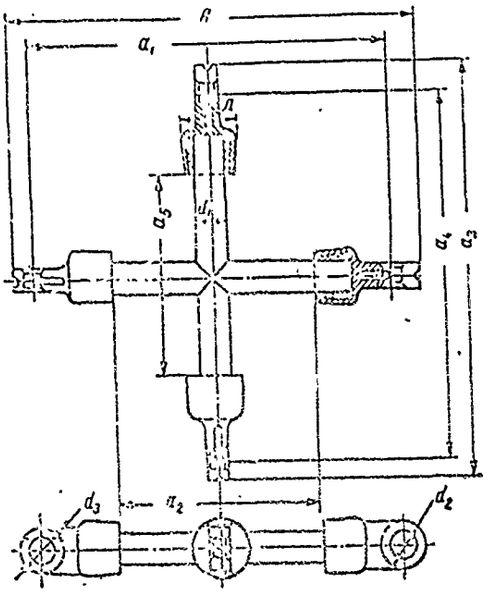

Figure H.V.1b.

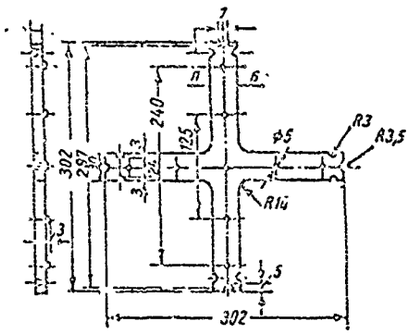

Figure H.V.2. Cruciform spreader.

Insulator-condenser for traveling wave antenna BYe (fig. H.V.3, Table H.V.7).

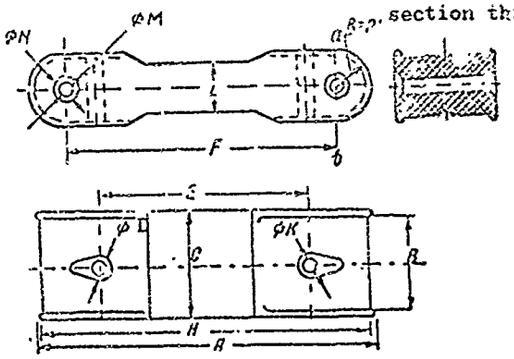

Figure H.V.3.

Table H.V.7

Type	Material	Dimensions, mm											
		A	B	C	D	E	F	H	K	L	M	N	P
Insulator-condenser	Porcelain	112	30	34	10	70	90	108	6	14	6	10	12

(b) Feeder insulators

Insulator, feeder, transmitting, single-wire (fig. H.V.4, Table H.V.8) (Two of these insulators are used to suspend a two-wire line).

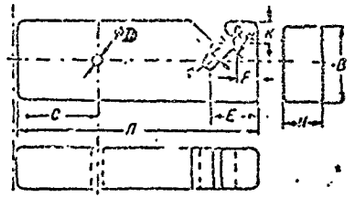

Figure H.V.4.

Table H.V.8.

Type	Dimensions, mm										Material
	A	B	C	D	E	F	H	K	L	α	
feeder, single-wire	150	50	50	8	30	13	25	13	7	90°	Porcelain

Insulator, feeder, receiving, bar (fig. H.V.5, Table H.V.9).

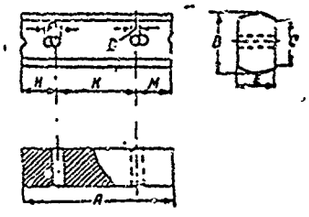

Figure H.V.5.

Table H.V.9

Type	Dimensions, mm									Material
	A	B	C	D	E	F	H	K	M	
Feeder, bar	63	22	16	5	16	7	15	33	15	Porcelain

Insulator, feeder, receiving, four-wire (fig. H.V.6, Table H.V.10).

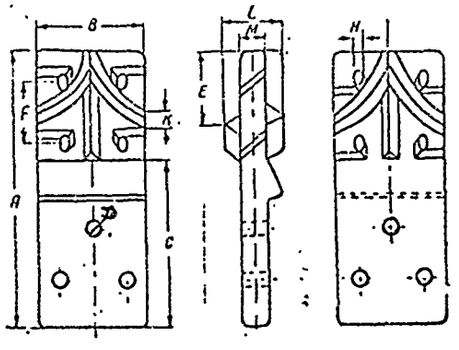

Figure H.V.6.

Table H.V.10

Type	Dimensions, mm										Weight (appr.), kg	Material
	A	B	C	D	E	F	H	K	L	M		
Feeder, four-wire	147	60	89	8	40	35	3	10	34	14	0,320	Porcelain

Insulators, feeder, partition (fig. H.V.7, Table H.V.11).

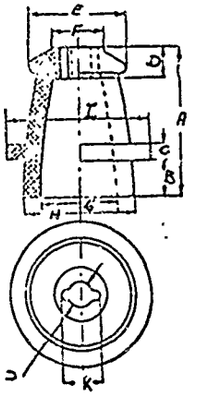

Figure H.V.7.

Table H.V.11

Type	Dimensions, mm											Weight (appr.) kg	Material
	A	B	C	D	E	F	G	H	I	J	K		
PR-1	42	10	5	8	30	16	22	32	42	6	9	0,044	porcelain
PR-2	60	15	6	12	42	22	32	45	60	12	17	0,180	
PR-3	75	20	7	16	52	28	44	58	74	14	20	0,245	
PR-4	90	25	8	13	58	35	56	70	86	16	21	0,380	
PR-5	160	33	12	20	90	60	90	125	155	30	40	1,900	

(c) Rigging insulators

Insulators, rigging, saddle (fig. H.V.8, Table H.V.12).

Figure H.V.8.

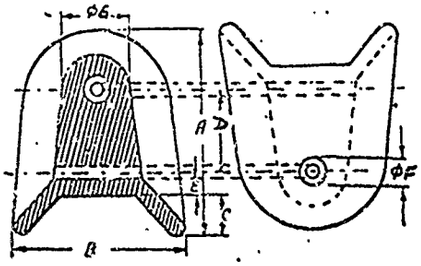

Table H.V.12

Type	Dimensions, mm							Рабочее напряжение, кв	Сухоразрядное напряжение, кв	Допустимая нагрузка, кг	Диаметр троса, мм	Вес (приближенно), кг	Материал
	A	B	C	D	E	F	G						
								1	2	3	4	5	6
RCA-3	93	81	18	27	7	12	32/34	3	30	6,50	6-8	0,383	Фарфор
RCA-6	129	106	25	35	9	16	46/48	6	43	15,00	8-12	0,850	
RCA-11	152	122	30	38	9	18	54/58	10	55	23,00	10-16	1,310	
													7

Key: 1 - operating voltage, kv, 2 - dry discharge voltage, kv, 3 - permissible load, kg, 4 - wire cable diameter, mm; 5 - weight (approximate), kg; 6 - material; 7 - porcelain.

The voltages indicated are for 50 hertz AC.

Insulators, rigging, type IT (fig. H.V.9; Table H.V.13).

Figure H.V.9.

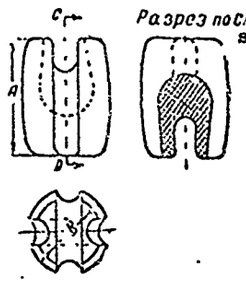

section through CD

Table H.V.13

1 Тип	2 Размеры мм		3 Разрядное напряжение при 50 гц кв		6 Разрушающая нагрузка т	7 Средний вес изолятора кг	8 Диаметры тросов (приближённо) мм	9 Материал
	A	B	4 сухое	5 мокрое				
								10
IT-1	100	65	15	6	2,8	0,345	6—8	Фарфор
IT-2	136	95	35	12	4,1	0,753	9,5	«
IT-3	155	105	35	12	6,8	1,528	12,5	«
IT-4	170	120	35	12	13,0	2,300	15—17	«
IT-5	175	130	40	15	18,5	3,020	19—21	«

Key: 1 - type; 2 - dimensions, mm; 3 - discharge voltage at 50 hertz, kv; 4 - dry; 5 - wet; 6 - destructive load, tons; 7 - average insulator weight, kg; 8 - wire cable diameter (approximate), mm; 9 - material; 10 - porcelain.

Insulator, egg (fig. H.V.10, Table H.V.14).

Figure H.V.10.

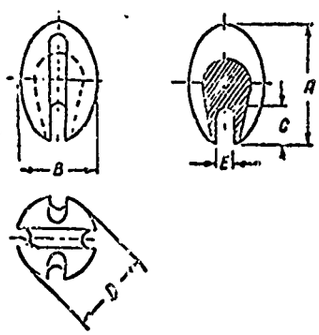

Table H.V.14

Type Тип	Dimensions, mm					Разрушающее усилие, 1 кг	Диаметр провода, 2 мм	Material
	A	B	C	D	E			
IAL-5	40	28	13	28	6	350	up to 5 mm	Porce-lain

Key: 1 - destructive force, kg; 2 - conductor diameter, mm.

H.VI. Sine and cosine integrals

$$\left.\begin{aligned} &\text{Sine integral} && \mathrm{si}(x) = -\int_x^\infty \frac{\sin u}{u}\,du \\ &\text{Cosine integral} && \mathrm{ci}(x) = -\int_x^\infty \frac{\cos u}{u}\,du \end{aligned}\right\} \qquad \text{(H.VI.1)}$$

si(x) and ci(x) can be expanded into the following series

$$\left.\begin{aligned} \mathrm{si}(x) &= x - \frac{1}{3}\cdot\frac{x^3}{3!} + \frac{1}{5}\cdot\frac{x^5}{5!} - \dots \\ \mathrm{ci}(x) &= E + \ln x - \frac{1}{2}\cdot\frac{x^2}{2!} + \frac{1}{4}\cdot\frac{x^4}{4!} - \dots \end{aligned}\right\} \qquad \text{(H.VI.2)}$$

E is Euler's constant,

$$E = 0.57721\,56649\dots$$

For large values, the argument for the series at (H.VI.2) will converge slowly and in such case the following, semiconverging series must be used:

$$\left.\begin{aligned} si(x) &= \frac{\pi}{2} - \frac{\cos x}{x}\left(1 - \frac{2!}{x^2} + \frac{4!}{x^4} - \dots\right) - \\ &\quad - \frac{\sin x}{x}\left(\frac{1}{x} - \frac{3!}{x^3} + \frac{5!}{x^5} - \dots\right) \\ ci(x) &= \frac{\sin x}{x}\left(1 - \frac{2!}{x^2} + \frac{4!}{x^4} - \dots\right) - \\ &\quad - \frac{\cos x}{x}\left(\frac{1}{x} - \frac{3!}{x^3} + \frac{5!}{x^5} - \dots\right) \end{aligned}\right| \qquad \text{(H.VI.3)}$$

The terms in these series decrease at first, but then increase to infinity.

When these series are used it must be borne in mind that the absolute error will always be less than the first discarded term. Consequently, the accuracy of the computation made using the semiconverging series can be defined by the minimum term in this series, directly ahead of which the summing must be stopped in order to obtain the greatest possible accuracy in the result.

In the tables that follow the functions have been given with an accuracy of within 0.001. The argument is expressed in parts of a circle (in 2π parts).

Table H.VI.1

Sine and Cosine Integrals

x	si $2\pi x$	Δ	ci $2\pi x$	Δ	x	si $2\pi x$	Δ	ci $2\pi x$	Δ
0,000	0,000	6	$-\infty$	∞	0,045	+0,281	7	−0,706	21
0,001	+0,006	7	−4,493	693	0,046	0,288	6	−0,685	21
0,002	0,013	6	−3,800	406	0,047	0,294	6	−0,664	20
0,003	0,019	6	−3,394	287	0,048	0,300	7	−0,644	20
0,004	0,025	6	−3,107	224	0,049	0,307	6	−0,624	19
0,005	0,031	7	−2,883	182	0,050	0 313	6	−0,605	19
0,006	0,038	6	−2,701	154	0,051	0,319	6	−0,586	18
0,007	0,044	6	−2,547	133	0,052	0,325	6	−0,568	18
0,008	0,050	6	−2,414	118	0,053	0,331	6	−0,550	18
0,009	0,056	7	−2,296	105	0,054	0,337	6	−0,532	17
0,010	0,063	6	−2,191	95	0,055	0,343	7	−0,515	17
0,011	0,069	6	−2,096	87	0,056	0,350	6	−0,498	16
0,012	0,075	7	−2,009	80	0,057	0,356	6	−0,482	17
0,013	0,082	6	−1,929	73	0,058	0,362	6	−0,465	16
0,014	0,088	6	−1,856	69	0,059	0,368	6	−0,449	15
0,015	0,094	6	−1,787	64	0,060	0,374	6	−0,434	16
0,016	0,100	7	−1,723	61	0,061	0,380	6	−0,418	15
0,017	0,107	6	−1,662	57	0,062	0,386	7	−0,403	15
0,018	0,113	6	−1,605	53	0,063	0,398	6	−0,388	14
0,019	0,119	7	−1,552	51	0,064	0,399	6	−0,374	14
0,020	0,126	6	−1,501	49	0,065	0,405	6	−0,360	14
0,021	0,132	6	−1,452	46	0,066	0,411	6	−0,346	14
0,022	0,138	6	−1,406	44	0,067	0,417	6	−0,332	14
0,023	0,144	7	−1,362	42	0,068	0,423	6	−0,318	13
0,024	0,151	5	−1,320	40	0,069	0,429	6	−0,305	13
0,025	0,157	6	−1,280	39	0,070	0,435	6	−0,292	13
0,026	0,163	6	−1,241	37	0,071	0,441	6	−0,279	12
0,027	0,169	7	−1,204	36	0,072	0,447	6	−0,267	13
0,028	0,176	6	−1,168	34	0,073	0,453	6	−0,254	12
0,029	0,182	6	−1,134	34	0,074	0,459	6	−0,242	12
0,030	0,188	6	−1,100	32	0,075	0,465	7	−0,230	12
0,031	0,194	7	−1,068	31	0,076	0,472	6	−0,218	11
0,032	0,201	6	−1,037	30	0,077	0,478	6	−0,207	12
0,033	0,207	6	−1,007	29	0,078	0,484	6	−0,195	11
0,034	0,213	6	−0,978	29	0,079	0,490	6	−0,184	11
0,035	0,219	7	−0,949	27	0,080	0,496	6	−0,173	11
0,036	0,225	6	−0,922	27	0,081	0,502	6	−0,162	10
0,037	0,232	6	−0,895	26	0,082	0,508	6	−0,152	11
0,038	0,238	6	−0,869	25	0,083	0,514	6	−0,141	10
0,039	0,244	7	−0,844	24	0,084	0,520	6	−0,131	10
0,040	0,251	6	−0,820	24	0,085	0,526	6	−0,121	10
0,041	0,257	6	−0,796	24	0,086	0,532	6	−0,111	10
0,042	0,263	6	−0,772	22	0,087	0,538	6	−0,101	10
0,043	0,269	6	−0,750	22	0,088	0,544	6	−0,091	10
0,044	0,275	6	−0,728	22	0,089	0,550	6	−0,081	9
0,045	+0,281		−0,706		0,090	+0,556		−0,072	10

(continued)

x	si $2\pi x$	Δ	ci $2\pi x$	Δ	x	si $2\pi x$	Δ	ci $2\pi x$	Δ
0,090	+0,556	5	−0,072	10	0,135	+0,815	6	+0,238	5
0,091	0,561	6	−0,062	9	0,136	0,821	5	+0,243	5
0,092	0,567	6	−0,053	9	0,137	0,826	6	+0,248	4
0,093	0,573	6	−0,044	9	0,138	0,832	5	+0,252	5
0,094	0,579	6	−0,035	8	0,139	0,837	6	+0,257	5
0,095	0,585	6	−0,027	9	0,140	0,843	5	+0,262	4
0,096	0,591	6	−0,018	8	0,141	0,848	6	+0,266	5
0,097	0,597	6	−0,010	9	0,142	0,854	5	+0,271	4
0,098	0,603	6	−0,001	8	0,143	0,859	6	+0,275	4
0,099	0,609	6	+0,007	8	0,144	0,865	5	+0,279	5
0,100	0,615	6	+0,015	8	0,145	0,870	5	+0,284	4
0,101	0,621	5	+0,023	8	0,146	0,876	6	+0,288	4
0,102	0,626	6	+0,031	8	0,147	0,881	5	+0,292	4
0,103	0,632	6	+0,039	8	0,148	0,886	6	+0,296	4
0,104	0,638	6	+0,047	7	0,149	0,892	5	+0,300	4
0,105	0,644	6	+0,054	8	0,150	0,897	6	+0,304	4
0,106	0,650	6	+0,062	7	0,151	0,903	5	+0,308	4
0,107	0,656	5	+0,069	8	0,152	0,908	5	+0,312	3
0,108	0,661	6	+0,077	7	0,153	0,913	6	+0,315	4
0,109	0,667	6	+0,084	7	0,154	0,919	5	+0,319	4
0,110	0,673	6	+0,091	7	0,155	0,924	5	+0,323	3
0,111	0,679	6	+0,098	7	0,156	0,929	6	+0,326	4
0,112	0,685	5	+0,105	6	0,157	0,935	5	+0,330	3
0,113	0,690	6	+0,111	7	0,158	0,940	5	+0,333	4
0,114	0,696	6	+0,118	7	0,159	0,945	6	+0,337	3
0,115	0,702	6	+0,125	6	0,160	0,951	5	+0,340	4
0,116	0,708	5	+0,131	6	0,161	0,956	5	+0,344	3
0,117	0,713	6	+0,137	7	0,162	0,961	5	+0,347	3
0,118	0,719	6	+0,144	6	0,163	0,966	6	+0,350	3
0,119	0,725	6	+0,150	6	0,164	0,972	5	+0,353	3
0,120	0,731	5	+0,156	6	0,165	0,977	5	+0,356	3
0,121	0,736	6	+0,162	6	0,166	0,982	5	+0,359	3
0,122	0,742	6	+0,168	6	0,167	0,987	5	+0,362	3
0,123	0,748	5	+0,174	6	0,168	0,992	6	+0,365	3
0,124	0,753	6	+0,180	5	0,169	0,998	5	+0,368	3
0,125	0,759	6	+0,185	6	0,170	1,003	5	+0,371	3
0,126	0,765	5	+0,191	6	0,171	1,008	5	+0,374	3
0,127	0,770	6	+0,197	5	0,172	1,013	5	+0,377	2
0,128	0,776	6	+0,202	5	0,173	1,018	5	+0,379	3
0,129	0,782	5	+0,207	6	0,174	1,023	5	+0,382	3
0,130	0,787	6	+0,213	5	0,175	1,028	5	+0,385	2
0,131	0,793	5	+0,218	5	0,176	1,033	5	+0,387	3
0,132	0,798	6	+0,223	5	0,177	1,038	6	+0,390	2
0,133	0,804	5	+0,228	5	0,178	1,044	5	+0,392	3
0,134	0,809	6	+0,233	5	0,179	1,049	5	+0,395	2
0,135	+0,815		+0,238		0,180	+1,054		+0,397	

(continued)

x	si $2\pi x$	Δ	ci $2\pi x$	Δ	x	si $2\pi x$	Δ	ci $2\pi x$	Δ
0,180	+1,054	5	+0,397	2	0,225	+1,266	4	+0,464	0
0,181	1,059	5	+0,399	3	0,226	1,270	5	+0,464	1
0,182	1,064	5	+0,402	2	0,227	1,275	4	+0,465	1
0,183	1,069	5	+0,404	2	0,228	1,279	4	+0,466	0
0,184	1,074	5	+0,406	2	0,229	1,283	5	+0,466	1
0,185	1,079	5	+0,408	2	0,230	1,288	4	+0,467	0
0,186	1,084	4	+0,410	3	0,231	1,292	4	+0,467	1
0,187	1,088	5	+0,413	2	0,232	1,296	4	+0,468	0
0,188	1,093	5	+0,415	2	0,233	1,300	5	+0,468	1
0,189	1,098	5	+0,417	2	0,234	1,305	4	+0,469	0
0,190	1,103	5	+0,419	1	0,235	1,309	4	+0,469	0
0,191	1,108	5	+0,420	2	0,236	1,313	4	+0,469	1
0,192	1,113	5	+0,422	2	0,237	1,317	5	+0,470	0
0,193	1,118	5	+0,424	2	0,238	1,322	4	+0,470	0
0,194	1,123	5	+0,426	2	0,239	1,326	4	+0,470	1
0,195	1,128	4	+0,428	1	0,240	1,330	4	+0,471	0
0,196	1,132	5	+0,429	2	0,241	1,334	4	+0,471	0
0,197	1,137	5	+0,431	2	0,242	1,338	4	+0,471	0
0,198	1,142	5	+0,433	1	0,243	1,342	4	+0,471	1
0,199	1,147	4	+0,434	2	0,244	1,346	4	+0,472	0
0,200	1,151	5	+0,436	1	0,245	1,350	5	+0,472	0
0,201	1,156	5	+0,437	2	0,246	1,355	4	+0,472	0
0,202	1,161	5	+0,439	1	0,247	1,359	4	+0,472	0
0,203	1,166	4	+0,440	2	0,248	1,363	4	+0,472	0
0,204	1,170	5	+0,442	1	0,249	1,367	4	+0,472	0
0,205	1,175	5	+0,443	2	0,250	1,371	4	+0,472	0
0,206	1,180	4	+0,445	1	0,251	1,375	4	+0,472	0
0,207	1,184	5	+0,446	1	0,252	1,379	4	+0,472	0
0,208	1,189	5	+0,447	1	0,253	1,383	4	+0,472	0
0,209	1,194	4	+0,448	2	0,254	1,387	3	+0,472	0
0,210	1,198	5	+0,450	1	0,255	1,390	4	+0,472	0
0,211	1,203	5	+0,451	1	0,256	1,394	4	+0,472	1
0,212	1,208	4	+0,452	1	0,257	1,398	4	+0,471	0
0,213	1,212	5	+0,453	1	0,258	1,402	4	+0,471	0
0,214	1,217	4	+0,454	1	0,259	1,406	4	+0,471	0
0,215	1,221	5	+0,455	1	0,260	1,410	4	+0,471	0
0,216	1,226	4	+0,456	1	0,261	1,414	4	+0,471	1
0,217	1,230	5	+0,457	1	0,262	1,418	3	+0,470	0
0,218	1,235	4	+0,458	1	0,263	1,421	4	+0,470	0
0,219	1,239	5	+0,459	1	0,264	1,425	4	+0,470	1
0,220	1,244	4	+0,460	1	0,265	1,429	4	+0,469	0
0,221	1,248	5	+0,461	0	0,266	1,433	3	+0,469	0
0,222	1,253	4	+0,461	1	0,267	1,436	4	+0,469	1
0,223	1,257	4	+0,462	1	0,268	1,440	4	+0,468	0
0,224	1,261	5	+0,463	1	0,269	1,444	4	+0,468	1
0,225	+1,266		+0,464		0,270	+1,448		+0,467	

(continued)

x	si $2\pi x$	Δ	ci $2\pi x$	Δ	x	si $2\pi x$	Δ	ci $2\pi x$	Δ
0,270	+1,448	3	+0,467	0	0,315	+1,596	3	+0,427	1
0,271	1,451	4	+0,467	1	0,316	1,599	3	+0,426	1
0,272	1,455	3	+0,463	0	0,317	1,602	3	+0,425	2
0,273	1,458	4	+0,466	1	0,318	1,605	2	+0,423	1
0,274	1,462	4	+0,465	0	0,319	1,607	3	+0,422	1
0,275	1,466	3	+0,465	1	0,320	1,610	3	+0,421	2
0,276	1,469	4	+0,464	1	0,321	1,613	3	+0,419	1
0,277	1,473	3	+0,463	0	0,322	1,616	3	+0,418	1
0,278	1,476	4	+0,463	1	0,323	1,619	2	+0,417	2
0,279	1,480	3	+0,462	0	0,324	1,621	3	+0,415	1
0,280	1,483	4	+0,462	1	0,325	1,624	3	+0,414	1
0,281	1,487	3	+0,461	1	0,326	1,627	3	+0,413	2
0,282	1,490	4	+0,460	1	0,327	1,630	2	+0,411	1
0,283	1,494	3	+0,459	0	0,328	1,632	3	+0,410	2
0,284	1,497	4	+0,459	1	0,329	1,635	3	+0,408	1
0,285	1,501	3	+0,458	1	0,330	1,638	2	+0,407	2
0,286	1,504	4	+0,457	1	0,331	1,640	3	+0,405	1
0,287	1,508	3	+0,456	0	0,332	1,643	3	+0,404	2
0,288	1,511	3	+0,456	1	0,333	1,646	2	+0,402	1
0,289	1,514	4	+0 455	1	0,334	1,648	3	+0,401	2
0,290	1,518	3	+0,454	1	0,335	1,651	2	+0,399	1
0,291	1,521	3	+0,453	1	0,336	1,653	3	+0,398	2
0,292	1,524	4	+0,452	1	0,337	1,656	2	+0,396	1
0,293	1,528	3	+0,451	1	0,338	1,658	3	+0,395	2
0,294	1,531	3	+0,450	1	0,339	1,661	2	+0,393	1
0,295	1,534	3	+0,449	1	0,340	1,663	3	+0,392	2
0,296	1,537	4	+0,448	1	0,341	1,666	2	+0,390	2
0,297	1,541	3	+0,447	1	0,342	1,668	3	+0,388	1
0,298	1,544	3	+0,446	1	0,343	1,671	2	+0,387	2
0,299	1,547	3	+0,445	1	0,344	1,673	3	+0,385	1
0,300	1,550	3	+0,444	1	0,345	1,676	2	+0,384	2
0,301	1,553	4	+0,443	1	0,346	1,678	2	+0,382	2
0,302	1,557	3	+0,442	1	0,347	1,680	3	+0,380	1
0,303	1,560	3	+0,441	1	0,348	1,683	2	+0,379	2
0,304	1,563	3	+0,440	1	0,349	1,685	2	+0,377	2
0,305	1,566	3	+0,439	1	0,350	1,687	3	+0,375	1
0,306	1,569	3	+0,438	1	0,351	1,690	2	+0,374	2
0,307	1,572	3	+0,437	1	0,352	1,692	2	+0,372	2
0,308	1,575	3	+0,436	1	0,353	1,694	2	+0,370	1
0,309	1,578	3	+0,435	2	0,354	1,696	3	+0,369	2
0,310	1,581	3	+0,433	1	0,355	1,699	2	+0,367	2
0,311	1,584	3	+0,432	1	0,356	1,701	2	+0,365	2
0,312	1,587	3	+0,431	1	0,357	1,703	2	+0,363	1
0,313	1,590	3	+0,430	2	0,358	1,705	2	+0,362	2
0,314	1,593	3	+0,428	1	0,359	1,707	3	+0,360	2
0,315	+1,596		+0,427		0,360	+1,710		+0,358	

(continued)

x	si 2πx	Δ	ci 2πx	Δ	x	si 2πx	Δ	ci 2πx	Δ
0,360	+1,710	2	+0,358	2	0,405	+1,789	1	+0,271	2
0,361	1,712	2	+0,356	2	0,406	1,790	2	+0,269	2
0,362	1,714	2	+0,351	1	0,407	1,792	1	+0,267	2
0,363	1,716	2	+0,353	2	0,408	1,793	1	+0,265	2
0,364	1,718	2	+0,351	2	0,409	1,794	2	+0,263	2
0,365	1,720	2	+0,349	2	0,410	1,796	1	+0,261	2
0,366	1,722	2	+0,347	2	0,411	1,797	1	+0,259	2
0,367	1,724	2	+0,345	1	0,412	1,798	1	+0,257	2
0,368	1,726	2	+0,344	2	0,413	1,799	2	+0,255	2
0,369	1,728	2	+0,342	2	0,414	1,801	1	+0,253	2
0,370	1,730	2	+0,340	2	0,415	1,802	1	+0,251	2
0,371	1,732	2	+0,338	2	0,416	1,803	1	+0,249	2
0,372	1,734	2	+0,336	2	0,417	1,804	1	+0,247	2
0,373	1,736	2	+0,334	2	0,418	1,805	2	+0,245	2
0,374	1,738	2	+0,332	1	0,419	1,807	1	+0,243	3
0,375	1,740	2	+0,331	2	0,420	1,808	1	+0,240	2
0,376	1,742	1	+0,329	2	0,421	1,809	1	+0,238	2
0,377	1,743	2	+0,327	2	0,422	1,810	1	+0,236	2
0,378	1,745	2	+0,325	2	0,423	1,811	1	+0,234	2
0,379	1,747	2	+0,323	2	0,424	1,812	1	+0,232	2
0,380	1,749	2	+0,321	2	0,425	1,813	1	+0,230	2
0,381	1,751	2	+0,319	2	0,426	1,814	1	+0,228	2
0,382	1,753	1	+0,317	2	0,427	1,815	1	+0,226	2
0,383	1,751	2	+0,315	2	0,428	1,816	1	+0,224	2
0,384	1,756	2	+0,313	2	0,429	1,817	1	+0,222	3
0,385	1,758	1	+0,311	2	0,430	1,818	1	+0,219	2
0,386	1,759	2	+0,309	1	0,431	1,819	1	+0,217	2
0,387	1,761	2	+0,308	2	0,432	1,820	1	+0,215	2
0,388	1,763	1	+0,306	2	0,433	1,821	1	+0,213	2
0,389	1,764	2	+0,304	2	0,434	1,822	1	+0,211	2
0,390	1,766	2	+0,302	2	0,435	1,823	1	+0,209	2
0,391	1,768	1	+0,300	2	0,436	1,824	1	+0,207	2
0,392	1,769	2	+0,298	2	0,437	1,825	1	+0,205	2
0,393	1,771	2	+0,296	2	0,438	1,826	1	+0,203	2
0,394	1,773	1	+0,294	2	0,439	1,827	1	+0,201	3
0,395	1,774	2	+0,292	2	0,440	1,828	0	+0,198	2
0,396	1,776	1	+0,290	2	0,441	1,828	1	+0,196	2
0,397	1,777	2	+0,288	2	0,442	1,829	1	+0,194	2
0,398	1,779	1	+0,286	2	0,443	1,830	1	+0,192	2
0,399	1,780	2	+0,284	2	0,444	1,831	1	+0,190	2
0,400	1,782	1	+0,282	2	0,445	1,832	0	+0,188	2
0,401	1,783	2	+0,280	2	0,446	1,832	1	+0,186	2
0,402	1,785	1	+0,278	2	0,447	1,833	1	+0,184	3
0,403	1,786	1	+0,276	3	0,448	1,834	1	+0,181	2
0,404	1,787	2	+0,273	2	0,449	1,835	0	+0,179	2
0,405	+1,789		+0,271		0,450	+1,835		+0,177	

(continued)

x	si $2\pi x$	Δ	ci $2\pi x$	Δ	x	si $2\pi x$	Δ	ci $2\pi x$	Δ
0,450	+1,835	1	+0,177	2	0,495	+1,852	0	+0,081	2
0,451	1,836	1	+0,175	2	0,496	1,852	0	+0,082	2
0,452	1,837	0	+0,173	2	0,497	1,852	0	+0,080	2
0,453	1,837	1	+0,171	2	0,498	1,852	0	+0,078	2
0,454	1,838	0	+0,169	2	0,499	1,852	0	+0,076	2
0,455	1,838	1	+0,167	2	0,50	1,852	1	+0,074	20
0,456	1,839	1	+0,165	3	0,51	1,851	2	+0,054	19
0,457	1,840	0	+0,162	2	0,52	1,849	2	+0,035	19
0,458	1,840	1	+0,160	2	0,53	1,847	5	+0,016	19
0,459	1,841		+0,158	2	0,54	1,842	5	−0,003	17
0,460	1,841	1	+0,156	2	0,55	1,837	6	−0,020	17
0,461	1,842	0	+0,154	2	0,56	1,831	7	−0,037	16
0,462	1,842	1	+0,152	2	0,57	1,824	8	−0,053	16
0,463	1,843	0	+0,150	2	0,58	1,816	8	−0,069	15
0,464	1,843	1	+0,148	2	0,59	1,808	10	−0,084	13
0,465	1,844	0	+0,146	2	0,60	1,798	10	−0,097	13
0,466	1,844	1	+0,144	3	0,61	1,788	11	−0,110	13
0,467	1,845	0	+0,141	2	0,62	1,777	11	−0,123	11
0,468	1,845	1	+0,139	2	0,63	1,766	12	−0,134	10
0,469	1,846	0	+0,137	2	0,64	1,754	12	−0,144	10
0,470	1,846	0	+0,135	2	0,65	1,742	13	−0,154	8
0,471	1,846	1	+0,133	2	0,66	1,729	13	−0,162	8
0,472	1,847	0	+0,131	2	0,67	1,716	13	−0,170	7
0,473	1,847	1	+0,129	2	0,68	1,703	13	−0,177	6
0,474	1,848	0	+0,127	2	0,69	1,690	14	−0,183	5
0,475	1,848	0	+0,125	2	0,70	1,676	13	−0,188	4
0,476	1,848	1	+0,123	2	0,71	1,663	14	−0,192	3
0,477	1,849	0	+0,121	2	0,72	1,649	14	−0,195	2
0,478	1,849	0	+0,119	3	0,73	1,635	13	−0,197	1
0,479	1,849	0	+0,116	2	0,74	1,622	14	−0,198	0
0,480	1,849	1	+0,114	2	0,75	1,608	13	−0,198	0
0,481	1,850	0	+0,112	2	0,76	1,595	13	−0,198	1
0,482	1,850	0	+0,110	2	0,77	1,582	13	−0,197	2
0,483	1,850	0	+0,108	2	0,78	1,569	12	−0,195	3
0,484	1,850	0	+0,106	2	0,79	1,557	12	−0,192	4
0,485	1,850	1	+0,104	2	0,80	1,545	12	−0,188	4
0,486	1,851	0	+0,102	2	0,81	1,533	11	−0,184	5
0,487	1,851	0	+0,100	2	0,82	1,522	11	−0,179	5
0,488	1,851	0	+0,098	2	0,83	1,511	10	−0,174	6
0,489	1,851	0	+0,096	2	0,84	1,501	10	−0,168	7
0,490	1,851	0	+0,094	2	0,85	1,491	9	−0,161	7
0,491	1,851	1	+0,092	2	0,86	1,482	9	−0,154	8
0,492	1,852	0	+0,090	2	0,87	1,473	8	−0,146	8
0,493	1,852	0	+0,088	2	0,88	1,465	7	−0,138	8
0,494	1,852	0	+0,086	2	0,89	1,458	7	−0,130	9
0,495	+1,852		+0,084		0,90	+1,451		−0,121	

(continued)

x	si $2\pi x$	Δ	ci $2\pi x$	Δ	x	si $2\pi x$	Δ	ci $2\pi x$	Δ
0,90	+1,451	7	−0,121	9	1,35	+1,628	6	+0,101	5
0,91	1,444	5	−0,112	10	1,36	1,634	5	+0,096	5
0,92	1,439	5	−0,102	9	1,37	1,639	5	+0,091	5
0,93	1,434	4	−0,093	10	1,38	1,644	5	+0,086	5
0,94	1,430	4	−0,083	10	1,39	1,649	5	+0,081	6
0,95	1,426	3	−0,073	10	1,40	1,654	4	+0,075	6
0,96	1,423	2	−0,063	10	1,41	1,658	3	+0,069	6
0,97	1,421	2	−0,053	10	1,42	1,661	3	+0,063	6
0,98	1,419	1	−0,043	10	1,43	1,664	3	+0,057	7
0,99	1,418	0	−0,033	10	1,44	1,667	2	+0,050	6
1,00	1,418	0	−0,023	10	1,45	1,669	2	+0,044	7
1,01	1,418	1	−0,013	10	1,46	1,671	2	+0,037	6
1,02	1,419	2	−0,003	10	1,47	1,673	1	+0,031	7
1,03	1,421	2	+0,007	9	1,48	1,674	1	+0,024	7
1,04	1,423	3	+0,016	9	1,49	1,675	0	+0,017	6
1,05	1,426	3	+0,025	9	1,50	1,675	0	+0,011	7
1,06	1,429	4	+0,034	9	1,51	1,675	1	+0,004	7
1,07	1,433	4	+0,043	8	1,52	1,674	1	−0,003	6
1,08	1,437	5	+0,051	8	1,53	1,673	1	−0,009	7
1,09	1,442	5	+0,059	8	1,54	1,672	2	−0,016	6
1,10	1,447	5	+0,067	7	1,55	1,670	2	−0,022	6
1,11	1,452	6	+0,074	7	1,56	1,668	3	−0,028	6
1,12	1,458	6	+0,081	6	1,57	1,665	3	−0,034	5
1,13	1,464	7	+0,087	6	1,58	1,662	3	−0,039	6
1,14	1,471	7	+0,093	5	1,59	1,659	4	−0,045	5
1,15	1,478	7	+0,098	5	1,60	1,655	3	−0,050	5
1,16	1,485	7	+0,103	4	1,61	1,652	5	−0,055	4
1,17	1,492	8	+0,107	4	1,62	1,647	4	−0,059	5
1,18	1,500	8	+0,111	4	1,63	1,643	5	−0,064	4
1,19	1,508	8	+0,115	2	1,64	1,638	4	−0,068	4
1,20	1,516	8	+0,117	3	1,65	1,634	5	−0,072	3
1,21	1,524	8	+0,120	2	1,66	1,629	5	−0,075	3
1,22	1,532	8	+0,122	1	1,67	1,624	6	−0,078	3
1,23	1,540	8	+0,123	1	1,68	1,618	5	−0,081	2
1,24	1,548	8	+0,124	0	1,69	1,613	6	−0,083	2
1,25	1,556	8	+0,124	0	1,70	1,607	5	−0,085	2
1,26	1,564	8	+0,124	1	1,71	1,602	6	−0,087	1
1,27	1,572	7	+0,123	1	1,72	1,596	6	−0,088	1
1,28	1,579	8	+0,122	2	1,73	1,590	6	−0,089	0
1,29	1,587	7	+0,120	2	1,74	1,584	5	−0,089	1
1,30	1,594	8	+0,118	3	1,75	1,579	6	−0,090	1
1,31	1,602	7	+0,115	3	1,76	1,573	6	−0,089	0
1,32	1,609	6	+0,112	3	1,77	1,567	5	−0,089	1
1,33	1,615	7	+0,109	4	1,78	1,562	6	−0,088	1
1,34	1,622	6	+0,105	4	1,79	1,556	5	−0,087	2
1,35	+1,628		+0,101		1,80	+1,551		−0,085	

(continued)

x	si $2\pi x$	Δ	ci $2\pi x$	Δ	x	si $2\pi x$	Δ	ci $2\pi x$	Δ
1,80	+1,551	5	−0,085	2	2,25	+1,566	4	+0,079	1
1,81	1,516	5	−0,083	2	2,26	1,570	5	+0,076	1
1,82	1,541	5	−0,081	2	2,27	1,575	4	+0,070	1
1,83	1,536	5	−0,079	3	2,28	1,579	4	+0,069	0
1,84	1,531	4	−0,076	3	2,29	1,583	5	+0,068	0
1,85	1,527	5	−0,073	3	2,30	1,588	4	+0,067	2
1,86	1,522	4	−0,070	4	2,31	1,592	4	+0,065	2
1,87	1,518	3	−0,066	4	2,32	1,596	3	+0,063	1
1,88	1,515	4	−0,062	4	2,33	1,599	4	+0,062	3
1,89	1,511	3	−0,058	4	2,34	1,603	4	+0,059	2
1,90	1,508	3	−0,054	4	2,35	1,607	3	+0,057	3
1,91	1,505	3	−0,050	5	2,36	1,610	3	+0,054	2
1,92	1,502	2	−0,045	4	2,37	1,613	3	+0,052	3
1,93	1,500	2	−0,041	5	2,38	1,616	3	+0,049	4
1,94	1,498	2	−0,036	5	2,39	1,619	2	+0,045	3
1,95	1,496	1	−0,031	5	2,40	1,621	3	+0,042	3
1,96	1,495	1	−0,026	5	2,41	1,624	2	+0,039	4
1,97	1,494	1	−0,021	5	2,42	1,626	2	+0,035	4
1,98	1,493	1	−0,016	5	2,43	1,628	1	+0,031	3
1,99	1,492	0	−0,011	5	2,44	1,629	2	+0,028	4
2,00	1,492	0	−0,006	5	2,45	1,631	1	+0,024	4
2,01	1,492	1	−0,001	5	2,46	1,632	1	+0,020	4
2,02	1,493	1	+0,004	5	2,47	1,633	0	+0,016	4
2,03	1,494	1	+0,009	4	2,48	1,633	1	+0,012	4
2,04	1,495	1	+0,013	5	2,49	1,634	0	+0,008	4
2,05	1,496	2	+0,018	5	2,50	1,634	0	+0,004	4
2,06	1,498	2	+0,023	4	2,51	1,634	1	0,000	4
2,07	1,500	2	+0,027	5	2,52	1,633	0	−0,004	4
2,08	1,502	2	+0,031	5	2,53	1,633	1	−0,008	4
2,09	1,504	3	+0,036	4	2,54	1,632	1	−0,012	4
2,10	1,507	3	+0,040	3	2,55	1,631	1	−0,016	3
2,11	1,510	3	+0,043	4	2,56	1,630	2	−0,019	4
2,12	1,513	3	+0,047	3	2,57	1,628	2	−0,023	3
2,13	1,516	4	+0,050	3	2,58	1,626	2	−0,026	4
2,14	1,520	3	+0,053	3	2,59	1,624	2	−0,030	3
2,15	1,523	4	+0,056	3	2,60	1,622	2	−0,033	3
2,16	1,527	4	+0,059	2	2,61	1,620	3	−0,036	3
2,17	1,531	4	+0,061	2	2,62	1,617	2	−0,039	2
2,18	1,535	5	+0,063	2	2,63	1,615	3	−0,041	3
2,19	1,540	4	+0,065	2	2,64	1,612	3	−0,044	2
2,20	1,544	4	+0,067	1	2,65	1,609	3	−0,046	2
2,21	1,548	5	+0,068	1	2,66	1,606	4	−0,048	2
2,22	1,553	4	+0,069	1	2,67	1,602	3	−0,050	2
2,23	1,557	4	+0,070	0	2,68	1,599	3	−0,052	1
2,24	1,561	5	+0,070	0	2,69	1,596	4	−0,053	2
2,25	+1,566		+0,070		2,70	+1,592		−0,055	

(continued)

x	si $2\pi x$	Δ	ci $2\pi x$	Δ	x	si $2\pi x$	Δ	ci $2\pi x$	Δ
2,70	+1,592	3	−0,055	1	3,15	+1,539	3	+0,036	2
2,71	1,589	4	−0,056	0	3,16	1,542	3	+0,041	2
2,72	1,585	4	−0,056	1	3,17	1,545	2	+0,043	1
2,73	1,581	3	−0,057	0	3,18	1,547	3	+0,044	1
2,74	1,578	4	−0,057	1	3,19	1,550	3	+0,045	1
2,75	1,574	4	−0,058	1	3,20	1,553	3	+0,046	1
2,76	1,570	3	−0,057	0	3,21	1,556	3	+0,047	1
2,77	1,567	4	−0,057	1	3,22	1,559	3	+0,048	0
2,78	1,563	3	−0,056	0	3,23	1,562	3	+0,048	1
2,79	1,560	4	−0,056	1	3,24	1,565	3	+0,049	0
2,80	1,556	3	−0,055	1	3,25	1,568	4	+0,049	0
2,81	1,553	3	−0,054	2	3,26	1,572	3	+0,049	1
2,82	1,550	3	−0,052	2	3,27	1,575	3	+0,048	0
2,83	1,547	3	−0,050	1	3,28	1,578	3	+0,048	1
2,84	1,544	3	−0,049	2	3,29	1,581	2	+0,047	1
2,85	1,541	3	−0,047	2	3,30	1,583	3	+0,046	1
2,86	1,538	3	−0,045	3	3,31	1,586	3	+0,045	1
2,87	1,535	2	−0,042	2	3,32	1,589	3	+0,044	1
2,88	1,533	2	−0,040	3	3,33	1,592	2	+0,043	2
2,89	1,531	3	−0,037	2	3,34	1,594	3	+0,041	1
2,90	1,528	2	−0,034	2	3,35	1,597	2	+0,040	2
2,91	1,526	1	−0,032	3	3,36	1,599	2	+0,038	2
2,92	1,525	2	−0,029	3	3,37	1,601	2	+0,036	2
2,93	1,523	1	−0,026	4	3,38	1,603	2	+0,034	3
2,94	1,522	1	−0,022	3	3,39	1,605	2	+0,031	2
2,95	1,521	1	−0,019	3	3,40	1,607	2	+0,029	2
2,96	1,520	1	−0,016	3	3,41	1,609	1	+0,027	3
2,97	1,519	1	−0,013	4	3,42	1,610	2	+0,024	2
2,98	1,518	0	−0,009	3	3,43	1,612	1	+0,022	3
2,99	1,518	0	−0,006	3	3,44	1,613	1	+0,019	3
3,00	1,518	0	−0,003	4	3,45	1,614	1	+0,016	3
3,01	1,518	0	+0,001	3	3,46	1,615	0	+0,013	2
3,02	1,518	1	+0,004	3	3,47	1,615	1	+0,011	3
3,03	1,519	1	+0,007	3	3,48	1,616	0	+0,008	3
3,04	1,520	1	+0,010	3	3,49	1,616	0	+0,005	3
3,05	1,521	1	+0,013	4	3,50	1,616	0	+0,002	3
3,06	1,522	1	+0,017	3	3,51	1,616	0	−0,001	3
3,07	1,523	1	+0,020	2	3,52	1,616	1	−0,004	2
3,08	1,524	2	+0,022	3	3,53	1,615	0	−0,006	3
3,09	1,526	2	+0,025	3	3,54	1,615	1	−0,009	3
3,10	1,528	2	+0,028	2	3,55	1,614	1	−0,012	3
3,11	1,530	2	+0,030	3	3,56	1,613	1	−0,015	2
3,12	1,532	2	+0,033	2	3,57	1,612	1	−0,017	3
3,13	1,534	3	+0,035	2	3,58	1,611	2	−0,020	2
3,14	1,537	2	+0,037	2	3,59	1,609	1	−0,022	2
3,15	+1,539		+0,039		3,60	+1,608		−0,024	

(continued)

x	si $2\pi x$	Δ	ci $2\pi x$	Δ	x	si $2\pi x$	Δ	ci $2\pi x$	Δ
3,60	+1,608	2	—0,021	3	4,05	+1,533	1	+0,011	2
3,61	1,606	2	—0,027	2	4,06	1,531	1	+0,013	2
3,62	1,604	2	—0,029	2	4,07	1,535	1	+0,015	2
3,63	1,602	2	—0,031	1	4,08	1,536	1	+0,017	3
3,64	1,600	2	—0,032	2	4,09	1,537	2	+0,020	2
3,65	1,598	2	—0,034	2	4,10	1,539	1	+0,022	1
3,66	1,596	3	—0,036	1	4,11	1,540	2	+0,023	2
3,67	1,593	2	—0,037	1	4,12	1,542	1	+0,025	2
3,68	1,591	3	—0,038	1	4,13	1,543	2	+0,027	2
3,69	1,588	2	—0,039	1	4,14	1,545	2	+0,029	1
3,70	1,586	3	—0,040	1	4,15	1,547	2	+0,030	1
3,71	1,583	2	—0,041	1	4,16	1,549	2	+0,031	2
3,72	1,581	3	—0,042	0	4,17	1,551	2	+0,033	1
3,73	1,578	3	—0,042	0	4,18	1,553	3	+0,034	1
3,74	1,575	2	—0,042	0	4,19	1,556	2	+0,035	1
3,75	1,573	3	—0,042	0	4,20	1,558	2	+0,036	0
3,76	1,570	3	—0,042	0	4,21	1,560	2	+0,036	1
3,77	1,567	2	—0,042	0	4,22	1,562	3	+0,037	0
3,78	1,565	3	—0,042	1	4,23	1,565	2	+0,037	0
3,79	1,562	2	—0,041	1	4,24	1,567	2	+0,037	0
3,80	1,560	3	—0,040	1	4,25	1,569	3	+0,037	0
3,81	1,557	2	—0,039	1	4,26	1,572	2	+0,037	0
3,82	1,555	3	—0,038	1	4,27	1,574	2	+0,037	0
3,83	1,552	2	—0,037	1	4,28	1,576	3	+0,037	1
3,84	1,550	2	—0,036	2	4,29	1,579	2	+0,036	0
3,85	1,548	2	—0,034	1	4,30	1,581	2	+0,036	1
3,86	1,546	2	—0,033	2	4,31	1,583	2	+0,035	1
3,87	1,544	2	—0,031	2	4,32	1,585	2	+0,034	1
3,88	1,542	2	—0,029	2	4,33	1,587	2	+0,033	1
3,89	1,540	1	—0,027	2	4,34	1,589	2	+0,032	2
3,90	1,539	2	—0,025	2	4,35	1,591	2	+0,030	1
3,91	1,537	1	—0,023	2	4,36	1,593	2	+0,029	2
3,92	1,536	1	—0,021	2	4,37	1,595	1	+0,027	1
3,93	1,535	1	—0,019	3	4,38	1,596	2	+0,026	2
3,94	1,534	1	—0,016	2	4,39	1,598	1	+0,024	2
3,95	1,533	1	—0,014	2	4,40	1,599	2	+0,022	2
3,96	1,532	0	—0,012	3	4,41	1,601	1	+0,020	2
3,97	1,532	1	—0,009	2	4,42	1,602	1	+0,018	2
3,98	1,531	0	—0,007	3	4,43	1,603	1	+0,016	2
3,99	1,531	0	—0,004	2	4,44	1,604	0	+0,014	2
4,00	1,531	0	—0,002	3	4,45	1,604	1	+0,012	2
4,01	1,531	0	+0,001	2	4,46	1,605	0	+0,010	2
4,02	1,531	0	+0,003	3	4,47	1,605	1	+0,008	2
4,03	1,532	0	+0,006	2	4,48	1,606	0	+0,006	3
4,04	1,532	1	+0,008	3	4,49	1,606	0	+0,003	2
4,05	+1,533		+0,011		4,50	+1,606		+0,001	

(continued)

x	si 2πx	Δ	ci 2πx	Δ	x	si 2πx	Δ	ci 2πx	Δ
4,50	+1,606	0	+0,001	2	4,95	+1,511	1	−0,011	2
4,51	1,606	0	−0,001	2	4,96	1,510	0	−0,009	2
4,52	1,606	1	−0,003	2	4,97	1,510	1	−0,007	2
4,53	1,605	0	−0,005	3	4,98	1,509	0	−0,005	2
4,54	1,605	1	−0,008	2	4,99	1,509	0	−0,003	2
4,55	1,604	0	−0,010	2	5,00	1,509	0	−0,001	2
4,56	1,604	1	−0,012	2	5,01	1,509	0	+0,001	2
4,57	1,603	1	−0,014	2	5,02	1,509	1	+0,003	2
4,58	1,602	1	−0,016	2	5,03	1,510	0	+0,005	2
4,59	1,601	2	−0,018	1	5,04	1,510	1	+0,007	2
4,60	1,599	1	−0,019	2	5,05	1,511	0	+0,009	2
4,61	1,598	1	−0,021	2	5,06	1,511	1	+0,011	1
4,62	1,597	2	−0,023	1	5,07	1,512	1	+0,012	2
4,63	1,595	1	−0,024	2	5,08	1,513	1	+0,014	2
4,64	1,594	2	−0,026	1	5,09	1,514	1	+0,016	2
4,65	1,592	2	−0,027	1	5,10	1,515	1	+0,018	1
4,66	1,590	2	−0,028	1	5,11	1,516	2	+0,019	2
4,67	1,588	2	−0,029	1	5,12	1,518	1	+0,021	1
4,68	1,586	2	−0,030	1	5,13	1,519	1	+0,022	1
4,69	1,584	2	−0,031	1	5,14	1,520	2	+0,023	1
4,70	1,582	2	−0,032	0	5,15	1,522	1	+0,024	1
4,71	1,580	2	−0,032	1	5,16	1,523	2	+0,025	1
4,72	1,578	2	−0,033	0	5,17	1,525	2	+0,026	1
4,73	1,576	2	−0,033	0	5,18	1,527	2	+0,027	1
4,74	1,574	2	−0,033	0	5,19	1,529	1	+0,028	1
4,75	1,572	2	−0,033	0	5,20	1,530	2	+0,029	0
4,76	1,570	2	−0,033	0	5,21	1,532	2	+0,029	1
4,77	1,568	2	−0,033	0	5,22	1,534	2	+0,030	0
4,78	1,566	2	−0,033	1	5,23	1,535	2	+0,030	0
4,79	1,564	2	−0,032	0	5,24	1,538	2	+0,030	0
4,80	1,562	2	−0,032	1	5,25	1,540	2	+0,030	0
4,81	1,560	2	−0,031	1	5,26	1,542	2	+0,030	0
4,82	1,558	2	−0,030	1	5,27	1,544	2	+0,030	0
4,83	1,556	2	−0,029	1	5,28	1,546	1	+0,030	1
4,84	1,554	2	−0,028	1	5,29	1,547	2	+0,029	0
4,85	1,552	1	−0,027	1	5,30	1,549	2	+0,029	1
4,86	1,551	2	−0,026	1	5,31	1,551	2	+0,028	1
4,87	1,549	1	−0,025	2	5,32	1,553	1	+0,027	0
4,88	1,548	2	−0,023	1	5,33	1,554	2	+0,027	1
4,89	1,546	1	−0,022	2	5,34	1,556	2	+0,026	1
4,90	1,545	1	−0,020	2	5,35	1,558	1	+0,025	2
4,91	1,544	1	−0,018	2	5,36	1,559	1	+0,023	1
4,92	1,543	1	−0,016	1	5,37	1,560	2	+0,022	1
4,93	1,542	1	−0,015	2	5,38	1,562	1	+0,021	2
4,94	1,541	0	−0,013	2	5,39	1,563	1	+0,019	1
4,95	+1,541		−0,011		5,40	+1,564		+0,018	

(continued)

x	si $2\pi x$	Δ	ci $2\pi x$	Δ	x	si $2\pi x$	Δ	ci $2\pi x$	Δ
5,40	+1,594	1	+0,018	2	5,85	+1,555	1	−0,022	1
5,41	1,595	1	+0,016	1	5,86	1,554	1	−0,021	1
5,42	1,596	1	+0,015	2	5,87	1,553	1	−0,020	1
5,43	1,597	1	+0,013	1	5,88	1,552	2	−0,019	1
5,44	1,598	0	+0,012	2	5,89	1,550	1	−0,018	2
5,45	1,598	1	+0,010	2	5,90	1,549	1	−0,016	1
5,46	1,599	0	+0,008	2	5,91	1,548	0	−0,015	1
5,47	1,599	0	+0,006	2	5,92	1,548	1	−0,014	2
5,48	1,599	1	+0,004	1	5,93	1,547	1	−0,012	1
5,49	1,600	0	+0,003	2	5,94	1,546	0	−0,011	2
5,50	1,600	0	+0,001	2	5,95	1,546	1	−0,009	2
5,51	1,600	1	−0,001	2	5,96	1,545	0	−0,007	1
5,52	1,599	0	−0,003	2	5,97	1,545	0	−0,005	2
5,53	1,599	1	−0,005	1	5,98	1,545	1	−0,004	2
5,54	1,599	1	−0,006	2	5,99	1,544	0	−0,002	1
5,55	1,598	0	−0,008	2	6,00	1,544	0	−0,001	2
5,56	1,598	1	−0,010	1	6,01	1,544	1	+0,001	2
5,57	1,597	1	−0,011	2	6,02	1,545	0	+0,003	1
5,58	1,596	1	−0,013	2	6,03	1,545	0	+0,004	2
5,59	1,595	1	−0,015	1	6,04	1,545	1	+0,006	1
5,60	1,594	1	−0,016	1	6,05	1,546	0	+0,007	2
5,61	1,593	1	−0,017	2	6,06	1,546	1	+0,009	2
5,62	1,592	1	−0,019	1	6,07	1,547	1	+0,011	1
5,63	1,591	2	−0,020	1	6,08	1,548	0	+0,012	1
5,64	1,589	1	−0,021	1	6,09	1,548	1	+0,013	2
5,65	1,588	1	−0,022	1	6,10	1,549	1	+0,015	1
5,66	1,587	2	−0,023	1	6,11	1,550	1	+0,016	1
5,67	1,585	2	−0,024	1	6,12	1,551	2	+0,017	1
5,68	1,583	1	−0,025	1	6,13	1,553	1	+0,018	2
5,69	1,582	2	−0,026	0	6,14	1,554	1	+0,020	1
5,70	1,580	2	−0,026	1	6,15	1,555	1	+0,021	0
5,71	1,578	1	−0,027	0	6,16	1,556	2	+0,021	1
5,72	1,577	2	−0,027	0	6,17	1,558	1	+0,022	1
5,73	1,575	2	−0,027	1	6,18	1,559	2	+0,023	1
5,74	1,573	1	−0,028	0	6,19	1,561	1	+0,024	0
5,75	1,572	2	−0,028	0	6,20	1,562	2	+0,024	1
5,76	1,570	2	−0,028	1	6,21	1,561	1	+0,025	0
5,77	1,568	2	−0,027	0	6,22	1,565	2	+0,025	0
5,78	1,566	1	−0,027	0	6,23	1,567	2	+0,025	0
5,79	1,565	2	−0,027	1	6,24	1,569	1	+0,025	0
5,80	1,563	2	−0,026	0	6,25	1,570	2	+0,025	0
5,81	1,561	1	−0,026	1	6,26	1,572	1	+0,025	0
5,82	1,560	1	−0,025	1	6,27	1,573	2	+0,025	0
5,83	1,559	2	−0,024	1	6,28	1,575	2	+0,025	0
5,84	1,557	2	−0,023	1	6,29	1,577	1	+0,025	1
5,85	+1,555		−0,022		6,30	+1,578		+0,024	

(continued)

x	si $2\pi x$	Δ	ci $2\pi x$	Δ	x	si $2\pi x$	Δ	ci $2\pi x$	Δ
6,30	+1,578	1	+0,021	0	6,75	+1,571	1	−0,024	0
6,31	1,579	2	+0,021	1	6,76	1,570	2	−0,024	1
6,32	1,581	1	+0,023	1	6,77	1,568	1	−0,023	0
6,33	1,582	2	+0,022	0	6,78	1,567	2	−0,023	0
6,34	1,584	1	+0,022	1	6,79	1,565	1	−0,023	1
6,35	1,585	1	+0,021	1	6,80	1,564	1	−0,022	0
6,36	1,586	1	+0,020	1	6,81	1,563	2	−0,022	1
6,37	1,587	2	+0,019	1	6,82	1,561	1	−0,021	0
6,38	1,589	1	+0,018	2	6,83	1,560	1	−0,021	1
6,39	1,590	1	+0,016	1	6,84	1,559	1	−0,020	1
6,40	1,591	0	+0,015	1	6,85	1,558	2	−0,019	1
6,41	1,591	1	+0,014	2	6,86	1,556	1	−0,018	1
6,42	1,592	1	+0,012	1	6,87	1,555	1	−0,017	1
6,43	1,593	1	+0,011	1	6,88	1,554	1	−0,016	1
6,44	1,591	0	+0,010	2	6,89	1,553	1	−0,015	1
6,45	1,591	0	+0,008	1	6,90	1,552	0	−0,014	1
6,46	1,594	1	+0,007	2	6,91	1,552	1	−0,013	1
6,47	1,595	0	+0,005	1	6,92	1,551	1	−0,012	2
6,48	1,595	0	+0,004	2	6,93	1,550	0	−0,010	1
6,49	1,595	0	+0,002	1	6,94	1,550	1	−0,009	1
6,50	1,595	0	+0,001	2	6,95	1,549	0	−0,008	2
6,51	1,595	0	−0,001	1	6,96	1,549	1	−0,006	1
6,52	1,595	0	−0,002	2	6,97	1,548	0	−0,005	2
6,53	1,595	1	−0,001	1	6,98	1,548	0	−0,003	1
6,54	1,594	0	−0,005	2	6,99	1,548	0	−0,002	1
6,55	1,594	0	−0,007	1	7,00	1,548	0	−0,001	2
6,56	1,594	1	−0,008	2	7,01	1,548	0	+0,001	1
6,57	1,593	1	−0,010	1	7,02	1,548	0	+0,002	2
6,58	1,592	1	−0,011	1	7,03	1,548	1	+0,004	1
6,59	1,591	0	−0,012	2	7,04	1,549	0	+0,005	1
6,60	1,591	1	−0,014	1	7,05	1,549	1	+0,006	2
6,61	1,590	1	−0,015	1	7,06	1,550	0	+0,008	1
6,62	1,589	1	−0,016	1	7,07	1,550	1	+0,009	1
6,63	1,588	2	−0,017	1	7,08	1,551	1	+0,010	2
6,64	1,586	1	−0,018	1	7,09	1,552	0	+0,012	1
6,65	1,585	1	−0,019	1	7,10	1,552	1	+0,013	1
6,66	1,584	1	−0,020	1	7,11	1,553	1	+0,014	1
6,67	1,583	2	−0,021	0	7,12	1,554	1	+0,015	1
6,68	1,581	1	−0,021	1	7,13	1,555	1	+0,016	1
6,69	1,580	1	−0,022	0	7,14	1,556	1	+0,017	1
6,70	1,579	2	−0,022	1	7,15	1,557	1	+0,018	0
6,71	1,577	1	−0,023	0	7,16	1,558	1	+0,018	1
6,72	1,576	2	−0,023	0	7,17	1,559	2	+0,019	1
6,73	1,574	1	−0,023	1	7,18	1,561	1	+0,020	0
6,74	1,573	2	−0,024	0	7,19	1,562	1	+0,020	1
6,75	+1,571		−0,024		7,20	+1,563		+0,021	

(continued)

x	si $2\pi x$	Δ	ci $2\pi x$	Δ	x	si $2\pi x$	Δ	ci $2\pi x$	Δ
7,20	+1,563	2	+0,021	0	7,65	+1,583	1	−0,017	0
7,21	1,565	1	+0,021	1	7,66	1,582	1	−0,017	1
7,22	1,566	2	+0,022	0	7,67	1,581	1	−0,018	1
7,23	1,568	1	+0,022	0	7,68	1,580	1	−0,019	0
7,24	1,569	1	+0,022	0	7,69	1,579	1	−0,019	1
7,25	1,570	2	+0,022	0	7,70	1,578	2	−0,020	0
7,26	1,572	1	+0,022	0	7,71	1,576	1	−0,020	0
7,27	1,573	1	+0,022	0	7,72	1,575	1	−0,020	0
7,28	1,574	2	+0,022	1	7,73	1,574	1	−0,020	0
7,29	1,576	1	+0,021	0	7,74	1,573	2	−0,020	1
7,30	1,577	1	+0,021	1	7,75	1,571	1	−0,021	1
7,31	1,578	2	+0,020	0	7,76	1,570	1	−0,020	0
7,32	1,580	1	+0,020	1	7,77	1,569	2	−0,020	0
7,33	1,581	1	+0,019	0	7,78	1,567	1	−0,020	0
7,34	1,582	1	+0,019	1	7,79	1,566	1	−0,020	0
7,35	1,583	1	+0,018	1	7,80	1,565	1	−0,020	1
7,36	1,584	1	+0,017	1	7,81	1,564	2	−0,019	0
7,37	1,585	1	+0,016	1	7,82	1,562	1	−0,019	1
7,38	1,586	1	+0,015	1	7,83	1,561	1	−0,018	1
7,39	1,587	1	+0,014	1	7,84	1,560	1	−0,017	0
7,40	1,588	1	+0,013	1	7,85	1,559	1	−0,017	1
7,41	1,589	0	+0,012	1	7,86	1,558	1	−0,016	1
7,42	1,589	1	+0,011	1	7,87	1,557	1	−0,015	1
7,43	1,590	0	+0,010	2	7,88	1,556	0	−0,014	1
7,44	1,590	1	+0,008	1	7,89	1,556	1	−0,013	1
7,45	1,591	0	+0,007	1	7,90	1,555	1	−0,012	1
7,46	1,591	1	+0,006	2	7,91	1,554	1	−0,011	1
7,47	1,592	0	+0,004	1	7,92	1,553	0	−0,010	1
7,48	1,592	0	+0,003	1	7,93	1,553	1	−0,009	1
7,49	1,592	0	+0,002	2	7,94	1,552	0	−0,008	1
7,50	1,592	0	0,000	1	7,95	1,552	0	−0,007	2
7,51	1,592	0	−0,001	1	7,96	1,552	1	−0,005	1
7,52	1,592	0	−0,002	2	7,97	1,551	0	−0,004	1
7,53	1,592	1	−0,001	1	7,98	1,551	0	−0,003	1
7,54	1,591	0	−0,005	1	7,99	1,551	0	−0,002	2
7,55	1,591	0	−0,006	1	8,00	1,551	0	0,000	1
7,56	1,591	1	−0,007	2	8,01	1,551	0	+0,001	1
7,57	1,590	1	−0,009	1	8,02	1,551	0	+0,002	1
7,58	1,589	0	−0,010	1	8,03	1,551	1	+0,003	2
7,59	1,589	1	−0,011	1	8,04	1,552	0	+0,005	1
7,60	1,588	1	−0,012	1	8,05	1,552	0	+0,006	1
7,61	1,587	1	−0,013	1	8,06	1,552	1	+0,007	1
7,62	1,586	1	−0,014	1	8,07	1,553	0	+0,008	1
7,63	1,585	1	−0,015	1	8,08	1,553	1	+0,009	1
7,64	1,584	1	−0,016	1	8,09	1,554	1	+0,010	1
7,65	+1,583		−0,017		8,10	+1,555		+0,011	

(continued)

x	si $2\pi x$	Δ	ci $2\pi x$	Δ	x	si $2\pi x$	Δ	ci $2\pi x$	Δ
8,10	+1,555	0	+0,011	1	8,55	+1,589	1	−0,005	2
8,11	1,555	1	+0,012	1	8,56	1,588	0	−0,007	1
8,12	1,556	1	+0,013	1	8,57	1,588	1	−0,008	1
8,13	1,557	1	+0,014	1	8,58	1,587	0	−0,009	1
8,14	1,558	1	+0,015	1	8,59	1,587	1	−0,010	1
8,15	1,559	1	+0,016	0	8,60	1,586	1	−0,011	1
8,16	1,560	1	+0,016	1	8,61	1,585	1	−0,012	0
8,17	1,561	1	+0,017	0	8,62	1,584	0	−0,012	1
8,18	1,562	1	+0,017	1	8,63	1,584	1	−0,013	1
8,19	1,563	1	+0,018	0	8,64	1,583	1	−0,014	1
8,20	1,564	2	+0,018	1	8,65	1,582	1	−0,015	0
8,21	1,566	1	+0,019	0	8,66	1,581	1	−0,015	1
8,22	1,567	1	+0,019	0	8,67	1,580	1	−0,016	0
8,23	1,568	1	+0,019	0	8,68	1,579	1	−0,016	1
8,24	1,569	1	+0,019	0	8,69	1,578	1	−0,017	0
8,25	1,570	2	+0,019	0	8,70	1,577	1	−0,017	1
8,26	1,572	1	+0,019	0	8,71	1,576	1	−0,018	0
8,27	1,573	1	+0,019	0	8,72	1,575	2	−0,018	0
8,28	1,574	1	+0,019	0	8,73	1,573	1	−0,018	0
8,29	1,575	1	+0,019	1	8,74	1,572	1	−0,018	0
8,30	1,576	2	+0,018	0	8,75	1,571	1	−0,018	0
8,31	1,578	1	+0,018	1	8,76	1,570	1	−0,018	0
8,32	1,579	1	+0,017	0	8,77	1,569	1	−0,018	0
8,33	1,580	1	+0,017	1	8,78	1,568	1	−0,018	0
8,34	1,581	1	+0,016	0	8,79	1,567	1	−0,018	1
8,35	1,582	1	+0,016	1	8,80	1,566	2	−0,017	0
8,36	1,583	1	+0,015	1	8,81	1,564	1	−0,017	1
8,37	1,584	0	+0,014	1	8,82	1,563	1	−0,016	0
8,38	1,584	1	+0,013	1	8,83	1,562	1	−0,016	1
8,39	1,585	1	+0,012	1	8,84	1,561	1	−0,015	0
8,40	1,586	1	+0,011	1	8,85	1,560	0	−0,015	1
8,41	1,587	0	+0,010	1	8,86	1,560	1	−0,014	1
8,42	1,587	1	+0,009	1	8,87	1,559	1	−0,013	1
8,43	1,588	0	+0,008	1	8,88	1,558	1	−0,012	0
8,44	1,588	1	+0,007	1	8,89	1,558	0	−0,012	1
8,45	1,589	0	+0,006	1	8,90	1,557	1	−0,011	1
8,46	1,589	0	+0,005	1	8,91	1,556	1	−0,010	1
8,47	1,589	0	+0,004	1	8,92	1,555	0	−0,009	1
8,48	1,589	0	+0,003	1	8,93	1,555	1	−0,008	1
8,49	1,589	1	+0,002	2	8,94	1,554	0	−0,007	1
8,50	1,590	1	0,000	1	8,95	1,554	0	−0,006	1
8,51	1,589	0	−0,001	1	8,96	1,554	1	−0,005	1
8,52	1,589	0	−0,002	1	8,97	1,553	0	−0,001	1
8,53	1,589	0	−0,003	1	8,98	1,553	0	−0,003	2
8,54	1,589	0	−0,004	1	8,99	1,553	0	−0,001	1
8,55	+1,589		−0,005		9,00	+1,553		0,000	

(continued)

x	si $2\pi x$	Δ	ci $2\pi x$	Δ	x	si $2\pi x$	Δ	ci $2\pi x$	Δ
9,00	+1,553	0	0,000	1	9,45	+1,587	0	+0,005	1
9,01	1,553	0	+0,001	1	9,46	1,587	0	+0,001	1
9,02	1,553	0	+0,002	1	9,47	1,587	0	+0,003	1
9,03	1,553	1	+0,003	1	9,48	1,587	1	+0,002	1
9,04	1,551	0	+0,001	1	9,49	1,588	0	+0,001	1
9,05	1,551	0	+0,005	1	9,50	1,588	0	0,000	1
9,06	1,551	1	+0,006	1	9,51	1,588	1	−0,001	1
9,07	1,553	0	+0,007	1	9,52	1,587	0	−0,002	1
9,08	1,555	1	+0,008	1	9,53	1,587	0	−0,003	1
9,09	1,556	0	+0,009	1	9,54	1,587	0	−0,001	1
9,10	1,556	1	+0,010	1	9,55	1,587	1	−0,005	1
9,11	1,557	1	+0,011	1	9,56	1,586	0	−0,006	1
9,12	1,558	1	+0,012	0	9,57	1,586	1	−0,007	1
9,13	1,559	0	+0,012	1	9,58	1,585	0	−0,008	1
9,14	1,559	1	+0,013	1	9,59	1,585	1	−0,009	1
9,15	1,560	1	+0,014	0	9,60	1,584	0	−0,010	0
9,16	1,561	1	+0,014	1	9,61	1,584	1	−0,010	1
9,17	1,562	1	+0,015	1	9,62	1,583	1	−0,011	1
9,18	1,563	1	+0,016	0	9,63	1,582	0	−0,012	1
9,19	1,564	1	+0,016	0	9,64	1,582	1	−0,013	0
9,20	1,565	1	+0,016	1	9,65	1,581	1	−0,013	1
9,21	1,566	1	+0,017	0	9,66	1,580	1	−0,014	0
9,22	1,567	1	+0,017	0	9,67	1,579	1	−0,014	1
9,23	1,568	1	+0,017	0	9,68	1,578	1	−0,015	0
9,24	1,569	1	+0,017	0	9,69	1,577	1	−0,015	1
9,25	1,570	2	+0,017	0	9,70	1,576	1	−0,016	0
9,26	1,572	1	+0,017	0	9,71	1,575	1	−0,016	0
9,27	1,573	1	+0,017	0	9,72	1,574	1	−0,016	0
9,28	1,574	1	+0,017	0	9,73	1,573	1	−0,016	0
9,29	1,575	1	+0,017	1	9,74	1,572	1	−0,016	0
9,30	1,576	1	+0,016	0	9,75	1,571	1	−0,016	0
9,31	1,577	1	+0,016	0	9,76	1,570	1	−0,016	0
9,32	1,578	1	+0,016	1	9,77	1,569	1	−0,016	0
9,33	1,579	1	+0,015	0	9,78	1,568	1	−0,016	0
9,34	1,580	1	+0,015	1	9,79	1,567	1	−0,016	0
9,35	1,581	0	+0,014	1	9,80	1,566	1	−0,016	1
9,36	1,581	1	−0,013	0	9,81	1,565	1	−0,015	0
9,37	1,582	1	+0,013	1	9,82	1,564	1	−0,015	1
9,38	1,583	1	+0,012	1	9,83	1,563	1	−0,014	0
9,39	1,584	0	+0,011	1	9,84	1,562	0	−0,014	1
9,40	1,584	1	+0,010	1	9,85	1,562	1	−0,013	0
9,41	1,585	0	+0,009	1	9,86	1,561	1	−0,013	1
9,42	1,585	1	+0,008	1	9,87	1,560	1	−0,012	1
9,43	1,586	0	+0,007	1	9,88	1,559	0	−0,011	1
9,44	1,586	1	+0,006	1	9,89	1,559	1	−0,010	0
9,45	+1,587		+0,005		9,90	+1,558		−0,010	
9,90	+1,558	1	−0,010	1	9,95	+1,556	1	−0,005	1
9,91	1,557	0	−0,009	1	9,96	1,555	0	−0,004	1
9,92	1,557	1	−0,008	1	9,97	1,555	0	−0,003	1
9,93	1,556	0	−0,007	1	9,98	1,555	0	−0,002	1
9,94	1,556	0	−0,006	1	9,99	1,555	0	−0,001	1
9,95	+1,556		−0,005		10,00	+1,555		0,000	

H.VII. Diagrams for determining input impedance

The practical work involved in the antenna field often involves computing the input impedances of lines loaded with known resistances. Despite the simplicity of these computations they are extremely cumbersome and difficult to do.

Figure H.VII.1 contains a diagram which can be used to compute the input impedance if a lossless line is loaded by any complex impedance.

Without dwelling on the theory behind these diagrams, we will limit ourselves to an explanation of the rules for using them. The explanation of how the diagrams are used will be made by using concrete examples of the computation.

Example 1

Given is a line with the following data:

(1) characteristic impedance, W = 600 ohms;

(2) line length, $l = 0.3\ \lambda$;

(3) load impedance is

$$Z = R + iX = (360 + i360) \text{ ohms.}$$

Find the input impedance.

(1) We find

$$Z' = Z/W = R' + iX' = 0.5 + i0.6.$$

(2) We find on the diagram that point corresponding to the above values for R' and X'.

On the diagram the various values of $R' = R/W$ correspond to the various solid line circles with centers on the vertical axis.

The various values of $X' = X/W$ correspond to the arcs of circles also drawn in solid lines. The centers of the circles of which these arcs are parts are outside the diagram in Figure H.VII.1. The right-hand system of arcs has positive X' values, the left-hand system negative X' values.

The point corresponding to the circle for R' = 0.5 and the arc for X' = 0.6, that is, the point of intersection of the circle for R' = 0.5 and the arc for X' = 0.6, is designated by the figure 1' in Figure H.VII.1.

(3) Let us draw a straight line 1-1'-2' passing through point 1', which we have found, and point 1 on vertical axis ab.

(4) We determine on the circular scale designated "length (wavelength)" the magnitude corresponding to the line 1-1'-2'. In our case this magnitude equals 0.0995.

(5) We read the magnitude equal to l/λ from the point found on the "length" scale. In this case this magnitude equals 0.3, and we find the value 0.0995 + 0.3 = 0.3998 on the "length" scale.

(6) We draw a line connecting point 1 on the vertical axis ab with the point we have found (the line 1-3').

(7) The sought-for value of the input impedance is determined by the point of intersection of line 1-3' and the circle with center at point 1 on the vertical axis ab and the radius 1-1'.

A series of dotted circles with their centers at point 1 are drawn in in Figure H.VII.1. In the case specified not one of the dotted circles passes through the point 1'. Point 1' lies between the dotted circles which intersect the ab axis at points 2, 6, and 3.

The circle with its center at point 1 on the ab axis and radius 1-1' intersects the line 1-3' at point 4'. Point 4' corresponds to the numerical values $R'_1 = 0.505$ and $X'_1 = -0.604$. The sought-for impedance equals

$$Z_{in} = (R'_1 + iX'_1)W = (0.505 - i\,0.604)\,600 = (303 - i\,362.4) \text{ ohms.}$$

Example 2

Find the input impedance of a line with the following data:

(1) W = 200 ohms;

(2) $l = 0.6\,\lambda$;

(3) load impedance Z = (360 - i 400) ohms.

Solution

(1) We determine

$$Z' = R' + iX' = Z/W = 1.8 - i2.$$

(2) We find the point corresponding to

$$R' = R/W = 1.8 \quad \text{and} \quad X' = X/W = -2$$

on the diagram.

This point is designated by the number 1" in Figure H.VII.1.

(3) We draw the line 1-1" to the intersection with the "length (wavelength)" scale (the line 1-1"-2").

This line intersects the scale at the point 0.2946.

(4) We add the magnitude l/λ to the value found on the "length" scale. Since the line's input impedance does not change when it is shortened, or lengthened, by the integer $0.5\,\lambda$, we can, in the case specified, take it that the line length is equal to $0.6\,\lambda - 0.5\,\lambda = 0.1\,\lambda$.

Adding 0.1 to the value 0.2946 we have found, we obtain the point 0.3946 on the "length" scale.

(5) We draw the line 1-3" passing through point 1 on the ab axis and the point corresponding to the value 0.3946 on the circular "length" scale.

(6) Using the radius equal to 1-1", we inscribe a circle with its center at point 1. The intersection of this circle with the line 1-3" (point 4") yields the values

$$R'_1 = 0.35 \qquad \text{and} \qquad X'_1 = -0.735.$$

The sought-for input impedance equals

$$Z_{in} = (0.35 - i0.735)W = (70 - i147) \text{ ohms.}$$

Similar diagrams can also be used to compute Z_{in} for a line in which attenuation is present.

Impedance diagram.

A - negative reactance;
B - positive reactance;
C - active component;
D - length (wavelength).

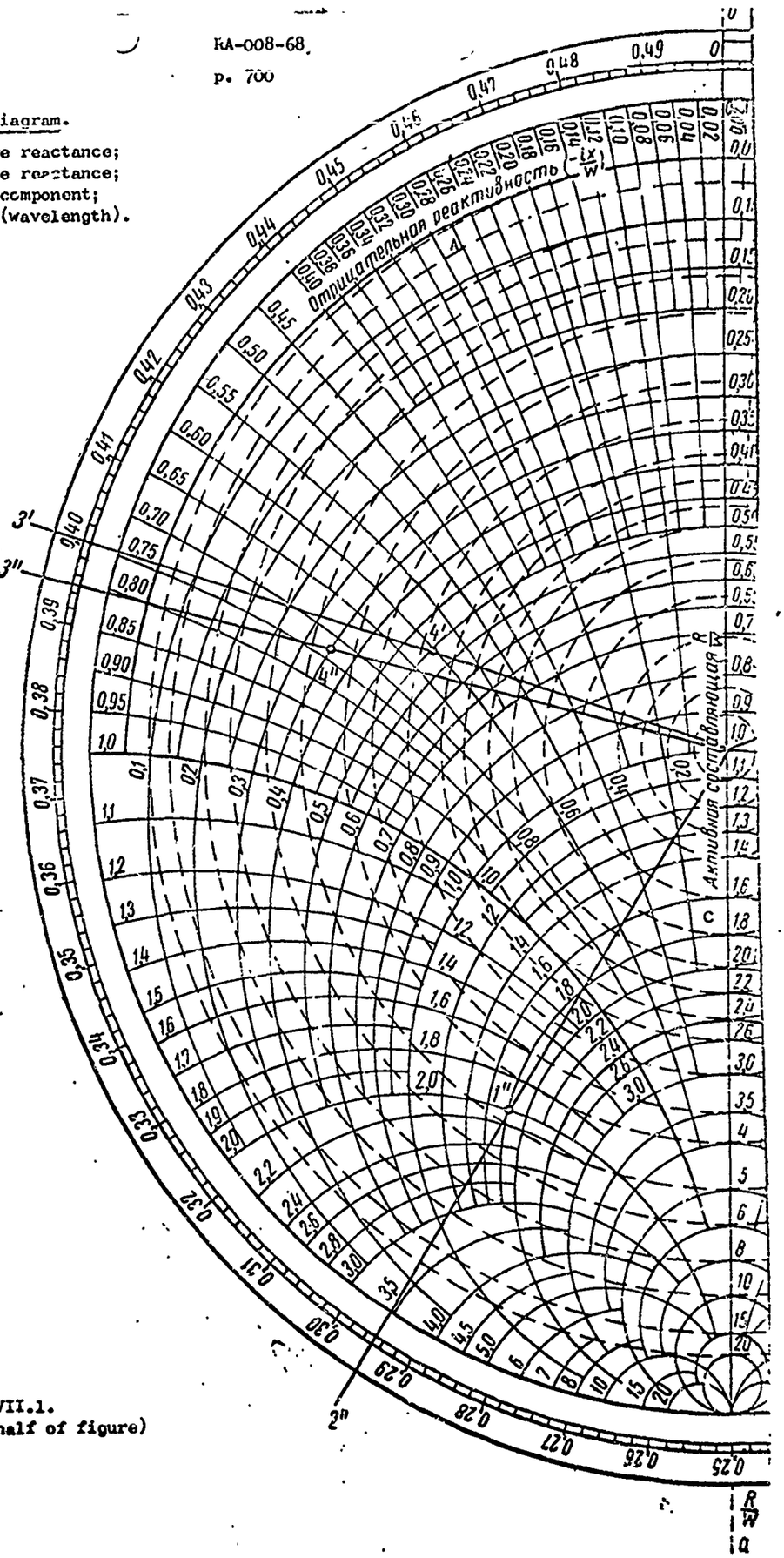

Figure H.VII.1.
(left half of figure)

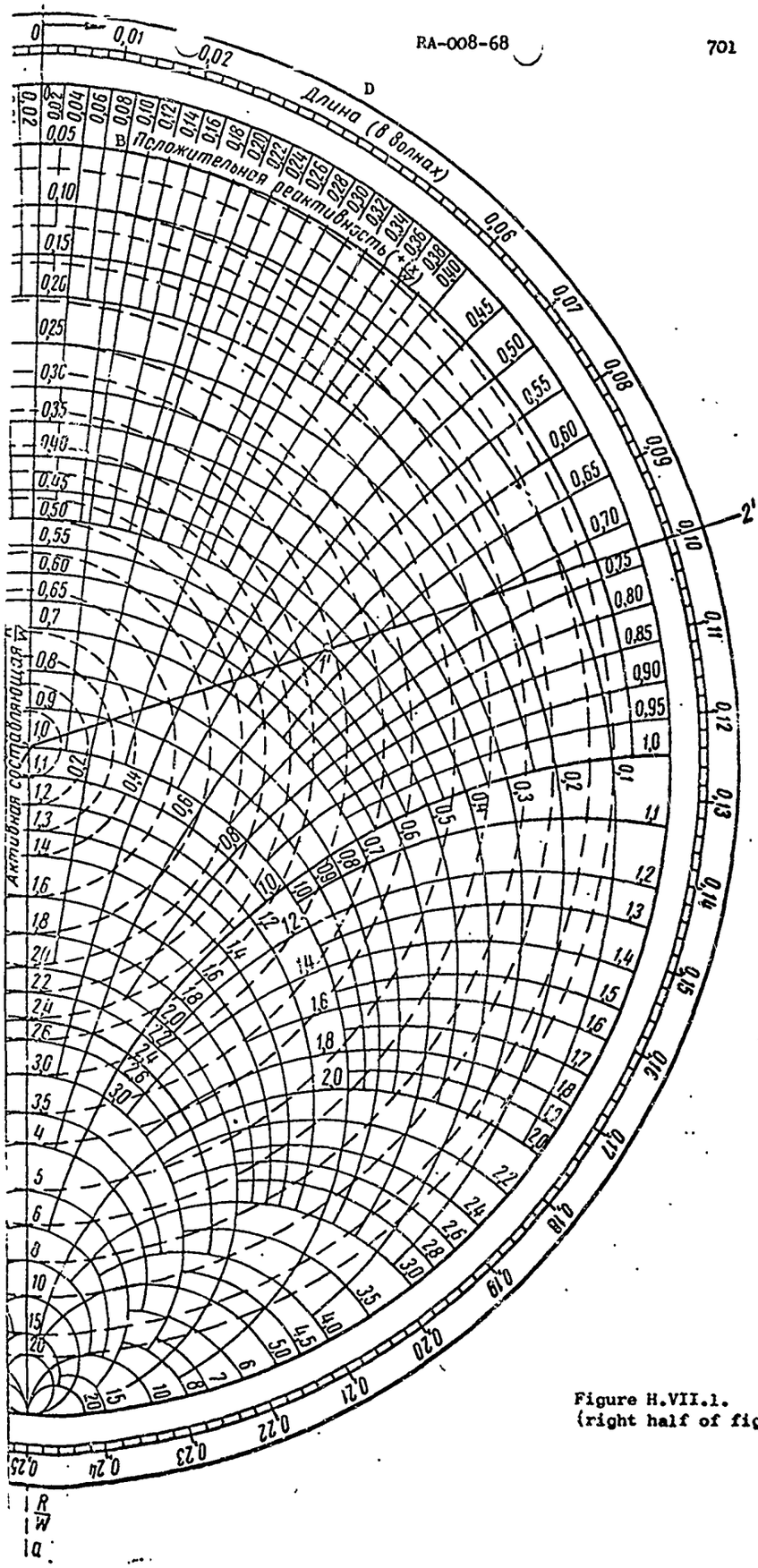

Figure H.VII.1.
(right half of figure)

TABLE OF CONTENTS

Chapter XIX. Feeders. Switching for Antennas and Feeders.

Chapter XX. Tuning and Testing Antennas.

Appendices

Handbook Section

UNCLASSIFIED
Security Classification

DOCUMENT CONTROL DATA - R & D

(Security classification of title, body of abstract and indexing annotation must be entered when the overall report is classified)

1. ORIGINATING ACTIVITY *(Corporate author)*
Foreign Science and Technology Center
US Army Materiel Command
Department of the Army

2a. REPORT SECURITY CLASSIFICATION
UNCLASSIFIED

2b. GROUP

3. REPORT TITLE
SHORTWAVE ANTENNAS

4. DESCRIPTIVE NOTES *(Type of report and inclusive dates)*
Translation

5. AUTHOR(S) *(First name, middle initial, last name)*
G. Z. Ayzenberg

6. REPORT DATE	7a. TOTAL NO. OF PAGES	7b. NO. OF REFS
2 March 70		N/A

8a. CONTRACT OR GRANT NO	9a. ORIGINATOR'S REPORT NUMBER(S)
b. PROJECT NO.	FSTC-HT-23-829-70
c. 02RD500 2301	9b. OTHER REPORT NO(S) *(Any other numbers that may be assigned this report)*
d. Redstone Arsenal	RA-008-68

10. DISTRIBUTION STATEMENT
This document has been approved for public release and sale; its distribution is unlimited.

11. SUPPLEMENTARY NOTES	12. SPONSORING MILITARY ACTIVITY
	US Army Foreign Science and Technology Center

13. ABSTRACT

This is a reprint of RA-008-68 prepared for Missile Intelligence Directorate, Redstone Arsenal.

The monograph is a revision of the book Antennas for Shortwave Radio Communication published in 1948. Included are such newer antennas as broadside multiple tuned antennas and in particular broadside antennas with untuned reflectors (chapter XII), traveling wave antennas with pure resistance coupling (chapter XIV), logarithmic antennas (chapter XVI), multiple-tuned shut dipoles (chapter IX) and others. The material on rhombic antennas was expanded and new chapters on single-wire traveling antennas and on the comparative noise stability of various receiving antennas.

DD FORM 1 NOV 68 1473 REPLACES DD FORM 1473, 1 JAN 64, WHICH IS OBSOLETE FOR ARMY USE.

711

UNCLASSIFIED
Security Classification

UNCLASSIFIED
Security Classification

14. KEY WORDS	LINK A		LINK B		LINK C	
	ROLE	WT	ROLE	WT	ROLE	WT
Antennas Short wave Communication radio						

UNCLASSIFIED
Security Classification